TECHNISCHE UNIVERSITÄT
KAISERSLAUTERN

Dr.-Ing. Michael Meurer

Empfängerorientierte Funkkommunikation – Grundzüge, Potential und Ausgestaltung einer unkonventionellen Übertragungstechnik für die Mobilkommunikation

Forschungsberichte Mobilkommunikation Band 19

Herausgegeben von Prof. Dr.-Ing. habil. Dr.-Ing. E.h. P.W. Baier

HS

Bibliografische Information der Deutschen Bibliothek

Die Deutsche Bibliothek verzeichnet diese Publikation in der Deutschen Nationalbiografie; detaillierte bibliografische Daten sind im Internet über **http://dnb.ddb.de** abrufbar.

Bibliographic information published by Die Deutsche Bibliothek

Die Deutsche Bibliothek lists this publication in the Deutsche Nationalbiografie; detailed bibliographic data are available in the Internet at **http://dnb.ddb.de**.

Herausgeber:	Prof. Dr.–Ing. habil. Dr.–Ing. E.h. P.W. Baier Lehrstuhl für hochfrequente Signalübertragung und -verarbeitung Technische Universität Kaiserslautern Postfach 3049 67653 Kaiserslautern
Verfasser:	Michael Meurer
Verlag:	Technische Universität Kaiserslautern
Druck:	Technische Universität Kaiserslautern ZBT – Abteilung Foto-Repro-Druck
	D-386

Als Manuskript gedruckt. Printed in Germany.

ISSN 1438–6720
ISBN 3–936890–81–1

Dr.-Ing. Michael Meurer
Auf dem Bännjerrück 22
D–67663 Kaiserslautern

Empfängerorientierte Funkkommunikation — Grundzüge, Potential und Ausgestaltung einer unkonventionellen Übertragungstechnik für die Mobilkommunikation

Vom Fachbereich Elektrotechnik und Informationstechnik
der Technischen Universität Kaiserslautern
zur Erlangung der Lehrbefugnis für das Fachgebiet
Nachrichtentechnik
angenommene Habilitationsschrift

von

Dr.-Ing. Michael Meurer,
wohnhaft in D–67663 Kaiserslautern, Auf dem Bännjerrück 22,
geboren am 21. Februar 1974 in Dernbach / Ww.

Kaiserslautern, den 01. Juni 2005

Vorwort

Die vorliegende Arbeit entstand in der Zeit von Februar 2003 bis Februar 2005 im Rahmen meiner Tätigkeit als wissenschaftlicher Assistent am Lehrstuhl für hochfrequente Signalübertragung und -verarbeitung der Technischen Universität Kaiserslautern. Ich möchte all jenen danken, die mich während der Entstehung dieser Arbeit unterstützt haben.

Mein besonderer Dank gilt Herrn Prof. Dr.-Ing. habil. Dr.-Ing. E.h. P.W. Baier für die Anregung, die Betreuung und die Förderung meiner Arbeit. Durch seine stete Diskussionsbereitschaft sowie durch zahlreiche Ratschläge und hilfreiche Hinweise hat er wesentlich zum Gelingen dieser Arbeit beigetragen.

Herrn Prof. Dr.-Ing. habil. Dr.-Ing. E.h. N. Fliege danke ich für das Interesse an dieser Arbeit, die kritisch-kooperative Durchsicht der Habilitationsschrift und für die Übernahme des Korreferats. Weiterhin danke ich dem Vorsitzenden der Habilitationskommission, Herrn Prof. Dr.-Ing. R. Urbansky, sowie allen weiteren Mitgliedern der Habilitationskommission.

Den jetzigen und den ehemaligen Kollegen am Lehrstuhl für hochfrequente Signalübertragung und –verarbeitung gebührt Dank für die angenehme Arbeitsatmosphäre und für viele fruchtbare Diskussionen, die mir oftmals weitergeholfen haben. Ein besonderer Dank ergeht an die Herren Dipl.-Ing. S. Heilmann, Dr.-Ing. C.A. Jötten, Dr.-Ing. W. Qiu, Dr.-Ing. H. Tröger und Dr.-Ing. habil. T. Weber für die erfolgreiche und angenehme Zusammenarbeit in gemeinsamen Projekten. Ebenso danke ich allen Studenten, die im Rahmen von Studienarbeiten, Diplomarbeiten, Masterarbeiten und als wissenschaftliche Hilfskräfte unter meiner Anleitung Beiträge zu dieser Arbeit geleistet haben. Insbesondere danke ich den Herren A. Bruhn, M. Cuntz und C. Lautensack für die tatkräftige Unterstützung beim Erstellen des Manuskripts der Habilitationsschrift.

Die in dieser Arbeit präsentierten theoretischen Grundlagen entstanden im Rahmen von Forschungsvorhaben, die durch die Deutsche Forschungsgemeinschaft (DFG) gefördert wurden. Für die wissenschaftliche Diskussionsplattform, die die DFG mir auf diese Weise bot, wie auch die finanzielle Förderung danke ich herzlich. In diesem Zusammenhang möchte ich insbesondere die enge Kooperation und die hilfreichen wissenschaftlichen Diskussionen mit Arbeitsgruppen der TU München (Prof. Dr. techn. J.A. Nossek, Prof. Dr.-Ing. W. Utschick, Dr.-Ing. M. Joham), der TU Dresden (Prof. Dr.-Ing. G. Fettweis, Dr.-Ing. R. Irmer), der Universität Erlangen-Nürnberg (Prof. Dr.-Ing. J. Huber, Priv.-Doz. Dr.-Ing. habil. R. Fischer, Dr.-Ing. C. Windpassinger), der TU Hamburg-Harburg (Prof. Dr. rer. nat. H. Rohling, Dipl.-Ing. C. Stimming), der TU Berlin bzw. des Fraunhofer Instituts für Nachrichtentechnik Heinrich-Hertz-Institut (Prof. Dr.-Ing. Dr. rer. nat. H. Boche, Dr.-Ing. M. Schubert, Dr.-Ing. G. Wunder, Dr. rer. nat. V. Jungnickel) und des Forschungszentrums Telekommunikation Wien (Prof. Dr.-Ing. R.R. Müller) nennen, woraus wichtige Hinweise für meine Arbeit resultierten.

Wesentliche Teile der Arbeit entstanden im Rahmen der Kooperation des Lehrstuhls für hochfrequente Signalübertragung und -verarbeitung mit der Fa. Siemens, u.a. im EU-Projekt FLOWS (Flexible Convergence of Wireless Standards and Services). Für zahlreiche Anregungen aus der industriellen Praxis sowie die finanzielle Förderung sei den Herren Dipl.-Ing. H. von der Neyen, Dipl.-Ing. G. Lehmann, Dr.-Ing. E. Schulz, Dipl.-Ing. W. Zirwas und Dipl.-Ing. L. Jarbot herzlich gedankt.

Der Technischen Universität Kaiserslautern danke ich für die Möglichkeit der Benutzung leistungsfähiger Rechnersysteme des Regionalen Hochschulrechenzentrums Kaiserslautern (RHRK). Den Mitarbeitern des RHRK sei für die Beratung in Softwarefragen gedankt.

Besonders herzlichen Dank schulde ich meiner Familie, insbesondere meinen Eltern. Sie haben mir das Studium der Elektrotechnik ermöglicht und mir immer ihre uneingeschränkte Unterstützung zukommen lassen. Schließlich danke ich meiner Freundin Rebecca, die mir beim Entstehen der Habilitationsschrift einen entscheidenden Rückhalt gab. Ihnen dreien widme ich diese Arbeit.

Kaiserslautern, im Juni 2005

Michael Meurer

Übersicht

Seit den ersten Anfängen der elektrischen Informationsübertragung bis in heutige Zeiten arbeiten konventionelle Funkkommunikationssysteme senderorientiert. Dies bedeutet, daß beim Entwurf solcher Systeme zunächst festgelegt wird, was im Sender geschieht, und nach dieser Festlegung hat sich dann der Empfänger beim Schätzen der gesendeten Informationen mit entsprechenden Algorithmen zu richten. Die senderseitig verwendeten Signalverarbeitungsalgorithmen werden also a priori festgelegt, und hieraus ergeben sich die empfängerseitig zu benutzenden Signalverarbeitungsalgorithmen a posteriori. Anstelle dieser herkömmlichen A-priori-Festlegung der senderseitig anzuwendenden Algorithmen kann man beim Systementwurf alternativ auch a priori mit den im Empfänger einzusetzenden Algorithmen beginnen und daraus a posteriori die senderseitig anzuwendenden Algorithmen festlegen. Diese nicht herkömmliche, mit der Bezeichnung „Empfängerorientierung“ zu kennzeichnende Vorgehensweise war bis in die jüngste Vergangenheit noch vollkommen unbekannt und wird daher nach Kenntnis des Verfassers im Bereich der Funkkommunikation bisher nicht eingesetzt. Dies ist erstaunlich, da Empfängerorientierung doch unter anderem folgende Vorteile bieten kann:

- Die a priori zu bestimmenden Empfängeralgorithmen können so gewählt werden, daß man sehr einfache Empfänger erhält.
- Kanalzustandsinformation ist lediglich senderseitig nötig, so daß auf das Übertragen von Trainingssignalen und empfängerseitig auf den Einsatz komplexer Kanalschätzalgorithmen verzichtet werden kann.
- Durch das senderseitige Einbeziehen von Kanalzustandsinformation läßt sich gegenüber herkömmlichen Systemen die Sendeleistung reduzieren.

Ziel der vorliegenden Schrift ist es, das Potential des Konzepts der Empfängerorientierung in der Mobilkommunikation eingehend zu beleuchten sowie verschiedene vorteilhafte Ausgestaltungsmöglichkeiten dieser Grundidee herauszuarbeiten und der praktischen Anwendung näherzubringen.

Der Verfasser hat maßgebliche Beiträge zur Etablierung und Ausgestaltung der Grundidee der Empfängerorientierung geleistet. Diese Beiträge manifestieren sich in zahlreichen Veröffentlichungen auf internationalen Konferenzen und in internationalen Zeitschriften sowie in mehreren Patentanmeldungen. Die vorliegende Habilitationsschrift ist in Form einer kumulativen Zusammenstellung der wichtigsten Veröffentlichungen des Verfassers zum genannten Themengebiet gestaltet und läßt so die Originalität dieser Beiträge erkennen. Eine die eingebundenen Veröffentlichungen einordnende Einleitung und Inhaltsübersicht, die auch gegenseitige Bezüge der in diesen Werken behandelten Teilgebiete darlegt, ist den Veröffentlichungen vorangestellt. Eine Zusammenfassung wesentlicher Resultate findet sich im Anschluß.

Inhaltsverzeichnis

Verzeichnis ausgewählter eingebundener Veröffentlichungen des Verfassers

Kapitel 1
Einleitung und Inhaltsübersicht

1.1 Grundlagen der Mobilkommunikation

1.1.1 Begriffe und Architekturprinzipien

Vorrangige Aufgabe der Mobilkommunikation ist das Übertragen von Informationen zwischen mindestens zwei Kommunikationspartnern, wobei mindestens einer der Kommunikationspartner nicht ortsfest, sondern mobil ist [Meu03]. Die Kommunikationspartner werden auch Teilnehmer, die technischen Einrichtungen, die Mobilkommunikation ermöglichen, Mobilkommunikationssysteme [Web00] genannt. Neben dem Übertragen von Informationen ist es primäres Ziel der Mobilkommunikation, möglichst freizügige Mobilität mindestens einer der Kommunikationspartner zu gewährleisten. Aus diesem Grund und aufgrund der unter Umständen großen zu überbrückenden Distanzen zwischen den Kommunikationspartnern bedienen sich alle heute bekannten Mobilkommunikationssysteme elektromagnetischer Wellen im Frequenzbereich einiger hundert Megahertz bis weniger Gigahertz zum Übertragen von Informationen. Elektromagnetische Wellen dieses Frequenzbereichs, die sich im Raum ausbreiten, werden als Funkwellen bezeichnet [Web00]. Daher heißen derartige Mobilkommunikationssysteme auch Mobilfunksysteme [Meu03]. Das Übertragen von Informationen erfolgt bei Mobilfunksystemen durch Übertragen informationstragender Daten, die den verwendeten Funkwellen aufgeprägt werden. Das von den mobilen Teilnehmern eingesetzte Endgerät, das die Kommunikation mit Funkwellen ermöglicht, wird als Mobilstation (MS) oder mobiles Terminal (engl. mobile terminal, MT) bezeichnet.

Der oben angesprochene Frequenzbereich der für den Mobilfunk eingesetzten Funkwellen ist eine äußerst knappe, kostbare und begrenzte Ressource, die effizient genutzt werden sollte [Ste96, DB96]. Effizientes Nutzen bedeutet hierbei, daß eine möglichst große Anzahl koexistierender Informationsübertragungen von Paaren von Kommunikationspartnern ermöglicht werden soll, wobei das Mobilfunksystem zu diesem Zweck wiederum ein Minimum des für Mobilfunksysteme zur Verfügung stehenden Frequenzbereichs nutzt [Meu03]. Neben physikalischen Gründen, die vor allem die Ausbreitungseigenschaften der Funkwellen betreffen, sind besonders wirtschaftliche Belange zu nennen, die die Kostbarkeit des angesprochenen Mediums Funkwelle ausmachen. Dies wurde beispielsweise im Jahr 2000 in Deutschland sehr eindrucksvoll bei der Versteigerung der Lizenzen für die Nutzung der Frequenzspektrumsressourcen des UMTS-Mobilfunksystems demonstriert, bei der letztlich die Zuschläge für ein Gesamtgebot von 50 Mrd. Euro erteilt wurden [ntz00a, ntz00b]. Folglich ist es unerläßlich, daß die Informationsübertragungen mehrerer Paare von Kommunikationspartnern im selben Frequenzbereich erfolgen – für die Kommunikation mehrerer Paare von Kommunikationspartnern also Funkwellen des gleichen Frequenzbereichs eingesetzt werden. Mehrere Informationsübertragungen nutzen somit gleichzeitig ein gemeinsames Übertragungsmedium. Empfängt ein Teilnehmer, der im folgenden als Referenzteilnehmer bezeichnet wird, Funkwellen, die für diesen Referenzteilnehmer Daten, also ein Nutzsignal tragen, so empfängt der Referenzteilnehmer folglich unweigerlich neben diesen nützlichen Funkwellen im allgemeinen auch weitere Funkwellen, die unerwünschte Signale tragen. Derartige unerwünschte Funkwellen gehen vorrangig auf systemfremde Störsignale, die Störung, aber auch auf solche Funkwellen zurück, die für andere Teilnehmer Daten tragen. Für andere Teilnehmer Daten tragende Funkwellen werden als Interferenz bezeichnet und wirken primär schädlich hinsichtlich der Informationsübertragung des Referenzteilnehmers. In Analogie hierzu heißen die mit den als Interferenz wirkenden Funkwellen transportierten Signale Interferenzsignale [Meu03]. Der Begriff der Interferenz wird hier in einem allgemeineren Sinn als in der Physik üblich verwendet. In der Physik bezeichnet Interferenz die kohärente Überlagerung von Wellen [GKV98], während im Mobilfunk unter Interferenz allgemein die Überlagerung beliebiger deterministischer Signale verstanden wird. Unter der schädlichen Wirkung oder kurz der Schädlichkeit von Interferenz versteht man die Schädlichkeit der Interferenzsignale hinsichtlich der fehlerfreien Informationsübertragung des Referenzteilnehmers. Für die Schädlichkeit von Interferenz sind insbesondere die folgenden beiden Gesichtspunkte entscheidend:

- Die Leistung der Interferenzsignale, denn Interferenzsignale verschwindenden Beitrags zum Empfangssignal des Referenzteilnehmers können vernachlässigt werden, und

- die strukturelle Ähnlichkeit des Interferenzsignals mit dem durch den Referenzteilnehmer zu empfangenen Nutzsignal.

Soll die Schädlichkeit von Interferenz auf ein Mindestmaß reduziert werden, so bieten sich demzufolge die folgenden vier Möglichkeiten:

- Der gemeinsame Zugriff unterschiedlicher Paare von Kommunikationspartnern auf das gemeinsam genutzte Medium Funkwelle sollte in organisierter und koordinierter Form, also einem gewissen Verhaltenscodex entsprechend, erfolgen.

- Die Leistung, der zur Informationsübertragung eingesetzten Funksignale sollte möglichst klein sein, um so die schädliche Wirkung der durch diese verursachten Interferenz zu minimieren.

- Die von verschiedenen Kommunikationspartnern verwendeten Funksignale sollten so gestaltet werden, daß vom Referenzteilnehmer empfangene Interferenzsignale strukturell möglichst geringe Ähnlichkeit mit dem vom Referenzteilnehmer empfangenen Nutzsignal haben und somit möglichst wenig schädlich wirken.

- Die selbst bei gegebenenfalls großer struktureller Ähnlichkeit bestehenden strukturellen Unterschiede zwischen vom Referenzteilnehmer empfangenen Nutzsignal und Interferenzsignalen sollten empfängerseitig möglichst effizient genutzt werden, um die schädliche Wirkung der Interferenz zu minimieren.

Die erstgenannte Möglichkeit bildet die Grundlage der wohlbekannten Vielfachzugriffsverfahren (engl. multiple access techniques), die einen derartigen Verhaltenscodex beschreiben und Stand der Technik sind. Bekannte elementare Vielfachzugriffsverfahren sind Frequenzmultiplex (engl. frequency division multiple access, FDMA), Zeitmultiplex (engl. time division multiple access, TDMA), Codemultiplex (engl. code division multiple access, CDMA) und Raummultiplex (engl. space division multiple access, SDMA), auf deren detaillierte Beschreibung hier jedoch verzichtet wird. Der interessierte Leser sei beispielsweise auf [MG62, Cal88, Ste92, SOSL88, LL86, BJK91, MR00, Meu00] verwiesen.

Die drei letztgenannten Möglichkeiten bilden den Kern zahlreicher in den letzten Jahren durchgeführter und teils noch andauernder Forschungsarbeiten in unter anderem folgenden Themenbereichen:

- Verfahren der Sendeleistungsregelung [Aei73, Zan92a, Zan92b, GZ94, GVGZ93, NA83, GVG94, AN82, LLS95, HWL97, SW96],

- Verfahren der Mehrantennentechniken [Koh94, LB00, LBM01, MM80, LR99, Hay85, WS85, God97a, God97b, Rap98, Fuh97, KV96, AMVW91, TVP96, App76, Gab76, WMGG67, Pap00, Wec02, Bla98, Jöt03, Lu02, JMB01, JBM01, JMT02],

- gemeinsame Empfangssignalverarbeitung [MJWT01, Meu03, Web02] und Mehrteilnehmerdetektion (engl. multiuser detection, MUD) [Sch79, Sch80, Ver86, Ver88, LV89, VA89, KIHP90, LV90, VA90, XSR90, VA91, AF92, DH92, BFKM93, DH93, Ver93, ASF94, KKKB94, PF94, RV94, WDH94, YR94, DH95, TAS95, Kle96, KKKB96, ARS97, Ver98, ZB98, ARAS99, Kar99, HMC99, BNK00, Poo00, TR00, Jar01, JD01, WM02b, WOWB02, WM02a, KTF04, KBF05, MW03a, MW03b] und

- gemeinsame Sendesignalerzeugung (engl. joint transmission, JT) [BMWT00, KM00, MBL$^+$00, MBW$^+$00, PMWB00, TMW00, GC01, INBF01, JU01, JUN01, JWJH01, LMTB01, LTM01, MTWB01b, MTWB01a, TWMB01b, TWMB01a, WR01, BM02, CM02a, CM02b, GC02, IF02b, IF02a, JKG+02, JKUN02, ML02, MTJ02, QTM02, RIF02, SSB+02, TQMJ02, TWL+02, WIF02, BM03, BQT+03, BZT+03, CM03, CML03, DHJU03, FW03, JIB+03, Geo03, HSB03, IHRF03, IRF03b, IRF03a, JIB+03, MQW03, Trö03, WCS03, WM03d, WM03e, WM03c, WM03b, WMS03, WVF03b, BHMW04, BJM+04, BM04, CM04d, CM04a, CM04c, CM04b, IGF04, IHRF04b, JBU04, JBVU04, Joh04, MBQ04, Meu04b, Meu04a, MQS+04, MW04a, MW04b, MWQ04b, MWQ04a, Skl04, Qiu05] und Precoding [VJ98, BPD00, CLM01, FTH01, Fis02, FWLH02b, FWLH02a, FWLH02c, WF03, WVF03a, WES04, Win04].

Der letztgenannte Bereich ist ein zentrales Thema der vorliegenden Schrift.

Betrachtet man die Gesamtsituation der Funkkommunikation in einem mehrere Teilnehmer umfassenden Mobilfunksystem, so lassen sich anhand dessen, ob die einzelnen Teilnehmer eine Senderrolle oder eine Empfängerrolle einnehmen, die im folgenden beschriebenen und in Bild 1.1 dargestellten vier Grundarchitekturen der Funkkommunikation definieren:

- Kommuniziert ein einziger Sender (engl. transmitter, Tx) mit einem einzigen Empfänger (engl. receiver, Rx), so spricht man von einer Punkt-zu-Punkt-Übertragung (engl. point-to-point, P2P), siehe auch Bild 1.1a.

- Kommuniziert ein einziger Sender mit N_O, das heißt mehreren Empfängern, so spricht man von einer Punkt-zu-Mehrpunkt-Übertragung (engl. point-to-multipoint, P2MP), siehe auch Bild 1.1b. In der Literatur [Cov72, CT91, Cov98] wird eine derartige Grundarchitektur der Funkkommunikation auch als Broadcast (BC) bezeichnet. Entgegen alternativen, anders lautenden Definitionen dieses Begriffs in der Literatur [OPM98, Rei98] ist es bei der hier verwendeten unerheblich, ob die verschiedenen Empfänger gleiche oder unterschiedliche Daten erhalten sollen.

- Kommunizieren N_I, das heißt mehrere Sender mit einem einzigen Empfänger, so spricht man von einer Mehrpunkt-zu-Punkt-Übertragung (engl. multipoint-to-point, MP2P), siehe auch Bild 1.1c. Eine derartige Grundarchitektur wird auch als Multiple Access (MA) bezeichnet.

- Kommunizieren N_I, das heißt mehrere Sender mit N_O, das heißt mehreren Empfängern, so spricht man von einer Mehrpunkt-zu-Mehrpunkt-Übertragung (engl. multipoint-to-multipoint, MP2MP), siehe auch Bild 1.1d.

Ein Mobilfunksystem kann mehreren der oben genannten Grundarchitekturen der Funkkommunikation genügen, wenn diese Grundarchitekturen beispielsweise zu verschiedenen Zeiten oder für verschiedene unabhängige Übertragungsmedien, also Funkwellen verschiedener Frequenzbereiche, verwendet werden.

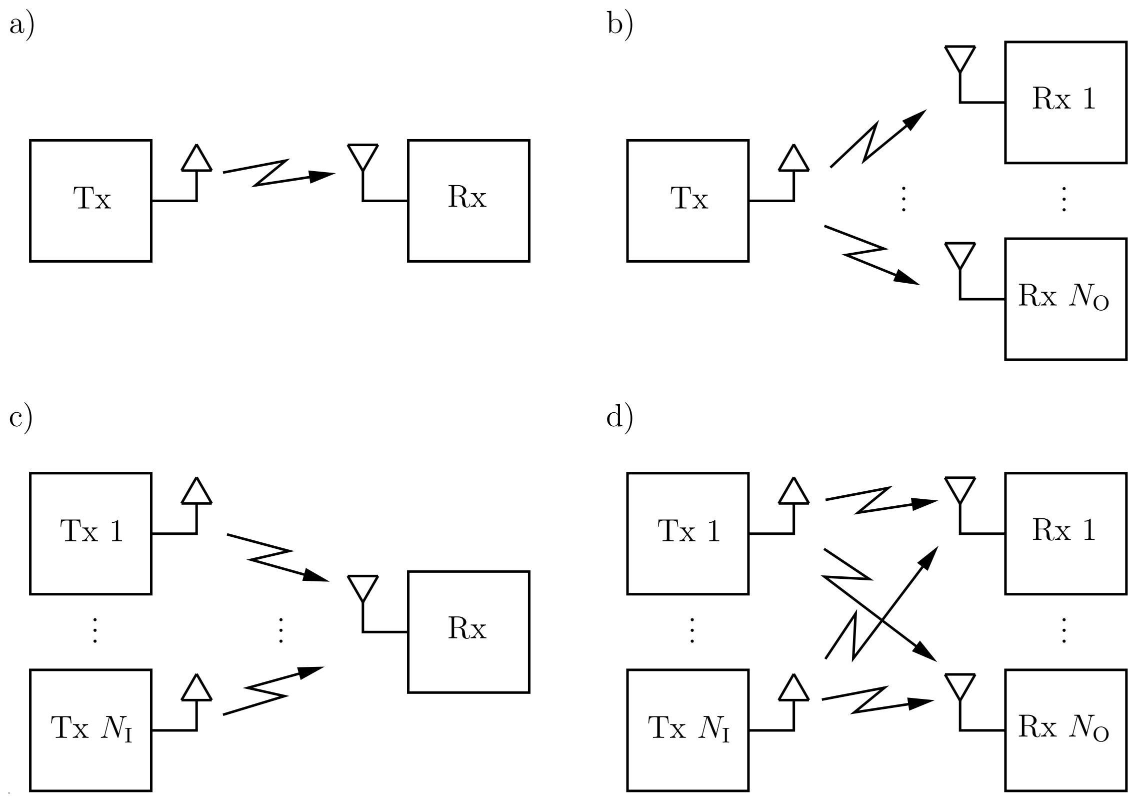

Bild 1.1. Grundarchitekturen der Funkkommunikation zwischen mindestens einem Sender (Tx) und mindestens einem Empfänger (Rx):

a) Punkt-zu-Punkt-Übertragung,
b) Punkt-zu-Mehrpunkt-Übertragung (Broadcast),
c) Mehrpunkt-zu-Punkt-Übertragung (Multiple Access) und
d) Mehrpunkt-zu-Mehrpunkt-Übertragung

Betrachtet man eine Punkt-zu-Punkt-Übertragung zwischen einem mit einer Sendeantenne ausgestatteten Sender und einem mit einer Empfangsantenne versehenen Empfänger, so ist die Menge der fehlerfrei übertragbaren Information pro Zeit entsprechend der Theorie von Shannon begrenzt [Sha48, CT91, Roh95]. Dies ist ein wenig befriedigender Zustand, da in den letzten Jahren die Anforderungen an die Menge der fehlerfrei übertragbaren Information pro Zeit mit Einführung neuer mobiler Dienste, wie beispielsweise Wireless Application Protocol (WAP), elektronische Post (engl. electronic mail, email), World Wide Web (WWW), Multimedia Messaging Service (MMS), Bildtelefonie, Videoübertragung (engl. streaming video) und mobiles Fernsehen stetig zunahmen. Aus diesem Grund wurden in jüngster Vergangenheit intensiv Möglichkeiten diskutiert, diese Informationsmenge durch Verfolgen einer recht einfachen Grundidee zu steigern. Diese Grundidee besteht darin, mehrere Antennen am Sender und/oder meh-

Tabelle 1.1. Grundlegende Antennenkonfigurationen

<table>
<tr><td colspan="2" rowspan="2"></td><td colspan="2">Anzahl der Empfangsantennen</td></tr>
<tr><td>$= 1$</td><td>> 1</td></tr>
<tr><td rowspan="2">Anzahl der Sendeantennen</td><td>$= 1$</td><td>SISO</td><td>SIMO</td></tr>
<tr><td>> 1</td><td>MISO</td><td>MIMO</td></tr>
</table>

rere Antennen am Empfänger einzusetzen, um so die aus der Shannonschen Theorie folgenden Grenzen hinauszuschieben [Fos96, FG98, WFGV98, FGVW99, Tel99]. In der Literatur wurden sowohl theoretische Arbeiten [Tel99, FG98] vorgestellt, die eine Analyse der auf diese Weise maximal erzielbaren fehlerfrei übertragbaren Informationsmengen pro Zeit betreffen, als auch solche Arbeiten [FG98, WFGV98, FGVW99, GFVW99, CRFLL00, BTT02, WVF03b, CM04d] präsentiert, die speziell auf die praktische Umsetzung dieser Grundidee eingehen. Als Konsequenz dessen lassen sich heute, je nach Anzahl der Sende- und Empfangsantennen, die vier in Tabelle 1.1 dargestellten Antennenkonfigurationen

- Single-Input-Single-Output (SISO),
- Single-Input-Multiple-Output (SIMO),
- Multiple-Input-Single-Output (MISO) und
- Multiple-Input-Multiple-Output (MIMO)

unterscheiden, die bei Mobilfunksystemen eingesetzt werden.

Durch Kombination der vier Grundarchitekturen der Funkkommunikation mit den vier Antennenkonfigurationen kann eine Vielzahl $2^{N_\mathrm{I}+N_\mathrm{O}}$ unterschiedlicher Ausprägungen von Grundstrukturen der Kommunikation in Mobilfunksystemen definiert werden, wie beispielsweise MIMO-Broadcast. Um eine kompakte nachrichtentechnische Behandlung derartiger Grundstrukturen zu ermöglichen, ist es hilfreich, ein alle angesprochenen Ausprägungen umfassendes gemeinsames Rahmenwerk bereitzustellen. Ein derartiges Rahmenwerk bildet das in Bild 1.2 dargestellte verallgemeinerte

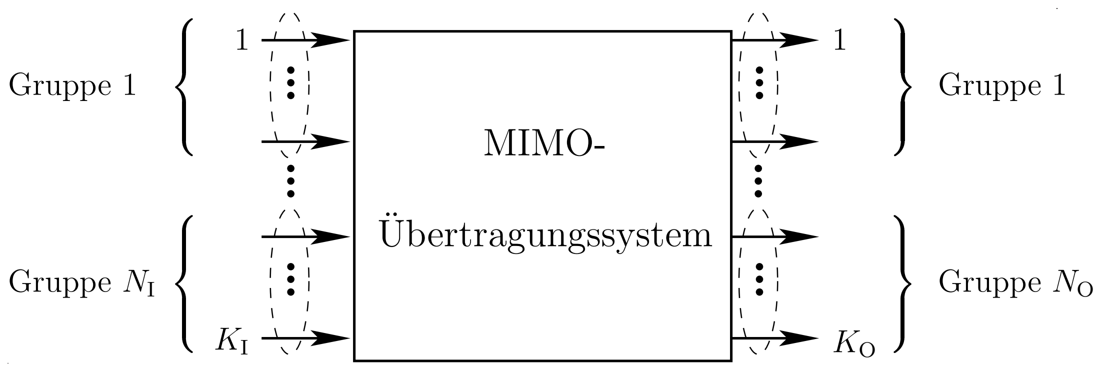

Bild 1.2. Verallgemeinertes MIMO-Übertragungssystem mit K_I Eingängen und K_O Ausgängen; die K_I Ein- bzw. K_O Ausgänge sind in N_I bzw. N_O Gruppen gegliedert, die jeweils hinsichtlich der senderseitigen bzw. empfängerseitigen Signalverarbeitung kooperativ bedienbare Ein- bzw. Ausgänge bündeln.

MIMO-Übertragungssystem, denn unabhängig davon, welche konkrete Ausprägung betrachtet wird, läßt sich der bei den verschiedenen Ausprägungen eingesetzte Mobilfunkkanal stets als ein Spezialfall des in Bild 1.2 dargestellten verallgemeinerten MIMO-Übertragungssystems interpretieren. Ein derartiges verallgemeinertes MIMO-Übertragungssystem verfügt im allgemeinen über K_I Eingänge – dies sind im obigen Fall die Eingänge der Sendeantennen der Sender – und K_O Ausgänge – dies sind im obigen Fall die Ausgänge der Empfangsantennen der Empfänger –, die eingangsseitig zu N_I und ausgangsseitig zu N_O Gruppen zusammengefaßt sind. Jeder Eingang ist genau einer der N_I eingangsseitigen Gruppen, jeder Ausgang genau einer der N_O ausgangsseitigen Gruppen zugeordnet. Eingänge beziehungsweise Ausgänge, die der gleichen Gruppe zugeordnet sind, können eingangsseitig beziehungsweise ausgangsseitig in einer kooperativen Weise, das heißt gemeinsam bedient werden. Dies gilt im obigen Fall beispielsweise für Eingänge, die zu verschiedenen Sendeantennen ein und desselben Senders gehören, wie auch für Ausgänge, die zu verschiedenen Empfangsantennen ein und desselben Empfängers gehören. Demgegenüber können Eingänge beziehungsweise Ausgänge unterschiedlicher Gruppen nur in nicht kooperativer Weise, das heißt unabhängig voneinander bedient werden, beispielsweise weil diese zu Sendeantennen unterschiedlicher nicht kooperierender Sender beziehungsweise zu Empfangsantennen verschiedener nicht kooperierender Empfänger gehören. Die Gruppen sind in Bild 1.2 durch gestrichelt gezeichnete Ellipsen graphisch veranschaulicht.

Aus der Vielzahl aller in den letzten Jahrzehnten entstandenen oben charakterisierten Mobilfunksysteme hat sich die Klasse der infrastrukturbasierten Mobilfunksysteme als die bedeutsamste herauskristallisiert. Die Bedeutung derartiger infrastrukturbasierter Mobilfunksysteme, zu denen unter anderem die erfolgreichen (kommerziellen)

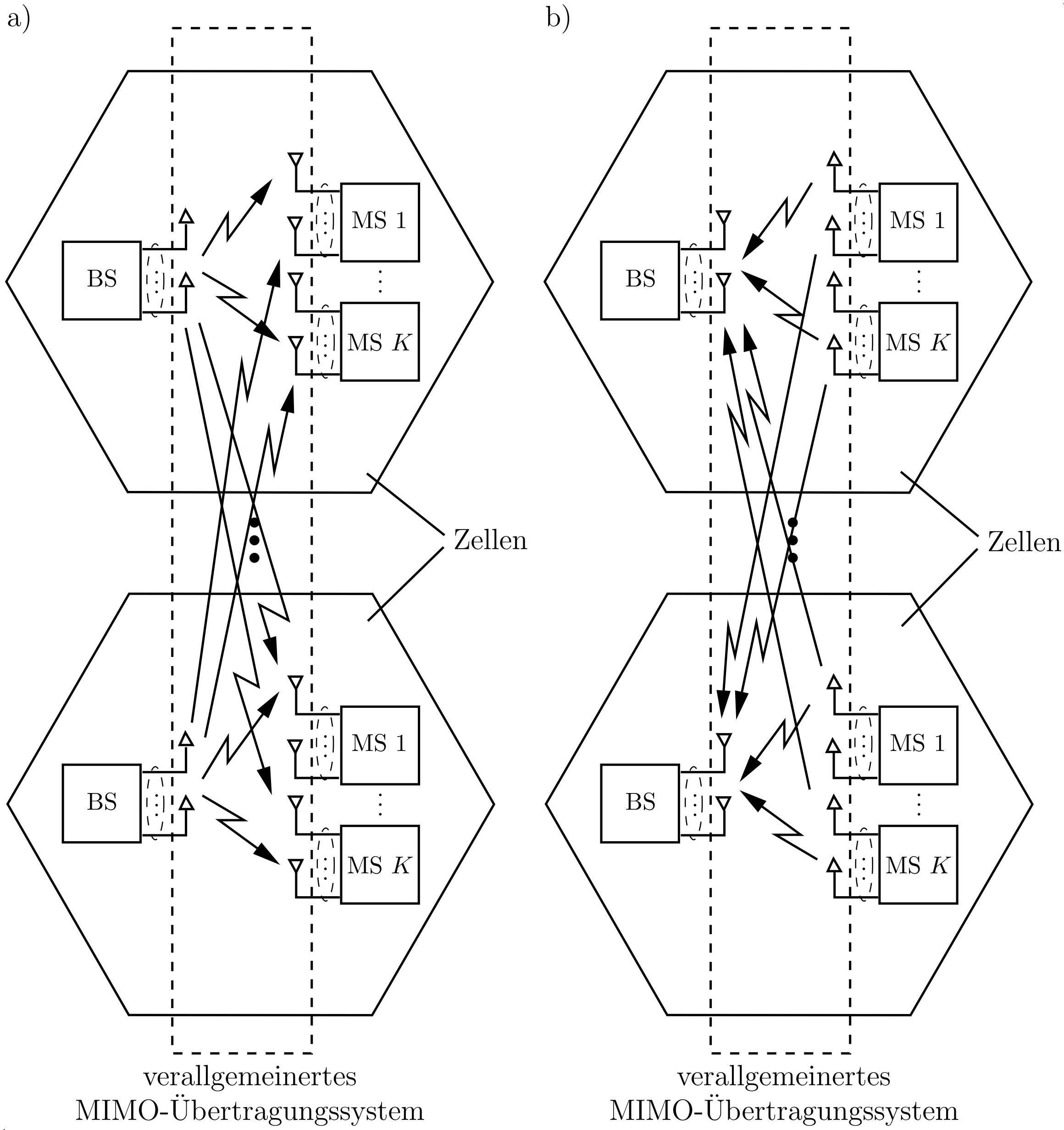

Bild 1.3. Interpretation des in infrastrukturbasierten Mobilfunksystemen genutzten Mobilfunkkanals als verallgemeinertes MIMO-Übertragungssystem:

a) Abwärtsstrecke und

b) Aufwärtsstrecke

zellularen Mobilfunksysteme [SG91, Pad94, KKLN98, OP98, HT00, AS97, CMO99, DGNS98, ASS98, FST+96, Wal98b, Huf79, You79, Kam84, Kam85, HS87, Wes02] wie auch infrastrukturbasierte drahtlose Funknetzwerke (engl. wireless local area networks, WLAN) [CWKS97, EMSW02, Wal98a] zählen, gründet insbesondere auf der herausragenden wirtschaftlichen Bedeutung, die infrastrukturbasierte Mobilfunksysteme im

Vergleich zu andersartigen Mobilfunksystemen erlangt haben [DAI96]. Weltweit stetig ansteigende Nutzerzahlen derartiger infrastrukturbasierter Mobilfunksysteme betonen diese Erkenntnis zunehmend von Jahr zu Jahr [DAI96, Rab01]. Aus diesem Grund beschränkt sich der Autor im weiteren Verlauf dieser Schrift der Übersichtlichkeit halber exemplarisch auf die Betrachtung infrastrukturbasierter Mobilfunksysteme. Es sei jedoch angemerkt, daß sämtliche gemachten allgemeinen Betrachtungen prinzipiell nicht auf derartige infrastrukturbasierte Mobilfunksysteme beschränkt sind.

In infrastrukturbasierten Mobilfunksystemen sind einige der Kommunikationspartner ortsfest. Die von diesen Kommunikationspartnern zur Funkkommunikation verwendeten Endgeräte sind demzufolge Feststationen, die auch Basisstationen (engl. base station, BS) oder Zugriffspunkte (engl. access points, AP) genannt werden. Mobile Endgeräte werden weiterhin als Mobilstationen oder mobile Terminals bezeichnet. Da die Distanz zwischen einer Mobilstation und deren Kommunikationspartner sehr groß sein kann, wodurch eine direkte Funkübertragung zwischen der Mobilstation und ihrem Kommunikationspartner sehr erschwert wird, oder der Kommunikationspartner sogar Teilnehmer eines anderen, beispielsweise leitungsgebundenen Kommunikationssystems sein kann [Web02], verwendet man in infrastrukturbasierten Mobilfunksystemen typischerweise eine einheitliche indirekte Informationsübertragung [Gib99, Ste92, DB96, Wes02, Tan92]. Zu diesem Zweck kommuniziert die Mobilstation ausschließlich mit den ortsfesten Basisstationen, die ihrerseits, eventuell über weitere Zwischenstationen, mit dem letztlich gewünschten Kommunikationspartner kommunizieren und somit als Transitsystem dienen [EF86, Web00, Meu03]. In Mobilfunksystemen wird eine Duplexübertragung [Gib99, Ste92, DB96] realisiert [Lee90]. Dabei wird die Übertragung von der Mobilstation zur Basisstation als Aufwärtsstrecke (engl. uplink, UL) bezeichnet, wohingegen die entgegengesetzt gerichtete Übertragung von der Basisstation zur Mobilstation als Abwärtsstrecke (engl. downlink, DL) bezeichnet wird [Meu03]. Sinnvollerweise kommuniziert eine Mobilstation mit dieser Basisstation, für die die Übertragungseigenschaften des zwischen Mobilstation und Basisstation wirksamen Mobilfunkkanals bestmöglich sind — insbesondere die Dämpfung minimal ist —, und die typischerweise, aber nicht notwendigerweise aus Sicht der Mobilstation die nächstgelegene ist. In natürlicher Art und Weise ergibt sich somit eine Partitionierung des Mobilfunksystems in Zellen, die jeweils aus genau einer Basisstation und den zugeordneten Mobilstationen bestehen [MD79, Gib99, DB96, Wes02]. Infrastrukturbasierte Mobilfunksysteme mit mindestens zwei Zellen werden daher auch zellulare Mobilfunksysteme genannt, und die Gesamtheit aller Zellen wird als Zellnetz bezeichnet. Bild 1.3 zeigt ein derartiges Zellnetz eines zellularen Mobilfunksystems, wobei, wie in den folgenden Betrachtungen ebenfalls, angenommen wird, daß pro Zelle K Mobilstationen zu versorgen sind.

Betrachtet man die Funkkommunikation innerhalb eines infrastrukturbasierten Mobilfunksystems, so fällt auf, daß entsprechend den oben gemachten Ausführungen die Gesamtheit aller zwischen Basisstationen und Mobilstationen bestehenden wirksamen Funkkanäle als verallgemeinertes MIMO-Übertragungssystem nach Bild 1.2 angesehen werden kann, vergleiche auch Bild 1.3. Im Falle der Abwärtsstrecke bilden dabei die Eingänge der Sendeantennen aller Basisstationen die K_{I} Eingänge des verallgemeinerten MIMO-Übertragungssystems, wohingegen die Ausgänge der Empfangsantennen aller Mobilstationen die K_{O} Ausgänge dieses verallgemeinerten MIMO-Übertragungssystems sind. Im Falle der Aufwärtsstrecke gilt entsprechendes für die Eingänge der Sendeantennen aller Mobilstationen beziehungsweise die Ausgänge der Empfangsantennen aller Basisstationen.

Betrachtet man exemplarisch die Abwärtsstrecke, siehe Bild 1.3a – in der Aufwärtsstrecke gelten die folgenden Ausführungen analog –, so ist es infolge der räumlichen Separierung der verschiedenen Mobilstationen einsichtig, daß die Verarbeitung der durch die Mobilstationen empfangenen Signale vorzugsweise nur mobilstationsweise, also in einer nicht kooperativen Weise erfolgen kann. Demgegenüber können die von verschiedenen Empfangsantennen ein und derselben Mobilstation empfangene Signale prinzipiell gemeinsam behandelt werden, da diese am gleichen Endgerät bereitstehen. Folgerichtig bilden die zu verschiedenen Empfangsantennen ein und derselben Mobilstation gehörigen Ausgänge des verallgemeinerten MIMO-Übertragungssystems jeweils eine der N_{O} Gruppe im zuvor dargelegten Sinne. Hinsichtlich der Gruppierung der K_{I} Eingänge des verallgemeinerten MIMO-Übertragungssystems, das heißt der Eingänge der Sendeantennen aller Basisstationen, ist festzustellen, daß grundsätzlich ein gemeinsames, das heißt in kooperativer Weise erfolgendes Bedienen der Sendeantennen aller Basisstation möglich ist. Im Gegensatz zu den Mobilstationen sind Basisstationen eines infrastrukturbasierten Mobilfunksystems nämlich typischerweise in der Lage, durch leitungsgebundene oder drahtlose Netzwerke untereinander zu kommunizieren, was die Grundlage für die genannte Kooperation ist. Erste eine derartige Kooperation betreffende theoretische Ansätze wurden in jüngster Vergangenheit in der Literatur bereits vorgeschlagen [SWM01, WMSL02, SWBC02, WSLW03, SWWM04]. Die praktische Relevanz derartiger Vorschläge ist jedoch in heutigen infrastrukturbasierten Mobilfunksystemen aus folgenden Gründen noch gering:

- Die Kapazität der zwischen verschiedenen Basisstationen bestehenden Übertragungskanäle ist in heutigen infrastrukturbasierten Mobilfunksystemen typischerweise stark begrenzt. Für eine umfassende Kooperation im obigen Sinne ist diese Kapazität unterdimensioniert und daher nicht ausreichend.

- Ein umfassendes kooperatives Bedienen der Sendeantennen aller Basisstationen ist nur dann sinnvoll möglich, wenn die Kenntnis aller zwischen Basisstationen und Mobilstationen wirksamen Funkkanäle insbesondere über Zellgrenzen hinweg vorliegt [Fis97, Win04]. Eine derartige Kenntnis ist jedoch nicht a priori vorhanden, sondern muß durch geeignete Verfahren des Kanalschätzens verfügbar gemacht werden. Der Aufwand zum Schätzen aller genannten Funkkanäle steigt je nach verwendetem Verfahren mindestens quadratisch mit der Anzahl der Basisstationen [WM03a, WM04a]. Es ist daher einleuchtend, daß im Falle eines großen Zellnetzes die angesprochene Kenntnis über die wirksamen Funkkanäle kaum oder nur für einen sehr hohen Preis zu erlagen ist.

Als Folge der oben dargelegten Ausführungen arbeiten alle heutigen infrastrukturbasierten Mobilfunksysteme im Sinne der oben dargelegten Kooperation ausschließlich basisstationsweise. Es ist davon auszugehen, daß die geschilderten Schwierigkeiten aufgrund ihres grundsätzlichen Charakters kurzfristig nicht auszuräumen sind. Daher ist auch bei infrastrukturbasierten Mobilfunksystemen der nahen Zukunft ein basisstationsweises Bedienen der Sendeantennen der Basisstationen zu erwarten. Da eine derartige Annahme die grundsätzlichen im Rahmen dieser Arbeit gemachten Betrachtungen nicht betrifft, soll in der vorliegenden Schrift im folgenden ebenfalls vereinfachend von basisstationsweisem Vorgehen ausgegangen werden. Erfolgt das Speisen der Sendeantennen verschiedener Basisstationen in der beschriebenen nicht kooperativen Weise, so zerfällt das dargestellte verallgemeinerte MIMO-Übertragungssystem in zellenspezifische unabhängige Übertragungssysteme, die ausschließlich durch wechselseitige Interferenz, sogenannte Interzellinterferenz [Web02, Meu03], gekoppelt sind. Die Funkkommunikation in der Abwärtsstrecke eines zellularen Mobilfunksystems kann daher vereinfachend für jede Zelle separat behandelt werden, wobei dabei auftretende Interzellinterferenz zu berücksichtigen ist. Gleiches gilt für die Aufwärtsstrecke eines zellularen Mobilfunksystems in analoger Weise. Im Rahmen der vorliegenden Schrift beschränkt sich der Autor daher der Übersichtlichkeit halber vorzugsweise auf die Betrachtung der Funkkommunikation in einer derartigen Zelle, die im folgenden als Referenzzelle bezeichnet wird. Auf andere Zellen zurückgehende Interzellinterferenz wird durch zufällige additive Störsignale modelliert, siehe auch Abschnitt 1.1.2. Für Betrachtungen, die das gesamte zellulare Mobilfunksystem betreffen, sei der interessierte Leser beispielsweise auf [PMWB00, BZT+03, Trö03] verwiesen.

1.1.2 Systemmodell

Verfahren und Systeme zur Funkkommunikation können nur entwickelt und untersucht werden, wenn geeignete mathematische Hilfsmittel zum Beschreiben aller beteiligten relevanten Signale, Größen und Übertragungssysteme vorhanden sind. Das Ziel dieses

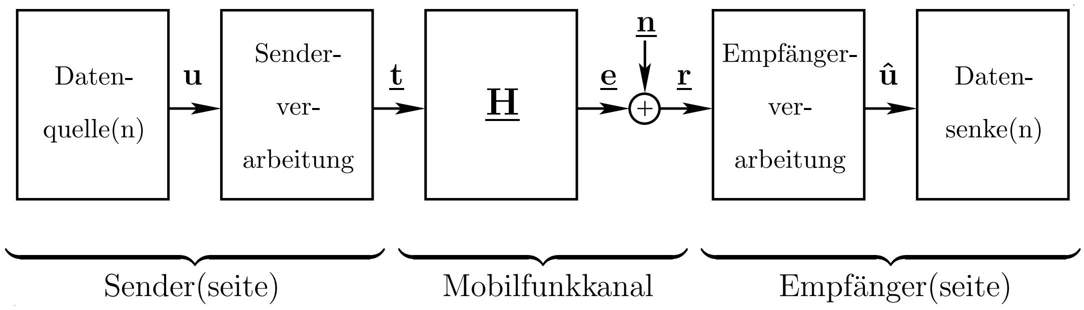

Bild 1.4. Allgemeines Modell der Funkkommunikation innerhalb einer Referenzzelle mit mindestens einem Sender und mindestens einem Empfänger

Unterkapitels besteht darin, solche mathematischen Hilfsmittel vorzustellen und basierend auf diesen ein mathematisches Modell für alle beteiligten relevanten Signale, Größen und Übertragungssysteme zu entwickeln.

Die mathematischen Darstellungen in dieser Schrift erfolgen im zeitdiskreten äquivalenten Tiefpaßbereich [SJ67, Pro95, Kle96]. Vektoren werden mit fettgedruckten Kleinbuchstaben, Matrizen mit fettgedruckten Großbuchstaben bezeichnet. Komplexe Größen, seien es skalare Größen, Vektoren oder Matrizen, werden unterstrichen. Das Bilden der Vektornorm, die komplexe Konjugation und die Transposition werden mit $||\cdot||$, $(\cdot)^*$ beziehungsweise $(\cdot)^{\mathrm{T}}$, der hermitesche Operator mit $(\cdot)^{\mathrm{H}}$ bezeichnet. Wahrscheinlichkeiten werden mit $\mathrm{P}(\cdot)$, Wahrscheinlichkeitsdichten mit $\mathrm{p}(\cdot)$ bezeichnet. Der Erwartungswert und die Varianz einer Zufallsgröße sind durch $\mathrm{E}\{\cdot\}$ beziehungsweise $\mathrm{var}\{\cdot\}$ gekennzeichnet.

Betrachtet man die Funkkommunikation in der in Unterkapitel 1.1.1 beschriebenen Referenzzelle eines infrastrukturbasierten Mobilfunksystems, so fällt auf, daß die Funkkommunikation in der Abwärtsstrecke der Grundarchitektur Broadcast, die Funkkommunikation in der Aufwärtsstrecke der Grundarchitektur Multiple Access genügt. Diesen beiden Grundarchitekturen der Funkkommunikation kommt demzufolge eine besondere Bedeutung zu. Aus diesem Grund sollen die genannten Grundarchitekturen der Funkkommunikation im folgenden besonders beleuchtet werden. Eine separate Behandlung der Grundarchitektur Punkt-zu-Punkt-Übertragung ist dabei nicht erforderlich, da diese einen entarteten Spezialfall der Grundarchitektur Broadcast für einen einzigen Empfänger beziehungsweise der Grundarchitektur Multiple Access für einen einzigen Sender darstellt und daher implizit abgedeckt ist. Unabhängig davon, ob die Abwärtsstrecke – also Funkkommunikation der Grundarchitektur Broadcast – oder die Aufwärtsstrecke – also Funkkommunikation der Grundarchitektur Multiple Access – betrachtet wird, läßt sich ein einheitliches Modell für die Kommunikation in der Referenzzelle definieren. Ein derartiges Modell ist in Bild 1.4 dargestellt. In diesem Bild ist die Senderseite, die den mindestens einen Sender der Referenzzelle umfaßt, und die die Empfängerseite, die den mindestens einen Empfänger der Referenzzelle umfaßt, gekennzeichnet. Im Rahmen der vorliegenden Schrift werden alle relevanten Signale als näherungsweise zeit- und bandbegrenzte Signale betrachtet. Die Konzentration auf näherungsweise sowohl zeit- als auch bandbegrenzte Signale ist aus den folgenden Gründen keine große Einschränkung [Web02]:

- Eine Bandbreitenbegrenzung der Signale eines Mobilfunksystems ist bei Verwenden realer Komponenten, wie beispielsweise realer Verstärker, Antennen, etc. aus physikalischen Gründen ohnehin unumgänglich [MG86].

- Die Sendesignale in Mobilfunksystemen müssen aus regulatorischen Gründen in guter Näherung auf begrenzte Frequenzbänder limitiert sein.

- Eine Zeitbegrenzung der Signale ist in Mobilfunksystemen mit Zeitmultiplexkomponente ohnehin gegeben und läßt sich in Mobilfunksystemen ohne eine derartige Komponente durch Betrachten zeitbegrenzter Signalausschnitte erzeugen. Der durch Betrachten derartiger zeitbegrenzter Signalausschnitte resultierende Modellierungsfehler kann durch Wahl hinreichend langer Ausschnitte beliebig gering gestaltet und darüber hinaus durch spezielle Signalverarbeitungstechniken [Ver88, Ver93, WNM92, WNM93, WNM96, Bra97, JA97, ML01, MJWT01, Meu03] weiter reduziert werden.

Näherungsweise zeit- und bandbegrenzte Signale lassen sich mathematisch kompakt durch Vektoren repräsentieren. Daher soll im folgenden ein auf dieser Darstellung beruhendes Modell der Funkkommunikation innerhalb der Referenzzelle vorgestellt werden.

In einer eine Basisstation und K Mobilstationen umfassenden Referenzzelle eines heutigen infrastrukturbasierten Mobilfunksystems liegen die L Nutzdaten $u_l^{(k)}$, $l = 1 \dots L$, die zwischen der Basisstation und einer Mobilstation k, $k = 1 \dots K$, das heißt einem mobilen Teilnehmer, auszutauschen sind, senderseitig typischerweise in binärer Form vor, das heißt es gilt

$$u_l^{(k)} \in \mathbb{B} \tag{1.1}$$

mit

$$\mathbb{B} = \{0, 1\}. \tag{1.2}$$

Dies gilt unabhängig vom zu realisierenden mobilen Dienst und wird beispielsweise im Falle von Sprachtelefonie durch geeignete Verfahren der Abtastung [Lük79, Lük99, GR91], Analog-Digital-Wandlung [Max60, Lük79, Llo82, Meu00, MR00] und Quellcodierung [VHH98, Jax02] ermöglicht. Derartige Verfahren sind Stand der Technik und werden daher in der vorliegenden Schrift nicht weiter beleuchtet. Durch Zusammenfassen aller L Nutzdaten $u_l^{(k)}$, $l = 1 \ldots L$, eines Teilnehmers erhält man den teilnehmerspezifischen Nutzdatenvektor

$$\mathbf{u}^{(k)} = \left(u_1^{(k)} \ldots u_L^{(k)}\right)^{\mathrm{T}} \in \mathbb{B}^L, \tag{1.3}$$

der alle für den Teilnehmers k, $k = 1 \ldots K$, zu übertragenden Nutzdaten kompakt beschreibt. Durch weiteres Kombinieren der K teilnehmerspezifischen Nutzdatenvektoren $\mathbf{u}^{(k)}$, $k = 1 \ldots K$, nach (1.3) folgt der totale Nutzdatenvektor

$$\mathbf{u} = \left(\mathbf{u}^{(1)\mathrm{T}} \ldots \mathbf{u}^{(K)\mathrm{T}}\right)^{\mathrm{T}} \in \mathbb{B}^{KL}, \tag{1.4}$$

der Dimension KL.

Wie bereits erwähnt, fungieren in der Abwärtsstrecke die Basisstation, in der Aufwärtsstrecke die K Mobilstationen als Sender. Unabhängig davon, ob die Abwärtsstrecke oder die Aufwärtsstrecke betrachtet wird, bilden die Nutzdaten $u_l^{(k)}$, $l = 1 \ldots L$, $k = 1 \ldots K$, nach (1.1) dabei die Basis für das Erzeugen von Sendesignalen durch diesen einen Sender in der Abwärtsstrecke beziehungsweise die mehreren Sender in der Aufwärtsstrecke. Unter einem Sendesignal wird in diesem Zusammenhang das in eine Sendeantenne eingespeiste Signal verstanden. Den beschriebenen Prozeß des Erzeugens der Sendesignale durch alle Sender auf Basis der Nutzdaten wird im folgenden als senderseitige Signalverarbeitung oder kurz Senderverarbeitung bezeichnet. Wie im folgenden Unterkapitel 1.2 genauer erläutert wird, läßt sich das Ergebnis der Senderverarbeitung, das heißt die Gesamtheit aller in die Sendeantennen aller Sender eingespeisten Sendesignale, kompakt durch den totalen Sendesignalvektor $\underline{\mathbf{t}}$ beschreiben, der im folgenden auch als totales Sendesignal [MBW+00, BQT+03, MBQ04] bezeichnet wird, siehe auch Bild 1.4.

Die Sendesignale, die in die im allgemeinen mehreren Sendeantennen eingespeist werden, erzeugen durch Übertragen über den Mobilfunkkanal im allgemeinen an allen Empfangsantennen aller Empfänger der Referenzzelle — dies sind in der Abwärtsstrecke die K Mobilstationen und in der Aufwärtsstrecke die Basisstation — jeweils ein ungestörtes Empfangssignal. Als ungestörtes Empfangssignal wird dabei das einer Empfangsantenne entnommene Signal bezeichnet, das ausschließlich auf das dem mindestens einen Sender entstammende totale Sendesignal $\underline{\mathbf{t}}$ und nicht auf andere Signale oder Quellen zurückgeht. In ähnlicher Weise zur Definition des totalen Sendesignals $\underline{\mathbf{t}}$ ist es möglich, die Gesamtheit aller ungestörten Empfangssignale, die den Empfangsantennen aller Empfänger entnommenen werden, kompakt durch den totalen ungestörten Empfangssignalvektor $\underline{\mathbf{e}}$ oder kurz das totale ungestörte Empfangssignal $\underline{\mathbf{e}}$ zu beschreiben, siehe Bild 1.4.

Der Mobilfunkkanal ordnet jedem totalen Sendesignal $\underline{\mathbf{t}}$ eindeutig ein totales ungestörtes Empfangssignal $\underline{\mathbf{e}}$ zu. Die Struktur dieses Zusammenhangs folgt aus den charakteristischen Eigenschaften

- Linearität,
- Mehrwegeausbreitung und daraus folgender Frequenzselektivität und
- Zeitvarianz

des physikalischen Mobilfunkkanals [Par92, Bel63, Lor85, Ste92, Pät99, Web02]. Der physikalischen Mobilfunkkanal kann demzufolge nachrichtentheoretisch als lineares, zeitvariantes Übertragungssystem modelliert werden [Rup93], das sich mathematisch mit einer linearen Abbildung beschreiben läßt. Sind die Signale des weiteren auf Zeitintervalle begrenzt, die so kurz sind, daß sich in ihnen der Mobilfunkkanal nur unwesentlich ändert — und davon soll im folgenden vereinfachend ausgegangen werden —, so kann der Mobilfunkkanal als lineares, zeitinvariantes Übertragungssystem angesehen werden [Rup93]. Die angesprochene lineare Abbildung wird zweckmäßigerweise durch die totale Kanalmatrix $\underline{\mathbf{H}}$ charakterisiert, die den Zusammenhang

$$\underline{\mathbf{e}} = \underline{\mathbf{H}}\,\underline{\mathbf{t}} \tag{1.5}$$

zwischen totalem Sendesignal $\underline{\mathbf{t}}$ und totalem ungestörten Empfangssignal $\underline{\mathbf{e}}$ herstellt [MBW+00, BMWT00].

Typischerweise empfängt jeder Empfänger in der Referenzzelle eines zellularen Mobilfunksystems außer den Signalen, die auf Sender der Referenzzelle zurückgehen, auch solche Signale, die nicht auf Sender der Referenzzelle zurückgehen und hinsichtlich der Informationsübertragung innerhalb der Referenzzelle ausschließlich schädlich wirken. Derartige schädliche Signale schließen beispielsweise Interzellinterferenz, siehe auch Unterkapitel 1.1.1, oder systemfremde Störungen ein, die im folgenden zusammenfassend als Rauschen bezeichnet werden. Das Rauschen hat zur Folge, daß die den Empfangsantennen entnommenen Empfangssignale im allgemeinen von den oben diskutierten ungestörten Empfangssignalen abweichen. Es ist daher zweckmäßig, in Analogie zur Definition des totalen ungestörten Empfangssignals $\underline{\mathbf{e}}$ des weiteren das totale Empfangssignal $\underline{\mathbf{r}}$ einzuführen, das die Gesamtheit aller gegebenenfalls gestörten Empfangssignale aller Empfänger der Referenzzelle beschreibt und das totale Rauschen

$$\underline{\mathbf{n}} = \underline{\mathbf{r}} - \underline{\mathbf{e}} \tag{1.6}$$

beinhaltet. Durch Kombinieren von (1.5) und (1.6) erhält man zusammenfassend

$$\underline{\mathbf{r}} = \underline{\mathbf{H}}\,\underline{\mathbf{t}} + \underline{\mathbf{n}}. \tag{1.7}$$

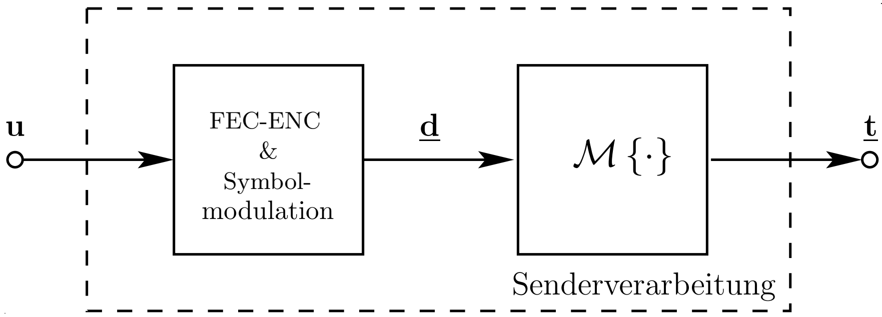

Bild 1.5. Spezielle Ausgestaltung der Senderverarbeitung bestehend in der seriellen Verkettung von Fehlerschutzcodieren (FEC-ENC) & Symbolmodulation und weiterer durch den Modulatoroperator $\mathcal{M}\{\cdot\}$ beschriebenen Sendesignalerzeugung

Empfängerseitig werden beruhend auf dem totalen Empfangssignal $\underline{\mathbf{r}}$ durch geeignete empfängerseitige Signalverarbeitung, die im folgenden als Empfängerverarbeitung bezeichnet wird, Schätzungen $\widehat{u}_l^{(k)}$ jedes der L Nutzdaten $u_l^{(k)}$, $l = 1 \dots L$, aller Teilnehmer k, $k = 1 \dots K$, bestimmt. Diese Schätzungen $\widehat{u}_l^{(k)}$ werden in Analogie zu (1.3) und (1.4) zur Schätzung

$$\widehat{\mathbf{u}}^{(k)} = \left(\widehat{u}_1^{(k)} \dots \widehat{u}_L^{(k)}\right)^{\mathrm{T}} \in \mathbb{B}^L, \tag{1.8}$$

des teilnehmerspezifischen Nutzdatenvektors $\mathbf{u}^{(k)}$, sowie zur Schätzung

$$\widehat{\mathbf{u}} = \left(\widehat{\mathbf{u}}^{(1)\mathrm{T}} \dots \widehat{\mathbf{u}}^{(K)\mathrm{T}}\right)^{\mathrm{T}} \in \mathbb{B}^{KL}, \tag{1.9}$$

des totalen Nutzdatenvektors zusammengefaßt. Bild 1.4 veranschaulicht die oben beschriebenen Zusammenhänge graphisch.

In der Literatur [Lük79, Pro95, Roh95, Kle96] hat sich der Einfachheit halber in den letzten Jahren eine spezielle Ausgestaltung der Senderverarbeitung durchgesetzt, die in Bild 1.5 skizziert ist und die auch im Rahmen dieser Schrift exemplarisch betrachtet werden soll. Diese spezielle Ausgestaltung besteht in der seriellen Verkettung von Fehlerschutzcodieren & Symbolmodulation einerseits und weiterer Sendesignalerzeugung andererseits. Dabei werden aus den Nutzdaten $u_l^{(k)}$, $l = 1 \dots L$, eines Teilnehmers k, $k = 1 \dots K$, zuerst durch Codierungstechniken und Symbolmodulationstechniken [Bos92, Pro95, Roh95, Fri96] in einer eineindeutigen Art und Weise, das heißt informationsverlustfrei, N Datensymbole $\underline{d}_n^{(k)}$ erzeugt, die jeweils dem Repertoire

$$\mathbb{V}_{\mathrm{d}} = \left\{\underline{\nu}_1 \dots \underline{\nu}_M\right\} \subseteq \mathbb{C} \tag{1.10}$$

der Kardinalität M entnommen werden. Dieses Repertoire $\mathbb{V}_{\mathrm{d}}$ beschreibt alle M zulässigen Realisierungen $\underline{\nu}_m$, $m = 1 \dots M$, eines Datensymbols $\underline{d}_n^{(k)}$ und wird daher im folgenden auch als Datensymbolalphabet bezeichnet. In analoger Weise zu (1.3) und

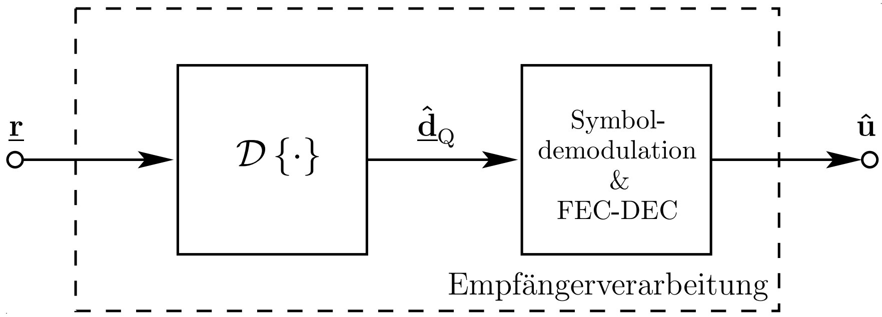

Bild 1.6. Spezielle Ausgestaltung der Empfängerverarbeitung bestehend in der seriellen Verkettung von durch den Detektoroperator $\mathcal{D}\{\cdot\}$ beschriebener Signalverarbeitung und Symboldemodulation & Fehlerschutzdecodieren (FEC-DEC)

(1.4) erhält man durch Zusammenstellen aller N Datensymbole $\underline{d}_n^{(k)}$, $n = 1 \ldots N$, den zu Teilnehmer k, $k = 1 \ldots K$, gehörigen teilnehmerspezifischen Datenvektor

$$\underline{\mathbf{d}}^{(k)} = \left(\underline{d}_1^{(k)} \ldots \underline{d}_N^{(k)}\right)^{\mathrm{T}} \in \mathbb{V}_{\mathrm{d}}^{N} \tag{1.11}$$

sowie den alle Datensymbole $\underline{d}_n^{(k)}$, $n = 1 \ldots N$, aller Teilnehmer k, $k = 1 \ldots K$, umfassenden totalen Datenvektor

$$\underline{\mathbf{d}} = \left(\underline{\mathbf{d}}^{(1)\mathrm{T}} \ldots \underline{\mathbf{d}}^{(K)\mathrm{T}}\right)^{\mathrm{T}} \in \mathbb{V}_{\mathrm{d}}^{KN}. \tag{1.12}$$

In einem zweiten Schritt wird aus dem totalen Datenvektor $\underline{\mathbf{d}}$ nach (1.12) durch weitere Sendesignalerzeugung das totale Sendesignal $\underline{\mathbf{t}}$ ermittelt. Das Erzeugen des totalen Sendesignals $\underline{\mathbf{t}}$ auf Basis des totalen Datenvektors $\underline{\mathbf{d}}$ läßt sich mathematisch als eine Abbildung interpretieren. Diese Abbildung kann kompakt durch den Modulatoroperator $\mathcal{M}\{\cdot\}$ beschrieben werden, so daß für das totale Sendesignal

$$\underline{\mathbf{t}} = \mathcal{M}\{\underline{\mathbf{d}}\} \tag{1.13}$$

folgt. Wie sich unter anderem im folgenden Abschnitt 1.1.3 herausstellen wird, ist der Modulatoroperator $\mathcal{M}\{\cdot\}$ im allgemeinen nicht trivial und nichtlinear in $\underline{\mathbf{d}}$ und wird daher im Rahmen dieser Schrift noch genauer beleuchtet.

Die in Bild 1.4 dargestellte Senderverarbeitung und Empfängerverarbeitung sind nicht unabhängig voneinander wählbar, wenn — und dies ist, wie bereits erläutert, das primäre Ziel von Mobilkommunikation — eine möglichst fehlerfreie Informationsübertragung von der Senderseite zu der Empfängerseite ermöglicht werden soll, denn, wie in Abschnitt 1.1.1 erläutert, gilt es nämlich, die schädliche Wirkung von Interferenz möglichst gering zu halten. Ausgehend von der in Bild 1.5 vorgeschlagenen und zuvor ausgeführten Ausgestaltung der Senderverarbeitung läßt sich die in Bild 1.6

gezeigte, zu Bild 1.5 gehörige Ausgestaltung der Empfängerverarbeitung finden. Die dargestellte spezielle Ausgestaltung der Empfängerverarbeitung hat sich aufgrund ihrer Einfachheit in der Literatur [Lük79, Pro95, Roh95, SRAX96, Kle96, ARS97, Wil98] als bevorzugte Wahl herauskristallisiert und besteht in der seriellen Verkettung einer im folgenden genauer spezifizierten Empfangssignalverarbeitung und Symboldemodulation & Fehlerschutzdecodieren. Gemäß Bild 1.6 werden in einem ersten Schritt typischerweise basierend auf dem totalen Empfangssignal $\underline{\mathbf{r}}$ Schätzungen $\widehat{\underline{d}}_{\mathrm{Q},n}^{(k)}$ aller Datensymbole $\underline{d}_n^{(k)}$, $n = 1 \ldots N$, aller Teilnehmer k, $k = 1 \ldots K$, ermittelt. Diese Schätzungen $\widehat{\underline{d}}_{\mathrm{Q},n}^{(k)}$ lassen sich zur Schätzung

$$\widehat{\underline{\mathbf{d}}}_{\mathrm{Q}}^{(k)} = \left(\widehat{\underline{d}}_{\mathrm{Q},1}^{(k)} \ldots \widehat{\underline{d}}_{\mathrm{Q},N}^{(k)}\right)^{\mathrm{T}} \in \mathbb{V}_{\mathrm{d}}^{N}, \tag{1.14}$$

des zu Teilnehmer k, $k = 1 \ldots K$, gehörigen Datenvektors $\underline{\mathbf{d}}^{(k)}$ nach (1.11) und des weiteren zur Schätzung

$$\widehat{\underline{\mathbf{d}}}_{\mathrm{Q}} = \left(\widehat{\underline{\mathbf{d}}}_{\mathrm{Q}}^{(1)\mathrm{T}} \ldots \widehat{\underline{\mathbf{d}}}_{\mathrm{Q}}^{(K)\mathrm{T}}\right)^{\mathrm{T}} \in \mathbb{V}_{\mathrm{d}}^{KN}. \tag{1.15}$$

des totalen Datenvektors $\underline{\mathbf{d}}$ nach (1.12) zusammenfassen. Das auf $\underline{\mathbf{r}}$ nach (1.7) basierende, durch geeignete Signalverarbeitung erfolgende Ermitteln von $\widehat{\underline{\mathbf{d}}}_{\mathrm{Q}}$ nach (1.15) läßt sich als eindeutige Zuordnung zwischen $\underline{\mathbf{r}}$ und $\widehat{\underline{\mathbf{d}}}_{\mathrm{Q}}$ interpretieren. In einer zum Beschreiben der Senderverarbeitung nach Bild 1.5 analogen Weise läßt sich diese Zuordnung mathematisch durch den Detektoroperator $\mathcal{D}\{\cdot\}$ beschreiben, der jedem totalen Empfangssignal $\underline{\mathbf{r}}$ eindeutig eine Schätzung $\widehat{\underline{\mathbf{d}}}_{\mathrm{Q}}$ nach (1.15) des totalen Datenvektors $\underline{\mathbf{d}}$ gemäß

$$\widehat{\underline{\mathbf{d}}}_{\mathrm{Q}} = \mathcal{D}\{\underline{\mathbf{r}}\} \tag{1.16}$$

zuordnet. In einem zweiten Schritt werden den gewonnenen Schätzungen $\widehat{\underline{d}}_{\mathrm{Q},n}^{(k)}$ der Datensymbole $\underline{d}_{\mathrm{Q},n}^{(k)}$, $n = 1 \ldots N$, jedes Teilnehmers k, $k = 1 \ldots K$, durch Verfahren der Symboldemodulation und des Fehlerschutzdecodierens [Bos92, Pro95, Roh95, Fri96] Schätzungen $\widehat{u}_l^{(k)}$ der L Nutzdaten $u_l^{(k)}$, $l = 1 \ldots L$, dieses Teilnehmers k zugeordnet, aus denen die Schätzungen $\widehat{\mathbf{u}}^{(k)}$ nach (1.8) und $\widehat{\mathbf{u}}$ nach (1.9) folgen. Derartige Verfahren der Symboldemodulation und des Fehlerschutzdecodierens sind Stand der Technik und sollen daher hier nicht weiter vertieft werden [Bos92, Pro95, Roh95, Vit95, Fri96].

In den letzten Jahren wurde in der Literatur [DHHZ95, GW96, Poo00, ARAS99, SS01, Moh98, WP99, RSAA98, Hag96, AGR98, VW98, Wer94, HS96, WM02b, BJW01a, BJW01b, WO01, WBOW00, WOWB02, RF96] herausgearbeitet, daß ein gemäß den obigen Ausführungen erfolgendes Aufspalten der Empfängerverarbeitung bei gegebener Senderverarbeitung im allgemeinen suboptimal hinsichtlich der erzielbaren Qualität der Informationsübertragung ist — beispielsweise der unter gegebenen Randbedingungen minimalen Übertragungsfehlerwahrscheinlichkeit. Suboptimal heißt in diesem Zusammenhang, daß das Aufspalten mit einem Informationsverlust verbunden ist, der

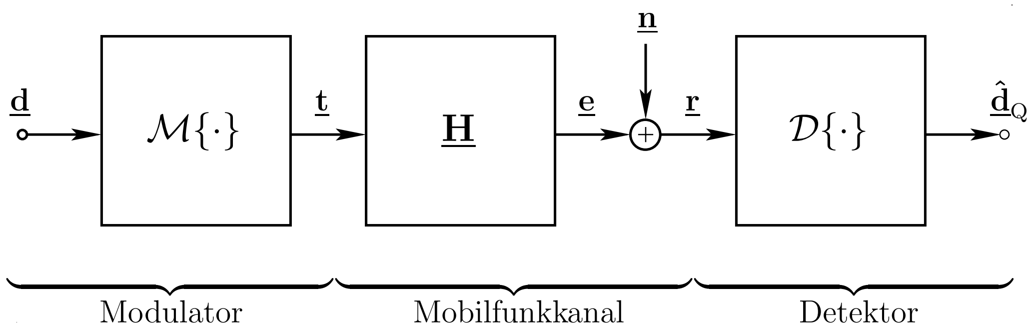

Bild 1.7. Vereinfachtes Modell der Funkkommunikation innerhalb einer Referenzzelle

sich darin äußerst, daß nicht die gesamte im totalen Empfangssignal $\underline{\mathbf{r}}$ enthaltende Information über $\mathbf{u}$ nutzbar gemacht werden kann, um $\widehat{\mathbf{u}}$ möglichst zuverlässig zu bestimmen. In der Literatur sind mittlerweile auch in dieser Hinsicht optimale [DHHZ95, GW96] oder unter gewissen Randbedingungen asymptotisch optimale Ansätze [Poo00, ARAS99, SS01, Moh98, WP99, RSAA98, Hag96, AGR98, VW98, Wer94, HS96, WM02b, BJW01a, BJW01b, WO01, WBOW00, WOWB02, RF96] verfügbar, die dieses Problem umschiffen. Derartige Ansätze, die teilweise iterativ arbeiten, sind jedoch typischerweise sehr aufwendig oder bilden lediglich einen mehr oder weniger guten Kompromiß zwischen Rechenkomplexität, erzielbarer Übertragungsqualität und Stabilität. Aus diesem Grund und da für solche Mobilfunksysteme, die den Kern dieser Schrift darstellen, vergleiche auch Unterkapitel 1.2, bisher keine praktikablen Ansätze der beschriebenen Art bekannt sind, soll im Rahmen dieser Schrift auf derartige optimale oder asymptotisch optimale Ansätze nicht weiter eingegangen werden.
Um prinzipiell eine fehlerfreie Informationsübertragung von der Sender- zur Empfängerseite zu ermöglichen, sind das in Bild 1.5 eingeführte Fehlerschutzcodieren und die dort genannte Symbolmodulation derart auszuführen, daß die gesamte Information über den totalen Nutzdatenvektor $\mathbf{u}$ im totalen Datenvektor $\underline{\mathbf{d}}$ enthalten ist. Dies ist genau dann der Fall, wenn stets eine fehlerfreie Rekonstruktion von $\mathbf{u}$ auf Basis von $\underline{\mathbf{d}}$ möglich ist. Darüber hinaus läßt sich feststellen, daß in der Schätzung $\underline{\mathbf{d}}_{\mathrm{Q}}$ nach (1.15) des totalen Datenvektors $\underline{\mathbf{d}}$ nach (1.12) die gesamte Information über $\widehat{\mathbf{u}}$ nach (1.9) enthalten ist. Denn $\widehat{\mathbf{u}}$ nach (1.9) folgt gemäß Bild 1.6 ausschließlich als Resultat des Verarbeitens von $\underline{\mathbf{d}}_{\mathrm{Q}}$. Als Essenz der obigen beiden Beobachtungen lassen sich die folgenden Schlußfolgerungen ziehen:

- Eine Analyse der in Bild 1.6 dargestellten Funkkommunikation kann auf die informationstheoretisch äquivalente Analyse des Zusammenhangs zwischen totalem Datenvektor $\underline{\mathbf{d}}$ und der zugehörigen Schätzung $\widehat{\underline{\mathbf{d}}}$ reduziert werden.

- Der Entwurf der durch den Modulatoroperator $\mathcal{M}\{\cdot\}$ beschriebenen Sendesignalerzeugung und der durch den Detektoroperator $\mathcal{D}\{\cdot\}$ beschriebenen Empfangssignalverarbeitung kann ausschließlich auf Basis des zuvor genannten Zusammenhangs erfolgen.

Durch Kombinieren der in den Bildern 1.4 bis 1.6 dargestellten Modelle kann das in Bild 1.7 gezeigte vereinfachte Modell der Funkkommunikation innerhalb der Referenzzelle definiert werden. In Bild 1.7 wird die durch den Modulatoroperator $\mathcal{M}\{\cdot\}$ beschriebene Sendesignalerzeugung nach (1.13) verkürzt durch die Bezeichnung Modulator, die durch den Detektoroperator $\mathcal{D}\{\cdot\}$ beschriebene Empfangssignalverarbeitung nach (1.16) durch die Bezeichnung Detektor gekennzeichnet. Als Konsequenz der vorgenannten Schlußfolgerungen beschreibt das vereinfachte Modell die Funkkommunikation innerhalb der Referenzzelle vollständig in einem informationstheoretischen Sinne. Daher wird dieses vereinfachte Modell ohne Einschränkung der Allgemeinheit als Basis für alle weiteren Betrachtungen innerhalb der vorliegenden Schrift herangezogen.

1.1.3 Klassifikation von Funkkommunikation

Für einen Mobilfunkkanal gegebener Eigenschaften, das heißt für eine bekannte Kanalmatrix $\underline{\mathbf{H}}$ nach (1.5), hängt die Leistungsfähigkeit der Funkkommunikation in einer Referenzzelle neben der Abhängigkeit von weiteren Einflußfaktoren vorrangig davon ab, inwieweit es gelingt, die gewünschten Informationen zu übertragen und gleichzeitig die in Abschnitt 1.1.1 erläuterten schädlichen Interferenzen weitestgehend zu vermeiden oder unschädlich zu machen. Dieses Gelingen wird ausschließlich von der Ausgestaltung der Sendesignalerzeugung auf der Senderseite, das heißt dem Modulatoroperator $\mathcal{M}\{\cdot\}$, und der Ausgestaltung der Empfangssignalverarbeitung auf der Empfängerseite, das heißt dem Detektoroperator $\mathcal{D}\{\cdot\}$, bestimmt. Hinsichtlich des Entwurfs eines leistungsfähigen Mobilfunksystems ist es daher entscheidend, sich mit der Wahl dieser beiden Operatoren $\mathcal{M}\{\cdot\}$ und $\mathcal{D}\{\cdot\}$ genauer zu befassen.

Wie oben bereits angesprochen, kann die Wahl des Modulatoroperators $\mathcal{M}\{\cdot\}$ und des Detektoroperators $\mathcal{D}\{\cdot\}$ nicht unabhängig voneinander erfolgen, wenn eine leistungsfähige, möglichst fehlerfreie Funkkommunikation ermöglicht werden soll. Daher wird im folgenden stets auf die gemeinsame Wahl beider Operatoren eingegangen. Im weiteren Verlauf wird klar werden, daß bei dieser gemeinsamen Wahl des Modulatoroperators $\mathcal{M}\{\cdot\}$ und des Detektoroperators $\mathcal{D}\{\cdot\}$ grundsätzlich verschiedene Grundkonzepte unterschieden werden können.

Neben der Leistungsfähigkeit eines Mobilfunksystems spielen in der Praxis beim Systementwurf noch weitere Belange, wie beispielsweise

- die verfahrenstechnische Komplexität der Sendesignalerzeugung und der Empfangssignalverarbeitung,

- die Kosten der zur Bewältigung der vorgenannten Komplexität benötigten Hardwarekomponenten und
- die elektrischen Leistungsaufnahmen der einzelnen Komponenten des Mobilfunksystems, das heißt die zu erwartenden Energiekosten,

eine erhebliche Rolle. Wie sich im folgenden zeigen wird, hängen die Vor- und Nachteile der verschiedenen möglichen Grundkonzepte maßgeblich von diesen weiteren Belangen ab. Daher werden diese Belange im Rahmen dieser Schrift noch eine besondere Bedeutung erlangen.

Die Anwendung sich im Raum ausbreitender elektromagnetischer Wellen, also von Funkwellen, zur Kommunikation hat ihren Ursprung in den im Jahr 1895 von Guglielmo Marchese Marconi (1874-1937) in der Nähe von Bologna durchführten Experimenten. In diesen Experimenten zeigte Marconi erstmals, daß es möglich ist, Informationen mittels Funkwellen — deren Existenz im übrigen erst zehn Jahre zuvor von Heinrich Hertz (1857-1894) experimentell in Karlsruhe nachgewiesen werden konnte — drahtlos zu übertragen, wofür ihm 1909 der Nobelpreis für Physik verliehen wurde [Asc84]. Schon in diesen ersten Experimenten wie auch in praktisch allen heute oder in der Vergangenheit bedeutsamen Funkkommunikationssystemen startete der Systementwurf auf der Senderseite. Dabei wurde in einem ersten Schritt das senderseitige Erzeugen der Sendesignale auf Basis der zu übertragenden Information festgelegt und in einem zweiten Schritt erfolgte dann das empfängerseitige Verarbeiten der Empfangssignale zum Extrahieren der übertragenen Information als Konsequenz der erstgemachten, den Sender betreffenden Festlegung [BQT+03, MBQ04]. Verallgemeinert und auf das in Bild 1.7 eingeführte allgemeine Modell der Funkkommunikation übertragen bedeutet dies, daß

1. der Modulator, also der Modulatoroperator $\mathcal{M}\{\cdot\}$, a priori gewählt wird, und
2. der Detektor, also der Detektoroperator $\mathcal{D}\{\cdot\}$, a posteriori daran und gegebenenfalls an weitere Informationen, die vom betrachteten Funkszenario und Funksystem abhängen, adaptiert wird, beispielsweise im Sinne einer Minimierung der schädlichen Wirkung von Interferenz.

In einer derart organisierten Funkkommunikation spielen die Sender die Rolle der Meister (engl. masters), die die zu befolgenden Regeln festlegen, wohingegen die Empfänger die Rolle von Sklaven (engl. slaves) einnehmen, die sich den gesetzten Regeln anzupassen haben [Trö03]. Ein derartiges Grundkonzept wird daher als Senderorientierung (engl. transmitter orientation, Tx orientation) bezeichnet.

Infolge der großen Freiheit, die sich bei der A-priori-Wahl der Sender, also des Modulators, bietet, erlaubt es die Senderorientierung, Sender zu entwerfen, die hinsichtlich eines gewünschten Optimierungskriteriums besonders ausgezeichnet sind. Wird als Optimierungskriterium die Minimierung der Komplexität der an den Sendern zu leistenden Sendesignalerzeugung gewählt — und dies ist eine häufig anzutreffende Wahl des Optimierungskriteriums [BQT+03] —, so ist es bei Senderorientierung insbesondere möglich, besonders einfache Sender zu entwerfen. Wie sich im folgenden Unterkapitel 1.2 zeigen wird, ist dieser Aspekt für die Praxis von besonderer Bedeutung. Der Preis, der für diese Vereinfachung im allgemeinen zu zahlen ist, manifestiert sich in einer im Vergleich zur Sendesignalerzeugung typischerweise deutlich höheren Komplexität der Empfangssignalverarbeitung und damit der Empfänger.

Alternativ zur Senderorientierung kann der Systementwurf jedoch auch von der Empfängerseite starten. Dabei wird

1. a priori der Detektor, also der die Empfangssignalverarbeitung beschreibende Detektoroperator $\mathcal{D}\{\cdot\}$, gewählt, und
2. der Modulator, das heißt der die Sendesignalerzeugung charakterisierende Modulatoroperator $\mathcal{M}\{\cdot\}$, folgt a posteriori daraus, wiederum beispielsweise im Sinne der zuvor angesprochenen Minimierung der schädlichen Wirkung von Interferenz.

Da nun die Empfänger die Rolle der Meister übernehmen, wohingegen die Sender die Rolle der Sklaven einnehmen, spricht man bei einer derartigen Organisation der Funkkommunikation vom Grundkonzept der Empfängerorientierung (engl. receiver orientation, Rx orientation), das den Kern der vorliegenden Schrift ausmacht. In Analogie zur Senderorientierung ist es bei der Empfängerorientierung möglich, Empfänger zu entwerfen, die hinsichtlich des gewünschten Optimierungsziels besonders ausgezeichnet sind. Beispielsweise können auf diese Weise sehr einfache Empfänger geschaffen werden, wohingegen die zugehörigen Sender, die zum Erzielen einer möglichst fehlerfreien Funkkommunikation nötig sind, im allgemeinen komplizierter sind. Dieses Grundkonzept der Organisation ist im Bereich der Funkkommunikation recht neu, wenig untersucht und daher unkonventionell. Dies ist erstaunlich, da, wie im folgenden Unterkapitel 1.2 herausgestellt wird, beide Grundkonzepte der Organisation, Senderorientierung und Empfängerorientierung, je nach gegebenen Rahmenbedingungen ihre Vorzüge haben. Offensichtlich verfügt das üblicherweise verfolgte Prinzip der Senderorientierung über eine außergewöhnliche natürliche Anziehungskraft auf Entwickler von Funksystemen, was dazu führte, daß in den letzten mehr als 100 Jahren der Entwicklung von Funksystemen praktisch ausschließlich dieses Prinzip Bedeutung erlangte. Eine systematische Untersuchung des Grundkonzepts der Empfängerorientierung ist demzufolge in der Literatur praktisch nicht verfügbar. In den letzten wenigen Jahren entstanden, teilweise unter anderem angestoßen durch zahlreiche Veröffentlichungen des

Autors und seiner Kollegen am Lehrstuhl für hochfrequente Signalübertragung und -verarbeitung der Technischen Universität Kaiserslautern [BM04, BM03, BMWT00, BQT+03, BZT+03, LMTB01, LTM01, Meu04b, Meu04a, MBL+00, MBQ04, MBW+00, MQW03, MTJ02, MW04b, MW04a, MWQ04a, MWQ04b, PMWB00, QMBW04, QTM02, TMW00, TWMB01b, TWMB01a, WLMM03, WM04a, WM04b, WM03c, WM03d, WM03b, WM03e, WMS03, WSM04], erste die Empfängerorientierung betreffende Arbeiten [KM00, GC01, INBF01, JU01, JUN01, JWJH01, WR01, CM02a, CM02b, GC02, IF02b, IF02a, JKG+02, JKUN02, ML02, RIF02, SSB+02, TWL+02, WIF02, CM03, CML03, DHJU03, FW03, JIB+03, Geo03, HSB03, IHRF03, IRF03b, IRF03a, JIB+03, WCS03, WVF03b, BHMW04, CM04d, CM04a, CM04c, CM04b, IGF04, IHRF04b, JBU04, JBVU04, Joh04], wobei dabei auch die alternativen Bezeichnungen Joint Transmission, Joint Predistortion und Precoding verwendet wurden. Es ist jedoch festzustellen, daß naturbedingt die Zahl der verfügbaren, die Senderorientierung betreffenden Veröffentlichungen noch um Größenordnungen höher liegt, als die der Veröffentlichungen, die auf Empfängerorientierung eingehen. Insbesondere sind für das Grundkonzept der Senderorientierung umfassende Werke in der Literatur publiziert [Kle96, Ver98], die systematisch auf verschiedene im Rahmen dieses Grundkonzepts relevanten Aspekte, Ausgestaltungsmöglichkeiten und zu klärenden Kernfragen eingehen. Demgegenüber sind im Bereich der Empfängerorientierung bisher vorrangig solche Werke verfügbar, die ausschließlich eng begrenzte spezielle Detailaspekte dieses Grundkonzepts behandeln. Eine systematische Gegenüberstellung prinzipieller möglicher Ausgestaltungsmöglichkeiten der Empfängerorientierung sowie eine grundlegende Diskussion der zu klärenden Kernfragen fehlt bisher. Es ist daher ein vorrangiges Ziel der vorliegenden Schrift, diesen Überblick zu schaffen und auf diese Weise einen Beitrag dazu zu leisten, der Empfängerorientierung den Weg in künftige Mobilfunksysteme zu ebnen.

Die Begriffe Senderorientierung und Empfängerorientierung wurden vom Autor der vorliegenden Schrift sowie seinen Kollegen am Lehrstuhl für hochfrequente Signalübertragung und -verarbeitung der Technischen Universität Kaiserslautern geprägt [BM04, BM03, BQT+03, Meu04b, Meu04a, MBQ04, MQW03, MW04b, MW04a, MWQ04a, MWQ04b, QMBW04, WLMM03, WM04a, WM04b, WM03c, WM03d, WM03b, WM03e, WMS03, WSM04] und werden mittlerweile auch in Werken anderer Autoren [BZT+03, TWL+02, Bur05] verwendet.

Sowohl beim Grundkonzept der Senderorientierung als auch beim Grundkonzept der Empfängerorientierung spielt Kanalzustandsinformation eine wichtige Rolle, da das Adaptierung von Empfänger(n), das heißt des Detektoroperators $\mathcal{D}\{\cdot\}$, beziehungsweise Sender(n), das heißt des Modulatoroperators $\mathcal{M}\{\cdot\}$, im allgemeinen Kenntnis über die zwischen Sender(n) und Empfänger(n) wirksamen Mobilfunkkanäle voraussetzt. Wird das Grundkonzept der Senderorientierung verfolgt, so ist dabei Kanalzustandsinformation auf der Empfängerseite nötig, während auf der Senderseite darauf vollständig verzichtet wird [BQT+03, MWQ04b]. Die Kanalzustandsinformation auf der Empfängerseite wird üblicherweise durch Übertragen von empfängerseitig bekannten Trainingssequenzen und anschließendes Kanalschätzen verfügbar gemacht [SB93, SJ94, Ste95, SMWB01, MWSL02, BDT95, ASA97, WMZ05]. Des weiteren sind in der Literatur halbblinde oder vollständig blinde Verfahren [BA94, MDCM95, MLW+02] zum Bereitstellen von Kanalzustandsinformation verfügbar, die nur Teilinformationen über die zum Kanalschätzen verwendeten Funksignale einsetzen.

Beim Grundkonzept der Empfängerorientierung ist Kanalzustandsinformation auf der Senderseite (engl. transmitter sided channel state information, TxCSI) nötig, während auf der Empfängerseite darauf vollständig verzichtet wird [BQT+03, MWQ04b, Trö03]. Diese Kanalzustandsinformation muß daher durch geeignete Methoden [KM00, FWLH02c, JBMW02b, JBM+02, JBMW02a, DHJU03, CM04a, WSLW03, SWWM04, Skl04] auf der Senderseite verfügbar gemacht werden, die in dieser Schrift im Rahmen des folgenden Unterkapitels 1.2 und des Kapitels 6 genauer beleuchtet werden.

In der Literatur wurden differentielle Verfahren der Funkkommunikation vorgeschlagen, die weder senderseitig noch empfängerseitig Kanalzustandsinformation voraussetzen [Hug00, MFP97, TJ00, LSF03, SL04b, SL04a]. Diese Verfahren sind jedoch in ihrer Leistungsfähigkeit gegenüber solchen Verfahren, die senderseitig und/oder empfängerseitig Kanalzustandsinformation einbeziehen, beschränkt und haben daher bisher keine Bedeutung in wirtschaftlich relevanten Mobilfunksystemen erlangt. Der Autor der vorliegenden Schrift verzichtet daher auf die Betrachtung derartiger Verfahren. Der interessierte Leser sei beispielsweise auf [Hug00, MFP97, TJ00, LSF03, SL04b, SL04a] verwiesen.

Des weiteren sind Verfahren der Funkkommunikation bekannt [JVP98, YR94, IF02b, MTWB01b, MTWB01a, BQT+03, MT03, QTMJ03], die sowohl sender- als auch empfängerseitig Kanalzustandsinformation voraussetzen. Derartige Verfahren

- haben jedoch meist höhere Komplexität als solche Verfahren, die ausschließlich auf einer der beiden Seiten Kanalzustandsinformation voraussetzen [BQT+03, MT03, QTMJ03] und
- erfordern typischerweise eine verstärkte Kommunikation zwischen Sender- und Empfängerseite zur Organisation der Funkkommunikation.

Vorgenannte Verfahren werden daher bisher nur bedingt in Mobilfunksystemen eingesetzt und sollen im Rahmen dieser Schrift ausschließlich in Form eines Ausblicks in Kapitel 7 berücksichtigt werden.

1.2 Empfängerorientierung in der Mobilkommunikation

Der Ursprung des Grundkonzepts der Empfängerorientierung liegt im Bereich der drahtgebundenen Kommunikation. Bereits in den 70er Jahren des letzten Jahrhunderts entstanden in diesem Bereich die ersten wissenschaftlichen Veröffentlichungen [Tom71, HM72], die sich dieses Grundkonzept zu Nutze machen. Ziel der in [Tom71, HM72] vorgeschlagenen Verfahren ist es, drahtgebundene Kommunikation über dispersive Übertragungsmedien zu ermöglichen, wobei dazu ausschließlich Empfänger einer sehr einfachen Bauart eingesetzt werden sollen.

Im Bereich der drahtlosen Kommunikation, also vorrangig der Funkkommunikation, ist das Grundkonzept der Empfängerorientierung hingegen erst in den letzten wenigen Jahren in den Fokus der Forschungsaktivitäten gerückt und daher recht neu [MBQ04]. Aus diesem Grund wird Empfängerorientierung nach Kenntnis des Autors dieser Schrift noch in keinem kommerziellen Mobilfunksystem eingesetzt.

Soll eine Funkkommunikation zwischen mindestens einem Sender und einem Empfänger etabliert werden, so erlaubt Empfängerorientierung, wie bereits in Abschnitt 1.1.3 erläutert, die A-priori-Wahl der Empfänger. Es bietet sich an, diese Wahlmöglichkeit geschickt zu nutzen, um vorzugsweise die Komplexität der Empfänger auf ein Minimum zu reduzieren. Unter Komplexität wird dabei die Implementierungskomplexität der (digitalen) Basisbandsignalverarbeitung verstanden, die sich unmittelbar in den Anforderungen an die empfängerseitig verwendete Hardware niederschlägt. In der Praxis gehen niedrigere Anforderungen an die Hardware typischerweise einher mit unter anderem

- niedrigerem Herstellungspreis,
- geringerem Gewicht,
- kleinerer Baugröße und
- geringerem Energieverbrauch

der betrachteten Hardware [KM00]. Die sich somit ergebenden prinzipiellen Vorteile der Empfängerorientierung wiegen besonders schwer, wenn die Empfänger in großen Stückzahlen für den Endkundenmarkt verfügbar gemacht werden sollen. Im Falle der Senderorientierung gilt gleiches für die Sender, das heißt einfache Sender werden zum Preis einer erhöhten Komplexität an den Empfängern ermöglicht.

Betrachtet man die zuvor angesprochenen wirtschaftlich bedeutenden infrastrukturbasierten Mobilfunksysteme — und um diese soll es, wie bereits erwähnt, in dieser Schrift vorrangig gehen —, so ist es als Folge der obigen Ausführungen erstrebenswert, in der Abwärtsstrecke derartiger Mobilfunksysteme die Funkkommunikation gemäß Empfängerorientierung zu organisieren. In diesem Fall sind nämlich die mobilen Endgeräte der Endkunden, also die Mobilstationen, die Empfänger, wohingegen die ortsfesten Basisstationen die Sender sind. Vergleich man eine gemäß Senderorientierung gestaltete Abwärtsstreckenübertragung mit einer Abwärtsstreckenübertragung, die gemäß Empfängerorientierung gestaltet ist, so lassen sich somit auf Kosten erhöhter Anforderungen an die Basisstationen die obigen prinzipiellen Vorteile der Empfängerorientierung unmittelbar in die im folgenden erläuterten Vorteile einer empfängerorientierten Abwärtsstrecke überführen:

- Infolge der gegenüber dem klassischen Prinzip der Senderorientierung mäßigen Komplexitätsanforderungen an die Hardware der Empfänger der Mobilstationen können kostengünstigere mobile Endgeräte auf dem Endkundenmarkt angeboten werden. Beim Verkauf dieser Endgeräte ist der Verkaufspreis ein entscheidender, die Kaufentscheidungen der potentiellen Kunden und somit die Absatzzahlen bestimmender Einflußfaktor [WHL+03]. Gelingt es dem Hersteller mobiler Endgeräte, diesen Verkaufspreis auf die oben dargestellte Weise zu verringern, so besteht darin ein entscheidender Geschäftsvorteil gegenüber Konkurrenten. Für die Netzbetreiber, die die zur zellularen Mobilkommunikation benötigte Infrastruktur und damit auch die — im Falle von Empfängerorientierung gegebenenfalls aufwendigen und teuren — Basisstationen bereitstellen, ist dies jedoch nicht ausschließlich mit gewinnreduzierenden Mehraufwendungen verbunden. Es ist nämlich davon auszugehen, daß auch ein Netzbetreiber, der beispielsweise im Gegensatz zur Konkurrenz Empfängerorientierung in seinem Netz einsetzt, von den höhere Absatzzahlen der kostengünstigen mobilen Endgeräten insofern profitieren kann, als zusätzliche Einnahmen im Bereich der fixen oder dienstbezogenen variablen Mobilfunkgebühren möglich werden.

- Die mobilen Endgeräte können infolge der reduzierten Komplexität der Empfänger kompakter, mit kleinerer Baugröße und geringerem Gewicht gestaltet werden. Auch dieser Aspekt ist als nicht unerheblicher Geschäftsvorteil auf dem Endkundenmarkt zu bewerten.

- Mobile Endgeräte, die aufgrund der genannten Vereinfachungen der Empfänger eine geringere elektrische Leistungsaufnahme haben, können im Vergleich zu mobilen Endgeräten ohne diesen Vorzug bei gleicher Batterieausstattung längere Batterielaufzeiten bieten oder bei gleichen Batterielaufzeiten mit einer geringeren Batterieausstattung arbeiten. Eine Reduktion der Batterieausstattung bewirkt unmittelbar eine vorteilhafte weitere Gewichts- und Volumeneinsparung der mobilen Endgeräte.

Der letztgenannte der drei Aspekte spielt dabei eine besondere Rolle, da sich in den letzten Jahren im Bereich der konventionellen senderorientierten Funkkommunikation eine nicht zu unterschätzende Entwicklung abzeichnet. Es kann festgestellt werden, daß im Verlauf der letzten Jahre die Implementierungskomplexität der Empfänger im Bereich der Senderorientierung typischerweise stets zunahm [LW04]. Hinsichtlich der Größe und des Gewichts der zum Bewältigen dieser Komplexität benötigten Hardware konnte dieser Entwicklung durch den rasanten Fortschritt im Bereich der Mikroelektronik weitestgehend, stets dem Moore'schen Gesetz [Sch97] folgend, entsprochen werden [Rab00, Rab01, Aar03]. Die Leistungsaufnahme dieser stetig komplexer werdenden Empfänger ist jedoch trotz vieler Bemühungen [KMGW03, KW04, WZW04a, WZW04b] im Bereich der Mikroelektronik [Rab00, Rab01, Aar03] ebenso gestiegen. Diesem Anstieg der Leistungsaufnahme konnte in den letzten Jahren kein entsprechender Anstieg der Energiedichten verfügbarer Batterien entgegengesetzt werden [Rab00, Rab01], so daß die gestiegene Empfängerkomplexität unmittelbar durch geringere Batterielaufzeiten oder größere Batterieausstattungen der mobilen Endgeräte mit den genannten Gewichts- und Volumenproblemen zu bezahlen war. In den nächsten Jahren ist zu erwarten, daß diese Diskrepanz zwischen der Entwicklung der Empfängerkomplexität einerseits und dem Fortschritt im Bereich der Mikroelektronik und der Energiespeicher andererseits sich weiter vergrößern wird. Es ist demzufolge von besonderer Bedeutung, Prinzipien wie Empfängerorientierung, die diesen Mißstand ausräumen oder zumindest mildern, zu entwickeln und zu studieren.

Neben den oben genannten, eher aus der Praxis motivierten Vorteilen der Empfängerorientierung existieren noch weitere Vorteile, die es zu diskutieren gilt:

- Im Bereich der Empfängerorientierung ist empfängerseitig keine Kanalzustandsinformation erforderlich. Daher kann auf das Übertragen von Trainingssignalen, die im Bereich der Senderorientierung üblich sind, verzichtet werden. Die dadurch frei werdenden Übertragungskapazitäten können nunmehr ganz oder teilweise zum Übertragen von Nutzdaten eingesetzt werden. Dieser Aspekt ist besonders zu betonen, da in den nächsten Jahren Kapazitätsengpässe vorwiegend in der Abwärtsstrecke erwartet werden, die somit als Flaschenhals (engl. bottle neck) der Funkkommunikation zwischen Basisstationen und Mobilstationen gilt [BM04, BM02, SWWM04]. Diese Einschätzung resultiert vor allem aus der zunehmenden Bedeutung asymmetrischer Dienste, wie beispielsweise des mobilen Fernsehens oder des Abrufs von Inhalten des World Wide Web (WWW), im Mobilfunk, die vorrangig hohe Übertragungskapazitäten in der Abwärtsstrecke voraussetzen.

Wird empfängerseitig keine Kanalzustandsinformation benötigt, so ist dort keine Kanalschätzung erforderlich. Die für Empfänger, die gemäß Senderorientierung entworfenen sind, in Verbindung mit dem Ermitteln von Kanalschätzungen bestehenden Implementierungsaufwände können daher durch Empfängerorientierung eingespart werden, was über die bisher genannten Aspekte hinaus erlaubt, die Empfängerkomplexität zu reduzieren. Kritisch ist an dieser Stelle jedoch anzumerken, daß es im Sinne des Verfügbarmachens von Kanalzustandsinformation für den Sender, das heißt für die Basisstation, unter Umständen doch notwendig werden kann, Kanalschätzungen empfängerseitig zu bestimmen und durch geeignete Signalisierungsverfahren der Basisstation zu übermitteln. Eine detaillierte Beschreibung dieses Sachverhalts finden sich in Kapitel 6.

- Empfängerorientierte Funkkommunikation kann im Vergleich mit senderorientierter Funkkommunikation bei gegebener Störsituation an den Empfängern die gleiche Übertragungsqualität erzielen, wobei dazu eine geringere totale Sendeleistung benötigt wird. Die totale Sendeleistung bezeichnet dabei die insgesamt vom Sender für die Versorgung aller Empfänger abgestrahlte Leistung. Folglich läßt sich durch Empfängerorientierung die in einem gegebenen Zeitintervall abgestrahlte Energie bei gegebener Übertragungsqualität reduzieren, was in der Literatur [MWQ04b, QMBW04, MQW03] auch als erhöhte Energieeffizienz bezeichnet wird. Dieser Vorzug beruht insbesondere darauf, daß das für Empfängerorientierung typische senderseitige Einbeziehen von Kanalzustandsinformation ein leistungs- und energieeffizientes Versorgen der Empfänger erlaubt. Unter leistungseffizient wird dabei verstanden, daß vom Sender keine Sendesignalkomponenten abgestrahlt werden, die infolge widriger Übertragungseigenschaften des Mobilfunkkanals keinen signifikanten Beitrag zur Informationsübertragung zum gewünschten Empfänger leisten. Derartige nutzlose Sendesignalkomponenten, die Sendeleistung binden, können durch Empfängerorientierung prinzipiell reduziert oder gar vollständig vermieden werden. Inwiefern dieses gelingt, ist unter anderem Thema dieser Schrift und wird in den Kapiteln 2 bis 5 behandelt. Das Einsparen von totaler Sendeleistung ist aus verschiedenen Gründen besonders bedeutend:

  - In der Bevölkerung ist eine stetig zunehmende Elektrophobie, das heißt Sensibilisierung gegenüber Sendeanlagen, wie beispielsweise Basisstationen, zu beobachten. In den letzten zehn Jahren hat die Anzahl der Mobilfunknutzer weltweit stark zugenommen. Die Omnipräsenz von Mobiltelefonen hat daher zu verstärkten Bedenken in der Bevölkerung hinsichtlich der davon ausgehenden Gesundheitsgefahren geführt. Studien und wissenschaftliche Untersuchungen dieser biologisch-technologischen Wechselwirkungen wurden durchgeführt. Da solche Untersuchungen jedoch sehr zeitaufwendig und äußerst schwierig sind, sind diese immer noch im Gange [KBL97, HNP+99, IEE01]. Eine endgültige Klarheit über mögliche Gesundheitsgefahren besteht noch nicht, die Diskussionen dauern an. Das Problem geht dabei weit über das Technologische und Biologische hinaus und ist daher äußerst komplex. Unabhängig davon, zu welchem Resultat die laufenden Diskussionen führen, ist jedoch klar, daß eine sinnvolle Antwort von Seiten der Technologie ist, Verfahren mit reduzierten Leistungsemissionen zu forcieren, um damit Befürchtungen und Ängsten entgegenzuwirken.

– Wird Empfängerorientierung in der Abwärtsstrecke eines zellularen Mobilfunksystems eingesetzt, um die Sendeleistung mindestens einer einzelnen Basisstation bei gegebener Übertragungsqualität zu reduzieren, so bewirkt dies, daß die von dieser Basisstation ausgehende Interzellinterferenz im gleichen Maß wie die Sendeleistung reduziert wird. Die Funkkommunikation in zu anderen Basisstationen gehörigen Zellen kann daher mit verbesserter Übertragungsqualität oder, bei gleichbleibender Übertragungsqualität, mit erhöhten Datenraten erfolgen. Wird Empfängerorientierung in der Abwärtsstrecke jeder Zelle eingesetzt, so verbessert sich folglich die Gesamtqualität des zellularen Mobilfunksystems.

- Max H. M. Costa zeigte im Jahr 1983 in seinem grundlegenden Artikel [Cos83], daß bei gegebener Sendeleistung ein Punkt-zu-Punkt-SISO-Funkübertragungssystem, das durch eine ausschließlich dem Sender bekannte (quasi-)zufällige Störung, beispielsweise Interferenz, gestört wird, zumindest theoretisch die gleiche Leistungsfähigkeit erzielen kann wie ein gleichartiges Funkübertragungssystem, in dem diese bekannte Störung nicht vorhanden ist. Diese auf zuvor publizierten Arbeiten [EGC80, EGH81, EGH83] von Cover, El Gamal und Heegard basierende und in Arbeiten [YSJ+01, CL02] von Chiang, Cover, Cohen, Julian, Lapidoth, Sutivang und Yu weiter vertiefte theoretische Erkenntnis läßt sich für in der Abwärtsstrecke eingesetzte empfängerorientierte Funkkommunikation innerhalb einer K Mobilstationen und eine Basisstation umfassenden Referenzzelle grundsätzlich interpretieren, wie im folgend geschilderten Gedankenexperiment klar wird: Sendet in einem ersten Schritt die Basisstation der Referenzzelle ein Funksignal zur Versorgung einer Mobilstation k, so kann die Basisstation, aufgrund senderseitig vorhandener Kanalzustandsinformation — und diese ist im Fall von Empfängerorientierung verfügbar — und der Kenntnis dieses für Mobilstation k gesendeten Funksignals, die an allen anderen Mobilstationen k', $k' = 1 \dots K$, $k \neq k'$, entstehende Interferenz prognostizieren. In einem zweiten Schritt soll nun eine weitere Mobilstation k', $k' = 1 \dots K$, $k \neq k'$, der Referenzzelle durch dieselbe Basisstation zusätzlich versorgt werden. In diesem Fall stellt sich der Basisstation die Situation nach Costa, das heißt, es ist die Informationsübertragung von einem Sender, der Basisstation, zu einem Empfänger, der Mobilstation k', zu bewerkstelligen, wobei eine dem Sender bekannte Störung, die Interferenz infolge des zur Versorgung von Mobilstation k gesendeten Funksignals, vorhanden ist. Damit ist als Folge des theoretischen Ergebnises nach Costa klar, daß diese Informationsübertragung, dem oben geschilderten Costa'schen Prinzip folgend, prinzipiell mit der Leistungsfähigkeit erfolgen kann, die erzielbar gewesen wäre, wenn Mobilstation k zuvor nicht versorgt worden wäre. Das Versorgen einer weiteren Mobilstation k' ist folglich unabhängig von dem Versorgen von Mobilstation k ohne jegliche, als Folge der Versorgung von Mobilstation k auftretende Einbußen möglich. Es ist jedoch anzumerken, daß diese Unabhängigkeit im Sinne vermiedener wechselseitiger Störung nicht in umgekehrter Richtung gilt. Denn das im zweiten Schritt zur Versorgung von Mobilstation k' abgestrahlte Funksignal, das im allgemeinen Interferenz auch für Mobilstation k bedeutet, kann nicht im zuvor erfolgenden ersten Schritt im Costa'schen Sinne als dem Sender bekannte Störung berücksichtigt werden. Das geschilderte Vorgehen, das auch als Costa-Precoding bezeichnet wird [HSB03, AFHS04], kann für weitere Mobilstationen wiederholt werden, bis schließlich sämtliche Mobilstationen versorgt sind.

Als Essenz der obigen Ausführungen wird klar, daß Empfängerorientierung im Gegensatz zu Senderorientierung die Möglichkeit bietet, Interferenzen zu prognostizieren, die aus Wechselwirkungen zwischen den für verschiedene Empfänger gesendeten Funksignalen resultieren. Daher kann prinzipiell, dem Costa'schen Ergebnis folgend, der Preis, der für das gleichzeitige Versorgen mehrerer Empfänger zu zahlen ist, sehr klein werden. Neben den zuvor genannten Vorzügen der Empfängerorientierung macht dies den Einsatz von Empfängerorientierung in zukünftigen Mobilfunksystemen äußerst lukrativ. Die Arbeit Costas hat ausschließlich theoretischen Charakter und gibt leider keinerlei Aufschluß darüber, wie das Anpassen des Senders an die sich stellende senderseitig bekannte Störung konkret und in einer praktisch realisierbaren Weise zu erfolgen hat. Es ist das Thema dieser Schrift, die Vielzahl der praktisch umsetzbaren Möglichkeiten dieses Prinzips zwecks Erzeugung geeigneter Sendesignale systematisch zu erschließen und die darin verborgenen Grundprinzipien aufzuzeigen.

Als Folge der Vielzahl der oben angeführten Resultate gilt Empfängerorientierung als äußerst lukrativ für die Abwärtsstrecke zellularer Mobilfunksysteme [KM00, GC01, INBF01, JU01, JWJH01, WR01, CM02b, GC02, IF02b, SSB+02, WIF02, Geo03, HSB03, IHRF03, Joh04, BM04, BMWT00, BQT+03, MBL+00, MW04a, MWQ04a, MWQ04b, PMWB00, WLMM03, WMS03, WSM04].

In der Aufwärtsstrecke hingegen, wird — wie bereits heute üblich — sinnvollerweise das Grundkonzept der Senderorientierung eingesetzt. Es ist nämlich dieses Grundkonzept, das den Einsatz einfacher Sender erlaubt — und dies sind in der Aufwärtsstrecke die mobilen Endgeräte. Wie bereits angesprochen, entspricht Senderorientierung dem heutigen Stand der Technik und ist demzufolge in großer Tiefe und Ausführlichkeit in der Literatur behandelt [Sch79, Sch80, Ver86, Ver88, LV89, VA89, KIHP90, LV90, VA90, XSR90, VA91, AF92, DH92, BFKM93, DH93, Ver93, ASF94, KKKB94, PF94, RV94, WDH94, YR94, DH95, TAS95, Kle96, KKKB96, ARS97, Ver98, ZB98, ARAS99, Kar99, HMC99, BNK00, Poo00, TR00, Jar01, JD01, MJWT01, WM02b, WOWB02, WM02a, Meu03, KTF04, KBF05]. Aus diesem Grund soll im Rahmen dieser Schrift nicht genauer darauf eingegangen werden. Der interessierte Leser sei diesbezüglich auf die vorgenannten Quellen verwiesen.

Infrastrukturbasierte Mobilfunksysteme sollten sich aus den zahlreichen vorgenannten Gründen eine vorteilhafte Symbiose beider Grundkonzepte der Funkkommunikation zu Nutze machen. Dabei sollte Empfängerorientierung in der Abwärtsstrecke und Senderorientierung in der Aufwärtsstrecke eingesetzt werden. In der Literatur [WMSL02, TWL+02, WSLW03, BJM+04, WMZ04b, SWWM04] sind in jüngster Vergangenheit erste diesbezüglich Vorschläge unterbreitet worden. Dabei ist auch die Kombination beider Grundkonzepte mit dem Prinzip des orthogonalen Frequenzmultiplex (engl. orthogonal frequency division multiplex, OFDM) in Diskussion, das voraussichtlich nach herrschender Meinung eine Basis von Mobilfunksystemen der vierten Generation sein wird [vNP00, KS01, BM04].

Es ist das Ziel der vorliegenden Schrift, Klarheit über die prinzipiellen Einsatz- und Ausgestaltungsmöglichkeiten der Empfängerorientierung zu schaffen. Daher soll im folgenden, wie zuvor motiviert, im Detail ausschließlich die Abwärtsstrecke in einer Referenzzelle eines zellularen Mobilfunksystems betrachtet werden. Aus diesem Grund ist in Bild 1.8 eine spezielle Ausgestaltung des in Bild 1.7 dargestellten und in Abschnitt 1.1.2 eingeführten vereinfachten Modells der Funkkommunikation in der betrachteten Referenzzelle wiedergegeben. Diese Ausgestaltung spiegelt speziell die Gegebenheiten in einer MIMO-Abwärtsstrecke wider und wird daher im folgenden als vereinfachtes Modell der Funkkommunikation in der MIMO-Abwärtsstrecke der Referenzzelle, oder kurz Modell der MIMO-Abwärtsstrecke, bezeichnet. Dabei wird davon ausgegangen, daß in der Referenzzelle K Mobilstationen zu versorgen sind. Tabelle 1.2 faßt kompakt alle für dieses Modell relevanten Formelzeichen zusammen. Das in Bild 1.8 vorgestellte und in Tabelle 1.2 mathematisch fixierte Modell der MIMO-Abwärtsstrecke soll, soweit explizit nicht anders vereinbart, als Basis aller weiteren Analysen dienen, die die Abwärtsstrecke innerhalb einer Referenzzelle eines infrastrukturbasierten Mobilfunksystems betreffen.

Soll Empfängerorientierung in der beschriebenen MIMO-Abwärtsstrecke eingesetzt werden, so sind, wie bereits zuvor erläutert, zwei Teilaufgaben zu bewältigen:

1. die A-priori-Wahl der Empfänger der Mobilstationen und
2. das A-posteriori-Adaptieren des Senders der Basisstation an die gewählten Empfänger und die wirksamen Mobilfunkkanäle, das heißt das Erzeugen geeigneter Sendesignale durch den Sender.

Diese beiden Teilaufgaben betreffen die zu klärenden Kernfragen im Bereich der Empfängerorientierung und sollen daher im Rahmen dieser Schrift genauer studiert werden. Die bei der Wahl der Empfänger der Mobilstationen verfolgbaren Grundprinzipien sind dabei Thema des folgenden Unterkapitels 1.3. Die zweitgenannte der obigen Teilaufgabe, das heißt die Sendesignalerzeugung, stellt die weitaus größere der beiden Herausforderung dar. Soll nämlich der zuvor erläuterte schädliche Einfluß von Interferenz möglichst minimiert werden, so setzt dies voraus, daß alle von der Basisstation zur Versorgung der K Mobilstationen übertragenen Nachrichten so in ein totales Sendesignal $\underline{\mathbf{t}}$ nach (1.13) überführt werden, daß diese Nachrichten untereinander möglichst geringe oder keine wechselseitige Interferenz verursachen. Es ist prinzipiell möglich, sofern einige im folgenden noch genau zu diskutierenden Rahmenbedingungen erfüllt sind, den Beitrag jedes Datensymbols $\underline{d}_n^{(k)}$, $n = 1 \ldots N$, $k = 1 \ldots K$, zum totalen Sendesignal $\underline{\mathbf{t}}$ so zu gestalten, daß der Empfang anderer Datensymbole $\underline{d}_{n'}^{(k')}$, $n' = 1 \ldots N$, $k' = 1 \ldots K$, $n \neq n' \vee k \neq k'$, nicht oder nur in begrenztem Maße gestört wird. Diese Gestaltung resultiert in der Notwendigkeit, die Gesamtheit der zur Versorgung aller K Mobilstationen zu sendenden Datensymbole $\underline{d}_n^{(k)}$, $n = 1 \ldots N$, $k = 1 \ldots K$, gemeinsam zu verarbeiten, um somit unmittelbar ein totales Sendesignal $\underline{\mathbf{t}}$ unter Berücksichtigung des angesprochenen Ziels der Interferenzvermeidung zu erzeugen. Dieses Vorgehen unterscheidet sich maßgeblich von dem aus dem Bereich der Senderorientierung bekannten teilnehmerweisen oder datensymbolweisen Erzeugen von Sendesignalen [Kle96, Ver98] und ist ungleich komplexer. Naturgemäß ist demzufolge dem Themenkomplex der gemeinsamen Sendesignalerzeugung im Rahmen dieser Schrift eine umfassende Diskussion im Unterkapitel 1.4 und den Kapiteln 2 bis 5 gewidmet.

Eine essentielle Voraussetzung für eine gemäß Empfängerorientierung erfolgte gemeinsame Sendesignalerzeugung durch die Basisstation ist das basisstationsseitige Vorhandensein von Kanalzustandsinformation über die zwischen Basisstation und Mobilstationen wirksamen Mobilfunkkanäle in der MIMO-Abwärtsstrecke. Diese Information ist typischerweise auf Seiten der Basisstation nicht a priori vorhanden, sondern muß

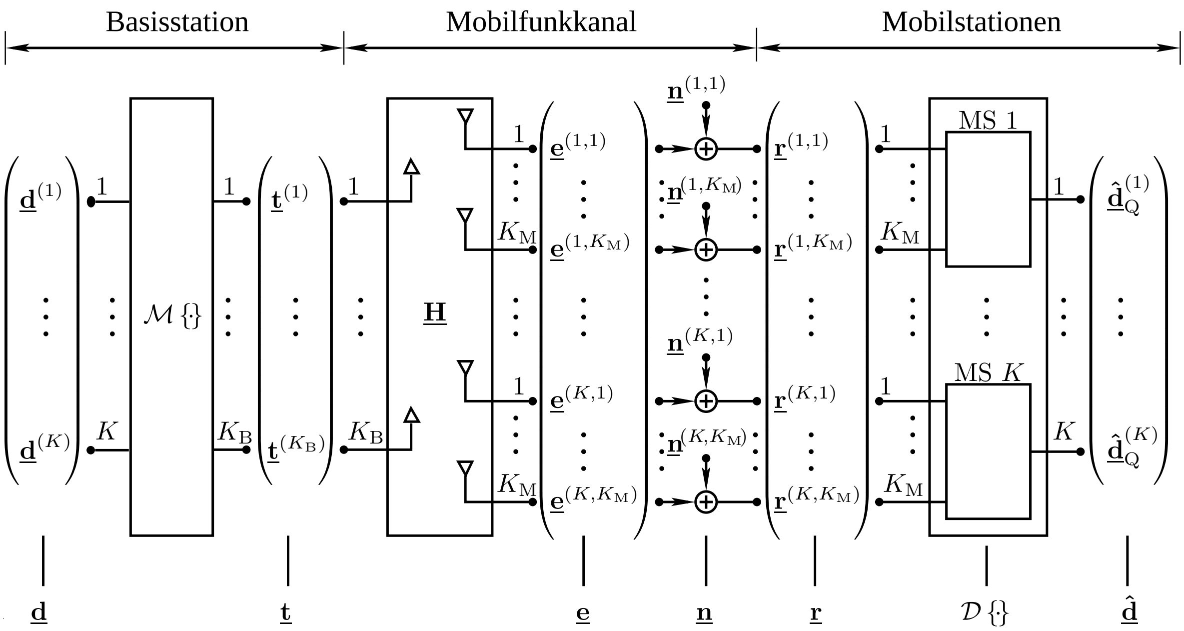

Bild 1.8. Vereinfachtes Modell der Funkkommunikation in der MIMO-Abwärtsstrecke der Referenzzelle

durch geeignete Maßnahmen verfügbar gemacht werden. In zellularen Mobilfunksystemen wird, wie bereits in Abschnitt 1.1.1 erläutert, eine Duplexübertragung realisiert. Dies kann genutzt werden, um die für die Abwärtsstreckenübertragung benötigte Kanalzustandsinformation während der Aufwärtsstreckenübertragung zu gewinnen. Ein derartiges Vorgehen setzt jedoch voraus, daß die Mobilfunkkanäle, die in beiden Übertragungsrichtungen genutzt werden, reziprok sind [Par92]. Dies ist genau dann gegeben, wenn zur Organisation der Aufwärtsstrecken- und Abwärtsstreckenübertragung [Web02]

- das Zeitduplexverfahren (engl. time division duplex, TDD) eingesetzt wird und die zwischen Kanalschätzen in der Aufwärtsstrecke und Nachrichtenübertragung gemäß Empfängerorientierung in der Abwärtsstrecke verstreichende Zeitspanne deutlich kleiner ist als die Korrelationsdauern der wirksamen Mobilfunkkanäle oder

- das Frequenzduplexverfahren (engl. frequency division duplex, FDD) eingesetzt wird und die Differenz der Mittenfrequenzen der für die beiden Übertragungsrichtungen verwendeten Frequenzbänder deutlich kleiner als die Kohärenzbandbreiten der wirksamen Mobilfunkkanäle ist.

Tabelle 1.2. Mathematische Formelzeichen im vereinfachten Modell nach Bild 1.8 der Funkkommunikation in der MIMO-Abwärtsstrecke der Referenzzelle

Kategorie	Formelzeichen	dargestellte Größe	Bemerkung
BS	K_B	Anzahl der Sendeantennen der BS	—
	N	Anzahl der Datensymbole pro MS	—
	$\underline{\mathbf{d}}^{(k)}$	zu MS k gehöriger teilnehmerspezifischer Datenvektor	—
	$\underline{\mathbf{d}}$	totaler Datenvektor	$\underline{\mathbf{d}}=\left(\underline{\mathbf{d}}^{(1)\mathrm{T}}\ldots\underline{\mathbf{d}}^{(K)\mathrm{T}}\right)^\mathrm{T}$
	$\underline{\mathbf{t}}^{(k_\mathrm{B})}$	sendeantennenspezifisches Sendesignal der k_B-ten Sendeantenne der BS	—
	$\underline{\mathbf{t}}$	totales Sendesignal	$\underline{\mathbf{t}}=\left(\underline{\mathbf{t}}^{(1)\mathrm{T}}\ldots\underline{\mathbf{t}}^{(K_\mathrm{B})\mathrm{T}}\right)^\mathrm{T}$
Mobilfunkkanal	$\underline{\mathbf{H}}^{(k,k_\mathrm{B},k_\mathrm{M})}$	sende- und empfangsantennenspezifische Kanalmatrix der k_B-ten Sendeantenne der BS und k_M-ten Empfangsantenne der MS k	—
	$\underline{\mathbf{H}}^{(k,k_\mathrm{B})}$	sendeantennenspezifische Kanalmatrix der k_B-ten Sendeantenne der BS und MS k	$\underline{\mathbf{H}}^{(k,k_\mathrm{B})}=\left(\underline{\mathbf{H}}^{(k,k_\mathrm{B},1)\mathrm{T}}\ldots \ldots\underline{\mathbf{H}}^{(k,k_\mathrm{B},K_\mathrm{M})\mathrm{T}}\right)^\mathrm{T}$
	$\underline{\mathbf{H}}^{(k)}$	teilnehmerspezifische Kanalmatrix der MS k	$\underline{\mathbf{H}}^{(k)}=\left(\underline{\mathbf{H}}^{(k,1)}\ldots\underline{\mathbf{H}}^{(k,K_\mathrm{B})}\right)$
	$\underline{\mathbf{H}}$	totale Kanalmatrix	$\underline{\mathbf{H}}=\left(\underline{\mathbf{H}}^{(1)\mathrm{T}}\ldots\underline{\mathbf{H}}^{(K)\mathrm{T}}\right)^\mathrm{T}$
	$\underline{\mathbf{n}}^{(k,k_\mathrm{M})}$	antennenspezifisches Rauschen der k_M-ten Empfangsantenne von MS k	—
	$\underline{\mathbf{n}}^{(k)}$	teilnehmerspezifisches Rauschen der MS k	$\underline{\mathbf{n}}^{(k)}=\left(\underline{\mathbf{n}}^{(k,1)\mathrm{T}}\ldots\underline{\mathbf{n}}^{(k,K_\mathrm{M})\mathrm{T}}\right)^\mathrm{T}$
	$\underline{\mathbf{n}}$	totales Rauschen	$\underline{\mathbf{n}}=\left(\underline{\mathbf{n}}^{(1)\mathrm{T}}\ldots\underline{\mathbf{n}}^{(K)\mathrm{T}}\right)^\mathrm{T}$
MS	K	Anzahl der Mobilstationen bzw. Teilnehmer	—
	K_M	Anzahl der Empfangsantennen pro MS	—
	$\hat{\underline{\mathbf{d}}}_\mathrm{Q}^{(k)}$	Schätzung von $\underline{\mathbf{d}}^{(k)}$	—
	$\hat{\underline{\mathbf{d}}}_\mathrm{Q}$	Schätzung von $\underline{\mathbf{d}}$	$\hat{\underline{\mathbf{d}}}_\mathrm{Q}=\left(\hat{\underline{\mathbf{d}}}_\mathrm{Q}^{(1)\mathrm{T}}\ldots\hat{\underline{\mathbf{d}}}_\mathrm{Q}^{(K)\mathrm{T}}\right)^\mathrm{T}$
	$\underline{\mathbf{e}}^{(k,k_\mathrm{M})}$	ungestörtes antennenspezifisches Empfangssignal der k_M-ten Empfangsantenne von MS k	—
	$\underline{\mathbf{e}}^{(k)}$	ungestörtes teilnehmerspezifisches Empfangssignal der MS k	$\underline{\mathbf{e}}^{(k)}=\left(\underline{\mathbf{e}}^{(k,1)\mathrm{T}}\ldots\underline{\mathbf{e}}^{(k,K_\mathrm{M})\mathrm{T}}\right)^\mathrm{T}$
	$\underline{\mathbf{e}}$	ungestörtes totales Empfangssignal	$\underline{\mathbf{e}}=\left(\underline{\mathbf{e}}^{(1)\mathrm{T}}\ldots\underline{\mathbf{e}}^{(K)\mathrm{T}}\right)^\mathrm{T}$
	$\underline{\mathbf{r}}^{(k,k_\mathrm{M})}$	(gestörtes) antennenspezifisches Empfangssignal der k_M-ten Empfangsantenne von MS k	—
	$\underline{\mathbf{r}}^{(k)}$	(gestörtes) teilnehmerspezifisches Empfangssignal der MS k	$\underline{\mathbf{r}}^{(k)}=\left(\underline{\mathbf{r}}^{(k,1)\mathrm{T}}\ldots\underline{\mathbf{r}}^{(k,K_\mathrm{M})\mathrm{T}}\right)^\mathrm{T}$
	$\underline{\mathbf{r}}$	(gestörtes) totales Empfangssignal	$\underline{\mathbf{r}}=\left(\underline{\mathbf{r}}^{(1)\mathrm{T}}\ldots\underline{\mathbf{r}}^{(K)\mathrm{T}}\right)^\mathrm{T}$

Ist einer der beiden oben dargelegten Fälle gegeben, so kann die angesprochene Kanalzustandsinformation, die für eine Abwärtsstreckenübertragung gemäß Empfängerorientierung benötigt wird, am Ort der Basisstation durch Schätzen während der Aufwärtsstreckenübertragung verfügbar gemacht werden. Erfolgt die Aufwärtsstreckenübertragung gemäß Senderorientierung — und dies ist typischerweise der Fall und auch Vorschlag des Verfassers —, so ist diese Kanalzustandsinformation ohnehin für die mit Senderorientierung einhergehende, an der Basisstation durchgeführte durch den Detektoroperator $\mathcal{D}\{\cdot\}$ beschriebene Empfangssignalverarbeitung, siehe auch Bild 1.7, nötig und daher auch für die Abwärtsstreckenübertragung verfügbar.

Gilt das Reziprozitätsprinzip nicht, beispielsweise weil das Frequenzduplexverfahren eingesetzt wird und die für Abwärtsstrecken- und Aufwärtsstreckenübertragung verwendeten Frequenzbänder frequenzmäßig voneinander um mehr als die Kohärenzbandbreite mindestens eines der wirksamen Mobilfunkkanäle separiert sind, so kann nach dem oben geschilderten Prinzip keine Kanalzustandsinformation über die Mobilfunkkanäle in der MIMO-Abwärtsstrecke verfügbar gemacht werden. Die zum Schätzen dieser Kanalzustandsinformation nötigen Beobachtungen der Mobilfunkkanäle können lediglich an den Orten der Empfänger, also den Mobilstationen, gemacht werden und müssen somit auf eine geschickte Art und Weise als explizite oder implizite Kanalzustandsinformation an den Sender, das heißt die Basisstation, rücksignalisiert werden. Details beider Vorgehensweisen, das heißt dem auf Reziprozität basierenden und dem aus Rücksignalisieren basierenden Vorgehen, werden in Kapitel 6 detailliert erläutert. Gemein ist diesen beiden Vorgehensweise jedoch, daß zwischen dem Zeitpunkt des Ermittelns der Kanalzustandsinformation und dem Nutzen dieser Kanalzustandsinformation zum Adaptieren des Senders im Sinne einer gemeinsamen Sendesignalerzeugung stets eine gewisse Totzeit T_{tot} verstreicht. Wenn die zwischen Basisstation und den K Mobilstationen wirksamen Mobilfunkkanäle zeitvariant sind — und dies ist, wie bereits in Abschnitt 1.1.2 erläutert, in typischen Mobilfunksystemen der Fall — und sich diese innerhalb der Zeit T_{tot} signifikant verändern, so kann das bei Empfängerorientierung nötige Adaptieren des Senders an die Empfänger und die wirksamen Mobilfunkkanäle nur in imperfekter Weise erfolgen. Derartige Imperfektionen gehen zu Lasten der Leistungsfähigkeit des betrachteten zellularen Mobilfunksystems. Eine detaillierte Studie der Grundprinzipien dieses Zusammenhangs ist in Kapitel 6 dieser Schrift nachzulesen. Anschaulich ist jedoch klar, daß das Einsatzgebiet von Empfängerorientierung in der Abwärtsstrecke zellularer Mobilfunksysteme durch die Variationsgeschwindigkeit der in der Abwärtsstrecke wirksamen Mobilfunkkanäle begrenzt ist. Praktisch bedeutet dies, daß bei gegebener Totzeit T_{tot} — und diese hängt ausschließlich vom Entwurf des Mobilfunksystems ab — und gegebener Mittenfrequenz des zur Abwärtsstreckenübertragung eingesetzten

Frequenzbandes die Geschwindigkeiten der Mobilstationen limitiert sind. Die für die Geschwindigkeiten geltenden weichen Grenzen lassen sich durch geeignete Verfahren wie beispielsweise Kanalprädiktionsverfahren [DHJU03, Win04, CM04a, CM03, Lay00] nach oben verschieben, sind jedoch prinzipiell stets vorhanden und unumgänglich.

1.3 Prinzipien der Empfängergestaltung

1.3.1 Grundlegendes

Der vermutlich bedeutsamste Vorteil von Empfängerorientierung besteht in der bereits mehrfach angesprochenen Möglichkeit, einfache Empfänger an den Mobilstationen zu verwenden und somit die Vielzahl der damit verbundenen in Unterkapitel 1.2 im Detail ausgeführten Vorzüge greifbar zu machen. Um diese Möglichkeit auszuschöpfen, sollte demnach bei der A-priori-Wahl der Empfänger der Mobilstationen eine möglichst einfache empfängerseitige Signalverarbeitung angestrebt werden. In der Literatur werden im Kontext von Empfängerorientierung eine verwirrende Vielzahl von Vorschlägen hinsichtlich der Wahl der Empfänger unterbreitet [EN93, ESN93, TC94, Wei94, ESN95, RV95, MSN97, JN98, MGS98a, MGS98b, VJ98, KSS99, SP99, WZZY99, BPD00, NBF00, BMWT00, KM00, MBL+00, MBW+00, PMWB00, TMW00, CLM01, FTH01, GC01, INBF01, JU01, JUN01, JWJH01, LMTB01, LTM01, MTWB01b, MTWB01a, SSP01, TWMB01b, TWMB01a, UY01, WR01, BM02, CM02a, CM02b, Fis02, FWLH02b, FWLH02a, FWLH02c, GC02, HvHJ+02, IF02b, IF02a, JHJvH02, JKG+02, JKUN02, ML02, MTJ02, NB02, QTM02, RIF02, SSB+02, TWL+02, WIF02, BM03, BQT+03, BZT+03, CM03, CML03, DHJU03, FW03, JIB+03, Geo03, HSB03, IHRF03, IRF03b, IRF03a, JIB+03, MQW03, PHS03, Trö03, WCS03, WF03, WVF03a, WM03d, WM03e, WM03c, WM03b, WMS03, WVF03b, BHMW04, BJM+04, BM04, CM04d, CM04a, CM04c, CM04b, IGF04, IHRF04b, JBU04, JBVU04, Joh04, MBQ04, Meu04b, Meu04a, MQS+04, MW04a, MW04b, MWQ04b, MWQ04a, NJU04, QMBW04, QMB+04, Skl04, SSH04, SWWM04, WES04, Win04, WM04a, WM04b, WMZ04a, WMZ04b, Qiu05, QMWB05]. Eine systematische Studie der sich bei der Wahl der Empfänger bietenden prinzipiellen Gestaltungsmöglichkeiten ist nach Kenntnis des Autors der vorliegenden Schrift jedoch nicht in der Literatur verfügbar. Dies ist insbesondere darin begründet, daß die zahlreichen die Wahl der Empfänger betreffenden Vorschläge typischerweise isoliert, meist im Kontext eines Beispielsystems unterbreitet werden und eine Gegenüberstellung der sich bietenden Möglichkeiten daher nicht thematisiert wird. In der vorliegenden Schrift soll daher in diesem Unterkapitel die sich bietende Vielfalt der in der Literatur verfügbaren relevanten Gestaltungsmöglichkeiten der Empfänger systematisiert, vervollständigt und im Grundsätzlichen beleuchtet werden.

Digitale Signalverarbeitung, die ausschließlich auf nicht iterativen Strukturen basiert, ist typischerweise hinsichtlich einer hardwaremäßigen Implementierung unproblematischer als eine solche, die auf iterativen Strukturen beruht. Für Funkkommunikation gemäß Empfängerorientierung ist daher eine Empfangssignalverarbeitung, die der Klasse der auf nicht iterativen Strukturen basierenden Signalverarbeitungen entstammt, besonders interessant. Darüber hinaus bietet eine der obigen Klasse entstammende, sich nicht an den Mobilfunkkanal adaptiv anpassende lineare empfängerseitige Signalverarbeitung den Vorteil, daß diese durch einfach realisierbare digitale lineare Filter mit festen Filterkoeffizienten beziehungsweise mit einfachen digitalen Korrelatoren implementiert werden kann. Folgerichtig haben sich in der Literatur im Kontext von Empfängerorientierung ausschließlich derartige nicht iterative Ausprägungen der Empfangssignalverarbeitung, die weitestgehend auf linearer Verarbeitung beruhen, etabliert [EN93, TC94, JN98, MGS98a, VJ98, SP99, BPD00, NBF00, BMWT00, KM00, MBL$^+$00, MBW$^+$00, CLM01, GC01, INBF01, JUN01, SSP01, UY01, CM02b, GC02, HvHJ$^+$02, JKG$^+$02, NB02, WIF02, BM03, BZT$^+$03, Geo03, MQW03, Trö03, BM04, MBQ04]. Im Rahmen der vorliegenden Schrift sollen daher ausschließlich derartige Ausgestaltungen der Empfangssignalverarbeitung der Empfänger und damit des Detektoroperators $\mathcal{D}\{\cdot\}$ nach (1.16) berücksichtigt werden.

Die in der Abwärtsstrecke zu übertragenden Datensymbole $\underline{d}_n^{(k)}$, $n = 1 \dots N$, $k = 1 \dots K$, sind, wie in Abschnitt 1.1.2 erläutert, einem diskreten Datensymbolalphabet $\mathbb{V}_\mathrm{d}$ nach (1.10) entnommen. Soll die durch die Datensymbole $\underline{d}_n^{(k)}$ getragene Information an den Empfängern wieder verfügbar gemacht werden, so ist es folglich unumgänglich, daß auch die empfängerseitig ermittelten Schätzungen $\widehat{\underline{d}}_{\mathrm{Q},n}^{(k)}$ dieser Datensymbole $\underline{d}_n^{(k)}$ dem Datensymbolalphabet $\mathbb{V}_\mathrm{d}$ nach (1.10) entnommen werden, also ausschließlich zwischen den verschiedenen Elementen von $\mathbb{V}_\mathrm{d}$ entschieden wird. Derartige Entscheidungen können durch eine ausschließlich lineare Empfangssignalverarbeitung nicht geleistet werden, sondern erfordern eine (teilweise) nichtlineare Empfangssignalverarbeitung. Sämtliche der oben angesprochenen, in der Literatur verfügbaren relevanten Ausprägungen der Empfangssignalverarbeitung und damit Ausgestaltungen des zugehörigen Detektoroperators $\mathcal{D}\{\cdot\}$ nach (1.16) lassen sich daher einheitlich als serielle Verkettung einer linearen Signalverarbeitung und einer nichtlinearen Signalverarbeitung beschreiben, wobei die zweitgenannte die notwendige Wertediskretheit der Schätzungen $\widehat{\underline{d}}_{\mathrm{Q},n}^{(k)}$ der Datensymbole $\underline{d}_n^{(k)}$, $n = 1 \dots N$, $k = 1 \dots K$, herbeiführt. Bild 1.9 veranschaulicht diese in der beschriebenen seriellen Verkettung bestehende Ausgestaltung des Detektoroperators $\mathcal{D}\{\cdot\}$ nach (1.16) graphisch. Die lineare Signalverarbeitung in Bild 1.9 hat die Aufgabe, auf Basis des totalen Empfangssignals $\underline{\mathbf{r}}$ nach (1.7) wer-

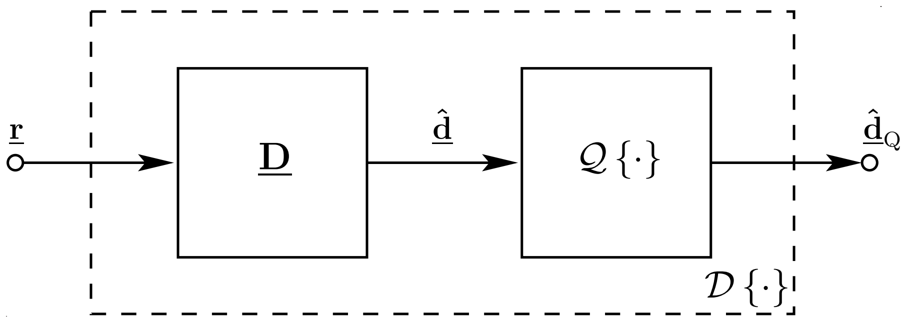

Bild 1.9. In der Literatur bedeutsame spezielle Ausgestaltung des Detektoroperators $\mathcal{D}\{\cdot\}$ nach (1.16) bestehend in der seriellen Verkettung einer durch die (totale) Demodulatormatrix $\underline{\mathbf{D}}$ beschriebenen linearen Signalverarbeitung und einer durch den Quantisierungsoperator $\mathcal{Q}\{\cdot\}$ beschriebenen nichtlinearen Signalverarbeitung

tekontinuierliche Schätzungen $\widehat{\underline{d}}_n^{(k)}$ der Datensymbole $\underline{d}_n^{(k)}$, $n = 1 \dots N$, $k = 1 \dots K$, zu ermitteln, die zu der wertekontinuierlichen Schätzung

$$\widehat{\underline{\mathbf{d}}}^{(k)} = \left(\widehat{\underline{d}}_1^{(k)} \dots \widehat{\underline{d}}_N^{(k)}\right)^{\mathrm{T}} \tag{1.17}$$

des teilnehmerspezifischen Datenvektors $\underline{\mathbf{d}}^{(k)}$, $k = 1 \dots K$, nach (1.11) und zu der wertekontinuierlichen Schätzung

$$\widehat{\underline{\mathbf{d}}} = \left(\widehat{\underline{\mathbf{d}}}^{(1)^{\mathrm{T}}} \dots \widehat{\underline{\mathbf{d}}}^{(K)^{\mathrm{T}}}\right)^{\mathrm{T}} \tag{1.18}$$

des totalen Datenvektors $\underline{\mathbf{d}}$ nach (1.12) zusammengefaßt werden. Mathematisch läßt sich eine derartige lineare Signalverarbeitung als linearer Operator interpretieren, der durch die (totale) Demodulatormatrix (engl. demodulator matrix) $\underline{\mathbf{D}}$ beschrieben werden kann und den Zusammenhang

$$\widehat{\underline{\mathbf{d}}} = \underline{\mathbf{D}}\,\underline{\mathbf{r}} \tag{1.19}$$

zwischen dem totalen Empfangssignal $\underline{\mathbf{r}}$ nach (1.7) und der wertekontinuierlichen Schätzung $\widehat{\underline{\mathbf{d}}}$ nach (1.18) des totalen Datenvektors $\underline{\mathbf{d}}$ nach (1.12) herstellt.

Die Schätzung $\widehat{\underline{\mathbf{d}}}_{\mathrm{Q}}$ nach (1.15) des totalen Datenvektors $\underline{\mathbf{d}}$ folgt entsprechend Bild 1.9 wiederum durch nichtlineare Signalverarbeitung der wertekontinuierlichen Schätzung $\widehat{\underline{\mathbf{d}}}$ nach (1.18). Diese nichtlineare Signalverarbeitung läßt sich in Analogie zu dem Vorgehen bei der erstgenannten linearen Signalverarbeitung durch einen nichtlinearen Quantisierungsoperator $\mathcal{Q}\{\cdot\}$ beschreiben, der durch Anwenden die Schätzung

$$\widehat{\underline{\mathbf{d}}}_{\mathrm{Q}} = \mathcal{Q}\left\{\widehat{\underline{\mathbf{d}}}\right\} \tag{1.20}$$

liefert. In der Literatur wird einheitlich mit nur wenigen Ausnahmen [Fis02, FSW03, WFH04] vorgeschlagen, die durch $\mathcal{Q}\{\cdot\}$ beschriebene nichtlineare Signalverarbeitung symbolweise durchzuführen, das heißt symbolweise zu quantisieren. Dieser Vorschlag resultiert vorrangig als Konsequenz aus der angestrebten Einfachheit der empfängerseitigen Signalverarbeitung und unterstützt somit einen der bedeutendsten der in Unterkapitel 1.2 erläuterten Vorzüge von Empfängerorientierung. Aus diesem Grund sollen im Rahmen dieser Schrift ausschließlich derartige Ausgestaltungen des Quantisierungsoperator $\mathcal{Q}\{\cdot\}$ betrachtet werden. Darüber hinaus soll angenommen werden, daß das symbolweise Quantisieren der wertekontinuierlichen Schätzungen $\underline{\widehat{d}}_{n}^{(k)}$ aller Datensymbole $\underline{d}_n^{(k)}$, $n = 1 \dots N$, $k = 1 \dots K$, in identischer Weise erfolgt. Beide vorgenannten Annahmen stellen keine signifikante Einschränkung hinsichtlich der in dieser Schrift behandelten Funkkommunikationssysteme dar, denn

- diese Annahmen tangieren nicht das behandelte Grundprinzip der Empfängerorientierung, und
- alle präsentierten Ergebnisse lassen sich prinzipiell in einfacher geradliniger Weise auch auf andere Fälle erweitern.

Erfolgt die nichtlineare Signalverarbeitung symbolweise, so läßt sich der nichtlineare Quantisierungsoperator $\mathcal{Q}\{\cdot\}$ durch die Quantisierungsfunktion $\mathrm{Q}(\cdot)$ gemäß

$$\mathcal{Q}\{\cdot\} : \underline{\widehat{\mathbf{d}}} \longmapsto \underline{\widehat{\mathbf{d}}}_{\mathrm{Q}}, \quad \text{mit} \quad \underline{\widehat{d}}_{\mathrm{Q},n}^{(k)} = \mathrm{Q}\left(\underline{\widehat{d}}_{n}^{(k)}\right), n = 1 \dots N, k = 1 \dots K, \tag{1.21}$$

darstellen, auf die in Abschnitt 1.3.3 noch genauer eingegangen wird. Wie sich zeigen wird, bildet die Quantisierungsfunktion $\mathrm{Q}(\cdot)$ nach (1.21) neben der totalen Demodulatormatrix $\underline{\mathbf{D}}$ nach (1.19) einen entscheidenden Freiheitsgrad bei der A-priori-Wahl der Empfänger der Mobilstationen.

1.3.2 Ausgestaltung der Demodulatormatrix

Typischerweise sind in einem infrastrukturbasierten Mobilfunksystem die Mobilstationen räumlich voneinander separiert und, infolge der ausschließlich verwendeten indirekten Informationsübertragung, nicht in der Lage, direkt untereinander Informationen auszutauschen. Folglich kann eine Mobilstation k, $k = 1 \dots K$, nur Kenntnis über die durch diese Mobilstation gewonnenen antennenspezifischen Empfangssignale $\underline{\mathbf{r}}^{(k,k_\mathrm{M})}$, $k_\mathrm{M} = 1 \dots K_\mathrm{M}$, also die Ausgangssignale der an diese Mobilstation angeschlossenen Empfangsantennen, erlangen. Diese Separierung resultiert zwangsläufig darin, daß die von verschiedenen Mobilstationen k und k', $k, k' = 1 \dots K$, $k \neq k'$, empfangenen antennenspezifischen Empfangssignale $\underline{\mathbf{r}}^{(k,k_\mathrm{M})}$, $k_\mathrm{M} = 1 \dots K_\mathrm{M}$, beziehungsweise $\underline{\mathbf{r}}^{(k',k_\mathrm{M}')}$,

$k_\mathrm{M}{}' = 1 \ldots K_\mathrm{M}$, lediglich in einer nicht kooperativen Weise auf der Empfängerseite verarbeitet werden können, um die zu den Mobilstationen gehörigen Schätzungen $\widehat{\underline{\mathbf{d}}}_\mathrm{Q}^{(k)}$ beziehungsweise $\widehat{\underline{\mathbf{d}}}_\mathrm{Q}^{(k')}$ der teilnehmerspezifischen Datenvektoren $\underline{\mathbf{d}}^{(k)}$ beziehungsweise $\underline{\mathbf{d}}^{(k')}$ zu ermitteln. Demgegenüber sind verschiedene antennenspezifische Empfangssignale $\underline{\mathbf{r}}^{(k,k_\mathrm{M})}$ und $\underline{\mathbf{r}}^{(k,k_\mathrm{M}{}')}$, $k_\mathrm{M}, k_\mathrm{M}{}' = 1 \ldots K_\mathrm{M}$, $k_\mathrm{M} \neq k_\mathrm{M}{}'$, ein und derselben Mobilstation k, $k = 1 \ldots K$, am gleichen Ort verfügbar und können daher in kooperativer Weise empfängerseitig ausgewertet werden. Es läßt sich somit festhalten, daß infolge der beschriebenen Gegebenheiten nicht jedes Element der Schätzung $\widehat{\underline{\mathbf{d}}}_\mathrm{Q}$ nach (1.15) des totalen Datenvektors $\underline{\mathbf{d}}$ nach (1.12) durch jedes Element des totalen Empfangssignals $\underline{\mathbf{r}}$ nach (1.7) beeinflußt wird. Es gilt vielmehr, daß die durch eine Mobilstation k ermittelte Schätzung $\widehat{\underline{\mathbf{d}}}_\mathrm{Q}^{(k)}$ des zugehörigen teilnehmerspezifischen Datenvektors $\underline{\mathbf{d}}^{(k)}$ ausschließlich von den antennenspezifischen Empfangssignalen $\underline{\mathbf{r}}^{(k,k_\mathrm{M})}$, $k_\mathrm{M} = 1 \ldots K_\mathrm{M}$, dieser Mobilstation k, das heißt zusammenfassend vom teilnehmerspezifischen Empfangssignals $\underline{\mathbf{r}}^{(k)}$ der Mobilstation k nach Tabelle 1.2 abhängt. Diese Beobachtung hat zur Folge, daß die in Bild 1.9 dargestellte totale Demodulatormatrix $\underline{\mathbf{D}}$ nach (1.19) bei Wahl der in dieser Schrift gültigen Notation gemäß Tabelle 1.2 stets die in Bild 1.10 gezeigte Blockdiagonalstruktur hat, das heißt sich mit den teilnehmerspezifischen Demodulatormatrizen $\underline{\mathbf{D}}^{(k)}$, $k = 1 \ldots K$, gemäß

$$\underline{\mathbf{D}} = \mathrm{blockdiag}\left(\underline{\mathbf{D}}^{(1)} \ldots \underline{\mathbf{D}}^{(K)}\right) \tag{1.22}$$

ausdrücken läßt. In Bild 1.10 sind nicht durch Schraffur gekennzeichnete Elemente der totalen Demodulatormatrix $\underline{\mathbf{D}}$ identisch null.

Betrachtet man die n-te Zeile, $n = 1 \ldots N$, einer zur Mobilstation k, $k = 1 \ldots K$, gehörigen teilnehmerspezifischen Demodulatormatrix $\underline{\mathbf{D}}^{(k)}$ nach (1.22), so beschreibt diese Zeile, wie die wertekontinuierliche Schätzung $\widehat{\underline{d}}_n^{(k)}$ des Datensymbols $\underline{d}_n^{(k)}$ auf Basis des zu Mobilstation k gehörigen teilnehmerspezifischen Empfangssignals $\underline{\mathbf{r}}^{(k)}$ ermittelt wird, denn es gilt in Analogie zu (1.19)

$$\widehat{\underline{\mathbf{d}}}^{(k)} = \underline{\mathbf{D}}^{(k)}\,\underline{\mathbf{r}}^{(k)}, k = 1 \ldots K. \tag{1.23}$$

Sollen mehrere Datensymbole $\underline{d}_n^{(k)}$, $n = 1 \ldots N$, $N > 1$, an eine Mobilstation k, $k = 1 \ldots K$, übertragen werden — und das ist typischerweise der Fall —, so bestehen hinsichtlich der Organisation dieser Übertragung, das heißt bezüglich des Multiplex, vielerlei Ausgestaltungsmöglichkeiten, die sich auch in der Gestaltung der zugehörigen teilnehmerspezifischen Demodulatormatrix $\underline{\mathbf{D}}^{(k)}$ niederschlagen. Diese Ausgestaltungsmöglichkeiten des Multiplex lassen sich im Falle von Empfängerorientierung danach klassifizieren, welche Anteile des von einer Mobilstation k empfangenen teilnehmerspezifischen Empfangssignals $\underline{\mathbf{r}}^{(k)}$ zum Schätzen der jeweiligen Datensymbole $\underline{d}_n^{(k)}$,

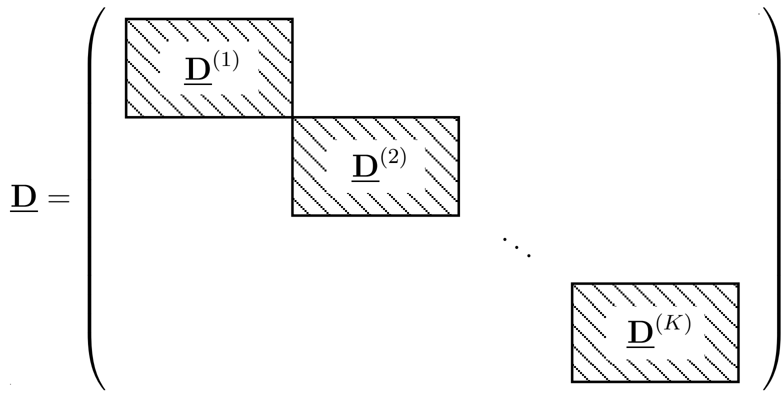

Bild 1.10. Blockdiagonalstruktur der totalen Demodulatormatrix $\underline{\mathbf{D}}$ nach (1.19)

$n = 1 \ldots N$, beitragen. An dieser Stelle sei darauf hingewiesen, daß eine derartige Betrachtungsweise des Multiplex von der im Bereich der Senderorientierung üblichen [Gib99, Ste92, DB96, Wes02, Meu00, MR00] erheblich abweicht, denn im Bereich der Senderorientierung dient ausschließlich die Zuordnung der mehreren zu übertragenden Datensymbole zu Anteilen des vom Sender abgestrahlten Sendesignals zur Klassifizierung der Ausgestaltungsmöglichkeiten des Multiplex.

Im Falle von Empfängerorientierung lassen sich, ähnlich wie bei der Senderorientierung, drei elementare Ausgestaltungsmöglichkeiten der Organisation der Übertragung mehrerer Datensymbole definieren:

- Zeitmultiplex (engl. time division multiplex, TDM): Die wertekontinuierlichen Schätzungen $\widehat{\underline{d}}_n^{(k)}$ beziehungsweise $\widehat{\underline{d}}_{n'}^{(k)}$, $n, n' = 1 \ldots N$, $n \neq n'$, verschiedener Datensymbole $\underline{d}_n^{(k)}$ beziehungsweise $\underline{d}_{n'}^{(k)}$ basieren auf zu verschiedenen Zeiten empfangenen Signalkomponenten des teilnehmerspezifischen Empfangssignals $\underline{\mathbf{r}}^{(k)}$ der Mobilstation k, $k = 1 \ldots K$.

- Raummultiplex (engl. space division multiplex, SDM): Die wertekontinuierlichen Schätzungen $\widehat{\underline{d}}_n^{(k)}$ beziehungsweise $\widehat{\underline{d}}_{n'}^{(k)}$, $n, n' = 1 \ldots N$, $n \neq n'$, verschiedener Datensymbole $\underline{d}_n^{(k)}$ beziehungsweise $\underline{d}_{n'}^{(k)}$ basieren auf an verschiedenen Empfangsantennen empfangenen Signalkomponenten des teilnehmerspezifischen Empfangssignals $\underline{\mathbf{r}}^{(k)}$ der Mobilstation k, $k = 1 \ldots K$.

- Codemultiplex (engl. code division multiplex, CDM): Die wertekontinuierlichen Schätzungen $\widehat{\underline{d}}_n^{(k)}$ beziehungsweise $\widehat{\underline{d}}_{n'}^{(k)}$, $n, n' = 1 \ldots N$, $n \neq n'$, verschiedener Datensymbole $\underline{d}_n^{(k)}$ beziehungsweise $\underline{d}_{n'}^{(k)}$ basieren auf zu gleichen Zeiten und an gleichen Empfangsantennen empfangenen Signalkomponenten des teilnehmerspezifischen Empfangssignals $\underline{\mathbf{r}}^{(k)}$ der Mobilstation k, $k = 1 \ldots K$, unterscheiden sich

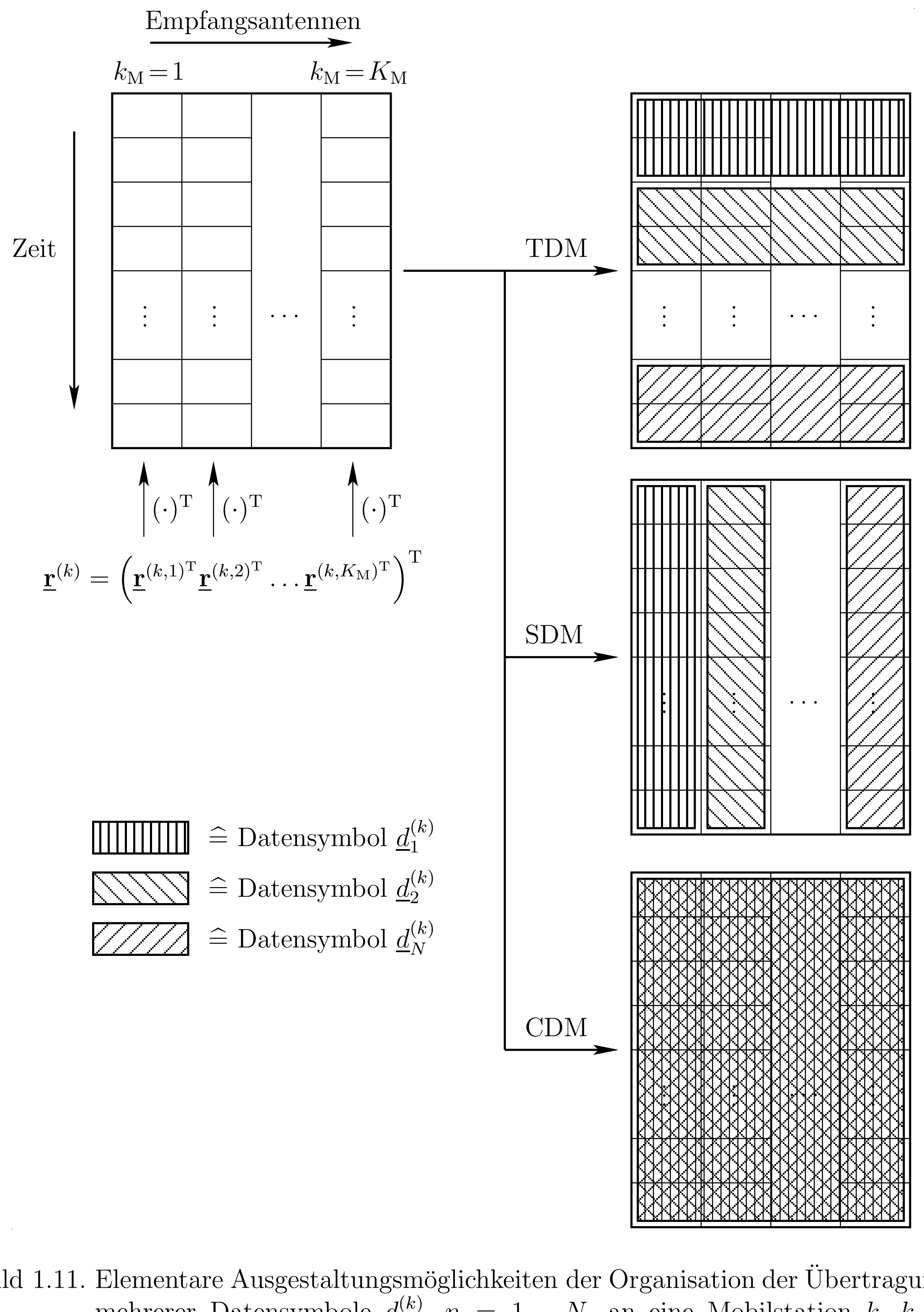

Bild 1.11. Elementare Ausgestaltungsmöglichkeiten der Organisation der Übertragung mehrerer Datensymbole $\underline{d}_n^{(k)}$, $n = 1 \ldots N$, an eine Mobilstation k, $k = 1 \ldots K$, mittels Zeitmultiplex (TDM), Raummultiplex (SDM) und Codemultiplex (CDM)

jedoch durch einzigartige Codes, das heißt unterschiedliche zugehörige Zeilen in der zu Mobilstation k gehörigen teilnehmerspezifischen Demodulatormatrix $\underline{\mathbf{D}}^{(k)}$.

Im allgemeinen sind auch Mischformen dieser elementaren Ausgestaltungsmöglichkeiten denkbar, die als hybride Multiplexverfahren bezeichnet werden. Bild 1.11 faßt die oben beschriebenen elementaren Ausgestaltungsmöglichkeiten des Multiplex graphisch zusammen. Dabei sind das von einer Mobilstation k, $k = 1 \ldots K$, empfangene teilnehmerspezifische Empfangssignal $\underline{\mathbf{r}}^{(k)}$ in Raum und Zeit sowie die Zuordnung der einzelnen Komponenten dieses Empfangssignals $\underline{\mathbf{r}}^{(k)}$ in Raum und Zeit zu Datensymbolen $\underline{d}_n^{(k)}$, $n = 1 \ldots N$, graphisch veranschaulicht.

Jede Ausgestaltungsmöglichkeit des Multiplex resultiert in einer charakteristischen Struktur der teilnehmerspezifischen Demodulatormatrix $\underline{\mathbf{D}}^{(k)}$ nach (1.22). Bild 1.12 zeigt diese charakteristische Strukturen für die oben genannten elementaren Ausgestaltungsmöglichkeiten Zeitmultiplex, Raummultiplex und Codemultiplex. Potentiell von Null verschiedene Elemente der teilnehmerspezifischen Demodulatormatrix $\underline{\mathbf{D}}^{(k)}$ sind dabei durch eine Schraffur gekennzeichnet. Unterschiedliche Schraffuren symbolisieren zu verschiedenen Datensymbolen $\underline{d}_n^{(k)}$, $n = 1 \ldots N$, gehörige Matrixelemente. Dabei ist besonders herauszuheben:

- Im Falle des Zeitmultiplex beinhaltet jede Spalte von $\underline{\mathbf{D}}^{(k)}$ nur höchstens ein von Null verschiedenes Element. Die potentiell von Null verschiedenen Elemente in der n-ten Zeile von $\underline{\mathbf{D}}^{(k)}$ sind in K_{M} Blöcken organisiert, die im folgenden als Codeblöcke bezeichnet werden, wobei jeder Codeblock zu einer der K_{M} Empfangsantennen gehört. Da zum Ermitteln der wertekontinuierlichen Schätzung $\widehat{\underline{d}}_n^{(k)}$, $n = 1 \ldots N$, eines Datensymbols $\underline{d}_n^{(k)}$ lediglich ein zeitlich stark begrenzter, kurzer Abschnitt des teilnehmerspezifischen Empfangssignals $\underline{\mathbf{r}}^{(k)}$ genutzt wird — also ausschließlich Codeblöcke verwendet werden, die aus deutlich weniger Elemente aufgebaut sind als die antennenspezifischen Empfangssignale $\underline{\mathbf{r}}^{(k,k_{\mathrm{M}})}$ —, bietet Zeitmultiplex nur wenig Zeitdiversität [Bla98]. Demgegenüber werden jedoch die antennenspezifischen Empfangssignale $\underline{\mathbf{r}}^{(k,k_{\mathrm{M}})}$ aller Empfangsantennen $k_{\mathrm{M}} = 1 \ldots K_{\mathrm{M}}$, zum Ermitteln der genannte Schätzung $\widehat{\underline{d}}_n^{(k)}$ einbezogen. Zeitmultiplex bietet daher ein hohes Maß an Empfangsantennendiversität beziehungsweise Raumdiversität [Bla98]. Die beschriebene Vorgehensweise des Zeitmultiplex ist hinsichtlich der Separierung der Übertragung verschiedener Datensymbole $\underline{d}_n^{(k)}$ und $\underline{d}_{n'}^{(k)}$, $n, n' = 1 \ldots N$, $n \neq n'$, das heißt dem Vermeiden schädlicher Interferenz, vorteilhaft, da durch die beschriebene zeitliche Organisation eine gewisse Separierung a priori erfolgt. Im allgemeinen können die zu verschiedenen Datensymbolen $\underline{d}_n^{(k)}$ und $\underline{d}_{n'}^{(k)}$, $n, n' = 1 \ldots N$, $n \neq n'$, gehörigen Codeblöcke gleich oder verschieden sein. Gleiches gilt für die zu unterschiedlichen Empfangsantennen gehörigen Codeblöcke ein und desselben Datensymbols $\underline{d}_n^{(k)}$. Eine häufig in

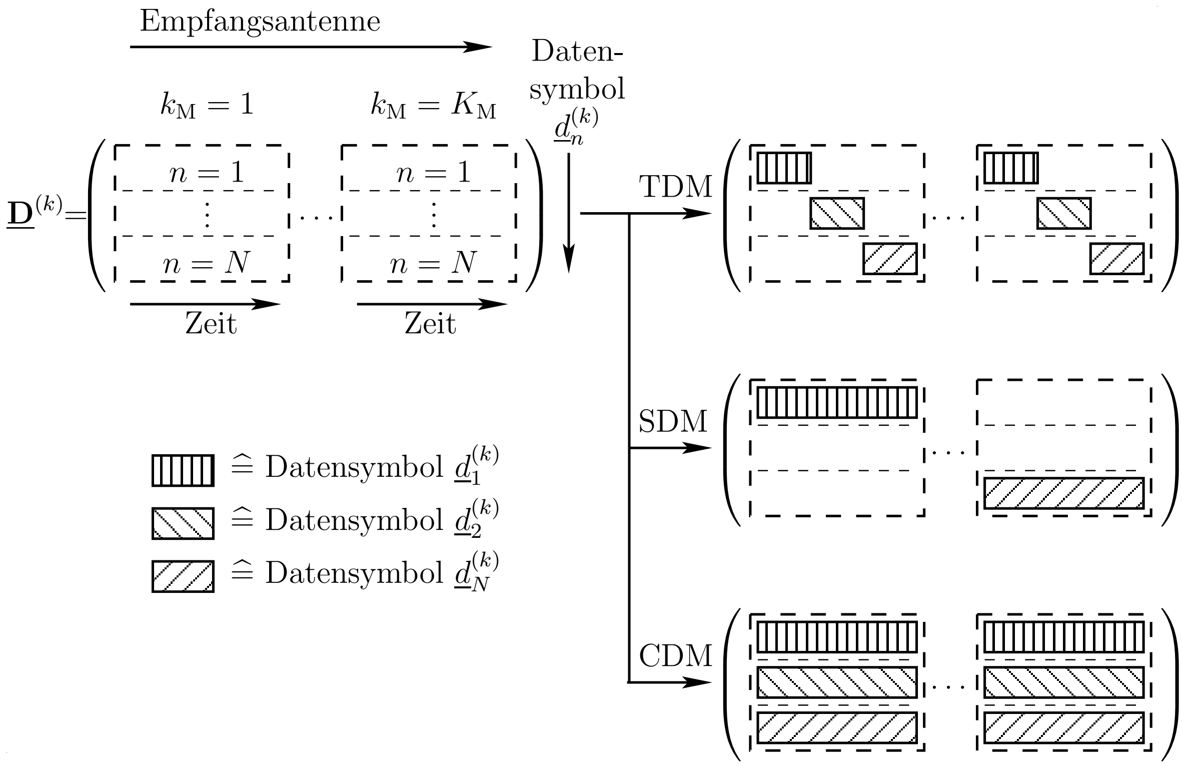

Bild 1.12. Ausgestaltung der teilnehmerspezifischen Demodulatormatrix $\underline{\mathbf{D}}^{(k)}$ nach (1.22) für die drei in Bild 1.11 dargestellten Ausgestaltungsmöglichkeiten Zeitmultiplex (TDM), Raummultiplex (SDM) und Codemultiplex (CDM)

der Literatur vorgeschlagene Vorgehensweise [VJ98, BPD00, BMWT00, KM00, BZT$^+$03, GC02, ESN93, IGF04, LMTB01, MBW$^+$00, MQW03, MTJ02, PMWB00, QTM02, JUN99, JU00, JU01, WIF02, TWL$^+$02, IRF03a, JIB$^+$03, Trö03, IGF04, BJM$^+$04] besteht in der Verwendung

- gleicher Codeblöcke für alle Empfangsantennen k_M, $k_\mathrm{M} = 1 \ldots K_\mathrm{M}$, und alle Datensymbole $\underline{d}_n^{(k)}$, $n = 1 \ldots N$, einer Mobilstation k, $k = 1 \ldots K$, und
- verschiedener Codeblöcke für unterschiedliche Mobilstation k und k', $k, k' = 1 \ldots K$, $k \neq k'$, wobei die für unterschiedliche Mobilstationen verwendeten Codeblöcke möglichst orthogonal oder zumindest mit günstigen Kreuzkorrelationseigenschaften gestaltet sind.

- Im Falle des Raummultiplex wird jedes antennenspezifische Empfangssignal $\underline{\mathbf{r}}^{(k,n)}$ einer Mobilstation k, $k = 1 \ldots K$, exklusiv jedoch im allgemeinen vollständig zum Schätzen eines Datensymbols $\underline{d}_n^{(k)}$, $n = 1 \ldots N$, verwendet. Die Anzahl N der gleichzeitig übertragbaren Datensymbole $\underline{d}_n^{(k)}$, $n = 1 \ldots N$, ist somit auf die Anzahl K_M der Empfangsantennen beschränkt, was Raummultiplex vorrangig als Teilkomponente hybrider Multiplexverfahren interessant macht. Jede Spalte von $\underline{\mathbf{D}}^{(k)}$ beinhaltet, ebenso wie beim Zeitmultiplex, nur höchstens ein einziges von Null verschiedenes Element; die potentiell von Null verschiedenen Elemente in der n-ten Zeile von $\underline{\mathbf{D}}^{(k)}$ sind in genau einem Codeblock organisiert. Für das Ermitteln der wertekontinuierlichen Schätzung $\widehat{\underline{d}}_n^{(k)}$, $n = 1 \ldots N$, eines Datensymbols $\underline{d}_n^{(k)}$ wird das gesamte antennenspezifische Empfangssignal $\underline{\mathbf{r}}^{(k,n)}$ ausgewertet. Raummultiplex bietet daher ein hohes Maß an Zeitdiversität [Bla98], wohingegen keine Empfangsantennendiversität beziehungsweise Raumdiversität geboten wird.

- Im Falle des Codemultiplex sind typischerweise in jeder Spalte und jeder Zeile der Matrix $\underline{\mathbf{D}}^{(k)}$ alle Elemente von Null verschieden. Die n-te Zeile von $\underline{\mathbf{D}}^{(k)}$ bildet somit einen alle Elemente umfassenden, für das Datensymbol $\underline{d}_n^{(k)}$ charakteristischen Codeblock, der daher auch als datensymbolspezifischer Code bezeichnet wird. Für das Ermitteln der wertekontinuierlichen Schätzung $\widehat{\underline{d}}_n^{(k)}$, $n = 1 \ldots N$, eines Datensymbols $\underline{d}_n^{(k)}$ wird demzufolge im allgemeinen das gesamte teilnehmerspezifische Empfangssignal $\underline{\mathbf{r}}^{(k)}$ der Mobilstation k, $k = 1 \ldots K$, ausgewertet. Codemultiplex bietet daher ein hohes Maß an Zeitdiversität und Empfangsantennen- beziehungsweise Raumdiversität [Bla98], wohingegen keine explizite Separierung der zu übertragenden Datensymbole $\underline{d}_n^{(k)}$, $n = 1 \ldots N$, a priori erfolgt. In der Literatur [CM02a, MBQ04, BZT+03, Meu04b, Meu04a, MWQ04b, MWQ04a, NJU04, QMBW04] ist es üblich, für die datensymbolspezifischen Codes
  - Zufallscodes oder
  - speziell gezüchtete Code mit beispielsweise guten Kreuzkorrelationseigenschaften

  einzusetzen.

Die grundsätzlichen Vor- und Nachteile der oben dargelegten elementaren Multiplexverfahren sind kompakt in Tabelle 1.3 zusammengefaßt. Dabei wird das Potential dieser Multiplexverfahren hinsichtlich Zeitdiversität, Raumdiversität, der einfachen Separierbarkeit der Übertragung verschiedener Datensymbole und hinsichtlich der Skalierbarkeit, das heißt der Freiheit, die sich bei der Wahl der Anzahl N der zu übertragenden Datensymbole bietet, bewertet.

Sowohl Zeitmultiplex als auch Raummultiplex können als entartete Spezialfälle des Codemultiplex mit speziellen datensymbolspezifischen Codes interpretiert werden. Gleiches gilt auch für den infolge der geringen Relevanz in der Literatur hier nicht genauer betrachteten (orthogonalen) Frequenzmultiplex (engl. (orthogonal) frequency division multiplex, (O)FDM), bei dem abgetastete harmonische Grundfunktionen verschiedener

Tabelle 1.3. Vorteile und Nachteile der elementare Ausgestaltungsmöglichkeiten der Organisation der Übertragung mehrerer Datensymbole; Klassifikation: positiv (+), neutral (0), negativ (–)

Multiplex-verfahren	Zeit-diversität	Raum-diversität	Separier-barkeit	Skalier-barkeit
Zeitmultiplex	–	+	+	0
Raummultiplex	+	–	0	–
Codemultiplex	+	+	–	+

Frequenz als datensymbolspezifische Codes eingesetzt werden. Aus diesem Grund kann für die weitere Diskussion von Empfängerorientierung ohne Beschränkung der Allgemeinheit einheitlich von einer Organisation der Übertragung mehrerer Datensymbole $\underline{d}_n^{(k)}$, $n = 1 \dots N$, an eine Mobilstation k, $k = 1 \dots K$, mittels Codemultiplex ausgegangen werden.

1.3.3 Wahl der Quantisierungsfunktion

Neben der Wahl der totalen Demodulatormatrix $\underline{\mathbf{D}}$ nach (1.19) besteht in der Wahl der nichtlinearen Quantisierungsfunktion $\mathrm{Q}(\cdot)$ nach (1.21) ein wesentlicher Freiheitsgrad bei der Empfängergestaltung. Daher soll diese Quantisierungsfunktion $\mathrm{Q}(\cdot)$ und das durch diese realisierte Quantisierungsschema im folgenden genauer betrachtet werden. Wie bereits erläutert, werden die zu übertragenden Datensymbole $\underline{d}_n^{(k)}$, $n = 1 \dots N$, $k = 1 \dots K$, dem diskreten Datensymbolalphabet $\mathbb{V}_\mathrm{d}$ nach (1.10) entnommen. Folglich ist es möglich, durch Übertragen eines Datensymbols $\underline{d}_n^{(k)}$ genau M gleich $\|\mathbb{V}_\mathrm{d}\|$ unterschiedliche Nachrichten, siehe auch (1.10), zu übermitteln, die durch M unterschiedliche Datensymbolrealisierungen $\underline{v}_m$, $m = 1 \dots M$, repräsentiert werden. Die Aufgabe der Quantisierungsfunktion $\mathrm{Q}(\cdot)$ besteht darin, der wertekontinuierlichen Schätzung $\widehat{\underline{d}}_n^{(k)}$ des Datensymbols $\underline{d}_n^{(k)}$ wieder eindeutig eine der Nachrichten, also eine Datensymbolrealisierung $\underline{v}_m$ aus $\mathbb{V}_\mathrm{d}$ zuzuordnen. Im mathematischen Sinne handelt es sich bei der Quantisierungsfunktion $\mathrm{Q}(\cdot)$ daher um eine Abbildung, die gemäß einer als die Quantisierungsschema bezeichneten Vorschrift eine wertekontinuierliche komplexwertige Größe $\underline{\widehat{d}}_n^{(k)}$ auf eine wertediskrete komplexwertige Größe $\underline{\widehat{d}}_{\mathrm{Q},n}^{(k)}$ abbildet. Eine derartige Abbildung läßt sich kompakt durch die Mengen $\mathbb{Q}_m \subset \mathbb{C}$, $m = 1 \dots M$, beschreiben, für die

$$\bigcup_{m=1}^{M} \mathbb{Q}_m = \mathbb{C} \tag{1.24}$$

und

$$\mathbb{Q}_m \cap \mathbb{Q}_{m'} = \emptyset, \forall m, m' = 1 \dots M, m \neq m', \tag{1.25}$$

gilt, das heißt, die die Menge $\mathbb{C}$ der komplexen Zahlen vollständig überlappungsfrei überdecken. Die Mengen $\mathbb{Q}_m$, $m = 1 \dots M$, bilden somit eine Partition von $\mathbb{C}$. Jedes $\mathbb{Q}_m$, $m = 1 \dots M$, faßt dabei alle möglichen Wertigkeiten der wertekontinuierlichen Schätzung $\underline{\widehat{d}}_n^{(k)}$ des Datensymbols $\underline{d}_n^{(k)}$ zusammen, die zur Schätzung der gleichen Nachricht m und damit dem gleichen $\underline{\widehat{d}}_{\mathrm{Q},n}^{(k)}$ führen. Daher heißen die Mengen $\mathbb{Q}_m$, $m = 1 \dots M$, auch Entscheidungsgebiete beziehungsweise Quantisierungsgebiete. Unter Ausnutzen dieser Nomenklatur folgt für die Quantisierungsfunktion nach (1.21)

$$\mathrm{Q}\left(\underline{d}_n^{(k)}\right) = \underline{\nu}_m, \quad \text{mit } \underline{d}_n^{(k)} \in \mathbb{Q}_m. \tag{1.26}$$

Je nach Eigenschaften der Mengen $\mathbb{Q}_m$, $m = 1 \dots M$, lassen sich verschiedene Klassen von Quantisierungsfunktionen $\mathrm{Q}(\cdot)$ und damit Klassen von Quantisierungsschemata definieren:

- Beschreiben alle $\mathbb{Q}_m$, $m = 1 \dots M$, einfach zusammenhängende Entscheidungsgebiete [Bai86], dann spricht man von einer konventionellen Quantisierungsfunktion $\mathrm{Q}(\cdot)$ beziehungsweise einem konventionellen Quantisierungsschema. Die auf $\mathrm{Q}(\cdot)$ basierende Verarbeitungseinheit in Bild 1.9 heißt demzufolge einfacher oder konventioneller Quantisierer. Die Empfänger von Mobilstationen, die derartige einfache Quantisierer nutzen, werden bezüglich der Quantisierung als konventionelle Empfänger bezeichnet. In der Literatur ist es üblich, jedem der einfach zusammenhängenden Entscheidungsgebiete $\mathbb{Q}_m$, $m = 1 \dots M$, einen Repräsentant $\underline{q}_m \in \mathbb{C}$ zuzuordnen, der typischerweise im Entscheidungsgebiet $\mathbb{Q}_m$, $m = 1 \dots M$, liegt und identisch mit $\underline{\nu}_m$ gewählt wird. Die Entscheidungsgebiete $\mathbb{Q}_m$, $m = 1 \dots M$, sind üblicherweise als Voronoi-Regionen [CS82] der M Repräsentanten $\underline{q}_m$, $m = 1 \dots M$, ausgeführt. Dieses stellt sicher, daß im Falle zufälligen totalen Rauschens $\underline{\mathbf{n}}$, das auf einen zirkular symmetrischen Gaußprozeß zurückgeht — und dieses ist ein typischer Fall im Mobilfunk [Pro95, Meu03] — und M unterschiedlicher gleichwahrscheinlicher zu übertragender Nachrichten eine minimalen Fehlentscheidwahrscheinlichkeit beim Quantisieren auftritt. Darüber hinaus ist diese Wahl von $\underline{q}_m$ und $\mathbb{Q}_m$, $m = 1 \ldots M$, einfach und praktikabel und ist daher etabliert [VJ98, BPD00, BMWT00, KM00, BZT+03, GC02, ESN93, IGF04, LMTB01, MBW+00, MQW03, MTJ02, PMWB00, QTM02, JUN99, JU00, JU01, WIF02, TWL+02, IRF03a, JIB+03, Trö03, IGF04, BJM+04].

- Beschreibt mindestens ein $\mathbb{Q}_m$, $m = 1 \ldots M$, ein mehrfach zusammenhängendes Entscheidungsgebiet [Bai86, MWQ04b, WMZ04a], dann spricht man von einer unkonventionellen Quantisierungsfunktion $\mathrm{Q}(\cdot)$ beziehungsweise einem unkonventionellen Quantisierungsschema. Die auf $\mathrm{Q}(\cdot)$ basierende Verarbeitungseinheit in Bild 1.9 heißt demzufolge unkonventioneller Quantisierer, die Empfänger von Mobilstationen, die derartige unkonventionelle Quantisierer nutzen, heißen bezüglich der Quantisierung unkonventionelle Empfänger. Jedes der $P^{(m)}$-fach zusammenhängenden Entscheidungsgebiete $\mathbb{Q}_m$, $m = 1 \ldots M$, läßt sich mathematisch durch $P^{(m)}$ einfach zusammenhängende Teilgebiete $\mathbb{Q}_{m,p}$, $p = 1 \ldots P^{(m)}$, in der Form

$$\mathbb{Q}_m = \bigcup_{p=1}^{P^{(M)}} \mathbb{Q}_{m,p} \tag{1.27}$$

beschreiben. In Analogie zu dem Vorgehen im Falle konventioneller Quantisierungsfunktionen $\mathrm{Q}(\cdot)$ kann jedem dieser Teilgebiete ein Repräsentant $\underline{q}_{m,p} \in \mathbb{C}$ zugeordnet werden, der typischerweise im entsprechenden Teilgebiet $\mathbb{Q}_{m,p}$, $p = 1 \ldots P^{(m)}$, $m = 1 \ldots M$, liegt. Die Teilgebiete $\mathbb{Q}_{m,p}$, $p = 1 \ldots P^{(m)}$, $m = 1 \ldots M$, sind aus den oben geschilderten Gründen üblicherweise als Voronoi-Regionen [CS82] der Repräsentanten $\underline{q}_{m,p}$, $p = 1 \ldots P^{(m)}$, $m = 1 \ldots M$, ausgeführt [MWQ04b, WMZ04a].

  In der Literatur hat sich insbesondere eine spezielle regelmäßige auf einer Gitterstruktur basierende Wahl der Repräsentanten $\underline{q}_{m,p}$, $p = 1 \ldots P^{(m)}$, $m = 1 \ldots M$, etabliert [Fis02, MBQ04, WMZ04a, FTH01, FWLH02b, FWLH02a, FWLH02c, HSB03, FW03, WF03, WVF03a, WVF03b, BHMW04, CM04d, JBU04, JBVU04, Joh04, NJU04, Win04]. Diese Gitterstruktur wird auch Lattice oder Lattice-Struktur genannt [CS88, Fis02], und das durch die Repräsentanten $\underline{q}_{m,p}$, $p = 1 \ldots P^{(m)}$, $m = 1 \ldots M$, definierte Quantisierungsschema heißt Latticequantisierungsschema. Der Vorzug dieser zu einer regelmäßigen Partition von $\mathbb{C}$ führenden Wahl der Repräsentanten liegt vor allem in der einfachen Implementierung der zugehörigen Quantisierungsfunktionen $\mathrm{Q}(\cdot)$, was hinsichtlich des Ziels, einfache Empfänger zu ermöglichen, von großer Bedeutung ist. Im Falle der angesprochenen Wahl der Repräsentanten $\underline{q}_{m,p}$, $p = 1 \ldots P^{(m)}$, werden typischerweise abzählbar unendlich viele Repräsentanten einer Nachricht m, $m = 1 \ldots M$, gewählt — das heißt $P^{(m)}$ geht gegen Unendlich —, die sich stets mit den beiden ganzen Zahlen k_1 und k_2 sowie geeignet gewählten komplexwertigen Konstanten

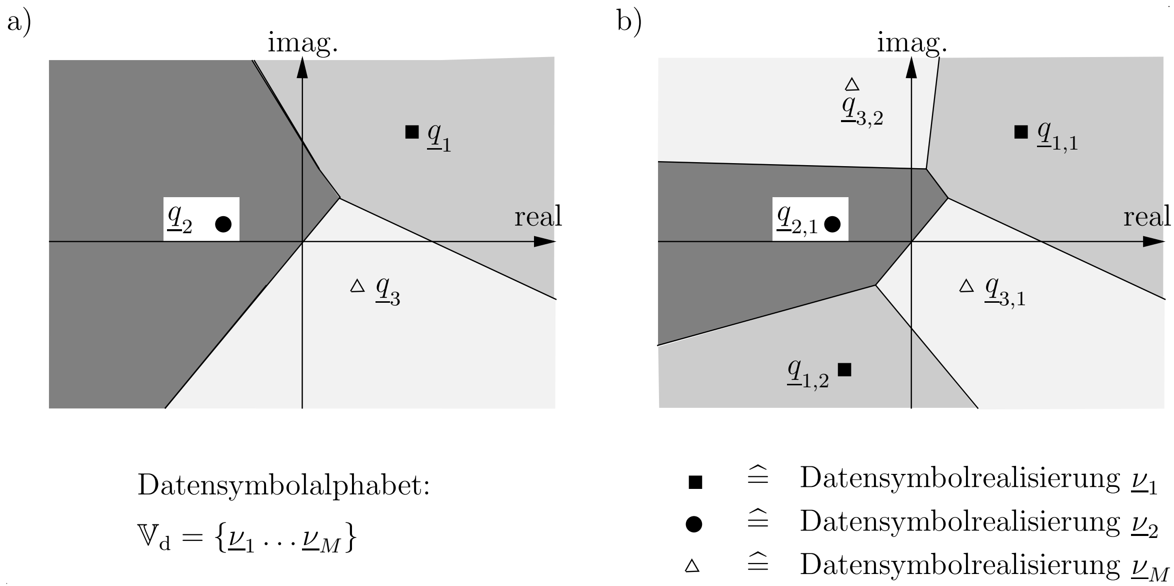

Bild 1.13. Beispiel eines durch $\mathrm{Q}(\cdot)$ nach (1.21) charakterisierten Quantisierungsschemas für ein Datensymbolalphabet $\mathbb{V}_{\mathrm{d}}$ der Kardinalität M gleich drei:

a) konventionelles Quantisierungsschema mit einfach zusammenhängenden Entscheidungsgebieten $\mathbb{Q}_m$, $m = 1 \ldots M$,
b) unkonventionelles Quantisierungsschema mit mehrfach zusammenhängenden Entscheidungsgebieten $\mathbb{Q}_m$, $m = 1 \ldots M$

$\underline{\alpha}_1$ und $\underline{\alpha}_2$ durch

$$\underline{q}_{m,p} = \underline{\nu}_m + k_1\underline{\alpha}_1 + k_2\underline{\alpha}_2, \quad \underline{\alpha}_1, \underline{\alpha}_2 \in \mathbb{C}, k_1, k_2 \in \mathbb{Z}, \tag{1.28}$$

beschreiben lassen [Fis02]. Bei entsprechender Sortierung besteht dabei zwischen der natürlichen Zahl p und dem Paar (k_1, k_2) dieser ganzen Zahlen stets ein eineindeutiger Zusammenhang

$$\begin{aligned} p \;&=\; \frac{k_1' + k_2' - 2}{2}(k_1' + k_2' - 1) + k_2', \\ &\quad \text{mit } k_i' = 2|k_i| + \frac{1}{2}\big[\mathrm{sgn}\,(k_i + 0,5) + 1\big], i = 1, 2. \end{aligned} \tag{1.29}$$

Bild 1.13 verdeutlicht die beiden dargelegten Klassen von Quantisierungsfunktionen graphisch.

Im Bereich der Empfängerorientierung werden Empfänger eingesetzt, die auf Quantisierungsfunktionen beider Klassen aufbauen. Dabei werden, wie bereits angesprochen, konventionelle Empfänger und unkonventionelle Empfänger unterschieden. Als ein wesentliches Ergebnis dieser Schrift wird sich herausstellen, daß beide Klassen von Empfängern ihre Vor- und Nachteile haben. Die sich zwischen beiden Klassen ergebenden Unterschiede liegen dabei vorrangig im Bereich der unterschiedlichen erzielbaren Leistungsfähigkeit von empfängerorientierter Funkkommunikation, die derartige

Empfänger einsetzt. Dieser Aspekt ist unter anderem Thema des folgenden Unterkapitels 1.4 und der Kapitel 2 bis 5 dieser Schrift.

1.4 Neuartige Verfahren der gemeinsamen Sendesignalerzeugung

Wie bereits in Abschnitt 1.1.3 erläutert, besteht Empfängerorientierung in der Abwärtsstrecke einer Referenzzelle eines zellularen Mobilfunksystems darin, die empfängerseitige Signalverarbeitung an den Mobilstationen a priori zu wählen und die senderseitige Signalverarbeitung der Basisstation an die gewählten Empfänger und die wirksamen relevanten Funkkanäle a posteriori zu adaptieren. Die sinnvolle Ausgestaltung der Empfänger und damit die A-priori-Wahl der empfängerseitigen, durch den Detektoroperator $\mathcal{D}\{\cdot\}$ nach (1.16) eindeutig charakterisierten Signalverarbeitung wurde in Unterkapitel 1.3 eingehend beleuchtet. Die Adaption der senderseitigen Signalverarbeitung, das heißt die Ausgestaltung des Modulatoroperators $\mathcal{M}\{\cdot\}$ nach (1.13) hingegen, ist eine noch zu klärende Frage.

Die Aufgabe einer im obigen Sinne adaptierten senderseitigen Signalverarbeitung besteht darin, auf Basis aller an die Mobilstationen zu übertragenden Datensymbole $\underline{d}_n^{(k)}$, $n = 1 \dots N$, $k = 1 \dots K$, das heißt des totalen Datenvektors $\underline{\mathbf{d}}$, ein totales Sendesignal $\underline{\mathbf{t}}$ zu erzeugen. Die Frage nach der geeigneten Adaption der senderseitigen Signalverarbeitung ist daher äquivalent zur Frage nach der Sendesignalerzeugung, das heißt der Erzeugung eines geeigneten totalen Sendesignals $\underline{\mathbf{t}}$ auf Basis des totalen Datenvektors $\underline{\mathbf{d}}$. Soll die Adaption der senderseitigen Signalverarbeitung beispielsweise derart erfolgen, daß die Entstehung der in Abschnitt 1.1.1 erläuterten schädlichen Interferenzen vermieden oder zumindest begrenzt wird — und dieses ist im Sinne einer möglichst leistungsfähigen fehlerfreien Übertragung sinnvoll —, so resultiert dies im allgemeinen in der Notwendigkeit, die Gesamtheit der zur Versorgung aller K Mobilstationen zu sendenden Datensymbole $\underline{d}_n^{(k)}$, $n = 1 \dots N$, $k = 1 \dots K$, gemeinsam zu verarbeiten, um somit unmittelbar ein totales Sendesignal $\underline{\mathbf{t}}$ unter Berücksichtigung des angesprochenen Ziels der Interferenzvermeidung zu erzeugen. Daher handelt es sich bei der Sendesignalerzeugung im allgemeinen um eine gemeinsame Sendesignalerzeugung. Verfahren, die eine derartige Sendesignalerzeugung erlauben, heißen daher auch Verfahren der gemeinsamen Sendesignalerzeugung oder Joint-Transmission-Verfahren. Sowohl die detaillierte Studie von Verfahren der gemeinsamen Sendesignalerzeugung als auch die Analyse der diesen Verfahren zugrundeliegenden Gütekriterien sind zentrale Themen dieser Arbeit und sollen in diesem Unterkapitel und den Kapiteln 2 bis 5 genauer betrachtet werden.

Im Bereich der gemeinsamen Sendesignalerzeugung ist in den letzten wenigen Jahren eine verwirrende Vielfalt von Verfahren [EN93, ESN93, TC94, Wei94, ESN95, RV95, MSN97, JN98, MGS98a, MGS98b, VJ98, KSS99, SP99, WZZY99, BPD00, NBF00, BMWT00, KM00, MBL+00, MBW+00, PMWB00, TMW00, CLM01, FTH01, GC01, INBF01, JU01, JUN01, JWJH01, LMTB01, LTM01, MTWB01b, MTWB01a, SSP01, TWMB01b, TWMB01a, UY01, WR01, BM02, CM02a, CM02b, Fis02, FWLH02b, FWLH02a, FWLH02c, GC02, HvHJ+02, IF02b, IF02a, JHJvH02, JKG+02, JKUN02, ML02, MTJ02, NB02, QTM02, RIF02, SSB+02, TWL+02, WIF02, BM03, BQT+03, BZT+03, CM03, CML03, DHJU03, FW03, JIB+03, Geo03, HSB03, IHRF03, IRF03b, IRF03a, JIB+03, MQW03, PHS03, Trö03, WCS03, WF03, WVF03a, WM03d, WM03e, WM03c, WM03b, WMS03, WVF03b, BHMW04, BJM+04, BM04, CM04d, CM04a, CM04c, CM04b, IGF04, IHRF04b, JBU04, JBVU04, Joh04, MBQ04, Meu04b, Meu04a, MQS+04, MW04a, MW04b, MWQ04b, MWQ04a, NJU04, QMBW04, QMB+04, Skl04, SSH04, SWWM04, WES04, Win04, WM04a, WM04b, WMZ04a, WMZ04b, Qiu05, QMWB05] entstanden, die es schwer macht, das gesamte Feld der gemeinsamen Sendesignalerzeugung zu durchdringen. Diese Schwierigkeiten resultieren im wesentlichen daraus, daß die genannten Verfahren der gemeinsamen Sendesignalerzeugung typischerweise stets isoliert oder in einer konkreten Anwendung betrachtet werden. Eine vergleichende Darstellung, die prinzipielle Gemeinsamkeiten und Unterschiede der verschiedenen vorgeschlagenen Verfahren herausarbeitet, fehlt. Daher ist es ein Ziel dieser Schrift, das gesamte Repertoire der bedeutenden, das heißt der relevanten Verfahren der gemeinsamen Sendesignalerzeugung systematisch darzustellen und zu komplettieren. Dabei soll auf die in Unterkapitel 1.3 beschriebene und in Bild 1.9 dargestellte vorteilhafte Ausgestaltung des Detektoroperators $\mathcal{D}\{\cdot\}$ zurückgegriffen werden.

Bild 1.14 zeigt schematisch die vom Autor favorisierte und im folgenden geschilderte systematische Gliederung der Vielfalt der relevanten Verfahren der gemeinsamen Sendesignalerzeugung. Der Verfasser schlägt vor, diese Verfahren in die beiden Klassen

- Verfahren der gemeinsamen Sendesignalerzeugung für konventionelle Empfänger und
- Verfahren der gemeinsamen Sendesignalerzeugung für unkonventionelle Empfänger

einzuteilen. Diese beiden Klassen unterscheiden sich im wesentlichen darin, daß bei den Verfahren der zweitgenannten Art bei der gemeinsamen Sendesignalerzeugung ein weiterer Freiheitsgrad verfügbar ist, den Verfahren der erstgenannten Art nicht bieten. Wie in Abschnitt 1.3.3 erläutert, stehen im Falle unkonventioneller Empfänger und damit unkonventioneller Quantisierungsschemata mehrere Repräsentanten $\underline{q}_{m,p}$, $p = 1 \ldots P^{(m)}$, und damit mehrere Teilgebiete $\mathbb{Q}_{m,p}$, $p = 1 \ldots P^{(m)}$, pro Nachricht

m, $m = 1 \ldots M$, zur Verfügung. Soll die Schätzung $\widehat{\underline{d}}_{\mathrm{Q},n}^{(k)}$ nach (1.14) eines Datensymbols $\underline{d}_n^{(k)}$, $n = 1 \ldots N$, $k = 1 \ldots K$, fehlerfrei sein, so ist es lediglich nötig, daß die wertekontinuierliche Schätzung $\widehat{\underline{d}}_n^{(k)}$ nach (1.17) dieses Datensymbols in einem der Teilgebiete $\mathbb{Q}_{m,p}$, $p = 1 \ldots P^{(m)}$, liegt. Dieses gelingt, zumindest im Falle verschwindenden totalen Rauschens $\underline{\mathbf{n}}$ nach (1.6), durch Erzeugen eines geeigneten totalen Sendesignals $\underline{\mathbf{t}}$. Im Rahmen der gemeinsamen Sendesignalerzeugung bietet sich daher die Wahlmöglichkeit zwischen $P^{(m)}$ Repräsentanten $\underline{q}_{m,p}$, $p = 1 \ldots P^{(m)}$, beziehungsweise Teilgebieten $\mathbb{Q}_{m,p}$, $p = 1 \ldots P^{(m)}$, der jeweiligen zu sendenden Nachricht m, $m = 1 \ldots M$. Diese Wahlmöglichkeit kann genutzt werden, um die Eignung des zu erzeugenden totalen Sendesignals $\underline{\mathbf{t}}$ hinsichtlich der noch genauer zu beleuchtenden Gütekriterien zu optimieren. Verfahren der gemeinsamen Sendesignalerzeugung der zweitgenannten Klasse sind demzufolge generell durch Entscheidungen zwischen verschiedenen Repräsentanten $\underline{q}_{m,p}$, $p = 1 \ldots P^{(m)}$, ein und derselben Nachricht m, $m = 1 \ldots M$, geprägt und daher stets nichtlinear in $\underline{\mathbf{d}}$.

Energie- beziehungsweise Leistungseffizienz sind aus den in Abschnitt 1.2 im Detail dargelegten Gründen im Kontext zellularen Mobilfunks besonders wichtig. Daher betreffen die bei der gemeinsamen Sendesignalerzeugung verwendeten und zu optimierenden Gütekriterien typischerweise, unabhängig davon, ob Verfahren der erstgenannten Art oder solche der zweitgenannten Art betrachtet werden, die Minimierung der abgestrahlten Energie

$$T = \frac{1}{2}\underline{\mathbf{t}}^{\mathrm{H}}\underline{\mathbf{t}} \tag{1.30}$$

des totalen Sendesignals $\underline{\mathbf{t}}$, oder kurz der totalen Sendeenergie T, bei gegebener zu erzielender Übertragungsqualität. Äquivalent wird auch das Maximieren der Übertragungsqualität bei gegebener Energie T nach (1.30) des totalen Sendesignals $\underline{\mathbf{t}}$ betrachtet. Unter dem Maximieren der Übertragungsqualität versteht man dabei, daß eine möglichst fehlerfreie Funkkommunikation gewährleistet werden soll. Dieses ist, je nach Ausgestaltung dann erreicht, wenn die Wahrscheinlichkeit dafür, daß ein Übertragungsfehler, beispielsweise eines Datensymbols $\underline{d}_n^{(k)}$,$n = 1 \ldots N$, $k = 1 \ldots K$, eines durch diese Datensymbole getragenen Nutzdatums $u_l^{(k)}$, $l = 1 \ldots L$, $k = 1 \ldots K$, oder der Gesamtheit aller an eine Mobilstation k, $k = 1 \ldots K$, zu übertragenden Nutzdaten $\mathbf{u}^{(k)}$, minimiert wird.

Historisch gesehen sind im Bereich der empfängerorientierten Funkkommunikation die Verfahren der erstgenannten Art die ältesten, die daher im folgenden zuerst betrachtet werden sollen. In [EN93, TC94, JN98, MGS98a, VJ98, SP99, BPD00, NBF00, BMWT00, KM00, MBL+00, MBW+00, CLM01, GC01, INBF01, JUN01, SSP01, UY01, CM02b, GC02, HvHJ+02, JKG+02, NB02, WIF02, BM03, BZT+03, Geo03, MQW03, Trö03, BM04, MBQ04] wurden Verfahren der gemeinsamen Sendesignalerzeugung vorgeschlagen, die entsprechend den obigen Ausführungen unter gewissen im folgenden

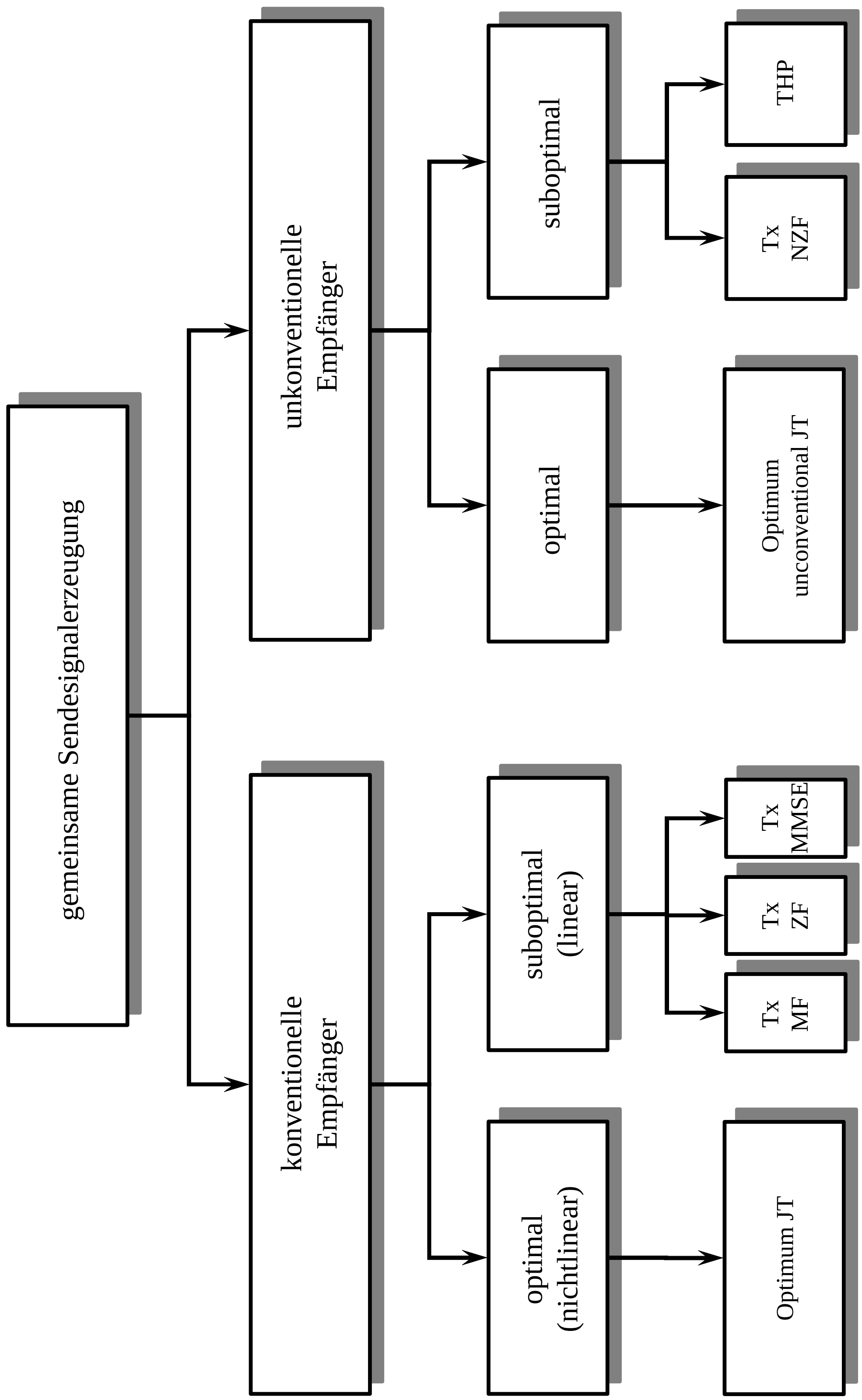

Bild 1.14. Systematische Gliederung bedeutender Verfahren der gemeinsamen Sendesignalerzeugung in der empfängerorientierten Funkkommunikation

noch beleuchteten Nebenbedingungen für eine angestrebte Übertragungsqualität auf die Minimierung der totalen Sendeenergie T nach (1.30) des totalen Sendesignals $\underline{\mathbf{t}}$ abzielen. Als Maß der bereits angesprochenen Übertragungsqualität der Funkkommunikation werden jedoch nicht die Wahrscheinlichkeiten von Übertragungsfehlern, sondern vereinfachend Signal-zu-Rausch-und-Interferenz-Verhältnisse (engl. signal to noise and interference ratio, SNIR) der wertekontinuierlichen Schätzungen $\widehat{\underline{d}}_n^{(k)}$ der Datensymbole $\underline{d}_n^{(k)}$, $n = 1 \dots N$, $k = 1 \dots K$, explizit oder implizit betrachtet. Diese Vereinfachung führt in [EN93, TC94, JN98, MGS98a, VJ98, SP99, BPD00, NBF00, BMWT00, KM00, MBL+00, MBW+00, CLM01, GC01, INBF01, JUN01, SSP01, UY01, CM02b, GC02, HvHJ+02, JKG+02, NB02, WIF02, BM03, BZT+03, Geo03, MQW03, Trö03, BM04, MBQ04] zu Verfahren der gemeinsamen Sendesignalerzeugung, die hinsichtlich der Erzeugung des totalen Sendesignals $\underline{\mathbf{t}}$ linear in $\underline{\mathbf{d}}$ sind und daher als lineare Verfahren der gemeinsamen Sendesignalerzeugung bezeichnet werden. Lineare Verfahren der gemeinsamen Sendesignalerzeugung können mit der Modulatormatrix $\underline{\mathbf{M}}$ durch einen linearen Modulatoroperator

$$\mathcal{M}\{\underline{\mathbf{d}}\} = \underline{\mathbf{M}}\,\underline{\mathbf{d}} \tag{1.31}$$

eindeutig beschrieben werden. Je nach Art der bereits oben angesprochenen Nebenbedingung lassen sich daraus, dual zu den aus dem Bereich der Senderorientierung bekannten linearen Verfahren der gemeinsamen Empfangssignalverarbeitung [Kle96, Ver98, Meu03], verschiedene lineare Grundverfahren der gemeinsamen Sendesignalerzeugung ableiten, die demzufolge zu unterschiedlichen Modulatormatrizen $\underline{\mathbf{M}}$ nach (1.31) führen:

- Senderseitige signalangepaßte Filterung (engl. transmit matched filter, TxMF) [EN93, JN98, MGS98a, WZZY99, NBF00, CLM01, GC01, INBF01, JUN01, NB02, BM03, BQT+03, BZT+03, Geo03, MQW03, Trö03, Joh04, MBQ04, Win04]: Das SNIR jedes Datensymbols $\underline{d}_n^{(k)}$, $n = 1 \dots N$, $k = 1 \dots K$, wird für eine gegebene totale Sendeenergie T unter Vernachlässigung der auftretenden Interferenzen maximiert. Diese Vorgehensweise liefert ein totales Sendesignal $\underline{\mathbf{t}}$, das zu wertekontinuierlichen Schätzungen $\widehat{\underline{d}}_n^{(k)}$ der Datensymbole $\underline{d}_n^{(k)}$, $n = 1 \dots N$, $k = 1 \dots K$, führt, die möglichst robust hinsichtlich des auftretenden totalen Rauschens $\underline{\mathbf{n}}$ nach (1.6) sind. Soll insgesamt nur ein einziges Datensymbol übertragen werden, so ist die angesprochene durch das SNIR quantifizierte Übertragungsqualität bei gemeinsamer Sendesignalerzeugung gemäß TxMF optimal. Werden jedoch mehrere Datensymbole $\underline{d}_n^{(k)}$, $n = 1 \dots N$, an eine oder mehrere Mobilstationen k, $k = 1 \dots K$, übertragen, so sind infolge der Vernachlässigung des Entstehens schädlicher Interferenz die angesprochenen wertekontinuierlichen Schätzungen $\widehat{\underline{d}}_n^{(k)}$ jedoch unter Umständen stark von Interferenz beeinflußt und daher von mäßiger Qualität. In der Literatur wird das beschriebene Grundverfahren der gemeinsamen Sendesignalerzeugung auch als Pre-Rake bezeichnet [EN93, ESN93, ESN95, BF99, NBF00, JUN01, CM02b].

- Senderseitige Interferenzeliminierung (engl. transmit zero forcing, TxZF) [TC94, MSN97, VJ98, KSS99, BPD00, BMWT00, KM00, MBL+00, MBW+00, GC01, JU01, JWJH01, WR01, CM02a, GC02, HvHJ+02, NB02, WIF02, BZT+03, Geo03, Trö03, IHRF04b, Joh04, MBQ04, WES04, Win04]: Unter Vernachlässigung des totalen Rauschens $\underline{\mathbf{n}}$ nach (1.6) wird das SNIR jedes Datensymbols $\underline{d}_n^{(k)}$, $n = 1 \dots N$, $k = 1 \dots K$, für eine gegebene totale Sendeenergie T maximiert. Eine derartige Vorgehensweise liefert ein totales Sendesignal $\underline{\mathbf{t}}$, das im rauschfreien Fall zu wertekontinuierlichen Schätzungen $\widehat{\underline{d}}_n^{(k)}$ der Datensymbole $\underline{d}_n^{(k)}$, $n = 1 \dots N$, $k = 1 \dots K$, führt, die frei von Interferenzen sind. Tritt jedoch Rauschen auf, so sind, infolge der Vernachlässigung des Rauscheinflusses, die angesprochenen wertekontinuierlichen Schätzungen $\widehat{\underline{d}}_n^{(k)}$ jedoch unter Umständen stark von Rauschen beeinflußt — stärker als bei TxMF – und daher rauschsensitiv. In der Literatur wird dieses interferenzvermeidende Grundverfahren der gemeinsamen Sendesignalerzeugung auch als „klassisches“ Joint Transmission (JT) [BMWT00, MBW+00, PMWB00, GC01, MTWB01b, TWL+02, HSB03, WM03d], Joint Pre-Distortion [KM00, WR01, TWL+02], Pre-Equalization [GC01, MPGF01, Geo03] oder Kanalinversion (engl. channel inversion) [HvHJ+02, JHJvH02, HSB03, Meu04b] bezeichnet.

- Senderseitiges Minimieren des mittleren quadratischen Schätzfehlers (engl. transmit minimum mean square error, TxMMSE) [KSS99, SP99, UY01, CM02b, GC02, JKG+02, WIF02, BM03, BZT+03, Joh04, MBQ04, Win04, Qiu05]: Die Qualität der wertekontinuierlichen Schätzungen $\widehat{\underline{d}}_n^{(k)}$ der Datensymbole $\underline{d}_n^{(k)}$, $n = 1 \dots N$, $k = 1 \dots K$, wird unter Berücksichtigung sowohl des Rauschens als auch der Interferenz optimiert. Dabei wird aus Gründen, die in Kapitel 3 noch genauer erläutert werden, ein alle Datensymbole $\underline{d}_n^{(k)}$, $n = 1 \dots N$, $k = 1 \dots K$, einschließendes SNIR maximiert. Dazu wird senderseitig, das heißt an der Basisstation, neben der Kenntnis der wirksamen Mobilfunkkanäle, das heißt der totalen Kanalmatrix $\underline{\mathbf{H}}$, und der durch den Detektoroperator $\mathcal{D}\{\cdot\}$ beschriebenen Empfangssignalverarbeitung auch Kenntnis über die Leistung des empfängerseitigen totalen Rauschens $\underline{\mathbf{n}}$ benötigt. In der Literatur [JKG+02, JKUN02, DHJU03, IHRF03, JIB+03, IGF04, NJU04] wird das beschriebene Grundverfahren der gemeinsamen Sendesignalerzeugung auch als senderseitiges Wiener-Filter (engl. transmit Wiener filter, TxWF) bezeichnet.

Über die oben beschriebenen Grundverfahren hinaus werden in der Literatur [BZT+03, MTJ02] auch weitere lineare Verfahren der gemeinsamen Sendesignalerzeugung in der Referenzzelle vorgeschlagen, die nicht auf die Minimierung der totalen Sendeenergie T

nach (1.30), sondern auf die Minimierung der Interferenzwirkung des erzeugten totalen Sendesignals $\underline{\mathbf{t}}$ bei potentiell gestörten, nicht der Referenzzelle angehörigen Empfängern abzielt.

Lineare Verfahren der gemeinsamen Sendesignalerzeugung sind recht einfach, lassen sich mit mäßiger Implementierungskomplexität realisieren, wie anhand einschlägiger Komplexitätsuntersuchungen gezeigt wurde [KM00, WIF02, Geo03, IGF04, MQS^{+}04, Win04], und werden daher bevorzugt in der Literatur betrachtet. Eine systematische detaillierte Darstellung der Vielzahl der relevanten linearen Verfahren der gemeinsamen Sendesignalerzeugung einschließlich einer vergleichenden Bewertung der Leistungsfähigkeit dieser Verfahren ist Thema von Kapitel 3 dieser Schrift.

Hinsichtlich der erzielten Übertragungsqualität ist das oben eingeführte SNIR, das bei linearen Verfahren der gemeinsamen Sendesignalerzeugung als Bewertungsmaß verwendet wird, nur ein unzureichendes Vehikel. Denn das SNIR ist infolge der nichttrivialen Statistik der aus Interferenz und Rauschen bestehenden Störung $\widehat{\underline{d}}_n^{(k)} - \underline{d}_n^{(k)}$ der wertekontinuierlichen Schätzung $\widehat{\underline{d}}_n^{(k)}$ eines jeden Datensymbols $\underline{d}_n^{(k)}$, $n = 1 \ldots N$, $k = 1 \ldots K$, nicht eineindeutig funktional mit der Wahrscheinlichkeit eines Übertragungsfehlers verkoppelt [IHRF03, WM03d, WM03e]. Daher ist ein Maximieren des SNIR nicht dem Minimieren der angesprochenen Übertragungsfehlerwahrscheinlichkeit äquivalent. Folgerichtig sind lineare Verfahren der gemeinsamen Sendesignalerzeugung hinsichtlich der oben eingeführten, auf Übertragungsfehlerwahrscheinlichkeiten basierenden Übertragungsqualität suboptimal [IHRF03, WM03d, WM03e].

Die linearen Verfahren der gemeinsamen Sendesignalerzeugung zielen ausschließlich auf die Gestaltung von wertekontinuierlichen Schätzungen $\widehat{\underline{d}}_n^{(k)}$ der Datensymbole $\underline{d}_n^{(k)}$, $n = 1 \ldots N$, $k = 1 \ldots K$, ab, die nach den beschriebenen Kriterien günstig sind. Lineare Verfahren können folglich die wertediskrete Natur der Datensymbole $\underline{d}_n^{(k)}$, die durch das Datensymbolalphabet $\mathbb{V}_{\mathrm{d}}$ nach (1.10) gegeben ist, beim Minimieren der Übertragungsfehlerwahrscheinlichkeit nicht berücksichtigen. In [IHRF03, IRF03b, IRF03a, WM03d, WM03e, WMS03, IHRF04b, Skl04] wird daher unter anderem durch den Autor der vorliegenden Schrift vorgeschlagen, diese wertediskrete Natur der Datensymbole $\underline{d}_n^{(k)}$, $n = 1 \ldots N$, $k = 1 \ldots K$, beim gemeinsamen Sendesignalerzeugen im Sinne der Minimierung einer über alle Datensymbole gemittelten Übertragungsfehlerwahrscheinlichkeit zu nutzen. Derartige Verfahren werden in der Literatur als optimale Joint-Transmission-Verfahren (engl. optimum joint transmission, optimum JT) [WM03d, WM03e, WMS03, Skl04] oder Minimal-Bitfehlerraten-Mehrteilnehmerübertragungs-Verfahren (engl. minimum bit-error rate multiuser transmission, Min. BER MUT) [IHRF03, IRF03b, IRF03a, IHRF04b] bezeichnet. Die genannten Verfahren maximieren bei gegebener totaler Sendeenergie T

nach (1.30) die Übertragungsqualität — und darunter wird im Rahmen dieser Schrift, sofern nicht explizit anders erwähnt, die Wahrscheinlichkeit von Übertragungsfehlern verstanden — beziehungsweise minimieren die zum Erreichen einer gewünschten Übertragungsqualität benötigte totale Sendeenergie T. Aus diesem Grund werden diese Verfahren, die die wertediskrete Natur der Datensymbole $\underline{d}_n^{(k)}$, $n = 1 \dots N$, $k = 1 \dots K$, ausnutzen, im folgenden als optimale Verfahren der gemeinsamen Sendesignalerzeugung für konventionelle Empfänger bezeichnet. Nachteilig ist bei den optimalen Verfahren der gemeinsamen Sendesignalerzeugung zu erwähnen, daß diese senderseitig gegenüber den linearen Verfahren der gemeinsamen Sendesignalerzeugung erheblich komplexer sind. Somit wird durch erhöhten senderseitigen Aufwand — und das ist in der Abwärtsstrecke der Referenzzelle die Basisstation — die verbesserte Übertragungsqualität zwischen Sender und Empfänger — und dies sind in der Referenzzelle die Mobilstationen — erkauft. Die detaillierte Vorstellung der optimalen Verfahren der gemeinsamen Sendesignalerzeugung für konventionelle Empfänger wie auch die Analyse der Leistungsfähigkeit dieser Verfahren ist Thema von Kapitel 2.

Motiviert durch die Vorarbeiten von Tomlinson [Tom71] und Harashima/Miyakawa [HM72] aus den frühen 70er Jahren des letzten Jahrhunderts zur Vorentzerrung im Kontext drahtgebundener Kommunikation über dispersive Übertragungsmedien kam ab dem Jahr 2002 der Vorschlag [FWLH02b] auf, die Übertragungsqualität von empfängerorientierter Funkkommunikation in MIMO-Abwärtsstrecken durch Methoden zu verbessern, die mit den Ideen von Tomlinson, Harashima und Miyakawa eng verwandt sind. Die Herausforderung lag im wesentlichen darin, diese Ideen, die auf drahtgebundene SISO-Punkt-zu-Punkt-Kommunikationssysteme beschränkt waren, auf Funkkommunikationssysteme der Grundarchitekturen Punkt-zu-Punkt und Punkt-zu-Mehrpunkt zu übertragen und dabei gegebenenfalls mehrere Sendeantennen wie auch mehrere Empfangsantennen einzubeziehen [FWLH02b, FWLH02a, FWLH02c, FW03, HSB03, WVF03b, BHMW04, JBU04, Joh04, Win04]. Die innovative Neuerung bestand vorrangig darin,

- anstelle der bisher üblichen konventionellen Empfänger unkonventionelle Empfänger vorzusehen, siehe auch Unterkapitel 1.3, die auf unkonventionellen Quantisierungsschemata aufbauen, und

- daran angepaßte Verfahren der gemeinsamen Sendesignalerzeugung für unkonventionelle Empfänger einzusetzen, also Verfahren der auf Seite 51 eingeführten zweitgenannten Klasse.

Dadurch wurde es prinzipiell möglich, bei gegebener totaler Sendeenergie T eine höhere Übertragungsqualität zu erzielen als die mit den oben dargelegten optimalen Verfahren der gemeinsamen Sendesignalerzeugung für konventionelle Empfänger erreichbare.

Erste Arbeiten zu diesem als Tomlinson-Harashima-Precoding (THP) oder MIMO-Tomlinson-Harashima-Precoding (MIMO-THP) bekannten Vorgehen betreffen MIMO-Funkkommunikation der Grundarchitekturen Punkt-zu-Punkt [FWLH02b] und Punkt-zu-Mehrpunkt [FWLH02a, FWLH02c], wobei dabei, ähnlich den Vorschlägen von Tomlinson, Harashima und Miyakawa spezielle Empfänger eingesetzt werden, die gemäß dem allgemeinen, in dieser Schrift entwickelten Rahmenwerk als Spezialfälle eines unkonventionellen Empfängers zu bezeichnen sind. Diese unkonventionellen Empfänger beruhen auf einer speziellen Wahl des Datensymbolalphabets $\mathbb{V}_{\mathrm{d}}$ nach (1.10), dem Spezialfall des Latticequantisierungsschemas nach (1.28) und einer quadratischen Demodulatormatrix $\underline{\mathbf{D}}$ nach (1.19) mit Diagonalstruktur und speziell gewählten Diagonalelementen $[\underline{\mathbf{D}}]_{n,n}$. Das Erzeugen des totalen Sendesignals $\underline{\mathbf{t}}$ erfolgt gemäß einem iterativen datensymbolweisen Vorgehen.

In [BZT$^+$03, MQW03, BM04, MQS$^+$04, QMBW04, QMB$^+$04, WM04b, WMZ04a] werden die vorgenannten Arbeiten verallgemeinert und durch den Autor der vorliegenden Schrift für den allgemeinen Fall unkonventioneller Empfänger und beliebiger Datensymbolalphabete $\mathbb{V}_{\mathrm{d}}$ nach (1.10) vorgeschlagen. Das daraus resultierende Verfahren der gemeinsamen Sendesignalerzeugung namens senderseitige nichtlineare Interferenzeliminierung (engl. transmit nonlinear zero forcing, TxNZF) erlaubt das iterative Erzeugen des totalen Sendesignals $\underline{\mathbf{t}}$ durch gruppenweises Erzeugen der Beiträge der einzelnen Datensymbole $\underline{d}_n^{(k)}$ zum totalen Sendesignal $\underline{\mathbf{t}}$. TxNZF schließt die zuvor genannten Verfahren Tomlinson-Harashima-Precoding und MIMO-Tomlinson-Harashima-Precoding als Spezialfall ein.

Beim gemeinsamen Sendesignalerzeugen durch alle oben angesprochenen Verfahren wird wieder das von den linearen Verfahren der gemeinsamen Sendesignalerzeugung für konventionelle Empfänger bekannte SNIR der wertekontinuierlichen Schätzungen $\widehat{\underline{d}}_n^{(k)}$ der Datensymbole $\underline{\mathbf{d}}_n^{(k)}$ für eine gegebene totale Sendeenergie T maximiert, oder, äquivalent, die totale Sendeenergie T für ein gefordertes SNIR minimiert. Dabei ist jedoch im nun betrachteten Falle unkonventioneller Empfänger der zusätzliche Freiheitsgrad der Wahl der Repräsentanten bei der Definition des SNIR in der Art und Weise zu berücksichtigen, daß als Nutzsignalbeitrag von $\widehat{\underline{d}}_n^{(k)}$ stets der günstigste Repräsentant der jeweiligen Nachricht betrachtet wird. Je nach Ausgestaltung lassen sich bei den zuvor genannten Verfahren der gemeinsamen Sendesignalerzeugung für unkonventionelle Empfänger wieder in analoger Weise zu den linearen Verfahren der gemeinsamen Sendesignalerzeugung für konventionelle Empfänger die beiden Verfahrensvarianten der Interferenzeliminierung (engl. zero forcing, ZF) [FTH01, FWLH02b, FWLH02a, FWLH02c, FW03, HSB03, WF03, WVF03a, WVF03b, BHMW04, CM04d, JBU04, JBVU04, Joh04, NJU04, Win04] und des Minimierens des mittleren quadratischen Schätzfehlers (engl. minimum mean square error, MMSE) [JBU04, JBVU04, Joh04] finden.

Tabelle 1.4. Wichtige ausgewählte Veröffentlichungen aus dem Themenkomplex der gemeinsamen Sendesignalerzeugung (kursiv gedruckt sind Arbeiten, die unter Mitwirkung des Verfassers entstanden sind)

Empfänger-typ	Verfahrens-klasse	Literatur-referenz	Anmerkung/ Einordnung
konven-tionell	suboptimal (linear)	[EN93, ESN93, ESN95, JN98, MGS98a, WZZY99, NBF00, CLM01, GC01, INBF01, JUN01, CM02b, IF02b, IF02a, IF02a, JKUN02, Geo03, NB02, RIF02, *BM03, BQT$^+$03, BZT$^+$03*, JIB$^+$03, CML03, *MQW03*, Trö03, *BM04*, CM04c, Joh04, *MBQ04, MQS$^+$04, MWQ04b, MWQ04a*, NJU04, *QMB$^+$04*, Win04, *WMZ04a*]	TxMF, Pre-Rake
		[TC94, MSN97, MGS98a, VJ98, KSS99, BPD00, *BMWT00*, KM00, *MBL$^+$00, MBW$^+$00, PMWB00*, GC01, JU01, *LMTB01, MTWB01b, TWMB01b*, WR01, *BM02*, CM02a, GC02, JHJvH02, JKUN02, ML02, *MTJ02*, NB02, TWL$^+$02, WIF02, *BM03, BQT$^+$03, BZT$^+$03*, JIB$^+$03, Geo03, HSB03, IHRF03, Trö03, WCS03, *BJM$^+$04, BM04*, CM04a, IGF04, IHRF04b, Joh04, *MBQ04, MWQ04b*, NJU04, *QMBW04, QMB$^+$04*, Skl04, SSH04, *SWWM04*, Win04, *WMZ04b*]	TxZF, „klassisches“ Joint Transmission (JT)
		[RV95, KSS99, SP99, SSP01, UY01, CM02b, GC02, JKG$^+$02, JKUN02, ML02, SSB$^+$02, WIF02, *BM03, BZT$^+$03*, CM03, IHRF03, JIB$^+$03, WCS03, CM04a, CM04c, IGF04, IHRF04b, Joh04, *MBQ04, MQS$^+$04*, NJU04, *QMB$^+$04*, Win04, *WMZ04a*, Qiu05]	TxMMSE, TxWF
	optimal (nichtlinear)	[IHRF03, IRF03b, IRF03a, *WM03d, WM03e, WMS03*, IHRF04b, Skl04]	Optimum JT, Min. BER MUT
unkonven-tionell	suboptimal	[FTH01, Fis02, FWLH02b, FWLH02a, FWLH02c, HSB03, FW03, WF03, WVF03a, WVF03b, BHMW04, CM04d, JBU04, JBVU04, Joh04, NJU04, Win04]	THP mit Latticequanti-sierungschema
		[Wei94, *BZT$^+$03, MQW03, BM04, QMBW04, QMB$^+$04, MWQ04b, MQS$^+$04, WM04b, WMZ04a*, Qiu05, QMWB05]	TxNZF mit allg. Quanti-sierungsschema
	optimal	[PHS03, *MWQ04b*]	totale Interfe-renzeliminierung

Grundlage der vorgenannten Verfahren der gemeinsamen Sendesignalerzeugung sind, wie bereits erwähnt, die SNIRs der wertekontinuierlichen Schätzungen $\widehat{\underline{d}}_n^{(k)}$ der Datensymbole $\underline{d}_n^{(k)}$, $n = 1 \ldots N$, $k = 1 \ldots K$, wohingegen die Wahrscheinlichkeit eines Übertragungsfehlers nicht berücksichtigt wird. Hinsichtlich des Ziels der Maximierung der Übertragungsqualität — und darunter soll im Rahmen dieser Schrift sofern nicht explizit anderes vereinbart, vorrangig die Minimierung der Übertragungsfehlerwahrscheinlichkeit verstanden werden — sind diese Verfahren daher suboptimal.

Die vorgenannten Verfahren der gemeinsamen Sendesignalerzeugung für unkonventionelle Empfänger sind, wie bereit zuvor erläutert, dadurch gekennzeichnet, daß für jedes zu übertragende Datensymbol $\underline{d}_n^{(k)}$, $n = 1 \ldots N$, $k = 1 \ldots K$, eine Wahl zwischen den verschiedenen Repräsentanten $\underline{q}_{m,p}$, $p = 1 \ldots P^{(m)}$, der jeweils zu sendenden Nachricht m, $m = 1 \ldots M$, zu treffen ist. Diese Wahl erfolgt bei den zuvor erläuterten Verfahren typischerweise in einer heuristischen Art und Weise und nicht im Sinne eines Optimierens der Übertragungsqualität bei gegebener totaler Sendeenergie T beziehungsweise im Sinne des Minimierens der totalen Sendeenergie T für eine geforderte Übertragungsqualität. Daher sind die bisher vorgestellten Verfahren der gemeinsamen Sendesignalerzeugung für unkonventionelle Empfänger auch in dieser zweiten Hinsicht suboptimal bezüglich des zuvor erläuterten Optimierungsziels. Nichtsdestoweniger sind derartige Verfahren infolge des sich in ihnen widerspiegelnden guten Kompromisses zwischen Implementierungskomplexität und Leistungsfähigkeit für die Praxis äußerst interessant [FWLH02b, QMBW04]. Kapitel 5 dieser Schrift befaßt sich daher eingehend mit Verfahren der gemeinsamen Sendesignalerzeugung der beschriebenen Art.

Soll die Übertragungsfehlerwahrscheinlichkeit bei gegebener totaler Sendeenergie T nach (1.30) minimiert werden oder, äquivalent, bei einzuhaltender gegebener Übertragungsfehlerwahrscheinlichkeit die totale Sendeenergie T minimiert werden, so ist die oben erläuterte Wahl der Repräsentanten für die Datensymbole $\underline{d}_n^{(k)}$, $n = 1 \ldots N$, $k = 1 \ldots K$, im allgemeinen nicht unabhängig und daher gemeinsam zu treffen. Unter der Nebenannahme, daß schädliche Interferenzen in den wertekontinuierlichen Schätzungen $\widehat{\underline{d}}_n^{(k)}$ aller Datensymbole $\underline{d}_n^{(k)}$, $n = 1 \ldots N$, $k = 1 \ldots K$, vollständig vermieden werden sollen, wird in [PHS03] für unkonventionelle, auf dem speziellen Latticequantisierungsschema beruhende Empfänger ein Verfahren zur Erzeugung des totalen Sendesignals $\underline{\mathbf{t}}$ vorgeschlagen. Dieses Verfahren erzielt unter der genannten Nebenbedingung bei Einhaltung einer gegebenen Übertragungsfehlerwahrscheinlichkeit eine minimale totale Sendeenergie T und ist daher im Kontext der angesprochenen Nebenbedingung im hier betrachteten Sinne optimal. Nachteilig ist jedoch, daß das gemeinsame Wählen der optimalen Repräsentanten für alle Datensymbole $\underline{d}_n^{(k)}$, $n = 1 \ldots N$, $k = 1 \ldots K$, sehr aufwendig ist und im allgemeinen nur über eine erschöpfende Suche (engl. exhaustive search) erfolgen kann. In [MWQ04b] wird dieses Verfahren der gemeinsamen Sendesignalerzeugung auf den Fall allgemeiner unkonventioneller Empfänger erweitert, und darüber hinaus werden aufwandsgünstige suboptimale Approximationen des Verfahrens vorgeschlagen. In beiden Vorschlägen [PHS03] und [MWQ04b] wird von der Nebenbedingung der Interferenzfreiheit ausgegangen. Ein Verfahren der gemeinsamen Sendesignalerzeugung für unkonventionelle Empfänger, das ohne diese Nebenbedingung die Übertragungsfehlerwahrscheinlichkeit für eine gegebene totale Sendeenergie T minimiert oder, äquivalent, für eine gegebene nicht zu überschreitende Übertragungsfehlerwahrscheinlichkeit die totale Sendeenergie T minimiert, ist nach Kenntnis des Autors der vorliegenden Schrift bisher nicht bekannt und Thema weiterer Forschungsaktivitäten. Aus diesem Grund werden im Rahmen dieser Schrift die oben genannten Verfahren der gemeinsamen Sendesignalerzeugung nach [PHS03] und [MWQ04b] als optimale Verfahren bezeichnet, da diese im Kontext der erwähnten Nebenbedingung optimal sind. Kapitel 4 befaßt sich im Detail mit diesen optimalen Verfahren der gemeinsamen Sendesignalerzeugung für unkonventionelle Empfänger.

In Tabelle 1.4 sind ausgewählte wichtige Veröffentlichungen zum Themenkomplex der gemeinsamen Sendesignalerzeugung nach Kategorien gegliedert aufgelistet. In der vorliegenden Schrift werden die relevanten, aus der Literatur bekannten Verfahren der gemeinsamen Sendesignalerzeugung rekapituliert, systematisiert und neuartige Verfahren vorgeschlagen, die die Vielfalt der verfügbaren Verfahren komplettieren. Bei den vorgeschlagenen Verfahren handelt es sich um Ergebnisse von Arbeiten an der Technischen Universität Kaiserslautern, die im Rahmen verschiedener Drittmittelprojekte sowohl mit Auftraggebern aus der Industrie, bei der Europäischen Union und bei der Deutschen Forschungsgemeinschaft, im Rahmen internationaler Kooperationen im Bereich COST (Cooperation on the Field of Science and Technology) und dem EU-Projekt FLOWS (Flexible Convergence of Wireless Standards and Services) und im Rahmen von Promotionsvorhaben, die unter Mitbetreuung durch den Verfasser durchgeführt wurden, entstanden sind.

1.5 Ziele der Schrift und Inhaltsübersicht

Trotz oder vielleicht auch gerade wegen der Vielzahl der in jüngster Vergangenheit entstandenen Arbeiten zur Empfängerorientierung fehlt heute ein Überblick über die im Zusammenhang mit Empfängerorientierung zu klärenden Fragestellungen, die zugehörigen prinzipiellen Lösungansätze, deren grundsätzlichen Stärken und Schwächen sowie die prinzipiellen Anwendungsmöglichkeiten. Bisher ist in der Literatur nicht einmal eine klare Herausarbeitung der gemeinsamen Basis „Empfängerorientung“, die allen angesprochenen Arbeiten zugrunde liegt, vorhanden. Dies ist eine angesichts der großen wirtschaftlichen Bedeutung von Performanzsteigerung und Endgeräteverbesserung im Mobilfunk eine unbefriedigende Situation, da eine direkte Einschätzung der durch Empfängerorientierung erzielbaren Verbesserungen und eine bestmögliche Mobilfunksystemauslegung so nicht möglich ist. Die vorliegende Schrift will hier Abhilfe schaffen. Hierzu ist das aus der Literatur bekannte Wissen über Empfängerorientierung zusammenzutragen, durch neue Ideen zu ergänzen, zu vervollständigen und zu systematisieren, im allgemeinen darzustellen und durch geeignete Methoden zu bewerten. Im einzelnen müssen folgende Aspekte geklärt werden:

- Das Grundprinzip der Empfängerorientierung muß herausgearbeitet werden und vom klassischen Grundprinzip der Senderorientierung abgegrenzt werden.
- Die bei der A-priori-Wahl der Empfänger geltenden relevanten Prinzipien sind zu betrachten und zu systematisieren.
- Das Repertoire der zur gemeinsamen Sendesignalerzeugung eingesetzten Verfahren ist durch ein Literaturstudium zu erarbeiten, durch neuartige Vorschläge zu ergänzen, zu strukturieren und systematisieren, um somit eine Übersicht über die verfügbare Vielfalt zu erlangen.
- Die Prinzipien der im Rahmen der gemeinsamen Sendesignalerzeugung verfügbaren Vorgehensweisen müssen herausgearbeitet werden und Verwandtschaftsbeziehungen zwischen verschiedenen Verfahren der gemeinsamen Sendesignalerzeugung aufgezeigt werden.
- Die Leistungsfähigkeiten der verschiedenen relevanten Verfahren der gemeinsamen Sendesignalerzeugung sind zu bewerten und zu vergleichen.
- Essentielle Voraussetzungen von Empfängerorientierung, wie beispielsweise die Verfügbarkeit und notwendige Güte senderseitiger Kanalzustandsinformation, sind im Grundsätzlichen zu beleuchten.
- Der durch Empfängerorientierung im Vergleich zur klassischen Senderorientierung erzielbare Nutzeffekt ist abzuschätzen, und das Potential von Empfängerorientierung im Mobilfunk ist zu bewerten.
- Mögliche Wege der Weiterentwicklung des Grundprinzips der Empfängerorientierung sind aufzuzeigen.

Wie bereits in Unterkapitel 1.4 klar wurde, besteht die Hauptaufgabe im Bereich der Empfängerorientierung im Finden geeigneter Verfahren der gemeinsamen Sendesignalerzeugung. Naturgemäß liegt daher der Schwerpunkt dieser Schrift bei der Vorstellung, Entwicklung und systematischen Analyse derartiger Verfahren.

Um den Fokus der Arbeit auf das Wesentliche zu beschränken, sollen bei den durchzuführenden Arbeiten einige Nebenbedingungen gelten:

- Die aktiven Empfänger, das heißt Mobilstationen, und deren Ausgestaltung, das heißt die Empfangssignalverarbeitung, sind dem Sender der Basisstation perfekt bekannt.
- Die zeitliche Synchronisierung des Senders der Basisstation und der Empfänger der Mobilstationen ist perfekt.
- Der Abgleich der vom Sender der Basisstation und den Empfängern der Mobilstationen verwendeten Trägerfrequenzen ist perfekt.
- Nichtlineare Störeffekte durch zur Realisierung eingesetzte nichtlineare Komponenten wie beispielsweise nichtlineare Verstärker, Analog-Digital-Wandler [Naß95, MR00, Meu00] oder infolge begrenzter Rechengenauigkeiten [Sch99, ID96] werden nicht berücksichtigt.

Um den Einsatz von empfängerorientierter Funkkommunikation in der Praxis zu ermöglichen, ist die Klärung derartiger Aspekte von großer Wichtigkeit. Derartige Aspekte betreffen jedoch nicht das Grundprinzip der Empfängerorientierung als solches. Es ist jedoch vorrangiges Ziel dieser Schrift, die grundsätzliche Herangehensweise Empfängerorientierung zu beleuchten und die sich im Grundsätzlichen bietenden Möglichkeiten aufzuzeigen und zu systematisieren. Daher wird an dieser Stelle darauf verzichtet, genauer auf oben genannte Aspekte einzugehen. In der Literatur sind bereits einige Arbeiten zu derartigen Aspekten verfügbar. Der interessierte Leser sei daher zur Klärung der obigen Fragen beispielsweise auf [KM00, FTH01, Fis02, HvHJ+02, TWL+02, Trö03] verwiesen.

Nachdem in diesem Kapitel 1 bereits die Grundzüge der Empfängerorientierung, der Empfängergestaltung sowie eine Klassifizierung der relevanten Verfahren der gemeinsamen Sendesignalerzeugung vorgestellt wurde, wird zunächst in Kapitel 2 auf die gemeinsame Sendesignalerzeugung für konventionelle Empfänger eingegangen. Dabei wird klar, daß zur optimalen Auslegung empfängerorientierter Funkkommunikation die Minimierung der Übertragungsfehlerwahrscheinlichkeit bei gegebener totaler Sendeenergie T nach (1.30) angestrebt werden sollte. Infolge der Natur des Problems der gemeinsamen Sendesignalerzeugung ist dabei jedoch stets ein Kompromiß zwischen den Übertragungsqualitäten aller zu übertragenden Datensymbole einzugehen, so daß exemplarisch über alle Datensymbole $\underline{d}_n^{(k)}$, $n = 1 \ldots N$, $k = 1 \ldots K$, gemittelte Übertragungsfehlerwahrscheinlichkeit betrachtet werden. Für das Entwurfsziel minimaler mittlere Bitfehlerwahrscheinlichkeit wird gezeigt, wie das totale Sendesignal $\underline{\mathbf{t}}$ bei gegebenen konventionellen Empfängern zu gestalten ist und welche Leistungsfähigkeit das vorgestellte optimale Verfahren im Vergleich mit aufwandsgünstigen suboptimalen Verfahren der gemeinsamen Sendesignalerzeugung zeigt. Darüber hinaus wird die Leistungsfähigkeit einer auf dem vorgestellten optimalen Verfahren beruhenden empfängerorientierten Funkkommunikation und klassischer senderorientierter Funkkommunikation verglichen.

Da das in Kapitel 2 behandelte optimale Verfahren der gemeinsamen Sendesignalerzeugung sehr aufwendig ist, wird in Kapitel 3 auf aufwandsgünstige suboptimale lineare Verfahren der gemeinsamen Sendesignalerzeugung für konventionelle Empfängern eingegangen. Diese Verfahren lassen sich durch eine lineare senderseitige Signalverarbeitung beschreiben. Aus diesem Grund wird zuerst basierend auf dem allgemeinen Systemmodell nach Abschnitt 1.1.2 ein vereinfachtes lineares Systemmodell hergeleitet. Basierend auf dem vereinfachten linearen Systemmodell läßt sich das SNIR der wertekontinuierlichen Schätzungen $\widehat{\underline{d}}_n^{(k)}$ der Datensymbole $\underline{d}_n^{(k)}$, $n = 1 \ldots N$, $k = 1 \ldots K$, mathematisch erfassen, aus dem sich die Verfahren der gemeinsamen Sendesignalerzeugung TxMF, TxZF, TxMMSE herleiten lassen. Dabei werden Dualitäten zwischen den im Kontext von Empfängerorientierung entworfenen Verfahren der gemeinsamen Sendesignalerzeugung TxMF, TxZF und TxMMSE und den aus dem Kontext von Senderorientierung bekannten dualen Verfahren der gemeinsamen Empfangssignalverarbeitung RxMF, RxZF und RxMMSE aufgezeigt. Darüber hinaus wird die Leistungsfähigkeit der verschiedenen Verfahrensausprägungen für die beiden Herangehensweisen Empfängerorientierung und Senderorientierung verglichen. Zum gerechten Bewerten der Leistungsfähigkeit der linearen Verfahren zur gemeinsamen Sendesignalerzeugung, werden die Gütemaße SNR-Degradation, Sendungseffizienz (engl. transmission efficiency) und Sendeeffizienz (engl. transmit efficiency) sowie die für eine einzuhaltende Übertragungsqualität benötigte totale Sendeenergie T analytisch beziehungsweise simulativ betrachtet. Die Analyse ergibt, daß die Leistungsfähigkeit der linearen Verfahren der Sendesignalerzeugung, beispielsweise die Sendeeffizienz und die totale Sendeenergie T, vorrangig durch die Systemlast innerhalb der betrachteten Referenzzelle bestimmt werden.

Kapitel 4 befaßt sich mit dem optimalen Verfahren der gemeinsamen Sendesignalerzeugung für unkonventionelle Empfänger, das als optimale senderseitige nichtlineare Interferenzeliminierung (engl. optimum transmit nonlinear zero forcing, opt. TxNZF) bezeichnet wird. Ausgehend von den Verfahren der gemeinsamen Sendesignalerzeugung für konventionelle Empfänger wird verdeutlicht, infolge welcher Grundprinzipien die Leistungsfähigkeit von Empfängerorientierung durch den Einsatz unkonventioneller Empfänger gesteigert werden kann. Für den allgemeinen Fall eines empfängerseitig eingesetzten allgemeinen unkonventionellen Quantisierungsschemas wird gezeigt, wie die gemeinsame Sendesignalerzeugung in einer hinsichtlich der Übertragungsqualität optimalen Art und Weise zu erfolgen hat. Da dieses Verfahren im allgemeinen sehr aufwendig ist, wird eine auf Gruppenbildung und gruppenweisem Sendesignalerzeugen basierende Approximation des optimalen Verfahrens der gemeinsamen Sendesignalerzeugung für unkonventionelle Empfängern vorgeschlagen. Die dabei gegenüber Verfahren der gemeinsamen Sendesignalerzeugung für konventionelle Empfänger erzielbaren Gewinne werden sowohl analytisch abgeschätzt wie auch durch detaillierte Simulationen beurteilt. Es zeigt sich, daß das (approximative) optimale Verfahren der gemeinsamen Sendesignalerzeugung für unkonventionelle Empfängern insbesondere in Mobilfunkszenarien mit mehreren Mobilstationen, die Mobilfunkkanäle erheblich unterschiedlicher Kanaldämpfungen haben, große Vorteile hinsichtlich der erzielbaren Leistungsfähigkeit gegenüber Verfahren der gemeinsamen Sendesignalerzeugung für konventionelle Empfänger zeigt.

Da das optimale Verfahren nach Kapitel 4 im allgemeinen sehr aufwendig ist, beschäftigt sich Kapitel 5 mit aufwandsgünstigen suboptimalen Verfahren der gemeinsamen Sendesignalerzeugung bei unkonventionellen Empfängern. Dazu wird das auf Gruppenbildung aufbauende iterative Verfahren TxNZF vorgestellt, das auch die aus der Literatur bekannten Verfahren THP und MIMO-THP [FWLH02b, FWLH02a, FWLH02c, FW03, HSB03, WVF03b, BHMW04, JBU04, Joh04, Win04] als Spezialfälle einschließt. Basierend auf exemplarischen Szenarien wird die Leistungsfähigkeit dieses suboptimalen aufwandsgünstigen Verfahrens der gemeinsamen Sendesignalerzeugung für unkonventionelle Empfänger analytisch und durch Simulationen abgeschätzt. Eine wesentliche Motivation des Verfahrens TxNZF ist die Reduktion der senderseitigen Implementierungskomplexität. Daher wird für das Verfahren TxNZF gezeigt, wie dieses auf Basis des mathematischen, aus der linearen Algebra entstammenden Kunstgriffes der QR-Zerlegung aufwandsgünstig implementiert werden kann.

Alle im Rahmen dieser Schrift betrachteten Verfahren der gemeinsamen Sendesignalerzeugung basieren auf dem senderseitigen Vorliegen von Kanalzustandsinformation (engl. transmitted sided channel state information, TxCSI). Kapitel 6 beschäftigt sich daher mit dem zur Verfügung Stellen dieser Information. Es wird gezeigt, daß im Falle von Mobilfunksystemen mit Zeitmultiplex infolge von Kanalreziprozität unter gewissen Nebenbedingungen die zur gemeinsamen Sendesignalerzeugung in der Abwärtsstrecke benötigte Kanalzustandsinformation durch Schätzen in der Aufwärtsstrecke verfügbar gemacht werden kann. Ist dies beispielsweise infolge fehlender Kanalreziprozität nicht möglich, so muß diese Kanalzustandsinformation an den Empfängern, das heißt den Mobilstationen, ermittelt und dem Sender, das heißt der Basisstation, durch Rücksignalisieren verfügbar gemacht werden. Wie dieses Rücksignalisieren aufwandsgünstig gelingen kann, das heißt mit möglichst geringem Rücksignalisiervolumen, wird in Kapitel 6 dargestellt und bewertet. Bei beiden

Vorgehensweisen des Bereitstellens von Kanalzustandsinformation sind die Zeitpunkte des Erfassens der Kanalzustandsinformation und des Nutzens dieser Information zum gemeinsamen Sendesignalerzeugen typischerweise nicht gleich. Bei zeitvarianten Mobilfunkkanälen ist daher ein Verwenden von mehr oder weniger veralteter Kanalzustandsinformation zur gemeinsamen Sendesignalerzeugung nicht vermeidbar. Daher werden im Rahmen des Kapitels 6 die zu erwartenden, in guter Näherung zufälligen Fehler in der Kanalzustandsinformation in Form von mittleren quadratischen Fehlern der Elemente der Kanalmatrix $\underline{\mathbf{H}}$ beschrieben sowie die Auswirkungen dieser Fehler auf die durch Empfängerorientierung erzielbare Übertragungsqualität, beispielsweise die Übertragungsfehlerwahrscheinlichkeit, analytisch und simulativ bewertet.

Kapitel 7 betrachtet mögliche Weiterentwicklungen des Grundkonzepts der Empfängerorientierung. Als wesentliches Grundproblem der Empfängerorientierung wird dabei identifiziert, daß aufgrund fehlender Kanalzustandsinformation an den Empfängern ein Adaptieren der Empfänger an die sich bietenden zeitlichen und räumlichen Eigenschaften der wirksamen relevanten Mobilfunkkanäle nicht möglich ist. Daher ist es denkbar, daß die empfängerseitige mobilfunkkanalunabhängige Signalverarbeitung ausschließlich solche Komponenten des totalen Empfangssignals $\underline{\mathbf{r}}$ auswertet, die, je nach Mobilfunkkanal, senderseitig nur schwer, das heißt mit großer totaler Sendeenergie T oder gar nicht beeinflußt werden können. Um dieses zu umgehen, wird in Kapitel 7 vorgeschlagen, die Leistungsfähigkeit der Funkkommunikation durch Nutzen von Kanalzustandsinformation auch an den Empfängern zu steigern. Das Grundkonzept der Empfängerorientierung wandelt sich demzufolge in ein neuartiges Grundkonzept, das als Kanalorientierung [BQT+03, BZT+03] bezeichnet werden kann. Es werden Vorschläge unterbreitet, wie das empfängerseitige Einbeziehen von Kanalzustandsinformation erfolgten kann, und es wird aufgezeigt, welche Steigerungen der Leistungsfähigkeit der Funkkommunikation möglich sind. Besteht die Möglichkeit der freien zeitlichen Organisation der Informationsübertragung der Basisstation an die Mobilstationen, so können weitere Erhöhungen der Leistungsfähigkeit der empfängerorientierten Funkkommunikation durch ein Anpassen dieser zeitlichen Organisation an die zeitlich wechselnden Eigenschaften der relevanten wirksamen Mobilfunkkanäle erzielt werden. Diese Vorgehensweise, die als opportunistisches Übertragen bezeichnet wird, läßt sich unmittelbar mit Empfängerorientierung kombinieren.

Kapitel 8 bringt schließlich eine bewertende Zusammenfassung in deutscher und englischer Sprache.

Kapitel 2

Optimale nichtlineare Verfahren der gemeinsamen Sendesignalerzeugung bei konventionellen Empfängern

Dieses Kapitel 2 befaßt sich mit optimalen Verfahren der gemeinsamen Sendesignalerzeugung für konventionelle Empfänger. Entsprechend den in Kapitel 1 dargelegten Zielen beim Entwurf eines zellularen Mobilfunksystems, ist eine bestmögliche Qualität der Informationsübertragung zwischen Basisstationen und Mobilstationen dann gegeben, wenn die Wahrscheinlichkeit eines Übertragungsfehlers bei gegebener totaler Sendeenergie T nach (1.30) minimal wird. Unter einem Übertragungsfehler versteht man dabei, die fehlerhafte Übertragung eines Datums $u_l^{(k)}$, $l = 1 \dots L$, $k = 1 \dots K$, nach (1.1), eines Datensymbols $\underline{d}_n^{(k)}$, $n = 1 \dots N$, $k = 1 \dots K$, nach (1.11) oder des totalen Datenvektors $\underline{\mathbf{d}}$ nach (1.12). Wie in Unterkapitel 1.4 bereits angesprochen, ist es im Bereich der Empfängerorientierung infolge der Natur des Problems der gemeinsamen Sendesignalerzeugung nicht möglich, durch geeignetes Erzeugen eines totalen Sendesignals $\underline{\mathbf{t}}$ gegebener totaler Sendeenergie T die Wahrscheinlichkeit eines Übertragungsfehlers individuell für sämtliche Daten $u_l^{(k)}$, $l = 1 \dots L$, $k = 1 \dots K$, nach (1.1) beziehungsweise sämtliche Datensymbole $\underline{d}_n^{(k)}$, $n = 1 \dots N$, $k = 1 \dots K$, nach (1.11) zu minimieren. Soll nämlich für ein Datum $u_l^{(k)}$, $l = 1 \dots L$, $k = 1 \dots K$, beziehungsweise ein Datensymbol $\underline{d}_n^{(k)}$, $n = 1 \dots N$, $k = 1 \dots K$, nach (1.11) die Übertragungsfehlerwahrscheinlichkeit unter den obigen Voraussetzungen minimiert werden, so ist dies nur durch Einsetzen der gesamten totalen Sendeenergie T zur Übertragung des jeweiligen Datums beziehungsweise Datensymbols möglich. Andere Daten $u_{l'}^{(k')}$, $l' = 1 \dots L$, $k' = 1 \dots K$, $l \neq l' \vee k \neq k'$, beziehungsweise Datensymbole $\underline{d}_{n'}^{(k')}$, $n' = 1 \dots N$, $k' = 1 \dots K$, $n \neq n' \vee k \neq k'$, werden dann nicht mehr übertragen. Dieses Vorgehen ist zwar optimal im obigen Sinne, jedoch für Mobilfunksysteme ist diese Vorgehensweise im Hinblick auf die Qualität des gesamten Systems unzulänglich. Die geschilderte Situation unterscheidet sich erheblich von der Situation, die sich typischerweise im Bereich der senderorientierten Funkkommunikation stellt. Im Falle von Senderorientierung ist es nämlich prinzipiell stets möglich, durch individuelles Empfangssignalverarbeiten für jedes Datum $u_l^{(k)}$, $l = 1 \dots L$, $k = 1 \dots K$, beziehungsweise jedes Datensymbol $\underline{d}_n^{(k)}$, $n = 1 \dots N$, $k = 1 \dots K$, nach (1.11) eines Schätzung $\widehat{u}_l^{(k)}$ beziehungsweise $\widehat{\underline{d}}_n^{(k)}$ zu ermitteln, die die obige Übertragungsfehlerwahrscheinlichkeit minimiert. Als Konsequenz dieser Gegebenheiten werden in diesem Kapitel exemplarisch über alle Datensymbole $\underline{d}_n^{(k)}$, $n = 1 \dots N$, $k = 1 \dots K$, gemittelte Übertragungsfehlerwahrscheinlichkeiten von

Tabelle 2.1. Wesentliche Unterschiede der Notationen nach Tabelle 1.2 und der Notation nach [WM03d]

dargestellte Größe	Formelzeichen nach Tab. 1.2	Formelzeichen nach [WM03d]
totales Empfangssignal	$\underline{\mathbf{r}}$	$\underline{\mathbf{e}}$
totales Sendesignal	$\underline{\mathbf{t}}$	$\underline{\mathbf{s}}$

Datensymbolen betrachtet werden. Für das Entwurfsziel minimaler mittlere Datensymbolfehlerwahrscheinlichkeit bei gegebener totaler Sendeenergie T wird im Rahmen der folgenden Veröffentlichung [WM03d] gezeigt,

- wie das totale Sendesignal $\underline{\mathbf{t}}$ bei gegebenen konventionellen Empfängern zu gestalten ist,
- welche Leistungsfähigkeit das vorgeschlagene optimale Verfahren der gemeinsamen Sendesignalerzeugung im Vergleich mit den in Unterkapitel 1.4 übersichtsartig dargelegten und in Kapitel 3.2 detailliert behandelten suboptimalen aufwandsgünstigen Verfahren der gemeinsamen Sendesignalerzeugung zeigt und
- welche Unterschiede sich hinsichtlich der erzielbaren Übertragungsqualität ergeben zwischen dem vorgeschlagenen optimalen empfängerorientierten und dem aus der Literatur [Ver98] bekannten optimalen senderorientierten Vorgehen.

Im Gegensatz zu dem aus Tabelle 1.2 bekannten Systemmodell werden in [WM03d] einige wenige Größen durch eine modifizierte Notation beschrieben. Tabelle 2.1 listet die wesentlichen Unterschiede in kompakter Form auf.

[WM03d] Weber, T.; Meurer, M.: "Optimum joint transmission: Potentials and dualities". *Proc. 6th International Symposium on Wireless Personal Multimedia Communications (WPMC'03)*, Bd. 1, Yokosuka, 2003, S. 79–83.

Optimum Joint Transmission: Potentials and Dualities

Tobias Weber, Michael Meurer
Research Group for RF Communications, University of Kaiserslautern,
D–67653 Kaiserslautern, Germany, email: tweber@rhrk.uni-kl.de

Abstract

Recently, receiver oriented signal processing techniques for multiple access interference reduction by joint transmission in the downlink of mobile radio systems attained great interest. Up to now investigations focused on linear joint transmission, first investigations of nonlinear joint transmission and capacity calculations based on dirty paper precoding. A major advantage of linear joint transmission over dirty paper precoding based techniques is that conventional simple receivers designed for single user systems can be employed. Unfortunately, the performance of linear joint transmission suffers from the fact that the discreteness of the data symbols to be transmitted can not be exploited for interference reduction. In the present paper novel nonlinear joint transmission techniques which exploit the knowledge of the a-priori given nonlinear receivers and thus combine the advantages of linear joint transmission with the improved performance of nonlinear techniques are investigated. It is shown that, in contrast to linear joint transmission which is dual to linear joint detection, nonlinear joint transmission exploiting the knowledge of the modulation alphabet is not dual to nonlinear optimum joint detection. Depending on the performance criterion, nonlinear joint transmission allows significant performance improvements over linear joint transmission.

1 Introduction

A particularly favorable configuration for multiple access interference reduction in mobile radio systems, which results in low complexity mobile terminals (MTs), is the application of joint detection (JD) in uplink (UL) transmission and joint transmission (JT) in downlink (DL) transmission. The basic idea of JD is to jointly estimate the data transmitted by the different MTs in the central unit (CU) [14]. For doing so, channel knowledge is assumed, which can be obtained, e.g., by joint channel estimation in the UL [11]. Both suboptimum linear and optimum nonlinear signal processing techniques for JD [14] and theoretical capacity bounds [2] are well known. The basic idea of joint transmission (JT) is to design the transmit signal in such a way that the interferences in the received signals are a-priori avoided [8]. For doing so channel knowledge, which can be obtained by channel estimation in the UL if time division duplexing is used, is exploited in the transmitter. Up to now investigations focused on linear JT [8, 4, 5, 6], nonlinear transmission schemes including receiver modifications [16, 3] and theoretical capacity investigations [1, 16]. A still open question, for which a first answer is given in the present paper, is how the discreteness of the modulation alphabet can be exploited for improving the performance of JT in practice.

In the following a mobile radio system without spreading where each MT is equipped with a single antenna and the CU has multiple antennas, is considered. In order to enable multiple access interference reduction by linear transmission techniques, the number of antennas at the CU must be at least as large as the number of MTs. The radio channel between the antennas of the CU and the entirety of all antennas of the MTs constitutes a MIMO channel. In the following for simplicity only flat fading MIMO channels will be considered. An exemplary mobile radio system concept which fulfills the above made assumptions is the JOINT concept for beyond 3G mobile radio systems presented in [15]. The time discrete equivalent lowpass representation of signals is chosen [9]. Consequently, signals are represented by vectors or matrices, which are printed in boldface. In the present paper $[\cdot]_{k,k}$ denotes the k-th diagonal element of a matrix

2 Data transmission model

The data symbol to be transmitted for user $k \in \{1 \ldots K\}$ is denoted by $\underline{d}^{(k)}$. For simplicity it is assumed that the data symbols are BPSK modulated in the following:

$$\underline{d}^{(k)} \in \{-1, +1\}\,,\; k = 1 \ldots K. \tag{1}$$

All K data symbols of the different users are compiled in the data vector

$$\underline{\mathbf{d}} = \left(\underline{d}^{(1)} \ldots \underline{d}^{(k)}\right)^{\mathrm{T}}. \tag{2}$$

On the transmitter side transmit signals for K_{I} inputs to the mobile radio channel are generated. The transmit signal for input k_{I}, which corresponds to transmit antenna k_{I}, is characterized by the complex value $\underline{s}^{(k_{\mathrm{I}})}$, which may be thought of as a sample of the signal in the equivalent lowpass domain or a complex amplitude. From all K_{I} transmit signals the transmit vector

$$\underline{\mathbf{s}} = \left(\underline{s}^{(1)} \ldots \underline{s}^{(K_{\mathrm{I}})}\right)^{\mathrm{T}} \tag{3}$$

is formed. In the UL case

$$K_{\mathrm{I}} = K \tag{4}$$

holds and the element $\underline{s}^{(k)}$ of the transmit vector $\underline{\mathbf{s}}$, which is the transmit signal of MT k, can only depend on the corresponding data symbol $\underline{d}^{(k)}$ due to the spatial separation of the MTs. In the DL case in general the elements $\underline{s}^{(k_{\mathrm{I}})}$, $k_{\mathrm{I}} = 1 \ldots K_{\mathrm{I}}$, of the transmit vector $\underline{\mathbf{s}}$ are generated depending on all data symbols $\underline{d}^{(k)}$, $k = 1 \ldots K$, of the data vector $\underline{\mathbf{d}}$ in the CU.

The receive signal of output k_{O}, which corresponds to receive antenna k_{O}, is also characterized by a complex value $\underline{e}^{(k_{\mathrm{O}})}$. From all K_{O} received signals the receive vector

$$\underline{\mathbf{e}} = \left(\underline{e}^{(1)} \ldots \underline{e}^{(k_{\mathrm{O}})}\right)^{\mathrm{T}} \tag{5}$$

is formed. In the DL case

$$K_{\mathrm{O}} = K \tag{6}$$

holds.

The receive signals $\underline{e}^{(k_0)}$, $k_\mathrm{O} = 1 \ldots K_\mathrm{O}$, are linear functions of the transmit signals $\underline{s}^{(k_\mathrm{I})}$, $1 \ldots K_\mathrm{I}$, plus some noise $\underline{n}^{(k_\mathrm{O})}$, $k_\mathrm{O} = 1 \ldots K_\mathrm{O}$. With the channel matrix

$$\underline{\mathbf{H}} = \begin{pmatrix} \underline{H}^{(1,1)} & \ldots & \underline{H}^{(1,K_\mathrm{I})} \\ \vdots & & \vdots \\ \underline{H}^{(K_\mathrm{O},1)} & \ldots & \underline{H}^{(K_\mathrm{O},K_\mathrm{I})} \end{pmatrix} \tag{7}$$

describing the linear MIMO channel and the noise vector

$$\underline{\mathbf{n}} = \left(\underline{n}^{(1)} \ldots \underline{n}^{(K_\mathrm{O})}\right)^\mathrm{T} \tag{8}$$

follows

$$\underline{\mathbf{e}} = \underline{\mathbf{H}} \cdot \underline{\mathbf{s}} + \underline{\mathbf{n}}. \tag{9}$$

The element $\underline{H}^{(k_\mathrm{O},k_\mathrm{I})}$ of the channel matrix $\underline{\mathbf{H}}$ is the channel coefficient characterizing the the channel from input k_I to output k_O. For the considered reciprocal channels the channel matrix $\underline{\mathbf{H}}_\mathrm{DL}$ in the DL case is the transpose of the channel matrix $\underline{\mathbf{H}}_\mathrm{UL}$ in the UL case, i.e.,

$$\underline{\mathbf{H}}_\mathrm{UL} = \underline{\mathbf{H}}_\mathrm{DL}^\mathrm{T} \tag{10}$$

holds.

For simplicity it is assumed in the following, that the elements $\underline{n}^{(k_\mathrm{O})}$, $k_\mathrm{O} = 1 \ldots K_\mathrm{O}$, of the noise vector $\underline{\mathbf{n}}$ are uncorrelated, gaussian distributed with variance σ^2 of real and imaginary part [9].

On the receiver side, estimates $\hat{\underline{d}}^{(k)}$ of the transmitted data symbols $\underline{d}^{(k)}$, $k = 1 \ldots K$, are obtained. All K estimated data symbols are compiled in the estimated data vector

$$\hat{\underline{\mathbf{d}}} = \left(\hat{\underline{d}}^{(1)} \ldots \hat{\underline{d}}^{(K)}\right)^\mathrm{T}. \tag{11}$$

In the UL case the complete receive vector $\underline{\mathbf{e}}$ is available for estimating the data vector $\underline{\mathbf{d}}$ in the CU whereas in the DL case the estimate $\hat{\underline{d}}^{(k)}$ has to be determined from the corresponding receive signal $\underline{e}^{(k)}$ of MT k alone due to the spatial separation of the MTs.

3 Linear data transmission

3.1 Generalized linear data transmission in UL and DL

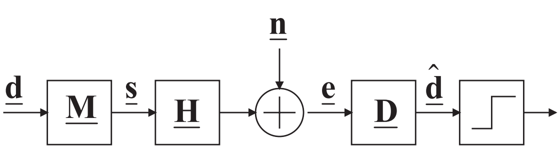

Figure 1: Generalized linear data transmission system

In the case of linear data transmission the transmit vector $\underline{\mathbf{s}}$ is a linear function of the data vector $\underline{\mathbf{d}}$ to be transmitted and the estimate $\hat{\underline{\mathbf{d}}}$ is a linear function of the receive vector $\underline{\mathbf{e}}$, see Fig. 1. The linear function of the transmitter can be described by a modulator matrix $\underline{\mathbf{M}}$, i.e.,

$$\underline{\mathbf{s}} = \underline{\mathbf{M}} \cdot \underline{\mathbf{d}} \tag{12}$$

holds. In the UL case there is the restriction that this modulator matrix has to be a diagonal matrix due to the spatial separation of the MTs.

The linear function of the receiver can be described by a demodulator matrix $\underline{\mathbf{D}}$, i.e.,

$$\hat{\underline{\mathbf{d}}} = \underline{\mathbf{D}} \cdot \underline{\mathbf{e}} \tag{13}$$

holds. In the DL case the demodulator matrix $\underline{\mathbf{D}}$ has to be a diagonal matrix due to the spatial separation of the MTs. In the following only linear transmission schemes which provide unbiased, i.e., interference free estimates $\hat{\underline{\mathbf{d}}}$ will be considered. With the $K \times K$ identity matrix $\mathbf{I}$,

$$\underline{\mathbf{D}} \cdot \underline{\mathbf{H}} \cdot \underline{\mathbf{M}} = \mathbf{I} \tag{14}$$

must hold in order to obtain unbiased estimates $\hat{\underline{\mathbf{d}}}$.

In the considered case of digital transmission, see (1), the data symbols $\underline{d}^{(k)}$, $k = 1 \ldots K$, are from a discrete valued modulation alphabet and the estimates $\hat{\underline{d}}^{(k)}$ are quantized in a following step.

As a prerequisite for studying the performance of linear data transmission the optimum system for the transmission of a single data symbol over the given MIMO channel characterized by the channel matrix $\underline{\mathbf{H}}$ without any restrictions going beyond (14) for the modulator matrix $\underline{\mathbf{M}}$ and the demodulator matrix $\underline{\mathbf{D}}$ is studied. In this single symbol case the transmit vector $\underline{\mathbf{s}}$ should correspond to the eigenvector belonging to the maximum eigenvalue of $\underline{\mathbf{H}}^{*\mathrm{T}}\underline{\mathbf{H}}$, which is also known as the spectral radius $\rho\left(\underline{\mathbf{H}}^{*\mathrm{T}}\underline{\mathbf{H}}\right)$, in order to obtain the maximum possible receive energy $E_\mathrm{b,opt}$ with given transmit energy

$$T = \frac{1}{2}\underline{\mathbf{s}}^{*\mathrm{T}}\underline{\mathbf{s}}. \tag{15}$$

For the receive energy

$$E_\mathrm{b,opt} = T \cdot \rho\left(\underline{\mathbf{H}}^{*\mathrm{T}}\underline{\mathbf{H}}\right) \tag{16}$$

folows. For the bit error probability of this optimum reference system

$$P_\mathrm{b,opt} = \frac{1}{2}\,\mathrm{erfc}\left(\sqrt{\frac{E_\mathrm{b,opt}}{\sigma^2}}\right) \tag{17}$$

is obtained [9].

The requirement to eliminate interferences in the multiuser system under consideration means

- that transmit energy can not be transformed as efficiently into receive energy as in the single symbol case and
- that not all the receive energy can be used.

The first point is obvious as the structure of the transmit signals of the different data symbols must be different, i.e., the optimum eigenvector of $\underline{\mathbf{H}}^{*\mathrm{T}}\underline{\mathbf{H}}$ can not be used for the transmission of all data symbols. The relative loss of receive energy as compared to the optimum single symbol case for given transmit energy T is described by the transmission efficiency [13]

$$\tau^{(k)} = \frac{\left[\underline{\mathbf{M}}^{*\mathrm{T}}\underline{\mathbf{H}}^{*\mathrm{T}}\underline{\mathbf{H}}\,\underline{\mathbf{M}}\right]_{k,k}}{\rho(\underline{\mathbf{H}}^{*\mathrm{T}}\underline{\mathbf{H}}) \cdot \left[\underline{\mathbf{M}}^{*\mathrm{T}}\underline{\mathbf{M}}\right]_{k,k}}, \tag{18}$$

which is smaller than one.

On the receiver side the parts of the received vector stemming from the transmission of different data symbols are in general not orthogonal. However, if interferences should be avoided only the orthogonal parts can be used by a linear receiver, i.e., only a part of the received energy, described by multiuser efficiency [14]

$$\eta^{(k)} = \frac{1}{\left[\underline{\mathbf{M}}^{*\mathrm{T}}\underline{\mathbf{H}}^{*\mathrm{T}}\underline{\mathbf{H}}\,\underline{\mathbf{M}}\right]_{k,k}\cdot\left[\underline{\mathbf{D}}\,\underline{\mathbf{D}}^{*\mathrm{T}}\right]_{k,k}}, \quad (19)$$

which is smaller than one, can be used.

The performance degradations described by the transmission efficiency $\tau^{(k)}$ and the multiuser efficiency $\eta(k)$ are also heavily influenced by the fact that not always all transmit signals $\underline{s}^{(k_\mathrm{I})}$, $k_\mathrm{I} = 1\ldots K_\mathrm{I}$, and receive signals $\underline{e}^{(k_\mathrm{O})}$, $k_\mathrm{O} = 1\ldots K_\mathrm{O}$, are available for the transmission of the considered data symbol $\underline{d}^{(k)}$ due to the spatial separation of the MTs.

Due to the energy losses $\tau^{(k)}$ and $\eta^{(k)}$ the bit error probability

$$\begin{aligned} P_\mathrm{b}^{(k)} &= \frac{1}{2}\,\mathrm{erfc}\left(\sqrt{\frac{E_\mathrm{b,opt}\tau^{(k)}\eta^{(k)}}{\sigma^2}}\right) \\ &= \frac{1}{2}\,\mathrm{erfc}\left(\sqrt{\frac{T}{\sigma^2\left[\underline{\mathbf{D}}\,\underline{\mathbf{D}}^{*\mathrm{T}}\right]_{k,k}\cdot\left[\underline{\mathbf{M}}^{*\mathrm{T}}\underline{\mathbf{M}}\right]_{k,k}}}\right) \quad (20) \end{aligned}$$

when estimating $\underline{d}^{(k)}$ in the multiuser case is larger than in the optimum single symbol case, see (17). Although the bit error probability $P_\mathrm{b}^{(k)}$ of (20) at first sight only depends on the modulator matrix $\underline{\mathbf{M}}$ and the demodulator matrix $\underline{\mathbf{D}}$, it also depends on the channel matrix $\underline{\mathbf{H}}$ due to the requirement (14).

3.2 Linear JD in the UL

The linear data estimator which maximizes the SNR of the estimates $\hat{\underline{d}}^{(k)}$, $k = 1\ldots K$, under the side condition that (14) is fulfilled is the zero-forcing-estimator [14, 7]. For the demodulator matrix

$$\underline{\mathbf{D}} = \left(\underline{\mathbf{M}}^{*\mathrm{T}}\underline{\mathbf{H}}_\mathrm{UL}^{*\mathrm{T}}\underline{\mathbf{H}}_\mathrm{UL}\,\underline{\mathbf{M}}\right)^{-1}\underline{\mathbf{M}}^{*\mathrm{T}}\underline{\mathbf{H}}_\mathrm{UL}^{*\mathrm{T}} \quad (21)$$

follows. If the same transmit energy T is used for all data symbols $\underline{d}^{(k)}$, $k = 1\ldots K$,

$$\underline{\mathbf{M}} = \sqrt{2T}\cdot\mathbf{I} \quad (22)$$

follows for the modulator matrix. It should be stressed that neither the modulator matrix $\underline{\mathbf{M}}$ nor the transmit energies are a function of the actual value of the data vector $\underline{\mathbf{d}}$ in the case of linear JD. With this the transmission efficiencies (18), multiuser efficiencies (19) and bit error probabilities (20) can be easily calculated. For the bit error probabilities

$$P_\mathrm{b}^{(k)} = \frac{1}{2}\,\mathrm{erfc}\left(\sqrt{\frac{T}{\sigma^2\left[\left(\underline{\mathbf{H}}_\mathrm{UL}^{*\mathrm{T}}\underline{\mathbf{H}}_\mathrm{UL}\right)^{-1}\right]_{k,k}}}\right),\ k = 1\ldots K, \quad (23)$$

is obtained.

3.3 Linear JT in the DL

The modulator matrix which fulfills (14) and simultaneously minimizes the transmit energies is obtained as [8, 6]

$$\underline{\mathbf{M}} = \underline{\mathbf{H}}_\mathrm{DL}^{*\mathrm{T}}\underline{\mathbf{D}}^{*\mathrm{T}}\left(\underline{\mathbf{D}}\,\underline{\mathbf{H}}_\mathrm{DL}\underline{\mathbf{H}}_\mathrm{DL}^{*\mathrm{T}}\underline{\mathbf{D}}^{*\mathrm{T}}\right)^{-1}. \quad (24)$$

The demodulator matrix $\underline{\mathbf{D}}$ must be a diagonal matrix due to the spatial separation of the MTs. For a fair comparison of JD and JT the same transmit energy T should be used for each data symbol $\underline{d}^{(k)}$, $k = 1\ldots K$, on the average. Mathematically this can be achieved by an appropriate scaling of the demodulator matrix

$$\underline{\mathbf{D}} = \sqrt{2T\cdot\mathrm{diag}\left(\left(\underline{\mathbf{H}}_\mathrm{DL}\underline{\mathbf{H}}_\mathrm{DL}^{*\mathrm{T}}\right)^{-1}\right)}. \quad (25)$$

It must be stressed that only the average transmit energies for all possible data vectors $\underline{\mathbf{d}}$ are fixed in the case of linear JT as the contributions to the transmit signal $\underline{\mathbf{s}}$ resulting from different data symbols $\underline{d}^{(k)}$ are correlated. With (25) the transmission efficiencies (18), multiuser efficiencies (19) and bit error probabilities (20) can be easily calculated. For the bit error probabilities

$$P_\mathrm{b}^{(k)} = \frac{1}{2}\mathrm{erfc}\left(\sqrt{\frac{T}{\sigma^2\left[\left(\underline{\mathbf{H}}_\mathrm{DL}\underline{\mathbf{H}}_\mathrm{DL}^{*\mathrm{T}}\right)^{-1}\right]_{k,k}}}\right),\ k = 1\ldots K, \quad (26)$$

is obtained. Taking into consideration that the DL channel matrix is the transpose of the UL channel matrix, see (10), this is the same result as obtained in (23) for linear JD, i.e., the performances of linear JD in the UL and linear JT in the DL are the same.

4 Optimum nonlinear data transmission

4.1 Maximum-likelihood-JD in the UL

Linear JD based on the zero-forcing-estimator, see (21), is suboptimum since the a priori knowledge of the discrete modulation alphabet (1) is not exploited when separating the signals from the different users. An optimum nonlinear data estimation which takes the knowledge of the modulation alphabet into consideration is the maximum-likelihood-vector-estimator [9, 14, 12] described by

$$\hat{\underline{\mathbf{d}}} = \underset{\underline{\mathbf{d}}\in\{-1,+1\}^K}{\arg\max}\left\{\mathrm{p}\left(\underline{\mathbf{e}}\middle|\,\underline{\mathbf{d}}\right)\right\}, \quad (27)$$

which in the case of white gaussian noise is equivalent to

$$\hat{\underline{\mathbf{d}}} = \underset{\underline{\mathbf{d}}\in\{-1,+1\}^K}{\arg\min}\left\{\|\underline{\mathbf{e}} - \underline{\mathbf{H}}_\mathrm{UL}\cdot\underline{\mathbf{d}}\|^2\right\}. \quad (28)$$

4.2 Potentials of nonlinear JT

The significant performance improvements by nonlinear JD, see Section 4.1, directly lead to the question whether it is possible also to improve JT by exploiting the knowledge of the modulation alphabet (1) in the transmitter. In general this would lead to nonlinear transmitters. In the present paper a first answer to this question based on a scenario with two MTs, two APs and the parametric MIMO channel described by the channel matrix

$$\underline{\mathbf{H}}_\mathrm{UL} = \begin{pmatrix} 1 & \rho_1 \\ \rho_2 & 1 \end{pmatrix}, \quad (29)$$

see Fig. 2, is given.

As the channel matrix of (29) is real and only the real parts of the received signals $\underline{e}^{(k)}$, $k = 1,\ 2$, are relevant in the considered case of BPSK modulation, only the real parts of the transmit signals $\underline{s}^{(k)}$, $k = 1,\ 2$, can cause useful received signals. Thus, only real transmit signals $s^{(k)}$, $k = 1,\ 2$, need to be

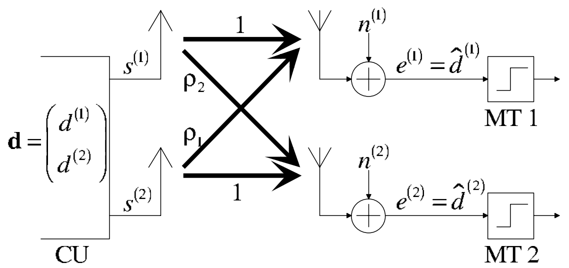

Figure 2: Exemplary DL scenario

considered in the following. Furthermore, only the real part of the Gaussian noise $n^{(k)}$, $k = 1,\ 2$, is effective and the data symbols $d^{(k)}$, $k = 1,\ 2$, and their estimates $\hat{d}^{(k)}$, $k = 1,\ 2$, are real. The transmit signals $s^{(k)}$, $k = 1,\ 2$, are in general nonlinear functions of the data symbols $d^{(k)}$, $k = 1,\ 2$, to be transmitted. These nonlinear functions have to be optimized in the following.

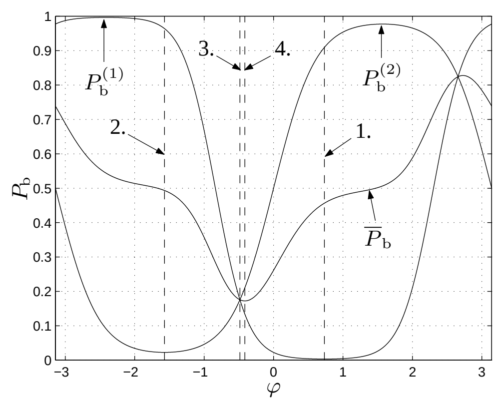

Figure 3: Bit error probabilities as a function of the transmitted signal characterized by φ; Parameters: $\sqrt{\frac{T}{\sigma^2}} = 1$, $\rho_1 = 0.9$, $\rho_2 = 0.0$, $d^{(1)} = +1$, $d^{(2)} = -1$;

For a fair optimization the transmit energy should be fixed in the first step. This means that the two dimensional transmit signal $s^{(k)}$, $k = 1,\ 2$, with the total transmit energy $2T$ for the two data symbols $d^{(k)}$, $k = 1,\ 2$, can be described by a single parameter φ:

$$\begin{aligned} s^{(1)} &= 2\sqrt{T}\cos(\varphi)\,, \\ s^{(2)} &= 2\sqrt{T}\sin(\varphi)\,. \end{aligned} \tag{30}$$

With the variance σ^2 of the Gaussian noise one can calculate the resulting bit error probabilities

$$P_\mathrm{b}^{(1)} = \frac{1}{2}\,\mathrm{erfc}\left(\pm\sqrt{2T}\frac{\cos(\varphi) + \rho_1 \sin(\varphi)}{\sigma}\right),\ \text{for } \underline{d}^{(1)} = \pm 1, \tag{31}$$

$$P_\mathrm{b}^{(2)} = \frac{1}{2}\,\mathrm{erfc}\left(\pm\sqrt{2T}\frac{\rho_2\cos(\varphi) + \sin(\varphi)}{\sigma}\right),\ \text{for } \underline{d}^{(2)} = \pm 1, \tag{32}$$

and the average bit error probability

$$\overline{P}_\mathrm{b} = \frac{1}{2}\left(P_\mathrm{b}^{(1)} + P_\mathrm{b}^{(2)}\right). \tag{33}$$

These bit error probabilities are depicted in Fig. 3 versus φ for one exemplary scenario and data vector to be transmitted. The parameter values φ characterizing transmit signals for

1. minimum bit error probability $P_\mathrm{b}^{(1)}$ of user 1,
2. minimum bit error probability $P_\mathrm{b}^{(2)}$ of user 2,
3. linear JT with fixed transmit energy and
4. minimum average bit error probability $\overline{P}_\mathrm{b}$

are marked. For linear JT with fixed transmit energy

$$\varphi = \mathrm{atan}\left(\frac{d^{(1)} - \rho_2 d^{(1)}}{d^{(1)} - \rho_1 d^{(2)}}\right) \tag{34}$$

holds [8].

In contrast to optimum JD it is obviously not possible to simultaneously minimize the bit error probabilities for all users in JT, i.e., one has to find a compromise. One possible compromise is to design the transmit signal in such a way that the bit error probabilities are the same for all users, or equivalently to minimize the maximum bit error probability. This is achieved by linear JT. Another compromise, which is studied in the following, is to minimize the average bit error probability $\overline{P}_\mathrm{b}$.

In general the transmit signal for minimum average bit error probability $\overline{P}_\mathrm{b}$ can only be found by numerical minimization [10]. In the considered scenario only the optimum value for φ has to be found and thus the numerical minimization is a quite simple one dimensional minimization problem. For a fixed channel and variance σ^2 of the noise the minimization has to be done only once and the outcome is a table describing which transmit signal has to be used for the transmission of each of the possible data vectors.

Whereas the total transmit energy in JD is always independent of the data vector $\underline{\mathbf{d}}$ to be transmitted, one has to distinguish JT schemes with fixed transmit energy, i.e., a transmit energy independent of the data vector $\underline{\mathbf{d}}$, and JT schemes with variable transmit energy, i.e., a transmit energy which depends on the data vector $\underline{\mathbf{d}}$ with only a given average transmit energy for all possible data vectors $\underline{\mathbf{d}}$. One example for a JT scheme with variable transmit energy is the linear JT described in Subsection 3.3 and an example for a JT scheme with fixed transmit energy is the optimum nonlinear JT described in this Section. However, it is also possible to scale the transmit signal $\underline{\mathbf{s}}$ obtained by linear JT in such a way that the transmit energy is fixed, i.e., the transmit energy is independent of the actual value of the data vector $\underline{\mathbf{d}}$ to be transmitted. Furthermore one can also think of optimum nonlinear JT schemes with variable transmit energy. The average bit error probability can be further reduced by using different transmit energies for different values of the data vector $\underline{\mathbf{d}}$. Of course the average transmit energy for all possible data vectors $\underline{\mathbf{d}}$ must remain the same in order to allow a fair comparison. Practically this means that one has to simultaneously optimize the transmit signals for all possible data vectors $\underline{\mathbf{d}}$ and the transmit energies under the side condition of a fixed average transmit energy. Even in the considered simple scenario this clearly is multi dimensional opimization problem.

5 Numerical results

In Fig. 4 the different transmission schemes are compared for the exemplary MIMO channel described by (29) and (10) with $\rho_1 = 0.9$ and $\rho_2 = 0.0$. It can be seen from Fig. 4 that all JT schemes with fixed transmit energy show approximately the same performance which is the worst of all transmission schemes. So it is crucial to allow a variable transmit energy for JT. In the case of variable transmit energy the performance of optimum JT is significantly better than the performance of the linear transmission schemes but the performance of optimum JD can not be reached.

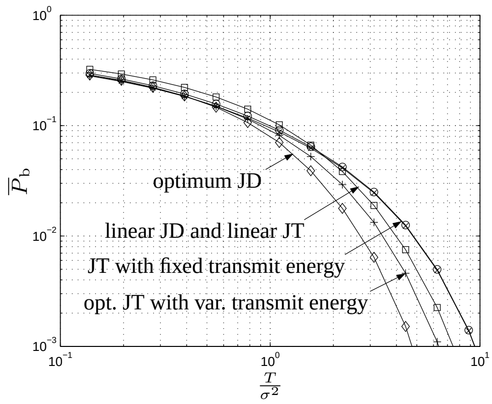

Figure 4: Average bit error probability $\overline{P}_{\mathrm{b}}$; Parameters $\rho_1 = 0.9$, $\rho_2 = 0$

6 Conclusions

In the present paper it is shown that linear JD in the UL and linear JT in the DL are dual and yield the same performance. However, if optimum nonlinear signal processing techniques are taken into consideration the UL with JD and the DL with JT are not dual anymore. It is shown that it is crucial to only fix the average transmit energy for all possible data vectors in order to obtain a good performance of JT. Nevertheless the performance of the DL with optimum nonlinear JT is worse than the performance of the UL with optimum nonlinear JD.

Acknowledgements

The authors gratefully appreciate the stimulating discussions and the fruitful exchange of ideas with P.W. Baier and their colleagues at the Research Group for RF Communications, University of Kaiserslautern, and Siemens AG. The invaluable support of the supercomputing staff at the central computer facility (RHRK) is highly acknowledged.

References

[1] Costa, M. H. M.: Writing on dirty paper. *IEEE Transactions on Information Theory*, vol. 29, 1983, pp. 439–441.

[2] Cover, T. M.; Thomas, J. A.: *Elements of Information Theory*. John Wiley & Sons, 1991.

[3] Fischer, R. F. H.: *Precoding and Signal Shaping for Digital Transmission*. New York: John Wiley & Sons, 2002.

[4] Joham, M.; Kusume, K.; Gzara, M. H.; Utschick, W.; Nossek, J. A.: Transmit Wiener filter for the downlink of TDD DS-CDMA systems. *Proc. IEEE 7th International Symposium on Spread Spectrum Techniques & Applications (ISSSTA'02)*, vol. 1, Prague, 2002, pp. 9–13.

[5] Joham, M.; Utschick, W.: Downlink processing for mitigation of intracell interference in DS-CDMA systems. *Proc. IEEE 6th International Symposium on Spread Spectrum Techniques & Applications (ISSSTA'00)*, vol. 1, Parsippany, 2000, pp. 15–19.

[6] Kowalewski, F.; Mangold, P.: Joint predistortion and transmit diversity. *Proc. IEEE Global Telecommunications Conference (GLOBECOM'00)*, vol. 1, San Francisco, 2000, pp. 245–249.

[7] Lupas, R.; Verdú, S.: Linear multiuser detectors for synchronous code-division multiple-access channels. *IEEE Transactions on Information Theory*, vol. 35, 1989, pp. 123–136.

[8] Meurer, M.; Baier, P. W.; Weber, T.; Lu, Y.; Papathanassiou, A.: Joint transmission: advantageous downlink concept for CDMA mobile radio systems using time division duplexing. *IEE Electronics Letters*, vol. 11, 2000, pp. 900–901.

[9] Proakis, J. G.: *Digital Communications*. 3. edition. New York: McGraw-Hill, 1995.

[10] Press, W. H.; Teukolsky, S. A.; Vetterling, W. T.; Flannery, B. P.: *Numerical Recipes in C*. 2. edition. New York: Cambridge University Press, 1992.

[11] Steiner, B.; Baier, P. W.: Low cost channel estimation in the uplink receiver of CDMA mobile radio systems. *Frequenz*, vol. 47, 1993, pp. 292–298.

[12] Schneider, K. S.: Optimum detection for code division multiplexed signals. *IEEE Transactions on Aerospace and Electronic Systems*, vol. 15, 1979, pp. 181–185.

[13] Tröger, H.; Weber, T.; Meurer, M.; Baier, P. W.: Performance assessment of joint transmission (JT) multi-user downlinks with multi-element transmit antennas. *European Transactions on Telecommunications*, vol. 12, 2001, pp. 407–415.

[14] Verdú, S.: *Multiuser Detection*. Cambridge: Cambridge University Press, 1998.

[15] Weber, T.; Maniatis, I.; Sklavos, A.; Liu, Y.: Joint transmission and detection integrated network (JOINT), a generic proposal for beyond 3G systems. *Proc. 9th International Conference on Telecommunications (ICT'02)*, vol. 3, Beijing, 2002, pp. 479–483.

[16] Yu, W.; Cioffi, J. M.: Trellis precoding for the broadcast channel. *Proc. IEEE Global Telecommunications Conference (GLOBECOM'01)*, vol. 2, San Antonio, 2001, pp. 1344–1348.

Kapitel 3

Suboptimale lineare Verfahren der gemeinsamen Sendesignalerzeugung bei konventionellen Empfängern

3.1 Modell linearer empfängerorientierter Übertragungssysteme

Da das in Kapitel 2 behandelte optimale Verfahren der gemeinsamen Sendesignalerzeugung sehr aufwendig ist, wurden bereits in Unterkapitel 1.4 aufwandsgünstige linearen Verfahren der gemeinsamen Sendesignalerzeugung für konventionelle Empfänger angesprochen. Bei diesen linearen Verfahren läßt sich der Modulatoroperator $\mathcal{M}\{\cdot\}$ nach (1.13) gemäß (1.31) durch die Modulatormatrix $\underline{\mathbf{M}}$ eindeutig beschreiben. Im Rahmen dieser Schrift soll vorrangig die in der Literatur bedeutende Ausgestaltung des Detektoroperators $\mathcal{D}\{\cdot\}$ nach Bild 1.9 betrachtet werden. Werden daher senderseitig lineare Verfahren der gemeinsamen Sendesignalerzeugung eingesetzt, so können diese Verfahren Entscheidungen, die empfängerseitig durch den Quantisierungsoperator $\mathcal{Q}\{\cdot\}$ getroffen werden, infolge ihrer linearen Natur nicht berücksichtigen. Dies hat zur Folge, daß sämtliche linearen Verfahren der gemeinsamen Sendesignalerzeugung ausschließlich auf die Gestaltung möglichst zuverlässiger wertekontinuierlichen Schätzungen $\widehat{\underline{d}}_n^{(k)}$ nach (1.17) der übertragenen Datensymbole $\underline{d}_n^{(k)}$, $n = 1 \ldots N$, $k = 1 \ldots K$, abzielen und daher hinsichtlich des in Kapitel 1 erläuterten Ziels des Minimierens von Übertragungsfehlerwahrscheinlichkeiten suboptimal sind.

Durch Kombinieren der linearen Wahl des Modulatoroperators $\mathcal{M}\{\cdot\}$ nach (1.31), des vereinfachten Modells der Funkkommunikation innerhalb einer Referenzzelle nach Bild 1.7 und der Ausgestaltung des Detektoroperators $\mathcal{D}\{\cdot\}$ nach Bild 1.9 ergibt sich das in Bild 3.1 wiedergegebene vereinfachte lineare Modell der Funkkommunikation innerhalb einer Referenzzelle. Dabei wird der Zusammenhang zwischen totalem Datenvektor $\underline{\mathbf{d}}$ nach (1.12) und dessen wertekontinuierlicher Schätzung $\widehat{\underline{\mathbf{d}}}$ nach (1.18) in Abhängigkeit von der Modulatormatrix $\underline{\mathbf{M}}$ nach (1.31), der totalen Kanalmatrix $\underline{\mathbf{H}}$ nach (1.5) und der totalen Demodulatormatrix $\underline{\mathbf{D}}$ nach (1.19) veranschaulicht.

Ausgehend von dem in Bild 3.1 dargelegten vereinfachten Modell läßt sich der einfache Zusammenhang

$$\widehat{\underline{\mathbf{d}}} = \underline{\mathbf{D}}\,\underline{\mathbf{H}}\,\underline{\mathbf{M}}\,\underline{\mathbf{d}} + \underline{\mathbf{D}}\,\underline{\mathbf{n}} \tag{3.1}$$

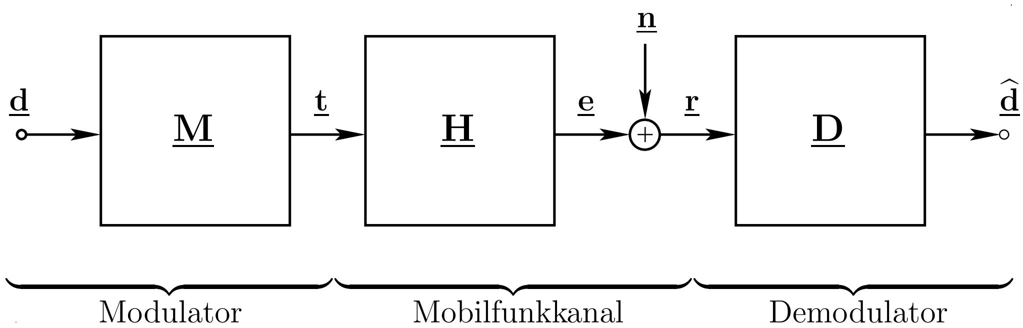

Bild 3.1. Vereinfachtes lineares Modell der Funkkommunikation innerhalb einer Referenzzelle

zwischen totalem Datenvektor $\underline{\mathbf{d}}$ nach (1.12) und dessen wertekontinuierlicher Schätzung $\widehat{\underline{\mathbf{d}}}$ nach (1.18) angeben. Die Schätzung $\widehat{\underline{d}}_n^{(k)}$ eines jeden Datensymbols $\underline{d}_n^{(k)}$, $n = 1 \ldots N$, $k = 1 \ldots K$, setzt sich im allgemeinen aus den drei Komponenten

$$\widehat{\underline{d}}_{\mathrm{useful},n}^{(k)} = \Big[\underline{\mathbf{D}}\,\underline{\mathbf{H}}\,\underline{\mathbf{M}}\Big]_{N(k-1)+n,N(k-1)+n} \underline{d}_n^{(k)}, \tag{3.2}$$

$$\widehat{\underline{d}}_{\mathrm{int},n}^{(k)} = \Big[\overline{\mathrm{diag}}\left(\underline{\mathbf{D}}\,\underline{\mathbf{H}}\,\underline{\mathbf{M}}\right)\underline{\mathbf{d}}\Big]_{N(k-1)+n} \tag{3.3}$$

und

$$\widehat{\underline{d}}_{\mathrm{noise},n}^{(k)} = \Big[\underline{\mathbf{D}}\,\underline{\mathbf{n}}\Big]_{N(k-1)+n} \tag{3.4}$$

gemäß

$$\widehat{\underline{d}}_n^{(k)} = \widehat{\underline{d}}_{\mathrm{useful},n}^{(k)} + \widehat{\underline{d}}_{\mathrm{int},n}^{(k)} + \widehat{\underline{d}}_{\mathrm{noise},n}^{(k)} \tag{3.5}$$

zusammen. Diese Komponenten beschreiben den gewünschten, das heißt auf die Übertragung des betrachteten Datensymbols $\underline{d}_n^{(k)}$ zurückgehenden Beitrag $\widehat{\underline{d}}_{\mathrm{useful},n}^{(k)}$, den auf die Übertragung anderer Datensymbole $\underline{d}_{n'}^{(k')}$, $n' = 1 \ldots N$, $k' = 1 \ldots K$, $n \neq n' \;\vee k \neq k'$, zurückgehenden Interferenzbeitrag $\widehat{\underline{d}}_{\mathrm{int},n}^{(k)}$ und den Beitrag $\widehat{\underline{d}}_{\mathrm{noise},n}^{(k)}$ des totalen Rauschens $\underline{\mathbf{n}}$ nach (1.6) zu $\widehat{\underline{d}}_n^{(k)}$.

3.2 Verfahren der gemeinsamen Sendesignalerzeugung

Basierend auf dem vereinfachten linearen Systemmodell nach (3.1) und Bild 3.1 lassen sich verschiedene linearen Verfahren der gemeinsamen Sendesignalerzeugung finden, die die Beiträge $\widehat{\underline{d}}_{\mathrm{useful},n}^{(k)}$, $\widehat{\underline{d}}_{\mathrm{int},n}^{(k)}$, und $\widehat{\underline{d}}_{\mathrm{noise},n}^{(k)}$ nach (3.2) bis (3.4) zu $\widehat{\underline{d}}_n^{(k)}$ nach (3.5) nach jeweils unterschiedlichen Gesichtspunkten ausbalancieren. Im einzelnen sind dabei vorrangig die Verfahren TxMF, TxZF und TxMMSE, zu nennen, die bereits in

Tabelle 3.1. Wesentliche Unterschiede der Notationen nach Tabelle 1.2 und der Notation nach [MBW+00, MBL+00, BMWT00, TMW00, MTJ02]

dargestellte Größe	nach Tab. 1.2	nach [·]	Bemerkung/ geltend für
Anzahl der Teilnehmer	K	U	[BMWT00]
totales Sendesignal	$\underline{\mathbf{t}}$	$\underline{\mathbf{s}}$	[MBW+00],[MBL+00], [BMWT00],[TMW00],[MTJ02]
totale Demodulatormatrix	$\underline{\mathbf{D}}$	$\underline{\mathbf{C}}^{*\mathrm{T}}$	[MBW+00, MBL+00]

Unterkapitel 1.4 eingeführt wurden. In den folgenden Veröffentlichungen [MBW+00, MBL+00, BMWT00, TMW00, MTJ02, MBQ04] werden diese linearen Verfahren der gemeinsamen Sendesignalerzeugung für konventionelle Empfänger detailliert betrachtet. Dabei wird unter anderem folgendes beleuchtet:

- Es wird erläutert, nach welchen Gesichtspunkten die oben genannten Beiträge $\widehat{\underline{d}}^{(k)}_{\mathrm{useful},n}$, $\widehat{\underline{d}}^{(k)}_{\mathrm{int},n}$, und $\widehat{\underline{d}}^{(k)}_{\mathrm{noise},n}$ nach (3.2) bis (3.4) zu $\widehat{\underline{d}}^{(k)}_{n}$ nach (3.5) durch die gemeinsamen Sendesignalerzeugung ausbalanciert werden.

- Die Berechnung der den jeweiligen Verfahren zugehörigen Modulatormatrizen $\underline{\mathbf{M}}$ wird mathematisch erläutert, wobei dabei auch die Verwendung von mehreren Sendeantennen an der Basisstation und/oder mehreren Empfangsantennen an den Mobilstationen berücksichtigt wird.

- Dualitäten zwischen den aus dem Bereich der Empfängerorientierung stammenden Verfahren der gemeinsamen Sendesignalerzeugung TxMF, TxZF und TxMMSE und den aus der Literatur [Kle96, Ver98] bekannten, aus dem Bereich der Senderorientierung stammenden Verfahren der gemeinsamen Sendesignalverarbeitung (engl. joint data detection) „empfängerseitige signalangepaßte Filterung (engl. receive matched filter, RxMF)“, „empfängerseitige Interferenzeliminierung (engl. receive zero forcing, RxZF)“ und „empfängerseitiges Minimieren des mittleren quadratischen Schätzfehlers (engl. receive minimum mean square error, RxMMSE)“ werden aufgezeigt sowie vergleichende Untersuchungen der Leistungsfähigkeit durchgeführt.

Im Gegensatz zu dem aus Tabelle 1.2 bekannten Systemmodell werden in [MBW+00, MBL+00, BMWT00, TMW00, MTJ02] einige wenige Größen durch eine modifizierte Notation beschrieben. Tabelle 3.1 listet die wesentlichen Unterschiede in kompakter Form auf.

[MBW+00] Meurer, M.; Baier, P. W.; Weber, T.; Lu, Y.; Papathanassiou, A.: "Joint transmission: advantageous downlink concept for CDMA mobile radio systems using time division duplexing". *IEE Electronics Letters*, Bd. 36, 2000, S. 900–901.

Joint transmission: advantageous downlink concept for CDMA mobile radio systems using time division duplexing

M. Meurer, P.W. Baier, T. Weber, Y. Lu and A. Papathanassiou

A novel downlink transmission scheme for time-slotted CDMA employing time-division duplexing (TDD) is proposed. It utilises the knowledge of the channel impulse responses at the BS transmitter in such a way that at the receivers of the MSs channel estimators are no longer required and the computational expense of data detection is dramatically reduced.

Introduction: In mobile radio systems employing time division duplexing (TDD) the same channel impulse responses are valid for both the uplink and the downlink if – and this is assumed in this Letter – the time between the uplink and downlink transmissions is sufficiently small. In this Letter, a novel downlink transmission scheme for time-slotted CDMA is proposed, which utilises the knowledge of the channel impulse reponses at the base station (BS) transmitter in such a way that channel estimators are no longer required at the receivers of the mobile stations (MSs). This implies that, compared to conventional time-slotted CDMA [1], the computational expense of data detection in the MSs is dramatically reduced, and system capacity is enhanced simultaneously, because no resources have to be allocated to the transmission of training signals [2]. The crux of the proposed approach consists in jointly determining at the BS one common transmit signal for the service of all MSs which, after having passed the mobile radio channels, at each MS yields the data sent for this MS by simple filtering. The authors propose to term this approach joint transmission (JT), because its rationale is the inverse of that in joint detection (JD) [1], where a received signal common to all users is jointly processed at the receiver. In this Letter, time discrete equivalent lowpass signal representation is chosen. Consequently, signals and channel impulse responses are represented by complex vectors or matrices [1], which are printed in bold face.

Signal transmission model: At the BS an array of *Ka* transmit antenna elements is utilised, whereas each MS μ_k, $k = 1, ..., K$, has a single element receiving antenna. The channel impulse response

$$\underline{\mathbf{h}}^{(k,k_a)} = \left(\underline{h}_1^{(k,k_a)} \cdots \underline{h}_W^{(k,k_a)}\right)^T \quad k = 1,...,K, k_a = 1,...,K_a \tag{1}$$

of length W characterises the signal transmission between the input of the transmit antenna element k_a and the output of the receiving antenna of MS μ_k. Into each of the K_a transmit antenna elements a signal

$$\underline{\mathbf{s}}^{(k_a)} = \left(\underline{s}_1^{(k_a)} \cdots \underline{s}_S^{(k_a)}\right)^T \quad k_a = 1,...,K_a \tag{2}$$

of length S is fed. The K_a signals $\underline{\mathbf{s}}^{(k_a)}$ of eqn. 2 can be compiled to form the total transmit signal

$$\underline{\mathbf{s}} = \left(\underline{\mathbf{s}}^{(1)T} \cdots \underline{\mathbf{s}}^{(K_a)T}\right)^T \tag{3}$$

of length K_aS. With the channel impulse responses $\underline{\mathbf{h}}^{(k,k_a)}$ of eqn. 1 the $(S + W - 1) \times S$ matrices

$$\underline{\mathbf{H}}^{(k,k_a)} = \left(\underline{H}_{i,j}^{(k,k_a)}\right) \quad i = 1,...,S+W-1, j = 1,...,S$$
$$\underline{H}_{i,j}^{(k,k_a)} = \begin{cases} \underline{h}_{i-j+1}^{(k,k_a)} & \text{for } 1 \le i-j+1 \le W \\ 0 & \text{otherwise} \end{cases}$$
$$k = 1,...,K, k_a = 1,...,K_a \tag{4}$$

and the $(S + W - 1) \times (K_aS)$ matrices

$$\underline{\mathbf{H}}^{(k)} = \left(\underline{\mathbf{H}}^{(k,1)} \cdots \underline{\mathbf{H}}^{(k,K_a)}\right) \quad k = 1,...,K \tag{5}$$

can be formed. The signal originating in $\underline{\mathbf{s}}$ of eqn. 3 and received at MS μ_k then becomes

$$\underline{\mathbf{e}}^{(k)} = \underline{\mathbf{H}}^{(k)}\underline{\mathbf{s}} \quad k = 1,...,K \tag{6}$$

The K received signals $\underline{\mathbf{e}}^{(k)}$ of eqn. 6 can be arranged in a vector

$$\underline{\mathbf{e}} = \left(\underline{\mathbf{e}}^{(1)T} \cdots \underline{\mathbf{e}}^{(K)T}\right)^T \tag{7}$$

of length $K(S + W - 1)$, which is termed the total received signal. The K matrices $\underline{\mathbf{H}}^{(k)}$ of eqn. 5 can be arranged in the $[K(S + W - 1)] \times (K_aS)$ matrix

$$\underline{\mathbf{H}} = \left(\underline{\mathbf{H}}^{(1)T} \cdots \underline{\mathbf{H}}^{(K)T}\right)^T \tag{8}$$

The total received signal of eqn. 7 can then be concisely expressed as

$$\underline{\mathbf{e}} = \underline{\mathbf{H}}\underline{\mathbf{s}} \tag{9}$$

Data transmission and detection: It is assumed that, per burst, N data symbols have to be transmitted from the BS to each MS μ_k, $k = 1, ..., K$. The data symbols intended for MS μ_k are arranged in the data vector

$$\underline{\mathbf{d}}^{(k)} = \left(\underline{d}_1^{(k)} \cdots \underline{d}_N^{(k)}\right)^T \quad k = 1,...,K \tag{10}$$

The K data vectors $\underline{\mathbf{d}}^{(k)}$ are put together to form the total data vector

$$\underline{\mathbf{d}} = \left(\underline{\mathbf{d}}^{(1)T} \cdots \underline{\mathbf{d}}^{(K)T}\right)^T = (\underline{d}_1 \cdots \underline{d}_{KN})^T \tag{11}$$

of length KN.

In the downlink of conventional TD-CDMA [1], one of K CDMA codes

$$\underline{\mathbf{c}}^{(k)} = \left(\underline{c}_1^{(k)} \cdots \underline{c}_Q^{(k)}\right)^T \quad k = 1,...,K \tag{12}$$

of length Q is uniquely assigned to each MS μ_k, $k = 1, ..., K$. In the case of additive white Gaussian noise (AWGN) transmission, the optimum linear single user detector at each MS μ_k would then consist of a filter matched to the CDMA code $\underline{\mathbf{c}}^{(k)}$. As the main feature of the proposed scheme JT, this simple detector would also be maintained if the radio channels were no longer AWGN channels, but showed multipath behaviour, and if antenna arrays were employed at the BSs. Nevertheless, it would be necessary to ensure, as in the case of employing JD, that intersymbol interference and intracell multiple access interference did not occur at the detector outputs. We now show that these goals can be achieved by properly designing the total transmit signal $\underline{\mathbf{s}}$ of eqn. 3. As in conventional time-slotted CDMA [3], the length of the signals $\underline{\mathbf{s}}^{(k_a)}$ of eqn. 2 is assumed to be

$$S = QN \tag{13}$$

Given the CDMA codes $\underline{\mathbf{c}}^{(k)}$ of eqn. 12 the CDMA code matrix

$$\underline{\mathbf{C}} = \text{blockdiag}\left[\underline{\mathbf{C}}^{(1)} \cdots \underline{\mathbf{C}}^{(K)}\right] \tag{14}$$

with

$$\underline{\mathbf{C}}^{(k)} = \left(\underline{C}_{i,j}^{(k)}\right) \quad i = 1,...,QN+W-1, j = 1,...,N,$$
$$k = 1,...,K$$
$$\underline{C}_{i,j}^{(k)} = \begin{cases} \underline{c}_{i-Q(j-1)}^{(k)} & \text{for } 1 \le i - Q(j-1) \le Q \\ 0 & \text{else} \end{cases} \tag{15}$$

can be established. Using this matrix, the matched filtering of the received signals $\underline{\mathbf{e}}^{(k)}$ is equivalent to forming the matrix-vector-product $\underline{\mathbf{C}}^{*T}\underline{\mathbf{e}}$ with $\underline{\mathbf{e}}$ of eqn. 9. The requirement that filtering of $\underline{\mathbf{e}}^{(k)}$ of eqn. 6 yields the data vectors $\underline{\mathbf{d}}^{(k)}$ of eqn. 10 at MS μ_k can then be expressed in the form

$$\underline{\mathbf{C}}^{*T}\underline{\mathbf{e}} \stackrel{!}{=} \underline{\mathbf{d}} \tag{16}$$

Substituting eqn. 9 in eqn. 16 yields

$$\underline{\mathbf{C}}^{*T}\underline{\mathbf{H}}\,\underline{\mathbf{s}} = \underline{\mathbf{d}} \tag{17}$$

In what follows we assume

$$K_aQN > KN \tag{18}$$

which is also a reasonable requirement in conventional time-slotted CDMA employing JD in order to keep the SNR-degradation sufficiently low. Eqn. 18 means that the system of equations given by eqn. 17 is under-determined, and, consequently, has infinitely many solutions $\underline{\mathbf{s}}$. The solution of minimum energy $\|\underline{\mathbf{s}}\|^2/2$ is obtained by setting

$$\underline{\mathbf{s}} = \underline{\mathbf{H}}^{*T}\underline{\mathbf{C}}\left(\underline{\mathbf{C}}^{*T}\underline{\mathbf{H}}\,\underline{\mathbf{H}}^{*T}\underline{\mathbf{C}}\right)^{-1}\underline{\mathbf{d}} \tag{19}$$

[4]. This solution has been adopted in this Letter because it is optimum in the sense that the transmit power and, consequently, multiple access interference are minimised.

13 March 2000
Electronics Letters Online No: 20000671
DOI: 10.1049/el:20000671

M. Meurer, P.W. Baier, T. Weber, Y. Lu and A. Papathanassiou (*Research Group for RF Communications, University of Kaiserlautern, PO Box 3049, D-67653 Kaiserlautern, Germany*)

E-mail: meurer@rhrk.uni-kl.de

References

1 KLEIN, A.: 'Multi-user detection of CDMA-signals – algorithms and their application to cellular mobile radio', *Fortschrittberichte VDI*, 1996, **10**, (VDI-Verlag, Düsseldorf)

2 STEINER, B.: 'Ein Beitrag zur Mobilfunkkanalschätzung unter besonderer Berücksichtigung synchroner CDMA-Mobilfunksysteme mit Joint Detection', *Fortschrittberichte VDI*, 1995, **10**, (VDI-Verlag, Düsseldorf)

3 PAPATHANASSIOU, A., FURIO, I., BLANZ, J.J., and BAIER, P.W.: 'Smart antennas with two-dimensional array configurations for performance enhancement of a joint detection CDMA mobile radio system', *Wireless Personal Commun.*, 1999, **11**, (1) pp. 89–108

4 BEN-ISRAEL, A., and GREVILLE, T.N.E.: 'Generalized inverses: theory and applications' (Wiley-Interscience, New York, 1974)

[MBL+00] Meurer, M.; Baier, P. W.; Lu, Y.; Papathanassiou, A.; Weber, T.: "TD-CDMA downlink: Optimum transmit signal design reduces receiver complexity and enhances system performance". *Proc. 7th International Conference on Telecommunications (ICT'00)*, Bd. 1, Acapulco, 2000, S. 300–305.

TD-CDMA Downlink: Optimum Transmit Signal Design Reduces Receiver Complexity and Enhances System Performance

Michael Meurer, Paul Walter Baier, Yang Lu, Apostolos Papathanassiou, Tobias Weber
Research Group for RF Communications, University of Kaiserslautern
P.O. Box 3049, D–67653 Kaiserslautern, Germany
phone/fax: +49 631 205 2084/3612; e–mail: meurer@rhrk.uni–kl.de

Abstract— **In the 3rd Generation Partnership Project (3GPP) Time Division CDMA (TD–CDMA) has been selected as the air interface for the TDD (Time Division Duplexing) bands of 3rd generation mobile radio systems (3G systems). In the case of TDD the same channel impulse responses are valid for both uplink and downlink. In state–of–the–art TD–CDMA characterized by joint data detection (JD) this equality cannot be exploited for enhancing system performance and reducing system complexity. In the paper a novel TD–CDMA downlink transmission scheme is proposed. This scheme is termed joint transmission (JT). It utilizes the knowledge of the channel impulse responses gained by channel estimation at the base station in such a way that at the mobile stations channel estimators are no longer required and the computational expense of data detection is dramatically reduced.**

Keywords— **TD–CDMA downlink, joint transmission, TDD in 3G systems, signal processing for wireless communications.**

I. Introduction

TD-CDMA is a promising air interface for third generation mobile radio systems (3G systems). Among other advantages, TD-CDMA easily lends itself to the application of joint detection (JD) [1], which, by eliminating intracell multiple access interference (MAI) and intersymbol interference (ISI), considerably enhances system performance [2] as compared to single user detection. Thanks to its TDMA component, TD-CDMA is especially suited for applications in unpaired frequency bands. No wonder that TD-CDMA has been selected by 3GPP [3] as the standard for the Time Division Duplexing (TDD) mode of the 3G system International Mobile Telecommunications 2000 (IMT-2000), and that also the Chinese 3G air interface TD-SCDMA [4], where S stands for synchronous, relies on time slotted CDMA. In the case of TDD the same channel impulse responses are valid for both the uplink and the downlink, if – and this is assumed in what follows – the time elapsing between uplink and downlink transmissions is sufficiently small compared to the coherence time of the mobile radio channels. However, this equality of uplink and downlink channel impulse responses cannot be exploited in state–of–the–art TD-CDMA operation, which requires channel estimators at the receivers of both the base stations (BS) and the mobile stations (MS). This is true because the knowledge of the channel impulse responses is needed for performing JD. In this paper, a novel TD-CDMA downlink transmission scheme is proposed, which utilizes the knowledge of the channel impulse reponses at the BS transmitter in such a way that channel estimators are no longer required at the receivers of the MSs. In addition, compared to conventional TD-CDMA, the computational expense of data detection in the MSs is dramatically reduced and simultaneously system performance is enhanced by this transmission scheme. The crux of the proposed approach consists in determining at the BS one common transmit signal for the service of all MSs which, after having passed the mobile radio channels, at each MS yields the data sent for this MS by simple filtering. The authors propose to term this approach joint transmission (JT), because its rationale is the inverse of the one followed in JD, where a received signal common to all users is jointly processed at the receiver. In a way JT is related to known CDMA concepts using transmit signals which originate by predistortion of CDMA coded signals [5, 6]. However, JT is much more general because the transmit signals are directly generated and do not result by first generating and then distorting CDMA coded signals.

The paper is structured as follows. In Section II the signal transmission model of JT is developed. Section III deals with data transmission and detection in TD-CDMA systems utilizing JT. In Section IV a performance assessment method of JT in TD-CDMA is proposed. This method is applied in Section V, where simulation results for an example scenario are presented. Finally, the paper is concluded by Section VI. In the paper the time discrete equivalent low–pass representation of signals is chosen. Consequently, signals and channel impulse responses are represented by complex vectors or matrices [1], which are printed in bold face.

II. Signal Transmission model

At the BS an array of K_a transmit antenna elements is utilized, whereas each MS μ_k, $k = 1\ldots K$, disposes of a single element receiving antenna. For each MS this situation can be modeled by a MS specific network with K_a input ports and a single output port, see Fig. 1. In this network the channel impulse response

$$\underline{\boldsymbol{h}}^{(k,k_\mathrm{a})} = \left(\underline{h}_1^{(k,k_\mathrm{a})} \ldots \underline{h}_W^{(k,k_\mathrm{a})}\right)^\mathrm{T}, k = 1\ldots K, \quad k_\mathrm{a} = 1\ldots K_\mathrm{a} \tag{1}$$

of length W characterizes signal transmission between the input of the transmit antenna element k_a and the output of the receiving antenna of MS μ_k. Into each of the K_a transmit antenna elements a signal

$$\underline{\boldsymbol{s}}^{(k_\mathrm{a})} = \left(\underline{s}_1^{(k_\mathrm{a})} \ldots \underline{s}_S^{(k_\mathrm{a})}\right)^\mathrm{T}, k_\mathrm{a} = 1\ldots K_\mathrm{a}, \tag{2}$$

of length S is fed. The K_a signals $\underline{\boldsymbol{s}}^{(k_\mathrm{a})}$ of (2) can be compiled to form the total transmit signal

$$\underline{\boldsymbol{s}} = \left(\underline{\boldsymbol{s}}^{(1)\mathrm{T}} \ldots \underline{\boldsymbol{s}}^{(K_\mathrm{a})\mathrm{T}}\right)^\mathrm{T} \tag{3}$$

of length $K_\mathrm{a}S$. $\underline{\boldsymbol{s}}$ of (3) represents the transmission of one TDMA burst of TD–CDMA. With the channel impulse responses $\underline{\boldsymbol{h}}^{(k,k_\mathrm{a})}$ of (1) the $(S+W-1)\times S$ matrices

$$\underline{\boldsymbol{H}}^{(k,k_\mathrm{a})} = \left(\underline{H}_{i,j}^{(k,k_\mathrm{a})}\right), i = 1\ldots S+W-1, \quad j = 1\ldots S,$$

$$\underline{H}_{i,j}^{(k,k_\mathrm{a})} = \begin{cases} \underline{h}_{i-j+1}^{(k,k_\mathrm{a})} & \text{for } 1 \le i-j+1 \le W, \\ 0 & \text{otherwise,} \end{cases} \tag{4}$$

$$k = 1\ldots K, k_\mathrm{a} = 1\ldots K_\mathrm{a}, \tag{5}$$

can be formed. The K_a matrices $\underline{\boldsymbol{H}}^{(k,k_\mathrm{a})}$ valid for a given value k , that is for a given MS μ_k, can be arranged in an $(S+W-1)\times(K_\mathrm{a}S)$ matrix

$$\underline{\boldsymbol{H}}^{(k)} = \left(\underline{\boldsymbol{H}}^{(k,1)} \ldots \underline{\boldsymbol{H}}^{(k,K_\mathrm{a})}\right), k = 1\ldots K. \tag{6}$$

Now, the signal originating in $\underline{\boldsymbol{s}}$ of (3) and received at MS μ_k becomes

$$\underline{\boldsymbol{e}}^{(k)} = \underline{\boldsymbol{H}}^{(k)}\underline{\boldsymbol{s}}, k = 1\ldots K. \tag{7}$$

The K received signals $\underline{\boldsymbol{e}}^{(k)}$ of (7) can be arranged in a vector

$$\underline{\boldsymbol{e}} = \left(\underline{\boldsymbol{e}}^{(1)\mathrm{T}} \ldots \underline{\boldsymbol{e}}^{(K)\mathrm{T}}\right)^\mathrm{T} \tag{8}$$

of length $K(S+W-1)$, which is termed the total received signal and corresponds to one TDMA burst of TD–CDMA. The K matrices $\underline{\boldsymbol{H}}^{(k)}$ of (6) can be arranged in the $[K(S+W-1)]\times(K_\mathrm{a}S)$ matrix

$$\underline{\boldsymbol{H}} = \left(\underline{\boldsymbol{H}}^{(1)\mathrm{T}} \ldots \underline{\boldsymbol{H}}^{(K)\mathrm{T}}\right)^\mathrm{T}. \tag{9}$$

Then, the total received signal of (8) can be concisely expressed as

$$\underline{\boldsymbol{e}} = \underline{\boldsymbol{H}}\,\underline{\boldsymbol{s}}. \tag{10}$$

Note that the signal $\underline{\boldsymbol{e}}$ of (10) cannot be observed at a single MS. It consists of K sections $\underline{\boldsymbol{e}}^{(k)}$, see (8), which are received at the K different MSs.

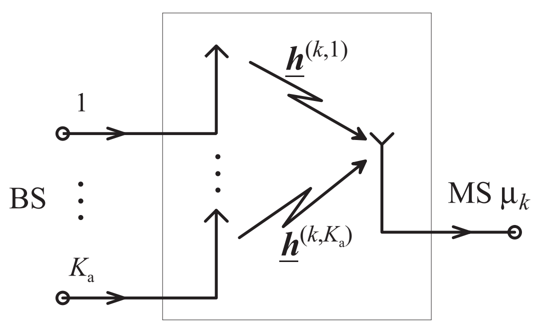

Fig. 1. Network with K_a input ports and one output port modeling the channel between the inputs of the K_a BS array elements and the antenna output of MS μ_k

III. Data transmission and detection

In Section II no specifications concerning the component values $\underline{s}_s^{(k_\mathrm{a})}$, $s = 1\ldots S$, $k_\mathrm{a} = 1\ldots K_\mathrm{a}$, of the transmit signals $\underline{\boldsymbol{s}}^{(k_\mathrm{a})}$ of (2), and, consequently, the component values of the total transmit signal $\underline{\boldsymbol{s}}$ of (3) were established. Now, these signals shall be determined in such a way that data transmission from the BS to the MSs μ_k, $k = 1\ldots K$, can be performed. It is assumed that per burst N data symbols have to be transmitted from the BS to each MS μ_k, $k = 1\ldots K$. The data symbols for MS μ_k are arranged in the data vector

$$\underline{\boldsymbol{d}}^{(k)} = \left(\underline{d}_1^{(k)} \ldots \underline{d}_N^{(k)}\right)^\mathrm{T}, k = 1\ldots K. \tag{11}$$

The K data vectors $\underline{\boldsymbol{d}}^{(k)}$ are put together to form the total data vector

$$\underline{\boldsymbol{d}} = \left(\underline{\boldsymbol{d}}^{(1)\mathrm{T}} \ldots \underline{\boldsymbol{d}}^{(K)\mathrm{T}}\right)^\mathrm{T} = \left(\underline{d}_1 \ldots \underline{d}_{KN}\right)^\mathrm{T} \tag{12}$$

of length KN.

In the downlink of conventional TD–CDMA [1] one of K CDMA codes

$$\underline{\boldsymbol{c}}^{(k)} = \left(\underline{c}_1^{(k)} \ldots \underline{c}_Q^{(k)}\right)^\mathrm{T}, k = 1\ldots K, \tag{13}$$

of length Q is uniquely assigned to each MS μ_k, $k = 1 \ldots K$, with all K CDMA codes $\underline{\boldsymbol{c}}^{(k)}$, $k = 1 \ldots K$, constituting an orthogonal set. Then, in the case of AWGN transmission, the optimum linear detector at each MS μ_k would consist of a filter matched to the CDMA code $\underline{\boldsymbol{c}}(k)$. As a main feature of the proposed scheme JT this simple and unexpensive detector shall be maintained also if the radio channels are no longer AWGN channels, but show multipath behaviour, and if antenna arrays are employed at the BSs. Nevertheless, it shall be required like in the case of employing JD that ISI and intracell MAI do not occur at the detector outputs. In what follows it will be shown that these goals can be achieved by properly designing the total transmit signal $\underline{\boldsymbol{s}}$ of (3). Like in conventional TD-CDMA [2], the length of the signals $\underline{\boldsymbol{s}}^{(k_\mathrm{a})}$ of (2) is assumed to be

$$S = QN\,. \tag{14}$$

Consequently, the lenght of $\underline{\boldsymbol{s}}$ of (3) becomes

$$K_\mathrm{a}S = K_\mathrm{a}QN\,. \tag{15}$$

As mentioned above, it is required that filtering of the signal $\underline{\boldsymbol{e}}^{(k)}$ of (7) received by MS μ_k with a filter matched to CDMA code $\underline{\boldsymbol{c}}^{(k)}$ yields the data vector $\underline{\boldsymbol{d}}^{(k)}$ of (11) intended for MS μ_k. With the CDMA codes $\underline{\boldsymbol{c}}^{(k)}$ of (13) the CDMA code matrix

$$\underline{\boldsymbol{C}} = \mathrm{blockdiag}\left[\underline{\boldsymbol{C}}^{(1)} \ldots \underline{\boldsymbol{C}}^{(K)}\right] \tag{16}$$

with

$$\begin{aligned}
\underline{\boldsymbol{C}}^{(k)} &= \left(\underline{C}_{i,j}^{(k)}\right),\ i = 1 \ldots S + W - 1, \\
&\quad\ j = 1 \ldots N,\ k = 1 \ldots K, \qquad (17) \\
\underline{C}_{i,j}^{(k)} &= \begin{cases} \underline{c}_{i-Q(j-1)}^{(k)} & \text{for } 1 \le i - Q(j-1) \le Q, \\ 0 & \text{else,} \end{cases}
\end{aligned}$$

can be established. Using this matrix, said filtering of the received signals $\underline{\boldsymbol{e}}^{(k)}$ is equivalent to forming the matrix–vector–product $\underline{\boldsymbol{C}}^{*\mathrm{T}}\underline{\boldsymbol{e}}$ with $\underline{\boldsymbol{e}}$ of (10). Then, the requirement that filtering of $\underline{\boldsymbol{e}}^{(k)}$ of (7) yields the data vectors $\underline{\boldsymbol{d}}^{(k)}$ of (11) at Ms μ_k can be expressed in the form

$$\underline{\boldsymbol{C}}^{*\mathrm{T}}\underline{\boldsymbol{e}} \overset{!}{=} \underline{\boldsymbol{d}}\,. \tag{18}$$

Substituting (10) in (18) and introducing the $(KN) \times (K_\mathrm{a}QN)$ matrix

$$\underline{\boldsymbol{B}} = \underline{\boldsymbol{C}}^{*\mathrm{T}}\underline{\boldsymbol{H}} \tag{19}$$

which is termed system matrix yields

$$\underline{\boldsymbol{B}}\,\underline{\boldsymbol{s}} = \underline{\boldsymbol{d}}\,. \tag{20}$$

In the BS transmitter the system matrix $\underline{\boldsymbol{B}}$ as well as the total data vector $\underline{\boldsymbol{d}}$ to be transmitted are known. Consequently, (20) can be considered as a system of equations by the solution of which the unknown components of $\underline{\boldsymbol{s}}$ can be determined. According to (15) the number of unknowns in this system of equations is equal to $K_\mathrm{a}QN$. On the other hand, the number of equations is equal to the number KN of elements of $\underline{\boldsymbol{d}}$ of (12). In what follows we assume

$$K_\mathrm{a}QN > KN\,, \tag{21}$$

which is also a reasonable requirement in conventional TD–CDMA employing JD in order to keep the SNR–degradation sufficiently low [7]. (21) means that the system of equations given by (20) is under–determined, and, consequently, has infinitely many solutions $\underline{\boldsymbol{s}}$. The solution of minimum energy $\|\underline{\boldsymbol{s}}\|^2/2$ is obtained by setting

$$\underline{\boldsymbol{s}} = \underline{\boldsymbol{B}}^{*\mathrm{T}}\left(\underline{\boldsymbol{B}}\underline{\boldsymbol{B}}^{*\mathrm{T}}\right)^{-1}\underline{\boldsymbol{d}} \tag{22}$$

[8]. This solution is favoured in this paper, because it is optimum in the sense that the transmit power and, consequently, multiple access interference are minimized. Interestingly, to each component $\underline{d}_i$ of $\underline{\boldsymbol{d}}$ of (12) corresponds a partial transmit signal $\underline{\boldsymbol{s}}^{(i)}$. In order to determine $\underline{\boldsymbol{s}}^{(i)}$ we introduce the partial data vector $\underline{\boldsymbol{d}}^{(i)}$ of length KN, the components of which are all zero with the exception of the i^{th} component, which is equal to the i^{th} component $\underline{d}_i$ of $\underline{\boldsymbol{d}}$, see (12). Then, we obtain

$$\underline{\boldsymbol{s}}^{(i)} = \underline{\boldsymbol{B}}^{*\mathrm{T}}\left(\underline{\boldsymbol{B}}\,\underline{\boldsymbol{B}}^{*\mathrm{T}}\right)^{-1}\underline{\boldsymbol{d}}^{(i)}\,, \tag{23}$$

and the total transmit signal can be written as

$$\underline{\boldsymbol{s}} = \sum_{i=1}^{KN}\underline{\boldsymbol{s}}^{(i)}\,. \tag{24}$$

IV. Performance Assessment of Joint Transmission TD–CDMA

As shown in Section III, the complexity of the TD–CDMA receivers in the MSs is greatly reduced if JT is applied instead of JD. However, besides receiver complexity also system performance is an important issue when comparing JT and JD in a fair manner. As the basis for such a comparison the average transmit energies per TDMA burst required in both cases for obtaining the same SIR (Signal to Interference Ratio) at the detector outputs are suited. In this comparison the following assumptions are made:

- For the elements of the data vector $\underline{\boldsymbol{d}}$ of (11) holds

$$\|\underline{d}_i\| = 1,\ k = 1 \ldots KN\,. \tag{25}$$

- For the elements of the CDMA codes $\underline{\boldsymbol{c}}^{(k)}$ of (13) holds

$$\|\underline{c}_q^{(k)}\| = 1,\, q = 1\ldots Q,\, k = 1\ldots K\,. \tag{26}$$

- From TDMA burst to TDMA burst the total data vector $\underline{\boldsymbol{d}}$ of (11) fluctuates in such a way that the data symbols $\underline{d}_i$ are all statistically independent of each other.
- The channel impulse responses $\underline{\boldsymbol{h}}^{(k,k_\mathrm{a})}$ of (1) are subject to stationary fast fading, whereas slow fading is eliminated by transmit power control.
- Intercell MAI at the receiver inputs of the MSs is modelled as uncorrelated complex Gaussian noise with the same variance σ^2 of real and imaginary part at all MSs μ_k, $k = 1\ldots K$.

Under the above assumptions we obtain the SIR

$$\gamma_\mathrm{JT} = \frac{1}{2Q\sigma^2} \tag{27}$$

at the outputs of the filters utilized, according to (18), as detectors in the case of JT at the MS receivers. In order to determine the average transmit energy T_JT per TDMA burst required to obtain the SIR of (27), first the channel impulse responses $\underline{\boldsymbol{h}}^{(k,k_\mathrm{a})}$ of (1) are kept fixed, and averaging is performed only with respect to the data vectors $\underline{\boldsymbol{d}}$ of (11). Due to the assumed statistical independence of the data symbols $\underline{d}_i$ the average energy of the total transmit signal $\underline{\boldsymbol{s}}$ of (22) is equal to the sum of the average energies of the partial transmit signals $\underline{\boldsymbol{s}}^{(i)}$ of (23). Therefore, with $\underset{\mathrm{d}}{\mathrm{E}}\{\}$ symbolizing averaging with respect to the fluctuating $\underline{\boldsymbol{d}}$ of (11), we obtain for the average energy $\tilde{T}_\mathrm{JT}$ of $\underline{\boldsymbol{s}}$

$$\tilde{T}_\mathrm{JT} = \frac{1}{2}\underset{\mathrm{d}}{\mathrm{E}}\left\{\underline{\boldsymbol{s}}^{*\mathrm{T}}\underline{\boldsymbol{s}}\right\} = \frac{1}{2}\sum_{i=1}^{KN}\underset{\mathrm{d}}{\mathrm{E}}\left\{\underline{\boldsymbol{s}}^{(i)*\mathrm{T}}\underline{\boldsymbol{s}}^{(i)}\right\}\,. \tag{28}$$

Due to (28) the energies of the partial transmit signals $\underline{\boldsymbol{s}}^{(i)}$ do not fluctuate and are given by the corresponding diagonal elements of the matrix

$$\left[\underline{\boldsymbol{B}}^{*\mathrm{T}}\left(\underline{\boldsymbol{B}}\,\underline{\boldsymbol{B}}^{*\mathrm{T}}\right)^{-1}\right]^{*\mathrm{T}}\underline{\boldsymbol{B}}^{*\mathrm{T}}\left(\underline{\boldsymbol{B}}\,\underline{\boldsymbol{B}}^{*\mathrm{T}}\right)^{-1} = \left[\left(\underline{\boldsymbol{B}}\,\underline{\boldsymbol{B}}^{*\mathrm{T}}\right)^{-1}\right]^{*\mathrm{T}}\,. \tag{29}$$

Then, with $[\,]_{i,i}$ designating the i^th diagonal element of the matrix in brackets, (28) can be rewritten in the form

$$\tilde{T}_\mathrm{JT} = \frac{1}{2}\sum_{i=1}^{KN}\left[\left(\underline{\boldsymbol{B}}\,\underline{\boldsymbol{B}}^{*\mathrm{T}}\right)^{-1}\right]_{i,i}\,. \tag{30}$$

Now, an additional averaging with respect to the channel impulse responses $\underline{\boldsymbol{h}}^{(k,k_\mathrm{a})}$, see (1), of the fast fading channels is performed, which is symbolized by $\underset{\mathrm{h}}{\mathrm{E}}\{\}$. Then we finally obtain from (30) the average transmit energy

$$T_\mathrm{JT} = \underset{\mathrm{h}}{\mathrm{E}}\left\{\tilde{T}_\mathrm{JT}\right\} = \frac{1}{2}\sum_{i=1}^{KN}\underset{\mathrm{h}}{\mathrm{E}}\left\{\left[\left(\underline{\boldsymbol{B}}\,\underline{\boldsymbol{B}}^{*\mathrm{T}}\right)^{-1}\right]_{i,i}\right\} \tag{31}$$

per burst of TD–CDMA employing JT.

The usual TD–CDMA downlink transmission scheme when utilizing conventional JD is shown in Fig. 2 [9]. With $\underline{\boldsymbol{d}}^{(k)}$ of (11) and $\underline{\boldsymbol{c}}^{(k)}$ of (13) the convolution products $\underline{\boldsymbol{d}}^{(k)} * \underline{\boldsymbol{c}}^{(k)}$ are formed at the BS. Each of these products is fed to a power amplifier of power gain $g^{(k)}$. The output signal of each of these amplifiers is put into one of the K input ports of a weighting network with K_a output ports. At each output port k_a, $k_\mathrm{a} = 1\ldots K_\mathrm{a}$, of this network a linear combination of the K input signals appears, which is then passed to the transmit antenna element k_a, $k_\mathrm{a} = 1\ldots K_\mathrm{a}$. The K_a linear combinations are determined by the K signal specific weight vectors

$$\underline{\boldsymbol{w}}^{(k)} = \left(\underline{w}_1^{(k)}\ldots\underline{w}_{K_\mathrm{a}}^{(k)}\right),\, k = 1\ldots K\,, \tag{32}$$

with each weight vector being assigned to one of the signals $\underline{\boldsymbol{d}}^{(k)} * \underline{\boldsymbol{c}}^{(k)}$ generated and then amplified at the BS. The K_a signals fed into the transmit antenna elements are then radiated to each of the K MSs μ_k, $k = 1\ldots K$, via a network as shown in Fig. 2. A method to advantageously determine the weight vectors $\underline{\boldsymbol{w}}^{(k)}$ of (32) is presented in [9].

As shown in [9] the transmission from the BS to MS μ_k can be described by a system matrix $\underline{\tilde{\boldsymbol{A}}}^{(k)}$ which is determined by the CDMA codes $\underline{\boldsymbol{c}}^{(k)}$, $k = 1\ldots K$, of (13), the power gains $g^{(k)}$, $k = 1\ldots K$, the weight vectors $\underline{\boldsymbol{w}}^{(k)}$, $k = 1\ldots K$ and the K_a channel impulse responses $\underline{\boldsymbol{h}}^{(k,k_\mathrm{a})}$, $k_\mathrm{a} = 1\ldots K_\mathrm{a}$, of (1). With $\underline{\tilde{\boldsymbol{A}}}^{(k)}$ and $\underline{\boldsymbol{d}}$ of (12) the signal generated at the antenna of MS μ_k by the BS can be expressed as [9]

$$\underline{\boldsymbol{e}}^{(k)} = \underline{\tilde{\boldsymbol{A}}}^{(k)}\underline{\boldsymbol{d}}\,. \tag{33}$$

The system matrix for the special case that all power gains $g^{(k)}$, $k = 1\ldots K$, are set to 1 is termed $\underline{\boldsymbol{A}}^{(k)}$.

With

$$\delta^{(k)} = \left[\left(\underline{\boldsymbol{A}}^{(k)\,*\mathrm{T}}\underline{\boldsymbol{A}}^{(k)}\right)^{-1}\right]_{\mathrm{int}[N(k-0.5)],\,\mathrm{int}[N(k-0.5)]} \tag{34}$$

the SIR of the estimate $\underline{\hat{\boldsymbol{d}}}^{(k)}$ of the data vector $\underline{\boldsymbol{d}}^{(k)}$ desired at the JD output of MS μ_k can be well approximated by the expression [7]

$$\gamma_\mathrm{JD}^{(k)} = \frac{g^{(k)}}{2\sigma^2\delta^{(k)}}\,. \tag{35}$$

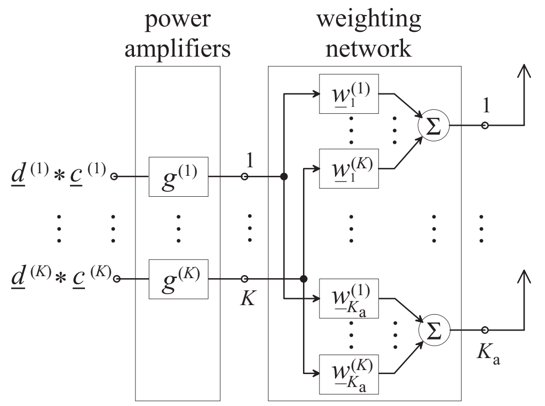

Fig. 2. TD-CDMA downlink transmission scheme suited for utilizing conventional JD at the MS receivers

In (35) it is assumed that the SNR degradations [7], which are slightly different for the data symbols in $\underline{\boldsymbol{d}}^{(k)}$ are replaced by the SNR degradation valid for the central data symbols of the TDMA burst.

As mentioned earlier in this section, JT and JD shall be compared based on equal SIRs at the detector outputs. Therefore, $\gamma_{\mathrm{JD}}^{(k)}$ of (35) has to be brought to the value of $\gamma_{\mathrm{JT}}^{(k)}$ of (27) by choosing the values

$$g^{(k)} = \frac{1}{Q}\delta^{(k)} \tag{36}$$

for the power gains. With (36) the energy transmitted by the BS to serve MS μ_k is [9]

$$T^{(k)} = \frac{1}{2} N g^{(k)} \underline{\boldsymbol{c}}^{(k)*\mathrm{T}} \underline{\boldsymbol{c}}^{(k)} \underline{\boldsymbol{w}}^{(k)*\mathrm{T}} \underline{\boldsymbol{w}}^{(k)} = \frac{N}{2Q} \delta^{(k)} \underline{\boldsymbol{c}}^{(k)*\mathrm{T}} \underline{\boldsymbol{c}}^{(k)} \underline{\boldsymbol{w}}^{(k)*\mathrm{T}} \underline{\boldsymbol{w}}^{(k)} . \tag{37}$$

From (37) follows the total transmit energy

$$\tilde{T}_{\mathrm{JD}} = \sum_{k=1}^{K} T^{(k)} \tag{38}$$

and the average transmit energy

$$T_{\mathrm{JD}} = \mathop{\mathrm{E}}_{\mathrm{h}}\left\{\tilde{T}_{JD}\right\} = \frac{N}{2Q} \sum_{k=1}^{K} \underline{\boldsymbol{c}}^{(k)*\mathrm{T}} \underline{\boldsymbol{c}}^{(k)} \underline{\boldsymbol{w}}^{(k)*\mathrm{T}} \underline{\boldsymbol{w}}^{(k)} \mathop{\mathrm{E}}_{\mathrm{h}}\left\{\delta^{(k)}\right\} \tag{39}$$

per TDMA burst in the case of JD.

The average transmit energies T_{JT} of (31) and T_{JD} of (39), respectively, required to obtain the same SIRs at the detector outputs when applying JT and JD, respectively, are suitable measures of the performance of these two transmission schemes. In Section V T_{JT} and T_{JD} will be determined by simulations for an example scenario.

V. Simulation results

As a basis for a fair comparison of time slotted CDMA employing JT and JD, respectively, the total transmit energies $\tilde{T}_{\mathrm{JT}}$ of (28) and $\tilde{T}_{\mathrm{JD}}$ of (38) required in both cases for obtaining the same SIR of (27) at the detector outputs will be determined. For the simulations the same assumptions as already described in Section IV are made. Further, the BS is equipped with a single antenna, that is K_{a} is equal to 1 and $\underline{w}_1^{(k)} = 1$, $k = 1 \ldots K$. The channel model utilized for the simulations is the well known rural area channel model (RA) proposed in [10].

For each possible realization of the channel impulse responses $\underline{\boldsymbol{h}}^{(k,k_{\mathrm{a}})}$ according to (1), a corresponding total transmit energy $\tilde{T}_{\mathrm{JT}}$ for JT and $\tilde{T}_{\mathrm{JD}}$ for JD, respectively, can be determined. For $N = 10$ and $Q = 16$, Fig. 3 shows the cumulative distribution function (CDF) of $\tilde{T}_{\mathrm{JT}}$ and $\tilde{T}_{\mathrm{JD}}$, respectively, if the channel impulse responses $\underline{\boldsymbol{h}}^{(k,k_{\mathrm{a}})}$ are randomly varied according to the RA channel model. The number K of served MSs is chosen between 2 and 8. In order to fairly compare $\tilde{T}_{\mathrm{JT}}$ and $\tilde{T}_{\mathrm{JD}}$ for several K, the total transmit energies depicted in Fig. 3 are normalized by the total number of transmitted data symbols. That is, the transmit energies $\tilde{T}_{\mathrm{JT}}/(NK)$ and $\tilde{T}_{\mathrm{JD}}/(NK)$ per data symbol are considered. Evidently, for both, JT and JD, the transmit energies $\tilde{T}_{\mathrm{JT}}/(NK)$ and $\tilde{T}_{\mathrm{JD}}/(NK)$ per data symbol increase with increasing K. In the case of JT, this effects directly results from (20). With increasing K, the number of individual equations in (20), that is the number of restrictions for $\underline{\boldsymbol{s}}$, also increases while the number of unknowns is fixed. Consequently, as the minimization of the energy $||\underline{\boldsymbol{s}}||^2/2$ of the total transmit signal $\underline{\boldsymbol{s}}$ has to be performed with regards to the increasing number of restrictions for $\underline{\boldsymbol{s}}$, that is the algorithm for determining $\underline{\boldsymbol{s}}$ has less degrees of freedom to minimize $||\underline{\boldsymbol{s}}||^2/2$, the achieved minimum energy for $\underline{\boldsymbol{s}}$ according to (22) also increases. For JD, the increasing transmit energy $\tilde{T}_{\mathrm{JD}}/(NK)$ per data symbol results from the increasing SNR-degradation [7].

When comparing JT and JD for a fixed K, almost no differences between JT and JD can be observed if $K = 2$ or $K = 4$. For $K = 6$ and $K = 8$, JD is slightly superior to JT with respect to the transmit energy per data symbol.

Fig. 4 shows the average transmit energies $T_{\mathrm{JT}}/(NK)$ and $T_{\mathrm{JD}}/(NK)$ per data symbol with $N = 10$ and $Q = 16$ depending on the number K of MSs. As already depicted in Fig. 3, for $K = 2$ and $K = 4$, $T_{\mathrm{JT}}/(NK)$ and $T_{\mathrm{JD}}/(NK)$ are very similar. In the case of $K = 6$ and $K = 8$, respectively, JT needs a slightly higher transmit energy $T_{\mathrm{JT}}/(NK)$ per data symbol than

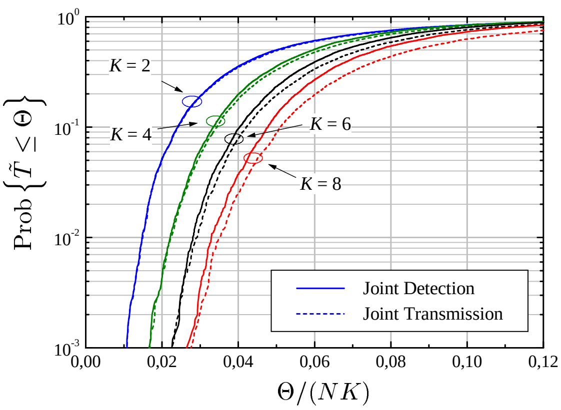

Fig. 3. CDF $\text{Prob}\left\{\tilde{T} \le \Theta\right\}$ of $\tilde{T} = \tilde{T}_{\text{JD}}$ and $\tilde{T} = \tilde{T}_{\text{JT}}$; $N = 10$, $Q = 16$, channel model RA

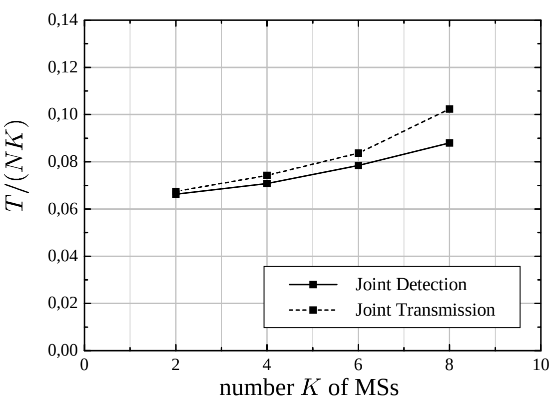

Fig. 4. Average transmit energy $T = T_{\text{JD}}$ of JD and $T = T_{\text{JT}}$ of JT; $N = 10$, $Q = 16$, channel model RA

JD which can for example be characterized by the ratio $T_{\text{JT}}/T_{\text{JD}} = 1.16$ for $K = 8$.

VI. Conclusions

In this paper a novel downlink scheme for time slotted CDMA is proposed, which utilizes the knowledge of the channel impulse responses at the BS transmitter in such a way that at the receivers of the MSs channel estimators are no longer required. Consequently, the computational expense of the data detection is dramatically reduced. Besides to lower receiver complexity, the presented scheme simultaneously enhances the system capacity, because no system resources are spent for the transmission of training signals.

When comparing JT with the state-of-the-art concept JD, it can be shown that the necessary average transmit energies of both schemes for obtaining the same SIR at the detector outputs are very similar. Only for $K = 6$ and $K = 8$, respectively, the average transmit energy for JT is slightly higher than the average transmit energy for JD. This is the low prize which must be paid for the simple receiver structure and enhancement of system capacity when applying JT as mentioned before. Overall, the advantages of JT predominate very much. JT is a very attractive approach for the downlink of time slotted CDMA.

Acknowledgement

The authors are indebted to Deutsche Forschungsgemeinschaft (DFG) for sponsoring part of this work within “DFG Schwerpunktprogramm Mobilkommunikation”. They are also grateful to the staffs of the Central Computer Facility (RHRK) and of the Center for Microelectronics of the University of Kaiserslautern for sustained technical support. Stimulating discussions with their colleagues at Siemens AG are gratefully acknowledged.

References

[1] A. Klein, *Multi–user detection of CDMA–signals — algorithms and their application to cellular mobile radio*, vol. 10 of *Fortschrittberichte VDI*, VDI–Verlag, Düsseldorf, 1996.

[2] A. Papathanassiou, I. Furio, J.J. Blanz, and P.W. Baier, “Smart antennas with two-dimensional array configurations for performance enhancement of a joint detection CDMA mobile radio system,” *Wireless Personal Communications*, vol. 11, no. 1, pp. 89–108, 1999.

[3] http://www.3gpp.org.

[4] Technical specification of IMT-2000 CDMA TDD (TD-SCDMA) by China Wireless Telecommunications Standard (CWTS). Published in Internet under the URL: http://www.cwts.org, 1999.

[5] H. Matsutani, Y. Sanada, and M. Nakagawa, “A forward link intracell orthogonalization technique using multicarrier predecorrelation for CDMA wireless local communication system,” in *IEEE 8th International Symposium on Personal, Indoor and Mobile Radio Communications (PIMRC’97)*, Helsinki, 1997, pp. 125–129.

[6] A. Noll-Barreto and G. Fettweis, “Performance improvement in DS-spread spectrum CDMA systems using a pre- and a post-rake,” in *2000 International Zurich Seminar on Broadband Communications (IZS’2000)*, Zurich, 2000, pp. 39–46.

[7] A. Papathanassiou, *Adaptive antennas for mobile radio systems using Time Division CDMA and joint detection*, Dissertation, Lehrstuhl für hochfrequente Signalübertragung und -verarbeitung. Universität Kaiserslautern, to be published in 2000.

[8] A. Ben-Israel and T.N.E. Greville, *Generalized inverses: theory and applications*, Wiley–Interscience, New York, 1974.

[9] Y. Lu and P.W. Baier, “Performance of adaptive antennas for the TD–CDMA downlink under special consideration of multidirectional channels and CDMA code pooling,” *accepted for publication in International Journal of Electronics and Communications (AEÜ: Archiv für Elektronik und Übertragungstechnik)*, 2000.

[10] COST 207, *Digital land mobile radio communications*, Office for Official Publications of the European Communities, Luxembourg, 1989.

[BMWT00] Baier, P. W.; Meurer, M.; Weber, T.; Tröger, H.: "Joint transmission (JT), an alternative rationale for the downlink of time division CDMA using multi-element transmit antennas". *Proc. IEEE 6th International Symposium on Spread Spectrum Techniques & Applications (ISSSTA'00)*, Bd. 1, Parsippany, 2000, S. 1–5.

IEEE 6th Int. Symp. on Spread-Spectrum Tech. & Appli., NJIT, New Jersey, USA, Sept. 6-8, 2000

Joint Transmission (JT), an alternative rationale for the downlink of Time Division CDMA using multi-element transmit antennas

P.W. Baier, M. Meurer, T. Weber, H. Tröger
Research Group for RF Communications,
University of Kaiserslautern,
P.O. Box 3049, D–67653 Kaiserslautern, Germany
e–mail: baier@rhrk.uni-kl.de

Abstract — **In the 3rd Generation Partnership Project (3GPP) Time Division CDMA (TD–CDMA) has been selected as the air interface for the TDD (Time Division Duplexing) bands of 3rd generation (3G) mobile radio systems . In the case of TDD the same channel impulse responses are valid for both the uplink and the downlink. In state–of–the–art TD–CDMA characterized by joint data detection (JD) this equality cannot be exploited for enhancing system performance and reducing system complexity. In the paper a novel TD–CDMA downlink transmission scheme is proposed. This scheme is termed joint transmission (JT). It utilizes the knowledge of the channel impulse responses gained by channel estimation at the base station in such a way that channel estimators are no longer required at the mobile stations and the computational expense of data detection is dramatically reduced. The scheme easily lends itself to the utilization of multi-element transmit antennas. Further, its application is not restricted to systems of the type TD–CDMA.**

I. Introduction

TD-CDMA [1] is based on time slotted CDMA, which utilizes a combination of the basic multiple access schemes FDMA, TDMA and CDMA, and is a promising air interface for third generation (3G) mobile radio systems. This air interface has been selected by 3GPP [2] as the standard for the Time Division Duplexing (TDD) mode of the 3G system International Mobile Telecommunications 2000 (IMT-2000). Also the Chinese 3G air interface TD-SCDMA [3] relies on time slotted CDMA and TDD and is closely related to TD-CDMA. In the case of TDD the same channel impulse responses are valid for both the uplink and the downlink, if – and this is assumed in what follows – the time elapsing between uplink and downlink transmissions is sufficiently small compared to the coherence time of the mobile radio channels. This equality of uplink and downlink channel impulse responses cannot be exploited in state–of–the–art TD-CDMA [1], which requires channel estimators at the receivers of both the base stations (BS) and the mobile stations (MS). This is true because the knowledge of the channel impulse responses is needed for performing joint detection (JD) [4], which is the preferred detection scheme in conventional TD-CDMA, because JD completely eliminates intracell multiple access interference (MAI) and intersymbol interference (ISI) . In this paper, a novel downlink transmission technique for TD-CDMA is proposed, which needs channel estimators only in the uplink receivers and which for the downlink transmission utilizes the knowledge of the channel impulse reponses at the BS transmitter in such a way that channel estimators are no longer required at the receivers of the MSs. In addition, compared to conventional TD-CDMA characterized by using JD, the computational expense of data detection in the MSs is dramatically reduced, and simultaneously system performance, especially capacity, is enhanced by this transmission scheme. The crux of the proposed scheme consists in determining one common transmit signal at each BS for the service of all MSs to be supported by this BS, which, after having passed the mobile radio channels, at each MS yields the data sent for this MS by simple linear filtering with a time invariant filter. The authors term this approach joint transmission (JT). Its rationale is the inverse of the one followed in JD, where a received signal common to all users is jointly processed at the receiver in order to obtain the data sent by the individual transmitters. In a way JT is related to known CDMA concepts using transmit signals which originate by predistortion of CDMA coded signals under consideration of the known channel impulse responses [5, 6, 7, 8, 9]. However, JT is more general, because the transmit signals are directly generated and do not result by first generating and then distorting CDMA coded signals. Therefore, the application of the proposed scheme JT is not restricted to time slotted CDMA systems, but is also applicable to other systems which have a TDMA component.

The paper is structured as follows. In Section II the signal transmission model of JT is developed. Section III deals with data transmission and detection in a general downlink system utilizing JT. In Section IV the application of JT in the TD–CDMA downlink is considered. The topic of Section V is a brief performance assessment of JT in TD-CDMA. Finally, the paper is concluded by Section VI. In the paper the time discrete equivalent low–pass representation of signals is chosen. Consequently, signals and channel impulse responses are represented by complex vectors or matrices [4], which are printed in bold face.

II. Signal Transmission model

At the BS an array of K_a transmit antenna elements is utilized, whereas each MS μ_u, $u = 1 \dots U$, disposes of a one element receiving antenna. For each MS this situation can be modeled by a MS specific network with K_a input ports and a single output port, see Fig. 1. In this network the channel impulse response

$$\underline{\boldsymbol{h}}^{(u,k_\mathrm{a})} = \left(\underline{h}_1^{(u,k_\mathrm{a})} \dots \underline{h}_W^{(u,k_\mathrm{a})}\right)^\mathrm{T}, u = 1 \dots U, \quad k_\mathrm{a} = 1 \dots K_\mathrm{a} \tag{1}$$

of length W characterizes signal transmission between the input of the transmit antenna element k_a and the output of the receiving antenna of MS μ_u. Into each of the K_a transmit antenna elements a signal

$$\underline{\boldsymbol{s}}^{(k_\mathrm{a})} = \left(\underline{s}_1^{(k_\mathrm{a})} \dots \underline{s}_S^{(k_\mathrm{a})}\right)^\mathrm{T}, k_\mathrm{a} = 1 \dots K_\mathrm{a}, \tag{2}$$

of length S is fed. The K_a signals $\underline{\boldsymbol{s}}^{(k_\mathrm{a})}$ of (2) can be compiled to form the total transmit signal

$$\underline{\boldsymbol{s}} = \left(\underline{\boldsymbol{s}}^{(1)\mathrm{T}} \dots \underline{\boldsymbol{s}}^{(K_\mathrm{a})\mathrm{T}}\right)^\mathrm{T} \tag{3}$$

of length $K_\mathrm{a}S$. $\underline{\boldsymbol{s}}$ of (3) represents the transmission of one TDMA burst. With the channel impulse responses $\underline{\boldsymbol{h}}^{(u,k_\mathrm{a})}$ of (1) the $(S+W-1)\times S$ matrices

$$\begin{aligned}
\underline{\boldsymbol{H}}^{(u,k_\mathrm{a})} &= \left(\underline{H}_{i,j}^{(u,k_\mathrm{a})}\right), i = 1 \dots S+W-1, \\
& \quad j = 1 \dots S, \\
\underline{H}_{i,j}^{(u,k_\mathrm{a})} &= \begin{cases} \underline{h}_{i-j+1}^{(u,k_\mathrm{a})} & \text{for } 1 \le i-j+1 \le W, \\ 0 & \text{otherwise,} \end{cases} && (4) \\
& \quad u = 1 \dots U, k_\mathrm{a} = 1 \dots K_\mathrm{a}, && (5)
\end{aligned}$$

can be formed. The K_a matrices $\underline{\boldsymbol{H}}^{(u,k_\mathrm{a})}$ valid for a given value u, that is for a given MS μ_u, can be arranged in an $(S+W-1)\times(K_\mathrm{a}S)$ matrix

$$\underline{\boldsymbol{H}}^{(u)} = \left(\underline{\boldsymbol{H}}^{(u,1)} \dots \underline{\boldsymbol{H}}^{(u,K_\mathrm{a})}\right), u = 1 \dots U. \tag{6}$$

Now, the signal originating in $\underline{\boldsymbol{s}}$ of (3) and received at MS μ_u can be represented by a column vector

$$\underline{\boldsymbol{e}}^{(u)} = \underline{\boldsymbol{H}}^{(u)}\underline{\boldsymbol{s}}, u = 1 \dots U \tag{7}$$

of length $S+W-1$. The U received signals $\underline{\boldsymbol{e}}^{(u)}$ of (7) can be arranged in a vector

$$\underline{\boldsymbol{e}} = \left(\underline{\boldsymbol{e}}^{(1)\mathrm{T}} \dots \underline{\boldsymbol{e}}^{(U)\mathrm{T}}\right)^\mathrm{T} \tag{8}$$

of length $U(S+W-1)$, which is termed the total received signal and corresponds to the reception of one TDMA burst. The U matrices $\underline{\boldsymbol{H}}^{(u)}$ of (6) can be arranged in the $[U(S+W-1)]\times(K_\mathrm{a}S)$ matrix

$$\underline{\boldsymbol{H}} = \left(\underline{\boldsymbol{H}}^{(1)\mathrm{T}} \dots \underline{\boldsymbol{H}}^{(U)\mathrm{T}}\right)^\mathrm{T}, \tag{9}$$

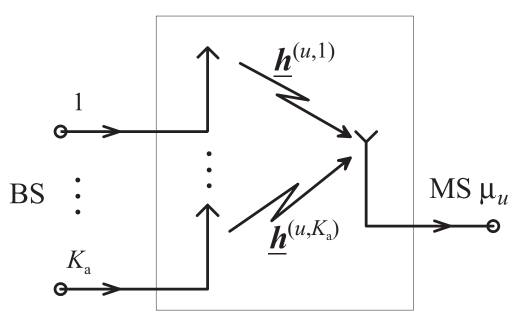

Fig. 1: Network with K_a input ports and one output port modeling the channel between the inputs of the K_a BS array elements and the antenna output of MS μ_u

which is termed channel matrix. In the case of time variant channels the elements of $\underline{\boldsymbol{H}}$ are non-constant. When designing a system it should be taken care that the correlation duration of the channels is sufficiently larger than the duration of the TDMA bursts. With $\underline{\boldsymbol{H}}$ of (9) the total received signal of (8) can be concisely expressed as

$$\underline{\boldsymbol{e}} = \underline{\boldsymbol{H}}\,\underline{\boldsymbol{s}}. \tag{10}$$

Note that the whole signal $\underline{\boldsymbol{e}}$ of (10) cannot be observed at a single MS. It consists of U received partial signals $\underline{\boldsymbol{e}}^{(u)}$, see (8), with each of these signals being received only at the corresponding MS μ_u.

III. Data transmission and detection, General case

In Section II the component values $\underline{s}_s^{(k_\mathrm{a})}$, $s = 1 \dots S$, $k_\mathrm{a} = 1 \dots K_\mathrm{a}$, of the transmit signals $\underline{\boldsymbol{s}}^{(k_\mathrm{a})}$ of (2), and, therefore, the component values of the total transmit signal $\underline{\boldsymbol{s}}$ of (3) have not yet been specified. In this section these values shall be determined in such a way that data transmission from the BS to the MSs μ_u, $u = 1 \dots U$, can be performed. It is assumed that per TDMA burst N_u data symbols have to be transmitted from the BS to the MS μ_u, $u = 1 \dots U$. The N_u data symbols meant for MS μ_u are arranged in the data vector

$$\underline{\boldsymbol{d}}^{(u)} = \left(\underline{d}_1^{(u)} \dots \underline{d}_{N_u}^{(u)}\right)^\mathrm{T}, u = 1 \dots U. \tag{11}$$

The U data vectors $\underline{\boldsymbol{d}}^{(u)}$ of (11) are put together to form, with the total number

$$N_\mathrm{t} = \sum_{u=1}^{U} N_u \tag{12}$$

of data symbols, the total data vector

$$\underline{\boldsymbol{d}} = \left(\underline{\boldsymbol{d}}^{(1)\mathrm{T}} \dots \underline{\boldsymbol{d}}^{(U)\mathrm{T}}\right)^\mathrm{T} = \left(\underline{d}_1 \dots \underline{d}_{N_\mathrm{t}}\right)^\mathrm{T} \tag{13}$$

of length N_t. With $\underline{\boldsymbol{s}}$ of (3), $\underline{\boldsymbol{d}}$ of (13) and a $K_\mathrm{a}S \times N_\mathrm{t}$-matrix $\underline{\boldsymbol{M}}$ to be determined in what follows, the linear modulation process to be performed at the transmitter can be represented by a matrix-vector operation

$$\underline{\boldsymbol{s}} = \underline{\boldsymbol{M}}\,\underline{\boldsymbol{d}}. \tag{14}$$

The matrix $\underline{\boldsymbol{M}}$ is termed modulator matrix and has to be known at the transmitter as a prerequisite for performing modulation.

In order to perform data detection at the MS μ_u a $N_u \times (S+W-1)$ matrix $\underline{\boldsymbol{D}}^{(u)}$ is multiplied by the partial signal $\underline{\boldsymbol{e}}^{(u)}$, see (7), received at this MS. The matrix $\underline{\boldsymbol{D}}^{(u)}$ has to be a priori agreed upon by the BS and MS μ_u. Therefore, $\underline{\boldsymbol{D}}^{(u)}$ can be assumed to be known both at the transmitter and the receiver. However, a great variety of possibilities to choose this matrix exists. This implies a high degree of freedom to the system designer, and finding optimum matrices $\underline{\boldsymbol{D}}^{(u)}$ is a challenge for further research. One of the possibilities to chose the matrices $\underline{\boldsymbol{D}}^{(u)}$ is considered in Section IV. Concerning the total transmit signal $\underline{\boldsymbol{s}}$ of (3) this signal has to be chosen such that said matrix-vector multiplication yields the desired data vector $\underline{\boldsymbol{d}}^{(u)}$ free from ISI and intracell MAI, that is

$$\underline{\boldsymbol{d}}^{(u)} = \underline{\boldsymbol{D}}^{(u)}\,\underline{\boldsymbol{e}}^{(u)}, \; u = 1 \dots U. \tag{15}$$

$$
\underline{\boldsymbol{D}} = \begin{pmatrix}
\underline{\boldsymbol{D}}^{(1)}_{1,1} & \underline{\boldsymbol{D}}^{(1)}_{N_1,1} & 0 & 0 & 0 & 0 \\
\underline{\boldsymbol{D}}^{(1)}_{1,2} & \underline{\boldsymbol{D}}^{(1)}_{N_1,2} & 0 & 0 & 0 & 0 \\
\underline{\boldsymbol{D}}^{(1)}_{1,3} & \underline{\boldsymbol{D}}^{(1)}_{N_1,3} & 0 & 0 & 0 & 0 \\
\underline{\boldsymbol{D}}^{(1)}_{1,S+W-1} & \underline{\boldsymbol{D}}^{(1)}_{N_1,S+W-1} & 0 & 0 & 0 & 0 \\
0 & 0 & \underline{\boldsymbol{D}}^{(2)}_{N_2,1} & 0 & 0 & 0 \\
0 & 0 & \underline{\boldsymbol{D}}^{(2)}_{N_2,2} & 0 & 0 & 0 \\
0 & 0 & \underline{\boldsymbol{D}}^{(2)}_{N_2,3} & 0 & 0 & 0 \\
0 & 0 & \underline{\boldsymbol{D}}^{(2)}_{N_2,S+W-1} & 0 & 0 & 0 \\
0 & 0 & 0 & \underline{\boldsymbol{D}}^{(U)}_{1,1} & \underline{\boldsymbol{D}}^{(U)}_{2,1} & \underline{\boldsymbol{D}}^{(U)}_{N_3,1} \\
0 & 0 & 0 & \underline{\boldsymbol{D}}^{(U)}_{1,2} & \underline{\boldsymbol{D}}^{(U)}_{2,2} & \underline{\boldsymbol{D}}^{(U)}_{N_3,2} \\
0 & 0 & 0 & \underline{\boldsymbol{D}}^{(U)}_{1,3} & \underline{\boldsymbol{D}}^{(U)}_{2,3} & \underline{\boldsymbol{D}}^{(U)}_{N_3,3} \\
0 & 0 & 0 & \underline{\boldsymbol{D}}^{(U)}_{1,S+W-1} & \underline{\boldsymbol{D}}^{(U)}_{2,S+W-1} & \underline{\boldsymbol{D}}^{(U)}_{N_3,S+W-1}
\end{pmatrix}^{\mathrm{T}}
$$

Fig. 2: Structure of the detector matrix $\underline{\boldsymbol{D}}$ for the example given by (18)

Substituting (7) in (15) yields

$$\underline{\boldsymbol{d}}^{(u)} = \underline{\boldsymbol{D}}^{(u)}\underline{\boldsymbol{H}}^{(u)}\underline{\boldsymbol{s}},\ u = 1 \dots U. \tag{16}$$

The U matrices $\underline{\boldsymbol{D}}^{(u)}$, $u = 1 \dots U$, can be put together to form the $N_\mathrm{t} \times [U(S+W-1)]$ matrix

$$\underline{\boldsymbol{D}} = \mathrm{blockdiag}\left[\underline{\boldsymbol{D}}^{(1)} \dots \underline{\boldsymbol{D}}^{(U)}\right] \tag{17}$$

which is termed detector matrix. As an example, the special case

$$S+W-1 = 4,\ U = 3,\ N_1 = 2,\ N_2 = 1,\ N_3 = 3 \tag{18}$$

is briefly considered. In this case the detector matrix takes the form illustrated in Fig. 2.

With the matrix $\underline{\boldsymbol{D}}$ of (17) and the matrix $\underline{\boldsymbol{H}}$ of (9) the matrix

$$\underline{\boldsymbol{B}} = \underline{\boldsymbol{D}}\,\underline{\boldsymbol{H}} \tag{19}$$

can be established, which is termed system matrix. Because both $\underline{\boldsymbol{D}}$ and $\underline{\boldsymbol{H}}$ are known at the transmitter, this is also true for $\underline{\boldsymbol{B}}$ of (19). With $\underline{\boldsymbol{B}}$ the U matrix-vector equations given by (16) can be put together to the single matrix-vector equation

$$\underline{\boldsymbol{d}} = \underline{\boldsymbol{B}}\,\underline{\boldsymbol{s}}. \tag{20}$$

In (20), $\underline{\boldsymbol{B}}$ and $\underline{\boldsymbol{d}}$ are known at the transmitter. Therefore, (20) can be considered as a system of equations by the solution of which the modulator matrix $\underline{\boldsymbol{M}}$ appearing in (14) and, based on $\underline{\boldsymbol{d}}$ of (13), the component values of the total transmit signal $\underline{\boldsymbol{s}}$ of (3) can be determined.

In (20) the total number of equations is N_t and the total number of unknowns is $K_\mathrm{a}S$. When determining the modulator matrix $\underline{\boldsymbol{M}}$ and the component values of $\underline{\boldsymbol{s}}$, the three cases

$$N_\mathrm{t} \lesseqqgtr K_\mathrm{a}S, \tag{21}$$

have to be distinguished. If "<" holds in (21), the system of equations (20) is under-determined and has infinitely many solutions $\underline{\boldsymbol{s}}$. One possible solution is in this case

$$\underline{\boldsymbol{s}} = \underbrace{\underline{\boldsymbol{B}}^{*\mathrm{T}}\left(\underline{\boldsymbol{B}}\,\underline{\boldsymbol{B}}^{*\mathrm{T}}\right)^{-1}}_{\underline{\boldsymbol{M}}}\underline{\boldsymbol{d}}. \tag{22}$$

This is the solution of minimum energy $\|\underline{\boldsymbol{s}}\|^2/2$ [10] and is optimum in the sense that the transmit power and, consequently, the multiple access interference caused by each BS in the cellular system are minimized.

If "=" is true in (21), the system of equations (20) is determined and has the unique solution

$$\underline{\boldsymbol{s}} = \underbrace{\underline{\boldsymbol{B}}^{-1}}_{\underline{\boldsymbol{M}}}\underline{\boldsymbol{d}}. \tag{23}$$

Finally, if ">" is true in (21), the system of equations (20) is over-determined and can be, in the Gaussian sense, approximately solved by

$$\underline{\boldsymbol{s}} = \underbrace{\left(\underline{\boldsymbol{B}}^{*\mathrm{T}}\underline{\boldsymbol{B}}\right)^{-1}\underline{\boldsymbol{B}}^{*\mathrm{T}}}_{\underline{\boldsymbol{M}}}\underline{\boldsymbol{d}}. \tag{24}$$

By (21) to (24) the problem posed by (14) concerning the determination of the modulator matrix $\underline{\boldsymbol{M}}$ has been solved.

In Fig. 3 the conventional transmission scheme, which for instance is applied in conventional TD–CDMA, and the novel transmission scheme JT are compared with each other. As shown in Fig. 3a and 3b, in both cases the transmission is determined by the three processes modulation, transmission over the mobile radio channel and detection, which are described by the matrices $\underline{\boldsymbol{M}}$, $\underline{\boldsymbol{H}}$ and $\underline{\boldsymbol{D}}$, respectively. Prior to detection a noise signal given by a vector $\underline{\boldsymbol{n}}$ of length $U(S+W-1)$ and representing thermal noise and intercell MAI is fed into the system. At the detector output an estimate $\hat{\underline{\boldsymbol{d}}}$ of the total data vector $\underline{\boldsymbol{d}}$ of (13) is obtained.

In the well known case of conventional transmission, see Fig. 3a, the modulator matrix $\underline{\boldsymbol{M}}$ is a priori given and determines, together with the channel matrix $\underline{\boldsymbol{H}}$, the system matrix [4]

$$\underline{\boldsymbol{A}} = \underline{\boldsymbol{H}}\,\underline{\boldsymbol{M}}. \tag{25}$$

The detector matrix is derived from $\underline{\boldsymbol{A}}$ of (25) and takes for instance the form [4]

$$\underline{\boldsymbol{D}} = \left(\underline{\boldsymbol{A}}^{*\mathrm{T}}\underline{\boldsymbol{A}}\right)^{-1}\underline{\boldsymbol{A}}^{*\mathrm{T}}, \tag{26}$$

if zero forcing linear equalization is utilized. If a multi-element antenna is applied at the BS, that is $K_\mathrm{a} > 1$, the antenna

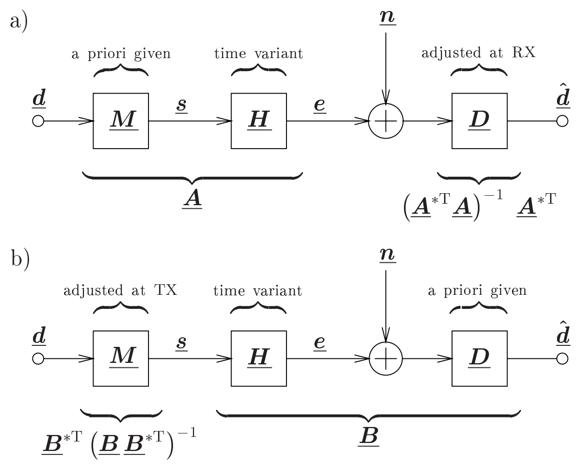

Fig. 3: Transmission schemes
a) conventional, used e.g. in state-of-the-art TD–CDMA
b) novel scheme joint transmission (JT)

weights have to be included in the channel matrix, see e.g. [11]. In the considered downlink situation only a section $\underline{\boldsymbol{A}}^{(u)}$ of the matrix $\underline{\boldsymbol{A}}$ of (25) and only a section $\underline{\boldsymbol{e}}^{(u)}$ of the total received vector $\underline{\boldsymbol{e}}$ of (8) are available at each MS μ_u, $u = 1 \ldots U$. This has to be considered, if the system shall be modeled in a realistic way.

In the case of JT the detector matrix $\underline{\boldsymbol{D}}$ is a priori given and determines, together with the channel matrix $\underline{\boldsymbol{H}}$, the system matrix $\underline{\boldsymbol{B}}$ of (19). The detector matrix $\underline{\boldsymbol{D}}$ is chosen for instance according to (22).

IV. Data transmission and detection, Special case TD–CDMA

Now

$$N_u = N \;\; \forall u = 1 \ldots U \tag{27}$$

is assumed. In the downlink of conventional TD–CDMA [1] one of U CDMA codes

$$\underline{\boldsymbol{c}}^{(u)} = \left(\underline{c}_1^{(u)} \ldots \underline{c}_Q^{(u)}\right)^{\mathrm{T}}, u = 1 \ldots U, \tag{28}$$

of length Q is uniquely assigned to each MS μ_u, $u = 1 \ldots U$, with all U CDMA codes $\underline{\boldsymbol{c}}^{(u)}$, $u = 1 \ldots U$, constituting an orthogonal set. Then, in the case of AWGN channels, the optimum linear detector at each MS μ_u would consist of a filter matched to the CDMA code $\underline{\boldsymbol{c}}^{(u)}$. As a main feature of the proposed scheme JT in connection with TD–CDMA [12] this simple and inexpensive detector shall be maintained also if the radio channels are no longer AWGN channels, but show multipath behaviour. Nevertheless, it shall be required like in the case of employing JD that ISI and intracell MAI do not occur at the detector outputs. Like in conventional TD-CDMA [1], the length of the K_a signals $\underline{\boldsymbol{s}}^{(k_\mathrm{a})}$ of (2) is assumed to be

$$S = QN. \tag{29}$$

Consequently, the lenght of $\underline{\boldsymbol{s}}$ of (3) becomes

$$K_\mathrm{a} S = K_\mathrm{a} QN. \tag{30}$$

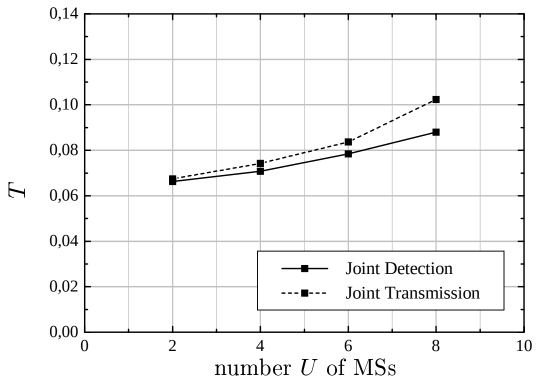

Fig. 4: Average transmit energy per symbol $T = T_\mathrm{JD}$ of JD and $T = T_\mathrm{JT}$ of JT versus number U of MSs; $N = 10$, $Q = 16$, channel model RA [13]

As shown in [12] the matrix $\underline{\boldsymbol{D}}$ of (17), which appears in (19), now takes the form

$$\underline{\boldsymbol{D}} = \mathrm{blockdiag}\left[\underline{\boldsymbol{C}}^{(1)} \ldots \underline{\boldsymbol{C}}^{(U)}\right]^{*\mathrm{T}} \tag{31}$$

with

$$\underline{\boldsymbol{C}}^{(u)} = \underline{\boldsymbol{D}}^{(u)\,*\mathrm{T}} \tag{32}$$

and

$$\begin{aligned} \underline{\boldsymbol{C}}^{(u)} &= \left(\underline{C}_{i,j}^{(u)}\right), \; i = 1 \ldots S + W - 1, \\ & \quad\; j = 1 \ldots N, \; u = 1 \ldots u, \\ \underline{C}_{i,j}^{(u)} &= \begin{cases} \underline{c}_{i-Q(j-1)}^{(u)} & \text{for } 1 \le i - Q(j-1) \le Q, \\ 0 & \text{else.} \end{cases} \end{aligned} \tag{33}$$

According to (30) the number of unknowns in the system of equations (20) is equal to $K_\mathrm{a} QN$. On the other hand, the number of equations is equal to the number UN of elements of $\underline{\boldsymbol{d}}$ of (13). In what follows we assume

$$K_\mathrm{a} QN > UN, \tag{34}$$

which is also a reasonable requirement in conventional TD–CDMA employing JD in order to keep the SNR–degradation sufficiently low [4]. (34) means that the system of equations given by (20) is under–determined.

V. Performance Assessment of Joint Transmission in TD–CDMA

As shown in Section IV, the complexity of the TD–CDMA receivers in the MSs is greatly reduced if JT is applied instead of JD. However, besides the receiver complexity also the system performance is an important issue when comparing JT and JD in a fair manner. As the basis for such a comparison the average transmit energies T_JT and T_JD, respectively, required per symbol in each case for obtaining the same SIR (Signal to Interference Ratio) at the detector outputs are suited. In this comparison the following assumptions are made:

- For the elements of the data vector $\underline{\boldsymbol{d}}$ of (13) holds

$$\|\underline{d}_i\| = 1,\ \forall i = 1 \dots UN\,. \tag{35}$$

- For the elements of the CDMA codes $\underline{\boldsymbol{c}}^{(u)}$ of (28) holds

$$\|\underline{c}_q^{(u)}\| = 1,\ \forall q = 1 \dots Q,\ \forall u = 1 \dots U\,. \tag{36}$$

- From TDMA burst to TDMA burst the total data vector $\underline{\boldsymbol{d}}$ of (13) fluctuates in such a way that the data symbols $\underline{d}_i$ are all statistically independent of each other.
- The channel impulse responses $\underline{\boldsymbol{h}}^{(u,k_\mathrm{a})}$ of (1) are subject to stationary fast fading, whereas slow fading is eliminated by transmit power control.
- Intercell MAI at the receiver inputs of the MSs is modelled as uncorrelated complex Gaussian noise with the same variance σ^2 of real and imaginary part at all MSs μ_u, $u = 1 \dots U$.

The average transmit energies T_JT and T_JD cannot be determined in closed form but have to be determined by simulations. Up to now simulation results for the following case are available [14]:

- Only one antenna element is utilized at the BS, that is K_a is equal to 1.
- The well known rural area (RA) channel model proposed in [13] is chosen.
- The length Q of the CDMA codes $\underline{\boldsymbol{c}}^{(u)}$ is 16, and N equal to 10 symbols are transmitted per burst and MS.

In Fig. 4 the average required transmit energies T_JD and T_JT are depicted versus the number U of MSs. For U equal to 2 and 4 the values of T_JT and T_JD are very similar. In the cases U equal to 6 and 8 JT needs a slightly higher transmit energy per data symbol than JD. This increase of the required transmit energy can for example be characterized by the ratio $T_\mathrm{JT}/T_\mathrm{JD}$ equal to 1.16 in the case U equal to 8.

VI. Conclusions

A novel scheme joint transmission (JT) for the downlink of mobile radio systems employing TDD is proposed, which utilizes the knowledge of the channel impulse responses at the BS transmitter in such a way that at the receivers of the MSs channel estimators are no longer required. Consequently, the computational expense of the data detection is dramatically reduced. Besides a lower receiver complexity, the presented scheme simultaneously enhances the system capacity, because no system resources have to be spent for the transmission of training signals. JT is especially suited for time slotted CDMA systems like TD–CDMA and easily lends itself to the application of multi-element transmit antennas.

Acknowledgments

The authors are indebted to Deutsche Forschungsgemeinschaft (DFG) for sponsoring part of this work within "DFG Schwerpunktprogramm Mobilkommunikation". They are also grateful to the staffs of the Central Computer Facility (RHRK) and of the Center for Microelectronics of the University of Kaiserslautern for sustained technical support. Stimulating discussions with Prof. J. Nossek of TU Munich and his group and with their colleagues at Siemens AG are gratefully acknowledged.

References

[1] M. Haardt, A. Klein, R. Koehn, S. Oestreich, M. Purat, V. Sommer and T. Ulrich, "The TD–CDMA based UTRA TDD mode," *IEEE Journal on Selected Areas in Communications*, vol. 18, to appear in August 2000 in the issue on Wideband CDMA, 2000.

[2] *http://www.3gpp.org.*

[3] *Technical specification of IMT-2000 CDMA TDD (TD-SCDMA) by China Wireless Telecommunications Standard (CWTS).* Published in Internet under the URL: *http://www.cwts.org*, 1999.

[4] A. Klein, *Multi–user detection of CDMA–signals — algorithms and their application to cellular mobile radio*, *Fortschrittberichte VDI*, series 10, no. 243, VDI–Verlag, Düsseldorf, 1996.

[5] H. Matsutani, Y. Sanada, and M. Nakagawa, "A forward link intracell orthogonalization technique using multicarrier pre-decorrelation for CDMA wireless local communication system," in *IEEE 8th International Symposium on Personal, Indoor and Mobile Radio Communications (PIMRC'97)*, Helsinki, 1997, pp. 125–129.

[6] A.N. Barreto and G. Fettweis, "Performance improvement in DS-spread spectrum CDMA systems using a pre- and a post-rake," in *2000 International Zurich Seminar on Broadband Communications (IZS'2000)*, Zurich, 2000, pp. 39–46.

[7] M. Brandt-Pearce and A. Dharap, "Transmitter-based multiuser interference rejection for the down-link of a wireless CDMA system in a multipath environment," *IEEE Journal on Selected Areas in Communications*, vol. 18, no. 3, pp. 407–417, 2000.

[8] B.R. Vojcic and J. W. Mee, "Transmitter precoding in synchronous multiuser communications," *IEEE Transactions on Communications*, vol. 46, pp. 1346–1355, 1998.

[9] M. Joham and W. Utschick, "Downlink processing for mitigation of intracell interference in DS-CDMA systems," to appear in *Proc. IEEE 6th International Symposium on Spread Spectrum Techniques & Applications (ISSSTA'2000)*, Parsippany/New Jersey, 2000.

[10] A. Ben-Israel and T.N.E. Greville, *Generalized inverses: theory and applications*, Wiley–Interscience, New York, 1974.

[11] Y. Lu and P.W. Baier, "Performance of adaptive antennas for the TD–CDMA downlink under special consideration of multi-directional channels and CDMA code pooling," accepted for publication in *International Journal of Electronics and Communications (AEÜ: Archiv für Elektronik und Übertragungstechnik)*, 2000.

[12] M. Meurer, P.W. Baier, T. Weber, Y. Lu and A. Papathanassiou, "Joint transmission, an advantageous downlink concept for CDMA mobile radio systems using time division duplexing," *IEE Electronics Letters*, vol. 36, pp. 900–901, 2000.

[13] COST 207, *Digital land mobile radio communications*, Office for Official Publications of the European Communities, Luxembourg, 1989.

[14] M. Meurer, P.W. Baier, Y. Lu, A. Papathanassiou and T. Weber, "TD-CDMA downlink: Optimum transmit signal design reduces receiver complexity and enhances system performance," in *Proc. 6th International Conference on Telecommunications (ICT 2000)*, Acapulco, 2000, pp. 300–305.

[TMW00] Tröger, H.; Meurer, M.; Weber, T.: "Adaptive antennas for the TD-CDMA downlink utilizing the novel concept joint transmission". *ITG Diskussionssitzung Antennen für mobile Systeme 2000*, Starnberg, 2000, S. 37–40.

Adaptive antennas for the TD-CDMA downlink utilizing the novel concept joint transmission

Hendrik Tröger, Michael Meurer, Tobias Weber
Research Group for RF Communications, University of Kaiserslautern
P.O. Box 3049, D–67653 Kaiserslautern, Germany
phone/fax: +49 631 205 2087/3612; e–mail: troeger@rhrk.uni–kl.de

Abstract—**In mobile radio systems employing TDD (Time Division Duplex) the same channel impulse responses are valid for both the uplink and the downlink, if the time elapsing between uplink and downlink transmission is sufficiently small compared to the coherence time of the mobile radio channels. Thus, the channel impulse responses of all mobile stations (MS) estimated at the base station (BS) in the uplink can be used to create a transmit signal for the downlink at the BS, which, after having passed the mobile radio channels, yields the data sent for each MS by simple linear filtering. This strategy is called joint transmission. In this paper, the application of joint transmission in multi-antenna configurations is investigated.**

I. Introduction

TD-CDMA is based on time slotted CDMA, which utilizes a combination of the three basic multiple access schemes FDMA, TDMA and CDMA. This air interface has been selected by 3GPP as the standard for the Time Division Duplexing (TDD) mode of the 3G system IMT-2000. In mobile radio systems employing TDD (Time Division Duplex) the same channel impulse responses are valid for both the uplink and the downlink, if - and this is assumed in what follows - the time elapsing between uplink and downlink transmission is sufficiently small compared to the coherence time of the mobile radio channels. This fact cannot be exploited in state-of-the-art TD-CDMA, where channel estimators are required at each MS to perform joint detection (JD), which eliminates intracell multiple access interference (MAI) and intersymbol interference (ISI). In this paper, a novel downlink transmission scheme is proposed, which reduces the receiver complexity and nevertheless eliminates MAI and ISI. This transmission technique needs channel estimators only in the uplink receivers and uses the channel impulse responses to create a common transmit signal for the downlink. This approach is termed joint transmission (JT) and is considered the inverse of the JD concept, where a received signal common to all users is jointly processed at the receiver in order to obtain the data sent by the individual transmitters. In a way JT is related to known CDMA concepts using transmit signals which originate from predistortion of CDMA coded signals under consideration of the known channel impulse responses. Nevertheless, JT is more general, because the transmit signals are directly generated. Therefore, the proposed scheme JT is not restricted to time slotted CDMA systems, but is also applicable to other systems which have a TDMA component.

This paper is structured as follows. In Section II the joint transmission concept is introduced. Section III deals with multi-antenna strategies. In Section IV the simulation environment is specified. The topic of Section V are the simulation results. Finally, the paper is concluded by Section VI. The time discrete equivalent low-pass representation of signals is chosen. Consequently, signals and channel impulse responses are represented by complex vectors or matrices [1], which are printed in bold face.

II. Joint Transmission Concept

In this paper a mobile radio system where each BS uses K_a transmit antenas, while each MS μ_k, $k = 1 \dots K$, disposes of a single receiving antenna will be considered [2]. For each MS this situation can be modeled by a MS specific network with K_a input ports and a single output port, see Fig. 1. In this network the channel impulse responses

$$\underline{\boldsymbol{h}}^{(k,k_\mathrm{a})} = \left(\underline{h}_1^{(k,k_\mathrm{a})} \dots \underline{h}_W^{(k,k_\mathrm{a})}\right)^\mathrm{T}, k = 1 \dots K, \quad k_\mathrm{a} = 1 \dots K_\mathrm{a} \qquad (1)$$

of the length W characterize the signal transmission between the input of the transmit antenna k_a and the output of the receiving antenna of the MS μ_k. Into each of the K_a transmit antennas an antenna specific signal

$$\underline{\boldsymbol{s}}^{(k_\mathrm{a})} = \left(\underline{s}_1^{(k_\mathrm{a})} \dots \underline{s}_S^{(k_\mathrm{a})}\right)^\mathrm{T}, k_\mathrm{a} = 1 \dots K_\mathrm{a}, \qquad (2)$$

of length S is fed. The K_a signals $\underline{\boldsymbol{s}}^{(k_\mathrm{a})}$ of (2) can be compiled to form the total transmit signal

$$\underline{\boldsymbol{s}} = \left(\underline{\boldsymbol{s}}^{(1)\mathrm{T}} \dots \underline{\boldsymbol{s}}^{(K_\mathrm{a})\mathrm{T}}\right)^\mathrm{T} \qquad (3)$$

of length $K_\mathrm{a}S$. With the channel impulse responses $\underline{\boldsymbol{h}}^{(k,k_\mathrm{a})}$ of (1) the $(S+W-1) \times S$ matrices

$$\underline{\boldsymbol{H}}^{(k,k_\mathrm{a})} = \left(\underline{H}_{i,j}^{(k,k_\mathrm{a})}\right), i = 1 \dots S+W-1, \; j = 1 \dots S,$$
$$\underline{H}_{i,j}^{(k,k_\mathrm{a})} = \begin{cases} \underline{h}_{i-j+1}^{(k,k_\mathrm{a})} & \text{for } 1 \le i-j+1 \le W, \\ 0 & \text{otherwise,} \end{cases}$$
$$k = 1 \dots K, \; k_\mathrm{a} = 1 \dots K_\mathrm{a}, \qquad (4)$$

and the $(S+W-1) \times (K_\mathrm{a}S)$ matrices

$$\underline{\boldsymbol{H}}^{(k)} = \left(\underline{\boldsymbol{H}}^{(k,1)} \dots \underline{\boldsymbol{H}}^{(k,K_\mathrm{a})}\right), k = 1 \dots K, \qquad (5)$$

can be formed. Now, the signal originating from $\underline{\boldsymbol{s}}$ of (3) and received at MS μ_k becomes

$$\underline{\boldsymbol{e}}^{(k)} = \underline{\boldsymbol{H}}^{(k)}\underline{\boldsymbol{s}}, \; k = 1 \dots K. \qquad (6)$$

The K received signals $\underline{\boldsymbol{e}}^{(k)}$ of (6) can be arranged in a total received signal

$$\underline{\boldsymbol{e}} = \left(\underline{\boldsymbol{e}}^{(1)\mathrm{T}} \dots \underline{\boldsymbol{e}}^{(K)\mathrm{T}}\right)^\mathrm{T} \qquad (7)$$

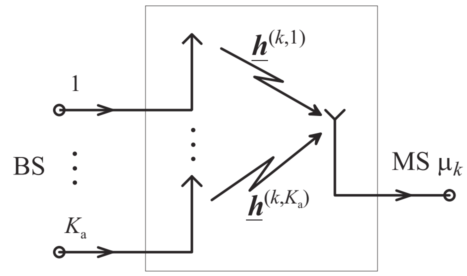

Fig. 1. Network modeling the channels between the inputs of the K_a BS antennas and the antenna output of MS μ_k

of length $K(S+W-1)$. The K matrices $\underline{\boldsymbol{H}}^{(k)}$ of (5) can be arranged in the $K(S+W-1) \times (K_a S)$ channel matrix

$$\underline{\boldsymbol{H}} = \left(\underline{\boldsymbol{H}}^{(1)\mathrm{T}} \ldots \underline{\boldsymbol{H}}^{(K)\mathrm{T}}\right)^{\mathrm{T}}. \tag{8}$$

Then, the total received signal of (7) can be concisely expressed as

$$\underline{\boldsymbol{e}} = \underline{\boldsymbol{H}}\,\underline{\boldsymbol{s}}. \tag{9}$$

The N data symbols meant for MS μ_k are arranged in the data vector

$$\underline{\boldsymbol{d}}^{(k)} = \left(\underline{d}_1^{(k)} \ldots \underline{d}_N^{(k)}\right)^{\mathrm{T}}, k = 1 \ldots K. \tag{10}$$

The K data vectors $\underline{\boldsymbol{d}}^{(k)}$ of (10) are put together to form the total data vector

$$\underline{\boldsymbol{d}} = \left(\underline{\boldsymbol{d}}^{(1)\mathrm{T}} \ldots \underline{\boldsymbol{d}}^{(K)\mathrm{T}}\right)^{\mathrm{T}} \tag{11}$$

of length NK. In order to perform data detection at MS μ_k a $N \times (S+W-1)$ matrix $\underline{\boldsymbol{D}}^{(k)}$ is multiplied by the signal $\underline{\boldsymbol{e}}^{(k)}$, see (6), received at this MS. $\underline{\boldsymbol{D}}^{(k)}$ can be assumed to be known at both the transmitter and the receiver. The total transmit signal $\underline{\boldsymbol{s}}$ of (3) has to be chosen in such a way that said matrix-vector multiplication yields the desired data vector $\underline{\boldsymbol{d}}^{(k)}$ free from ISI and intracell MAI, that is

$$\underline{\boldsymbol{d}}^{(k)} = \underline{\boldsymbol{D}}^{(k)}\,\underline{\boldsymbol{e}}^{(k)},\ k = 1 \ldots K. \tag{12}$$

Substituting (6) in (12) yields

$$\underline{\boldsymbol{d}}^{(k)} = \underline{\boldsymbol{D}}^{(k)}\underline{\boldsymbol{H}}^{(k)}\underline{\boldsymbol{s}},\ k = 1 \ldots K. \tag{13}$$

The K matrices $\underline{\boldsymbol{D}}^{(k)}$, $k = 1 \ldots K$, can be put together to form the $NK \times K(S+W-1)$ detector matrix

$$\underline{\boldsymbol{D}} = \text{blockdiag}\left[\underline{\boldsymbol{D}}^{(1)} \ldots \underline{\boldsymbol{D}}^{(K)}\right]. \tag{14}$$

With the detector matrix $\underline{\boldsymbol{D}}$ of (14) and the channel matrix $\underline{\boldsymbol{H}}$ of (8) the system matrix

$$\underline{\boldsymbol{B}} = \underline{\boldsymbol{D}}\,\underline{\boldsymbol{H}} \tag{15}$$

can be established. With $\underline{\boldsymbol{B}}$ the K matrix-vector equations given by (13) can be put together to the single matrix-vector equation

$$\underline{\boldsymbol{d}} = \underline{\boldsymbol{B}}\,\underline{\boldsymbol{s}}. \tag{16}$$

In (16), $\underline{\boldsymbol{B}}$ and $\underline{\boldsymbol{d}}$ are known at the transmitter. Therefore, (16) can be considered as a system of equations by the solution of which the component values of the total transmit signal $\underline{\boldsymbol{s}}$ of (3) can be determined. In (16) the total number of equations is NK and the total number of unknowns is $K_a S$. In the following

$$NK < K_a S, \tag{17}$$

will be assumed. Under this assumption, the system of equations (16) is under-determined and has infinitely many solutions $\underline{\boldsymbol{s}}$. One possible solution is

$$\underline{\boldsymbol{s}} = \underbrace{\underline{\boldsymbol{B}}^{*\mathrm{T}}\left(\underline{\boldsymbol{B}}\,\underline{\boldsymbol{B}}^{*\mathrm{T}}\right)^{-1}}_{\underline{\boldsymbol{M}}}\underline{\boldsymbol{d}}. \tag{18}$$

This is the solution of minimum energy $\|\underline{\boldsymbol{s}}\|^2/2$ [3] and is optimum in the sense that the transmit power and, consequently, the intercell multiple access interference are minimized. The matrix $\underline{\boldsymbol{M}}$ is termed modulator matrix

In the downlink of conventional TD–CDMA [1] one of K CDMA codes

$$\underline{\boldsymbol{c}}^{(k)} = \left(\underline{c}_1^{(k)} \ldots \underline{c}_Q^{(k)}\right)^{\mathrm{T}}, k = 1 \ldots K, \tag{19}$$

of length Q is uniquely assigned to each MS μ_k, $k = 1 \ldots K$, with all K CDMA codes $\underline{\boldsymbol{c}}^{(k)}$, $k = 1 \ldots K$, constituting an orthogonal set. Then, in the case of AWGN transmission, the optimum linear detector at each MS μ_k would consist of a filter matched to the CDMA code $\underline{\boldsymbol{c}}^{(k)}$. As a main feature of the proposed scheme JT this simple and inexpensive detector shall be maintained also if the radio channels are no longer AWGN channels, but show multipath behaviour. Nevertheless, ISI and intracell MAI can be eliminated by properly designing the transmit signal $\underline{\boldsymbol{s}}$ of (3), see (18). With the CDMA codes $\underline{\boldsymbol{c}}^{(k)}$ of (19) the CDMA code matrix

$$\underline{\boldsymbol{C}} = \text{blockdiag}\left[\underline{\boldsymbol{C}}^{(1)} \ldots \underline{\boldsymbol{C}}^{(K)}\right] \tag{20}$$

with

$$\begin{aligned} \underline{\boldsymbol{C}}^{(k)} &= \left(\underline{C}_{i,j}^{(k)}\right),\ i = 1 \ldots S+W-1, \\ & \quad j = 1 \ldots N,\ k = 1 \ldots K, \\ \underline{C}_{i,j}^{(k)} &= \begin{cases} \underline{c}_{i-Q(j-1)}^{(k)} & \text{for } 1 \le i - Q(j-1) \le Q, \\ 0 & \text{else,} \end{cases} \end{aligned} \tag{21}$$

can be established. Using this matrix, said filtering of the received signals $\underline{\boldsymbol{e}}^{(k)}$ can be described by the detector matrix

$$\underline{\boldsymbol{D}} = \underline{\boldsymbol{C}}^{*\mathrm{T}}. \tag{22}$$

Thus, substituting (22) in (15) the system matrix $\underline{\boldsymbol{B}}$ of (15) is given as

$$\underline{\boldsymbol{B}} = \underline{\boldsymbol{C}}^{*\mathrm{T}}\underline{\boldsymbol{H}}. \tag{23}$$

In Fig. 2 the conventional transmission scheme, which for instance is used in TD-CDMA, and the novel transmission scheme JT are compared with each other. In both cases the transmission is determined by the three steps

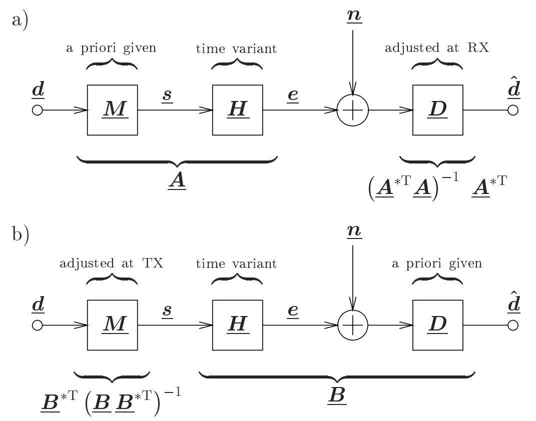

Fig. 2. Transmission schemes
a) conventional, used e.g. in state-of-the-art TD–CDMA
b) novel scheme joint transmission (JT)

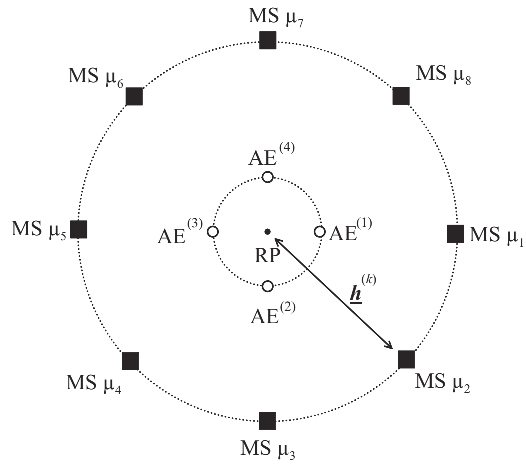

Fig. 3. Simulation model with $K = 8$ MS and $K_\mathrm{a} = 4$ antenna elements.

modulation, transmission over the mobile radio channel and detection, which are described by the matrices $\underline{\boldsymbol{M}}$, $\underline{\boldsymbol{H}}$ and $\underline{\boldsymbol{D}}$, respectively. Prior to detection a noise signal $\underline{\boldsymbol{n}}$ representing thermal noise and intercell MAI is fed into the system. At the detector output an estimate $\hat{\underline{\boldsymbol{d}}}$ of the total data vector $\underline{\boldsymbol{d}}$ of (11) is obtained. In the well known case of conventional transmission, see Fig. 2a, the modulator matrix $\underline{\boldsymbol{M}}$ is a priori given and determines, together with the channel matrix $\underline{\boldsymbol{H}}$, the system matrix [1]

$$\underline{\boldsymbol{A}} = \underline{\boldsymbol{H}}\,\underline{\boldsymbol{M}}. \tag{24}$$

The detector matrix is derived from $\underline{\boldsymbol{A}}$ of (24) and takes for instance the form [1]

$$\underline{\boldsymbol{D}} = \left(\underline{\boldsymbol{A}}^{*\mathrm{T}}\underline{\boldsymbol{A}}\right)^{-1}\underline{\boldsymbol{A}}^{*\mathrm{T}}, \tag{25}$$

if zero forcing linear equalization is utilized.

In the case of JT the detector matrix $\underline{\boldsymbol{D}}$ is a priori given and determines, together with the channel matrix $\underline{\boldsymbol{H}}$, the system matrix $\underline{\boldsymbol{B}}$ of (15).

III. Multi Antenna Structures

In the previous section the general mathematical formalism of JT, which is independent of the actual transmit antenna configuration, was introduced. The antenna configuration affects only the channel impulse responses $\underline{\boldsymbol{h}}^{(k,k_\mathrm{a})}$ describing signal transmission between transmit antenna element k_a and MS μ_k. In the following essential characteristics of the channel impulse responses $\underline{\boldsymbol{h}}^{(k,k_\mathrm{a})}$both for macro diversity and micro diversity scenarios are studied.

A) In macro diversity scenarios the antenna elements $\mathrm{AE}^{(k_\mathrm{a})}$, $k_\mathrm{a} = 1 \ldots K_\mathrm{a}$ are a few hundred wavelengths away from each other. The paths over which the radio waves propagate from the antenna elements $\mathrm{AE}^{(k_\mathrm{a})}$, $k_\mathrm{a} = 1 \ldots K_\mathrm{a}$ to a MS μ_k, $k = 1 \ldots K$, are totally independent for each antenna element. In this case the channel impulse responses $\underline{\boldsymbol{h}}^{(k,k_\mathrm{a})}$ can be considered as totally uncorrelated.

B) In micro diversity scenarios the antenna elements $\mathrm{AE}^{(k_\mathrm{a})}$, $k_\mathrm{a} = 1 \ldots K_\mathrm{a}$, are located close to each other, i.e. the distances between the antenna elements are in the order of the wavelength. The paths over which the radio waves propagate from the transmit antenna elements $\mathrm{AE}^{(k_\mathrm{a})}$, $k_\mathrm{a} = 1 \ldots K_\mathrm{a}$ to a MS μ_k, are the same for each antenna element. In the following it is assumed that the mobile radio channels for each MS μ_k are single direction channels, i.e. there is only a single direction of departure for each MS μ_k, see Fig 3. Now the channel impulse responses $\underline{\boldsymbol{h}}^{(k,k_\mathrm{a})}$ for different antenna elements $\mathrm{AE}^{(k_\mathrm{a})}$ are phase shifted versions of a single MS specific channel impulse response $\underline{\boldsymbol{h}}^{(k)}$ at a reference point RP.

IV. Simulation Environment

In this paper the system performance is surveyed for micro diversity scenarios in accordance with B). For the simulations a circular antenna array is assumed. The distance between two antenna elements $\mathrm{AE}^{(k_\mathrm{a})}$ and $\mathrm{AE}^{((k_\mathrm{a}+1) \bmod K_\mathrm{a})}$, $k_\mathrm{a} = 1 \ldots K_\mathrm{a}$, is one half of the wavelength. The directions of departure of the MSs μ_k, $k = 1 \ldots K$, are equally spaced, see Fig. 3. As the basis for a comparison of scenarios with different numbers K_a of antenna elements the average transmit energies per symbol $E\{T_\mathrm{s}\}$ required for obtaining the same SIR (Signal to Interference Ratio) at the detector outputs are suited. In this comparison the following assumptions are made:

- The data symbols $\underline{d}_i^{(k)}$, $k = 1 \ldots K$, $i = 1 \ldots N$ are statistically independent of each other.
- The channel impulse responses $\underline{\boldsymbol{h}}^{(k,k_\mathrm{a})}$ of (1) are subject to stationary fast fading, whereas slow fading is eliminated by transmit power control.
- Intercell MAI at the receiver inputs of the MSs is modelled as white Gaussian noise with the same variance at all MSs μ_k, $k = 1 \ldots K$.
- The well known rural area (RA) channel model proposed in [4] is chosen.
- The length Q of the CDMA codes $\underline{\boldsymbol{c}}^{(k)}$ is 16, and N equal to 10 symbols are transmitted per burst and MS μ_k.

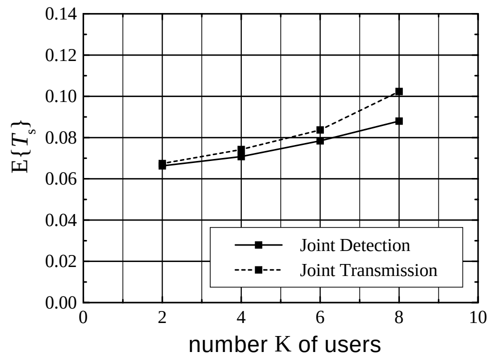

Fig. 4. Average transmit energy per symbol $E\{T_\mathrm{s}\}$ of JD and JT

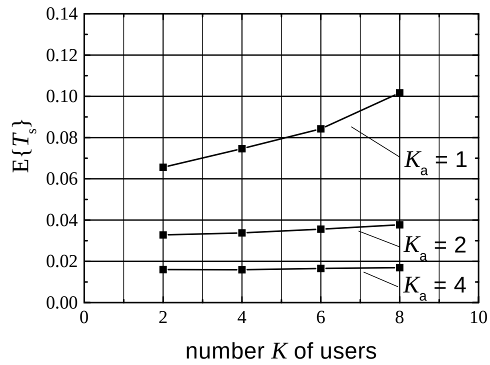

Fig. 5. Average transmit energy per symbol $E\{T_\mathrm{s}\}$ of JT for different numbers $K_\mathrm{a} = 1, 2, 4$ of antenna elements

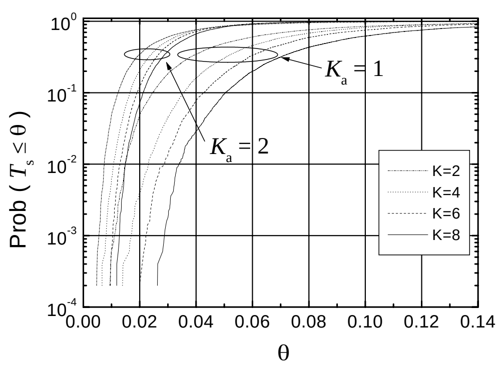

Fig. 6. Cumulative distribution function of the total transmit energy T_s per symbol

V. Simulation results

In [5] the novel downlink transmission scheme JT is compared to JD for the single antenna element case $K_\mathrm{a} = 1$. As shown in Fig. 4 there are almost no differences between JT and JD for $K = 2$ or $K = 4$. For $K = 6$ and $K = 8$, JD is slightly superior to JT with respect to the average transmit energy per data symbol $E\{T_\mathrm{s}\}$. In Fig. 5 the average transmit energy $E\{T_\mathrm{s}\}$ is shown for different numbers K_a of antenna elements, $K_\mathrm{a} = 1, 2, 4$. It is obvious that with increasing number K_a of antenna elements the average transmit energy per symbol $E\{T_\mathrm{s}\}$ goes down because the transmit energy can be better directed into the useful directions of the MSs μ_k. The other observable effect is the decreasing gradient of the curves for increasing number K_a of antenna elements. The ability of the JT scheme to spatially separate the MSs grows with increasing number K_a of antenna elements. Therefore the dependency of the average transmit energy per symbol $E\{T_\mathrm{s}\}$ on the number K of MSs μ_k decreases with increasing number K_a of antenna elements. Fig. 6 shows the cumulative distribution function (CDF) of the transmit energy per symbol T_s if the channel impulse responses $\underline{\boldsymbol{h}}^{(k,k_\mathrm{a})}$ are randomly varied according to the RA channel model. It can be seen that the transmit energies per symbol and the variance of the transmit energy per symbol go down with increasing number of antenna elements.

VI. Conclusions

The application of the novel scheme joint transmission (JT), proposed in [2, 5], in the downlink of mobile radio systems with multi-element transmit antennas is surveyed. It is shown that JT reduces receiver complexity compared to conventional joint detection (JD). With an increasing number K_a of transmit antennas joint transmission (JT) allows a reduction of the transmit power and consequently of the intercell interference.

Acknowledgments

The authors gratefully appreciate the fruitful exchange of ideas with Prof. Dr. Baier and the colleagues at the Research Group for RF Communications, University of Kaiserslautern. Moreover, special thanks should be expressed to Prof. Dr. Nossek for some stimulating discussions. The invaluable support of the supercomputer staff at the Regionales Hochschulrechenzentrum Kaiserslautern (RHRK) is highly acknowledged by the authors.

References

[1] A. Klein, *Multi-User Detection of CDMA Signals – Algorithms and their Application to Cellular Mobile Radio*, vol. 10 of *Fortschrittberichte VDI*, VDI–Verlag, Düsseldorf, 1996.

[2] P. W. Baier, M. Meurer, T. Weber, and H. Tröger, “Joint transmission (JT), an alternative rationale for the downlink of time division CDMA using multi-element transmit antennas” *To be published in: Proc. IEEE 6th International Symposium on Spread-Spectrum Tech. & Appl.*, 2000.

[3] A. Ben-Israel and T.N.E. Greville, *Generalized inverses: theory and applications*, Wiley–Interscience, New York, 1974.

[4] COST 207, *Digital land mobile radio communications*, Office for Official Publications of the European Communities, Luxembourg, 1989.

[5] A. Papathanassiou, M. Meurer, T. Weber, and P.W. Baier, “A novel multiuser transmission scheme requiring no channel estimation and no equalization at the mobile stations for the downlink of TD–CDMA operating in the TDD mode” *To be published in Proc. IEEE 52 th Vehicular Technology Conference (VTC Fall)*, 2000.

[MTJ02] Meurer, M.; Tröger, H.; Jötten, C. A.: "A novel generalized optimization criterion for transmit signal design in joint transmission (JT) multiuser downlinks". *Proc. 9th International Conference on Telecommunications (ICT'02)*, Bd. 1, Peking, 2002, S. 26–31.

A novel generalized optimization criterion for transmit signal design in Joint Transmission (JT) multiuser downlinks

M. Meurer, H. Tröger, C.A. Jötten
Research Group for RF Communications, University of Kaiserslautern,
P.O. Box 3049, D–67653 Kaiserslautern, Germany
e–mail: meurer@rhrk.uni-kl.de

Abstract— **Joint Transmission (JT), a novel downlink transmission scheme, was introduced and described in recent papers. The crux of JT consists in exploiting channel state knowledge at the base stations to jointly generate a common transmit signal for the support of all mobile terminals, with the aim to directly eliminate intersymbol interference and intracell multiple access interference while transmitting. The transmit signal design process offers further degrees of freedom for transmit signal optimization, which have only been insufficiently exploited yet. In this paper a generalized more sophisticated approach to transmit signal optimization is presented and demonstrated how to adapt the JT transmit signal design process correspondingly. A discussion of application aspects and exemplary numerical results completes the paper.**

I. Introduction

The conventional downlink transmission scheme in multi-user radio systems with multi-element transmit antennas can be characterized as follows [1]:

- In the base station (BS) the data to be transmitted to the mobile terminals (MTs) are modulated onto carrier signals according to an a priori determined modulation scheme, which also includes symbol mapping and, in the case of CDMA, spectral spreading.
- The modulated carrier signals are subject to antenna element specific and MT specific weighting, which can be considered as a part of the modulation, and then fed to the transmit antenna elements (AEs).
- At the MTs the received signals are demodulated with the goal to obtain estimates as accurate as possible of the transmitted data. The demodulators to be utilized result a posteriori from the modulation scheme chosen at the BS and from the impulse responses of the channels between the transmit AEs and the MTs.

This conventional approach to downlink transmission has the following disadvantages:

- The demodulators at the MTs need estimates of the channel impulse responses. This requires the transmission of training signals, which unfortunately consume part of the transmission capacity, and the implementation of rather expensive channel estimators at the MTs.
- The a posteriori determined demodulators may turn out to be rather complex, especially if the modulation comprises spectral spreading in the sense of CDMA, see for instance [1].

In [2, 3, 4, 5] an alternative rationale for downlink transmission termed Joint Transmission (JT) was presented, which is capable of avoiding the mentioned disadvantages. As explained in more detail in [2, 3, 4, 5], the term JT was chosen, because one common transmit signal for the support of all MTs is jointly generated at the BS. The crux of JT consists in

- setting out from a priori selected low cost demodulators,
- determining the modulator in the BS a posteriori based on the properties of the selected demodulators and the channel impulse responses, which are assumed to be known at the BS, in such a way that intersymbol interference (ISI) and intracell multiple access interference (MAI) are totally eliminated.

The knowledge of the channel impulse responses required at the BS in the case of JT can be assumed to be available – at least approximately – if we consider radio systems employing the duplexing scheme Time Division Duplex (TDD). In such systems the same channel impulse responses are valid for both the uplink and the downlink, which means that the channel impulse response estimates obtained at the BS as a prerequisite for uplink reception can be also utilized to perform JT in the downlink. Consequently, JT would be especially suited for the downlink of radio transmission systems employing TDD. In JT the transmit signal design ist based on channel state knowledge. In this sense JT is related to transmit signal preprocessing schemes published in [6, 7] for fixed wired transmission and in [8, 9, 10, 11, 12] for wireless transmission.

Besides to the elimination of ISI and MAI, JT offers the possibility to take further transmit signal optimization criteria into account while generating the common transmit signal. Whereas in [2, 3, 4, 5] only transmit signal energy minimization is pursued, in this paper, a novel generalized optimization criterion is presented and it is demonstrated how to incorporate this critrion into the JT transmit signal design. The paper is structured as follows: In Section II the basics of JT are briefly recapitulated in order to conveniently familiarize the reader with the contents of [2, 3, 4, 5] to a degree which is sufficient to follow the reasoning of this paper. In Section III a generalized optimization criterion for transmit signal design is proposed, and it is demonstrated how to adapt the JT transmit signal design process correspondingly. Transmit signal optimization with respect to the spatial characteristics of the radiated transmit signal in general is the topic of Section IV, and in Section V some special cases are considered. Section VI deals with application aspects of the proposed schemes for transmit signal design. In Section VII the results of an exemplary system evaluation are presented. Finally, Section VIII concludes the paper. In the paper the time discrete equivalent low-pass representation of signals is chosen. Consequently, signals and channel impulse responses are represented by complex vectors or matrices [13], which are printed in bold face.

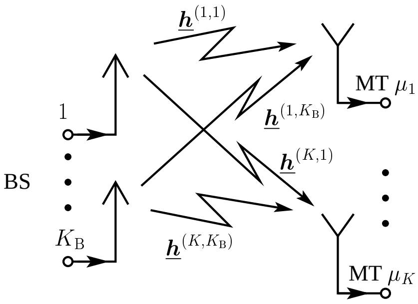

Fig. 1. Downlink multiple input/multiple output (MIMO) channel of a multi-user radio system with a multi-element transmit antenna.

II. Basics of JT

Fig. 1 shows the downlink multiple input/multiple output (MIMO) channel of a multi-user radio system with a multi-element transmit antenna. The BS equipped with K_B transmit AEs supports K MTs μ_k, $k = 1 \ldots K$, which possess a single element receive antenna each. The K_B AEs at the BS are assumed to be perfectly decoupled. In the structure shown in Fig. 1 the AE specific channel impulse responses [2, 3, 4, 5]

$$\underline{\boldsymbol{h}}^{(k,k_\mathrm{B})} = \left(\underline{h}_1^{(k,k_\mathrm{B})} \ldots \underline{h}_W^{(k,k_\mathrm{B})}\right)^\mathrm{T}, \qquad k = 1 \ldots K,\ k_\mathrm{B} = 1 \ldots K_\mathrm{B}, \tag{1}$$

of dimension W characterize the signal transmission between the input of the transmit AE k_B, $k_\mathrm{B} = 1 \ldots K_\mathrm{B}$, and the output of the receiving antenna of MT μ_k, $k = 1 \ldots K$. It is assumed that N data symbols have to be transmitted to each MT $\mu_k, k = 1 \ldots K$. The data symbols for MT μ_k are arranged in the column vector

$$\underline{\boldsymbol{d}}^{(k)} = \left(\underline{d}_1^{(k)} \ldots \underline{d}_N^{(k)}\right)^\mathrm{T}, k = 1 \ldots K, \tag{2}$$

of dimension N termed partial data vector. In total

$$N_\mathrm{t} = KN \tag{3}$$

data symbols have to be transmitted to the ensemble of K MTs. The stack

$$\underline{\boldsymbol{d}} = \left(\underline{\boldsymbol{d}}^{(1)\mathrm{T}} \ldots \underline{\boldsymbol{d}}^{(K)\mathrm{T}}\right)^\mathrm{T} = \left(\underline{d}_1 \ldots \underline{d}_{N_\mathrm{t}}\right)^\mathrm{T} \tag{4}$$

of the K partial data vectors $\underline{\boldsymbol{d}}^{(k)}$, $k = 1 \ldots K$, of (2) is termed the total data vector, which has the dimension N_t, see (3). In the BS, based on $\underline{\boldsymbol{d}}$ a partial transmit signal $\underline{\boldsymbol{s}}^{(k_\mathrm{B})}$, $k_\mathrm{B} = 1 \ldots K_\mathrm{B}$, of dimension S is generated for each of the K_B transmit AEs by a process termed modulation. If these K_B partial transmit signals $\underline{\boldsymbol{s}}^{(k_\mathrm{B})}$, $k_\mathrm{B} = 1 \ldots K_\mathrm{B}$, are compiled to the total transmit signal

$$\underline{\boldsymbol{s}} = \left(\underline{\boldsymbol{s}}^{(1)\mathrm{T}} \ldots \underline{\boldsymbol{s}}^{(K_\mathrm{B})\mathrm{T}}\right)^\mathrm{T} = \left(\underline{s}_1 \ldots \underline{s}_{K_\mathrm{B}S}\right)^\mathrm{T} \tag{5}$$

of dimension $K_\mathrm{B}S$, then, in the case of linear modulation, the process of modulation can be described by the $(K_\mathrm{B}S) \times N_\mathrm{t}$ modulator matrix $\underline{\boldsymbol{M}}$, which still has to be determined. With the modulator matrix $\underline{\boldsymbol{M}}$ and $\underline{\boldsymbol{d}}$ of (4) for the total transmit signal

$$\underline{\boldsymbol{s}} = \underline{\boldsymbol{M}}\, \underline{\boldsymbol{d}} \tag{6}$$

follows. Due to the transmission of $\underline{\boldsymbol{s}}$ of (6) a partial received signal $\underline{\boldsymbol{e}}^{(k)}$ of dimension $S+W-1$ arrives at each MT μ_k, $k = 1 \ldots K$, [2, 3, 4, 5]. The K partial received signals $\underline{\boldsymbol{e}}^{(k)}$, $k = 1 \ldots K$, can be stacked to form the total received signal

$$\underline{\boldsymbol{e}} = \left(\underline{\boldsymbol{e}}^{(1)\mathrm{T}} \ldots \underline{\boldsymbol{e}}^{(K)\mathrm{T}}\right)^\mathrm{T} \tag{7}$$

of dimension $K(S+W-1)$. As shown in [2, 3, 4, 5] the partial channel convolution matrices $\underline{\boldsymbol{H}}^{(k)}$, $k = 1 \ldots K$, of dimension $(S+W-1) \times (K_\mathrm{B}S)$ can be obtained by properly arranging the AE specific channel impulse responses $\underline{\boldsymbol{h}}^{(k,k_\mathrm{B})}$ of (1), and the matrices $\underline{\boldsymbol{H}}^{(k)}$ can be composed to form the total channel convolution matrix $\underline{\boldsymbol{H}}$ of dimension $[K(S+W-1)] \times (K_\mathrm{B}S)$. Then, in the case of absence of disturbing noise at the receiver inputs, the total received signal of (7) can be expressed as [2, 3, 4, 5]

$$\underline{\boldsymbol{e}} = \underline{\boldsymbol{H}}\, \underline{\boldsymbol{s}}. \tag{8}$$

At each MT μ_k the corresponding partial received signal $\underline{\boldsymbol{e}}^{(k)}$ is demodulated with the goal to obtain the corresponding partial data vector $\underline{\boldsymbol{d}}^{(k)}$. In the case of a linear demodulator the demodulation process at MT μ_k can be described by a demodulator matrix $\underline{\boldsymbol{D}}^{(k)}$ of dimension $N \times (S+W-1)$ [2, 3, 4, 5]:

$$\underline{\boldsymbol{d}}^{(k)} = \underline{\boldsymbol{D}}^{(k)} \underline{\boldsymbol{e}}^{(k)}, k = 1 \ldots K. \tag{9}$$

(9) implies the requirement already formulated in Section I that the data vector $\underline{\boldsymbol{d}}^{(k)}$ of (2) intended for MT μ_k is detected without ISI and intracell MAI.

By combining the K modulator matrices $\underline{\boldsymbol{D}}^{(k)}$, $k = 1 \ldots K$, the total demodulator matrix

$$\underline{\boldsymbol{D}} = \text{ blockdiag} \left[\underline{\boldsymbol{D}}^{(1)} \ldots \underline{\boldsymbol{D}}^{(K)}\right] \tag{10}$$

of dimension $N_\mathrm{t} \times [K(S+W-1)]$ is obtained. With (10) we can stack the K equations of (9) and obtain under consideration of (8) the single equation

$$\underline{\boldsymbol{d}} = \underline{\boldsymbol{D}}\, \underline{\boldsymbol{e}} = \underbrace{\underline{\boldsymbol{D}}\, \underline{\boldsymbol{H}}}_{\underline{\boldsymbol{B}}}\, \underline{\boldsymbol{s}}. \tag{11}$$

As already mentioned, in the case of JT the demodulators characterized by the total demodulator matrix $\underline{\boldsymbol{D}}$ of (10) are a priori agreed upon and, therefore, are also known at the BS. Also the AE specific channel impulse responses $\underline{\boldsymbol{h}}^{(k,k_\mathrm{B})}$ of (1) and, therefore, the channel convolution matrix $\underline{\boldsymbol{H}}$ are assumed to be known at the BS, see Section I. Then, the matrix $\underline{\boldsymbol{B}}$ defined in (11) is known at the BS as well. Consequently, (11) can be considered as a system of equations which determine the elements of the total transmit signal $\underline{\boldsymbol{s}}$ of (5) to be transmitted by the BS. From a mathematical point of view, (11) formulates the necessary condition for $\underline{\boldsymbol{s}}$ of (5) to obtain the desired partial data vectors $\underline{\boldsymbol{d}}^{(k)}$ at the MTs μ_k, $k = 1 \ldots K$, without any ISI and intracell MAI. If the dimension $K_\mathrm{B}S$ of $\underline{\boldsymbol{s}}$ is chosen larger than the dimension N_t of $\underline{\boldsymbol{d}}$ and if $\underline{\boldsymbol{B}}$ has maximum rank, i.e. if

$$\text{rank } \underline{\boldsymbol{B}} = N_\mathrm{t} < K_\mathrm{B}S, \tag{12}$$

holds – and this is assumed in the following – then the necessary condition expressed by (11) is an underdetermined system of equations with the set of solutions

$$\mathbb{L} = \left\{ \underline{\boldsymbol{s}} \in \mathbb{C}^{K_\mathrm{B}S} \middle| \underline{\boldsymbol{B}}\,\underline{\boldsymbol{s}} = \underline{\boldsymbol{d}} \right\} \tag{13}$$

of infinite cardinality. To definitely identify a certain solution $\underline{\boldsymbol{s}} \in \mathbb{L}$, i.e. to define a necessary and sufficient condition for the choice of $\underline{\boldsymbol{s}}$ of (5), in addition to fulfilling (11) a further condition for $\underline{\boldsymbol{s}}$ has to be introduced. The degree of freedom of choosing the further condition for $\underline{\boldsymbol{s}}$ offers the possibility of a further transmit signal optimization. In [2, 3, 4, 5] the solution

$$\underline{\boldsymbol{s}} = \underbrace{\underline{\boldsymbol{B}}^{*\mathrm{T}} \left(\underline{\boldsymbol{B}}\,\underline{\boldsymbol{B}}^{*\mathrm{T}} \right)^{-1}}_{\underline{\boldsymbol{M}}} \underline{\boldsymbol{d}} \tag{14}$$

out of $\mathbb{L}$ of (13) is chosen, which has minimum energy

$$T = \|\underline{\boldsymbol{s}}\|^2/2. \tag{15}$$

(14) describes the construction of the modulator matrix $\underline{\boldsymbol{M}}$ introduced in (6) and to be a posteriori determined in the BS transmitter [2, 3, 4, 5], see Section I.

III. JT WITH GENERALIZED OPTIMIZATION CRITERION

As explained in Section II, while determining the total transmit signal $\underline{\boldsymbol{s}}$ the necessary condition (11) leads to an infinite number of solutions $\underline{\boldsymbol{s}} \in \mathbb{L}$, c.f. (13), offering the potential for further transmit signal optimization. The choice of $\underline{\boldsymbol{s}}$ according to (14) and introduced in [2, 3, 4, 5] allows to minimize the energy T of (15), but is suboptimal with respect to other optimization criteria, i.e. other sufficient conditions. For this reason, the optimization criterion employed in JT and the corresponding transmit signal design of (14) should be generalized. As further motivated in Sections IV and V, the minimization of the hermitian form

$$E = \frac{1}{2}\underline{\boldsymbol{s}}^{*\mathrm{T}} \underline{\boldsymbol{R}}\,\underline{\boldsymbol{s}} \tag{16}$$

is an attractive choice for the optimization criterion, where $\underline{\boldsymbol{R}}$ of (16) is an hermitian matrix of dimension $(K_\mathrm{B}S) \times (K_\mathrm{B}S)$. By minimizing E of (16) the total transmit signal

$$\underline{\boldsymbol{s}} = \arg \min_{\forall \underline{\boldsymbol{s}}' \in \mathbb{L}} \frac{1}{2}\underline{\boldsymbol{s}}'^{*\mathrm{T}} \underline{\boldsymbol{R}}\,\underline{\boldsymbol{s}}' \tag{17}$$

follows, which satisfies the necessary condition expressed by (11) and optimizes the hermitian form of (16). Obviously, the minimization of the energy T of (15) introduced in Section II can be interpreted as a special case of (17) characterized by choosing

$$\underline{\boldsymbol{R}} = z\boldsymbol{I}^{(K_\mathrm{B}S)}, z \in \mathbb{R}\backslash\{0\}, \tag{18}$$

where $\boldsymbol{I}^{(K_\mathrm{B}S)}$ denotes the identity matrix of dimension $(K_\mathrm{B}S)\times(K_\mathrm{B}S)$. (17) represents an optimization problem with the side condition (11) and complex-valued unknowns. This kind of optimization problem can be transformed into an optimization problem without side condition by employing the Lagrange multiplier technique [14]. This proceeding leads to the Lagrange cost function

$$E_\mathrm{L} = \frac{1}{2}\underline{\boldsymbol{s}}^{*\mathrm{T}} \underline{\boldsymbol{R}}\,\underline{\boldsymbol{s}} - \left(\underline{\boldsymbol{B}}\,\underline{\boldsymbol{s}} - \underline{\boldsymbol{d}}\right)^{*\mathrm{T}} \underline{\boldsymbol{\mu}}, \tag{19}$$

which has to be minimized. $\underline{\boldsymbol{\mu}}$ in (19) is termed Lagrange multiplier. With the complex Nabla operator

$$\nabla_{\underline{\boldsymbol{s}}^*} = \frac{1}{2} \begin{bmatrix} \frac{\partial}{\partial \mathrm{Re}\{\underline{s}_1\}} + \mathrm{j}\frac{\partial}{\partial \mathrm{Im}\{\underline{s}_1\}} \\ \vdots \\ \frac{\partial}{\partial \mathrm{Re}\{\underline{s}_{K_\mathrm{B}S}\}} + \mathrm{j}\frac{\partial}{\partial \mathrm{Im}\{\underline{s}_{K_\mathrm{B}S}\}} \end{bmatrix} \tag{20}$$

originally introduced as Wirtinger derivative in [15], the cost function of (19) is minimized, if

$$\nabla_{\underline{\boldsymbol{s}}^*} E_\mathrm{L} = \boldsymbol{0}. \tag{21}$$

Substituting (19) in (21) yields

$$\begin{aligned} &\nabla_{\underline{\boldsymbol{s}}^*} \left(\frac{1}{2}\underline{\boldsymbol{s}}^{*\mathrm{T}} \underline{\boldsymbol{R}}\,\underline{\boldsymbol{s}} - \left(\underline{\boldsymbol{B}}\,\underline{\boldsymbol{s}} - \underline{\boldsymbol{d}}\right)^{*\mathrm{T}} \underline{\boldsymbol{\mu}} \right) \\ &= \frac{1}{2}\underline{\boldsymbol{R}}\,\underline{\boldsymbol{s}} - \underline{\boldsymbol{B}}^{*\mathrm{T}}\underline{\boldsymbol{\mu}} = \boldsymbol{0}. \end{aligned} \tag{22}$$

Assuming that $\underline{\boldsymbol{R}}$ of (22) is of full rank, (22) can be simplified to

$$\underline{\boldsymbol{s}} = 2\underline{\boldsymbol{R}}^{-1}\underline{\boldsymbol{B}}^{*\mathrm{T}}\underline{\boldsymbol{\mu}}. \tag{23}$$

Substituting $\underline{\boldsymbol{s}}$ of (23) in (11),

$$2\underline{\boldsymbol{B}}\,\underline{\boldsymbol{R}}^{-1}\underline{\boldsymbol{B}}^{*\mathrm{T}}\underline{\boldsymbol{\mu}} = \underline{\boldsymbol{d}} \tag{24}$$

follows. If $(\underline{\boldsymbol{B}}\,\underline{\boldsymbol{R}}^{-1}\,\underline{\boldsymbol{B}}^{*\mathrm{T}})$ is of full rank, and that is assumed in the following,

$$\underline{\boldsymbol{\mu}} = \frac{1}{2}\left(\underline{\boldsymbol{B}}\,\underline{\boldsymbol{R}}^{-1}\underline{\boldsymbol{B}}^{*\mathrm{T}}\right)^{-1}\underline{\boldsymbol{d}} \tag{25}$$

holds for the Lagrange multiplier of (19). Finally, by combining (23) and (25) the total transmit signal becomes

$$\underline{\boldsymbol{s}} = \underbrace{\underline{\boldsymbol{R}}^{-1}\underline{\boldsymbol{B}}^{*\mathrm{T}}\left(\underline{\boldsymbol{B}}\,\underline{\boldsymbol{R}}^{-1}\,\underline{\boldsymbol{B}}^{*\mathrm{T}}\right)^{-1}}_{\underline{\boldsymbol{M}}}\underline{\boldsymbol{d}}. \tag{26}$$

(26) describes the construction of the modulator matrix $\underline{\boldsymbol{M}}$ of (6) to be a posteriori determined in the BS transmitter, if JT is generalized utilizing transmit signal optimization with respect to the hermitian form of (16). For the fore mentioned special choice of $\underline{\boldsymbol{R}}$ expressed in (18), which corresponds to the conventional JT approach studied in [2, 3, 4, 5] and discussed in Section II, the expressions for $\underline{\boldsymbol{s}}$ of (26) and for $\underline{\boldsymbol{s}}$ of (14) are identical. A still open question concerns the proper choice of the hermitian matrix $\underline{\boldsymbol{R}}$. In the following sections some attractive approaches to this choice are discussed.

IV. OPTIMIZATION OF SPATIAL CHARACTERISTICS OF THE TOTAL TRANSMIT SIGNAL, GENERAL CASE

In what follows it is assumed that at the BS a microstructure [16] consisting of K_B transmit AEs is employed. The relativ position of each transmit AE k_B, $k_\mathrm{B} = 1 \ldots K_\mathrm{B}$, to the reference point (RP) is described by the position vector $\boldsymbol{r}^{(k_\mathrm{B})}$, see Fig. 2. With the direction of departure (DOD) characterized by the angle ϕ relative to the reference line (RL) and the vector

$$\beta(\phi) = \frac{2\pi}{\lambda}\left(\cos\phi, \sin\phi\right)^\mathrm{T}, \tag{27}$$

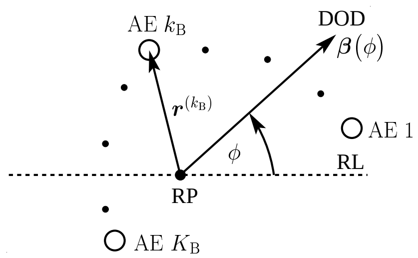

Fig. 2. Employed multi-element transmit antenna with K_B antenna elements (AEs), reference point (RP), reference line (RL) and DOD ϕ.

where λ is the wavelength of the used radio waves, the steering vector

$$\underline{\boldsymbol{a}}(\phi) = \left(\mathrm{e}^{-\mathrm{j}\boldsymbol{\beta}(\phi)^\mathrm{T}\boldsymbol{r}^{(1)}} \ldots \mathrm{e}^{-\mathrm{j}\boldsymbol{\beta}(\phi)^\mathrm{T}\boldsymbol{r}^{(K_\mathrm{B})}}\right)^\mathrm{T} \tag{28}$$

is introduced. Setting out from (28) and (5) a directional transmit signal

$$\underline{\boldsymbol{s}}_\mathrm{d}(\phi) = \left[\underline{\boldsymbol{a}}(\phi)^{*\mathrm{T}} \otimes \boldsymbol{I}^{(S)}\right] \underline{\boldsymbol{s}} \tag{29}$$

can be defined, which describes the signal radiated into the DOD ϕ by the antenna configuration of Fig. 2. In (29) the operator $\otimes$ denotes the Kronecker product of matrices and vectors [17], respectively. When optimizing the spatial characteristics of the total transmit signal $\underline{\boldsymbol{s}}$ of (5), the directional transmit signal $\underline{\boldsymbol{s}}_\mathrm{d}(\phi)$ of (29) has to be analyzed. An attractive optimization approach consists in minimizing the average energy T_d radiated into certain DODs or DOD regions. Setting out from the normalized weighting function $g(\phi) \in \mathbb{R}_0^+$, $\phi \in [0, 2\pi[$, with

$$\int_0^{2\pi} g(\phi)\mathrm{d}\phi = 1, \tag{30}$$

which describes the relevance of the DOD ϕ for the minimization of T_d, T_d can always be expressed as

$$T_\mathrm{d} = \int_0^{2\pi} \frac{1}{2}\underline{\boldsymbol{s}}_\mathrm{d}(\phi)^{*\mathrm{T}}\underline{\boldsymbol{s}}_\mathrm{d}(\phi)g(\phi)\mathrm{d}\phi. \tag{31}$$

Substituting (29) in (31) yields

$$T_\mathrm{d} = \frac{1}{2}\underline{\boldsymbol{s}}^{*\mathrm{T}} \underbrace{\left[\left(\int_0^{2\pi} \underline{\boldsymbol{a}}(\phi)\underline{\boldsymbol{a}}(\phi)^{*\mathrm{T}} g(\phi)\mathrm{d}\phi\right) \otimes \boldsymbol{I}^{(S)}\right]}_{\underline{\boldsymbol{R}} = \underline{\boldsymbol{R}}_\mathrm{s} \otimes \boldsymbol{I}^{(S)}} \underline{\boldsymbol{s}} \tag{32}$$

with

$$\underline{\boldsymbol{R}}_\mathrm{s} = \int_0^{2\pi} \underline{\boldsymbol{a}}(\phi)\underline{\boldsymbol{a}}(\phi)^{*\mathrm{T}} g(\phi)\mathrm{d}\phi. \tag{33}$$

$\underline{\boldsymbol{R}}_\mathrm{s}$ in (32) and (33) is termed spatial covariance matrix and has the dimension $K_\mathrm{B} \times K_\mathrm{B}$. For the elements $[\underline{\boldsymbol{R}}_\mathrm{s}]_{i,j}$, $i = 1 \ldots K_\mathrm{B}$, $j = 1 \ldots K_\mathrm{B}$, of $\underline{\boldsymbol{R}}_\mathrm{s}$ follows

$$[\underline{\boldsymbol{R}}_\mathrm{s}]_{i,j} = \int_0^{2\pi} \mathrm{e}^{-\mathrm{j}\boldsymbol{\beta}(\phi)^\mathrm{T}[\underline{\boldsymbol{r}}^{(i)} - \underline{\boldsymbol{r}}^{(j)}]}\, g(\phi)\, \mathrm{d}\phi. \tag{34}$$

Comparing (32) and (16) reveals that minimizing T_d of (32) can be interpreted as a special case of minimizing the hermitian form of (16). Consequently, the total transmit signal $\underline{\boldsymbol{s}}$ which minimizes T_d of (31) can be obtained by substituting $\underline{\boldsymbol{R}}$ of (32) in (26). According to the analysis presented in Section III, it has to be kept in mind that $\underline{\boldsymbol{R}}$ of (32) has to be of full rank.

V. Optimization of spatial characteristics of the total transmit signal, special cases

A. Discrete directions of departure

Let us assume that the average energy $T_\mathrm{d,dis}$ radiated into K_d discrete DODs $\phi^{(k_\mathrm{d})}$, $k_\mathrm{d} = 1 \ldots K_\mathrm{d}$, should be minimized. Setting out from the weighting function

$$g(\phi) = \frac{1}{K_\mathrm{d}} \sum_{k_\mathrm{d}=1}^{K_\mathrm{d}} \delta\left(\phi - \phi^{(k_\mathrm{d})}\right) \tag{35}$$

describing the K_d discrete DODs, with (33) the spatial covariance matrix

$$\underline{\boldsymbol{R}}_\mathrm{s} = \frac{1}{K_\mathrm{d}} \sum_{k_\mathrm{d}=1}^{K_\mathrm{d}} \underline{\boldsymbol{a}}\left(\phi^{(k_\mathrm{d})}\right) \underline{\boldsymbol{a}}\left(\phi^{(k_\mathrm{d})}\right)^{*\mathrm{T}} \tag{36}$$

with the elements

$$[\underline{\boldsymbol{R}}_\mathrm{s}]_{i,j} = \frac{1}{K_\mathrm{d}} \sum_{k_\mathrm{d}=1}^{K_\mathrm{d}} \mathrm{e}^{-\mathrm{j}\boldsymbol{\beta}(\phi^{(k_\mathrm{d})})^\mathrm{T}[\underline{\boldsymbol{r}}^{(i)} - \underline{\boldsymbol{r}}^{(j)}]}, \quad i = 1 \ldots K_\mathrm{B}, j = 1 \ldots K_\mathrm{B}, \tag{37}$$

follows. Utilizing $\underline{\boldsymbol{R}}_\mathrm{s}$ of (36) to obtain $\underline{\boldsymbol{R}}$ of (32) the total transmit signal $\underline{\boldsymbol{s}}$ can be determined by (26) by which minimum average energy is radiated into said K_d discrete DODs. To ensure that $\underline{\boldsymbol{R}}$ of (32) is of full rank, K_d has to be greater than or equal to K_B.

B. Omnidirectional uniform distribution of directions of departure

The average energy $T_\mathrm{d,omni}$ radiated in the azimuth should be minimized. Utilizing the weighting function

$$g(\phi) = \frac{1}{2\pi} \tag{38}$$

to describe the omnidirectional uniform distribution, with (33) the corresponding spatial covariance matrix

$$\underline{\boldsymbol{R}}_\mathrm{s} = \frac{1}{2\pi} \int_0^{2\pi} \underline{\boldsymbol{a}}(\phi)\underline{\boldsymbol{a}}(\phi)^{*\mathrm{T}} \mathrm{d}\phi \tag{39}$$

with the elements [14]

$$[\underline{\boldsymbol{R}}_\mathrm{s}]_{i,j} = \mathrm{J}_0\left(\frac{2\pi}{\lambda}\left\|\boldsymbol{r}^{(i)} - \boldsymbol{r}^{(j)}\right\|\right), i, j = 1 \ldots K_\mathrm{B}, \tag{40}$$

can be obtained. $\mathrm{J}_0(\cdot)$ in (40) denotes the Bessel function of first kind and zero order. (40) shows that each element $[\underline{\boldsymbol{R}}_{\mathrm{s}}]_{i,j}$, $i = 1 \dots K_{\mathrm{B}}$, $j = 1 \dots K_{\mathrm{B}}$, of $\underline{\boldsymbol{R}}_{\mathrm{s}}$ only depends on the wavelength λ and the distance $\|\boldsymbol{r}^{(i)} - \boldsymbol{r}^{(j)}\|$ between two AEs i and j. Setting out from $\underline{\boldsymbol{R}}_{\mathrm{s}}$ of (39), the total transmit signal $\underline{\boldsymbol{s}}$ can be determined in analogy to the proceeding presented in Subsection V-A. In contrast to $\underline{\boldsymbol{R}}_{\mathrm{s}}$ of (36), $\underline{\boldsymbol{R}}_{\mathrm{s}}$ of (39) is always of full rank if $\boldsymbol{r}^{(i)} \neq \boldsymbol{r}^{(j)}$ for all $i = 1 \dots K_{\mathrm{B}}$, $j = 1 \dots K_{\mathrm{B}}$, $i \neq j$.

VI. Application aspects

In the previous sections novel optimization criteria are presented and incorporated into the JT transmit signal design process. Up to now, the motivation for these new approaches is not discussed in detail. In this section such a discussion follows. In principle, the generalized optimization criterion presented in Section III offers the potential to exert more influence on the total transmit signals as compared to conventional JT introduced in [2, 3, 4, 5]. Especially the spatial optimization criteria studied in Sections IV and V allow to directly control the directional distribution of the radiated energy originating in the total transmit signals. Several applications of a control mechanism which is based on that kind of signal optimization are imaginable. In the following, one attractive application will be presented.

A cell of a cellular mobile radio system, termed reference cell, is considered. The MTs assigned to the reference cell are served by the BS of the reference cell by means of JT. Besides, around the reference cell other cells termed cochannel cells with MTs termed cochannel MTs are located, which use the same frequency bands as the reference cell. The total transmit signal radiated by the BS of the reference cell to serve the assigned MTs produces intercell interference and disturbes the data detection at the cochannel MTs. Especially cochannel MTs located close to the BS of the reference cell, e.g. which are at the cell borders, are disturbed by strong intercell interference. For this reason, in the following these cochannel MTs are termed relevant cochannel MTs. When designing a cellular mobile radio system, it has to be guaranteed that a certain upperbound for the service outage probability will no be exceeded. The service outage probability is massively influenced by the relevant cochannel MTs.

With the proposed technique for transmit signal optimization these relevant cochannel MTs can be explicitly taken into account. For instance, if at the BS of the reference cell the DODs of the paths leading to the relevant cochannel MTs are known, then the energy radiated into these directions can be controlled by the approach dicussed in Subsection V-A.

Often the BS of the reference cell has no knowledge about the DODs of the paths leading to the relevant cochannel MTs. In this case, it is admissible to assume that, seen from the BS of the reference cell, on the average the relevant cochannel MTs are uniformly distributed along the azimuth which leads to the approach discussed in Subsection V-B. Such an approach allows to minimize the mean intercell interference produced by the BS of the reference cell. Minimizing the mean intercell interference allows to significantly increase the capacity of the cellular mobile radio system.

TABLE I

DODs $\phi^{(k_{\mathrm{d}})}$, $k_{\mathrm{d}} = 1 \dots 4$, relative to the RL

k_{d}	1	2	3	4
$\phi^{(k_{\mathrm{d}})}/\mathrm{deg}$	145	215	254	345

VII. Exemplary system evaluation

A. Scenario and evaluation quantities

In this section, three approaches for transmit signal optimization for JT introduced in Sections II and V are evaluated by means of simulations. The following approaches are discussed: JT including transmit signal optimization with respect to

- minimum transmit energy T (approach 1), c.f. Section II,
- minimum average energy $T_{\mathrm{d,dis}}$ radiated into K_{d} equal to four discrete directions (approach 2), c.f. Subsection V-A, characterized by $\phi^{(k_{\mathrm{d}})}$, $k_{\mathrm{d}} = 1 \dots 4$, of Table I,
- minimum average energy $T_{\mathrm{d,omni}}$ radiated in the azimuth (approach 3), c.f. Subsection V-B.

In the evaluation the following assumptions are made:

- At the BS a circular array with K_{B} equal to four AEs is provided. The distance between adjacent AEs is one half of the wavelength λ.
- K equal to two MTs are assigned to the BS and are uniformly distributed on a circle around the BS in the farfield of the AEs.
- A set of fixed single-direction channels of dimension W equal to three with exponentially descending power delay profile is assumed between the RP of the transmit antenna of the BS and each MT μ_k, $k = 1 \dots 2$. The details on these channels can be found in [5]. Based on the channels and on the geometry of the configuration, the channel convolution matrix $\underline{\boldsymbol{H}}$ of (8) is determined.
- For each MT μ_k, $k = 1 \dots 2$, a demodulator matrix $\underline{\boldsymbol{D}}^{(k)}$ which is based on a MT specific CDMA signature $\underline{\boldsymbol{c}}^{(k)}$, is employed. The details on $\underline{\boldsymbol{D}}^{(k)}$ and $\underline{\boldsymbol{c}}^{(k)}$, $k = 1 \dots 2$, are presented in [5].
- The simulations are performed for the case that N equal to five data symbols $\underline{d}_n^{(k)}$ with $|\underline{d}_n^{(k)}| = 1$, $n = 1 \dots N$, are transmitted per MT μ_k, $k = 1 \dots 2$.

For the numerical evaluation four quantities are studied:

- directional distribution of the radiated energy $\underline{\boldsymbol{s}}_{\mathrm{d}}(\phi)^{*\mathrm{T}}\underline{\boldsymbol{s}}_{\mathrm{d}}(\phi)/2$ as function of $\phi \in [0, 2\pi[$,
- energy T of the total transmit signal,
- average energy $T_{\mathrm{d,dis}}$ radiated into the K_{d} desired discrete DODs of Table I.
- average energy $T_{\mathrm{d,omni}}$ radiated into the azimuth.

B. Simulation results

Table II shows the total transmit energy T, the average energy $T_{\mathrm{d,dis}}$ radiated into the discrete DODs of Table I and the average energy $T_{\mathrm{d,omni}}$ radiated into the azimuth, when applying approaches 1, 2 and 3 for transmit signal optimization. Each approach minimizes that quantity T, $T_{\mathrm{d,dis}}$ or $T_{\mathrm{d,omni}}$, respectively, for which it is optimized, see Sections II and V. However, the results for one certain quantity and several approaches show disparate behaviour. Whereas T only varies moderately when changing the approach for transmit signal optimization, $T_{\mathrm{d,dis}}$ and $T_{\mathrm{d,omni}}$ show dramatic changes. Approach 1 shows

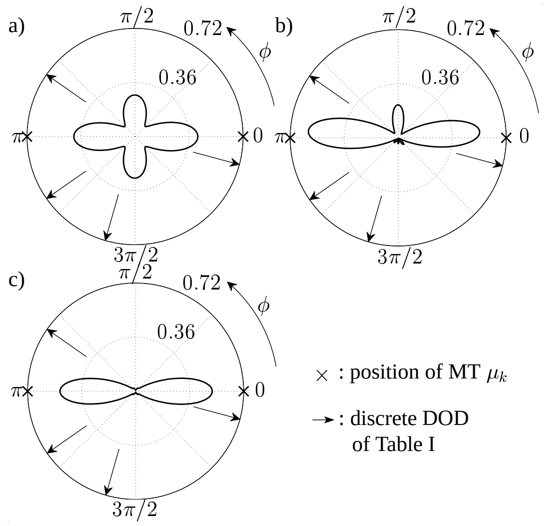

Fig. 3. directional distribution of the radiated energy $\underline{\boldsymbol{s}}_{\mathrm{d}}(\phi)^{*\mathrm{T}}\underline{\boldsymbol{s}}_{\mathrm{d}}(\phi)/2$ as function of the angle $\phi \in [0, 2\pi[$ to the RL when applying a) approach 1, b) approach 2 and c) approach 3.

the poorest performance and yields energies $T_{\mathrm{d,dis}}$ and $T_{\mathrm{d,omni}}$ which are more than 2000% and 700%, respectively, larger than the minimum energies $T_{\mathrm{d,dis}}$ and $T_{\mathrm{d,omni}}$ obtained by approach 2 and 3, respectively. The energies $T_{\mathrm{d,dis}}$ and $T_{\mathrm{d,omni}}$ for the approaches 2 and 3 show only marginal changes. This observation circumstantiates that approach 3 is an attractive one for transmit signal optimization, if no knowledge about the relevant DODs of Subsection V-A is available, see Section VI.

Fig. 3 shows the directional distribution of the radiated energy $\underline{\boldsymbol{s}}_{\mathrm{d}}(\phi)^{*\mathrm{T}}\underline{\boldsymbol{s}}_{\mathrm{d}}(\phi)/2$ for the three approaches introduced above. The DODs leading to the MTs to be served by the BS are marked with small crosses. The discrete DODs of Table I are indicated by arrows. These diagrams endorse the insights gained before. Focusing on Fig. 3a, the average energy radiated into the four given discrete DODs and radiated in the whole azimuth is obviously high, because the radiation pattern has very broad beams and no sharp nulls. In contrast to that, in Fig. 3b the average energy radiated into the four given discrete DODs is very low. The average energy radiated in the whole azimuth is small, but larger than in the case of Fig. 3c, which shows the directional distribution of the radiated energy when applying approach 3.

VIII. Conclusions

In this paper a generalized approach to transmit signal optimization in JT multiuser downlinks is presented. Based on the proposed generalized optimization criterion it is shown how to adapt the JT transmit signal design process correspondingly. A

TABLE II

ENERGIES T, $T_{\mathrm{d,dis}}$ AND $T_{\mathrm{d,omni}}$ FOR APPROACHES 1,2 AND 3.

approach	T	$T_{\mathrm{d,dis}}$	$T_{\mathrm{d,omni}}$
1	0.01785	0.22723	0.10764
2	0.02599	0.01016	0.01295
3	0.02227	0.01787	0.01279

discussion of application aspects and numerical results reveals that the intercell interference situation in cellular mobile radio systems employing the proposed scheme can be significantly improved.

Acknowledgment

The authors gratefully appreciate the fruitful exchange of ideas with their co-workers and Prof. P. W. Baier at the Research Group for RF Communications, University of Kaiserslautern. Moreover, thanks are expressed to Prof. M. Haardt of TU Ilmenau for stimulating discussions. Also the sustaining support by DFG, Siemens AG and by the supercomputer staff of the central computer facility (RHRK) of the University of Kaiserslautern is highly acknowledged.

References

[1] T. Ojanperä and R. Prasad, "An overview of air interface multiple access for IMT-2000/UMTS", *IEEE Communications Magazine*, vol. 36, no. 9, pp. 82–95, 1998.

[2] M. Meurer, P.W. Baier, T. Weber, Y. Lu and A. Papathanassiou, "Joint transmission, an advantageous downlink concept for CDMA mobile radio systems using time division duplexing", *IEE ELECTRONICS LETTERS*, vol. 36, no. 10, pp. 900–901, 2000.

[3] M. Meurer, P.W. Baier, Y. Lu, A. Papathanassiou and T. Weber, "TD-CDMA downlink: Optimum transmit signal design reduces receiver complexity and enhances system performance", *Proc. 7th International Conference on Telecommunications (ICT 2000), Acapulco*, pp. 300–305, 2000.

[4] P.W. Baier, M. Meurer, T. Weber and H. Tröger, "Joint transmission (JT), an alternative rationale for the downlink of time division CDMA using multi-element transmit antennas", *Proc. IEEE 6th International Symposium on Spread Spectrum Techniques & Applications (ISSSTA 2000), Parsippany*, pp. 1–5, 2000.

[5] H. Tröger, T. Weber, M. Meurer and P.W. Baier, "Performance assessment of Joint Transmission (JT) multi-user downlinks with multi-element transmit antennas", *European Transactions on Telecommunications*, vol. 12, no. 5, pp. 407–416, 2001.

[6] M. Tomlinson, "New automatic equalizer employing modulo arithmetic", *IEE ELECTRONICS LETTERS*, vol. 7, no. 5, pp. 138–139, 1971.

[7] H. Harashima and H. Miyakawa, "Matched-transmission technique for channels with intersymbol interference", *IEEE Transactions on Communications*, vol. COM-20, pp. 774–780, 1972.

[8] M. Joham and W. Utschick, "Downlink processing for mitigation of intracell interference in DS-CDMA systems", *Proc. IEEE 6th International Symposium on Spread Spectrum Techniques & Applications (ISSSTA 2000), Parsippany*, pp. 15–19, 2000.

[9] K. Ban, M. Katayama, T. Yamazato and A. Ogawa, "Joint optimization of transmitter/receiver with multiple transmit/receive antennas in band-limited channels", *IEICE Transactions on Communications*, vol. E83-B, no. 8, pp. 1697–1704, 2000.

[10] M. Brandt-Pearce and A. Dharap, "Transmitter-based multiuser interference rejection for the down-link of a wireless CDMA system in a multipath environment", *IEEE Journal on Selected Areas in Communications*, vol. 18, no. 3, pp. 407–417, 2000.

[11] B.R. Vojcic and J.W. Mee, "Transmitter precoding in synchronous multiuser communications", *IEEE Transactions on Communications*, vol. 46, no. 10, pp. 1346–1355, 1998.

[12] F. Kowalewski and P. Mangold, "Joint predistortion and transmit diversity", *Proc. IEEE Global Telecommunications Conference (GLOBECOM'00)*, pp. 245–249, 2000.

[13] A. Klein, *Multi-user detection of CDMA signals – algorithms and their application to cellular mobile radio*, Fortschrittberichte VDI, series 10, no. 423, VDI-Verlag, Düsseldorf, 1996.

[14] I.N. Bronstein and K.A. Semendjajew, *Taschenbuch der Mathematik*, Verlag Harry Deutsch, Frankfurt/Main, 1985.

[15] W. Wirtinger, "Zur formalen Theorie der Funktionen von mehreren komplexen Veränderlichen", *Mathematische Annalen*, vol. 97, pp. 357–376, 1927.

[16] P. W. Baier, J. J. Blanz and R. M. Schmalenberger, "Fundamentals of smart antennas for mobile radio applications", in *Wireless communications – TDMA versus CDMA*, S. G. Glisic and P. A. Leppänen, Eds., Kluwer, Dordrecht/The Netherlands, 1997, pp. 345–376.

[17] A. Graham, *Kronecker products and matrix calculus with applications*, Ellis Horwood, Chichester, 1981.

[MBQ04] Meurer, M.; Baier, P. W.; Qiu, W.: "Receiver Orientation versus Transmitter Orientation in Linear MIMO Transmission Systems". *EURASIP Journal on Applied Signal Processing*, Bd. 9, 2004, S. 1191–1198.

EURASIP Journal on Applied Signal Processing 2004:9, 1191–1198

Receiver Orientation versus Transmitter Orientation in Linear MIMO Transmission Systems

Michael Meurer
Research Group for RF Communications, University of Kaiserslautern, P.O. Box 3049, 67653 Kaiserslautern, Germany
Email: meurer@rhrk.uni-kl.de

Paul Walter Baier
Research Group for RF Communications, University of Kaiserslautern, P.O. Box 3049, 67653 Kaiserslautern, Germany
Email: baier@rhrk.uni-kl.de

Wei Qiu
Research Group for RF Communications, University of Kaiserslautern, P.O. Box 3049, 67653 Kaiserslautern, Germany
Email: wqiu@rhrk.uni-kl.de

Received 23 June 2003; Revised 13 February 2004

In conventional transmission schemes, the transmitter algorithms are a priori given, whereas the algorithms to be used by the receivers have to be a posteriori adapted. Such schemes can be termed transmitter (Tx) oriented and have the potential of simple transmitter implementations. The opposite to Tx orientation would be receiver (Rx) orientation in which the receiver algorithms are a priori given, and the transmitter algorithms have to be a posteriori adapted. An advantage of the rationale Rx orientation is the possibility to arrive at simple receiver structures. In this paper, linear versions of the rationales Tx orientation and Rx orientation are applied to radio transmission systems with multiantennas both at the transmitter and receiver. After the introduction of adequate models for such multiple-input multiple-output (MIMO) systems, different system designs are evaluated by simulations, and recommendations for proper system solutions are given.

Keywords and phrases: MIMO systems, transmitter orientation, receiver orientation.

1. INTRODUCTION

In conventional transmission schemes the transmitter algorithms are a priori given and made known to the receiver, whereas the algorithms to be used by the receivers have to be a posteriori adapted, possibly under consideration of channel information. For this approach, where the transmitter (Tx) is the master and the receiver (Rx) is the slave, the authors propose the term Tx orientation. The opposite to Tx orientation would be Rx orientation in which the receiver algorithms would be a priori given and made known to the transmitter, and the transmitter algorithms, again possibly under consideration of channel information, have to be a posteriori adapted correspondingly. Since the early times of radio communications, the rationale Tx orientation has been preferred because, seemingly, it has some kind of natural appeal to system designers. It was not before the 1990s that the first ideas of Rx orientation came up (cf. Table 1). It took another couple of years to clearly formulate this rationale in 2000 [1]. From then on, it attracted broader attention so that a systematical study could begin. This late perception of Rx orientation is astonishing because each of the two approaches, depending on the particular field of application, has its distinct pros. In the case of Tx orientation, the transmitter algorithms to be a priori determined can be chosen with a view to arrive at particularly simple transmitter implementations. On the other hand, in the case of Rx orientation, the receiver algorithms can be a priori determined in such a way that the receiver complexity is minimized. If we consider, as an important example of a radio transmission, mobile radio systems, the complexity of the mobile terminals (MT) should be as low as possible, whereas more complicated implementations can be tolerated at the base stations (BS). Having in mind the above-mentioned complexity features of the rationales Tx orientation and Rx orientation, this means that in the uplink (UL), the quasi natural choice would be Tx orientation, which leads to low-cost transmitters at the MTs, whereas in the downlink (DL), the rationale Rx orientation would be the favourite alternative because this results in simple receivers at the MTs. In [1, 2], the application of the rationale Rx orientation to mobile radio DLs is considered.

TABLE 1: Selected early publications on Rx-oriented transmission in chronological order.

References	Type of system, proposed techniques, and further remarks
[3, 4]	SISO, CDMA with spreading at Tx, design of FIR prefilter (MF criterion) ⇒ Pre-Rake
[5]	SISO, CDMA with spreading at Tx, pre-decorrelator (ZF criterion)
[6]	SISO, CDMA with spreading at Tx, pre-decorrelator (ZF criterion)
[7]	SISO, CDMA with spreading at Tx, pre-decorrelator (ZF criterion) and pre-MMSE (MMSE criterion)
[8]	MISO, CDMA with spreading at Tx, design of FIR prefilter (MF / ZF / MMSE criterion) ⇒ Pre-Rake
[9]	SISO, CDMA with spreading at Tx, design of FIR prefilter (MF criterion) ⇒ Pre-Rake
[10]	MIMO, MMSE processing (MMSE criterion)
[11]	MISO, CDMA, joint transmission (ZF criterion) ⇒ TxZF
[12]	MISO, CDMA, joint predistortion (ZF criterion) ⇒ TxZF
[13]	SISO, CDMA with spreading at Tx, design of FIR prefilter (ZF criterion)
[14]	MISO, CDMA, joint transmission (ZF criterion) ⇒ TxZF

As mentioned above, in the case of Tx orientation, channel knowledge would be desirable at the MTs, whereas in the case of Rx orientation, such knowledge should be available at the BSs. This means that, in the case of mobile radio systems, the above proposed combination of Tx orientation in the UL and Rx orientation in the DL is particularly easily feasible, if the utilized duplexing scheme is time division duplexing (TDD). In TDD, the UL and the DL use the same frequency in temporally separated periods so that, due to the reciprocity theorem, both links experience the same channel impulse responses as long as the time elapsing between UL and DL transmissions is not too large. Therefore, the channel knowledge needed by the BS receivers in the Tx-oriented UL and obtainable for instance based on the transmission of training signals by the MTs can be used also as the channel knowledge required for the Rx-oriented DL transmission. This approach to exploit channel knowledge available in the BS for DL transmission has the additional advantage that no resources have to be sacrificed for the transmission of training signals in the DL, which is, anyhow, capacity-wise the more critical one of the two links.

An important asset with respect to increasing the spectrum efficiency of radio transmission systems is the use of multiantennas instead of single antennas at both the transmitter and the receiver [15, 16]. Such multi-antenna structures were given the designation multiple input multiple output (MIMO). A series of theoretical results concerning the capacity of MIMO systems [17, 18] and the implementation of such systems [19, 20] came up in recent years. The present paper has the goal to study and compare the rationales Tx

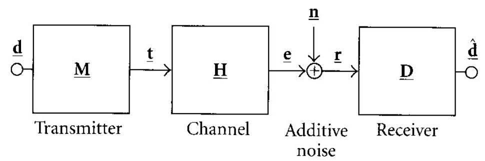

FIGURE 1: Generic model of a linear transmission system.

orientation and Rx orientation and to show some dualities and differences, if linear versions of these schemes are utilized in combination with MIMO antenna structures. Linear systems have, in contrast to nonlinear systems as for instance considered in [21], the advantage of lower complexity [22, 23]. Nevertheless, also in linear systems, a beneficial nonlinear feature can be introduced by operating the linear inner MIMO system in combination with outer FEC coding at the transmitter and FEC decoding at the receiver.

In Section 2, a generic model of linear transmission systems is developed. The topic of Section 3 is the detailed description of the rationales Tx orientation and Rx orientation under inclusion of the linear algorithms to be applied at the transmitters and receivers. In this section, also the quantity signal-to-noise-plus-interference ratio (SNIR) suitable for performance of comparisons of the two rationales is introduced. The generic model developed in Section 2 and the findings of Section 3 are adapted to linear MIMO transmission systems in Section 4. Section 5 presents the results of system simulations; these results help to decide in which cases Tx orientation or Rx orientation should be chosen. Finally, Section 6 summarizes the paper.

The investigations are performed in the time-discrete equivalent low-pass domain under utilization of the vector-matrix representation of signals and system components [24]. Consequently, signals and channel impulse responses are represented by complex vectors or matrices which are printed in bold face. In the analysis, $[\cdot]_{n,n}$ designates the nth diagonal element of a square matrix in brackets, $[\cdot]_n$ stands for the nth row of a matrix in brackets or the nth element of a vector in brackets, and $\|\cdot\|_2$ denotes the Euclidean norm of the vector in brackets. Moreover, the operation $\overline{\mathrm{diag}}(\cdot)$ yields a copy of the matrix in brackets with the diagonal elements being set to zero.

2. GENERIC MODEL OF LINEAR TRANSMISSION SYSTEMS

Figure 1 shows the generic model of a linear transmission system. In this model, the transmitter, the channel, and the receiver are described by the matrices $\underline{\mathbf{M}}$, $\underline{\mathbf{H}}$, and $\underline{\mathbf{D}}$, respectively [1]. $\underline{\mathbf{M}}$, $\underline{\mathbf{H}}$, and $\underline{\mathbf{D}}$ are termed modulator matrix, channel matrix, and demodulator matrix, respectively. The signals occurring in the structure of Figure 1 are represented by the following column vectors:

(i) $\underline{\mathbf{d}}$: data signal to be transmitted,
(ii) $\underline{\mathbf{t}}$: transmit signal,
(iii) $\underline{\mathbf{e}}$: useful receive signal at the channel output,

TABLE 2: Dimensions of the vectors and matrices used in the structure of Figure 1.

Vector or matrix, respectively	Dimensions
$\underline{\mathbf{d}} = (\underline{d}_1,\ldots,\underline{d}_N)^{\mathrm{T}}$	$\mathbb{C}^{N\times 1}$
$\underline{\mathbf{M}}$	$\mathbb{C}^{Q\times N}$, $Q \geq N$
$\underline{\mathbf{t}}$	$\mathbb{C}^{Q\times 1}$
$\underline{\mathbf{H}}$	$\mathbb{C}^{S\times Q}$
$\underline{\mathbf{e}}$	$\mathbb{C}^{S\times 1}$
$\underline{\mathbf{n}}$	$\mathbb{C}^{S\times 1}$
$\underline{\mathbf{r}}$	$\mathbb{C}^{S\times 1}$
$\underline{\mathbf{D}}$	$\mathbb{C}^{N\times S}$
$\hat{\underline{\mathbf{d}}}$	$\mathbb{C}^{N\times 1}$

(iv) $\underline{\mathbf{n}}$: Gaussian noise signal at the receiver input,
(v) $\underline{\mathbf{r}}$: disturbed signal at the receiver input,
(vi) $\hat{\underline{\mathbf{d}}}$: linear estimate of $\underline{\mathbf{d}}$ at the receiver output.

The dimensions of the vectors and matrices used in the structure of Figure 1 are specified in Table 2.

The elements $\underline{d}_n$, $n = 1,\ldots,N$, of $\underline{\mathbf{d}}$ are the data symbols to be transmitted and are taken from a finite symbol set

$$\mathbb{V} = \{\underline{v}_1 \cdots \underline{v}_M\} \tag{1}$$

of cardinality M. $\underline{\mathbf{d}}$ and $\underline{\mathbf{n}}$ are assumed to be wide-sense stationary with zero mean and the covariance matrices

$$\underline{\mathbf{R}}_{\mathrm{d}} = 2\sigma_{\mathrm{d}}^2 \mathbf{I}^{N\times N}, \tag{2}$$

$$\underline{\mathbf{R}}_{\mathrm{n}} = 2\sigma^2 \mathbf{I}^{S\times S}, \tag{3}$$

respectively. In the system of Figure 1, the estimate $\hat{\underline{\mathbf{d}}}$ of $\underline{\mathbf{d}}$ obtained at the receiver output can be expressed as

$$\begin{aligned}\hat{\underline{\mathbf{d}}} = (\hat{\underline{d}}_1 \cdots \hat{\underline{d}}_N)^{\mathrm{T}} &= \underline{\mathbf{D}}\,\underline{\mathbf{r}} = \underline{\mathbf{D}}(\underline{\mathbf{e}} + \underline{\mathbf{n}}) = \underline{\mathbf{D}}(\underbrace{\underline{\mathbf{H}}\,\underline{\mathbf{t}}}_{\underline{\mathbf{e}}} + \underline{\mathbf{n}}) \\ &= \underline{\mathbf{D}}(\underline{\mathbf{H}}\underbrace{\underline{\mathbf{M}}\,\underline{\mathbf{d}}}_{\underline{\mathbf{t}}} + \underline{\mathbf{n}}) = \underline{\mathbf{D}}\,\underline{\mathbf{H}}\,\underline{\mathbf{M}}\,\underline{\mathbf{d}} + \underline{\mathbf{D}}\,\underline{\mathbf{n}}.\end{aligned} \tag{4}$$

$\underline{\mathbf{D}}\,\underline{\mathbf{H}}\,\underline{\mathbf{M}}$ is a square matrix of dimension $N \times N$. Generally, each data symbol $\underline{d}_n$, $n = 1,\ldots,N$, has an influence on all Q elements of $\underline{\mathbf{t}}$. Therefore, Q can be considered as a spreading factor, where, as we will see in Section 4, spreading can have a temporal and a spatial component.

According to (2) and (4), the mean radiated energy invested for the data symbol $\underline{d}_n$ becomes

$$T_n = \frac{1}{2}\left\|[\underline{\mathbf{M}}^{\mathrm{T}}]_n\right\|_2^2 2\sigma_{\mathrm{d}}^2, \tag{5}$$

where the factor "1/2" results from the low-pass domain representation used within this contribution [25]. By averaging over all N data symbols $\underline{d}_n$, $n = 1,\ldots,N$, we obtain the mean radiated energy

$$T = \frac{\sigma_{\mathrm{d}}^2}{N}\sum_{n=1}^{N}\left\|[\underline{\mathbf{M}}^{\mathrm{T}}]_n\right\|_2^2 \tag{6}$$

per data symbol.

The estimate $\hat{\underline{d}}_n$ of the transmitted data symbol $\underline{d}_n$ consists of the sum of a useful part

$$\underline{d}_{\mathrm{useful},n} = [\underline{\mathbf{D}}\,\underline{\mathbf{H}}\,\underline{\mathbf{M}}]_{n,n}\underline{d}_n, \tag{7}$$

of an interference part

$$\underline{d}_{\mathrm{int},n} = [\overline{\mathrm{diag}}(\underline{\mathbf{D}}\,\underline{\mathbf{H}}\,\underline{\mathbf{M}})\underline{\mathbf{d}}]_n, \tag{8}$$

and of a noise part

$$\underline{d}_{\mathrm{noise},n} = [\underline{\mathbf{D}}\,\underline{\mathbf{n}}]_n; \tag{9}$$

see also [24]. In (8) and (9), the terms in brackets are column vectors. A concise and obvious quality measure for the estimates $\hat{\underline{d}}_n$ of (4) are the SNIRs γ_n [24]. With (2), (3), (7), (8), and (9), we obtain

$$\begin{aligned}\gamma_n &= \frac{\mathrm{E}\left\{|\underline{d}_{\mathrm{useful},n}|^2\right\}}{\mathrm{E}\left\{|\underline{d}_{\mathrm{noise},n}|^2\right\} + \mathrm{E}\left\{|\underline{d}_{\mathrm{int},n}|^2\right\}} \\ &= \frac{|[\underline{\mathbf{D}}\,\underline{\mathbf{H}}\,\underline{\mathbf{M}}]_{n,n}|^2\sigma_{\mathrm{d}}^2}{\|[\underline{\mathbf{D}}]_n\|_2^2\sigma^2 + \|[\overline{\mathrm{diag}}(\underline{\mathbf{D}}\,\underline{\mathbf{H}}\,\underline{\mathbf{M}})]_n\|_2^2\sigma_{\mathrm{d}}^2}.\end{aligned} \tag{10}$$

Even though in this paper, γ_n is adopted as the quality measure and quantitatively studied, ultimately the symbol error probabilities would be the proper measure. Fortunately, in many cases, noise plus interference can be modeled as white Gaussian noise with sufficient accuracy. Then, the error probabilities immediately follow from the values γ_n. Otherwise, also the probability density function of noise plus interference has to be taken into account.

3. TRANSMITTER ORIENTATION AND RECEIVER ORIENTATION

The a posteriori determination of $\underline{\mathbf{D}}$ in the case of linear Tx orientation or of $\underline{\mathbf{M}}$ in the case of linear Rx orientation have to be performed under the consideration of certain criteria. Depending on these criteria, different matrices $\underline{\mathbf{D}}$ or $\underline{\mathbf{M}}$, respectively, result. In what follows, first expressions for determining $\underline{\mathbf{D}}$ or $\underline{\mathbf{M}}$, respectively, are presented, and only then it will be explained which criteria stand behind these expressions. The authors believe that this procedure facilitates the understanding of the presentation, even though the said expressions are consequences of the related criteria.

In the case of Tx orientation, $\underline{\mathbf{M}}$ and $\underline{\mathbf{H}}$ are a priori given, whereas $\underline{\mathbf{D}}$ is a posteriori determined at the Rx based on the knowledge of $\underline{\mathbf{M}}$ and $\underline{\mathbf{H}}$. Well-known approaches for determining $\underline{\mathbf{D}}$ are the receive matched filter (RxMF), the receive zero forcer (RxZF), and the receive minimum mean square error estimator (RxMMSE) [24]. In these three cases, the demodulator matrix is a posteriori determined according to [24]

$$\underline{\mathbf{D}} = \begin{cases} (\underline{\mathbf{H}}\,\underline{\mathbf{M}})^{\mathrm{H}} & (\mathrm{RxMF}), \\ \left[(\underline{\mathbf{H}}\,\underline{\mathbf{M}})^{\mathrm{H}}\underline{\mathbf{H}}\,\underline{\mathbf{M}}\right]^{-1}(\underline{\mathbf{H}}\,\underline{\mathbf{M}})^{\mathrm{H}} & (\mathrm{RxZF}), \\ \left[(\underline{\mathbf{H}}\,\underline{\mathbf{M}})^{\mathrm{H}}\underline{\mathbf{H}}\,\underline{\mathbf{M}} + \sigma^2\mathbf{I}^{N\times N}\right]^{-1}(\underline{\mathbf{H}}\,\underline{\mathbf{M}})^{\mathrm{H}} & (\mathrm{RxMMSE}). \end{cases} \tag{11}$$

In the case of Rx orientation, $\underline{\mathbf{H}}$ and $\underline{\mathbf{D}}$ are a priori given, and $\underline{\mathbf{M}}$ is a posteriori determined at the Tx based on the knowledge of $\underline{\mathbf{H}}$ and $\underline{\mathbf{D}}$. Approaches meanwhile quite well known to determining $\underline{\mathbf{M}}$ are the transmit matched filter (TxMF) and the transmit zero forcer (TxZF) [1, 2]. For these, the modulator matrix is a posteriori determined as follows:

$$\underline{\mathbf{M}} = \begin{cases} (\underline{\mathbf{D}}\,\underline{\mathbf{H}})^{\mathrm{H}}, & (\mathrm{TxMF}) \\ (\underline{\mathbf{D}}\,\underline{\mathbf{H}})^{\mathrm{H}}\left[\underline{\mathbf{D}}\,\underline{\mathbf{H}}(\underline{\mathbf{D}}\,\underline{\mathbf{H}})^{\mathrm{H}}\right]^{-1}. & (\mathrm{TxZF}) \end{cases} \tag{12}$$

Other options for Rx orientation are various kinds of transmit minimum mean square error modulators (TxMMSE). In one version, which leads to a closed-form expression for $\underline{\mathbf{M}}$, we set out from a given average transmit energy T, see (6), and, under this condition, determine $\underline{\mathbf{M}}$ with a real scalar k according to

$$\begin{aligned} \underline{\mathbf{M}} &= k(\underline{\mathbf{D}}\,\underline{\mathbf{H}})^{\mathrm{H}}\left[\underline{\mathbf{D}}\,\underline{\mathbf{H}}(\underline{\mathbf{D}}\,\underline{\mathbf{H}})^{\mathrm{H}} + \frac{\sigma^2}{NT}\operatorname{trace}(\underline{\mathbf{D}}\,\underline{\mathbf{D}}^{\mathrm{H}})\mathbf{I}^{N\times N}\right]^{-1}, \\ \text{s.t.}\quad & \frac{\sigma_{\mathrm{d}}^2}{N}\sum_{n=1}^{N}\left\|\left[\underline{\mathbf{M}}^{\mathrm{T}}\right]_n\right\|_2^2 \\ &\overset{!}{=} T \quad \text{by proper choice of } k \quad (\mathrm{TxMMSE}). \end{aligned} \tag{13}$$

Equation (13) was first published in [26] in a somewhat different form.

Now we come to the said criteria behind the expressions (11) to (13). The criterion being fulfilled by the Tx-oriented schemes of (11) and the Rx-oriented schemes of (12) is the maximization of γ_n of (10) for a given mean transmit energy T_n per data symbol $\underline{d}_n$, see (5), and under different side conditions, namely [2, 24], the following.

(1) RxMF, TxMF: the impact of the interference term $\|[\overline{\operatorname{diag}}(\underline{\mathbf{D}}\,\underline{\mathbf{H}}\,\underline{\mathbf{M}})]_n\|^2\sigma_{\mathrm{d}}^2$ in the denominator on the right-hand side of (10) is neglected.

(2) RxZF, TxZF: the impact of the interference term $\|[\overline{\operatorname{diag}}(\underline{\mathbf{D}}\,\underline{\mathbf{H}}\,\underline{\mathbf{M}})]_n\|^2\sigma_{\mathrm{d}}^2$ in the denominator on the right-hand side of (10) is eliminated by forcing this term to zero.

(3) RxMMSE: an optimum compromise between the impact of the noise term $\|[\underline{\mathbf{D}}]_n\|^2\sigma^2$ and the interference term $\|[\overline{\operatorname{diag}}(\underline{\mathbf{D}}\,\underline{\mathbf{H}}\,\underline{\mathbf{M}})]_n\|^2\sigma_{\mathrm{d}}^2$ is brought about.

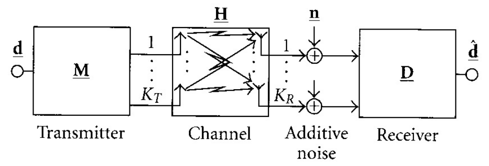

Figure 2: Linear MIMO transmission system.

In the case of the TxMMSE of (13), an average SNIR defined as

$$\gamma_{\mathrm{TxMMSE}} = \frac{\sigma_{\mathrm{d}}^2\sum_{n=1}^{N}\left|[\underline{\mathbf{D}}\,\underline{\mathbf{H}}\,\underline{\mathbf{M}}]_{n,n}\right|^2}{\sum_{n=1}^{N}\left\{\|[\underline{\mathbf{D}}]_n\|_2^2\sigma^2 + \|[\overline{\operatorname{diag}}(\underline{\mathbf{D}}\,\underline{\mathbf{H}}\,\underline{\mathbf{M}})]_n\|_2^2\sigma_{\mathrm{d}}^2\right\}} \tag{14}$$

is maximized for a given mean transmit energy T of (6) [26].

An important issue when evaluating the transmission schemes of (11) to (13) is the determination of the SNIRs for given mean transmit energies T_n of (5) or T of (6). Therefore, the question arises how these energies can be predetermined. In the case of the Tx-oriented schemes of (11), the mean transmit energies T_n per data symbol can be predetermined based on (5) when a priori establishing $\underline{\mathbf{M}}$ in a straightforward way. In the case of the TxMF and the TxZF, see (12), the predetermination of T_n has to be accomplished as follows:

(i) determine $\underline{\mathbf{M}}$ by using (12),

(ii) column-wise scale this $\underline{\mathbf{M}}$ in such a way that (5) yields the desired mean energies T_n.

In the case of the TxMMSE, see (13), the mean radiated energy T per data symbol can again be predetermined in a straightforward way.

The above theory is valid under the implicit understanding that the matrices to be inverted in (11) to (13) are nonsingular. This condition is usually fulfilled in reasonably designed systems. However, a closer look at this problem has yet to come.

4. LINEAR MIMO TRANSMISSION SYSTEMS

Figure 2 shows a linear MIMO transmission system with K_{T} antennas at the transmitter and K_{R} antennas at the receiver. The question is how in the case of such a MIMO system the vectors and matrices introduced in the generic transmission system of Section 2 have to be adjusted in order to make the equations derived in Sections 2 and 3 applicable.

We assume that each data symbol $\underline{d}_n$ is temporally spread over Q_{t} chips [2]. Then, with the K_{T} matrices

$$\underline{\mathbf{M}}^{(k_{\mathrm{T}})} = \begin{pmatrix} \underline{M}_{1,1}^{(k_{\mathrm{T}})} & \underline{M}_{1,2}^{(k_{\mathrm{T}})} & \cdots & \underline{M}_{1,N}^{(k_{\mathrm{T}})} \\ \underline{M}_{2,1}^{(k_{\mathrm{T}})} & \underline{M}_{2,2}^{(k_{\mathrm{T}})} & \cdots & \underline{M}_{2,N}^{(k_{\mathrm{T}})} \\ \vdots & \vdots & \ddots & \vdots \\ \underline{M}_{Q_{\mathrm{t}},1}^{(k_{\mathrm{T}})} & \underline{M}_{Q_{\mathrm{t}},2}^{(k_{\mathrm{T}})} & \cdots & \underline{M}_{Q_{\mathrm{t}},N}^{(k_{\mathrm{T}})} \end{pmatrix} \in \mathbb{C}^{Q_{\mathrm{t}}\times N} \tag{15}$$

termed transmit antenna specific modulator matrices, the (total) modulator matrix takes the form [2]

$$\underline{\mathbf{M}} = \left(\underline{\mathbf{M}}^{(1)^{\mathrm{T}}} \ \underline{\mathbf{M}}^{(2)^{\mathrm{T}}} \ \cdots \ \underline{\mathbf{M}}^{(K_{\mathrm{T}})^{\mathrm{T}}}\right)^{\mathrm{T}}, \quad \underline{\mathbf{M}} \in \mathbb{C}^{(Q_{\mathrm{t}}K_{\mathrm{T}})\times N}. \tag{16}$$

According to (16), the spreading factor Q introduced in Table 2 now reads

$$Q = Q_{\mathrm{t}}K_{\mathrm{T}}. \tag{17}$$

This shows that the total spreading quantified by Q results from a temporal spreading and a spatial spreading represented by Q_{t} and K_{T}, respectively.

The radio channel between transmit antenna k_{T}, $k_{\mathrm{T}} = 1,\ldots,K_{\mathrm{T}}$, and receive antenna $k_{\mathrm{R}}, k_{\mathrm{R}} = 1,\ldots,K_{\mathrm{R}}$, can be characterized by the transmit and receive antenna specific impulse response

$$\underline{\mathbf{h}}^{(k_{\mathrm{R}},k_{\mathrm{T}})} = \frac{1}{W}\left(\underline{h}_1^{(k_{\mathrm{R}},k_{\mathrm{T}})} \ \underline{h}_2^{(k_{\mathrm{R}},k_{\mathrm{T}})} \ \cdots \ \underline{h}_W^{(k_{\mathrm{R}},k_{\mathrm{T}})}\right)^{\mathrm{T}} \tag{18}$$

of dimension W [2]. Taking into account that each of the K_{T} transmit antennas radiates a signal of dimension $Q_{\mathrm{t}} \times 1$, the signal transmission from the transmit antenna k_{T}, $k_{\mathrm{T}} = 1,\ldots,K_{\mathrm{T}}$, to the receive antenna $k_{\mathrm{R}}, k_{\mathrm{R}} = 1,\ldots,K_{\mathrm{R}}$, can be described by the transmit and receive antenna specific channel matrix

$$\underline{\mathbf{H}}^{(k_{\mathrm{R}},k_{\mathrm{T}})} = \begin{pmatrix} \underline{h}_1^{(k_{\mathrm{R}},k_{\mathrm{T}})} & 0 & \cdots & 0 \\ \underline{h}_2^{(k_{\mathrm{R}},k_{\mathrm{T}})} & \underline{h}_1^{(k_{\mathrm{R}},k_{\mathrm{T}})} & \ddots & \vdots \\ \vdots & \underline{h}_2^{(k_{\mathrm{R}},k_{\mathrm{T}})} & \ddots & 0 \\ \underline{h}_W^{(k_{\mathrm{R}},k_{\mathrm{T}})} & \vdots & \ddots & \underline{h}_1^{(k_{\mathrm{R}},k_{\mathrm{T}})} \\ 0 & \underline{h}_W^{(k_{\mathrm{R}},k_{\mathrm{T}})} & \ddots & \underline{h}_2^{(k_{\mathrm{R}},k_{\mathrm{T}})} \\ \vdots & \ddots & \ddots & \vdots \\ 0 & \cdots & 0 & \underline{h}_W^{(k_{\mathrm{R}},k_{\mathrm{T}})} \end{pmatrix}, \quad \underline{\mathbf{H}}^{(k_{\mathrm{R}},k_{\mathrm{T}})} \in \mathbb{C}^{(Q_{\mathrm{t}}+W-1)\times Q_{\mathrm{t}}}. \tag{19}$$

The $K_{\mathrm{R}}K_{\mathrm{T}}$ transmit and receive antenna specific channel matrices $\underline{\mathbf{H}}^{(k_{\mathrm{R}},k_{\mathrm{T}})}$ of (19) can be stacked to the (total) channel matrix

$$\underline{\mathbf{H}} = \begin{pmatrix} \underline{\mathbf{H}}^{(1,1)} & \underline{\mathbf{H}}^{(1,2)} & \cdots & \underline{\mathbf{H}}^{(1,K_{\mathrm{T}})} \\ \underline{\mathbf{H}}^{(2,1)} & \underline{\mathbf{H}}^{(2,2)} & \cdots & \underline{\mathbf{H}}^{(2,K_{\mathrm{T}})} \\ \vdots & \vdots & \ddots & \vdots \\ \underline{\mathbf{H}}^{(K_{\mathrm{R}},1)} & \underline{\mathbf{H}}^{(K_{\mathrm{R}},2)} & \cdots & \underline{\mathbf{H}}^{(K_{\mathrm{R}},K_{\mathrm{T}})} \end{pmatrix}, \quad \underline{\mathbf{H}} \in \mathbb{C}^{[(Q_{\mathrm{t}}+W-1)K_{\mathrm{R}}]\times(Q_{\mathrm{t}}K_{\mathrm{T}})}. \tag{20}$$

According to (20), the quantity S introduced in Table 2 can be expressed as

$$S = (Q_{\mathrm{t}} + W - 1)K_{\mathrm{R}} \tag{21}$$

in the case of the considered MIMO system. Therefore, the signals $\underline{\mathbf{e}}$, $\underline{\mathbf{n}}$, and $\underline{\mathbf{r}}$, see Table 2, have the dimension $[(Q_{\mathrm{t}} + W - 1)K_{\mathrm{R}}] \times 1$. Consequently,

$$\underline{\mathbf{D}} \in \mathbb{C}^{N\times[(Q_{\mathrm{t}}+W-1)K_{\mathrm{R}}]} \tag{22}$$

holds for the demodulator matrix.

With the matrices $\underline{\mathbf{M}}$, $\underline{\mathbf{H}}$, and $\underline{\mathbf{D}}$ defined by (16), (20), and (22), respectively, the different transmission schemes specified by (11), (12), and (13) can be immediately applied to linear MIMO transmission systems.

5. SYSTEM EVALUATIONS BY SIMULATIONS

Based on the performance measure SNIR of (10), different versions of linear MIMO transmission systems can be compared and assessed. Questions to be answered by such comparisons concern

(i) the performance difference of Tx-oriented and Rx-oriented systems,
(ii) the influence of the antenna numbers K_{T} and K_{R} on the system performance.

Because a closed-form analysis is not possible, these questions will be addressed by simulations in what follows. Concerning the design of linear MIMO transmission systems, besides the distinction between Tx orientation and Rx orientation, we can choose from a great variety of system parametrizations and channel realizations. In this paper, only a limited selection of such variants can be considered, which, nevertheless, will allow some generally valid statements. In all simulations, we set

$$N = Q_{\mathrm{t}} = W = 4. \tag{23}$$

Simulations are performed for different pairs K_{T}, K_{R} of antenna numbers. For each such pair, many system realizations are investigated. In each realization, the elements of $\underline{\mathbf{h}}^{(k_{\mathrm{R}},k_{\mathrm{T}})}$ of (18) and—in the case of Tx orientation—the elements of $\underline{\mathbf{M}}$, or—in the case of Rx orientation—the elements of $\underline{\mathbf{D}}$ are chosen as independent realizations of a complex Gaussian random variable with variance 1 of its real and imaginary parts. For a given T/σ^2, by averaging over all N values γ_n of (10) and all realizations, the mean SNIR γ can be obtained as a function of T/σ^2. Concerning the predetermination of T, see the last paragraph of Section 3. The determination of $\underline{\mathbf{h}}^{(k_{\mathrm{R}},k_{\mathrm{T}})}$ described above means that all $K_{\mathrm{T}}K_{\mathrm{R}}$ channel impulse responses are totally uncorrelated. The opposite to this extreme case would be totally correlated channel impulse responses, which, however, are not considered in this paper.

In Figures 3a, 3b, 3c, 3d, 3e, and 3f, the mean SNIR γ is plotted versus T/σ^2 for different pairs K_{T}, K_{R} and different transmission schemes. The curves in these figures allow the following conclusions.

(1) Both in the case of Tx orientation and Rx orientation, the MF outperforms the ZF for small values of T/σ^2, and the ZF outperforms the MF for large values of T/σ^2. See Figures 3a, 3b, 3c, and 3d.

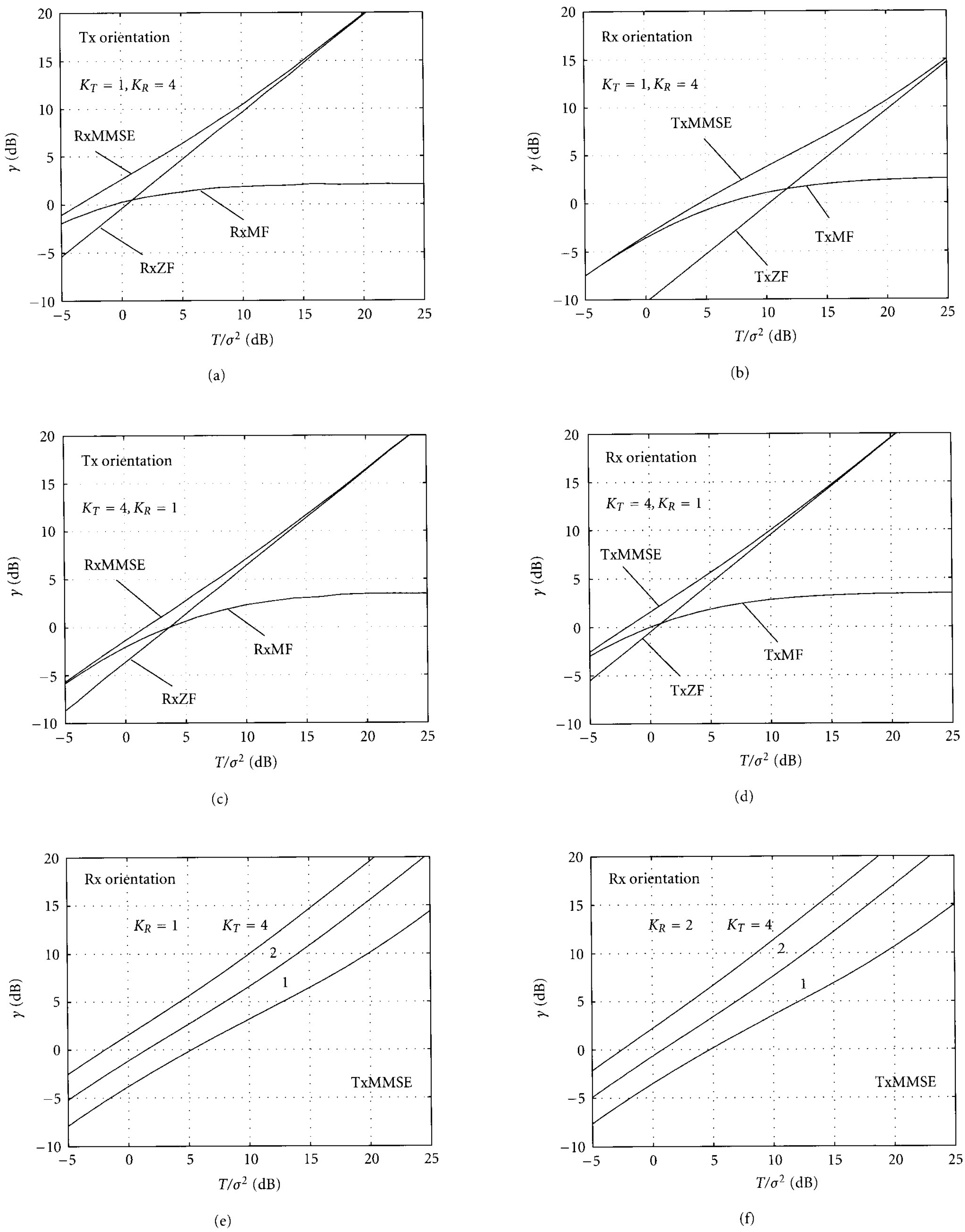

Figure 3: Mean SNIR γ versus T/σ^2 for the rationales Tx orientation and Rx orientation and for different combinations K_T, K_R; $N = Q_t = W = 4$.

(2) Both in the case of Tx orientation and Rx orientation, the MMSE outperforms the MF and the ZF. For small values of T/σ^2, the performance of the MMSE converges to the performance of the MF, and for large values of T/σ^2 to the performance of the ZF. See Figures 3a, 3b, 3c, and 3d.

(3) If the number K_R of receive antennas is larger than the number K_T of transmit antennas, Tx orientation should be chosen because it outperforms Rx orientation. If K_R is smaller than K_T, the opposite is true. Compare Figures 3a and 3b, and Figures 3c and 3d.

(4) The performance is enhanced with growing K_T and K_R. See Figures 3e and 3f.

If we compare the Tx-oriented schemes for $K_T = 1$ and $K_R = 4$ (see Figure 3a) with the Rx-oriented schemes for $K_T = 4$ and $K_R = 1$ (see Figure 3d) or if we compare the Tx-oriented schemes for $K_T = 4$, $K_R = 1$ (see Figure 3c) with the Rx-oriented schemes for $K_T = 1$, $K_R = 4$ (see Figure 3b), we can find a very interesting result: if the number of antennas in the two considered schemes both at the a priori given sides and at the a posteriori adapted sides are equal, then the Rx-oriented schemes perform worse than the Tx-oriented schemes. This effect results from the assumption of totally uncorrelated channel impulse responses of dimension W, which is larger than one.

6. SUMMARY

A system model for linear MIMO transmission systems is developed, and this model is worked out for the cases of Tx-oriented and Rx-oriented systems. Based on the system model, performance comparisons and evaluations are made in which the performance measure is the mean SNIR, and the recommendations concerning the system design are given.

ACKNOWLEDGMENTS

The authors gratefully appreciate the fruitful exchange of ideas with C. A. Jötten, H. Tröger, and T. Weber from the Research Group for RF Communications, University of Kaiserslautern (UKL). The support of individual parts of this work in the framework of the EU-IST-Project FLOWS (Flexible Convergence of Wireless Standards and Services), by DFG, by Siemens AG, and by the supercomputer staff of the central computer facility (RHRK) of the TUKL is highly acknowledged. Thanks are also extended to the anonymous reviewers for their valuable comments and to A. Bruhn and M. Cuntz for, despite all time pressure, carefully typesetting the manuscript in LaTeX.

REFERENCES

[1] P. W. Baier, M. Meurer, T. Weber, and H. Tröger, "Joint transmission (JT), an alternative rationale for the downlink of time division CDMA using multi-element transmit antennas," in *Proc. IEEE 6th International Symposium on Spread Spectrum Techniques and Applications (ISSSTA '00)*, vol. 1, pp. 1–5, Parsippany, NJ, USA, September 2000.

[2] P. W. Baier, W. Qiu, H. Tröger, C. A. Jötten, and M. Meurer, "Modelling and optimization of receiver oriented multi-user MIMO downlinks for frequency selective channels," in *Proc. 10th International Conference on Telecommunications (ICT '03)*, vol. 2, pp. 1547–1554, Papeete, French Polynesia, February 2003.

[3] R. Esmailzadeh and M. Nakagawa, "Pre-RAKE diversity combination for direct sequence spread spectrum mobile communications systems," *IEICE Transactions on Communications*, vol. 76, no. 8, pp. 1008–1015, 1993.

[4] R. Esmailzadeh, E. Sourour, and M. Nakagawa, "Pre-RAKE diversity combining in time division duplex CDMA mobile communications," in *Proc. IEEE 6th International Symposium on Personal, Indoor and Mobile Radio Communications (PIMRC '95)*, vol. 2, pp. 431–435, Toronto, Ontario, Canada, September 1995.

[5] Z. Tang and S. Cheng, "Interference cancellation for DS-CDMA systems over flat fading channels through pre-decorrelating," in *Proc. IEEE 5th International Symposium on Personal, Indoor and Mobile Radio Communications (PIMRC '94)*, vol. 2, pp. 435–438, The Hague, The Netherlands, September 1994.

[6] H. Matsutani, Y. Sanada, and M. Nakagawa, "A forward link intracell orthogonalization technique using multicarrier pre-decorrelation for CDMA wireless local communication system," in *Proc. IEEE 8th International Symposium on Personal, Indoor and Mobile Radio Communications (PIMRC '97)*, vol. 1, pp. 125–129, Helsinki, Finland, September 1997.

[7] B. Vojcic and W. M. Jang, "Transmitter precoding in synchronous multiuser communications," *IEEE Transactions on Communications*, vol. 46, no. 10, pp. 1346–1355, 1998.

[8] G. Montalbano, I. Ghauri, and D. T. M. Slock, "Spatio-temporal array processing for CDMA/SDMA downlink transmission," in *Proc. 32nd Asilomar Conference on Signals, Systems and Computers*, vol. 2, pp. 1337–1341, Pacific Grove, Calif, USA, November 1998.

[9] A. N. Barreto and G. Fettweis, "On the downlink capacity of TDD CDMA systems using a Pre-RAKE," in *IEEE Global Telecommunications Conference (GLOBECOM '99)*, vol. 1A, pp. 117–121, Rio de Janeiro, Brazil, December 1999.

[10] H. R. Karimi, M. Sandell, and J. Salz, "Comparison between transmitter and receiver array processing to achieve interference nulling and diversity," in *Proc. IEEE 10th International Symposium on Personal, Indoor and Mobile Radio Communications (PIMRC'99)*, vol. 3, pp. 997–1001, Osaka, Japan, September 1999.

[11] M. Meurer, P. W. Baier, T. Weber, Y. Lu, and A. Papathanassiou, "Joint transmission: advantageous downlink concept for CDMA mobile radio systems using time division duplexing," *IEE Electronics Letters*, vol. 11, no. 10, pp. 900–901, 2000.

[12] F. Kowalewski and P. Mangold, "Joint predistortion and transmit diversity," in *Proc. IEEE Global Telecommunications Conference(GLOBECOM '00)*, vol. 1, pp. 245–249, San Francisco, Calif, USA, 2000.

[13] M. Brandt-Pearce and A. Dharap, "Transmitter-based multiuser interference rejection for the down-link of a wireless CDMA system in a multipath environment," *IEEE Journal on Selected Areas in Communications*, vol. 18, no. 3, pp. 407–417, 2000.

[14] M. Joham and W. Utschick, "Downlink processing for mitigation of intracell interference in DS-CDMA systems," in *Proc. IEEE 6th International Symposium on Spread Spectrum Techniques and Applications (ISSSTA '00)*, vol. 1, pp. 15–19, Parsippany, NJ, USA, September 2000.

[15] G. G. Raleigh and J. M. Cioffi, "Spatio-temporal coding for wireless communication," *IEEE Transactions on Communications*, vol. 46, no. 3, pp. 357–366, 1998.

[16] D. Gesbert, M. Shafi, D.-S. Shiu, P. J. Smith, and A. Naguib, "From theory to practice: an overview of MIMO space-time coded wireless systems," *IEEE Journal on Selected Areas in Communications*, vol. 21, no. 3, pp. 281–302, 2003.

[17] G. J. Foschini and M. Gans, "On limits of wireless communications in a fading environment when using multiple antennas," *Wireless Personal Communications*, vol. 6, no. 3, pp. 311–335, 1998.

[18] I. E. Telatar, "Capacity of multi-antenna Gaussian channels," *European Transactions on Telecommunications*, vol. 10, no. 6, pp. 585–595, 1999.

[19] G. J. Foschini, "Layered space-time architecture for wireless communication in a fading environment when using multi-element antennas," *Bell Labs Technical Journal*, vol. 1, no. 2, pp. 41–59, 1996.

[20] P. Wolniansky, G. J. Foschini, G. D. Golden, and R. A. Valenzuela, "V-BLAST: An architecture for realizing very high data rates over the rich-scattering wireless channel," in *Proc. URSI International Symposium on Signals, Systems, and Electronics (ISSSE '98)*, pp. 295–300, Pisa, Italy, 1998.

[21] E. Biglieri, G. Taricco, and A. Tulino, "Decoding space-time codes with BLAST architectures," *IEEE Transactions on Signal Processing*, vol. 50, no. 10, pp. 2547–2552, 2002.

[22] T. Weber and M. Meurer, "Optimum joint transmission: Potentials and dualities," in *Proc. 6th International Symposium on Wireless Personal Multimedia Communications (WPMC '03)*, vol. 1, pp. 79–83, Yokosuka, Japan, October 2003.

[23] R. Irmer, W. Rave, and G. Fettweis, "Minimum BER transmission for TDD-CDMA in frequency-selective channels," in *Proc. IEEE 14th International Symposium on Personal, Indoor and Mobile Radio Communications (PIMRC '03)*, vol. 2, pp. 1260–1264, Beijing, China, September 2003.

[24] A. Klein, *Multi-User Detection of CDMA Signals— Algorithms and Their Application to Cellular Mobile Radio*, Number 423 in Fortschrittberichte VDI, Reihe 10. VDI-Verlag, Düsseldorf, Germany, 1996.

[25] S. Stein and J. J. Jones, *Modern Communication Principles*, McGraw-Hill, New York, NY, USA, 1967.

[26] M. Joham, K. Kusume, M. H. Gzara, W. Utschick, and J. A. Nossek, "Transmit Wiener filter for the downlink of TDD DS-CDMA systems," in *Proc. IEEE 7th International Symposium on Spread Spectrum Techniques and Applications (ISSSTA '02)*, vol. 1, pp. 9–13, Prague, Czech Republic, September 2002.

Michael Meurer was born in Dernbach (Westerwald), Germany, in 1974 and received the diploma in electrical engineering in 1998 and the doctoral degree in 2003, both from the University of Kaiserslautern, Germany. After graduation in October 1998, he joined the Research Group for RF Communications at the University of Kaiserslautern, Germany, as a Research Engineer, where he is presently active as a Senior Research Engineer and Senior Lecturer. His research interests are MIMO systems, receiver-oriented (joint transmission) and channel-oriented (joint transmitter and receiver optimization) transmission concepts, multiuser detection, and statistical signal processing. He is a Member of VDE/ITG and of the IEEE.

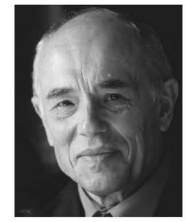

Paul Walter Baier was born in Backnang, Germany, in 1938, and graduated from the Technical University Munich, Germany. In 1970, he joined Siemens AG, Munich, where he was engaged in various topics of communications engineering. Since 1973, he has been a Professor for electrical communications and Director of the Institute for RF Communications and Fundamentals of Electronic Engineering at the University of Kaiserslautern, Germany. His main research interests are spread spectrum techniques, impulse compression and synthetic aperture radars, mobile radio systems, and adaptive antennas. The basics of the TD-CDMA component of the UMTS Terrestrial Radio Access System (UTRA) agreed upon by 3GPP were developed by him and his coworkers in cooperation with Siemens and in the framework of EU projects. He is a member of VDE/ITG, of the URSI Member Committee Germany, and a Fellow of the IEEE. He was a Scholar of the Japanese Society for the Promotion of Science in 1997 and was awarded the Innovation Prize of the Mannesmann Mobile Radio Foundation in 1999 and the Ring of Honor of VDE Association for Electrical, Electronic & Information Technologies in 2000. Since July 2002, he holds an honorary doctorate of the Technical University Munich.

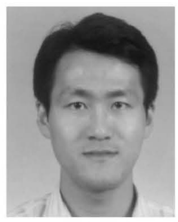

Wei Qiu was born in Jiangsu, China, in 1975. He received his B.E. degree from Tsinghua University, Beijing, China, in 1999, and his M.S. degree from University of Kaiserslautern, Kaiserslautern, Germany, in 2001, both in electrical engineering. Since 2001, he has been a Research Engineer with the Research Group for RF Communications, the University of Kaiserslautern. His research interests are mainly concentrated on mobile radio communications and on MIMO systems. He is a Student Member of IEEE.

3.3 Analyse der Übertragungsqualität

Zum gerechten Bewerten der Leistungsfähigkeit der in Unterkapitel 3.2 vorgeschlagenen linearen Verfahren der gemeinsamen Sendesignalerzeugung, werden in diesem Unterkapitel im Rahmen der Veröffentlichungen [TWMB01b, Meu04b, Meu04a, PMWB00] die Gütemaße

- SNR-Degradation,
- Sendungseffizienz (engl. transmission efficiency),
- Sendeeffizienz (engl. transmit efficiency),
- die für eine vorgegebene Übertragungsqualität benötige totale Sendeenergie T nach (1.30) sowie
- spektrale Effizienz (engl. spectrum efficiency)

vorgeschlagen. In diesen Werken wird die Leistungsfähigkeit empfängerorientierter Funkkommunikation auf Basis dieser Gütekriterien für exemplarische Mobilfunkszenarien bewertet. Dabei werden sowohl analytische als auch numerische Methoden eingesetzt.

Im Gegensatz zu dem aus Tabelle 1.2 bekannten Systemmodell werden in [TWMB01b, PMWB00] einige wenige Größen durch eine modifizierte Notation beschrieben. Tabelle 3.2 listet die wesentlichen Unterschiede in kompakter Form auf.

Tabelle 3.2. Wesentliche Unterschiede der Notationen nach Tabelle 1.2 und der Notation nach [TWMB01b, PMWB00]

dargestellte Größe	Formelzeichen nach Tab. 1.2	Formelzeichen nach [TWMB01b, PMWB00]
totales Sendesignal	$\underline{\mathbf{t}}$	$\underline{\mathbf{s}}$

[TWMB01b] Tröger, H.; Weber, T.; Meurer, M.; Baier, P. W.: "Performance assessment of joint transmission (JT) multi-user downlinks with multi-element transmit antennas". *European Transactions on Telecommunications*, Bd. 12, 2001, S. 407–415.

Smart Antennas

Performance Assessment of Joint Transmission (JT) Multi-User Downlinks with Multi-Element Transmit Antennas

HENDRIK TRÖGER, TOBIAS WEBER, MICHAEL MEURER, PAUL WALTER BAIER
Research Group for RF Communications, University of Kaiserslautern,
P.O. Box 3049, D-67653 Kaiserslautern, Germany
{*troeger, tweber, meurer, baier*}*@rhrk.uni-kl.de*

Abstract. Joint transmission (JT), a novel downlink transmission scheme, was introduced and described in recent papers. Questions still open concern the performance assessment of JT and the comparison of JT with conventional downlink transmission schemes. In order to answer these questions, quantities termed SNR degradation and transmission efficiency are presented in this paper. Based on these quantities, exemplary system assessments and comparisons are performed, which clearly show the suitability of these measures and also the advantages of the novel downlink transmission scheme JT.

1 INTRODUCTION

The conventional downlink transmission scheme in multi-user radio systems with multi-element transmit antennas can be characterized as follows [1]:

- In the base station (BS) the data to be transmitted to the mobile stations (MSs) are modulated onto carrier signals according to an a priori determined modulation scheme, which also includes symbol mapping and, in the case of CDMA, spectral spreading.
- The modulated carrier signals are subject to antenna element specific and MS specific weighting, which can be considered as part of the modulation, and then fed to the transmit antenna elements.
- At the MSs the received signals are demodulated with the goal to obtain estimates as accurate as possible of the transmitted data. The demodulators to be utilized result a posteriori from the modulation scheme chosen at the BS and from the impulse responses of the channels between the transmit antenna elements and the MSs.

This conventional approach to downlink transmission has the following disadvantages:

- The demodulators at the MSs need estimates of the channel impulse responses. This requires the transmission of training signals, which unfortunately consume part of the transmission capacity, and the implementation of rather expensive channel estimators at the MSs.
- The a posteriori determined demodulators may turn out to be rather complex, especially if the modulation comprises spectral spreading in the sense of CDMA, see for instance [1].

In [2, 3, 4] an alternative rationale for downlink transmission termed Joint Transmission (JT) was presented, which is capable of avoiding the mentioned disadvantages. As explained in more detail in [2, 3, 4], the term JT was chosen, because one common transmit signal for the support of all MSs is jointly generated at the BS. The crux of JT consists in

- setting out from a priori selected low cost demodulators,
- determining the modulator in the BS a posteriori based on the properties of the selected demodulators and the channel impulse responses, which are assumed to be known at the BS, in such a way that intersymbol interference (ISI) and intracell multiple access interference (MAI) are totally eliminated.

The knowledge of the channel impulse responses required at the BS in the case of JT can be assumed to be available – at least approximately –, if we consider radio systems employing the duplexing scheme Time Division Duplex (TDD). In such systems the same channel impulse responses are valid for both the uplink and the downlink, which means that the channel impulse response estimates obtained at the BS as a prerequisite for uplink reception can be also utilized to perform JT in the downlink. Consequently, JT would be especially suited for the downlink of radio transmission systems employing TDD. In JT the transmission signal design is based on channel state knowledge. In this sense JT is related to transmission signal preprocessing schemes published in [5, 6] for fixed wired transmission and in [7, 8, 9, 10] for wireless transmission.

In [2, 3, 4] the scheme JT is described in detail in the equivalent lowpass domain utilizing the matrix-vector representation explained for instance in [11]. In this representation signals are written as column vectors and convolutions as matrix-vector multiplications.

Questions still open concern adequate quantitative performance measures for JT which allow the concise characterization of the effects of parameter changes within a given JT system and the comparison of JT with conventional downlink transmission schemes. The goal of the paper is the proposal of such performance measures. The paper is structured as follows: In Section 2 the basics of JT are briefly recapitulated in order to conveniently familiarize the reader with the contents of [2, 3, 4] to a degree which is sufficient to follow the reasoning of this paper. In Section 3 a quantity termed SNR degradation is derived, which allows the assessment of the receiver performance of JT. Another quantity, termed transmission efficiency by the authors, is introduced in Section 4; this quantity allows to judge how efficiently the radiated energy is transformed into desired received energy at the MSs, if JT is applied. In Section 5 the results of exemplary system evaluations are presented with the focus on the quantities SNR degradation and transmission efficiency derived in Sections 3 and 4, respectively. Finally, Section 6 concludes the paper.

2 Basics of JT

Figure 1 shows the downlink multiple input/multiple output (MIMO) channel of a multi-user radio system with a multi-element transmit antenna. The BS equipped with K_a transmit antenna elements supports K MSs μ_k, $k = 1 \dots K$, which possess a single element receive antenna each. The K_a antenna elements at the BS are assumed to be perfectly decoupled. In the structure shown in figure 1 the antenna element specific channel impulse responses

$$\underline{\boldsymbol{h}}^{(k,k_\mathrm{a})} = \left(\underline{h}_1^{(k,k_\mathrm{a})} \dots \underline{h}_W^{(k,k_\mathrm{a})}\right)^\mathrm{T}, \qquad (1)$$
$$k = 1 \dots K,\ k_\mathrm{a} = 1 \dots K_\mathrm{a},$$

of dimension W characterize the signal transmission between the input of the transmit antenna element k_a, $k_\mathrm{a} = 1 \dots K_\mathrm{a}$, and the output of the receiving antenna of MS μ_k, $k = 1 \dots K$. It is assumed that N data symbols have

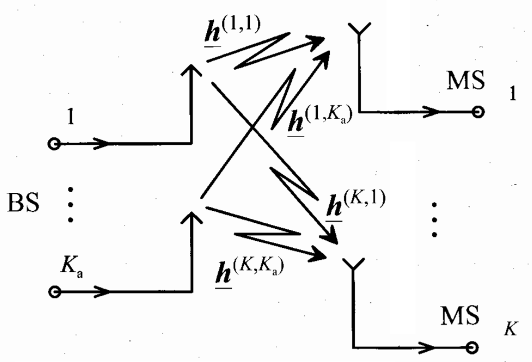

Figure 1: Downlink multiple input/multiple output (MIMO) channel of a multi-user radio system with a multi-element transmit antenna.

to be transmitted to each MS $\mu_k, k = 1 \dots K$. The data symbols for MS μ_k are arranged in the column vector

$$\underline{\boldsymbol{d}}^{(k)} = \left(\underline{d}_1^{(k)} \dots \underline{d}_N^{(k)}\right)^\mathrm{T}, k = 1 \dots K, \qquad (2)$$

of dimension N termed partial data vector. In total

$$N_\mathrm{t} = KN \qquad (3)$$

data symbols have to be transmitted to the ensemble of K MSs. The stack

$$\underline{\boldsymbol{d}} = \left(\underline{\boldsymbol{d}}^{(1)\mathrm{T}} \dots \underline{\boldsymbol{d}}^{(K)\mathrm{T}}\right)^\mathrm{T} = \left(\underline{d}_1 \dots \underline{d}_{N_\mathrm{t}}\right)^\mathrm{T} \qquad (4)$$

of the K partial data vectors $\underline{\boldsymbol{d}}^{(k)}$, $k = 1 \dots K$, of (2) is termed the total data vector, which has the dimension N_t, see (3). In the BS, based on $\underline{\boldsymbol{d}}$ a partial transmit signal $\underline{\boldsymbol{s}}^{(k_\mathrm{a})}$, $k_\mathrm{a} = 1 \dots K_\mathrm{a}$, of dimension S is generated for each of the K_a transmit antenna elements by a process termed modulation. If these K_a partial transmit signals $\underline{\boldsymbol{s}}^{(k_\mathrm{a})}$, $k_\mathrm{a} = 1 \dots K_\mathrm{a}$, are compiled to the total transmit signal

$$\underline{\boldsymbol{s}} = \left(\underline{\boldsymbol{s}}^{(1)\mathrm{T}} \dots \underline{\boldsymbol{s}}^{(K_\mathrm{a})\mathrm{T}}\right)^\mathrm{T} \qquad (5)$$

of dimension $K_\mathrm{a}S$, then, in the case of linear modulation, the process of modulation can be described with the $K_\mathrm{a}S \times N_\mathrm{t}$ modulator matrix $\underline{\boldsymbol{M}}$, which still has to be determined, and with $\underline{\boldsymbol{d}}$ of (4) as follows:

$$\underline{\boldsymbol{s}} = \underline{\boldsymbol{M}}\, \underline{\boldsymbol{d}}. \qquad (6)$$

Due to the transmission of $\underline{\boldsymbol{s}}$ of (6) a partial received signal $\underline{\boldsymbol{e}}^{(k)}$ of dimension $S + W - 1$ arrives at each MS μ_k, $k = 1 \dots K$, [2, 3, 4]. The K partial received signals $\underline{\boldsymbol{e}}^{(k)}$, $k = 1 \dots K$, can be stacked to form the total received signal

$$\underline{\boldsymbol{e}} = \left(\underline{\boldsymbol{e}}^{(1)\mathrm{T}} \dots \underline{\boldsymbol{e}}^{(K)\mathrm{T}}\right)^\mathrm{T} \qquad (7)$$

of dimension $K(S+W-1)$. As shown in [2, 3, 4] the partial channel matrices $\underline{\boldsymbol{H}}^{(k)}$, $k = 1\ldots K$, of dimension $(S+W-1)\times(K_\mathrm{a}S)$ can be obtained by properly arranging the antenna element specific channel impulse responses $\underline{\boldsymbol{h}}^{(k,k_\mathrm{a})}$ of (1), and the matrices $\underline{\boldsymbol{H}}^{(k)}$ can be composed to form the total channel matrix $\underline{\boldsymbol{H}}$ of dimension $[K\,(S+W-1)]\times(K_\mathrm{a}S)$. Then, in the case of absence of disturbing noise at the receiver inputs, the total received signal of (7) can be expressed as [2, 3, 4]

$$\underline{\boldsymbol{e}} = \underline{\boldsymbol{H}}\,\underline{\boldsymbol{s}}. \tag{8}$$

At each MS μ_k the corresponding partial received signal $\underline{\boldsymbol{e}}^{(k)}$ is demodulated with the goal to obtain the corresponding partial data vector $\underline{\boldsymbol{d}}^{(k)}$. In the case of a linear demodulator the demodulation process at MS μ_k can be described by a demodulator matrix $\underline{\boldsymbol{D}}^{(k)}$ of dimension $N\times(S+W-1)$ [2, 3, 4]:

$$\underline{\boldsymbol{d}}^{(k)} = \underline{\boldsymbol{D}}^{(k)}\underline{\boldsymbol{e}}^{(k)}, k = 1\ldots K. \tag{9}$$

(9) implies the requirement already formulated in Section 1 that the data vector $\underline{\boldsymbol{d}}^{(k)}$ of (2) intended for MS μ_k is detected without ISI and intracell MAI.

By combining the K modulator matrices $\underline{\boldsymbol{D}}^{(k)}$, $k = 1\ldots K$, the total demodulator matrix

$$\underline{\boldsymbol{D}} = \text{blockdiag}\left[\underline{\boldsymbol{D}}^{(1)}\ldots\underline{\boldsymbol{D}}^{(K)}\right] \tag{10}$$

of dimension $N_\mathrm{t}\times[K\,(S+W-1)]$ is obtained. With (10) we can stack the K equations of (9) and obtain under consideration of (8) the single equation

$$\underline{\boldsymbol{d}} = \underline{\boldsymbol{D}}\,\underline{\boldsymbol{e}} = \underbrace{\underline{\boldsymbol{D}}\,\underline{\boldsymbol{H}}}_{\underline{\boldsymbol{B}}}\,\underline{\boldsymbol{s}}. \tag{11}$$

As already mentioned, in the case of JT the demodulators characterized by the total demodulator matrix $\underline{\boldsymbol{D}}$ of (10) are a priori agreed upon and, therefore, also known at the BS. Also the antenna element specific channel impulse responses $\underline{\boldsymbol{h}}^{(k,k_\mathrm{a})}$ of (1) and, therefore, the channel matrix $\underline{\boldsymbol{H}}$ are assumed to be known at the BS, see Section 1. Then, the matrix $\underline{\boldsymbol{B}}$ defined in (11) is known at the BS as well. Consequently, (11) can be considered as a system of equations which determine the elements of the total transmit signal $\underline{\boldsymbol{s}}$ of (5) to be transmitted by the BS in order to obtain the desired partial data vectors $\underline{\boldsymbol{d}}^{(k)}$ at the MSs μ_k, $k = 1\ldots K$, without any ISI and intracell MAI. If the dimension $K_\mathrm{a}S$ of $\underline{\boldsymbol{s}}$ is chosen larger than the dimension N_t of $\underline{\boldsymbol{d}}$ – this is assumed to be the case in what follows –, then the system of equations of (11) is underdetermined. Among the infinitely many solutions, the solution

$$\underline{\boldsymbol{s}} = \underbrace{\underline{\boldsymbol{B}}^{*\mathrm{T}}\left(\underline{\boldsymbol{B}}\,\underline{\boldsymbol{B}}^{*\mathrm{T}}\right)^{-1}}_{\underline{\boldsymbol{M}}}\underline{\boldsymbol{d}} \tag{12}$$

of minimum energy $||\underline{\boldsymbol{s}}||^2/2$ [12] is chosen in what follows, because this solution is optimum in the sense that the transmit power and, consequently, the MAI caused by the BS in other networks or, if the BS is part of a cellular system, in other cells, is minimized. (12) describes the construction of the modulator matrix $\underline{\boldsymbol{M}}$ introduced in (6) and to be a posteriori determined in the BS transmitter, see Section 1.

3 SNR DEGRADATION

Now it is assumed that at the receiver input of MS μ_k, $k = 1\ldots K$, white Gaussian noise with the variances σ^2 of the real and imaginary parts occurs, which models intercell MAI and thermal noise. Then, in the case of JT the SNR of the data symbol $\underline{d}_n^{(k)}$, $k = 1\ldots K$, $n = 1\ldots N$, see (2), observed at the detector output of MS μ_k due to the reception of $\underline{\boldsymbol{e}}^{(k)}$ plus noise becomes, with $\underline{\boldsymbol{D}}^{(k)}$ of (9),

$$\gamma_{\mathrm{JT},n}^{(k)} = \frac{|\underline{d}_n^{(k)}|^2}{2\sigma^2\left[\underline{\boldsymbol{D}}^{(k)}\underline{\boldsymbol{D}}^{(k)*\mathrm{T}}\right]_{n,n}}, \tag{13}$$

where $[\cdot]_{i,i}$ denotes the i-th diagonal element of the matrix in brackets. The desired partial signal $\underline{\boldsymbol{e}}^{(k)}$ arriving at MS μ_k is a linear combination of signal portions originating in the individual transmitted data symbols $\underline{d}_1\ldots\underline{d}_{N_\mathrm{t}}$, see (4). The signal portion $\underline{\boldsymbol{e}}_n^{(k)}$ within $\underline{\boldsymbol{e}}^{(k)}$ representing the data symbol $\underline{d}_n^{(k)}$ at MS μ_k is given by the expression

$$\underline{\boldsymbol{e}}_n^{(k)} = \left[\underline{\boldsymbol{H}}^{(k)}\underline{\boldsymbol{M}}\right]_{(k-1)N+n}\underline{d}_n^{(k)}, \tag{14}$$

where $[\cdot]_i$ denotes a column vector which consists of the i-th column of the matrix in brackets, describing the received symbol waveform corresponding to the n-th symbol transmitted to the k-th MS. The energy of $\underline{\boldsymbol{e}}_n^{(k)}$ of (14) is

$$R_n^{(k)} = \frac{1}{2}\left[\left(\underline{\boldsymbol{H}}^{(k)}\underline{\boldsymbol{M}}\right)^{*\mathrm{T}}\underline{\boldsymbol{H}}^{(k)}\underline{\boldsymbol{M}}\right]_{(k-1)N+n,\,(k-1)N+n}\cdot|\underline{d}_n^{(k)}|^2. \tag{15}$$

Now, if we, instead of detecting the data according to (9), would employ matched filtering, i.e use a matched filter for the detection of $\underline{d}_n^{(k)}$ which is matched to the symbol waveform $\left[\underline{\boldsymbol{H}}^{(k)}\underline{\boldsymbol{M}}\right]_{(k-1)N+n}$ appearing in (14) and originating in data symbol $\underline{d}_n^{(k)}$, than the SNR at the output of this matched filter becomes

$$\gamma_{\mathrm{MF},n}^{(k)} = \frac{R_n^{(k)}}{\sigma^2} = \frac{\left[\left(\underline{\boldsymbol{H}}^{(k)}\underline{\boldsymbol{M}}\right)^{*\mathrm{T}}\underline{\boldsymbol{H}}^{(k)}\underline{\boldsymbol{M}}\right]_{(k-1)N+n,(k-1)N+n}|\underline{d}_n^{(k)}|^2}{2\sigma^2}. \tag{16}$$

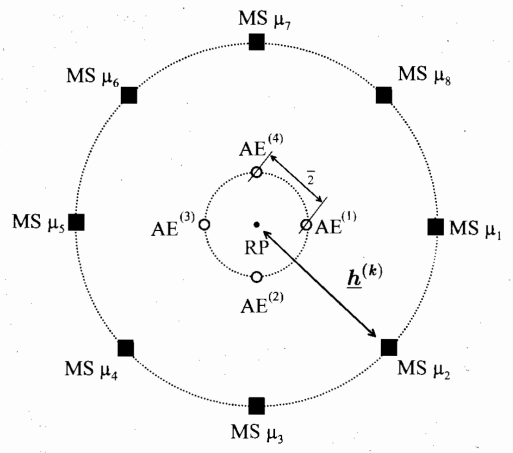

Figure 2: Considered configuration with $K = 8$ MSs and $K_{\mathrm{a}} = 4$ antenna elements.

As mentioned earlier, JT perfectly eliminates ISI and intracell MAI, whereas its SNR behavior, characterized by $\gamma_{\mathrm{JT},n}^{(k)}$ of (13), may be non-optimum. On the other hand, signal detection by matched filtering maximizes the SNR $\gamma_{\mathrm{MF},n}^{(k)}$ of (16), whereas ISI and intracell MAI may have a severe impact. As a suitable measure for symbolwise assessing the SNR behavior of JT for each symbol $\underline{d}_n^{(k)}$ the ratios

$$\begin{aligned}\delta_n^{(k)} &\doteq \frac{\gamma_{\mathrm{MF},n}^{(k)}}{\gamma_{\mathrm{JT},n}^{(k)}}\\ &= \left[\left(\underline{\boldsymbol{H}}^{(k)}\underline{\boldsymbol{M}}\right)^{*\mathrm{T}}\underline{\boldsymbol{H}}^{(k)}\underline{\boldsymbol{M}}\right]_{(k-1)N+n,(k-1)N+n}\\ &\quad\cdot\left[\underline{\boldsymbol{D}}^{(k)}\underline{\boldsymbol{D}}^{(k)*\mathrm{T}}\right]_{n,n},\\ &\quad k = 1\ldots K,\, n = 1\ldots N, \qquad (17)\end{aligned}$$

of $\gamma_{\mathrm{MF},n}^{(k)}$ of (16) and $\gamma_{\mathrm{JT},n}^{(k)}$ of (13) are proposed by the authors, which are termed the SNR degradations of JT. As $\gamma_{\mathrm{MF},n}^{(k)}$ of (16) describes the maximum SNR achievable with linear detectors, $\delta_n^{(k)}$ of (17) is always larger than or equal to one. The closer the quantities $\delta_n^{(k)}$ come to 1, the less severe the SNR degradations are.

4 TRANSMISSION EFFICIENCY

In the previous section the energy $R_n^{(k)}$ associated with the data symbol $\underline{d}_n^{(k)}$ at the input of the receiver of MS μ_k, $k = 1\ldots K$, was introduced, see (15). The energy of the total transmit signal $\underline{\boldsymbol{s}}$ of (6) is defined as

$$T = \frac{1}{2}\left(\underline{\boldsymbol{s}}^{*\mathrm{T}}\underline{\boldsymbol{s}}\right) = \frac{1}{2}\left(\left(\underline{\boldsymbol{M}}\,\underline{\boldsymbol{d}}\right)^{*\mathrm{T}}\underline{\boldsymbol{M}}\,\underline{\boldsymbol{d}}\right). \qquad (18)$$

If only the single data symbol $\underline{d}_n^{(k)}$ would be transmitted, i.e. all elements of $\underline{\boldsymbol{d}}$ of (4) would be zero except for $\underline{d}_n^{(k)}$, then, with $\underline{\boldsymbol{M}}$ of (12), the transmit energy required for this data symbol would be

$$T_n^{(k)} = \frac{1}{2}\left[\underline{\boldsymbol{M}}^{*\mathrm{T}}\underline{\boldsymbol{M}}\right]_{(k-1)N+n,(k-1)N+n}|\underline{d}_n^{(k)}|^2. \qquad (19)$$

Now, the ratio

$$\frac{R_n^{(k)}}{T_n^{(k)}} = \frac{\left[\left(\underline{\boldsymbol{H}}^{(k)}\underline{\boldsymbol{M}}\right)^{*\mathrm{T}}\underline{\boldsymbol{H}}^{(k)}\underline{\boldsymbol{M}}\right]_{(k-1)N+n,(k-1)N+n}}{\left[\underline{\boldsymbol{M}}^{*\mathrm{T}}\underline{\boldsymbol{M}}\right]_{(k-1)N+n,(k-1)N+n}} \qquad (20)$$

of the received energy $R_n^{(k)}$, see (15), and of the transmitted energy $T_n^{(k)}$, see (19), of the data symbol $\underline{d}_n^{(k)}$ can be formed. $\underline{\boldsymbol{M}}$ depends on the a priori determined demodulator matrices $\underline{\boldsymbol{D}}^{(k)}$ introduced in (9) and on the antenna element specific channel impulse responses $\underline{\boldsymbol{h}}^{(k,k_{\mathrm{a}})}$ of (1), see [2, 3, 4]. Therefore, the ratio $R_n^{(k)}/\,T_n^{(k)}$ of (20) also depends on $\underline{\boldsymbol{D}}^{(k)}$and $\underline{\boldsymbol{h}}^{(k,k_{\mathrm{a}})}$. It is desirable that the ratio $R_n^{(k)}/\,T_n^{(k)}$ of (20) attains large values, because then the energy radiated by the BS transmitter is efficiently transformed into desired received energy at the respective MS receiver inputs. However, the statement that this ratio should be large is a rather subjective one. In order to be able to quantitatively compare versions of JT systems characterized by different values of their system parameters, first a reference system should be defined. The energy ratio of (20) valid for the reference system is termed $\left(R_n^{(k)}/\,T_n^{(k)}\right)_{\mathrm{ref}}$. Now, the ratio

$$t_{\mathrm{r},n}^{(k)} = \frac{R_n^{(k)}/\,T_n^{(k)}}{\left(R_n^{(k)}/\,T_n^{(k)}\right)_{\mathrm{ref}}} \qquad (21)$$

of $R_n^{(k)}/\,T_n^{(k)}$ of (20) and $\left(R_n^{(k)}/\,T_n^{(k)}\right)_{\mathrm{ref}}$ can be formed. $t_{\mathrm{r},n}^{(k)}$ is termed the relative transmission efficiency of the JT system under discussion by the authors. The value of $t_{\mathrm{r},n}^{(k)}$ indicates to which degree the considered JT system outperforms or falls behind the chosen reference system.

In order to assess the benefits of JT, one has also to compare the performance of downlinks utilizing JT and the performance of conventional downlinks under the condition that both kinds of downlinks employ the same transmit antenna configurations and operate over the same radio channels. The structure of conventional downlinks is for instance described in [13] and is characterized by a weighting network, via which weighted versions of the k MS specific transmit signals are fed to the K_{a} antenna elements. As shown in [13] the KK_{a} antenna weights $\underline{w}_{k_{\mathrm{a}}}^{(k)}$, $k = 1\ldots K$, $k_{\mathrm{a}} = 1\ldots K_{\mathrm{a}}$, can be compiled to the K MS specific weight vectors

$$\underline{\boldsymbol{w}}^{(k)} = \left(\underline{w}_1^{(k)}\ldots\underline{w}_{K_{\mathrm{a}}}^{(k)}\right)^{\mathrm{T}},\, k = 1\ldots K. \qquad (22)$$

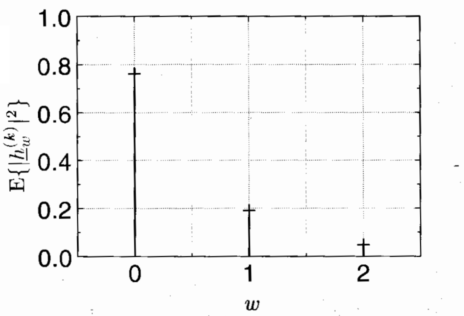

Figure 3: Power delay profile of the used channel impulse responses.

Let us assume that each data symbol $\underline{d}_n^{(k)}$ transmitted for MS μ_k is represented by a signature

$$\underline{c}^{(k)} = \left(\underline{c}_1^{(k)} \dots \underline{c}_Q^{(k)}\right)^{\mathrm{T}}, \; k = 1 \dots K, \tag{23}$$

of length Q with the elements $\underline{c}_q^{(k)}$, $q = 1 \dots Q$, at the BS transmitter [13]. Then, the total energy radiated by the K_a antenna elements in order to transmit $\underline{d}_n^{(k)}$ becomes [13]

$$T^{(k)} = \frac{1}{2}\,\underline{c}^{(k)*\mathrm{T}}\underline{c}^{(k)}\underline{\boldsymbol{w}}^{(k)*\mathrm{T}}\underline{\boldsymbol{w}}^{(k)}|\underline{d}_n^{(k)}|^2. \tag{24}$$

With the channel matrices

$$\underline{\boldsymbol{H}}_\mathrm{a}^{(k)} = \left(\underline{\boldsymbol{h}}^{(k,1)} \dots \underline{\boldsymbol{h}}^{(k,K_\mathrm{a})}\right), k = 1 \dots K, \tag{25}$$

resulting from the antenna element specific channel impulse responses $\underline{\boldsymbol{h}}^{(k,k_\mathrm{a})}$, $k = 1 \dots K$, $k_\mathrm{a} = 1 \dots K_\mathrm{a}$, of (1) and the signature matrices

$$\begin{aligned} \tilde{\underline{\boldsymbol{C}}}^{(k)} &= (\tilde{\underline{C}}_{l,w}^{(k)}), \; l = 1 \dots Q + W - 1, \\ & \qquad w = 1 \dots W, \; k = 1 \dots K, \\ \tilde{\underline{C}}_{l,w}^{(k)} &= \begin{cases} \underline{c}_{l-w+1}^{(k)} & \text{if} \quad 1 \le l - w + 1 \le Q, \\ 0 & \text{else} \end{cases} \end{aligned} \tag{26}$$

which are constructed by using the signature sequences $\underline{c}^{(k)}$ of (23) we can determine the energy $R^{(k)}$ received at MS μ_k due to transmitting $\underline{d}_n^{(k)}$ with the energy $T^{(k)}$ of (24):

$$R^{(k)} = \frac{1}{2}\underline{\boldsymbol{w}}^{(k)*\mathrm{T}}\underline{\boldsymbol{H}}_\mathrm{a}^{(k)*\mathrm{T}}\tilde{\underline{\boldsymbol{C}}}^{(k)*\mathrm{T}}\tilde{\underline{\boldsymbol{C}}}^{(k)}\underline{\boldsymbol{H}}_\mathrm{a}^{(k)}\underline{\boldsymbol{w}}^{(k)}|\underline{d}_n^{(k)}|^2. \tag{27}$$

From (24) and (27) we obtain

$$\frac{R^{(k)}}{T^{(k)}} = \frac{\underline{\boldsymbol{w}}^{(k)*\mathrm{T}}\underline{\boldsymbol{H}}_\mathrm{a}^{(k)*\mathrm{T}}\tilde{\underline{\boldsymbol{C}}}^{(k)*\mathrm{T}}\tilde{\underline{\boldsymbol{C}}}^{(k)}\underline{\boldsymbol{H}}_\mathrm{a}^{(k)}\underline{\boldsymbol{w}}^{(k)}}{\underline{c}^{(k)*\mathrm{T}}\underline{c}^{(k)}\underline{\boldsymbol{w}}^{(k)*\mathrm{T}}\underline{\boldsymbol{w}}^{(k)}}. \tag{28}$$

An obvious approach to choosing the K weight vectors $\underline{\boldsymbol{w}}^{(k)}$ of (22) consists in maximizing the K ratios $R^{(k)}/\,T^{(k)}$ of (28) [13], which leads to $\left(R^{(k)}/\,T^{(k)}\right)_{\max}$. This approach is followed by the authors.

With $R_n^{(k)}/T_n^{(k)}$ of (20) and $\left(R^{(k)}/T^{(k)}\right)_{\max}$ resulting from (28) by appropriately choosing the weight vectors $\underline{\boldsymbol{w}}^{(k)}$, the quantity

$$t_n^{(k)} = \frac{R_n^{(k)}/T_n^{(k)}}{\left(R^{(k)}/T^{(k)}\right)_{\max}} \tag{29}$$

is introduced. $t_n^{(k)}$ is termed transmission efficiency of JT by the authors. The larger $t_n^{(k)}$, the more efficiently the radiated energy is transformed into desired received energy by JT in comparison to a conventional downlink system.

5 Exemplary System Evaluation

In what follows an exemplary system evaluation is presented for the configuration shown in figure 2. At the BS a circular array with K_a antenna elements (AE) is provided, and K MSs are uniformly distributed on a circle around the BS in the farfield of the AEs. The distance between adjacent AEs is one half of the wavelength λ. From the reference point (RP), which is the center of the configuration, a single-direction channel in the line-of-sight direction with the channel impulse response

$$\underline{\boldsymbol{h}}^{(k)} = \left(\underline{h}_1^{(k)} \dots \underline{h}_W^{(k)}\right)^{\mathrm{T}}, \; k = 1 \dots K, \tag{30}$$

is assumed to each MS μ_k, $k = 1 \dots K$ [14]. Based on $\underline{\boldsymbol{h}}^{(k)}$ of (30) and on the geometry of the configuration shown in figure 2 the antenna element specific channel impulse responses $\underline{\boldsymbol{h}}^{(k,k_\mathrm{a})}$ of (1) can be determined [13].

Table 1: Parameter values chosen for the simulations.

parameter	value
K	8
N	5
Q	16
K_a	$1 \dots 32$
W	3

For each MS μ_k, $k = 1 \dots K$, a signature $\underline{c}^{(k)}$ is introduced with the K signatures $\underline{c}^{(k)}$ forming an orthogonal set. The signatures $\underline{c}^{(k)}$ are used on the one side to determine the K demodulator matrices introduced in (9) according to

$$\underline{\boldsymbol{D}}^{(k)} = \underline{\boldsymbol{C}}^{(k)*\mathrm{T}} \tag{31}$$

Table 2: Exemplary channel impulse responses $\underline{\mathbf{h}}^{(k)}$, $k = 1 \ldots 8$, see (30).

w	k			
	1	2	3	4
1	$0.7227 + \mathrm{j}\,0.4895$	$0.1498 - \mathrm{j}\,0.8599$	$0.1541 + \mathrm{j}\,0.8592$	$0.0885 + \mathrm{j}\,0.8684$
2	$0.3606 + \mathrm{j}\,0.2458$	$0.2569 + \mathrm{j}\,0.3528$	$-0.0984 - \mathrm{j}\,0.4252$	$-0.2464 - \mathrm{j}\,0.3602$
3	$0.1840 - \mathrm{j}\,0.1173$	$0.1649 + \mathrm{j}\,0.1429$	$-0.1195 + \mathrm{j}\,0.1826$	$-0.0157 + \mathrm{j}\,0.2177$
w	k			
	5	6	7	8
1	$-0.8295 + \mathrm{j}\,0.2717$	$-0.8540 + \mathrm{j}\,0.1806$	$-0.7346 + \mathrm{j}\,0.4715$	$0.7909 - \mathrm{j}\,0.3693$
2	$-0.2550 - \mathrm{j}\,0.3542$	$-0.4272 - \mathrm{j}\,0.0894$	$-0.3700 + \mathrm{j}\,0.2315$	$0.4196 + \mathrm{j}\,0.1200$
3	$0.0902 + \mathrm{j}\,0.1987$	$-0.1625 - \mathrm{j}\,0.1456$	$-0.0947 - \mathrm{j}\,0.1966$	$0.1934 - \mathrm{j}\,0.1011$

with

$$\underline{\mathbf{C}}^{(k)} = \left(\underline{C}_{i,j}^{(k)}\right),\ i = 1 \ldots S + W - 1,$$
$$j = 1 \ldots N,\ k = 1 \ldots K,$$
$$\underline{C}_{i,j}^{(k)} = \begin{cases} \underline{c}_{i-Q(j-1)}^{(k)} & \text{for } 1 \leq i - Q(j-1) \leq Q, \\ 0 & \text{else,} \end{cases} \tag{32}$$

and

$$S = NQ. \tag{33}$$

On the other side the signatures $\underline{\mathbf{c}}^{(k)}$ are used as the signatures appearing in (26). The simulations are performed for the parameter values, the signatures $\underline{\mathbf{c}}^{(k)}$, $k = 1 \ldots 8$, and the channel impulse responses $\underline{\mathbf{h}}^{(k)}$, $k = 1 \ldots 8$, shown in tables 1, 2 and 3, respectively. The channel impulse responses $\underline{\mathbf{h}}^{(k)}$, $k = 1 \ldots 8$, shown in table 2 are samples for only one exemplary snapshot corresponding to the power delay profile depicted in figure 3. According to table 1 different numbers K_a of AEs are considered. Concerning the relative transmission efficiency $t_{\mathrm{r},n}^{(k)}$ of (21), a JT system having only one AE, that is K_a equal to one, is chosen. For the situation characterized by figure 2 and tables 1, 2 and 3, figure 3 shows the SNR degradations $\delta_3^{(k)}$, $k = 1 \ldots 8$, of (17) of the third, that is the center data symbol of each MS, versus the number K_a of AEs with k as the parameter. In figure 5 the average $\overline{t_{\mathrm{r},3}^{(k)}}$ of the relative transmission efficiencies obtained by averaging over the eight values $t_{\mathrm{r},3}^{(k)}$, $k = 1 \ldots 8$, of (29) is depicted versus K_a. The simulations show that the 8 individual values $t_{\mathrm{r},3}^{(k)}$, $k = 1 \ldots 8$, deviate by less than 0.25 dB from the average $\overline{t_{\mathrm{r},3}^{(k)}}$. In figure 6 the transmission efficiencies $t_3^{(k)}$, $k = 1 \ldots 8$, of (29) are depicted versus K_a, again with k as the parameter.

Table 3: Orthogonal set of $K = 8$ signatures $\underline{\mathbf{c}}^{(k)}$ of dimension $Q = 16$, see (23).

q	k							
	1	2	3	4	5	6	7	8
1	-1	-1	-1	-1	-1	-1	-1	-1
2	1	-1	1	-1	1	-1	1	-1
3	-1	-1	1	1	-1	-1	1	1
4	1	-1	-1	1	1	-1	-1	1
5	-1	-1	-1	-1	1	1	1	1
6	-1	1	-1	1	1	-1	1	-1
7	-1	-1	1	1	1	1	-1	-1
8	1	-1	-1	1	-1	1	1	-1
9	-1	-1	-1	-1	-1	-1	-1	-1
10	1	-1	1	-1	1	-1	1	-1
11	1	1	-1	-1	1	1	-1	-1
12	-1	1	1	-1	-1	1	1	-1
13	1	1	1	1	-1	-1	-1	-1
14	1	-1	1	-1	-1	1	-1	1
15	1	1	-1	-1	-1	-1	1	1
16	1	-1	-1	1	-1	1	1	-1

In the figures 4 to 6 the third data symbols $\underline{d}_3^{(k)}$, $k = 1 \ldots K$ are considered, because for these symbols fringing effects which can be observed at the beginning and the end of each burst do not occur. Therefore, the SNR degradations $\delta_3^{(k)}$, $k = 1 \ldots 8$, the relative transmission efficiencies $t_{\mathrm{r},3}^{(k)}$, $k = 1 \ldots 8$, and the transmission efficiencies $t_3^{(k)}$, $k = 1 \ldots 8$, obtained for these center symbols are representative also for the corresponding quantities of longer bursts, that is for symbol numbers N larger than 5.

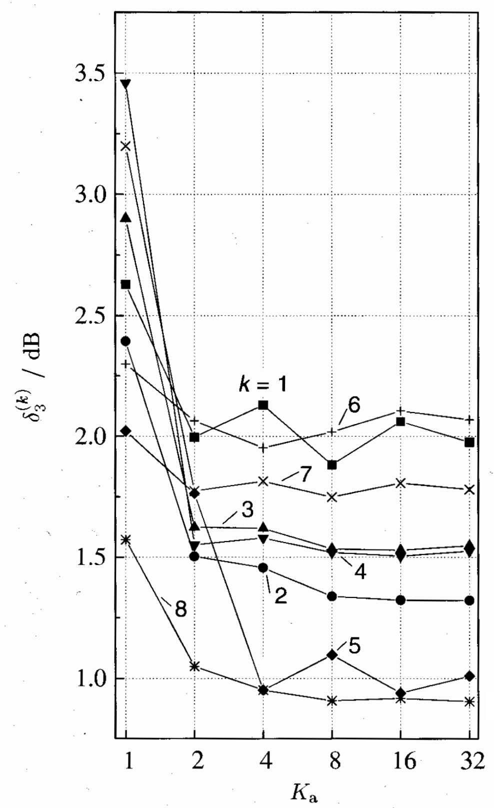

Figure 4: SNR degradations $\delta_3^{(k)}$, $k = 1 \ldots K$, of the 3[rd] data symbols versus K_a.

However, due to simulation complexity a small number of data symbols, that is $N = 5$ was chosen. The graphs of figure 4 show that the SNR degradations $\delta_3^{(k)}$, $k = 1 \ldots 8$, may differ significantly from MS to MS. These differences are due to interrelations between the individual channel impulse responses $\underline{\boldsymbol{h}}^{(k)}$, $k = 1 \ldots 8$, of (1) and the signatures $\underline{\boldsymbol{c}}^{(k)}$, $k = 1 \ldots 8$, of (23). For the case of a single transmit antenna element the quantity $\delta_3^{(k)}$ takes values between 1.5 dB and 3.3 dB, depending on the considered MS μ_k, $k = 1 \ldots 8$. As a general tendency, it can be stated that, the SNR degradations $\delta_3^{(k)}$, $k = 1 \ldots 8$, decrease with increasing number K_a of transmit antenna elements. As already mentioned, figure 5 shows the average of the relative transmission efficiencies $t_{\mathrm{r},3}^{(k)}$, $k = 1 \ldots 8$, of (21) versus K_a.

In the chosen logarithmic representation the graph is linear. For each doubling of K_a, the average over $t_{\mathrm{r},3}^{(k)}$, $k = 1 \ldots 8$, grows by approximately 3 dB. The values $t_3^{(k)}$, $k = 1 \ldots 8$, of (29) shown in figure 6 range between 0.5 dB and 2 dB.

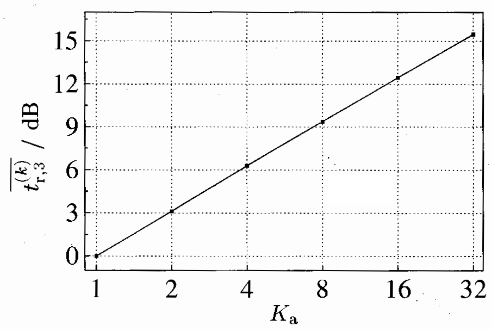

Figure 5: Average relative transmission efficiency $\overline{t_{\mathrm{r},3}^{(k)}}$ of the 3[rd] data symbols versus K_a.

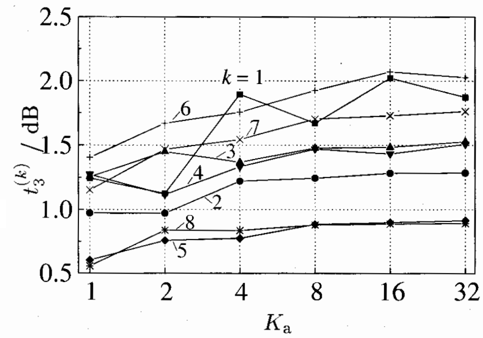

Figure 6: Transmission efficiencies $t_3^{(k)}$, $k = 1 \ldots K$, of the 3[rd] data symbols versus K_a.

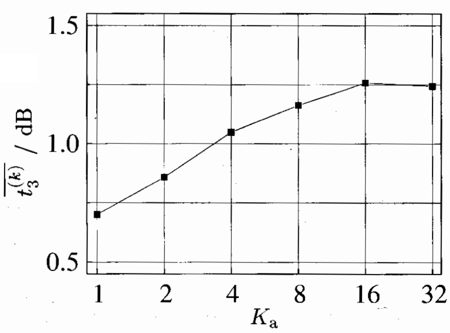

Figure 7: Mean transmission efficiency $\overline{t_3^{(k)}}$, $k = 1 \ldots K$, of the 3[rd] data symbols versus K_a.

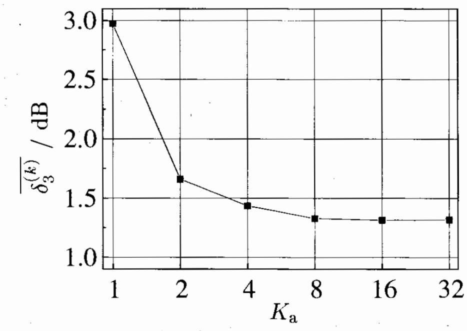

Figure 8: Mean SNR degradation $\overline{\delta_3^{(k)}}$, $k = 1 \ldots K$, of the 3rd data symbols versus K_a.

For six of the eight MSs served by the BS, $t_3^{(k)}$, $k = 1 \ldots 8$, is larger than 1 dB. However, this shows that, in all cases, the considered JT system utilizes the energy $T_3^{(k)}$ radiated per data symbol $\underline{d}_3^{(k)}$, $k = 1 \ldots 8$, more efficiently than the conventional reference system described in section 4. The achievable MS specific gains depend on the valid channel impulse responses $\underline{\boldsymbol{h}}^{(k)}$, $k = 1 \ldots 8$, and the signatures $\underline{c}^{(k)}$, $k = 1 \ldots 8$.

To create mean values $\overline{\delta_3^{(k)}}$ for the SNR degradation $\delta_3^{(k)}$, $k = 1 \ldots 8$, and mean values $\overline{t_3^{(k)}}$, $k = 1 \ldots 8$, for the transmission efficiency $t_3^{(k)}$, $k = 1 \ldots 8$, a simulation with 10 000 experiments, using the signatures $\underline{c}^{(k)}$, $k = 1 \ldots 8$, of (23) and channel impulse responses corresponding to the power delay profile shown in figure 3 are performed. In figure 8 mean values $\overline{\delta_3^{(k)}}$ of the SNR degradation $\delta_3^{(k)}$, $k = 1 \ldots 8$, are depicted versus K_a. Again, a decreasing tendency of the SNR degradation $\overline{\delta_3^{(k)}}$, $k = 1 \ldots 8$, can be observed with increasing number K_a. Finally, in figure 7 the mean values $\overline{t_3^{(k)}}$, $k = 1 \ldots 8$, for the transmission efficiency $t_3^{(k)}$, $k = 1 \ldots 8$, are depicted versus K_a. An increase of $\overline{t_3^{(k)}}$, $k = 1 \ldots 8$, for increasing the number K_a can be observed.

6 Conclusions

In order to enable quantitative performance assessments of the recently proposed downlink transmission scheme JT the measures SNR degradation and transmission efficiency are introduced. The SNR records how efficiently the energy received by the MSs is utilized for data detection. The transmission efficiency reflects the potential of JT to transform the energy radiated by the BS into received energy at the inputs of the MS receivers. Exemplary system assessments based on the introduced performance measures illustrate the benefits of JT.

Acknowledgment

The authors gratefully appreciate the fruitful exchange of ideas with their colleagues at the Research Group for RF Communications, University of Kaiserslautern. Moreover, thanks are expressed to Prof. Nossek of TU Munich and his co-workers for stimulating discussions. Also the sustaining support by DFG, Siemens AG and the supercomputer staff of Regionales Hochschulrechenzentrum Kaiserslautern (RHRK) is acknowledged.

Manuscript received on June 1, 2001.

References

[1] T. Ojanperä and R. Prasad. An overview of air interface multiple access for IMT-2000/UMTS. In *IEEE Communications Magazine*, Vol. 36, No. 9, pages 82–95, September 1998.

[2] M. Meurer, P.W. Baier, T. Weber, Y. Lu and A. Papathanassiou. Joint transmission, an advantageous downlink concept for CDMA mobile radio systems using time division duplexing. In *IEE ELECTRONICS LETTERS*, Vol. 36, No. 10, pages 900–901, May 2000.

[3] M. Meurer, P.W. Baier, Y. Lu, A. Papathanassiou and T. Weber. TD-CDMA downlink: Optimum transmit signal design reduces receiver complexity and enhances system performance. In *Proc. 7th International Conference on Telecommunications (ICT 2000), Acapulco*, pages 300–305, 2000.

[4] P.W. Baier, M. Meurer, T. Weber and H. Tröger. Joint transmission (JT), an alternative rationale for the downlink of time division CDMA using multi-element transmit antennas. In *Proc. 6th International Symposium on Spread Spectrum Techniques & Applications (ISSSTA 2000), Parsippany*, pages 1–5, 2000.

[5] M. Tomlinson. New automatic equalizer employing modulo arithmetic. In *IEE ELECTRONICS LETTERS*, Vol. 7, No. 5, pages 138–139, March 1971.

[6] H. Harashima and H. Miyakawa. Matched-transmission technique for channels with intersymbol interference. In *IEEE Transactions on Communications*, Vol. COM-20, pages 774–780, August 1972.

[7] M. Joham and W. Utschick. Downlink processing for mitigation of intracell interference in DS-CDMA systems. In *Proc. 6th International Symposium on Spread Spectrum Techniques & Applications (ISSSTA 2000), Parsippany*, pages 15–19, 2000.

[8] K. Ban, M. Katayama, T. Yamazato and A. Ogawa. Joint optimization of transmitter/receiver with multiple transmit/receive antennas in band-limited channels. In *IEICE Transactions on Communications*, Vol. E83-B, No. 8, pages 1697–1704, August 2000.

[9] M. Brandt-Pearce and A. Dharap. Transmitter-based multiuser interference rejection for the down-link of a wireless CDMA system in a multipath environment. In *IEEE Journal on Selected Areas in Communications*, Vol. 18, No. 3, pages 407–417, March 2000.

[10] B.R. Vojčić and J.W. Mee. Transmitter precoding in synchronous multiuser communications. In *IEEE Transactions on Communications*, Vol. 46, No. 10, pages 1346–1355, October 1998.

[11] A. Klein. *Multi-user detection of CDMA signals – algorithms and their application to cellular mobile radio*, Fortschrittberichte VDI, Reihe 10, Nr. 423, VDI-Verlag, Düsseldorf, 1996.

[12] A. Ben-Israel and T.N.E. Greville. *Generalized inverses: theory and applications*, Wiley–Interscience, New York, 1974.

[13] Y. Lu and P.W. Baier. Performance of adaptive antennas for the TD-CDMA downlink under special consideration of multi-directional channels and CDMA code pooling. In *International Journal of Electronics and Communications (AEÜ)*, Vol. 54, No. 5, pages 249–258, October 2000.

[14] A. Klein, W. Mohr and R. Thomas. Direction-of-arrival of partial waves in wideband mobile radio channels for intelligent antenna concepts. In *Proc. IEEE 46th Vehicular Technology Conference (VTC'96)*, pages 849 – 853, 1996.

[Meu04b] Meurer, M.: “On the transmit efficiency of multi-user MIMO transmission utilizing transmit zero-forcing”. Submitted for publication in *IEEE Transactions on Wireless Communications*, 2004.

On the transmit efficiency of multi-user MIMO transmission utilizing transmit zero-forcing

Michael Meurer, *Member*

Abstract—**Recently, receiver oriented transmission has attracted significant attention as a means to reduce receiver complexity and to increase the data throughput in mobile radio downlinks. Receiver oriented transmission is based on a suitable transmit signal design exploiting channel knowledge at the transmitter. In several contributions transmit signal design by Transmit Zero-Forcing (TxZF) is proposed. Up to now, the performance analysis of TxZF for scenarios with time-variant mobile radio channels has almost exclusively been performed by means of computer simulations. In this contribution an alternative analytical evaluation technique is proposed which relies on the achievements of random matrix theory. The analysis focuses on the quality criterion transmit efficiency and its statistical characteristics. The results obtained show that both the expectation and the variance of said criterion are primarily influenced by the system load.**

Keywords—Receiver orientation, transmit zero-forcing, MIMO

I. Introduction

In [1–4] and the references therein, the transmit signal design strategy Transmit Zero-Forcing (TxZF) has been proposed which allows to totally avoid interferences while transmitting. This strategy is especially suited for the downlink of mobile radio communications systems, i.e., broadcast situations, including MIMO (Multiple Input Multiple Output) systems [4]. Up to now, the performance analysis of TxZF for scenarios with time-variant mobile radio channels has mainly been performed by means of computer simulations [5–8]. Only few contributions exist [9–11] which address this issue by means of analytical methods. These contributions are limited to the asymptotic analysis of transmitted energies [10, 11] or even to the analysis of mean transmitted energies [9]. The mentioned transmitted energies are mainly influenced by the channel attenuations, if time-variant mobile radio channels are considered. However, the price to be paid for interference avoidance itself is not quantified by these results. Therefore, in this contribution, especially this price should be studied by analytical methods for time-variant mobile radio channels. The instruments used to obtain the desired results are based on random matrix theory [12, 13].

The paper is organized as follows: In Section II a generic model of linear multi-user MIMO transmission systems is developed. Section III deals with a short survey of the transmit signal design strategies Transmit Matched Filter (TxMF) and TxZF in order to conveniently familiarize the reader with the basics of these transmit signal design strategies to a degree sufficient to follow the reasoning of the paper. The crux of this paper is concentrated in Section IV, where the quality criterion for the performance of TxZF is introduced and analytically studied. This criterion is termed transmit efficiency. Section V concludes the paper.

The investigations are performed in the time discrete equivalent low pass domain under utilization of a vector-matrix representation [14]. Consequently, signals and system components are represented by complex vectors or matrices, respectively, which are printed in bold face. In the analysis, $[\cdot]_{n,m}$ designates the element in the n-th row and m-th column of the matrix in brackets, $[\cdot]_n$ stands for the n-th row of the matrix or the n-th element of the vector in brackets and $\|\cdot\|_2$ denotes the Euclidean norm.

Dr. M. Meurer is with the Research Group for RF Communications, University of Kaiserslautern, P.O. Box 3049, D–67653 Kaiserslautern, Germany. Contact via email: meurer@rhrk.uni-kl.de

II. Multi-user MIMO transmission model

A. Data Transmission

We consider a downlink situation, where an access point (AP) supports K mobile terminals (MTs) $k, k = 1 \dots K$. The AP is equipped with K_B transmit antennas, and each of the K MTs employs K_M receive antennas. Therefore, each link between the AP and one of the K MTs constitutes a MIMO structure, and the total system is a multi-user MIMO structure. N data symbols $\underline{d}_n^{(k)}, n = 1 \dots N$, have to be transmitted from the AP to each MT $k, k = 1 \dots K$. The N data symbols $\underline{d}_n^{(k)}, n = 1 \dots N$, intended for MT k are arranged in the MT specific data vector

$$\underline{\mathbf{d}}^{(k)} = \left(\underline{d}_1^{(k)} \dots \underline{d}_N^{(k)}\right)^\mathrm{T} \tag{1}$$

of dimension N. The K MT specific data vectors $\underline{\mathbf{d}}^{(k)}, k = 1 \dots K$, of (1) are stacked to the total data vector

$$\underline{\mathbf{d}} = \left(\underline{\mathbf{d}}^{(1)^\mathrm{T}} \dots \underline{\mathbf{d}}^{(K)^\mathrm{T}}\right)^\mathrm{T} = \left(\underline{d}_1 \dots \underline{d}_{N_\mathrm{t}}\right)^\mathrm{T} \tag{2}$$

of dimension

$$N_\mathrm{t} = KN. \tag{3}$$

$\underline{\mathbf{d}}$ of (2) is assumed to be wide sense stationary with zero mean and the covariance matrix

$$\underline{\mathbf{R}}_\mathrm{d} = \mathop{\mathrm{E}}_{\underline{\mathrm{d}}}\left\{\underline{\mathbf{d}}\,\underline{\mathbf{d}}^\mathrm{H}\right\} = E_\mathrm{d} \cdot \mathbf{I}^{(N_\mathrm{t})}. \tag{4}$$

By linear modulation based on $\underline{\mathbf{d}}$ of (2) for each of the K_B transmit antennas an antenna specific transmitted signal

$$\underline{\mathbf{t}}^{(k_\mathrm{B})} = \left(\underline{t}_1^{(k_\mathrm{B})} \dots \underline{t}_{Q_\mathrm{t}}^{(k_\mathrm{B})}\right)^\mathrm{T} \in \mathbb{C}^{Q_\mathrm{t}},\ k_\mathrm{B} = 1 \dots K_\mathrm{B}, \tag{5}$$

is generated. The K_B transmitted signals $\underline{\mathbf{t}}^{(k_\mathrm{B})}, k_\mathrm{B} = 1 \dots K_\mathrm{B}$, of (5) are stacked in the signal

$$\underline{\mathbf{t}} = \left(\underline{\mathbf{t}}^{(1)^\mathrm{T}} \dots \underline{\mathbf{t}}^{(K_\mathrm{B})^\mathrm{T}}\right)^\mathrm{T} \in \mathbb{C}^{(K_\mathrm{B}Q_\mathrm{t})} \quad (6)$$

termed (total) transmitted signal. The synthesis of $\underline{\mathbf{t}}$ of (6) based on $\underline{\mathbf{d}}$ of (2) is described by the $(K_\mathrm{B}Q_\mathrm{t}) \times N_\mathrm{t}$-matrix $\underline{\mathbf{M}}$ termed modulator matrix [2]. With $\underline{\mathbf{M}}$ one obtains

$$\underline{\mathbf{t}} = \underline{\mathbf{M}}\,\underline{\mathbf{d}}. \quad (7)$$

The ratio

$$\kappa = \frac{N_\mathrm{t}}{K_\mathrm{B}Q_\mathrm{t}} \quad (8)$$

which describes the ratio between the number N_t of columns and the number $K_\mathrm{B}Q_\mathrm{t}$ of rows of $\underline{\mathbf{M}}$ of (7) is termed system load. Via (7) the N_t components of $\underline{\mathbf{d}}$ of (2) are mapped onto the $K_\mathrm{B}Q_\mathrm{t}$ components of $\underline{\mathbf{t}}$ of (6). Setting out from (7) the energy invested to transmit $\underline{\mathbf{t}}$, which is termed transmitted energy in the following, becomes

$$T = \frac{1}{2}\underline{\mathbf{t}}^\mathrm{H}\underline{\mathbf{t}}. \quad (9)$$

The frequency selective MIMO channel between the AP and MT k is assumed to be linear and is characterized by the $KK_\mathrm{B}K_\mathrm{M}$ channel impulse responses [14]

$$\underline{\mathbf{h}}^{(k,k_\mathrm{B},k_\mathrm{M})} = \left(\underline{h}_1^{(k,k_\mathrm{B},k_\mathrm{M})} \dots \underline{h}_W^{(k,k_\mathrm{B},k_\mathrm{M})}\right)^\mathrm{T} \in \mathbb{C}^W, \quad (10)$$

where $\underline{\mathbf{h}}^{(k,k_\mathrm{B},k_\mathrm{M})}$ describes the channel between the k_B-th transmit antenna, $k_\mathrm{B} = 1 \dots K_\mathrm{B}$, of the AP and the k_M-th receive antenna, $k_\mathrm{M} = 1 \dots K_\mathrm{M}$, of MT $k, k = 1 \dots K$. With $\underline{\mathbf{h}}^{(k,k_\mathrm{B},k_\mathrm{M})}$ of (10) and Q_t, see (5), the $KK_\mathrm{B}K_\mathrm{M}$ MT transmit antenna and receive antenna specific channel matrices

$$\begin{aligned}
\underline{\mathbf{H}}^{(k,k_\mathrm{B},k_\mathrm{M})} &= \left(\underline{H}_{i,j}^{(k,k_\mathrm{B},k_\mathrm{M})}\right) \in \mathbb{C}^{(Q_\mathrm{t}+W-1)\times Q_\mathrm{t}}, \quad (11)\\
& i = 1 \dots Q_\mathrm{t} + W - 1, j = 1 \dots Q_\mathrm{t},\\
\underline{H}_{i,j}^{(k,k_\mathrm{B},k_\mathrm{M})} &= \begin{cases} \underline{h}_{i-j+1}^{(k,k_\mathrm{B},k_\mathrm{M})}, & 1 \le i - j + 1 \le W,\\ 0, & \text{else}, \end{cases}\\
k = 1 \dots K, & k_\mathrm{B} = 1 \dots K_\mathrm{B}, k_\mathrm{M} = 1 \dots K_\mathrm{M},
\end{aligned}$$

are established. With the $KK_\mathrm{B}K_\mathrm{M}$ matrices $\underline{\mathbf{H}}^{(k,k_\mathrm{B},k_\mathrm{M})}$ of (11) we form the KK_B MT and transmit antenna specific channel matrices

$$\begin{aligned}
\underline{\mathbf{H}}^{(k,k_\mathrm{B})} &= \left(\underline{\mathbf{H}}^{(k,k_\mathrm{B},1)^\mathrm{T}} .. \underline{\mathbf{H}}^{(k,k_\mathrm{B},K_\mathrm{M})^\mathrm{T}}\right)^\mathrm{T} \in \mathbb{C}^{[K_\mathrm{M}(Q_\mathrm{t}+W-1)]\times Q_\mathrm{t}},\\
& k = 1 \dots K, k_\mathrm{B} = 1 \dots K_\mathrm{B}, \quad (12)
\end{aligned}$$

the K MT specific channel matrices

$$\begin{aligned}
\underline{\mathbf{H}}^{(k)} &= \left(\underline{\mathbf{H}}^{(k,1)} \dots \underline{\mathbf{H}}^{(k,K_\mathrm{B})}\right) \in \mathbb{C}^{[K_\mathrm{M}(Q_\mathrm{t}+W-1)]\times(K_\mathrm{B}Q_\mathrm{t})},\\
& k = 1 \dots K, \quad (13)
\end{aligned}$$

and the total channel matrix

$$\underline{\mathbf{H}} = \left(\underline{\mathbf{H}}^{(1)^\mathrm{T}} \dots \underline{\mathbf{H}}^{(K)^\mathrm{T}}\right)^\mathrm{T} \in \mathbb{C}^{[KK_\mathrm{M}(Q_\mathrm{t}+W-1)]\times(K_\mathrm{B}Q_\mathrm{t})}. \quad (14)$$

With $\underline{\mathbf{H}}^{(k)}$ of (13) the transmitted signal $\underline{\mathbf{t}}$ of (6) yields in the noisefree case the received signal

$$\begin{aligned}
\underline{\mathbf{e}}^{(k)} &= \left(\underline{e}_1^{(k)} \dots \underline{e}_{K_\mathrm{M}(Q_\mathrm{t}+W-1)}^{(K)}\right)^\mathrm{T}\\
&= \underline{\mathbf{H}}^{(k)}\underline{\mathbf{t}} \in \mathbb{C}^{[K_\mathrm{M}(Q_\mathrm{t}+W-1)]} \quad (15)
\end{aligned}$$

of MT $k, k = 1 \dots K$. With $\underline{\mathbf{H}}$ of (14) the signals $\underline{\mathbf{e}}^{(k)}, k = 1 \dots K$, are stacked in the total signal

$$\underline{\mathbf{e}} = \left(\underline{\mathbf{e}}^{(1)^\mathrm{T}} \dots \underline{\mathbf{e}}^{(K)^\mathrm{T}}\right)^\mathrm{T} = \underline{\mathbf{H}}\,\underline{\mathbf{t}} \in \mathbb{C}^{[KK_\mathrm{M}(Q_\mathrm{t}+W-1)]} \quad (16)$$

received in the noisefree case. If $\underline{\mathbf{e}}^{(k)}$ of (15) is corrupted by an additive noise signal

$$\underline{\mathbf{n}}^{(k)} = \left(\underline{n}_1^{(k)} \dots \underline{n}_{K_\mathrm{M}(Q_\mathrm{t}+W-1)}^{(K)}\right)^\mathrm{T} \in \mathbb{C}^{[K_\mathrm{M}(Q_\mathrm{t}+W-1)]}, \quad (17)$$

then we obtain the noisy received signal

$$\underline{\mathbf{r}}^{(k)} = \underline{\mathbf{e}}^{(k)} + \underline{\mathbf{n}}^{(k)} = \underline{\mathbf{H}}^{(k)}\underline{\mathbf{t}} + \underline{\mathbf{n}}^{(k)} \in \mathbb{C}^{[K_\mathrm{M}(Q_\mathrm{t}+W-1)]}, \quad (18)$$

of MT k and the total noisy received signal

$$\underline{\mathbf{r}} = \left(\underline{\mathbf{r}}^{(1)^\mathrm{T}} \dots \underline{\mathbf{r}}^{(K)^\mathrm{T}}\right)^\mathrm{T} = \underline{\mathbf{e}} + \underline{\mathbf{n}} = \underline{\mathbf{H}}\,\underline{\mathbf{t}} + \underline{\mathbf{n}}, \quad (19)$$

where

$$\underline{\mathbf{n}} = \left(\underline{\mathbf{n}}^{(1)^\mathrm{T}} \dots \underline{\mathbf{n}}^{(K)^\mathrm{T}}\right)^\mathrm{T} \quad (20)$$

denotes the total noise signal.

B. Data Detection

The demodulator of each MT $k, k = 1 \dots K$, determines based on $\underline{\mathbf{r}}^{(k)}$ of (18) a linear estimate $\hat{\underline{\mathbf{d}}}^{(k)}$ of $\underline{\mathbf{d}}^{(k)}$ of (1). Stacking the estimates $\hat{\underline{\mathbf{d}}}^{(k)}, k = 1 \dots K$, results in a total data estimate

$$\hat{\underline{\mathbf{d}}} = \left(\hat{\underline{\mathbf{d}}}^{(1)^\mathrm{T}} \dots \hat{\underline{\mathbf{d}}}^{(K)^\mathrm{T}}\right)^\mathrm{T} = \left(\hat{\underline{d}}_1 \dots \hat{\underline{d}}_{N_\mathrm{t}}\right)^\mathrm{T}, \quad (21)$$

of the total data vector $\underline{\mathbf{d}}$ of (2). In analogy to the procedure of (7) the generation of $\hat{\underline{\mathbf{d}}}^{(k)}$ based on $\underline{\mathbf{r}}^{(k)}$ can be described by a MT specific $N \times [K_\mathrm{M}(Q_\mathrm{t}+W-1)]$ matrix termed demodulator matrix by

$$\hat{\underline{\mathbf{d}}}^{(k)} = \underline{\mathbf{D}}^{(k)}\underline{\mathbf{r}}^{(k)}. \quad (22)$$

With $\hat{\underline{\mathbf{d}}}^{(k)}, k = 1 \dots K$, of (22), one obtains the total data estimate

$$\hat{\underline{\mathbf{d}}} = \left(\hat{\underline{\mathbf{d}}}^{(1)^\mathrm{T}} \dots \hat{\underline{\mathbf{d}}}^{(K)^\mathrm{T}}\right)^\mathrm{T} = \left(\hat{\underline{d}}_1 \dots \hat{\underline{d}}_{N_\mathrm{t}}\right)^\mathrm{T}. \quad (23)$$

With the total demodulator matrix

$$\underline{\mathbf{D}} = \mathrm{blockdiag}\left(\underline{\mathbf{D}}^{(1)} .. \underline{\mathbf{D}}^{(K)}\right) \in \mathbb{C}^{(KN)\times[KK_\mathrm{M}(Q_\mathrm{t}+W-1)]} \quad (24)$$

(22) and (23) can be written in the comprehensive form

$$\hat{\underline{\mathbf{d}}} = \underline{\mathbf{D}}\,\underline{\mathbf{r}}. \quad (25)$$

Finally with (7), (19) and (25) one obtains

$$\hat{\underline{\mathbf{d}}} = \underbrace{\underline{\mathbf{D}}\,\underline{\mathbf{H}}}_{\underline{\mathbf{B}}}\,\underline{\mathbf{M}}\,\underline{\mathbf{d}} + \underline{\mathbf{D}}\,\underline{\mathbf{n}} \tag{26}$$

for the relation between $\hat{\underline{\mathbf{d}}}$ of (23) and $\underline{\mathbf{d}}$ of (2). In (26) the matrix $\underline{\mathbf{B}}$ of dimension $N_\mathrm{t} \times (K_\mathrm{B} Q_\mathrm{t})$ is termed system matrix and is composed of the data symbol specific combined signatures $\underline{\mathbf{b}}_n, n = 1 \ldots N_\mathrm{t}$, as follows:

$$\underline{\mathbf{B}} = \left(\underline{\mathbf{b}}_1^\mathrm{T} \ldots \underline{\mathbf{b}}_{N_\mathrm{t}}^\mathrm{T}\right)^\mathrm{T}. \tag{27}$$

According to (4) and (7) the mean transmitted energy invested for the data symbol $\underline{d}_n$ becomes

$$T_n = \frac{1}{2}\left\|\left[\underline{\mathbf{M}}^\mathrm{T}\right]_n\right\|_2^2 \cdot E_\mathrm{d} = \frac{1}{2}\left[\underline{\mathbf{M}}^\mathrm{H}\underline{\mathbf{M}}\right]_{n,n} \cdot E_\mathrm{d}. \tag{28}$$

III. Short review of the Transmit Matched Filter and the Transmit Zero-forcing Filter

The idea behind the Transmit Matched Filter (TxMF) is the minimization of T_n of (28) for each data symbol $\underline{d}_n$, $n = 1 \ldots N_\mathrm{t}$, under the side condition that interference is neglected and unbiased data transmission is desired. This leads to the modulator matrix [15–18]

$$\underline{\mathbf{M}}_\mathrm{TxMF} = \underline{\mathbf{B}}^\mathrm{H}\left[\mathrm{diag}\left(\underline{\mathbf{B}}\,\underline{\mathbf{B}}^\mathrm{H}\right)\right]^{-1}. \tag{29}$$

Due to the design criterion of TxMF explained above, the choice of (29) for the modulator matrix is optimum with respect to the minimization of the data symbol specific transmitted energies T_n of (28), if unbiased data transmission is established. The respective minimum data symbol specific transmitted energies read

$$T_{\mathrm{MF},n} = \frac{1}{2}\left(\left[\underline{\mathbf{B}}\,\underline{\mathbf{B}}^\mathrm{H}\right]_{n,n}\right)^{-1} E_\mathrm{d}. \tag{30}$$

However, if multiple data symbols are transmitted in parallel, quite strong interferences might occur.

TxZF totally eliminates interferences. Therefore, the interference contributions to $\hat{\underline{d}}_n$, $n = 1 \ldots N_\mathrm{t}$, of (21) are nulled. While ensuring unbiased data transmission, the remaining degrees of freedom in the choice of $\underline{\mathbf{M}}_\mathrm{TxZF}$ are exploited for the minimization of the required transmitted energy T of (9) and simultaneously the minimization of the data symbol specific energies T_n, $n = 1 \ldots N_\mathrm{t}$, of (28). Following this idea one obtains

$$\underline{\mathbf{M}}_\mathrm{TxZF} = \underline{\mathbf{B}}^\mathrm{H}\left(\underline{\mathbf{B}}\,\underline{\mathbf{B}}^\mathrm{H}\right)^{-1} \tag{31}$$

for the modulator matrix $\underline{\mathbf{M}}$ of (7) [2, 17, 18]. The price to be paid for the elimination of interferences is an increase of the data symbol specific energies

$$T_{\mathrm{ZF},n} = \frac{1}{2}\left[\left(\underline{\mathbf{B}}\,\underline{\mathbf{B}}^\mathrm{H}\right)^{-1}\right]_{n,n} E_\mathrm{d} \tag{32}$$

of (28) as compared to the TxMF.

IV. Transmit efficiency for TxZF

The just mentioned price is quantified by the transmit (Tx) efficiency $\eta_{\mathrm{TxZF},n}$ [19] which is defined as the ratio

$$\eta_{\mathrm{TxZF},n} = \frac{T_{\mathrm{MF},n}}{T_{\mathrm{ZF},n}} = \frac{1}{\left[\left(\underline{\mathbf{B}}\,\underline{\mathbf{B}}^\mathrm{H}\right)^{-1}\right]_{n,n} \cdot \left[\underline{\mathbf{B}}\,\underline{\mathbf{B}}^\mathrm{H}\right]_{n,n}} \tag{33}$$

of the symbol specific transmitted energies $T_{\mathrm{MF},n}$ of (30) and $T_{\mathrm{ZF},n}$ of (32), $n = 1 \ldots N_\mathrm{t}$, for TxMF and TxZF, respectively. Quite generally, as the Tx efficiency describes the degrading impact of interference suppression, it can be interpreted as a measure dual to the asymptotic multi-user efficiency [20], a measure which is quite common in the field of transmitter oriented transmission and multi-user detection, and which was originally introduced by Verdu [21]. Likewise, the transmit efficiency $\eta_{\mathrm{TxZF},n}$ takes values from 0 to 1, with 1 being the optimum. The quantity $\eta_{\mathrm{TxZF},n}$ of (33) depends on the number of additional constraints, which have to be satisfied to avoid interferences while designing the transmitted signal $\underline{\mathbf{t}}$ of (5), and on the total number of degrees of freedom for this design process. Unfortunately, a closed form analysis of these dependencies is not yet available in literature for Rx oriented transmission. In [9–11] some insights concerning the transmit energies $T_{\mathrm{ZF},n}$ of (32) have been gained. However, this insights do not allow to assess the impact of interference. In this paper this open point will be addressed by analyzing the transmit efficiencies $\eta_{\mathrm{TxZF},n}$, $n = 1 \ldots N_\mathrm{t}$. The instruments to derive the mentioned results are based on random matrix theory [12] and are related to the procedure described in [13].

With the diagonal scaling matrix $\sqrt{\mathbf{P}}$ of dimension $N_\mathrm{t} \times N_\mathrm{t}$ and the matrix $\tilde{\underline{\mathbf{B}}}$ with normalized rows $\tilde{\underline{\mathbf{b}}}_n$ the system matrix $\underline{\mathbf{B}}$ of (27) can be decomposed as

$$\underline{\mathbf{B}} = \underbrace{\mathrm{diag}\left(\sqrt{P_1} \ldots \sqrt{P_{N_\mathrm{t}}}\right)}_{\sqrt{\mathbf{P}}} \cdot \underbrace{\left(\tilde{\underline{\mathbf{b}}}_1^\mathrm{T} \ldots \tilde{\underline{\mathbf{b}}}_{N_\mathrm{t}}^\mathrm{T}\right)^\mathrm{T}}_{\tilde{\underline{\mathbf{B}}}}. \tag{34}$$

Each row $\tilde{\underline{\mathbf{b}}}_n$, $n = 1 \ldots N_\mathrm{t}$, of $\tilde{\underline{\mathbf{B}}}$, can be thought of being the result of normalizing a row vector

$$\tilde{\underline{\mathbf{g}}}_n = \left(\tilde{\underline{g}}_{n,1} \cdots \tilde{\underline{g}}_{n,K_\mathrm{B}Q_\mathrm{t}}\right) \tag{35}$$

to norm one, i.e.,

$$\tilde{\underline{\mathbf{b}}}_n = \tilde{\underline{\mathbf{g}}}_n / \left\|\tilde{\underline{\mathbf{g}}}_n\right\|_2 \tag{36}$$

holds. If the mobile radio channels are time-variant with random block-fading and/or the demodulator $\underline{\mathbf{D}}$ changes, $\underline{\mathbf{B}}$ of (27) varies with time and can, therefore, be regarded as a random matrix. Consequently, $\eta_{\mathrm{TxZF},n}$ of (33) is a random quantity. Therefore, an analysis of $\eta_{\mathrm{TxZF},n}$ can only be made on a stochastical basis taking the stochastical properties of $\underline{\mathbf{B}}$ and, therefore, of $\sqrt{\mathbf{P}}$ of (34) and $\tilde{\underline{\mathbf{g}}}_n$, $n = 1 \ldots N_\mathrm{t}$, of (35) into account. In the following it should be assumed that all elements $\tilde{\underline{g}}_{n,s}$, $s = 1 \ldots K_\mathrm{B} Q_\mathrm{t}$, of $\tilde{\underline{\mathbf{g}}}_n$, $n = 1 \ldots N_\mathrm{t}$, are independent identically distributed (i.i.d.) Gaussian variables with zero mean and unit standard deviation. This assumption is quite common for MIMO transmission systems [22] and holds in good approximation, e.g., if

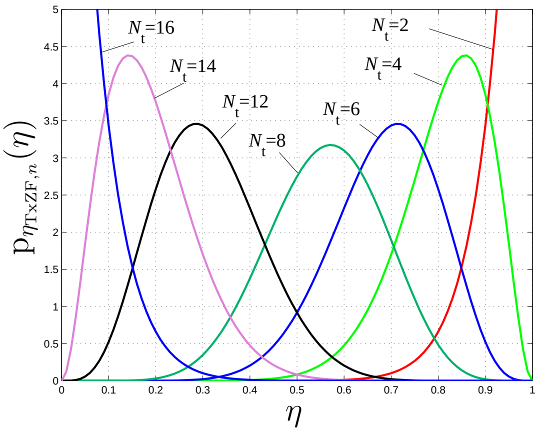

Fig. 1. pdf $\mathrm{p}_{\eta_{\mathrm{TxZF},n}}(\eta)$ of (38) for $K_\mathrm{B}=1$, $Q_\mathrm{t}=16$, $N_\mathrm{t}=2\dots16$

- for each k the elements $\underline{h}_w^{(k,k_\mathrm{B},k_\mathrm{M})}$, $k_\mathrm{B}=1\dots K_\mathrm{B}$, $k_\mathrm{M}=1\dots K_\mathrm{M}$, of (10) are i.i.d. Gaussian variables and
- the elements of each row of the MT specific demodulator matrices $\underline{\mathbf{D}}^{(k)}$ are independent random binary quantities with identical uniform distribution.

With the above made assumptions for $\underline{\tilde{\mathbf{g}}}_n$, $n=1\dots N_\mathrm{t}$, $\underline{\tilde{\mathbf{b}}}_n$ of (34) is spherically uniformly distributed [22]. Substituting (34) in (33) yields

$$\eta_{\mathrm{TxZF},n}=1\Big/\left[\left(\underline{\tilde{\mathbf{B}}}\,\underline{\tilde{\mathbf{B}}}^{\mathrm{H}}\right)^{-1}\right]_{n,n}. \qquad (37)$$

Obviously, $\eta_{\mathrm{TxZF},n}$ of (37) is independent of $\sqrt{\mathbf{P}}$ of (34) and, consequently, also independent of its probability distribution. Therefore, $\sqrt{\mathbf{P}}$ does not have to be considered in what follows. Using (37) and the assumptions made above for the distribution of the elements of $\underline{\mathbf{B}}$, the probability density function (pdf)

$$\mathrm{p}_{\eta_{\mathrm{TxZF},n}}(\eta)=\begin{cases}\frac{\eta^{K_\mathrm{B}Q_\mathrm{t}-N_\mathrm{t}}(1-\eta)^{N_\mathrm{t}-2}}{\mathrm{B}(K_\mathrm{B}Q_\mathrm{t}-N_\mathrm{t}+1,N_\mathrm{t}-1)}, & 0\le\eta\le1,\\ 0, & \text{else},\end{cases} \qquad (38)$$

of $\eta_{\mathrm{TxZF},n}$ can be derived as shown in the appendix. The function

$$\mathrm{B}(z,w)=\int_0^1 t^{z-1}(1-t)^{w-1}\mathrm{d}t=\frac{\Gamma(z)\cdot\Gamma(w)}{\Gamma(z+w)} \qquad (39)$$

in (38) denotes the beta-function [23]. Therefore, $\eta_{\mathrm{TxZF},n}$ of (37) is termed to be beta distributed [23]. Fig. 1 shows the pdf $\mathrm{p}_{\eta_{\mathrm{TxZF},n}}(\eta)$ of (38) for K_B equal to one and Q_t equal to 16 for different N_t. Obviously, with increasing N_t, the maximum of the pdf $\mathrm{p}_{\eta_{\mathrm{TxZF},n}}(\eta)$ tends to be shifted to lower η.

Based on (38) the m-th moment of $\eta_{\mathrm{TxZF},n}$ of (33) can be expressed as

$$\mathrm{E}\{\eta_{\mathrm{TxZF},n}^m\}=\frac{\Gamma(K_\mathrm{B}Q_\mathrm{t}-N_\mathrm{t}+m+1)}{\Gamma(K_\mathrm{B}Q_\mathrm{t}-N_\mathrm{t}+1)}\,\frac{\Gamma(K_\mathrm{B}Q_\mathrm{t})}{\Gamma(K_\mathrm{B}Q_\mathrm{t}+m)}. \qquad (40)$$

Using (40), the mean

$$\overline{\eta}_{\mathrm{TxZF}}=\mathrm{E}\{\eta_{\mathrm{TxZF},n}\}=\frac{K_\mathrm{B}Q_\mathrm{t}-(N_\mathrm{t}-1)}{K_\mathrm{B}Q_\mathrm{t}} \qquad (41)$$

and the variance

$$\begin{aligned}\mathrm{var}\left(\eta_{\mathrm{TxZF},n}\right)&=\mathrm{E}\{\eta_{\mathrm{TxZF},n}^2\}-\overline{\eta}_{\mathrm{TxZF}}^2\\&=\frac{[K_\mathrm{B}Q_\mathrm{t}-(N_\mathrm{t}-1)]\,(N_\mathrm{t}-1)}{(K_\mathrm{B}Q_\mathrm{t})^2\,(K_\mathrm{B}Q_\mathrm{t}+1)}\end{aligned} \qquad (42)$$

of $\eta_{\mathrm{TxZF},n}$ follow. Obviously, as already presumed before, $\overline{\eta}_{\mathrm{TxZF}}$ depends on the difference of two quantities,

- the number $K_\mathrm{B}Q_\mathrm{t}$ of degrees of freedom for the transmit signal design, i.e., the number of elements of the total transmitted signal $\underline{\mathbf{t}}$ of (5), and
- the number $(N_\mathrm{t}-1)$ of restrictions due to interference avoidance when designing the contribution of each data symbol $\underline{d}_n$, $n=1\dots N_\mathrm{t}$, to $\underline{\mathbf{t}}$.

If the number $K_\mathrm{B}Q_\mathrm{t}$ of degrees of freedom is large compared to $(N_\mathrm{t}-1)$, then $\overline{\eta}_{\mathrm{TxZF}}$ tends to be close to one; otherwise it is between zero and one. For a fixed system load κ of (8), (41) and (42) can be rewritten as

$$\overline{\eta}_{\mathrm{TxZF}}=1-\big(\kappa-1/(K_\mathrm{B}Q_\mathrm{t})\big), \qquad (43a)$$

$$\mathrm{var}\left(\eta_{\mathrm{TxZF},n}\right)=\frac{\left(1-\kappa+\frac{1}{K_\mathrm{B}Q_\mathrm{t}}\right)\left(\kappa-\frac{1}{K_\mathrm{B}Q_\mathrm{t}}\right)}{1+K_\mathrm{B}Q_\mathrm{t}}. \qquad (43b)$$

(43) discloses, if the system load κ is kept constant and $K_\mathrm{B}Q_\mathrm{t}$ is quite large, $\eta_{\mathrm{TxZF},n}$ tends to the asymptotic transmit efficiency $\eta_{\mathrm{TxZF}}^{\infty}$ with its mean

$$\overline{\eta}_{\mathrm{TxZF}}^{\infty}=\lim_{K_\mathrm{B}Q_\mathrm{t}\to\infty}\overline{\eta}_{\mathrm{TxZF}}=1-\kappa \qquad (44)$$

and its variance

$$\mathrm{var}\left(\eta_{\mathrm{TxZF}}^{\infty}\right)=\lim_{K_\mathrm{B}Q_\mathrm{t}\to\infty}\mathrm{var}\left(\eta_{\mathrm{TxZF},n}\right)=0, \qquad (45)$$

respectively. Therefore, for large systems with given system load κ the mean of the asymptotic transmit efficiency $\overline{\eta}_{\mathrm{TxZF}}^{\infty}$ is only a function of the system load κ, while the variance $\mathrm{var}\left(\eta_{\mathrm{TxZF}}^{\infty}\right)$ of $\eta_{\mathrm{TxZF},n}$ asymptotically goes to zero, resulting in the pdf

$$\mathrm{p}_{\eta_{\mathrm{TxZF}}^{\infty}}(\eta)=\delta\big(\eta-(1-\kappa)\big) \qquad (46)$$

of the asymptotic transmit efficiency $\eta_{\mathrm{TxZF}}^{\infty}$. This asymptotic behaviour is verified by the results depicted in Fig. 2 which shows the pdf $\mathrm{p}_{\eta_{\mathrm{TxZF},n}}(\eta)$ of (38) for a fixed system load κ of 0.5 and different values $K_\mathrm{B}Q_\mathrm{t}$.

V. Conclusions

Up to now, for scenarios with time-variant mobile radio channels the performance analysis of receiver oriented transmission systems has primarily been conducted by computer simulations. However, as shown in this contribution, also analytical methods are applicable to quantify this performance, e.g., in terms of the quality measure transmit efficiency – a measure quantifying the price for interference suppression. In contrast to performance results obtained by simulations, the analytically derived closed-form expressions for the statistical characteristics of the transmit efficiency allow a deeper understanding of the fundamental

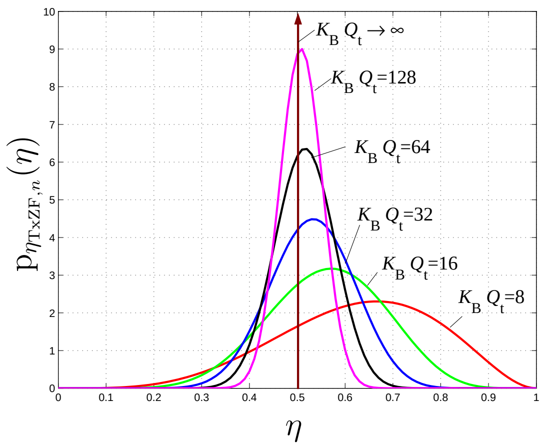

Fig. 2. pdf $\mathrm{p}_{\eta_{\mathrm{TxZF},n}}(\eta)$ of (38) for $\kappa = 0.5$, $K_{\mathrm{B}}Q_{\mathrm{t}} = 8\dots128$ and $K_{\mathrm{B}}Q_{\mathrm{t}} \to \infty$

interdependencies between system performance and system parameters. Especially the influences of the system load κ and the dimension $K_{\mathrm{B}}Q_{\mathrm{t}}$ of the total transmitted signal $\underline{\mathbf{t}}$ onto the system performance have been clarified. The insights gained are not only restricted to the analysis of TxZF but also have a significant importance for a profound understanding of recently proposed, more sophisticated non-linear transmit signal design strategies like for instance Transmit Nonlinear Zero-Forcing (TxNZF) [19] or Tomlinson-Harashima Precoding (THP) [24]. Those strategies can be interpreted as stepwise partially applying TxZF and, consequently, show a performance which is limited by the performance of those partial processing steps. Using the derived closed-form expressions for TxZF also the performance of said non-linear transmit signal design strategies can be demystified.

Appendix

Derivation of the PDF $\mathrm{p}_{\eta_{\mathrm{TxZF},n}}(\eta)$ of (38)

Based on (37) and using the auxiliary real-valued positive scalar s it can be shown by means of the matrix inversion lemma [25] that $\eta_{\mathrm{TxZF},n}$ of (33) can be written as

$$\eta_{\mathrm{TxZF},n} = \lim_{s\to 0}\left[\tilde{\underline{\mathbf{b}}}_n\Big(\underbrace{\left[\underline{\mathbf{B}}^{\mathrm{H}}\underline{\mathbf{B}} - \underline{\mathbf{b}}_n^{\mathrm{H}}\underline{\mathbf{b}}_n\right]}_{\underline{\mathbf{R}}_{\tilde{\mathrm{B}}}}/s + \mathbf{I}^{(K_{\mathrm{B}}Q_{\mathrm{t}})}\Big)^{-1}\tilde{\underline{\mathbf{b}}}_n^{\mathrm{H}}\right]. \tag{47}$$

By Eigenvalue decomposition follows

$$\underline{\mathbf{R}}_{\tilde{\mathrm{B}}} = \underline{\mathbf{U}}\boldsymbol{\lambda}\underline{\mathbf{U}}^{\mathrm{H}} \tag{48}$$

for the Hermitian matrix $\underline{\mathbf{R}}_{\tilde{\mathrm{B}}}$ of (47), where $\underline{\mathbf{U}}$ is a unitary matrix and

$$\boldsymbol{\lambda} = \mathrm{diag}(\lambda_1\dots\lambda_{N_{\mathrm{t}}-1},\ \underbrace{0\ \dots\ 0}_{(K_{\mathrm{B}}Q_{\mathrm{t}}-N_{\mathrm{t}}+1)-\mathrm{times}}\ ) \tag{49}$$

is a diagonal matrix with $(N_{\mathrm{t}}-1)$ non-zero Eigenvalues $\lambda_n, n = 1\dots N_{\mathrm{t}}-1$. Substituting (49) in (47), the transmit efficiency $\eta_{\mathrm{TxZF},n}$ of (33) reads

$$\begin{aligned}\eta_{\mathrm{TxZF},n} &= \lim_{s\to 0}\left[\tilde{\underline{\mathbf{b}}}_n\left(\underline{\mathbf{U}}\left(\boldsymbol{\lambda}/s + \mathbf{I}^{(K_{\mathrm{B}}Q_{\mathrm{t}})}\right)\underline{\mathbf{U}}^{\mathrm{H}}\right)^{-1}\tilde{\underline{\mathbf{b}}}_n^{\mathrm{H}}\right] \\ &= \lim_{s\to 0}\left[\underbrace{\tilde{\underline{\mathbf{b}}}_n\underline{\mathbf{U}}}_{\tilde{\tilde{\underline{\mathbf{b}}}}_n}\left(\boldsymbol{\lambda}/s + \mathbf{I}^{(K_{\mathrm{B}}Q_{\mathrm{t}})}\right)^{-1}\underbrace{\left(\tilde{\underline{\mathbf{b}}}_n\underline{\mathbf{U}}\right)^{\mathrm{H}}}_{\tilde{\tilde{\underline{\mathbf{b}}}}_n^{\mathrm{H}}}\right].\end{aligned} \tag{50}$$

As already explained, $\tilde{\underline{\mathbf{b}}}_n$ of (36) is spherically uniformly distributed. Therefore, this assumption also holds for the row vector $\tilde{\tilde{\underline{\mathbf{b}}}}_n$ in (50) of dimension $K_{\mathrm{B}}Q_{\mathrm{t}}$, as multiplying a spherically distributed vector by a unitary matrix $\underline{\mathbf{U}}$ does not change its probability distribution [22]. Therefore, in analogy to (35) and (36), $\tilde{\tilde{\underline{\mathbf{b}}}}_n$ of (50) can also be represented by

$$\tilde{\tilde{\underline{\mathbf{b}}}}_n = \tilde{\underline{\mathbf{b}}}_n\underline{\mathbf{U}} = \tilde{\tilde{\underline{\mathbf{g}}}}_n/\|\tilde{\tilde{\underline{\mathbf{g}}}}_n\|_2, \tilde{\tilde{\underline{\mathbf{g}}}}_n = \left(\tilde{\tilde{\underline{g}}}_{n,1}\dots\tilde{\tilde{\underline{g}}}_{n,K_{\mathrm{B}}Q_{\mathrm{t}}}\right)^{\mathrm{T}}, \tag{51}$$

where the elements $\tilde{\tilde{\underline{g}}}_{n,s}, s = 1\dots K_{\mathrm{B}}Q_{\mathrm{t}}$, of $\tilde{\tilde{\underline{\mathbf{g}}}}_n, n = 1\dots N_{\mathrm{t}}$, satisfy the same probability distribution as $\tilde{\underline{\mathbf{g}}}_n$ of (35). Substituting (49) in (50), the transmit efficiency can be calculated to be

$$\begin{aligned}\eta_{\mathrm{TxZF},n} &= \tilde{\tilde{\underline{\mathbf{b}}}}_n\lim_{s\to 0}\left[\mathrm{diag}\left(1+\frac{\lambda_1}{s}\dots 1+\frac{\lambda_{N_{\mathrm{t}}-1}}{s}, 1\dots 1\right)\right]^{-1}\tilde{\tilde{\underline{\mathbf{b}}}}_n^{\mathrm{H}} \\ &= \tilde{\tilde{\underline{\mathbf{b}}}}_n\lim_{s\to 0}\left[\mathrm{diag}\left(\frac{s}{s+\lambda_1}\dots\frac{s}{s+\lambda_{N_{\mathrm{t}}-1}}, 1\dots 1\right)\right]\tilde{\tilde{\underline{\mathbf{b}}}}_n^{\mathrm{H}} \\ &= \tilde{\tilde{\underline{\mathbf{b}}}}_n\mathrm{diag}\left(0\dots 0, 1\dots 1\right)\tilde{\tilde{\underline{\mathbf{b}}}}_n^{\mathrm{H}}.\end{aligned} \tag{52}$$

Using (51) and the quantities

$$X_1 = \sum_{s=N_{\mathrm{t}}}^{K_{\mathrm{B}}Q_{\mathrm{t}}}\left|\tilde{\tilde{\underline{g}}}_{n,s}\right|^2,\quad X_2 = \sum_{s=1}^{N_{\mathrm{t}}-1}\left|\tilde{\tilde{\underline{g}}}_{n,s}\right|^2, \tag{53}$$

$\eta_{\mathrm{TxZF},n}$ of (52) can be simplified to

$$\eta_{\mathrm{TxZF},n} = \frac{\sum\limits_{s=N_{\mathrm{t}}}^{K_{\mathrm{B}}Q_{\mathrm{t}}}\left|\tilde{\tilde{\underline{g}}}_{n,s}\right|^2}{\sum\limits_{s=1}^{K_{\mathrm{B}}Q_{\mathrm{t}}}\left|\tilde{\tilde{\underline{g}}}_{n,s}\right|^2} = \frac{X_1}{X_1+X_2}. \tag{54}$$

As stated in [23], both X_1 and X_2 are centrally χ^2-distributed random variables with $2(K_{\mathrm{B}}Q_{\mathrm{t}}-N_{\mathrm{t}}+1)$ and $2(N_{\mathrm{t}}-1)$ degrees of freedom, respectively. Thus, as shown in [23], $\eta_{\mathrm{TxZF},n}$ of (54) is beta distributed with the pdf $\mathrm{p}_{\eta_{\mathrm{TxZF},n}}(\eta)$ of (38).

Acknowledgment

The author gratefully appreciates the fruitful exchange of ideas with Prof. P. W. Baier, and his colleagues at the Research Group for RF Communications, University of Kaiserslautern, with T. Haustein, V. Jungnickel and M. Schubert from Prof. Boche's group at the Fraunhofer-Institute for Telecommunications, Heinrich-Hertz-Institut, and with R. R. Müller from Vienna Telecommunications Research Centre (ftw). The support of individual parts of this work in the framework of the EU-IST-Project FLOWS (Flexible Convergence of Wireless Standards and Services), by Siemens AG and by DFG as well as the assistance by the supercomputer staff of the central computer facility (RHRK) of the University of Kaiserslautern are highly acknowledged.

REFERENCES

[1] M. Meurer, P. W. Baier, T. Weber, Y. Lu, and A. Papathanassiou, "Joint transmission: advantageous downlink concept for CDMA mobile radio systems using time division duplexing," *IEE ELECTRONICS LETTERS*, vol. 11, pp. 900–901, 2000.

[2] P. W. Baier, M. Meurer, T. Weber, and H. Tröger, "Joint transmission (JT), an alternative rationale for the downlink of time division CDMA using multi-element transmit antennas," *Proc. IEEE 6th International Symposium on Spread Spectrum Techniques & Applications (ISSSTA'00)*, pp. 1–5, 2000.

[3] M. Joham and W. Utschick, "Downlink processing for mitigation of intracell interference in DS-CDMA systems," *Proc. IEEE 6th International Symposium on Spread Spectrum Techniques & Applications (ISSSTA'00)*, pp. 15–19, 2000.

[4] M. Meurer, P. W. Baier, and W. Qiu, "Receiver orientation versus transmitter orientation in linear MIMO transmission systems," *EURASIP Special Issue on Advances in Smart Antennas*, vol. 9, pp. 1–8, 2004.

[5] B. R. Vojcic and W. M. Jang, "Transmitter precoding in synchronous multiuser communications," *IEEE Transactions on Communications*, vol. 46, no. 10, pp. 1346–1355, 1998.

[6] F. Kowalewski and P. Mangold, "Joint predistortion and transmit diversity," *Proc. IEEE Global Telecommunications Conference (GLOBECOM'00)*, pp. 245–249, 2000.

[7] R. Irmer, A. Noll-Barreto, and G. Fettweis, "Transmitter precoding for spread-spectrum signals in frequency-selective fading channels," in *Proc. 3G Wireless 2001*, San Francisco, 2001, pp. 939–944.

[8] F. Dietrich, R. Hunger, M. Joham, and W. Utschick, "Linear precoding over time-varying channels in TDD systems," in *Proc. IEEE International Conference on Acoustics, Speech, and Signal Processing (ICASSP'03)*, Hong Kong, 2003, pp. 117–120.

[9] V. Jungnickel, T. Haustein, E. Jorswieck, and C. von Helmolt, "On linear pre-processing in multi-antenna systems," in *Proc. IEEE Global Telecommunications Conference (GLOBECOM'02)*, Taipei, 2002, pp. 1012–1016.

[10] E. Jorswieck, G. Wunder, V. Jungnickel, and T. Haustein, "Inverse eigenvalue statistics for Rayleigh and Rician MIMO channels," *IEE Professional Network on Antennas and Propagation*, pp. 3/1–3/6, 2001.

[11] T. Haustein, C. von Helmolt, E. Jorswieck, V. Jungnickel, and V. Pohl, "Performance of MIMO systems with channel inversion," in *Proc. IEEE 55th Vehicular Technology Conference (VTC'02)*, Birmingham, 2002, pp. 35–39.

[12] M. L. Mehta, *Random matrices*. San Diego: Academic Press, 1991.

[13] R. R. Müller, "Multiuser receivers for randomly spread signals: Fundamental limits with and without decision-feedback," *IEEE Transactions on Information Theory*, vol. 47, pp. 268–283, 2001.

[14] P. W. Baier, W. Qiu, H. Tröger, C. A. Jötten, and M. Meurer, "Modelling and optimization of receiver oriented multi-user MIMO downlinks for frequency selective channels," in *Proc. 10th International Conference on Telecommunications (ICT'03)*, Papeete, 2003, pp. 1547–1554.

[15] R. Esmailzadeh and M. Nakagawa, "Pre-RAKE diversity combining for direct sequence spread spectrum mobile communications systems," *IEICE Transactions on Communications*, vol. 76, pp. 1008–1015, 1993.

[16] A. Noll-Barreto and G. Fettweis, "Performance improvement in DS-spread spectrum CDMA systems using a pre- and a post-rake," in *Proc. 2000 International Zurich Seminar on Broadband Communications (IZS'2000)*, Zurich, 2000, pp. 39–46.

[17] M. Joham, K. Kusume, M. H. Gzara, W. Utschick, and J. A. Nossek, "Transmit Wiener Filter for the Downlink of TDD DS-CDMA Systems," in *Proc. IEEE 7th International Symposium on Spread Spectrum Techniques & Applications (ISSSTA'02)*, Prague, 2002, pp. 9–13.

[18] P. W. Baier and M. Meurer, "Receiver orientation, an unconventional approach to mobile radio downlink design," in *Proc. European Conference on Wireless Technology (ECWT'03)*, Munich, 2003, pp. 11–14.

[19] M. Meurer, T. Weber, and W. Qiu, "Transmit Nonlinear Zero Forcing: Energy efficient receiver oriented transmission in MIMO CDMA mobile radio downlinks," in *Proc. IEEE 8th International Symposium on Spread Spectrum Techniques & Applications (ISSSTA'04)*, Sydney, 2004.

[20] S. Verdú, *Multiuser detection*. Cambridge: Cambridge University Press, 1998.

[21] ——, "Optimum multiuser asymptotic efficiency," *IEEE Transactions on Communications*, vol. 34, pp. 890–897, 1986.

[22] I. E. Telatar, "Capacity of multi-antenna Gaussian channels," *European Transactions on Telecommunications*, no. 6, pp. 585–595, 1999.

[23] M. Abramowitz and I. Stegun, *Handbook of mathematical functions*. New York: Dover, 1965.

[24] R. F. H. Fischer, C. Windpassinger, A. Lampe, and J. B. Huber, "MIMO precoding for decentralized receivers," in *Proc. 2002 IEEE International Symposium on Information Theory (ISIT'2002)*, Lausanne, 2002, p. 496.

[25] H. Lütkepohl, *Handbook of Matrices*. England: John Wiley & Sons, 1996.

[Meu04a] Meurer, M.: "An analytical view on receiver oriented multi-user MIMO transmission over dispersive Rayleigh fading channels". Submitted for publication in *IEEE Transactions on Communications*, 2004.

An analytical view on receiver oriented multi-user MIMO transmission over dispersive Rayleigh fading channels

Michael Meurer, *Member, IEEE*

***Abstract*— Receiver orientation is a transmission conception which reduces receiver complexity and allows to increase the data throughput in mobile radio downlinks. The crux of receiver oriented transmission consists in a suitable transmit signal design exploiting channel knowledge at the transmitter. In numerous contributions transmit signal design by Transmit Zero-Forcing (TxZF) has been proposed. Up to now, the performance analysis of TxZF for scenarios with time-variant mobile radio channels has almost exclusively been performed by means of computer simulations. In this contribution an alternative analytical approach is proposed which relies on instruments borrowed from random matrix theory. The analysis focuses on the quality criteria transmitted energy and transmit efficiency and their statistical characteristics. The results obtained show that both these quality criteria are primarily influenced by the system load.**

***Index Terms*— Receiver orientation, MIMO, transmit zero-forcing, transmitted energy, transmit efficiency.**

I. Introduction

It is not long ago, since the transmit signal design strategy Transmit Zero-Forcing (TxZF) – also known as channel inversion [1–4] or Joint Transmission [5–8] – has been proposed, see [9–14], [15] and the references therein. This strategy belongs to the class of receiver (Rx) oriented transmission techniques [15] and allows to totally avoid interferences at the receiver side by proper measures at the transmitter side. In [6, 14] it has been shown that this strategy is especially suited for the downlink of mobile radio communications systems, i.e., broadcast situations [16], including multiple input multiple output (MIMO) systems [15, 17]. Up to now, the performance analysis of TxZF for scenarios with frequency selective time-variant mobile radio channels has mainly been performed by means of computer simulations [7, 12, 18, 19]. Only few contributions exist [1–3] which address this issue by means of analytical methods. These contributions are limited to the asymptotic analysis of transmitted energies for non frequency selective channels [2, 3] or even to the analysis of mean transmitted energies [1]. To the author's knowledge, for frequency selective time-variant channels no analytical performance results are available in the literature. In this contribution, this lack of analytical results shall be eliminated. Therefore, the performance of TxZF is systematically studied by means of instruments borrowed from random matrix theory [20, 21].

For a given noise situation at the receivers unbiased transmission by TxZF always yields the same performance [22] – both in terms of bit error probability and signal-to-noise-ratio (SNR). However, depending on the random channel conditions, e.g. the channel attenuation, and further conditions to be discussed in the following, different transmitted energies are required. Therefore, these energies are appropriate quantities for the evaluation of TxZF and will be analyzed in this paper. However, the price to be paid for interference avoidance itself in multi-user MIMO scenarios considered here is not totally quantified by transmitted energies – the transmitted energies are also significantly influenced by the channel attenuations for instance. Therefore, in this contribution also an alternative performance measure termed transmit efficiency [23] is derived and is studied by analytical methods for time-variant mobile radio channels.

The paper is organized as follows: In Section II a generic model of linear multi-user MIMO transmission systems is developed. Section III deals with a short survey of the transmit signal design strategies Transmit Matched Filter (TxMF) and TxZF in order to conveniently familiarize the reader with the basics of these transmit signal design strategies to a degree sufficient to follow the reasoning of the paper. The crux of this paper is concentrated in Sections IV and V. These sections present the performance analysis of TxZF based on transmitted energies and based on transmit efficiencies, respectively. The analytical results obtained in Sections IV and V are verified by some exemplary simulation results in Section VI. Section VII concludes the paper.

The investigations are performed in the time discrete equivalent low pass domain under utilization of a vector-matrix representation [24]. Consequently, signals and system components are represented by complex vectors or matrices, respectively, which are printed in bold face. In the analysis, $[\cdot]_{n,m}$ designates the element in the n-th row and m-th column of the matrix in brackets, $[\cdot]_n$ stands for the n-th row of the matrix or the n-th element of the vector in brackets, and $\|\cdot\|_2$ denotes the Euclidean norm.

II. Multi-user MIMO transmission model

A. Data Transmission

We consider a downlink situation, where an access point (AP) supports K mobile terminals (MTs) $k, k = 1\ldots K$. The AP is equipped with K_{B} transmit antennas, and each of the K MTs employs K_{M} receive antennas. Therefore, each link between the AP and one of the K MTs constitutes a MIMO structure, and the total system is a multi-user MIMO structure. N data symbols $\underline{d}_n^{(k)}, n = 1\ldots N$, have to be transmitted from the AP to each MT $k, k = 1\ldots K$. The N data symbols $\underline{d}_n^{(k)}, n = 1\ldots N$, intended for MT k are arranged in the MT

The material in this paper was presented in part at the 4th symposium of the ITG expert group "Angewandte Informationstheorie (applied information theory)", Kiel, Oct. 2004. Dr. M. Meurer is with the Research Group for RF Communications, University of Kaiserslautern, P.O. Box 3049, D–67653 Kaiserslautern, Germany. Contact via email: meurer@rhrk.uni-kl.de

specific data vector

$$\underline{\mathbf{d}}^{(k)} = \left(\underline{d}_1^{(k)} \ldots \underline{d}_N^{(k)}\right)^{\mathrm{T}} \tag{1}$$

of dimension N. The K MT specific data vectors $\underline{\mathbf{d}}^{(k)}, k = 1 \ldots K$, of (1) are further stacked to the total data vector

$$\underline{\mathbf{d}} = \left(\underline{\mathbf{d}}^{(1)\mathrm{T}} \ldots \underline{\mathbf{d}}^{(K)\mathrm{T}}\right)^{\mathrm{T}} = \left(\underline{d}_1 \ldots \underline{d}_{N_\mathrm{t}}\right)^{\mathrm{T}} \tag{2}$$

of dimension

$$N_\mathrm{t} = KN. \tag{3}$$

$\underline{\mathbf{d}}$ of (2) is assumed to be wide sense stationary with zero mean and the covariance matrix

$$\underline{\mathbf{R}}_\mathrm{d} = \mathop{\mathrm{E}}_{\underline{\mathrm{d}}}\left\{\underline{\mathbf{d}}\,\underline{\mathbf{d}}^{\mathrm{H}}\right\} = E_\mathrm{d} \cdot \mathbf{I}^{(N_\mathrm{t})}. \tag{4}$$

By linear modulation based on $\underline{\mathbf{d}}$ of (2) for each of the K_B transmit antennas an antenna specific transmitted signal

$$\underline{\mathbf{t}}^{(k_\mathrm{B})} = \left(\underline{t}_1^{(k_\mathrm{B})} \ldots \underline{t}_{Q_\mathrm{t}}^{(k_\mathrm{B})}\right)^{\mathrm{T}} \in \mathbb{C}^{Q_\mathrm{t}},\ k_\mathrm{B} = 1 \ldots K_\mathrm{B}, \tag{5}$$

is generated. The K_B transmitted signals $\underline{\mathbf{t}}^{(k_\mathrm{B})}, k_\mathrm{B} = 1 \ldots K_\mathrm{B}$, of (5) are stacked in the signal

$$\underline{\mathbf{t}} = \left(\underline{\mathbf{t}}^{(1)\mathrm{T}} \ldots \underline{\mathbf{t}}^{(K_\mathrm{B})\mathrm{T}}\right)^{\mathrm{T}} \in \mathbb{C}^{(K_\mathrm{B}Q_\mathrm{t})} \tag{6}$$

termed (total) transmitted signal. The synthesis of $\underline{\mathbf{t}}$ of (6) based on $\underline{\mathbf{d}}$ of (2) is described by the $(K_\mathrm{B}Q_\mathrm{t}) \times N_\mathrm{t}$-matrix $\underline{\mathbf{M}}$ termed modulator matrix [6]. With $\underline{\mathbf{M}}$ one obtains

$$\underline{\mathbf{t}} = \underline{\mathbf{M}}\,\underline{\mathbf{d}}. \tag{7}$$

The ratio

$$\kappa = \frac{N_\mathrm{t}}{K_\mathrm{B}Q_\mathrm{t}} \tag{8}$$

of the number N_t of columns and the number $K_\mathrm{B}Q_\mathrm{t}$ of rows of $\underline{\mathbf{M}}$ of (7) is termed system load. Via (7) the N_t components of $\underline{\mathbf{d}}$ of (2) are mapped onto the $K_\mathrm{B}Q_\mathrm{t}$ components of $\underline{\mathbf{t}}$ of (6). Setting out from (7) the energy invested to transmit $\underline{\mathbf{t}}$, which is termed transmitted energy in the following, becomes

$$T = \frac{1}{2}\underline{\mathbf{t}}^{\mathrm{H}}\underline{\mathbf{t}}. \tag{9}$$

The frequency selective MIMO channel between the AP and MT k is assumed to be linear and is characterized by the $KK_\mathrm{B}K_\mathrm{M}$ channel impulse responses [24]

$$\underline{\mathbf{h}}^{(k,k_\mathrm{B},k_\mathrm{M})} = \left(\underline{h}_1^{(k,k_\mathrm{B},k_\mathrm{M})} \ldots \underline{h}_W^{(k,k_\mathrm{B},k_\mathrm{M})}\right)^{\mathrm{T}} \in \mathbb{C}^{W}. \tag{10}$$

$\underline{\mathbf{h}}^{(k,k_\mathrm{B},k_\mathrm{M})}$ of (10) describes the channel between the k_B-th transmit antenna, $k_\mathrm{B} = 1 \ldots K_\mathrm{B}$, of the AP, and the k_M-th receive antenna, $k_\mathrm{M} = 1 \ldots K_\mathrm{M}$, of MT $k, k = 1 \ldots K$. With $\underline{\mathbf{h}}^{(k,k_\mathrm{B},k_\mathrm{M})}$ of (10) and Q_t, see (5), the $KK_\mathrm{B}K_\mathrm{M}$ MT transmit antenna and receive antenna specific channel matrices

$$\begin{aligned}
\underline{\mathbf{H}}^{(k,k_\mathrm{B},k_\mathrm{M})} &= \left(\underline{H}_{i,j}^{(k,k_\mathrm{B},k_\mathrm{M})}\right) \in \mathbb{C}^{(Q_\mathrm{t}+W-1)\times Q_\mathrm{t}}, \\
& i = 1 \ldots Q_\mathrm{t} + W - 1, j = 1 \ldots Q_\mathrm{t}, \\
\underline{H}_{i,j}^{(k,k_\mathrm{B},k_\mathrm{M})} &= \begin{cases} \underline{h}_{i-j+1}^{(k,k_\mathrm{B},k_\mathrm{M})}, & 1 \le i - j + 1 \le W, \\ 0, & \text{else}, \end{cases} \\
& k = 1 \ldots K, k_\mathrm{B} = 1 \ldots K_\mathrm{B}, k_\mathrm{M} = 1 \ldots K_\mathrm{M},
\end{aligned} \tag{11}$$

are established. With the $KK_\mathrm{B}K_\mathrm{M}$ matrices $\underline{\mathbf{H}}^{(k,k_\mathrm{B},k_\mathrm{M})}$ of (11) we form the KK_B MT and transmit antenna specific channel matrices

$$\begin{aligned}
\underline{\mathbf{H}}^{(k,k_\mathrm{B})} &= \left(\underline{\mathbf{H}}^{(k,k_\mathrm{B},1)\mathrm{T}} \ldots \underline{\mathbf{H}}^{(k,k_\mathrm{B},K_\mathrm{M})\mathrm{T}}\right)^{\mathrm{T}} \in \mathbb{C}^{[K_\mathrm{M}(Q_\mathrm{t}+W-1)]\times Q_\mathrm{t}}, \\
& k = 1 \ldots K, k_\mathrm{B} = 1 \ldots K_\mathrm{B},
\end{aligned} \tag{12}$$

the K MT specific channel matrices

$$\underline{\mathbf{H}}^{(k)} = \left(\underline{\mathbf{H}}^{(k,1)} \ldots \underline{\mathbf{H}}^{(k,K_\mathrm{B})}\right) \in \mathbb{C}^{[K_\mathrm{M}(Q_\mathrm{t}+W-1)]\times(K_\mathrm{B}Q_\mathrm{t})} \tag{13}$$

and the total channel matrix

$$\underline{\mathbf{H}} = \left(\underline{\mathbf{H}}^{(1)\mathrm{T}} \ldots \underline{\mathbf{H}}^{(K)\mathrm{T}}\right)^{\mathrm{T}} \in \mathbb{C}^{[KK_\mathrm{M}(Q_\mathrm{t}+W-1)]\times(K_\mathrm{B}Q_\mathrm{t})}. \tag{14}$$

With $\underline{\mathbf{H}}^{(k)}$ of (13) the transmitted signal $\underline{\mathbf{t}}$ of (6) yields in the noisefree case the received signal

$$\underline{\mathbf{e}}^{(k)} = \left(\underline{e}_1^{(k)} \ldots \underline{e}_{K_\mathrm{M}(Q_\mathrm{t}+W-1)}^{(K)}\right)^{\mathrm{T}} = \underline{\mathbf{H}}^{(k)}\underline{\mathbf{t}} \in \mathbb{C}^{[K_\mathrm{M}(Q_\mathrm{t}+W-1)]} \tag{15}$$

of MT $k, k = 1 \ldots K$. With $\underline{\mathbf{H}}$ of (14) the signals $\underline{\mathbf{e}}^{(k)}, k = 1 \ldots K$, are stacked in the total signal

$$\underline{\mathbf{e}} = \left(\underline{\mathbf{e}}^{(1)\mathrm{T}} \ldots \underline{\mathbf{e}}^{(K)\mathrm{T}}\right)^{\mathrm{T}} = \underline{\mathbf{H}}\,\underline{\mathbf{t}} \in \mathbb{C}^{[KK_\mathrm{M}(Q_\mathrm{t}+W-1)]} \tag{16}$$

received in the noisefree case. If $\underline{\mathbf{e}}^{(k)}$ of (15) is corrupted by an additive noise signal

$$\underline{\mathbf{n}}^{(k)} = \left(\underline{n}_1^{(k)} \ldots \underline{n}_{K_\mathrm{M}(Q_\mathrm{t}+W-1)}^{(K)}\right)^{\mathrm{T}} \in \mathbb{C}^{[K_\mathrm{M}(Q_\mathrm{t}+W-1)]}, \tag{17}$$

then we obtain the noisy received signal

$$\underline{\mathbf{r}}^{(k)} = \underline{\mathbf{e}}^{(k)} + \underline{\mathbf{n}}^{(k)} = \underline{\mathbf{H}}^{(k)}\underline{\mathbf{t}} + \underline{\mathbf{n}}^{(k)} \in \mathbb{C}^{[K_\mathrm{M}(Q_\mathrm{t}+W-1)]}, \tag{18}$$

of MT k and the total noisy received signal

$$\underline{\mathbf{r}} = \left(\underline{\mathbf{r}}^{(1)\mathrm{T}} \ldots \underline{\mathbf{r}}^{(K)\mathrm{T}}\right)^{\mathrm{T}} = \underline{\mathbf{e}} + \underline{\mathbf{n}} = \underline{\mathbf{H}}\,\underline{\mathbf{t}} + \underline{\mathbf{n}}, \tag{19}$$

where

$$\underline{\mathbf{n}} = \left(\underline{\mathbf{n}}^{(1)\mathrm{T}} \ldots \underline{\mathbf{n}}^{(K)\mathrm{T}}\right)^{\mathrm{T}} \tag{20}$$

denotes the total noise signal.

B. Data Detection

The demodulator of each MT $k, k = 1 \ldots K$, determines based on $\underline{\mathbf{r}}^{(k)}$ of (18) a linear estimate $\hat{\underline{\mathbf{d}}}^{(k)}$ of $\underline{\mathbf{d}}^{(k)}$ of (1). Stacking the estimates $\hat{\underline{\mathbf{d}}}^{(k)}, k = 1 \ldots K$, results in a total data estimate

$$\hat{\underline{\mathbf{d}}} = \left(\hat{\underline{\mathbf{d}}}^{(1)\mathrm{T}} \ldots \hat{\underline{\mathbf{d}}}^{(K)\mathrm{T}}\right)^{\mathrm{T}} = \left(\hat{\underline{d}}_1 \ldots \hat{\underline{d}}_{N_\mathrm{t}}\right)^{\mathrm{T}}, \tag{21}$$

of the total data vector $\underline{\mathbf{d}}$ of (2). In analogy to the procedure of (7) the generation of $\hat{\underline{\mathbf{d}}}^{(k)}$ based on $\underline{\mathbf{r}}^{(k)}$ can be described by an MT specific $N \times [K_\mathrm{M}(Q_\mathrm{t} + W - 1)]$ matrix termed demodulator matrix by

$$\hat{\underline{\mathbf{d}}}^{(k)} = \underline{\mathbf{D}}^{(k)}\underline{\mathbf{r}}^{(k)}. \tag{22}$$

With $\hat{\underline{\mathbf{d}}}^{(k)}, k = 1 \ldots K$, of (22), one obtains the total data estimate

$$\hat{\underline{\mathbf{d}}} = \left(\hat{\underline{\mathbf{d}}}^{(1)\mathrm{T}} \ldots \hat{\underline{\mathbf{d}}}^{(K)\mathrm{T}}\right)^{\mathrm{T}} = \left(\hat{\underline{d}}_1 \ldots \hat{\underline{d}}_{N_\mathrm{t}}\right)^{\mathrm{T}}. \tag{23}$$

With the total demodulator matrix

$$\underline{\mathbf{D}}=\text{blockdiag}\left(\underline{\mathbf{D}}^{(1)}\ldots\underline{\mathbf{D}}^{(K)}\right)\in\mathbb{C}^{(KN)\times[KK_{\mathrm{M}}(Q_{\mathrm{t}}+W-1)]} \quad (24)$$

(22) and (23) can be written in the comprehensive form

$$\hat{\underline{\mathbf{d}}}=\underline{\mathbf{D}}\,\underline{\mathbf{r}}. \quad (25)$$

Finally with (7), (19) and (25) one obtains

$$\hat{\underline{\mathbf{d}}}=\underbrace{\underline{\mathbf{D}}\,\underline{\mathbf{H}}}_{\underline{\mathbf{B}}}\,\underline{\mathbf{M}}\,\underline{\mathbf{d}}+\underline{\mathbf{D}}\,\underline{\mathbf{n}} \quad (26)$$

for the relation between $\hat{\underline{\mathbf{d}}}$ of (23) and $\underline{\mathbf{d}}$ of (2). In (26) the matrix $\underline{\mathbf{B}}$ of dimension $N_{\mathrm{t}}\times(K_{\mathrm{B}}Q_{\mathrm{t}})$ is termed system matrix and is composed of the data symbol specific combined signatures $\underline{\mathbf{b}}_n, n=1\ldots N_{\mathrm{t}}$, as follows:

$$\underline{\mathbf{B}}=\left(\underline{\mathbf{b}}_1^{\mathrm{T}}\ldots\underline{\mathbf{b}}_{N_{\mathrm{t}}}^{\mathrm{T}}\right)^{\mathrm{T}}. \quad (27)$$

According to (4) and (7) the mean transmitted energy invested for the data symbol $\underline{d}_n$ becomes

$$T_n=\frac{1}{2}\left\|\left[\underline{\mathbf{M}}^{\mathrm{T}}\right]_n\right\|_2^2\cdot E_{\mathrm{d}}=\frac{1}{2}\left[\underline{\mathbf{M}}^{\mathrm{H}}\underline{\mathbf{M}}\right]_{n,n}\cdot E_{\mathrm{d}}. \quad (28)$$

III. Short review of Transmit Matched Filter (TxMF) and Transmit Zero forcing (TxZF)

A. Transmit Matched Filter (TxMF)

The idea behind the Transmit Matched Filter (TxMF) is the minimization of T_n of (28) for each data symbol $\underline{d}_n$, $n=1\ldots N_{\mathrm{t}}$, under the side condition that interference is neglected and unbiased data transmission is desired. This leads to the modulator matrix [25–28]

$$\underline{\mathbf{M}}_{\mathrm{TxMF}}=\underline{\mathbf{B}}^{\mathrm{H}}\left[\text{diag}\left(\underline{\mathbf{B}}\,\underline{\mathbf{B}}^{\mathrm{H}}\right)\right]^{-1}. \quad (29)$$

Due to the design criterion of TxMF explained above, the choice of (29) for the modulator matrix is optimum, with respect to the minimization of the data symbol specific transmitted energies T_n of (28), if unbiased data transmission is established. The respective minimum data symbol specific transmitted energies read

$$T_{\mathrm{MF},n}=\frac{1}{2}\left(\left[\underline{\mathbf{B}}\,\underline{\mathbf{B}}^{\mathrm{H}}\right]_{n,n}\right)^{-1}E_{\mathrm{d}}. \quad (30)$$

However, if multiple data symbols are transmitted in parallel, quite strong interferences might occur.

B. Transmit Zero forcing (TxZF)

TxZF totally eliminates interferences. Therefore, the interference contributions to $\widehat{\underline{d}}_n$, $n=1\ldots N_{\mathrm{t}}$, of (21) are nulled. While ensuring unbiased data transmission, the remaining degrees of freedom in the choice of $\underline{\mathbf{M}}_{\mathrm{TxZF}}$ are exploited for the minimization of the required transmitted energy T of (9) and simultaneously the minimization of the data symbol specific energies T_n, $n=1\ldots N_{\mathrm{t}}$, of (28). Following this idea one obtains

$$\underline{\mathbf{M}}_{\mathrm{TxZF}}=\underline{\mathbf{B}}^{\mathrm{H}}\left(\underline{\mathbf{B}}\,\underline{\mathbf{B}}^{\mathrm{H}}\right)^{-1} \quad (31)$$

for the modulator matrix $\underline{\mathbf{M}}$ of (7) [6, 27, 28]. The price to be paid for the elimination of interferences is an increase of the data symbol specific energies

$$T_{\mathrm{ZF},n}=\frac{1}{2}\left[\left(\underline{\mathbf{B}}\,\underline{\mathbf{B}}^{\mathrm{H}}\right)^{-1}\right]_{n,n}E_{\mathrm{d}} \quad (32)$$

of (28) as compared to the TxMF, i.e.,

$$T_{\mathrm{ZF},n}\geq T_{\mathrm{MF},n} \quad (33)$$

holds for all $n=1\ldots N_{\mathrm{t}}$. Although this increase is somehow intuitively clear, to the author's knowledge the formal proof of this proposition (33) is not available in literature up to now. Therefore, as an additional novel achievement of this paper, the proof is included in Appendix I. The detailed further analysis of this increase is the topic of Section V.

IV. Analysis of the symbol specific transmitted energies for TxZF

Obviously, $T_{\mathrm{ZF},n}$ of (32) depends on the number of additional constrains, which have to be satisfied to avoid interferences while designing the transmitted signal $\underline{\mathbf{t}}$ of (5) and on the total number of degrees of freedom for this design process. Unfortunately, a full analytical analysis of these dependencies for Rx oriented transmission is not yet available in literature. Therefore, in the following the symbol specific transmitted energies $T_{\mathrm{ZF},n}$ of (32), $n=1\ldots N_{\mathrm{t}}$, will be analyzed. The instruments to derive the mentioned results are based on random matrix theory [20] and are related to the procedure in [21].

If the mobile radio channels are time-variant random block-fading channels and/or the demodulator $\underline{\mathbf{D}}$ changes, $\underline{\mathbf{B}}$ of (27) varies with time and can, therefore, be regarded as a random matrix. Consequently, $T_{\mathrm{ZF},n}$ of (32) is also a random quantity, and an analysis of $T_{\mathrm{ZF},n}$ can only be made on a statistical basis taking the statistical property of $\underline{\mathbf{B}}$ into account. As $\underline{\mathbf{B}}$ is a function of $\underline{\mathbf{D}}$ and $\underline{\mathbf{H}}$, the joint probability distribution of the elements of $\underline{\mathbf{B}}$ is in general a non-trivial function which is directly related to the considered statistics of $\underline{\mathbf{H}}$, i.e., the channel model, and the chosen model of the demodulator matrices $\underline{\mathbf{D}}^{(k)}$ of (22). However, as a simplification in the first step, in the following it will be assumed that all elements $\underline{b}_{n,s}$, $s=1\ldots K_{\mathrm{B}}Q_{\mathrm{t}}$, of $\underline{\mathbf{b}}_n$, $n=1\ldots N_{\mathrm{t}}$, are independent identically distributed (i.i.d.) Gaussian variables with zero mean and variance $2\sigma_n^2$. This supposition is quite common for MIMO transmission systems [29]. Especially, the assumption of identically distributed Gaussian variables is fulfilled, if the following conditions are satisfied:

- For each MT k the elements $\underline{h}_w^{(k,k_{\mathrm{B}},k_{\mathrm{M}})}$, $k_{\mathrm{B}}=1\ldots K_{\mathrm{B}}$, $k_{\mathrm{M}}=1\ldots K_{\mathrm{M}}$, of (10) are independent Gaussian variables with zero mean and such variances, that

$$\sum_{k_{\mathrm{M}}=1}^{K_{\mathrm{M}}}\mathrm{E}\left\{\left\|\underline{\mathbf{h}}^{(k,k_{\mathrm{B}},k_{\mathrm{M}})}\right\|_2^2\right\}=\text{const.}\ \forall k_{\mathrm{B}}=1\ldots K_{\mathrm{B}}. \quad (34)$$

  (34) is especially fulfilled if all elements $\underline{h}_w^{(k,k_{\mathrm{B}},k_{\mathrm{M}})}$, $k_{\mathrm{B}}=1\ldots K_{\mathrm{B}}$, $k_{\mathrm{M}}=1\ldots K_{\mathrm{M}}$, of (10) have the same variance $2{\sigma_{\mathrm{h}}^{(k)}}^2$, i.e., if the power delay profile is flat.

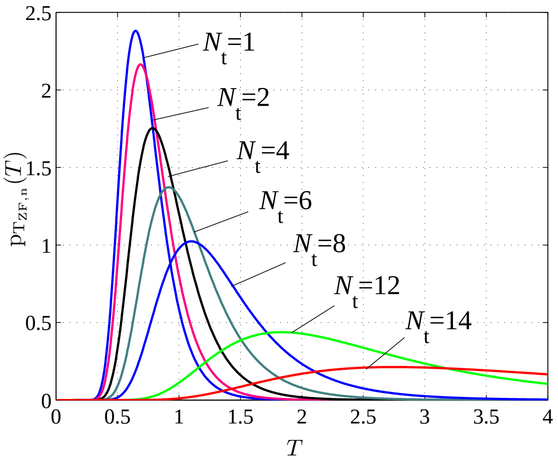

Fig. 1. pdf $p_{T_{ZF,n}}(T)$ of (37) for $K_B = 2$, $Q_t = 8$, $E_d = 2$, $\sigma_n^2 = 1/22$ and $N_t = 1 \dots 14$

- The elements of each row n, $n = 1 \dots N$, of the MT specific demodulator matrices $\underline{\mathbf{D}}^{(k)}$ are random independent identically uniformly distributed binary quantities of zero mean and variance $2\sigma_{d,n}^2$, i.e., the entirety of all elements of each row n, $n = 1 \dots N$, form a data symbol specific random binary code [6].

If the above described conditions are fulfilled, then

$$\sigma_n^2 = \sigma_{d,n}^2 \sum_{k_M=1}^{K_M} \mathrm{E}\left\{ \left\| \underline{\mathbf{h}}^{(k,k_B,k_M)} \right\|_2^2 \right\} \tag{35}$$

holds; for the special case of a flat power delay profile one obtains

$$\sigma_n^2 = 2\sigma_{d,n}^2 \sigma_h^2 K_M W. \tag{36}$$

Furthermore, any two elements $\underline{b}_{n+(k-1)N,s}$ and $\underline{b}_{n'+(k'-1)N,s'}$, $n, n' = 1 \dots N$, $k, k' = 1 \dots K$, $s, s' = 1 \dots K_B Q_t$, $n \neq n' \vee k \neq k' \vee s \neq s'$, can be shown to be pairwise uncorrelated. However, pairwise statistical independence is in general only given if k is not equal to k'. Nevertheless, as an approximation it will be assumed in the following that statistical independence holds for all elements of $\underline{\mathbf{B}}$. It will become clear in Section VI that this simplification is well justified by simulation results.

With the assumptions made above for the distribution of the elements of $\underline{\mathbf{B}}$, the probability density function (pdf)

$$p_{T_{ZF,n}}(T) = \begin{cases} \frac{4\sigma_n^2 \, \mathrm{e}^{-\frac{E_d}{4\sigma_n^2 T}}}{E_d (K_B Q_t - N_t)!} \left(\frac{E_d}{4\sigma_n^2 T}\right)^{K_B Q_t - N_t + 2}, & T \geq 0, \\ 0, & \text{otherwise}, \end{cases} \tag{37}$$

of $T_{ZF,n}$ of (32) can be derived as shown in Appendix II. Note that the pdf of (37) – which to the author's knowledge is not available in literature up to now – is not only a tool to evaluate the performance of the considered Rx oriented transmission transmission; it can also be used to determine the performance variability of TxZF based transmission and to study the fundamental impacts of system parameters on that.

Studies on the performance variability were previously only available through simulations [12, 7, 18, 19]. Fig. 1 shows the pdf $p_{T_{ZF,n}}(T)$ of (37) for K_B equal to two, Q_t equal to eight, E_d equal to two, σ_n^2 equal to $1/22$ and different N_t. With (37) the mean

$$\overline{T}_{ZF} = \frac{E_d}{4\sigma_n^2} \frac{1}{K_B Q_t - N_t} \tag{38}$$

and the variance

$$\mathrm{var}\left(T_{ZF}\right) = \left(\frac{E_d}{4\sigma_n^2}\right)^2 \frac{1}{(K_B Q_t - N_t)^2 (K_B Q_t - N_t + 1)} \tag{39}$$

of $T_{ZF,n}$ of (32) can be calculated. (38) confirms the statement made right at the beginning of this section: If the number $K_B Q_t$ of degrees of freedom for transmit signal design is large compared to the number N_t of constrains, then $\overline{T}_{ZF}$ is low. If N_t comes closer to $K_B Q_t$, $\overline{T}_{ZF}$ diverges to infinity. The result for the mean $\overline{T}_{ZF}$ of (38) has already been derived for the asymptotic case of infinitely large systems in [1–3] but is now proven to be a special case of the more general analysis presented in this paper, which incorporates frequency selective channels and more realistic finite dimensional systems.

V. Analysis of the Tx efficiency for TxZF

The data symbol specific transmitted energy $T_{ZF,n}$ massively depends on $\|\underline{\mathbf{b}}_n\|_2^2$, i.e., besides other influences on the channel attenuation which changes with time. Therefore, $T_{ZF,n}$ is not an adequate measure to quantify the price which has to be paid in TxZF solely due to interference avoidance. This price can be quantified by normalizing $T_{ZF,n}$ in an appropriate way, e.g., by normalizing it by $T_{MF,n}$. This leads to the transmit efficiency [23]

$$\eta_{TxZF,n} = \frac{T_{MF,n}}{T_{ZF,n}} = \frac{1}{\left[\left(\underline{\mathbf{B}}\,\underline{\mathbf{B}}^H\right)^{-1}\right]_{n,n} \cdot \left[\underline{\mathbf{B}}\,\underline{\mathbf{B}}^H\right]_{n,n}}, \tag{40}$$

which is the ratio of the symbol specific transmitted energies $T_{MF,n}$ of (30) and $T_{ZF,n}$ of (32), $n = 1 \dots N_t$, for TxMF and TxZF, respectively. Quite generally, as the Tx efficiency describes the degrading impact of interference suppression, it can be interpreted as a measure dual to the asymptotic multiuser efficiency [30], a measure which is quite common in the field of transmitter oriented transmission and multi-user detection, and which was originally introduced by Verdu [31]. Likewise, the transmit efficiency $\eta_{TxZF,n}$ takes values from 0 to 1, with 1 being the optimum. The quantity $\eta_{TxZF,n}$ of (40) depends on the number of additional constraints, which have to be satisfied to avoid interferences while designing the transmitted signal $\underline{\mathbf{t}}$ of (5), and on the total number of degrees of freedom for this design process. Unfortunately, a closed form analysis of these dependencies is not yet available in literature for Rx oriented transmission if $\underline{\mathbf{B}}$ is a random matrix, see Section IV. In this paper this open point will be addressed by analyzing the transmit efficiencies $\eta_{TxZF,n}$, $n = 1 \dots N_t$. The instruments to derive the mentioned results are related to those described in Section IV.

With the diagonal scaling matrix $\sqrt{\mathbf{P}}$ of dimension $N_t \times N_t$ and the matrix $\underline{\widetilde{\mathbf{B}}}$ with normalized rows $\underline{\widetilde{\mathbf{b}}}_n$ the system matrix

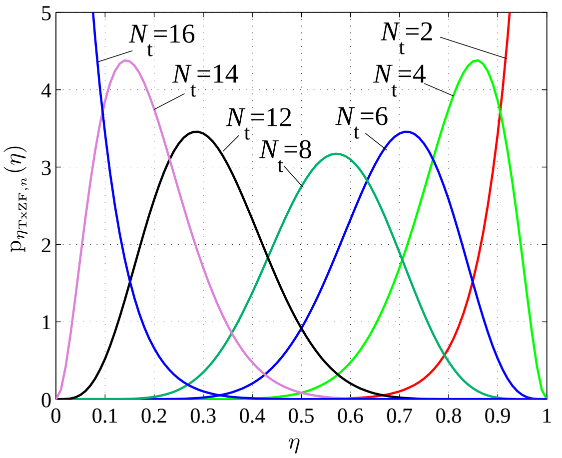

Fig. 2. pdf $p_{\eta_{\mathrm{TxZF},n}}(\eta)$ of (45) for $K_{\mathrm{B}}=2$, $Q_{\mathrm{t}}=8$, $N_{\mathrm{t}}=2\ldots16$

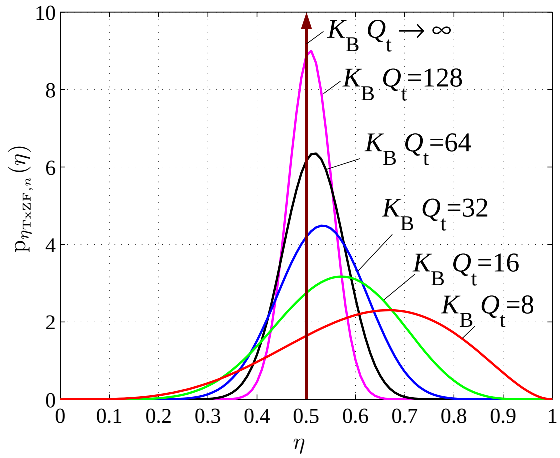

Fig. 3. pdf $p_{\eta_{\mathrm{TxZF},n}}(\eta)$ of (45) for $\kappa=0.5$, $K_{\mathrm{B}}Q_{\mathrm{t}}=8\ldots128$ and $K_{\mathrm{B}}Q_{\mathrm{t}}\rightarrow\infty$

$\underline{\mathbf{B}}$ of (27) can be decomposed as

$$\underline{\mathbf{B}} = \underbrace{\mathrm{diag}\left(\sqrt{P_1}\ldots\sqrt{P_{N_{\mathrm{t}}}}\right)}_{\sqrt{\mathbf{P}}}\cdot\underbrace{\left(\underline{\tilde{\mathbf{b}}}_1^{\mathrm{T}}\ldots\underline{\tilde{\mathbf{b}}}_{N_{\mathrm{t}}}^{\mathrm{T}}\right)^{\mathrm{T}}}_{\underline{\tilde{\mathbf{B}}}}. \tag{41}$$

Each row $\underline{\tilde{\mathbf{b}}}_n$, $n=1\ldots N_{\mathrm{t}}$, of $\underline{\tilde{\mathbf{B}}}$, can be thought of being the result of normalizing a row vector

$$\underline{\tilde{\mathbf{g}}}_n = \left(\underline{\tilde{g}}_{n,1}\cdots\underline{\tilde{g}}_{n,K_{\mathrm{B}}Q_{\mathrm{t}}}\right) \tag{42}$$

to norm one, i.e.,

$$\underline{\tilde{\mathbf{b}}}_n = \underline{\tilde{\mathbf{g}}}_n/\|\underline{\tilde{\mathbf{g}}}_n\|_2 \tag{43}$$

holds. Again the assumptions mentioned in Section IV for the statistical properties of the matrix $\underline{\mathbf{B}}$ should hold. Then also all elements $\underline{\tilde{g}}_{n,s}$, $s=1\ldots K_{\mathrm{B}}Q_{\mathrm{t}}$, of $\underline{\tilde{\mathbf{g}}}_n$, $n=1\ldots N_{\mathrm{t}}$, are independent identically distributed (i.i.d.) Gaussian variables with zero mean and unit standard deviation. With the above made assumptions for $\underline{\tilde{\mathbf{g}}}_n$, $n=1\ldots N_{\mathrm{t}}$, $\underline{\tilde{\mathbf{b}}}_n$ of (41) is spherically uniformly distributed [29]. Substituting (41) in (40) yields

$$\eta_{\mathrm{TxZF},n} = 1\Big/\left[\left(\underline{\tilde{\mathbf{B}}}\,\underline{\tilde{\mathbf{B}}}^{\mathrm{H}}\right)^{-1}\right]_{n,n}. \tag{44}$$

Obviously, $\eta_{\mathrm{TxZF},n}$ of (44) is independent of $\sqrt{\mathbf{P}}$ of (41) and, consequently, also independent of its probability distribution. Therefore, $\sqrt{\mathbf{P}}$ does not have to be considered in what follows. Using (44) and the assumptions made above for the distribution of the elements of $\underline{\mathbf{B}}$, the probability density function (pdf)

$$p_{\eta_{\mathrm{TxZF},n}}(\eta) = \begin{cases} \frac{\eta^{K_{\mathrm{B}}Q_{\mathrm{t}}-N_{\mathrm{t}}}(1-\eta)^{N_{\mathrm{t}}-2}}{B(K_{\mathrm{B}}Q_{\mathrm{t}}-N_{\mathrm{t}}+1,N_{\mathrm{t}}-1)}, & 0\leq\eta\leq1,\\ 0, & \text{else,}\end{cases} \tag{45}$$

of $\eta_{\mathrm{TxZF},n}$ can be derived as shown in Appendix III. The function

$$B(z,w) = \int_0^1 t^{z-1}(1-t)^{w-1}\mathrm{d}t = \frac{\Gamma(z)\cdot\Gamma(w)}{\Gamma(z+w)} \tag{46}$$

in (45) denotes the beta-function [32]. Therefore, $\eta_{\mathrm{TxZF},n}$ of (44) is termed to be beta distributed [32]. Fig. 2 shows the pdf $p_{\eta_{\mathrm{TxZF},n}}(\eta)$ of (45) for K_{B} equal to two, Q_{t} equal to eight and different N_{t}. Obviously, with increasing N_{t}, the maximum of the pdf $p_{\eta_{\mathrm{TxZF},n}}(\eta)$ of (45) tends to be shifted to lower η.

Based on (45) the m-th moment of $\eta_{\mathrm{TxZF},n}$ of (40) can be expressed as

$$\mathrm{E}\{\eta_{\mathrm{TxZF},n}^m\} = \frac{\Gamma(K_{\mathrm{B}}Q_{\mathrm{t}}-N_{\mathrm{t}}+m+1)}{\Gamma(K_{\mathrm{B}}Q_{\mathrm{t}}-N_{\mathrm{t}}+1)}\,\frac{\Gamma(K_{\mathrm{B}}Q_{\mathrm{t}})}{\Gamma(K_{\mathrm{B}}Q_{\mathrm{t}}+m)}. \tag{47}$$

Using (47), the mean

$$\overline{\eta}_{\mathrm{TxZF}} = \mathrm{E}\{\eta_{\mathrm{TxZF},n}\} = \frac{K_{\mathrm{B}}Q_{\mathrm{t}}-(N_{\mathrm{t}}-1)}{K_{\mathrm{B}}Q_{\mathrm{t}}} \tag{48}$$

and the variance

$$\begin{aligned}\mathrm{var}\left(\eta_{\mathrm{TxZF},n}\right) &= \mathrm{E}\{\eta_{\mathrm{TxZF},n}^2\} - \overline{\eta}_{\mathrm{TxZF}}^2\\ &= \frac{\left[K_{\mathrm{B}}Q_{\mathrm{t}}-(N_{\mathrm{t}}-1)\right](N_{\mathrm{t}}-1)}{(K_{\mathrm{B}}Q_{\mathrm{t}})^2\,(K_{\mathrm{B}}Q_{\mathrm{t}}+1)}.\end{aligned} \tag{49}$$

of $\eta_{\mathrm{TxZF},n}$ follow. Obviously, as already presumed before, $\overline{\eta}_{\mathrm{TxZF}}$ depends on the difference of two quantities, namely

- the number $K_{\mathrm{B}}Q_{\mathrm{t}}$ of degrees of freedom for transmit signal design, i.e. the number $K_{\mathrm{B}}Q_{\mathrm{t}}$ of elements of the total transmitted signal $\underline{\mathbf{t}}$ of (5), and
- the number $(N_{\mathrm{t}}-1)$ of restrictions due to interference avoidance while designing the contribution of each data symbol $\underline{d}_n$, $n=1\ldots N_{\mathrm{t}}$, to $\underline{\mathbf{t}}$.

If the number $K_{\mathrm{B}}Q_{\mathrm{t}}$ of degrees of freedom is large compared to $(N_{\mathrm{t}}-1)$, $\overline{\eta}_{\mathrm{TxZF}}$ tends to be close to one, otherwise it is between zero and one. For a fixed system load κ of (8), (48) and (49) can be rewritten as

$$\overline{\eta}_{\mathrm{TxZF}} = 1-\left(\kappa-1/(K_{\mathrm{B}}Q_{\mathrm{t}})\right), \tag{50a}$$

$$\mathrm{var}\left(\eta_{\mathrm{TxZF},n}\right) = \frac{\left(1-\kappa+\frac{1}{K_{\mathrm{B}}Q_{\mathrm{t}}}\right)\left(\kappa-\frac{1}{K_{\mathrm{B}}Q_{\mathrm{t}}}\right)}{1+K_{\mathrm{B}}Q_{\mathrm{t}}}. \tag{50b}$$

(50) discloses, if the system load κ is kept constant and $K_\mathrm{B}Q_\mathrm{t}$ is quite large, then $\eta_{\mathrm{TxZF},n}$ tends to the asymptotic transmit efficiency $\eta^\infty_\mathrm{TxZF}$ with its mean

$$\overline{\eta}^\infty_\mathrm{TxZF} = \lim_{K_\mathrm{B}Q_\mathrm{t}\to\infty} \overline{\eta}_\mathrm{TxZF} = 1-\kappa \qquad (51)$$

and its variance

$$\mathrm{var}\left(\eta^\infty_\mathrm{TxZF}\right) = \lim_{K_\mathrm{B}Q_\mathrm{t}\to\infty} \mathrm{var}\left(\eta_{\mathrm{TxZF},n}\right) = 0, \qquad (52)$$

respectively. Therefore, for large systems with given system load κ the mean of the asymptotic transmit efficiency $\overline{\eta}^\infty_\mathrm{TxZF}$ is only a function of the system load κ, while the variance $\mathrm{var}\left(\eta^\infty_\mathrm{TxZF}\right)$ of $\eta_{\mathrm{TxZF},n}$ asymptotically goes to zero, resulting in the pdf

$$\mathrm{p}_{\eta^\infty_\mathrm{TxZF}}(\eta) = \delta\big(\eta-(1-\kappa)\big) \qquad (53)$$

of the asymptotic transmit efficiency $\eta^\infty_\mathrm{TxZF}$. This asymptotic behaviour is verified by the results depicted in Fig. 3 which shows the pdf $\mathrm{p}_{\eta_{\mathrm{TxZF},n}}(\eta)$ of (45) for a fixed system load κ of 0.5 and different values $K_\mathrm{B}Q_\mathrm{t}$.

VI. Simulative verification of analytical results

In the previous Sections IV and V analytical results for both the pdf $\mathrm{p}_{T_{\mathrm{ZF},\mathrm{n}}}(T)$ of $T_{\mathrm{ZF},n}$ of (32) and for the pdf $\mathrm{p}_{\eta_{\mathrm{TxZF},n}}(\eta)$ of $\eta_{\mathrm{TxZF},n}$ of (40) have been derived. One key assumption made in the derivations was the statistical independence of the elements $\underline{b}_{n,s}$, $s=1\ldots K_\mathrm{B}Q_\mathrm{t}$, of $\underline{\mathbf{b}}_n$, $n=1\ldots N_\mathrm{t}$, of (27). As already explained in Section IV this statistical independence is in general not fulfilled in a strict mathematical sense. However, it will become clear in this section that the assumption of independence is a quite accurate approximation of reality. This perception is in full agreement with similar results often reported in the field of random matrix theory [33, 34].

To justify the mentioned approximation, in the following the theoretical results are validated by simulation results, which are based on realistic channel models. In the simulations the author restricts himself to the analysis of Rx oriented transmission systems operating over uncorrelated MIMO channels [29]. However, the results obtained, both by simulations and by the theoretical considerations of Sections IV and V, can also be regarded as an upper bound of the performance of Rx oriented MIMO transmission systems operating over correlated MIMO channels. The detailed analysis of systems of that kind is the topic of further research and is beyond the scope of this contribution.

For the simulations the following assumptions are made:

- The demodulator matrices $\underline{\mathbf{D}}^{(k)}$ of (22) are chosen according to the assumptions described in Section IV on page 4. For the variance $\sigma^2_{\mathrm{d},n}$ introduced in Section IV

$$\sigma^2_{\mathrm{d},n} = \frac{1}{2K_\mathrm{M}(Q_\mathrm{t}+W-1)}, n=1\ldots N_\mathrm{t}, \qquad (54)$$

  holds, i.e., each row of $\underline{\mathbf{D}}^{(k)}$ of (22) is normalized to one.
- The author considers an uncorrelated multi-user MIMO channel described by the channel impulse responses $\underline{\mathbf{h}}^{(k,k_\mathrm{B},k_\mathrm{M})}$, $k=1\ldots K$, $k_\mathrm{B}=1\ldots K_\mathrm{B}$, $k_\mathrm{M}=1\ldots K_\mathrm{M}$, of (10). Each element $\underline{h}_w^{(k,k_\mathrm{B},k_\mathrm{M})}$ of $\underline{\mathbf{h}}^{(k,k_\mathrm{B},k_\mathrm{M})}$ is a Gaussian distributed independent random variable with zero mean. The impulse responses $\underline{\mathbf{h}}^{(k,k_\mathrm{B},k_\mathrm{M})}$ are normalized in such a way that

$$\mathrm{E}\left\{\left\|\underline{\mathbf{h}}^{(k,k_\mathrm{B},k_\mathrm{M})}\right\|_2^2\right\} = 1 \qquad (55)$$

  holds for all $k=1\ldots K$, $k_\mathrm{B}=1\ldots K_\mathrm{B}$, $k_\mathrm{M}=1\ldots K_\mathrm{M}$. The variances of the elements $\underline{h}_w^{(k,k_\mathrm{B},k_\mathrm{M})}$ of each $\underline{\mathbf{h}}^{(k,k_\mathrm{B},k_\mathrm{M})}$ are assumed to fulfill with the constant α

$$\mathrm{E}\left\{\left|\underline{h}_w^{(k,k_\mathrm{B},k_\mathrm{M})}\right|_2^2\right\}=\alpha\mathrm{E}\left\{\left|\underline{h}_{w+1}^{(k,k_\mathrm{B},k_\mathrm{M})}\right|_2^2\right\}, w=1\ldots W-1, \qquad (56)$$

  while satisfying (55). The constant α in (56) describes the power delay profile (pdp) of the considered radio channel. For the simulations in this section the following two exemplary models are utilized:
  - $\alpha=1$ (model 1 – flat pdp) and
  - $\alpha=2$ (model 2 – exponentially decreasing pdp).

  The motivation for chosing these two models is based on the fact that, for a given dimension W of the channel impulse responses $\underline{\mathbf{h}}^{(k,k_\mathrm{B},k_\mathrm{M})}$, model 1 describes the worst case multipath situation, whereas model 2 is related to typical channel models often used in literature for quantitative performance analysis [35]. Therefore, both model 1 and model 2 are of special interest, when analyzing scenarios with dispersive multi-user MIMO channels. In the simulations W is assumed to be four.
- The temporal spreading factor Q_t is equal to eight, E_d is equal to two and N is equal to one.

With the above assumptions σ^2_n of (35) becomes $1/22$, which is also the figure which was considered for the numerical example in Section IV, c.f. Fig. 1.

Figs. 4 to 6 show both simulation results and analytical results for the pdf $\mathrm{p}_{T_{\mathrm{ZF},\mathrm{n}}}(T)$ of $T_{\mathrm{ZF},n}$ for K_B equal to two and different numbers K_M of receive antennas at the MTs. Comparing the results shown, one can make the following observations:

- Whereas the theoretical result of (37) is independent of K_M, the simulations yield different results for different K_M. However, for all K_M the simulation results and the theoretical result agree quite well. The reason for the remaining discrepancies is the already mentioned statistical independence of the elements $\underline{b}_{n,s}$ $n=1\ldots N_\mathrm{t}$, $s=1\ldots K_\mathrm{B}Q_\mathrm{t}$, of $\underline{\mathbf{B}}$. In the realistic scenarios considered in the simulations this statistical independence is only approximately fulfilled. However, this approximation gets more accurate the more Rx antennas are available at the MTs. Therefore, the mentioned discrepancy between theory and simulations vanishes with increasing K_M.
- The simulation results obtained for both channel models 1 and 2 do not differ significantly. The remaining slight differences between the obtained results trace back to the different grades of dispersion described by the models and, as a consequence of that, the different grade of the already mentioned remaining weak statistical dependencies between the elements $\underline{b}_{n,s}$ $n=1\ldots N_\mathrm{t}$, $s=1\ldots K_\mathrm{B}Q_\mathrm{t}$, of $\underline{\mathbf{B}}$. From that result it can be concluded

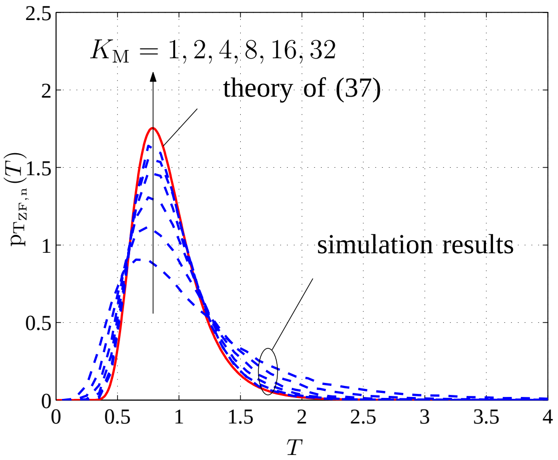

Fig. 4. comparison of simulation results (– – –) and of the theoretical result (——) of (37) for pdf $\mathrm{p}_{T_{\mathrm{ZF,n}}}(T)$ with $K_{\mathrm{B}} = 2, Q_{\mathrm{t}} = 8$, $E_{\mathrm{d}} = 2$, $K = 4$, $N = 1$, $W = 4$, model 1

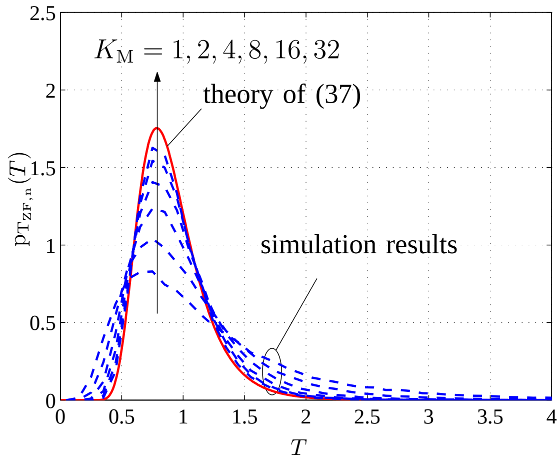

Fig. 6. comparison of simulation results (– – –) and of the theoretical result (——) of (37) for pdf $\mathrm{p}_{T_{\mathrm{ZF,n}}}(T)$ with $K_{\mathrm{B}} = 2, Q_{\mathrm{t}} = 8$, $E_{\mathrm{d}} = 2$, $K = 4$, $N = 1$, $W = 4$, model 2

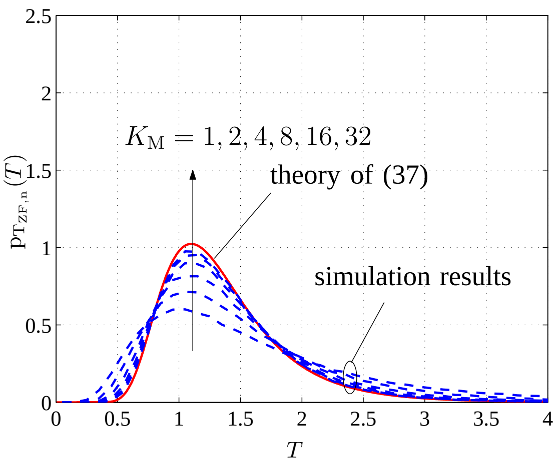

Fig. 5. comparison of simulation results (– – –) and of the theoretical result (——) of (37) for pdf $\mathrm{p}_{T_{\mathrm{ZF,n}}}(T)$ with $K_{\mathrm{B}} = 2, Q_{\mathrm{t}} = 8$, $E_{\mathrm{d}} = 2$, $K = 8$, $N = 1$, $W = 4$, model 1

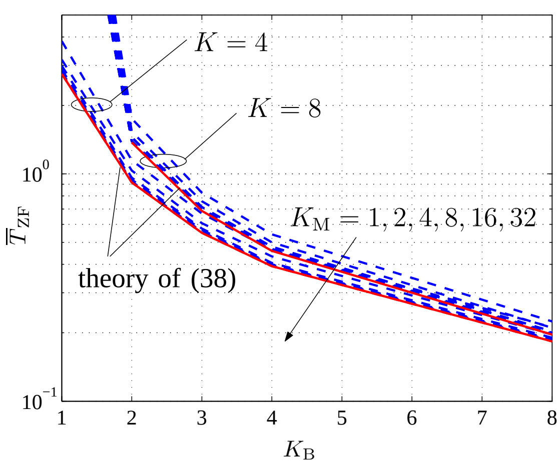

Fig. 7. comparison of simulation results (– – –) and of the theoretical result (——) of (38) for $\overline{T}_{\mathrm{ZF}}$ vs. K_{B} for $Q_{\mathrm{t}} = 8$, $E_{\mathrm{d}} = 2$, $K = 4, 8$, $N = 1$, $W = 4$, model 1

that the theoretical result of (37) is suitable to assess the performance of TxZF based transmission for a large variety of channel models. As explained, details of the considered channel model, like the pdp, do not play a significant role. Therefore, for simplicity only model 1 will be considered in the following within the simulative validation of the theoretical results.

- Comparing Figs. 4 and 5 shows that the congruence between the theoretical results and the simulation results does not depend significantly on the number K of MTs.

In Fig. 7 the average transmitted energy $\overline{T}_{\mathrm{ZF}}$ is depicted versus the number K_{B} of transmit antennas for channel model 1 and different K_{M}. K is set to four and eight, respectively. As could be expected from the results presented right before, the simulation results and the theoretical results of (38) for $\overline{T}_{\mathrm{ZF}}$ match quite well for all considered K_{M}. The remaining differences between both kinds of results converge to zero with increasing K_{M}.

In analogy to Figs. 4 to 7, Figs. 8 to 11 show both analytical results and simulation results for $\mathrm{p}_{\eta_{\mathrm{TxZF},n}}(\eta)$ of (45) and $\overline{\eta}_{\mathrm{TxZF}}$ of (48), respectively. The system parameters are chosen identical to those valid for Figs. 4 to 7. The most important observations to be made are:

- For all considered parameter combinations the theoretical results and the simulation results match almost perfectly. Even for a very low number K_{M} of receive antennas, e.g. K_{M} equal to one, the discrepancies between both results are negligibly small.
- The differences between the simulation results obtained for the channel models 1 and 2, respectively, are negligi-

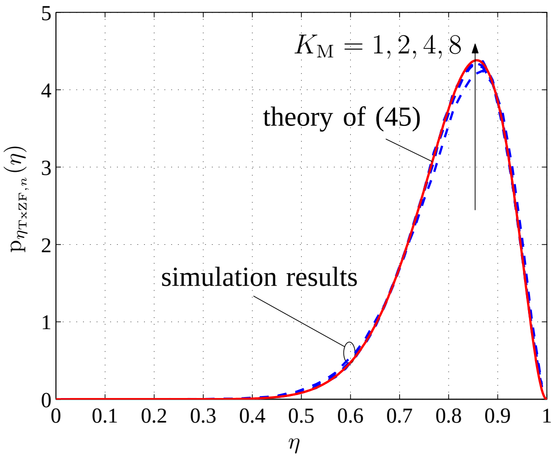

Fig. 8. comparison of simulation results (– – –) and of the theoretical result (——) of (45) for pdf $p_{\eta_{\mathrm{TxZF},n}}(\eta)$ with $K_\mathrm{B} = 2$, $Q_\mathrm{t} = 8$, $E_\mathrm{d} = 2$, $K = 4$, $N = 1$, $W = 4$, model 1

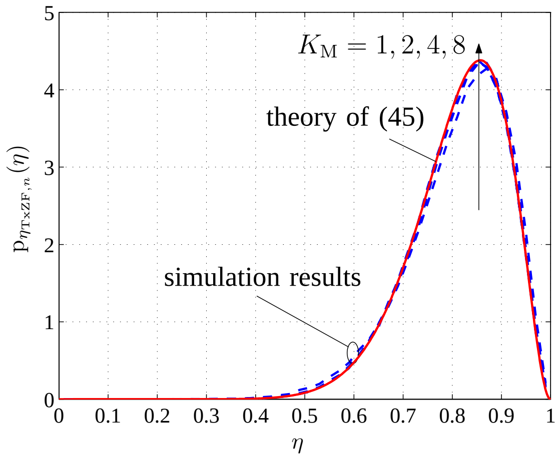

Fig. 10. comparison of simulation results (– – –) and of the theoretical result (——) of (45) for pdf $p_{T_{\mathrm{ZF},n}}(T)$ with $K_\mathrm{B} = 2$, $Q_\mathrm{t} = 8$, $E_\mathrm{d} = 2$, $K = 4$, $N = 1$, $W = 4$, model 2

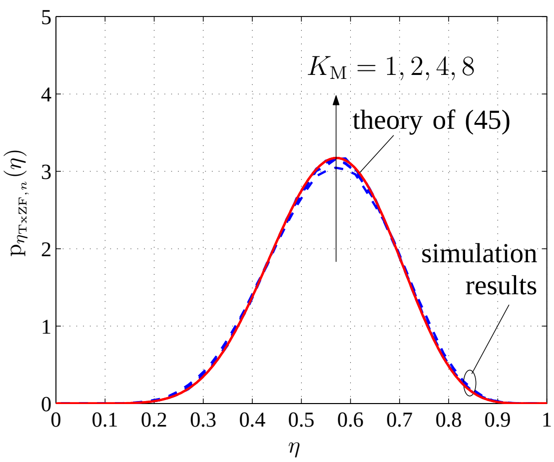

Fig. 9. comparison of simulation results (– – –) and of the theoretical result (——) of (45) for pdf $p_{T_{\mathrm{ZF},n}}(T)$ with $K_\mathrm{B} = 2$, $Q_\mathrm{t} = 8$, $E_\mathrm{d} = 2$, $K = 8$, $N = 1$, $W = 4$, model 1

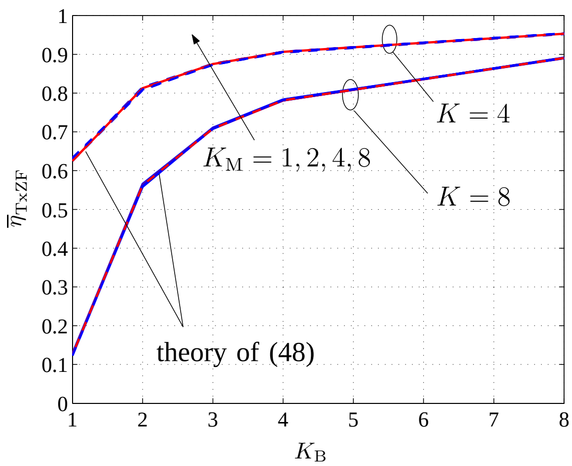

Fig. 11. comparison of simulation results (– – –) and of the theoretical result (——) of (48) for $\overline{\eta}_\mathrm{TxZF}$ vs. K_B for $Q_\mathrm{t} = 8$, $E_\mathrm{d} = 2$, $K = 4, 8$, $W = 4$, model 1

ble. The theoretical results of (45) and (48) are valid for both types of channels.

Summarizing, the results presented in this section show that the theoretical results of Sections IV and V match quite well with the obtained simulation results. Therefore, as already claimed in Section IV, the assumption of statistical independence of the elements $\underline{b}_{n,s}$ $n = 1 \ldots N_\mathrm{t}$, $s = 1 \ldots K_\mathrm{B} Q_\mathrm{t}$, of $\underline{\mathbf{B}}$ is fully justified and turns out to be tolerable.

VII. Conclusions

Up to now, for scenarios with time-variant mobile radio channels the performance analysis of receiver oriented transmission systems has primarily been conducted by computer simulations. However, as shown in this contribution, also analytical methods are applicable to quantify this performance, e.g., in terms of the quality measures transmitted energy and transmit efficiency – a measure quantifying the price for interference suppression. In contrast to performance results obtained by simulations, the analytically derived closed-form expressions for the statistical characteristics of the transmitted energies and of the transmit efficiencies allow a deeper understanding of the fundamental interdependencies between system performance and system parameters. Especially, the influences of the system load κ and the dimension $K_\mathrm{B} Q_\mathrm{t}$ of the total transmitted signal $\underline{\mathbf{t}}$ on the system performance have been clarified. The insights gained are not restricted to the analysis of TxZF but also have a significant importance for a profound understanding of recently proposed, more sophisticated non-linear transmit signal design strategies like for instance Transmit Nonlinear Zero-Forcing (TxNZF) [23] or Tomlinson-Harashima Precoding (THP) [36]. Those strategies can be interpreted as stepwise partially applying TxZF and, consequently, show a performance which is limited by the performance of those partial processing steps. Using the derived closed-form expressions for TxZF also the performance of said non-linear transmit signal design strategies can be demystified.

APPENDIX I
PROOF OF THE PROPOSITION OF (33)

In order to proof (33), we have to show that with the hermitian matrix

$$\underline{\mathbf{R}}_{\mathrm{B}} = \underline{\mathbf{B}}\,\underline{\mathbf{B}}^{\mathrm{H}} \tag{57}$$

for all $n = 1 \ldots N_{\mathrm{t}}$,

$$\left[(\underline{\mathbf{R}}_{\mathrm{B}})^{-1}\right]_{n,n} \geq \left([\underline{\mathbf{R}}_{\mathrm{B}}]_{n,n}\right)^{-1} \tag{58}$$

holds. In the following, only n equal to one is considered, the proof for $n = 2 \ldots N_{\mathrm{t}}$ is straightforward. $\underline{\mathbf{R}}_{\mathrm{B}}$ of (57) is an hermitian matrix of dimension $N_{\mathrm{t}} \times N_{\mathrm{t}}$. If N_{t} is equal to one the proof of (58) is trivial as both sides of that equation are identical. If N_{t} is larger than one – and that is basically the case we are interested in – with the column vector $\underline{\mathbf{r}}_{\mathrm{B}}$ and the hermitian matrix $\underline{\mathbf{R}}'_{\mathrm{B}}$ of dimension $(N_{\mathrm{t}}-1) \times (N_{\mathrm{t}}-1)$, $\underline{\mathbf{R}}_{\mathrm{B}}$ may be partitioned as

$$\underline{\mathbf{R}}_{\mathrm{B}} = \begin{pmatrix} [\underline{\mathbf{R}}_{\mathrm{B}}]_{1,1} & \underline{\mathbf{r}}_{\mathrm{B}}^{\mathrm{H}} \\ \underline{\mathbf{r}}_{\mathrm{B}} & \underline{\mathbf{R}}'_{\mathrm{B}} \end{pmatrix}. \tag{59}$$

The vector $\underline{\mathbf{r}}_{\mathrm{B}}$ in (59) denotes the first column of $\underline{\mathbf{R}}_{\mathrm{B}}$ without its first element $[\underline{\mathbf{R}}_{\mathrm{B}}]_{1,1}$. Then, according to the matrix inversion lemma for partitioned matrices [37], with

$$\zeta = \underline{\mathbf{r}}_{\mathrm{B}}^{\mathrm{H}} \underline{\mathbf{R}}'^{\,-1}_{\mathrm{B}} \underline{\mathbf{r}}_{\mathrm{B}} \tag{60}$$

the element $\left[\underline{\mathbf{R}}_{\mathrm{B}}^{-1}\right]_{1,1}$ of $\underline{\mathbf{R}}_{\mathrm{B}}^{-1}$ can be expressed as

$$\left[\underline{\mathbf{R}}_{\mathrm{B}}^{-1}\right]_{1,1} = \frac{1}{[\underline{\mathbf{R}}_{\mathrm{B}}]_{1,1} - \zeta}. \tag{61}$$

Since $\underline{\mathbf{B}}$ is assumed to be a non-singular matrix, $\underline{\mathbf{R}}_{\mathrm{B}}^{-1}$ is a positiv hermitian matrix. Therefore, ζ of (60) is an hermitian form which is by definition always non-negative, i.e.,

$$\zeta \geq 0. \tag{62}$$

With (61) and (62) follows

$$\left[\underline{\mathbf{R}}_{\mathrm{B}}^{-1}\right]_{1,1} = \left([\underline{\mathbf{R}}_{\mathrm{B}}]_{1,1} - \zeta\right)^{-1} \geq \left([\underline{\mathbf{R}}_{\mathrm{B}}]_{1,1}\right)^{-1} \tag{63}$$

which had to be shown. □

APPENDIX II
DERIVATION OF THE PDF $\mathrm{p}_{\mathrm{T}_{\mathrm{TxZF},n}}(T)$ OF (37)

Let us consider the scaled inverse

$$X_n = \frac{1}{2T_{\mathrm{ZF},n}} \cdot \frac{E_{\mathrm{d}}}{\sigma_n^2} = \frac{1}{\left[\left(\underline{\mathbf{B}}\,\underline{\mathbf{B}}^{\mathrm{H}}\right)^{-1}\right]_{n,n}} \frac{1}{\sigma_n^2} \tag{64}$$

of the symbol specific transmitted energy $T_{\mathrm{ZF},n}$ of (32). It can be shown that using the auxiliary real-valued positive scalar s and the matrix inversion lemma [37] that X_n of (64) can be rewritten as

$$X_n = \frac{1}{\sigma_n^2} \lim_{s\to 0}\left[\underline{\mathbf{b}}_n \Big(\underbrace{\left[\underline{\mathbf{B}}^{\mathrm{H}}\underline{\mathbf{B}} - \underline{\mathbf{b}}_n^{\mathrm{H}}\underline{\mathbf{b}}_n\right]}_{\widetilde{\underline{\mathbf{R}}}_{\mathrm{B}}}/s + \mathbf{I}^{(K_{\mathrm{B}}Q_{\mathrm{t}})}\Big)^{-1} \underline{\mathbf{b}}_n^{\mathrm{H}}\right]. \tag{65}$$

By Eigenvalue decomposition follows

$$\widetilde{\underline{\mathbf{R}}}_{\mathrm{B}} = \underline{\mathbf{U}}\boldsymbol{\lambda}\underline{\mathbf{U}}^{\mathrm{H}} \tag{66}$$

for the Hermitian matrix $\widetilde{\underline{\mathbf{R}}}_{\mathrm{B}}$ of (65), where $\underline{\mathbf{U}}$ is a unitary matrix and

$$\boldsymbol{\lambda} = \mathrm{diag}(\lambda_1 \ldots \lambda_{N_{\mathrm{t}}-1}, \underbrace{0 \,\ldots\, 0}_{(K_{\mathrm{B}}Q_{\mathrm{t}}-N_{\mathrm{t}}+1)-\mathrm{times}}) \tag{67}$$

is with probability one a diagonal matrix with $(N_{\mathrm{t}}-1)$ non-zero Eigenvalues $\lambda_n, n = 1 \ldots N_{\mathrm{t}}-1$. Substituting (67) in (65), X_n of (64) reads

$$\begin{aligned} X_n &= \frac{1}{\sigma_n^2} \lim_{s\to 0}\left[\underline{\mathbf{b}}_n \left(\underline{\mathbf{U}}\left(\boldsymbol{\lambda}/s^2 + \mathbf{I}^{(K_{\mathrm{B}}Q_{\mathrm{t}})}\right)\underline{\mathbf{U}}^{\mathrm{H}}\right)^{-1} \underline{\mathbf{b}}_n^{\mathrm{H}}\right] \\ &= \frac{1}{\sigma_n^2} \lim_{s\to 0}\left[\underbrace{\underline{\mathbf{b}}_n\underline{\mathbf{U}}}_{\underline{\mathbf{b}}'_n}\left(\boldsymbol{\lambda}/s + \mathbf{I}^{(K_{\mathrm{B}}Q_{\mathrm{t}})}\right)^{-1} \underbrace{(\underline{\mathbf{b}}_n\underline{\mathbf{U}})^{\mathrm{H}}}_{\underline{\mathbf{b}}'^{\mathrm{H}}_n}\right]. \end{aligned} \tag{68}$$

$\underline{\mathbf{b}}_n$ is Gaussian i.i.d. Therefore, this assumption also holds for the row vector

$$\underline{\mathbf{b}}'_n = \underline{\mathbf{b}}_n\underline{\mathbf{U}} = \left(\underline{b}'_{n,1} \ldots \underline{b}'_{n,K_{\mathrm{B}}Q_{\mathrm{t}}}\right)^{\mathrm{T}} \tag{69}$$

in (68) of dimension $K_{\mathrm{B}}Q_{\mathrm{t}}$, as multiplying a Gaussian i.i.d. vector by a unitary matrix $\underline{\mathbf{U}}$ does not change its probability distribution [29]. Substituting (67) in (68), X_n of (64) can be calculated to be

$$\begin{aligned} X_n &= \frac{1}{\sigma_n^2} \;\underline{\mathbf{b}}'_n \lim_{s\to 0}\left[\mathrm{diag}\left(1+\frac{\lambda_1}{s}\ldots 1+\frac{\lambda_{N_{\mathrm{t}}-1}}{s}, 1\ldots 1\right)\right]^{-1}\underline{\mathbf{b}}'^{\mathrm{H}}_n \\ &= \frac{1}{\sigma_n^2} \;\underline{\mathbf{b}}'_n \lim_{s\to 0}\left[\mathrm{diag}\left(\frac{s}{s+\lambda_1}\ldots \frac{s}{s+\lambda_{N_{\mathrm{t}}-1}}, 1\ldots 1\right)\right]\underline{\mathbf{b}}'^{\mathrm{H}}_n \\ &= \frac{1}{\sigma_n^2} \;\underline{\mathbf{b}}'_n \mathrm{diag}\Big(0\ldots 0, 1\ldots 1\Big)\underline{\mathbf{b}}'^{\mathrm{H}}_n. \end{aligned} \tag{70}$$

X_n of (70) can be simplified using (69) to

$$X_n = \sum_{s=N_{\mathrm{t}}}^{K_{\mathrm{B}}Q_{\mathrm{t}}} \left|\frac{\underline{b}'_{n,s}}{\sigma_n^2}\right|^2. \tag{71}$$

The real and imaginary parts of $\underline{b}'_{n,s}$, $s = 1 \ldots K_{\mathrm{B}}Q_{\mathrm{t}}$, are independent Gaussian distributed random variables with variances σ_n^2, which has the consequence that both real and imaginary part of $\underline{b}'_{n,s}/\sigma_n^2$ are independent Gaussian distributed random variables with zero-mean and unit variance. Therefore, X_n of (71) is centrally χ^2-distributed with

$$\nu = 2(K_{\mathrm{B}}Q_{\mathrm{t}} - N_{\mathrm{t}} + 1) \tag{72}$$

degrees of freedom. As stated in [32], X_n fulfills the pdf

$$\mathrm{p}_{\mathrm{X}_n}(X) = \begin{cases} \frac{1}{2^{\frac{\nu}{2}}\Gamma\left(\frac{\nu}{2}\right)} X^{\frac{\nu}{2}-1}\mathrm{e}^{-\frac{X}{2}}, & X \geq 0, \\ 0 & \text{otherwise.} \end{cases} \tag{73}$$

X_n is a function of the data symbol specific energy the $T_{\mathrm{ZF},n}$, c.f. (64). Therefore, based on (73) by a simple transformation of the random variable X_n and plugging in (72) the pdf $\mathrm{p}_{\mathrm{T}_{\mathrm{TxZF,n}}}(T)$ of (37) follows. □

APPENDIX III
DERIVATION OF THE PDF $\mathrm{p}_{\eta_{\mathrm{TxZF},n}}(\eta)$ OF (45)

The way to derive (45) is quite similar to the one used in Appendix II. Again, based on (44) and using the auxiliary real-valued positive scalar s it can be shown by means of the matrix inversion lemma [37] that $\eta_{\mathrm{TxZF},n}$ of (40) can be written as

$$\eta_{\mathrm{TxZF},n}=\lim_{s\to 0}\left[\underline{\widetilde{\mathbf{b}}}_n\Big(\underbrace{\left[\underline{\mathbf{B}}^{\mathrm{H}}\underline{\mathbf{B}}-\underline{\mathbf{b}}_n^{\mathrm{H}}\underline{\mathbf{b}}_n\right]}_{\underline{\widetilde{\mathbf{R}}}_{\mathrm{B}}}/s+\mathbf{I}^{(K_{\mathrm{B}}Q_{\mathrm{t}})}\Big)^{-1}\underline{\widetilde{\mathbf{b}}}_n^{\mathrm{H}}\right]. \tag{74}$$

Using the Eigenvalue decomposition of $\underline{\widetilde{\mathbf{R}}}_{\mathrm{B}}$ of (66) described in Appendix II and substituting (67) in (74), the transmit efficiency $\eta_{\mathrm{TxZF},n}$ of (40) reads

$$\begin{aligned}\eta_{\mathrm{TxZF},n}&=\lim_{s\to 0}\Big[\underline{\widetilde{\mathbf{b}}}_n\left(\underline{\mathbf{U}}\left(\boldsymbol{\lambda}/s+\mathbf{I}^{(K_{\mathrm{B}}Q_{\mathrm{t}})}\right)\underline{\mathbf{U}}^{\mathrm{H}}\right)^{-1}\underline{\widetilde{\mathbf{b}}}_n^{\mathrm{H}}\Big]\\&=\lim_{s\to 0}\Big[\underbrace{\underline{\widetilde{\mathbf{b}}}_n\underline{\mathbf{U}}}_{\underline{\widetilde{\widetilde{\mathbf{b}}}}_n}\left(\boldsymbol{\lambda}/s+\mathbf{I}^{(K_{\mathrm{B}}Q_{\mathrm{t}})}\right)^{-1}\underbrace{\left(\underline{\widetilde{\mathbf{b}}}_n\underline{\mathbf{U}}\right)^{\mathrm{H}}}_{\underline{\widetilde{\widetilde{\mathbf{b}}}}_n^{\mathrm{H}}}\Big].\end{aligned} \tag{75}$$

As already explained in Section V, $\underline{\widetilde{\mathbf{b}}}_n$ of (43) is spherically uniformly distributed. Therefore, this assumption also holds for the row vector $\underline{\widetilde{\widetilde{\mathbf{b}}}}_n$ in (75) of dimension $K_{\mathrm{B}}Q_{\mathrm{t}}$, as multiplying a spherically distributed vector by a unitary matrix $\underline{\mathbf{U}}$ does not change its probability distribution [38]. Therefore, in analogy to (42) and (43), $\underline{\widetilde{\widetilde{\mathbf{b}}}}_n$ of (75) can also be represented by

$$\underline{\widetilde{\widetilde{\mathbf{b}}}}_n=\underline{\widetilde{\mathbf{b}}}_n\underline{\mathbf{U}}=\underline{\widetilde{\widetilde{\mathbf{g}}}}_n/\|\underline{\widetilde{\widetilde{\mathbf{g}}}}_n\|_2,\underline{\widetilde{\widetilde{\mathbf{g}}}}_n=\left(\underline{\widetilde{\widetilde{g}}}_{n,1}\cdots\underline{\widetilde{\widetilde{g}}}_{n,K_{\mathrm{B}}Q_{\mathrm{t}}}\right)^{\mathrm{T}}, \tag{76}$$

where the elements $\underline{\widetilde{\widetilde{g}}}_{n,s}, s=1\ldots K_{\mathrm{B}}Q_{\mathrm{t}}$, of $\underline{\widetilde{\widetilde{\mathbf{g}}}}_n, n=1\ldots N_{\mathrm{t}}$, satisfy the same probability distribution as $\underline{\widetilde{\mathbf{g}}}_n$ of (42). Substituting (67) in (75), the transmit efficiency can be calculated to be

$$\begin{aligned}\eta_{\mathrm{TxZF},n}&=\underline{\widetilde{\widetilde{\mathbf{b}}}}_n\lim_{s\to 0}\left[\mathrm{diag}\left(1+\frac{\lambda_1}{s}\ldots1+\frac{\lambda_{N_{\mathrm{t}}-1}}{s},1\ldots1\right)\right]^{-1}\underline{\widetilde{\widetilde{\mathbf{b}}}}_n^{\mathrm{H}}\\&=\underline{\widetilde{\widetilde{\mathbf{b}}}}_n\lim_{s\to 0}\left[\mathrm{diag}\left(\frac{s}{s+\lambda_1}\ldots\frac{s}{s+\lambda_{N_{\mathrm{t}}-1}},1\ldots1\right)\right]\underline{\widetilde{\widetilde{\mathbf{b}}}}_n^{\mathrm{H}}\\&=\underline{\widetilde{\widetilde{\mathbf{b}}}}_n\mathrm{diag}\Big(0\ldots0,1\ldots1\Big)\underline{\widetilde{\widetilde{\mathbf{b}}}}_n^{\mathrm{H}}.\end{aligned} \tag{77}$$

Using (76) and the quantities

$$X_1=\sum_{s=N_{\mathrm{t}}}^{K_{\mathrm{B}}Q_{\mathrm{t}}}\left|\underline{\widetilde{\widetilde{g}}}_{n,s}\right|^2,\quad X_2=\sum_{s=1}^{N_{\mathrm{t}}-1}\left|\underline{\widetilde{\widetilde{g}}}_{n,s}\right|^2, \tag{78}$$

$\eta_{\mathrm{TxZF},n}$ of (77) can be simplified to

$$\eta_{\mathrm{TxZF},n}=\frac{\sum_{s=N_{\mathrm{t}}}^{K_{\mathrm{B}}Q_{\mathrm{t}}}\left|\underline{\widetilde{\widetilde{g}}}_{n,s}\right|^2}{\sum_{s=1}^{K_{\mathrm{B}}Q_{\mathrm{t}}}\left|\underline{\widetilde{\widetilde{g}}}_{n,s}\right|^2}=\frac{X_1}{X_1+X_2}. \tag{79}$$

As stated in [32], both X_1 and X_2 are centrally χ^2-distributed random variables with $2(K_{\mathrm{B}}Q_{\mathrm{t}}-N_{\mathrm{t}}+1)$ and $2(N_{\mathrm{t}}-1)$ degrees of freedom, respectively. Thus, as shown in [32], $\eta_{\mathrm{TxZF},n}$ of (79) is beta distributed with the pdf $\mathrm{p}_{\eta_{\mathrm{TxZF},n}}(\eta)$ of (45). □

ACKNOWLEDGMENTS

The author gratefully appreciates the fruitful exchange of ideas with his colleagues at the Research Group for RF Communications and Prof. P. W. Baier, University of Kaiserslautern, with T. Haustein, V. Jungnickel and M. Schubert from Prof. Boche's group at the Fraunhofer-Institute for Telecommunications, Heinrich-Hertz-Institut, and with R. R. Müller from Vienna Telecommunications Research Centre (ftw). Special thanks go to W. Qiu for supporting this work with some simulation results. The support of individual parts of this work in the framework of the EU-IST-Project FLOWS (Flexible Convergence of Wireless Standards and Services), by Siemens AG and by DFG as well as the assistance by the supercomputer staff of the central computer facility (RHRK) of the University of Kaiserslautern are highly acknowledged.

REFERENCES

[1] V. Jungnickel, T. Haustein, E. Jorswieck, and C. von Helmolt, "On linear pre-processing in multi-antenna systems," in *Proc. IEEE Global Telecommunications Conference (GLOBECOM'02)*, Taipei, 2002, pp. 1012–1016.

[2] E. Jorswieck, G. Wunder, V. Jungnickel, and T. Haustein, "Inverse eigenvalue statistics for Rayleigh and Rician MIMO channels," *IEE Professional Network on Antennas and Propagation*, pp. 3/1–3/6, 2001.

[3] T. Haustein, C. von Helmolt, E. Jorswieck, V. Jungnickel, and V. Pohl, "Performance of MIMO systems with channel inversion," in *Proc. IEEE 55th Vehicular Technology Conference (VTC'02)*, Birmingham, 2002, pp. 35–39.

[4] Q. H. Spencer, A. L. Swindlehurst, and M. Haardt, "Zero-forcing methods for downlink spatial multiplexing in multiuser MIMO channels," *IEEE Transactions on Signal Processing*, vol. 52, no. 2, pp. 461–471, 2004.

[5] M. Meurer, P. W. Baier, T. Weber, Y. Lu, and A. Papathanassiou, "Joint transmission: advantageous downlink concept for CDMA mobile radio systems using time division duplexing," *IEE Electronics Letters*, vol. 36, no. 10, pp. 900–901, 2000.

[6] P. W. Baier, M. Meurer, T. Weber, and H. Tröger, "Joint transmission (JT), an alternative rationale for the downlink of time division CDMA using multi-element transmit antennas," in *Proc. IEEE 6th International Symposium on Spread Spectrum Techniques & Applications (ISSSTA'00)*, Parsippany, 2000, pp. 1–5.

[7] F. Kowalewski and P. Mangold, "Joint predistortion and transmit diversity," in *Proc. IEEE Global Telecommunications Conference (GLOBECOM'00)*, San Francisco, 2000, pp. 245–249.

[8] X. Tao, S. Wang, Y. Li, B. Liu, and P. Zhang, "Pre-distortion based joint transmission," in *Proc. IEEE 55th Vehicular Technology Conference (VTC'02)*, Birmingham, 2002, pp. 493–496.

[9] S. Georgoulis and D. G. M. Cruickshank, "Pre-equalization, transmitter precoding and joint transmission techniques for time division duplex CDMA," in *Proc. International Conference on 3G Mobile Communications Technologies*, London, 2001, pp. 257–261.

[10] G. Caire and S. Shamai, "On the achievable throughput of a multiantenna Gaussian broadcast channel," *IEEE Transactions on Information Theory*, vol. 49, no. 7, pp. 1691–1706, 2003.

[11] C. Walke and B. Rembold, "Joint detection and joint pre-distortion techniques for SD/TD/CDMA systems," *Frequenz*, vol. 55, no. 7–8, pp. 204–213, 2001.

[12] B. R. Vojcic and W. M. Jang, "Transmitter precoding in synchronous multiuser communications," *IEEE Transactions on Communications*, vol. 46, no. 10, pp. 1346–1355, 1998.

[13] Z. Tang and S. Cheng, "Interference cancellation for DS-CDMA systems over flat fading channels through pre-decorrelating," in *Proc. IEEE 5th International Symposium on Personal, Indoor and Mobile Radio Communications (PIMRC'94)*, The Hague, 1994, pp. 435–438.

[14] M. Joham, R. Irmer, S. Berger, G. Fettweis, and W. Utschick, "Linear precoding approaches for the TDD DS-CDMA downlink," in *Proc. 6th International Symposium on Wireless Personal Multimedia Communications 2003 (WPMC'03)*, Yokosuka, 2003, pp. 323–327.

[15] M. Meurer, P. W. Baier, and W. Qiu, "Receiver orientation versus transmitter orientation in linear MIMO transmission systems," *EURASIP Special Issue on Advances in Smart Antennas*, vol. 2004, no. 9, pp. 1–8, 2004.

[16] T. M. Cover and J. A. Thomas, *Elements of Information Theory*. John Wiley & Sons, 1991.

[17] D. Gesbert, M. Shafi, D.-S. Shiu, P. J. Smith, and A. Naguib, "From theory to practice: an overview of MIMO space-time coded wireless systems," *IEEE Journal on Selected Areas in Communications*, vol. 21, no. 3, pp. 281–302, 2003.

[18] R. Irmer, A. Noll-Barreto, and G. Fettweis, "Transmitter precoding for spread-spectrum signals in frequency-selective fading channels," in *Proc. 3G Wireless 2001*, San Francisco, 2001, pp. 939–944.

[19] F. Dietrich, R. Hunger, M. Joham, and W. Utschick, "Linear precoding over time-varying channels in TDD systems," in *Proc. IEEE International Conference on Acoustics, Speech, and Signal Processing (ICASSP'03)*, Hong Kong, 2003, pp. 117–120.

[20] M. L. Mehta, *Random matrices*. San Diego: Academic Press, 1991.

[21] R. R. Müller, "Multiuser receivers for randomly spread signals: Fundamental limits with and without decision-feedback," *IEEE Transactions on Information Theory*, vol. 47, no. 1, pp. 268–283, 2001.

[22] H. Tröger, T. Weber, M. Meurer, and P. W. Baier, "Performance assessment of joint transmission (JT) multi-user downlinks with multi-element transmit antennas," *European Transactions on Telecommunications*, vol. 12, no. 5, pp. 407–415, 2001.

[23] M. Meurer, T. Weber, and W. Qiu, "Transmit Nonlinear Zero Forcing: Energy efficient receiver oriented transmission in MIMO CDMA mobile radio downlinks," in *Proc. IEEE 8th International Symposium on Spread Spectrum Techniques & Applications (ISSSTA'04)*, Sydney, 2004, pp. 260–269.

[24] P. W. Baier, W. Qiu, H. Tröger, C. A. Jötten, and M. Meurer, "Modelling and optimization of receiver oriented multi-user MIMO downlinks for frequency selective channels," in *Proc. 10th International Conference on Telecommunications (ICT'03)*, Papeete, 2003, pp. 1547–1554.

[25] R. Esmailzadeh and M. Nakagawa, "Pre-RAKE diversity combining for direct sequence spread spectrum mobile communications systems," *IEICE Transactions on Communications*, vol. 76, no. 8, pp. 1008–1015, 1993.

[26] A. Noll-Barreto and G. Fettweis, "Performance improvement in DS-spread spectrum CDMA systems using a pre- and a post-rake," in *Proc. 2000 International Zurich Seminar on Broadband Communications (IZS'2000)*, Zurich, 2000, pp. 39–46.

[27] M. Joham, K. Kusume, M. H. Gzara, W. Utschick, and J. A. Nossek, "Transmit Wiener Filter for the Downlink of TDD DS-CDMA Systems," in *Proc. IEEE 7th International Symposium on Spread Spectrum Techniques & Applications (ISSSTA'02)*, Prague, 2002, pp. 9–13.

[28] P. W. Baier and M. Meurer, "Receiver orientation, an unconventional approach to mobile radio downlink design," in *Proc. European Conference on Wireless Technology (ECWT'03)*, Munich, 2003, pp. 11–14.

[29] I. E. Telatar, "Capacity of multi-antenna Gaussian channels," *European Transactions on Telecommunications*, vol. 10, no. 6, pp. 585–595, 1999.

[30] S. Verdú, *Multiuser detection*. Cambridge: Cambridge University Press, 1998.

[31] ——, "Optimum multiuser asymptotic efficiency," *IEEE Transactions on Communications*, vol. 34, no. 9, pp. 890–897, 1986.

[32] M. Abramowitz and I. Stegun, *Handbook of mathematical functions*. New York: Dover, 1965.

[33] R. R. Müller, "A random matrix model of communication via antenna arrays," *IEEE Transactions on Information Theory*, vol. 48, no. 9, pp. 2495–2506, 2002.

[34] A. M. Tulino and S. Verdú, "Random matrix theory and wireless communications," *Foundations and Trends in Communications and Information Theory*, vol. 1, no. 1, 2004.

[35] 3rd Generation Partnership Project (3GPP), "Technical specification group radio access network, UTRA (BS) TDD, radio transmission and reception," 3GPP, Technical Specification TS 25.105 Version 3.5.0, 2000.

[36] R. F. H. Fischer, C. Windpassinger, A. Lampe, and J. B. Huber, "MIMO precoding for decentralized receivers," in *Proc. 2002 IEEE International Symposium on Information Theory (ISIT'2002)*, Lausanne, 2002, p. 496.

[37] H. Lütkepohl, *Handbook of Matrices*. England: John Wiley & Sons, 1996.

[38] T. L. Marzetta and B. M. Hochwald, "Capacity of a mobile multiple-antenna communication link in rayleigh flat fading," *IEEE Transactions on Information Theory*, vol. 45, no. 1, pp. 139–157, 1999.

[PMWB00] Papathanassiou, A.; Meurer, M.; Weber, T.; Baier, P. W.: "A novel multiuser transmission scheme requiring no channel estimation and no equalization at the mobile stations for the downlink of TD-CDMA operating in the TDD mode". *Proc. IEEE 52nd Vehicular Technology Conference (VTC'00-Fall)*, Bd. 1, Boston, 2000, S. 203–210.

A Novel Multiuser Transmission Scheme Requiring No Channel Estimation and No Equalization at the Mobile Stations for the Downlink of TD–CDMA Operating in the TDD Mode

A. Papathanassiou
Advanced Communication Technologies
Development Programmes Department
INTRACOM S.A.
19002 Peania, Greece
e-mail: apap@intracom.gr

M. Meurer, T. Weber and P.W. Baier
Research Group for RF Communications
University of Kaiserslautern
P.O. Box 3049
D–67653 Kaiserslautern, Germany
e-mail: meurer@rhrk.uni-kl.de

Abstract

In the 3rd Generation Partnership Project (3GPP) Time Division CDMA (TD–CDMA) has been selected as the air interface for the TDD (Time Division Duplexing) bands of 3rd Generation (3G) mobile radio systems. In this paper, a novel multiuser transmission scheme for the TD–CDMA downlink is presented, which in contrast to state of the art TD–CDMA transceivers utilizes the reciprocity of the mobile radio channels of the uplink and the downlink. It is shown that according to this scheme no channel estimation is necessary at the MSs and the data detection effort is dramatically reduced. The theoretical analysis of the paper is supported by computer simulation results which illustrate the superiority of the novel scheme in terms of the BER (bit error rate) performance and the system spectrum efficiency in the downlink of TD–CDMA.

1. Introduction

Time Division CDMA (TD–CDMA) is a time–slotted CDMA air interface, which is based on the combination of the multiple access schemes FDMA, TDMA and CDMA [1]. This air interface has been selected by the 3rd Generation Partnership Project (3GPP) as the standard for the TDD (Time Division Duplexing) mode of the 3rd Generation (3G) mobile radio system IMT-2000 (International Mobile Telecommunications 2000) [2]. In the case of TDD the channel impulse response between a mobile station (MS) and a base station (BS) is valid for both the uplink and the downlink, as long as the time elapsing between uplink and downlink transmission is sufficiently smaller than the coherence time [3] of the mobile radio channel. When the downlink of TD–CDMA is considered, the fact that this equality is not exploited by the state of the art TD–CDMA transceivers leads to two fundamental requirements, which can also be viewed as the main drawbacks of the TD–CDMA downlink.

These requirements can be described as follows:

- A user specific training sequence is mandatory in the burst format, which enables channel estimation at the MSs. However, since the support of high data rates up to 2 Mbit/s is required for 3G mobile radio systems [2], the use of training sequences considerably reduces the useful data rate in the downlink of TD–CDMA.
- A considerable computational effort has to be made for channel estimation [4] at the MS. In addition to this effort, the use of joint detection [1] for data detection results in a further increase of the computational effort required at the MSs. Although channel estimation and joint data detection fulfill the performance requirements for 3G mobile radio systems [1], their high computational effort constitutes a severe drawback for the implementation of low–cost mobile handsets.

The above described drawbacks of the TD–CDMA downlink can be overcome by the novel multiuser transmission scheme presented in the paper. The novelty of this scheme consists in determining a common transmit signal for the service of all MSs assigned to the considered BS by explicitly using the information about the channel impulse responses of all MSs assigned to the considered BS. Due to the rationale of this approach, the name Joint Transmission (JT) has already been proposed for the novel multiuser transmission scheme by the authors [5]. The information about the channel impulse responses is obtained from the previous time slot assigned to the uplink, i.e., this scheme takes advantage of the equality of the mobile radio channel impulse responses between the uplink and the downlink valid in the TDD mode. Then, the transmit signal from the BS, after passing through the mobile radio channels, yields the data sent for a specific MS by simple linear filtering of the received signal at that MS. In this way, two goals are achieved:

- First, no user specific training sequences are required in the burst format, which allows an increase of the offered useful data rate, compared to the use of the state of the art burst format in the TD–CDMA downlink [1].
- Second, since no channel estimation is necessary and only a single filter is needed at each MS in order to perform data detection, a dramatic reduction of the receiver computational effort is achieved, compared to the one required by the state of the art TD–CDMA receivers at the MSs.

As a final remark, although the novel multiuser transmission technique is presented in this paper for the downlink of TD–CDMA, its application is also feasible to other air interfaces having a TDMA component.

The paper is structured as follows: In Section 2 the system model is developed, where the case of using multiple antennas at the BS is also treated. In Section 3 the said common transmit signal at the BS is determined and data detection at the MSs is presented according to the novel multiuser transmission scheme. In Section 4 simulation results for the BER (bit error rate) performance and the system spectrum efficiency achieved by the novel scheme are presented and compared to the ones obtained by using the state of the art TD–CDMA downlink scheme. Finally, Section 5 summarizes the basic results and concludes the paper.

2. System model

In this section a time discrete system model in the equivalent lowpass domain is described for the downlink of TD–CDMA. A single cell of the cellular network is considered and the number of MSs served by the BS of this cell is equal to K. Further, the transmission of one TDMA burst in the downlink is treated. It is assumed that N data symbols have to be transmitted for each MS from the BS. The N data symbols from each user are arranged to the user specific data vector

$$\underline{\mathbf{d}}^{(k)} = \left[\underline{d}_1^{(k)} \dots \underline{d}_N^{(k)}\right]^{\mathrm{T}}, \quad k = 1 \dots K, \tag{1}$$

and all K data vectors are stacked to form the total data vector

$$\underline{\mathbf{d}} = \left[\underline{\mathbf{d}}^{(1)\mathrm{T}} \dots \underline{\mathbf{d}}^{(K)\mathrm{T}}\right]^{\mathrm{T}} \tag{2}$$

of length KN. Furthermore, as commonly assumed for TD–CDMA [1], a user specific CDMA code

$$\underline{\mathbf{c}}^{(k)} = \left[\underline{c}_1^{(k)} \dots \underline{c}_Q^{(k)}\right]^{\mathrm{T}}, \quad k = 1 \dots K, \tag{3}$$

of length Q is assigned to each MS k, $k = 1 \dots K$. The CDMA codes $\underline{\mathbf{c}}^{(k)}$, $k = 1 \dots K$, see (3), are arranged to the K matrices $\underline{\mathbf{C}}^{(k)}$, $k = 1 \dots K$, of dimension $(NQ + W - 1) \times N$ the elements of which are given by

$$\left[\underline{\mathbf{C}}^{(k)}\right]_{q+Q(n-1),n} = \begin{cases} \underline{c}_q^{(k)} & , q = 1 \dots Q, \\ & \quad n = 1 \dots N \\ 0 & , \text{otherwise.} \end{cases} \tag{4}$$

The K matrices $\underline{\mathbf{C}}^{(k)}$, $k = 1 \dots K$, of (4) are combined to the $K(NQ + W - 1) \times KN$ block diagonal matrix

$$\underline{\mathbf{C}} = \mathrm{blockdiag}\left[\underline{\mathbf{C}}^{(1)} \dots \underline{\mathbf{C}}^{(K)}\right]. \tag{5}$$

In the rest of this section, the signal transmission model is described. In a first step, a single antenna is assumed to be used at the BS. Then, the system model is extended to include the use of multi–antenna configurations at the BS.

When a single antenna is used at the BS, the mobile radio channel can be characterized by K channel impulse responses [1]

$$\underline{\mathbf{h}}^{(k)} = \left[\underline{h}_1^{(k)} \dots \underline{h}_W^{(k)}\right]^{\mathrm{T}}, \quad k = 1 \dots K, \tag{6}$$

each one valid for the connection of the BS and MS k, $k = 1 \dots K$. The BS is assumed to transmit a signal

$$\underline{\mathbf{s}}_{\mathrm{s}} = \left[\underline{s}_{\mathrm{s},1} \dots \underline{s}_{\mathrm{s},S}\right]^{\mathrm{T}} \tag{7}$$

of length S, which represents the transmission of one TDMA burst. $\underline{\mathbf{s}}_{\mathrm{s}}$ of (7) will be termed the total transmit signal, since it is valid for all MSs assigned to the considered BS. With the channel impulse responses $\underline{\mathbf{h}}^{(k)}$, $k = 1 \dots K$, see (6), a $(S + W - 1) \times S$ Toeplitz matrix $\underline{\mathbf{H}}_{\mathrm{s}}^{(k)}$, $k = 1 \dots K$, is formed, the elements of which are given by

$$\left[\underline{\mathbf{H}}_{\mathrm{s}}^{(k)}\right]_{s+w-1,s} = \begin{cases} \underline{h}_w^{(k)} & , w = 1 \dots W, \\ & \quad s = 1 \dots S \\ 0 & , \text{otherwise.} \end{cases} \tag{8}$$

All K matrices $\underline{\mathbf{H}}_{\mathrm{s}}^{(k)}$, $k = 1 \dots K$, are arranged to the matrix

$$\underline{\mathbf{H}}_{\mathrm{s}} = \left[\underline{\mathbf{H}}_{\mathrm{s}}^{(1)\mathrm{T}} \dots \underline{\mathbf{H}}_{\mathrm{s}}^{(K)\mathrm{T}}\right]^{\mathrm{T}}, \tag{9}$$

with the dimension $K(S + W - 1) \times S$. Then, the signal originating from $\underline{\mathbf{s}}_{\mathrm{s}}$, see (7), and received at MS k, $k = 1 \dots K$, is expressed as

$$\underline{\mathbf{e}}_{\mathrm{s}}^{(k)} = \underline{\mathbf{H}}_{\mathrm{s}}^{(k)} \underline{\mathbf{s}}_{\mathrm{s}}, \quad k = 1 \dots K, \tag{10}$$

and has length $S + W - 1$. The K received signals $\underline{\mathbf{e}}_{\mathrm{s}}^{(k)}$, $k = 1 \dots K$, of (10) are arranged to the vector

$$\underline{\mathbf{e}}_{\mathrm{s}} = \left[\underline{\mathbf{e}}_{\mathrm{s}}^{(1)\mathrm{T}} \dots \underline{\mathbf{e}}_{\mathrm{s}}^{(K)\mathrm{T}}\right]^{\mathrm{T}} \tag{11}$$

of length $K(S+W-1)$. $\underline{\mathbf{e}}$ of (11) corresponds to the reception of one TDMA burst from all K MSs. With the channel impulse response matrix $\underline{\mathbf{H}}_{\mathrm{s}}$, see (9), and the transmit signal $\underline{\mathbf{s}}_{\mathrm{s}}$, see (7), the total received signal at all K MSs can be written as

$$\underline{\mathbf{e}}_{\mathrm{s}} = \underline{\mathbf{H}}_{\mathrm{s}}\underline{\mathbf{s}}_{\mathrm{s}}. \tag{12}$$

Note that the total received signal $\underline{\mathbf{e}}_{\mathrm{s}}$ of (12) cannot be observed by a single MS k, $k = 1\ldots K$. A MS k, $k = 1\ldots K$, can only observe $\underline{\mathbf{e}}_{\mathrm{s}}^{(k)}$, $k = 1\ldots K$, of (10). However, the representation of the total received signal $\underline{\mathbf{e}}_{\mathrm{s}}$ in (12) will appear useful when determining the transmit signal $\underline{\mathbf{s}}_{\mathrm{s}}$ of (7), which is common for all MSs assigned to the considered BS.

When multi–antenna configurations of K_{a} antenna elements are used at the BS, the method for deriving the total received signal at all MSs is the same as the one presented above in this section for the use of a single antenna at the BS. However, in the case where multi–antenna configurations are used at the BS, the total transmit signal is the combined transmit signal from all K_{a} antenna elements expressed by

$$\underline{\mathbf{s}}_{\mathrm{m}} = \left[\underline{\mathbf{s}}_{\mathrm{m}}^{(1)\mathrm{T}}\ldots\underline{\mathbf{s}}_{\mathrm{m}}^{(K_{\mathrm{a}})\mathrm{T}}\right]^{\mathrm{T}}, \tag{13}$$

where $\underline{\mathbf{s}}_{\mathrm{m}}^{(k_{\mathrm{a}})}$, $k_{\mathrm{a}} = 1\ldots K_{\mathrm{a}}$, represents the transmit signal from antenna k_{a} and its structure is as the one in (7). Further, the mobile radio channel is characterized by KK_{a} channel impulse responses $\underline{\mathbf{h}}^{(k,k_{\mathrm{a}})}$, $k = 1\ldots K$, $k_{\mathrm{a}} = 1\ldots K_{\mathrm{a}}$, each valid for the connection of antenna k_{a} and MS k [1, 4]. All KK_{a} channel impulse responses $\underline{\mathbf{h}}^{(k,k_{\mathrm{a}})}$, $k = 1\ldots K$, $k_{\mathrm{a}} = 1\ldots K_{\mathrm{a}}$, are arranged to the matrix

$$\underline{\mathbf{H}}_{\mathrm{m}} = \left[\underline{\mathbf{H}}_{\mathrm{m}}^{(1)\mathrm{T}}\ldots\underline{\mathbf{H}}_{\mathrm{m}}^{(K)\mathrm{T}}\right]^{\mathrm{T}}, \tag{14}$$

$$\underline{\mathbf{H}}_{\mathrm{m}}^{(k)} = \left[\underline{\mathbf{H}}_{\mathrm{m}}^{(k,1)}\ldots\underline{\mathbf{H}}_{\mathrm{m}}^{(k,K_{\mathrm{a}})}\right], \tag{15}$$

$k = 1\ldots K$, where the structure of the $(S+W-1)\times S$ matrix $\underline{\mathbf{H}}_{\mathrm{m}}^{(k,k_{\mathrm{a}})}$, $k = 1\ldots K$, $k_{\mathrm{a}} = 1\ldots K_{\mathrm{a}}$, is as the one in (8). Then, with $\underline{\mathbf{H}}_{\mathrm{m}}$, see (14), and the total transmit signal $\underline{\mathbf{s}}_{\mathrm{m}}$, see (13), the total received signal at all K MSs can be written as

$$\underline{\mathbf{e}}_{\mathrm{m}} = \underline{\mathbf{H}}_{\mathrm{m}}\underline{\mathbf{s}}_{\mathrm{m}} \tag{16}$$

for the case where multi–antenna configurations are used at the BS.

Note that $\underline{\mathbf{e}}_{\mathrm{s}}$ of (12), which holds for the case that a single antenna is used at the BS, and $\underline{\mathbf{e}}_{\mathrm{m}}$ of (16), which holds for the case that multi–antenna configurations are used at the BS, have the same number of components $K(S+W-1)$. This observation will be used in the following section in order to provide a common analysis for determining the total transmit signal $\underline{\mathbf{s}}_{\mathrm{s}}$, see (7), or $\underline{\mathbf{s}}_{\mathrm{m}}$, see (13), independent of the number K_{a} of antennas used at the BS. For this purpose, in the rest of the paper the total received signal at all MSs is expressed by

$$\underline{\mathbf{e}} = \underline{\mathbf{H}}\,\underline{\mathbf{s}}, \tag{17}$$

where $\underline{\mathbf{e}}$, $\underline{\mathbf{H}}$ and $\underline{\mathbf{s}}$ of (17) stand for $\underline{\mathbf{e}}_{\mathrm{s}}$, $\underline{\mathbf{H}}_{\mathrm{s}}$ and $\underline{\mathbf{s}}_{\mathrm{s}}$, respectively, see (12), when a single antenna is used at the BS, and for $\underline{\mathbf{e}}_{\mathrm{m}}$, $\underline{\mathbf{H}}_{\mathrm{m}}$ and $\underline{\mathbf{s}}_{\mathrm{m}}$, respectively, see (16), when multi–antenna configurations are used at the BS.

3. Determination of the total transmit signal and data detection at the MSs

In Section 2 it is shown that the total received signal $\underline{\mathbf{e}}$ at all MSs is given by (17), which describes both the single antenna and the multi–antenna case. In this section the total transmit signal $\underline{\mathbf{s}}$, see (17), is determined so that the goals stated in Section 1 are achieved, i.e., no training sequences are needed in the format of the transmitted burst, no channel estimation is necessary at the MSs and data detection is performed by simple linear filtering of the received signals at the MSs.

Setting out from (17), the above mentioned goals, see also Section 1, can be achieved by requiring that each MS k is equipped with a single linear filter matched to the CDMA code $\underline{\mathbf{c}}^{(k)}$ assigned to MS k, $k = 1\ldots K$, and the output of the filter at MS k directly yields the data transmitted from the BS for MS k, $k = 1\ldots K$. It is reminded that the data for MS k is contained in the data vector $\underline{\mathbf{d}}^{(k)}$, $k = 1\ldots K$, see (1). Concerning the length S of the transmit signal from antenna k_{a} of the BS, it will be assumed in the following that

$$S = N\,Q\,. \tag{18}$$

In this way, a direct comparison of the proposed scheme with the state of the art TD–CDMA downlink transmission scheme [1] is possible. When the total received signal $\underline{\mathbf{e}}$, see (17), at all K MSs is considered, the above stated requirement is mathematically described for all K MSs assigned to the considered BS by

$$\underline{\mathbf{C}}^{*\mathrm{T}}\underline{\mathbf{e}} = \underline{\mathbf{d}}, \tag{19}$$

where $\underline{\mathbf{C}}$ is defined in (5) and $\underline{\mathbf{d}}$ is given by (2). By substituting $\underline{\mathbf{e}}$ in (19) by its representation in (17), (19) can be equivalently written as

$$\underline{\mathbf{C}}^{*\mathrm{T}}\underline{\mathbf{H}}\,\underline{\mathbf{s}} = \underline{\mathbf{d}}. \tag{20}$$

Under the assumption that the time elapsing from the previous time slot assigned to the uplink of TD–CDMA is sufficiently smaller than the coherence time of the mobile radio channel, in (20) $\underline{\mathbf{C}}$, $\underline{\mathbf{H}}$ and $\underline{\mathbf{d}}$ are known at the BS. Since

$$K\,N < K_\mathrm{a}\,N\,Q \qquad (21)$$

is a state of the art assumption for TD–CDMA independently of the number K_a of antenna elements used at the BS [1], (20) constitutes an optimization problem [6], where the number KN of restrictions, contained in the vector $\underline{\mathbf{d}}$ of length KN, is smaller than the number $K_\mathrm{a}NQ$ of degrees of freedom, expressed by the vector $\underline{\mathbf{s}}$ of length NQ. Therefore, the validity of (21) implies that (20) has infinitely many solutions $\underline{\mathbf{s}}$.In the following the solution $\underline{\mathbf{s}}$ with minimum energy will be used. It can be obtained from (20) by following standard Lagrange techniques [6]

$$\underline{\mathbf{s}} = \underline{\mathbf{H}}^{*\mathrm{T}}\underline{\mathbf{C}}\left(\underline{\mathbf{C}}^{*\mathrm{T}}\underline{\mathbf{H}}\,\underline{\mathbf{H}}^{*\mathrm{T}}\underline{\mathbf{C}}\right)^{-1}\underline{\mathbf{d}}. \qquad (22)$$

Minimizing the energy of $\underline{\mathbf{s}}$ means that the multiple access interference caused by a BS of the cellular network is also minimized. This advantageous property of the total transmit signal $\underline{\mathbf{s}}$ given by (22) will be illustrated by computer simulation results in Section 4, where the system spectrum efficiency achieved by the novel scheme presented in the paper is compared to the system spectrum efficiency achieved by the state of the art scheme for the TD–CDMA downlink [1].

Concerning data detection at the MSs, if the vector $\underline{\mathbf{n}}^{(k)}$ of length $(NQ + W - 1)$ expresses the influence of the additive intercell multiple access interference (MAI) at the input of MS k, $k = 1\ldots K$, it is easily shown from (20) and (22) that the estimate of the data vector $\underline{\mathbf{d}}^{(k)}$, see (1), transmitted for MS k, $k = 1\ldots K$, is given by

$$\hat{\underline{\mathbf{d}}}^{(k)} = \underline{\mathbf{d}}^{(k)} + \underline{\mathbf{C}}^{(k)\,*\mathrm{T}}\underline{\mathbf{n}}^{(k)}, k = 1\ldots K. \qquad (23)$$

As a final remark, if the input intercell MAI vector $\underline{\mathbf{n}}^{(k)}$, $k = 1\ldots K$, in (23) is white and Gaussian distributed with each component of $\underline{\mathbf{n}}^{(k)}$ having variance equal to σ^2, i.e., if its covariance matrix equals the $(NQ + W - 1) \times (NQ + W - 1)$ identity matrix multiplied by σ^2, the covariance matrix of the output intercell MAI vector $\underline{\mathbf{C}}^{(k)*\mathrm{T}}\underline{\mathbf{n}}^{(k)}$, $k = 1\ldots K$, see (23), equals $\sigma^2||\underline{\mathbf{c}}^{(k)}||^2\,\mathbf{I}^{(N)}$. This means that according to the presented scheme at the output of the matched filter of MS k, $k = 1\ldots K$, uncorrelated noise is present, whereas according to the state of the art scheme for TD–CDMA the output intercell MAI vector is highly correlated, since the latter scheme does not take advantage of the information about the channel impulse responses when determining the total transmit signal at the BS. This advantageous property of the presented scheme will be illustrated by computer simulation results in Section 4, where the BER performance of the novel scheme is compared to the BER performance of the state of the art scheme for the TD–CDMA downlink [1].

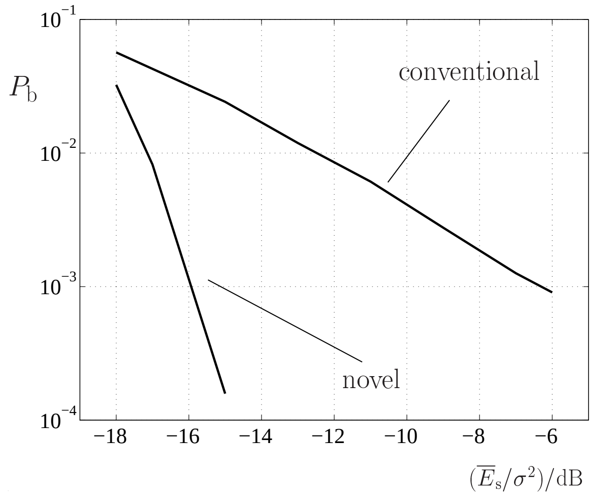

Figure 1. Coded BER P_b of user $k = 1$ versus $\bar{E}_\mathrm{s}/\sigma^2$; perfectly known channel impulse responses used at the BS; COST207 RA channel model; $K = 2$ users; mobile speed: 3 km/h

4. Simulation results

4.1. General

In this section the performance of the presented multiuser transmission scheme for the downlink of TD–CDMA is investigated by simulations and compared to the state of the art transmission scheme of the TD–CDMA downlink [1], which will be addressed as the conventional scheme from now on. First, in Section 4.2 the BER performance of the novel scheme is evaluated and compared to the performance of the conventional downlink scheme for TD–CDMA. This evaluation will illustrate the potential of the scheme presented in the paper for performance improvement, compared to the use of the conventional scheme for the TD–CDMA downlink. However, when considering a cellular mobile radio system, the ultimate goal should be the investigation of the applied scheme with respect to the system efficiency [7, 8]. The efficiency of mobile radio systems is evaluated through widely accepted performance measures, such as the spectrum efficiency. In addition to the possibility of comparing different mobile radio systems, the spectrum efficiency enables the comparison of different concepts within the same mobile radio system [7, 8]. Therefore, in Section 4.3 the spectrum efficiency of the TD–CDMA downlink is determined for both the novel and the conventional scheme for the downlink of TD–CDMA.

4.2. BER performance

In this section the BER performance of the novel scheme presented in the paper is evaluated by Monte Carlo simulations [9] and compared to the performance of the conventional downlink scheme for TD–CDMA [1]. In the simulations a single antenna is used at the BS and K equal to two users are assumed to be active within each TDMA burst. Each user moves with velocity equal to 3 km/h. The length Q of each CDMA code $\underline{\mathbf{c}}^{(k)}$, $k = 1, 2$, see (3), is equal to 16. Furthermore, a channel impulse response valid for the link between the BS and each of the two MSs is created according to the COST 207 channel model for transmission over Rural Area (RA) [10]. Since the BER performance is investigated, the influence of the intercell MAI is modelled by choosing the components of $\underline{\mathbf{n}}^{(k)}$, $k = 1, 2$, see (23), to be samples of independent complex Gaussian random variables with zero mean and variance equal to σ^2. The remaining parameters for TD–CDMA can be taken from [11].

In a first step, the channel impulse responses valid for the transmission of one downlink TDMA burst, i.e., for a single experiment, are assumed to be perfectly known at the BS. Although this assumption is somewhat optimistic for the real–time operation of TD–CDMA in the downlink, it offers the possibility of obtaining upper bounds for the performance of both the novel and the conventional downlink transmission scheme for TD–CDMA. In Fig. 1 the average coded BER P_b for MS $k = 1$ is illustrated versus the ratio of the average transmitted energy $\bar{E}_\mathrm{s}$ per symbol and user to σ^2 in dB, when the novel and the conventional scheme for the downlink of TD–CDMA are used. From Fig. 1, the dramatic performance improvement of the TD–CDMA downlink achieved by the novel scheme is obvious, compared to the use of the conventional downlink transmission scheme for TD–CDMA [1]. First, this improvement is expressed by an $\bar{E}_\mathrm{s}/\sigma^2$ gain of approximately 9 dB at a coded BER P_b equal to 10^{-3}. Second, there is a more rapid decrease of P_b as E_s/σ^2 increases, which is mainly due to the fact that uncorrelated noise is present at the CDMA code matched filter output prior to the implementation of channel decoding, see the analysis presented in the last part of Section 3, whereas the output intercell MAI vector in the conventional scheme is highly correlated due to the presence of ISI and MAI [1].

In a second step, a realistic operating situation for the downlink of TD–CDMA is considered with respect to the application of the novel scheme. According to this operating situation, the channel impulse responses of the two users are estimated in the previous TDMA burst assigned to the uplink. In order to obtain useful results for the downlink case, it is assumed that the signal–to–noise

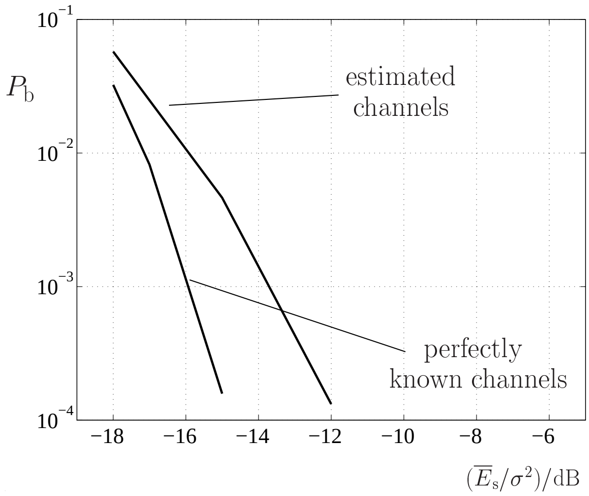

Figure 2. Coded BER P_b of user $k = 1$ versus $\bar{E}_\mathrm{s}/\sigma^2$; estimated channel impulse responses from the uplink used at the BS; COST207 RA channel model; $K = 2$ users; mobile speed: 3 km/h

ratio (SNR) at the input of the BS receiver during the uplink transmission takes values high enough so that an average coded BER P_b between 10^{-3} and 10^{-4} is achieved. In this way, the downlink BER performance can be investigated under the assumption that in the uplink of TD–CDMA the BER performance requirements for, at least, voice transmission [8] are met. Then, the total transmit signal $\underline{\mathbf{s}}$ is determined according to (22) by using the estimated channel impulse responses from the previous TDMA burst assigned to the uplink of TD–CDMA. The use of the estimated channel impulse responses from the uplink when determining $\underline{\mathbf{s}}$ from (22) constitutes a first source of error compared to the situation valid for the simulation results presented in Fig. 1. Furthermore, compared to the channel impulse responses valid for the transmission of the uplink TDMA burst, the channel impulse responses valid for the transmission of the downlink TDMA burst have slightly changed since the users move with velocity 3 km/h. This change constitutes a second source of error compared to the situation valid for the simulation results presented in Fig. 1. Under the described operating situation for the novel scheme, its BER performance is compared in Fig. 2 to the case where the channel impulse responses are perfectly known at the BS, see also the simulation results in Fig. 1 for the novel scheme. The remaining simulation parameters are as the ones valid for Fig. 1. From Fig. 2, a performance degradation of the novel scheme is observed when the estimated channel impulse responses from the uplink are used for determining the total transmit signal $\underline{\mathbf{s}}$ from (22), compared to the ideal case where the channel impulse responses are perfectly known at the BS prior to the downlink transmission. This degradation compared to the ideal case is expressed by an increase of the required $\bar{E}_{\mathrm{s}}/\sigma^2$ of approximately 2.5 dB in order to achieve an average coded BER P_{b} equal to 10^{-3}, see Fig. 2. However, this degradation is in the order of the one observed in the uplink of TD–CDMA when estimated channel impulse responses are used for data detection, compared to the case where the channel impulse responses are perfectly known at the BS uplink receiver [11]. Therefore, the simulation results of Fig. 2 illustrate the feasibility of using the novel multiuser transmission scheme presented in the paper for the downlink of TD–CDMA.

The simulation results presented in this section illustrate rather impressively that the BER performance of the novel scheme is superior to the BER performance of the conventional downlink transmission scheme for TD–CDMA. It may be argued though that one of the main reasons for this performance difference is related to the fact that in the simulations concerning the conventional scheme for the TD–CDMA downlink no kind of power control for the MSs assigned to the BS of the considered cell is applied, whereas in the simulations concerning the novel scheme the explicit use of the channel impulse responses, which do not have equal energies, when determining the transmit signal from the BS manages to overcome the problem of unequal received powers at the MSs in the downlink transmission. Therefore, in Section 4.3 the spectrum efficiency in the downlink of TD–CDMA is determined for both schemes. Thus, since the situation in the complete cellular network in the downlink is treated, a fair comparison of the two schemes is enabled.

4.3. Spectrum efficiency

One of the most widely accepted performance measures of a cellular mobile radio system is its spectrum efficiency η [7, 8]. In order to determine the spectrum efficiency, a single cell of the cellular network is considered. The spectrum efficiency relates the total available information rate within the considered cell to the total used system bandwidth [7, 8]. Based on the analysis presented in [7, 8], if r denotes the reuse factor, K is the total number of users active within each time slot and frequency band of bandwidth B and R stands for the information rate per active user in its assigned time slot, the spectrum efficiency of TD–CDMA operating in the TDD mode is given by

$$\eta = \frac{K\,R}{r\,B} \tag{24}$$

and measured in bit/(s $\cdot$ Hz) per cell. (24) shows that, for given values of R and B [12], η is determined by K and r. However, when choosing r and K such that η is maximized, the side condition of keeping the system performance sufficiently high has to be simultaneously fulfilled [7, 8]. To quantify the system performance, a quality of service (QoS) criterion is chosen which is defined as follows [7, 8]: The QoS criterion is met if the bit error probability P_{b} exceeds a given upper bound $P_{\mathrm{b}}^{\mathrm{M}}$ with a probability not greater than a given value $P_{\mathrm{o}}^{\mathrm{M}}$. The values $P_{\mathrm{b}}^{\mathrm{M}}$ and $P_{\mathrm{o}}^{\mathrm{M}}$ determine the required QoS. For each pair (r, K), a cumulative distribution function (CDF) $\mathrm{Prob}\{P_{\mathrm{b}} \le \Gamma\}$ holds. Then, the outage probability P_{o} is defined as [8]

$$P_{\mathrm{o}} = P_{\mathrm{o}}(\Gamma) = \mathrm{Prob}\{P_{\mathrm{b}} > \Gamma\} = 1 - \mathrm{Prob}\{P_{\mathrm{b}} \le \Gamma\}. \tag{25}$$

In order to test whether the QoS criterion specified by $P_{\mathrm{b}}^{\mathrm{M}}$ and $P_{\mathrm{o}}^{\mathrm{M}}$ is met, the value $P_{\mathrm{o}}(P_{\mathrm{b}}^{\mathrm{M}})$ has to be determined. Then, the following decision rule holds [7, 8]:

$$\begin{array}{ll} P_{\mathrm{o}}(P_{\mathrm{b}}^{\mathrm{M}}) > P_{\mathrm{o}}^{\mathrm{M}}: & \text{QoS criterion not fulfilled,} \\ P_{\mathrm{o}}(P_{\mathrm{b}}^{\mathrm{M}}) \le P_{\mathrm{o}}^{\mathrm{M}}: & \text{QoS criterion fulfilled.} \end{array} \tag{26}$$

If the QoS criterion is not fulfilled, r has to be increased and/or K has to be decreased until the QoS criterion is met. On the other hand, if the QoS criterion is met with a certain pair (r, K), one should try to increase K and/or decrease r with the goal to arrive at another pair (r, K), for which the QoS criterion is still fulfilled, however, with a larger spectrum efficiency η, see (24).

The above described procedure to determine η cannot be performed in a closed analytical way [7]. Extensive computer simulations are required to reach this goal. For the purpose of this section, the simulation method presented in [8], see also [13] for a detailed analysis, is used for determining the spectrum efficiency η in the downlink of TD–CDMA for both investigated downlink transmission schemes. The determination of η depends, on the one hand, on the pair (r, K) and, on the other hand, on a number of parameters which must be held fixed during the simulations. These parameters are [13]

- the propagation environment established by the used channel model,
- the mobile user velocity, and
- the antenna configuration used at the BS receiver,

and are addressed as the system operation situation [13].

The used simulation method [8] determines the outage probability P_{o} of (25) by Monte–Carlo simulations of data transmission in a reference cell embedded in a cellular environment. Each simulation experiment, which is performed for a certain combination (r, K) and a certain system operation situation, may be split into three steps [8]:

1. First, based on a Hata–like model for slow fading, an inhomogeneous directional distribution of the intercell interference is generated for the reference cell of the cellular network regarding both the average power and the DOA (Direction–Of–Arrival) associated with each interferer. The average power and the DOA associated with each interferer are available in the form of databases which contain different interference situations. These databases are distinguished by the combination (r, K). The main assumptions made when producing the said databases are listed in the following, see also [14, 13] for a more detailed analysis:
   - The locations of the BSs are chosen to form a regular hexagonal grid and at least two tiers of BSs around the reference cell are considered.
   - The locations of the MSs are randomly and uniformly distributed within the cellular network. The locations of any two MSs are statistically independent from each other.
   - The slow fading is described by a simple but widespread Hata–like link gain model which accounts for shadowing effects [14].
   - A power control algorithm is implemented for the complete cellular network. According to this algorithm, the transmit power at the BS for each MS is chosen in such a way that the average received carrier power at that MS has a constant value. This power control algorithm compensates only for large–scale variations of the received signals due to slow fading.
   - Handover is assumed to be perfectly power controlled.
2. Second, based on the COST 207 channel models [10] modeling the fast fading characteristics of the mobile radio channel, channel impulse responses are generated for the intracell interference, i.e., the connections between the MSs and the BS of the considered reference cell.
3. Third, data transmission is simulated for a small time duration T_{sim} under consideration of both the intercell interference, see the first step of the method, and the intracell interference, see the second step of the method. It is noted that the time duration of the data transmission is selected such that, on the one hand, the shadowing conditions do not change significantly within T_{sim} and, on the other hand, the number of counted bit errors is sufficiently large for determining a reliable value of P_{b} for each user active in the reference cell.

The outcome of each experiment is the value of P_{b} for each user from the third step. Then, after a great number of experiments is performed, the values of P_{b} from each experiment can be used for approximating the outage probability P_{o}, see (25). Certainly, if the outage probability P_{o} is available, then it can be decided if the QoS criterion, see (26), is fulfilled for the considered combination (r, K) and system operation situation. The combination which maximizes η, see (24), should be used for determining the spectrum efficiency for the considered system operation situation.

Table 1. Spectrum efficiency η of the TD–CDMA downlink according to (24) for the two investigated system operation situations; novel scheme

system operation situation	r	K	η in $\frac{\mathrm{bit/s}}{\mathrm{Hz}}$ per cell
COST 207 RA; $v = 3$ km/h; $K_{\mathrm{a}} = 1$	1	1	0.078
COST 207 BU; $v = 3$ km/h; $K_{\mathrm{a}} = 1$	1	2	0.156

Table 2. Spectrum efficiency η of the TD–CDMA downlink according to (24) for the two investigated system operation situations; conventional scheme

system operation situation	r	K	η in $\frac{\mathrm{bit/s}}{\mathrm{Hz}}$ per cell
COST 207 RA; $v = 3$ km/h; $K_{\mathrm{a}} = 1$	4	2	0.030
COST 207 BU; $v = 3$ km/h; $K_{\mathrm{a}} = 1$	4	4	0.06

The goal of the simulations performed by the described method is the fair comparison between the novel and the conventional scheme for the downlink of TD–CDMA in different macrocellular propagation environments. The parameters of TD–CDMA used in the simulations can be found in [13, 11]. Furthermore, the following system operation situations are investigated for both downlink transmission schemes:

- COST 207 rural area (RA) channel model, $v = 3$ km/h, $K_{\mathrm{a}} = 1$,
- COST 207 bad urban (BU) channel model, $v = 3$ km/h, $K_{\mathrm{a}} = 1$.

For specifying a QoS criterion, $P_{\mathrm{b}}^{\mathrm{M}}$ and $P_{\mathrm{o}}^{\mathrm{M}}$, see above in this section, are chosen to be equal to 10^{-3} and $5 \cdot 10^{-2}$, respectively. The chosen values for $P_{\mathrm{b}}^{\mathrm{M}}$ and $P_{\mathrm{o}}^{\mathrm{M}}$ are typical for speech services and are in accordance with [7, 8, 13]. Further, half of the time slots of a frame are used for downlink transmission. Finally, since the novel scheme does not require training sequences in the burst format, the information rate per user of the novel scheme, see the parameter R in (24), equals 1.3 times the information rate per user of the conventional scheme.

The combinations (r, K) which maximize the spectrum efficiency η, see (24), as well as the values of η achieved by the novel scheme for the two investigated system operation situations are presented in Table 1. The corresponding values achieved by the application of the conventional scheme for the two investigated system operation situations are presented in Table 2. By comparing Table 1 with Table 2 the superiority of the novel scheme with respect to the achieved system spectrum efficiency is obvious, compared to the conventional scheme. The improvement factor of the spectrum efficiency equals 2.6 for both COST 207 RA and COST 207 BU channel models, compare Table 1 with Table 2. Certainly, the increased diversity offered by the COST 207 BU channel models compared to the COST 207 RA channel models [1] leads to higher values of the spectrum efficiency for both the novel and the conventional scheme, see Table 1 and Table 2. As a final remark, the significant improvement of the spectrum efficiency of the TD–CDMA downlink achieved by the novel scheme, compared to the conventional one, is in accordance with the simulation results presented in Section 4.2 regarding the BER performance, i.e., the improvement achieved by the novel scheme concerning the BER performance of the TD–CDMA downlink, compared to the conventional scheme, is translated into an improvement of the spectrum efficiency of the TD–CDMA downlink.

5 Conclusions

In this paper, a novel multiuser transmission scheme is presented for the downlink of TD–CDMA operating in the TDD mode, which utilizes the equality of the mobile radio channel impulse responses between the uplink and the downlink, when TDD is applied. According to this scheme, no training sequences are mandatory in the downlink burst format, no channel estimation is necessary at the MSs and the data detection effort is dramatically reduced, compared to the the conventional TD–CDMA downlink concept. In addition to these advantages, the novel scheme outperforms the conventional one in terms of both the BER performance and the achieved spectrum efficiency. Therefore, the proposed multiuser transmission scheme constitutes a promising method for increasing the capacity of the downlink of TD–CDMA, while the implementation of low–cost mobile handsets is also feasible.

Acknowledgement

The authors are indebted to Deutsche Forschungsgemeinschaft (DFG) for sponsoring part of this work within “DFG Schwerpunktprogramm Mobilkommunikation”. They are also grateful to the staffs of the Central Computer Facility (RHRK) of the University of Kaiserslautern for sustained technical support. Stimulating discussions with Prof. J. Nossek of TU Munich and his group are gratefully acknowledged.

References

[1] A. Klein, *Multi–user detection of CDMA–signals — algorithms and their application to cellular mobile radio*, Fortschrittberichte VDI, series 10, no. 423, VDI–Verlag, Düsseldorf, 1996.

[2] E. Nikula, A. Toskala, E. Dahlman, Girard L. and A. Klein, “FRAMES multiple access for UMTS and IMT–2000”, *IEEE Personal Communications*, pp. 16–24, April 1998.

[3] J.D. Parsons, *The mobile radio propagation channel*, Pentech Press, London, 1992.

[4] B. Steiner and A. Klein, “Kanal– und Datenschätzung in synchronen CDMA–Mobilfunksystemen mit Interferenzeleminierung ”, *Kleinheubacher Berichte*, vol. 36, pp. 253–268, 1993.

[5] M. Meurer, P.W. Baier, T. Weber, Y. Lu, and A. Papathanassiou, “Joint transmission, an advantageous downlink concept for CDMA mobile radio systems using time division duplexing,” *IEE ELECTRONICS LETTERS*, vol. 36, pp. 900–901, 2000.

[6] G.R. Walsh, *Methods of optimization*, John Wiley and Sons, 1975.

[7] P.W. Baier, J.J. Blanz and R.M. Schmalenberger, “Fundamentals of smart antennas for mobile radio applications”, *Proc. IEEE* $8^{\rm th}$ *International Symposium on Personal, Indoor and Mobile Radio Communications (PIMRC’97)*, Helsinki, 1997, pp. 345–376.

[8] J.J. Blanz, R.M. Schmalenberger, A. Papathanassiou and P. Jung, “Smart antenna concepts for time-slotted CDMA”, *Proc. IEEE* $47^{\rm th}$ *Vehicular Technology Conference (VTC’97)*, pp. 11–15, Phoenix, 1997.

[9] M.C. Jeruchim, P. Balaban and K.S. Shanmugan, *Simulation of communication systems*, Plenum Press, New York, 1992.

[10] COST 207, *Digital land mobile radio communications*, Office for Official Publications of the European Communities, Luxembourg, 1989.

[11] A. Papathanassiou, J. Oster and P.W. Baier, “A novel simulation concept of reduced computational cost for TD–CDMA mobile radio systems with adaptive antennas”, *Proc. IEEE* $50^{\rm th}$ *Vehicular Technology Conference (VTC’99 Fall)*, pp. 218–222, Amsterdam, 1999.

[12] M. Haardt, A. Klein, R. Koehn, S. Oestreich, M. Purat, V. Sommer, and T. Ulrich, “The TD–CDMA based UTRA TDD mode,” *IEEE Journal on Selected Areas in Communications*, vol. 18, 2000, to appear in the august issue on Wideband CDMA.

[13] A. Papathanassiou, C. Hartmann and T. Weber, “Uplink spectrum efficiency and capacity of TD–CDMA with adaptive antennas”, *COST259 TD (99) 113*, Leidschendam, 1999.

[14] A. Steil, “Statistics of the carrier–to–interference ratio in C/TDMA cellular mobile radio systems applying multi–user detection”, *Wireless Personal Communications*, vol. 5, pp. 259–277, 1997.

Kapitel 4

Optimale Verfahren der gemeinsamen Sendesignalerzeugung bei unkonventionellen Empfängern

Das vorliegende Kapitel befaßt sich mit dem optimalen Verfahren der gemeinsamen Sendesignalerzeugung für unkonventionelle Empfänger, das als optimale senderseitige nichtlineare Interferenzeliminierung (engl. optimum transmit nonlinear zero forcing, opt. TxNZF) bezeichnet wird. Ausgehend von den in den Kapiteln 2 und 3 behandelten Verfahren der gemeinsamen Sendesignalerzeugung für konventionelle Empfänger wird im Rahmen der Veröffentlichung [MWQ04b] verdeutlicht, infolge welcher Grundprinzipien die Leistungsfähigkeit von Empfängerorientierung durch den Einsatz unkonventioneller Empfänger gesteigert werden kann. Für den allgemeinen Fall eines empfängerseitig eingesetzten allgemeinen unkonventionellen Quantisierungsschemas wird gezeigt, wie die gemeinsame Sendesignalerzeugung in einer hinsichtlich der Erzielung minimaler Übertragungsfehlerwahrscheinlichkeiten optimalen Art und Weise zu erfolgen hat. Dabei wird vereinfachend davon ausgegangen, daß Interferenz bei der empfängerorientierten Funkkommunikation vollständig vermieden werden soll. Ein hinsichtlich des genannten Ziels optimales Verfahren der gemeinsamen Sendesignalerzeugung, das nicht auf totale Interferenzeliminierung abzielt, ist nach Kenntnis des Verfassers bisher nicht bekannt und Gegenstand weiter Forschungsaktivitäten.

Im einzelnen werden in [MWQ04b] die folgenden wichtigen Aspekte behandelt:

- Ausgehend von empfängerorientierter Funkkommunikation mit konventionellen Empfängern werden die Prinzipien der Leistungssteigerung durch Verwenden unkonventioneller Empfänger aufgezeigt.
- Das zum Erzielen dieser Leistungssteigerung zu verwendende Verfahren der gemeinsamen Sendesignalerzeugung für unkonventionelle Empfänger opt. TxNZF wird mathematisch beschrieben und durch den zugehörigen Modulatoroperator $\mathcal{M}\{\cdot\}$ beschrieben.
- Die Gewinne, die durch das optimale Verfahren der gemeinsamen Sendesignalerzeugung für unkonventionelle Empfänger im Vergleich zu Verfahren der gemeinsamen Sendesignalerzeugung für konventionelle Empfänger erzielbar sind, werden sowohl analytisch abgeschätzt als auch durch detaillierte Simulationen beurteilt.

[MWQ04b] Meurer, M.; Weber, T.; Qiu, W.: "Transmit Nonlinear Zero Forcing: Energy efficient receiver oriented transmission in MIMO CDMA mobile radio downlinks". *Proc. IEEE 8th International Symposium on Spread Spectrum Techniques & Applications (ISSSTA'04)*, Sydney, 2004, S. 260–269.

Transmit Nonlinear Zero Forcing: Energy Efficient Receiver Oriented Transmission in MIMO CDMA Mobile Radio Downlinks

M. Meurer, T. Weber, W. Qiu
Research Group for RF Communications, University of Kaiserslautern
P.O. Box 3049, D-67653 Kaiserslautern, Germany, email: meurer@rhrk.uni-kl.de

Abstract— **For the downlink of MIMO TDD/CDMA mobile radio systems transmission schemes were recently proposed, which can be classified as receiver (Rx) oriented. A main asset of these schemes is their low receiver complexity. In addition, they do without sacrificing downlink transmission resources to training signals for channel estimation, which is beneficial for capacity. First investigations concerned linear transmitter (Tx) algorithms and nonlinear Tx algorithms based on the principle of Tomlinson-Harashima Precoding, which both, especially in scenarios with high system loads, show an unsatisfactory performance. Optimum nonlinear Tx algorithms studied later by Peel et al. circumvent this performance drawback but have been shown to be far from being feasible in today's mobile radio systems. In this paper we try to fill the gap between the feasible Tx algorithms with their performance drawback and the optimum Tx algorithm by a scalable nonlinear transmitter algorithm termed Transmit Nonlinear Zero Forcing (TxNZF). The crux of said Tx algorithm consists in designing the transmitted signal at the access point (AP) groupwise by a nonlinear approach, and in using multiply connected decision regions in the detectors of the mobile terminals (MT). Doing so TxNZF achieves almost optimum performance.**

Keywords— **CDMA, multi-user MIMO downlinks, Rx orientation, precoding**

I. INTRODUCTION

Conventional transmission schemes can be classified as Tx oriented [1]. The opposite to Tx orientation is Rx orientation [1], in which the receiver algorithms are *a priori* given and made known to the transmitter, whereas the transmitter algorithms, possibly under consideration of channel information, are *a posteriori* adapted correspondingly. Although ideas similar to the rationale Rx orientation came up more than five years ago [2–7], it was only recently that this rationale was clearly formulated and a systematical study has begun. This late perception of Rx orientation is astonishing, because each of the two approaches has its distinct pros. The most important advantage of Rx orientation might be that the *a priori* chosen receiver algorithms can be chosen with a view to arrive at particularly simple receiver structures. Therefore, if we consider as an important example of radio transmission, mobile radio systems, the quasi natural choice in the downlink (DL) would be Rx orientation, because this leads to low cost receivers at the mobile terminals (MTs) [8].

For multi-user CDMA mobile radio downlinks, the first proposals for Rx oriented transmission concerned linear transmission schemes which base on the rationales Transmit Matched Filter (TxMF) [2, 3, 9], Transmit Minimum Mean Square Error (TxMMSE) [4, 9] or Transmit Zero Forcing (TxZF) [4, 5, 7] and which were later extended to multi-user MIMO structures [1]. These three linear schemes differ from each other by the way in which the problems of intersymbol interference (ISI) and multiple access interference (MAI) are addressed when designing the transmitted signals [10]. Whereas in TxMF both ISI and MAI are totally neglected while maximizing the useful energies at the receivers, in TxZF both kinds of interferences are perfectly avoided for the price of reduced useful energies at the receivers. In TxMMSE a well balanced equilibrium between residual interferences and useful energies at the receivers is established. To summarize, there seems roughly speaking to be a rule, telling us, the less distinct the impact of residual interferences at the MTs, the smaller the useful energies at the MTs for a given energy of the transmitted signal.

For the robustness of the data transmission against transmission errors both the useful energies at the receivers, here at the MTs – which should be as high as possible – and the amount of residual interferences – which should be kept as small as possible – are important. Therefore, independent of which of the three mentioned approaches TxMF, TxMMSE or TxZF is chosen for data transmission, the mentioned robustness is limited by at least one of the two aforementioned factors. This drawback can only be overcome by investing sufficiently high transmit energies at the access point (AP) side, although in mobile radio applications these transmit energies should be as low as possible to keep intercell interferences low and, thereby, capacity high, and also with respect to the growing electro-phobia of the public.

To circumvent said drawback it was only recently [11, 12] that for Rx oriented transmission nonlinear approaches, which exploit the discrete nature of the data symbol alphabet and which focused on simply connected quantization schemes at the receivers attained attraction. However, it turned out that these techniques alone can not combat the problem of possibly high transmit energies [11, 12] [11, 12].

To overcome this problem Fischer et al. [13] and Erez et al. [14] proposed to further develop the idea of Tomlinson-Harashima Precoding (THP) already published more then 30 years ago [15, 16]. The crux of these approaches consists in resorting to lattice structured or, more generally, to multiply connected quantization schemes. It will become clear in the paper that this choice for the quantization scheme in combination with a suitable nonlinear signal processing at the transmitter is crucial to overcome the aforementioned problem of possibly high transmit energies. However, both approaches of [13] and [14] are known to be suboptimum [17], i.e., still show a rather moderate transmission performance, due to the symbol-by-symbol processing strategy followed therein. Peel et al. [18] have recently introduced a "vector perturbation technique" that circumvents this problem by jointly optimizing the transmitted signal taking simultaneously into account all data symbols to be transmitted. However, the technique proposed in [18]

- is only suitable for lattice structured quantization schemes and
- can only perform the mentioned joint optimization with a rather high signal processing effort if several MTs have to be served simultaneously.

In the present work we show how one might overcome these two problems by going to a novel more general framework for transmit signal design termed Transmit Nonlinear Zero Forcing (TxNZF). The crux of TxNZF consists in

- establishing a general framework which comprises both the suboptimum THP based approaches of Fischer et al. [13] and Erez et al. [14] and the optimum solution proposed by Peel et al. [18] as special cases,
- generalizing these results for arbitrary unconventional multiply connected quantization schemes and
- resorting in a novel way to a scalable groupwise processing strategy allowing to almost freely balance computational complexity versus transmission performance.

It turns out that this approach is particularly effective, i.e., achieves an almost optimum transmission performance with, compared to the approach of Peel et al. [18], a massively reduced computational complexity, if the channel attenuations from the AP to the individual MTs differ significantly, as it is usually the case in real world systems.

II. Generic multi-user MIMO downlink transmission model

A. Data transmission

We consider a situation, where an access point (AP) supports K MTs $k, k = 1 \dots K$. The AP is equipped with K_B transmit antennas and each of the K MTs employs K_M receive antennas. The N data symbols $\underline{d}_n^{(k)}, n = 1 \dots N$, to be transmitted from the AP to each MT $k, k = 1 \dots K$, are arranged in the MT specific data vector

$$\underline{\mathbf{d}}^{(k)} = \left(\underline{d}_1^{(k)} \dots \underline{d}_N^{(k)}\right)^\mathrm{T} \tag{1}$$

of dimension N and are stacked to the total data vector

$$\underline{\mathbf{d}} = \left(\underline{\mathbf{d}}^{(1)^\mathrm{T}} \dots \underline{\mathbf{d}}^{(K)^\mathrm{T}}\right)^\mathrm{T} = \left(\underline{d}_1 \dots \underline{d}_{N_\mathrm{t}}\right)^\mathrm{T} \tag{2}$$

of dimension N_t equal to KN. The elements $\underline{d}_n, n = 1 \dots N$, of $\underline{\mathbf{d}}$ of (2) are taken from a finite data symbol alphabet

$$\mathbb{V}_\mathrm{d} = \left\{\underline{\nu}_1 \dots \underline{\nu}_M\right\} \tag{3}$$

of cardinality M. Therefore each element $\underline{d}_n, n = 1 \dots N_\mathrm{t}$, of (2) is equal to a specific realization $\underline{\nu}_{m_n}$, where $m_n, m_n \in \{1 \dots M\}$, is a data symbol specific index describing which of the possible realizations the respective data symbol $\underline{d}_n$ takes. $\underline{\mathbf{d}}$ of (2) is assumed to be wide sense stationary with zero mean and the covariance matrix

$$\underline{\mathbf{R}}_\mathrm{d} = \mathop{\mathrm{E}}_{\underline{\mathrm{d}}}\left\{\underline{\mathbf{d}}\,\underline{\mathbf{d}}^\mathrm{H}\right\} = E_\mathrm{d} \cdot \mathbf{I}^{(N_\mathrm{t})}. \tag{4}$$

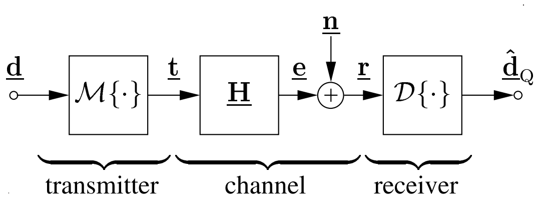

Fig. 1. Generic multi-user MIMO downlink transmission model

By modulation based on $\underline{\mathbf{d}}$ of (2) for each of the K_B transmit antennas an antenna specific transmitted signal $\underline{\mathbf{t}}^{(k_\mathrm{B})}$ of dimension Q_t is generated, which are stacked to the signal

$$\underline{\mathbf{t}} = \left(\underline{\mathbf{t}}^{(1)^\mathrm{T}} \dots \underline{\mathbf{t}}^{(K_\mathrm{B})^\mathrm{T}}\right)^\mathrm{T} \in \mathbb{C}^{(K_\mathrm{B} Q_\mathrm{t})} \tag{5}$$

termed (total) transmitted signal. The synthesis of $\underline{\mathbf{t}}$ of (5) based on $\underline{\mathbf{d}}$ of (2) can generally be described by

$$\underline{\mathbf{t}} = \mathcal{M}\{\underline{\mathbf{d}}\}, \tag{6}$$

where $\mathcal{M}\{\cdot\}$ denotes an operator termed modulator operator. Via (6) the N_t components of (2) are mapped onto the $K_\mathrm{B} Q_\mathrm{t}$ components of $\underline{\mathbf{t}}$ of (5). Setting out from (6) the energy invested to transmit $\underline{\mathbf{t}}$, which is termed transmitted energy in the following, becomes

$$T = \frac{1}{2} \underline{\mathbf{t}}^\mathrm{H} \underline{\mathbf{t}}. \tag{7}$$

The frequency selective MIMO channel between the AP and MT k is assumed to be linear and is characterized by the $K K_\mathrm{B} K_\mathrm{M}$ channel impulse responses $\underline{\mathbf{h}}^{(k,k_\mathrm{B},k_\mathrm{M})}$ of dimension W [1]. Using $\underline{\mathbf{h}}^{(k,k_\mathrm{B},k_\mathrm{M})}$ the K MT specific channel matrices $\underline{\mathbf{H}}^{(k)}$ of dimension $[K_\mathrm{M}(Q_\mathrm{t} + W - 1)] \times (K_\mathrm{B} Q_\mathrm{t})$ and the total channel matrix

$$\underline{\mathbf{H}} = \left(\underline{\mathbf{H}}^{(1)^\mathrm{T}} \dots \underline{\mathbf{H}}^{(K)^\mathrm{T}}\right)^\mathrm{T} \in \mathbb{C}^{[K K_\mathrm{M}(Q_\mathrm{t}+W-1)] \times (K_\mathrm{B} Q_\mathrm{t})} \tag{8}$$

can be established. The total transmitted signal $\underline{\mathbf{t}}$ of (5) leads to the noisefree received signals $\underline{\mathbf{e}}^{(k)}$ of dimension $[K_\mathrm{M}(Q_\mathrm{t} + W - 1)]$ of the MTs $k, k = 1 \dots K$, which are stacked in the total noisefree received signal

$$\underline{\mathbf{e}} = \left(\underline{\mathbf{e}}^{(1)^\mathrm{T}} \dots \underline{\mathbf{e}}^{(K)^\mathrm{T}}\right)^\mathrm{T} = \underline{\mathbf{H}}\,\underline{\mathbf{t}} \in \mathbb{C}^{[K K_\mathrm{M}(Q_\mathrm{t}+W-1)]}. \tag{9}$$

If $\underline{\mathbf{e}}^{(k)}$ is corrupted by an additive noise signal $\underline{\mathbf{n}}^{(k)}$ then we obtain the noisy received signal $\underline{\mathbf{r}}^{(k)}$ of MT k. By stacking $\underline{\mathbf{r}}^{(k)}$, $k = 1 \dots K$, follows the total noisy received signal

$$\underline{\mathbf{r}} = \left(\underline{\mathbf{r}}^{(1)^\mathrm{T}} \dots \underline{\mathbf{r}}^{(K)^\mathrm{T}}\right)^\mathrm{T} = \underline{\mathbf{e}} + \underline{\mathbf{n}} = \underline{\mathbf{H}}\,\underline{\mathbf{t}} + \underline{\mathbf{n}}, \tag{10}$$

where $\underline{\mathbf{n}}$ denotes the concatenation of $\underline{\mathbf{n}}^{(k)}$, $k = 1 \dots K$, termed total noise signal. $\underline{\mathbf{n}}$ of (10) is assumed to be Gaussian, wide sense stationary with zero mean, independent of $\underline{\mathbf{d}}$ of (2), and to have the covariance matrix

$$\underline{\mathbf{R}}_\mathrm{n} = \mathop{\mathrm{E}}_{\underline{\mathrm{n}}}\left\{\underline{\mathbf{n}}\,\underline{\mathbf{n}}^\mathrm{H}\right\}. \tag{11}$$

The signal transmission model developed in (1) – (10) is summarized in Fig. 1.

B. Data Detection

The detector of each MT $k, k = 1 \dots K$, determines based on $\underline{\mathbf{r}}^{(k)}$ of (10) an estimate $\underline{\widehat{\mathbf{d}}}_{\mathrm{Q}}^{(k)}$ of $\underline{\mathbf{d}}^{(k)}$ of (1). Stacking the estimates $\underline{\widehat{\mathbf{d}}}_{\mathrm{Q}}^{(k)}, k = 1 \dots K$, results in a total data estimate

$$\underline{\widehat{\mathbf{d}}}_{\mathrm{Q}} = \left(\underline{\widehat{\mathbf{d}}}_{\mathrm{Q}}^{(1)^{\mathrm{T}}} \dots \underline{\widehat{\mathbf{d}}}_{\mathrm{Q}}^{(K)^{\mathrm{T}}}\right)^{\mathrm{T}} = \left(\underline{\widehat{d}}_{\mathrm{Q},1} \dots \underline{\widehat{d}}_{\mathrm{Q},N_{\mathrm{t}}}\right)^{\mathrm{T}} \in \mathbb{V}_{\mathrm{d}}^{N_{\mathrm{t}}}, \quad (12)$$

of the total data vector $\underline{\mathbf{d}}$ of (2). In analogy to the procedure of (6) the generation of $\underline{\widehat{\mathbf{d}}}_{\mathrm{Q}}$ based on $\underline{\mathbf{r}}$ can generally be described by a detector operator $\mathcal{D}\{\cdot\}$ by

$$\underline{\widehat{\mathbf{d}}}_{\mathrm{Q}} = \mathcal{D}\{\underline{\mathbf{r}}\}. \quad (13)$$

In this contribution we focus on Rx oriented transmission which aims at a rather simple design of the receivers at the MTs. Therefore we assume that the generation of each element $\underline{\widehat{d}}_{\mathrm{Q},n}, n = 1 \dots N_{\mathrm{t}}$, of $\underline{\widehat{\mathbf{d}}}_{\mathrm{Q}}$ is performed in a quite simple two-step manner:

1. In a first step for each data symbol $\underline{d}_n^{(k)}, n = 1 \dots N$, of MT $k, k = 1 \dots K$, a continuous-valued estimate $\underline{\widehat{d}}_n^{(k)}$ is generated by linear filtering of $\underline{\mathbf{r}}^{(k)}$, i.e., the continuous-valued estimate $\underline{\widehat{\mathbf{d}}}^{(k)}$ of $\underline{\mathbf{d}}^{(k)}$ of (2) results from

$$\underline{\widehat{\mathbf{d}}}^{(k)} = \underline{\mathbf{D}}^{(k)}\underline{\mathbf{r}}^{(k)}, \quad (14)$$

where $\underline{\mathbf{D}}^{(k)}$ is a matrix of dimension $[N \times K_{\mathrm{M}}(Q_{\mathrm{t}}+W-1)]$ termed MT specific demodulator matrix. As we focus on CDMA mobile radio systems, the choice of $\underline{\mathbf{D}}^{(k)}$ depends on the CDMA code assigned to that MT k [8]. With $\underline{\widehat{\mathbf{d}}}^{(k)}, k = 1 \dots K$, of (14), one obtains the total continuous-valued data vector

$$\underline{\widehat{\mathbf{d}}} = \left(\underline{\widehat{\mathbf{d}}}^{(1)^{\mathrm{T}}} \dots \underline{\widehat{\mathbf{d}}}^{(K)^{\mathrm{T}}}\right)^{\mathrm{T}} = \left(\underline{\widehat{d}}_1 \dots \underline{\widehat{d}}_{N_{\mathrm{t}}}\right)^{\mathrm{T}}. \quad (15)$$

2. In a second step, to obtain $\underline{\widehat{d}}_{\mathrm{Q},n}$, each continuous-valued estimate $\underline{\widehat{d}}_n, n = 1 \dots N_{\mathrm{t}}$, is quantized according to

$$\underline{\widehat{d}}_{\mathrm{Q},n} = \mathrm{Q}\left(\underline{\widehat{d}}_n\right) \quad (16)$$

and therefore mapped to one of the elements of $\mathbb{V}_{\mathrm{d}}$ of (3) by means of the quantization function $\mathrm{Q}(\cdot)$.

Using the total demodulator matrix

$$\underline{\mathbf{D}} = \mathrm{blockdiag}\left(\underline{\mathbf{D}}^{(1)} \dots \underline{\mathbf{D}}^{(K)}\right) \in \mathbb{C}^{(KN) \times [KK_{\mathrm{M}}(Q_{\mathrm{t}}+W-1)]} \quad (17)$$

both steps can be described in the comprehensive form

$$\underline{\widehat{\mathbf{d}}} = \underline{\mathbf{D}}\,\underline{\mathbf{r}}, \ \ \underline{\widehat{\mathbf{d}}}_{\mathrm{Q}} = \mathrm{Q}\left(\underline{\widehat{\mathbf{d}}}\right) = \mathrm{Q}\left(\underline{\mathbf{D}}\,\underline{\mathbf{r}}\right), \quad (18)$$

where the notation $\mathrm{Q}\left(\underline{\widehat{\mathbf{d}}}\right)$ in (18) means that the quantization function $\mathrm{Q}(\cdot)$ of (16) is applied to each of the N_{t} components

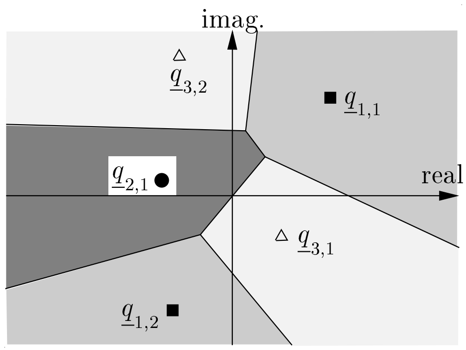

Fig. 2. Example of an unconventional quantization scheme for $M = 3$, $P^{(1)} = P^{(3)} = 2, P^{(2)} = 1$; same symbols correspond to the same realization $\underline{\nu}_m$

of the vector $\underline{\widehat{\mathbf{d}}}$. Finally with (6), (10) and (18) one obtains the total description

$$\underline{\widehat{\mathbf{d}}} = \underbrace{\underline{\mathbf{D}}\,\underline{\mathbf{H}}}_{\underline{\mathbf{B}}}\,\mathcal{M}\{\underline{\mathbf{d}}\} + \underline{\mathbf{D}}\,\underline{\mathbf{n}} \quad (19)$$

of the relation between $\underline{\widehat{\mathbf{d}}}$ of (15) and $\underline{\mathbf{d}}$ of (2). In (19) the matrix $\underline{\mathbf{B}}$ of dimension $N_{\mathrm{t}} \times (K_{\mathrm{B}}Q_{\mathrm{t}})$ is termed system matrix.

C. Quantization scheme

Concerning the quantization function $\mathrm{Q}\left(\underline{\widehat{d}}_n\right)$ of (16) for each possible realization $\underline{\nu}_m, m = 1 \dots M$, of a data symbol $\underline{d}_n, n = 1 \dots N_{\mathrm{t}}$, in general multiple, here $P^{(m)}$ representatives $\underline{q}_{m,p}, p = 1 \dots P^{(m)}$, exist. The entirety of all these representatives $\underline{q}_{m,p}, p = 1 \dots P^{(m)}$, valid for a certain realization $\underline{\nu}_m$ of a data symbol is represented by the data symbol realization specific set

$$\mathbb{V}_{\mathrm{q},m} = \left\{\underline{q}_{m,1} \cdots \underline{q}_{m,P^{(m)}}\right\}. \quad (20)$$

The Voronoi regions $\mathbb{Q}_{m,p}$ of the representatives $\underline{q}_{m,p}, p = 1 \dots P^{(m)}, m = 1 \dots M$, are termed partial decision regions in the following. Setting out from the $P^{(m)}$ partial decision regions $\mathbb{Q}_{m,p}, p = 1 \dots P^{(m)}$, corresponding to the realization $\underline{\nu}_m$ of a data symbol, one obtains the respective decision region

$$\mathbb{Q}_m = \bigcup_{p=1}^{P^{(m)}} \mathbb{Q}_{m,p}. \quad (21)$$

$\mathbb{Q}_m$ of (21) describes a region consisting of $P^{(m)}$ non-connected partial decision regions. Therefore $\mathbb{Q}_m$ is termed a $P^{(m)}$-fold, or generally multiply, connected decision region. For the special case $P^{(m)}$ equal to one, $\mathbb{Q}_m$ is termed simply connected. We term a quantization scheme, in which

- all decision regions $\mathbb{Q}_m, m = 1 \dots M$, are simply connected and
- each representative $\underline{q}_{m,1}, m = 1 \dots M$, is equal to the corresponding data symbol value $\underline{\nu}_m$,

a conventional simply connected quantization scheme. Otherwise we term it an unconventional multiply connected quantization scheme. Having the M decision regions $\mathbb{Q}_m, m = 1 \dots M$, the quantization function $\mathrm{Q}\left(\widehat{\underline{d}}_n\right)$ of (16) can easily be written as

$$\mathrm{Q}\left(\widehat{\underline{d}}_n\right) = \underline{\nu}_m \text{with } \widehat{\underline{d}}_n \in \mathbb{Q}_m. \tag{22}$$

Fig. 2 shows an example for an unconventional quantization scheme.

III. Transmit signal design for conventional quantization schemes

A. General

Techniques meanwhile quite well known to determine $\mathcal{M}\{\cdot\}$ based on $\underline{\mathbf{H}}$ and $\mathcal{D}\{\cdot\}$ can be classified as linear techniques and nonlinear techniques [11]. Nonlinear techniques allow to take the discrete nature of the data symbol alphabet $\mathbb{V}_\mathrm{d}$ of (3) into account and therefore have the potential to improve the transmission quality compared to linear techniques [11, 12]. However, it was shown in [11, 12] that the achievable gains for typical mobile radio scenarios are not significant. Moreover, it was one of the outcomes of [12] that the computational complexity is prohibitive for a practical implementation. Therefore, in this contribution the authors restrict themselves to linear techniques for transmit signal design if conventional quantization schemes are used at the MTs. It will become clear in the following Sections IV to VI why this focus is sufficient for the reasoning of the paper.

Linear techniques for transmit signal design are described by a linear modulator operator $\mathcal{M}\{\cdot\}$ of (6). With the $(K_\mathrm{B}Q_\mathrm{t}) \times N_\mathrm{t}$-matrix $\underline{\mathbf{M}}$ termed modulator matrix, one can write

$$\mathcal{M}\{\underline{\mathbf{d}}\} = \underline{\mathbf{M}}\,\underline{\mathbf{d}}. \tag{23}$$

In what follows, $[\cdot]_{n,n}$ designates the n-th diagonal element of a square matrix in brackets, and $[\cdot]_n$ stands for the n-th row of a matrix in brackets. Then, according to (4), (6) and (23) the mean transmitted energy invested for data symbol $\underline{d}_n$ becomes

$$T_n = \frac{1}{2}\left\|\left[\underline{\mathbf{M}}^\mathrm{T}\right]_n\right\|_2^2 \cdot E_\mathrm{d} = \frac{1}{2}\left[\underline{\mathbf{M}}^\mathrm{H}\underline{\mathbf{M}}\right]_{n,n} \cdot E_\mathrm{d}. \tag{24}$$

B. Transmit Matched Filter (TxMF)

The idea behind TxMF is the minimization of T_n for each data symbol $\underline{d}_n$, $n = 1 \ldots N_\mathrm{t}$, under the side condition that interference is neglected and unbiased data transmission is desired. This leads to the modulator matrix [2, 3, 9, 10]

$$\underline{\mathbf{M}}_\mathrm{TxMF} = \underline{\mathbf{B}}^\mathrm{H}\left[\mathrm{diag}\left(\underline{\mathbf{B}}\,\underline{\mathbf{B}}^\mathrm{H}\right)\right]^{-1}. \tag{25}$$

Due to the design criterion of TxMF explained above, the choice of (25) for the modulator matrix is optimum, with respect to the minimization of the data symbol specific transmitted energies $T_{\mathrm{MF},n}$ of (24), if unbiased data transmission is established. However if multiple data symbols are transmitted in parallel quite strong interferences might occur.

C. Transmit Zero forcing (TxZF)

TxZF totally eliminates interferences, both ISI and MAI. Therefore the inference contributions to $\widehat{\underline{d}}_n$, $n = 1 \ldots N_\mathrm{t}$, are made zero. While ensuring unbiased data transmission, the remaining degrees of freedom in the choice of $\underline{\mathbf{M}}_\mathrm{TxZF}$ are exploited for the minimization of the required transmitted energy T of (7) and simultaneously the minimization of the data symbol specific energies T_n, $n = 1 \ldots N_\mathrm{t}$, of (24). Following this idea one obtains

$$\underline{\mathbf{M}}_\mathrm{TxZF} = \underline{\mathbf{B}}^\mathrm{H}\left(\underline{\mathbf{B}}\,\underline{\mathbf{B}}^\mathrm{H}\right)^{-1} \tag{26}$$

for the modulator matrix $\underline{\mathbf{M}}$ of (23) [8–10]. The price to be paid for the elimination of interferences is an increase of the data symbol specific energies $T_{\mathrm{ZF},n}$ of (24) as compared to TxMF. This price is quantified by the transmit efficiency $\eta_{\mathrm{TxZF},n}$ which is defined as the ratio

$$\eta_{\mathrm{TxZF},n} = \frac{T_{\mathrm{MF},n}}{T_{\mathrm{ZF},n}} = \frac{1}{\left[\left(\underline{\mathbf{B}}\,\underline{\mathbf{B}}^\mathrm{H}\right)^{-1}\right]_{n,n} \cdot \left[\underline{\mathbf{B}}\,\underline{\mathbf{B}}^\mathrm{H}\right]_{n,n}} \tag{27}$$

of the symbol specific transmitted energies $T_{\mathrm{MF},n}$ and $T_{\mathrm{ZF},n}$, $n = 1 \ldots N_\mathrm{t}$, for TxMF and TxZF, respectively. The transmit efficiency $\eta_{\mathrm{TxZF},n}$ takes values from zero to one with one being the optimum. If the mobile radio channels are time-variant randomly block-fading channels and/or the demodulator $\underline{\mathbf{D}}$ changes, $\underline{\mathbf{B}}$ of (19) varies with time and can therefore be regarded as a random quantity. Consequently $\eta_{\mathrm{TxZF},n}$ of (27) is also a random quantity. An analysis of $\eta_{\mathrm{TxZF},n}$ preferably has to be done on a stochastical basis taking the stochastical properties of $\underline{\mathbf{B}}$ into account. If the elements of each row of $\underline{\mathbf{B}}$ are independent identically distributed (i.i.d.) Gaussian variables with zero mean and the same standard deviation, then the probability density function (pdf) of $\eta_{\mathrm{TxZF},n}$ can be derived in a closed form. As shown in detail in a further paper, one obtains

$$\mathrm{p}_{\eta_{\mathrm{TxZF},n}}(\eta) = \begin{cases} \frac{\eta^{K_\mathrm{B}Q_\mathrm{t}-N_\mathrm{t}}(1-\eta)^{N_\mathrm{t}-2}}{B(K_\mathrm{B}Q_\mathrm{t}-N_\mathrm{t}+1, N_\mathrm{t}-1)}, & 0 \le \eta \le 1, \\ 0, & \text{else,} \end{cases} \tag{28}$$

for the pdf of $\eta_{\mathrm{TxZF},n}$ of (27), where $B(\cdot,\cdot)$ denotes the beta-function [19]. Based on (28) the mean of $\eta_{\mathrm{TxZF},n}$ follows to be

$$\overline{\eta}_\mathrm{TxZF} = \mathrm{E}\{\eta_{\mathrm{TxZF},n}\} = \frac{K_\mathrm{B}Q_\mathrm{t} - (N_\mathrm{t}-1)}{K_\mathrm{B}Q_\mathrm{t}} \tag{29}$$

and the variance of $\eta_{\mathrm{TxZF},n}$ to be

$$\mathrm{var}\left(\eta_{\mathrm{TxZF},n}\right) = \frac{\left[K_\mathrm{B}Q_\mathrm{t} - (N_\mathrm{t}-1)\right](N_\mathrm{t}-1)}{\left(K_\mathrm{B}Q_\mathrm{t}\right)^2\left(K_\mathrm{B}Q_\mathrm{t}+1\right)}. \tag{30}$$

Obviously, $\overline{\eta}_\mathrm{TxZF}$ depends on the difference of two quantities,

- the number $K_\mathrm{B}Q_\mathrm{t}$ of degrees of freedom for transmit signal design, i.e., the number of elements of the total transmitted signal $\underline{\mathbf{t}}$ of (5), and
- the number $(N_\mathrm{t}-1)$ of restrictions due to interference avoidance while designing the contribution of each data symbol $\underline{d}_n$, $n = 1 \ldots N_\mathrm{t}$, to $\underline{\mathbf{t}}$.

If the number $K_\mathrm{B}Q_\mathrm{t}$ of degrees of freedom is large compared to $(N_\mathrm{t}-1)$, $\overline{\eta}_\mathrm{TxZF}$ tends to be close to one, otherwise it is between zero and one. A similar result to (29) has already been derived for the asymptotic case of infinitely large systems in [20] but is now proven to be a special case of the more general analysis presented in this paper. The result of (29) allows, roughly speaking to conclude a very fundamental rule which is also valid for other kinds for transmit signal design than TxZF: The more constrains have to be satisfied while designing the transmitted signal $\underline{\mathbf{t}}$ and the less degrees of freedom are available for this design process, the more transmitted energy has to be invested to achieve a desired transmission quality, i.e., the less energy efficient [1] is a technique for transmit signal design. Therefore, in order to achieve a desired transmission quality with moderate transmitted energy, in the following sections several measures are taken

- to decrease the number of constraints to be satisfied while designing the transmitted signal $\underline{\mathbf{t}}$ and
- to increase the number of degrees of freedom for transmit signal design.

IV. Transmit signal design for unconventional quantization schemes: optimum approach

A. Interference free transmission

If high quality data transmission between the AP and at least one MT should be established, the power of the noise at the inputs of the MTs has to be rather small compared to the available transmit powers. Therefore, interferences are the dominant performance limiting effects and have to be avoided. In the previous Section III it was shown that TxZF totally eliminates interferences. However, the dilemma of this and also other linear and nonlinear techniques for transmit signal design for receivers based on conventional quantization schemes is that it is generally not possible to simultaneously keep

- the impact of interferences low – or to totally avoid them –,
- the useful energies at the MTs high and
- the total transmitted energy T of (7) low.

This results, as already detailed in Section III, from the interaction between the number of degrees of freedom for transmit signal design and the number of restrictions to be satisfied thereby. If interference free transmission is desired, the number of restrictions is a fixed quantity. Therefore, the only possibility to relax the aforementioned dilemma is to increase the number of degrees of freedom for transmit signal design, preferably by resorting to multiply connected quantization schemes, which were already detailed in Section II. If multiply connected quantization schemes are applied, generally several representatives $\underline{q}_{m,p}$ are available for each data symbol realization $\underline{\nu}_m$. A technique for transmit signal design can exploit this additional degree of freedom in an advantageous way. About one year ago Peel et al. [18] proposed to go that way and showed how to exploit this potential in an optimal way, i.e., with the aim to invest a minimum transmitted energy T of (7). However, they only focused on multiply connected quantization schemes which base on a lattice structure. In this work we extend this idea to arbitrary multiply connected quantization schemes and use the gained insights to come up with a low-complexity near-optimum approximation termed Transmit Nonlinear Zero Forcing (TxNZF) detailed in the following Section V.

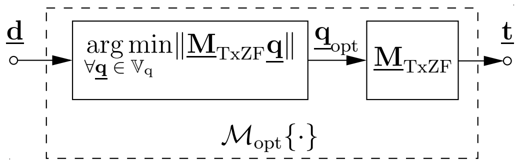

Fig. 3. Optimum transmit signal design for interference free transmission

If interference free unbiased data transmission should be established, then by properly designing the total transmitted signal $\underline{\mathbf{t}}$ of (5), for the expectation

$$\underline{q}_n = \mathop{\mathrm{E}}_{\underline{\mathrm{n}}}\left\{\widehat{\underline{d}}_n \middle| \underline{d}_n\right\} \tag{31}$$

of each continuous-valued estimate $\widehat{\underline{d}}_n$, $n = 1 \ldots N_{\mathrm{t}}$, $\underline{q}_n \in \mathbb{V}_{\mathrm{q},m_n}$ has to hold. Stacking the N_{t} values $\underline{q}_n$, $n = 1 \ldots N_{\mathrm{t}}$, one obtains a vector $\underline{\mathbf{q}}$ of dimension N_{t}, which describes the combination of selected representatives used to transmit a certain data vector $\underline{\mathbf{d}}$ without interferences. If $\underline{\mathbf{d}}$ is fixed, N_{q} equal to $P^{(m_1)} \cdot \ldots \cdot P^{(m_{N_{\mathrm{t}}})}$ different combinations of N_{t} representatives exist for $\underline{\mathbf{q}}$, which can be composed to the set

$$\mathbb{V}_{\mathrm{q}} = \left\{ \left(\underline{q}_1 \cdots \underline{q}_{N_{\mathrm{t}}}\right)^{\mathrm{T}} \middle| \underline{q}_n \in \mathbb{V}_{\mathrm{q},m_n}, \forall n = 1 \ldots N_{\mathrm{t}} \right\} \tag{32}$$

of cardinality N_{q}. Using the result of Section III for each possible choice of $\underline{\mathbf{q}} \in \mathbb{V}_{\mathrm{q}}$ a total transmitted signal

$$\underline{\mathbf{t}} = \underline{\mathbf{M}}_{\mathrm{TxZF}}\underline{\mathbf{q}} \tag{33}$$

can be compiled by TxZF. As shown in Section III, this choice for $\underline{\mathbf{t}}$ is optimum for the selected $\underline{\mathbf{q}}$ with respect to the minimization of the invested transmitted energy T of (7) and, at the same time, satisfies (31).

B. Optimum choice of $\underline{\mathbf{q}}$

The freedom of choosing for given $\underline{\mathbf{d}}$ a single combination $\underline{\mathbf{q}}$ out of N_{q} alternatives can be used to minimize the energy T of (7) of the transmitted total signal $\underline{\mathbf{t}}$ of (33). Doing so one obtains for the optimum choice

$$\underline{\mathbf{q}}_{\mathrm{opt}} = \arg\min_{\forall \underline{\mathbf{q}} \in \mathbb{V}_{\mathrm{q}}} \|\underline{\mathbf{M}}_{\mathrm{TxZF}}\underline{\mathbf{q}}\| \tag{34}$$

allowing to determine the corresponding optimum total transmitted signal

$$\underline{\mathbf{t}} = \underline{\mathbf{M}}_{\mathrm{TxZF}}\underline{\mathbf{q}}_{\mathrm{opt}}. \tag{35}$$

These two steps of (34) and (35) in combination with (20) and (32) define the mapping between the total data vector $\underline{\mathbf{d}}$ and the total transmitted signal $\underline{\mathbf{t}}$ and therefore constitute the optimum modulator operator $\mathcal{M}_{\mathrm{opt}}\{\cdot\}$ for interference free transmission. Fig. 3 summarizes this results.

Generally the minimization problem of (34) can only be solved by exhaustive search over all N_{q} possible choices for $\underline{\mathbf{q}}$, c.f. (32). Therefore the computational complexity increases exponentially in N_{t} and polynomially in $P^{(m)}$, $m = 1 \ldots M$. In [18] Peel et al. proposed to slightly relax this problem by using sphere-decoding strategies. Unfortunately, this approach still has exponential complexity [18] and is only applicable if the chosen multiply connected quantization scheme is based on a lattice structure [13]. However, for typical CDMA mobile radio systems where N_{t} is rather large, the complexity aspects are still prohibitive for the utilization of the optimum strategy for transmit signal design presented in this section. It is one of the main goals of this contribution to show how one might close the gap between the quite practical linear techniques of Section III with the explained performance drawbacks and the optimum strategy of this section with the mentioned complexity problem.

V. Transmit signal design for unconventional quantization schemes: low-complexity near-optimum approach

A. Basic concept

As motivated in Section IV, the usage of unconventional multiply connected quantization schemes is advantageous to overcome the problem of possibly high transmitted energies T. However, the optimum approach of Section IV suffers from its high computational complexity. Unfortunately, alternative strategies described in literature which base on extensions of THP [13, 14] and which show a significantly lower computational complexity than the optimum approach, show massive performance degradations compared to the optimum approach [17]. It is desirable to find a scalable technique which combines the advantages of both optimum approach and THP based approaches and which allows to almost freely balance computational complexity versus transmission performance.

In the following such a technique termed Transmit Nonlinear Zero Forcing (TxNZF) is described. The name TxNZF is motivated by the fact that both ISI and MAI are forced to zero by some sort of nonlinear signal processing.

The crux of TxNZF consists in a groupwise processing of the data symbols $\underline{d}_n$, $n = 1 \ldots N_{\mathrm{t}}$. For this reason the set

$$\mathbb{G} = \left\{ \underline{d}_1 \ldots \underline{d}_{N_{\mathrm{t}}} \right\} \tag{36}$$

containing all data symbols $\underline{d}_n$, $n = 1 \ldots N_{\mathrm{t}}$, to be transmitted from the AP to the K MTs is partitioned into G disjoint non-empty subsets $\mathbb{G}_g$, $g = 1 \ldots G$, termed groups, so that $\mathbb{G}$ is equal to $\mathbb{G}_1 \cup \ldots \cup \mathbb{G}_G$. Fig. 4 shows an example for such a partition for the case N_{t} equal to 8. For each group g, $g = 1 \ldots G$, a group specific transmitted signal $\underline{\mathbf{t}}_{\mathrm{G}}^{(g)}$ is generated. By superposition of all G group specific transmitted signals $\underline{\mathbf{t}}_{\mathrm{G}}^{(g)}$, $g = 1 \ldots G$, one obtains the total transmitted signal

$$\underline{\mathbf{t}} = \sum_{g=1}^{G} \underline{\mathbf{t}}_{\mathrm{G}}^{(g)}. \tag{37}$$

To answer the question how each group specific transmitted signal $\underline{\mathbf{t}}_{\mathrm{G}}^{(g)}$ is generated, the data symbols $\underline{d}_n$, $\underline{d}_n \in \mathbb{G}_g$, assigned to one and the same group g are combined to the group specific data vector

$$\underline{\mathbf{d}}_{\mathrm{G}}^{(g)} = \mathbf{S}_{\mathrm{G}}^{(g)} \underline{\mathbf{d}} \tag{38}$$

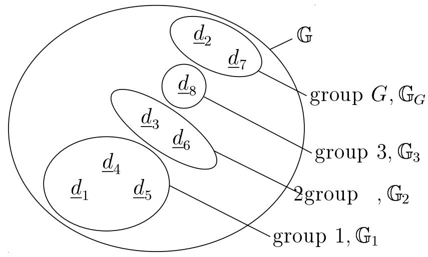

Fig. 4. Partition of set $\mathbb{G}_g$ of all data symbols into disjoint subsets $\mathbb{G}_g$, $g = 1 \ldots G$, termed groups

of dimension $\|\mathbb{G}_g\|$. The mapping between the total data vector $\underline{\mathbf{d}}$ of (2) and $\underline{\mathbf{d}}_{\mathrm{G}}^{(g)}$ is expressed by a $\|\mathbb{G}_g\| \times N_{\mathrm{t}}$-matrix $\mathbf{S}_{\mathrm{G}}^{(g)}$ termed selection matrix which has several properties:

- In each row of $\mathbf{S}_{\mathrm{G}}^{(g)}$ all elements are zero except of exactly one element which is one.
- Each column of $\mathbf{S}_{\mathrm{G}}^{(g)}$ only contains one element at most which is non-zero.

Even if a fixed partition $\mathbb{G}_g$, $g = 1 \ldots G$, of $\mathbb{G}$ of (36) is considered, generally different possibilities exist for the choice of the selection matrix $\mathbf{S}_{\mathrm{G}}^{(g)}$ due to different sorting orders of the data symbols $\underline{d}_n$, $\underline{d}_n \in \mathbb{G}_g$.

Based on $\mathbf{S}_{\mathrm{G}}^{(g)}$ of (38) the group specific system matrices

$$\underline{\mathbf{B}}_{\mathrm{G}}^{(g)} = \mathbf{S}_{\mathrm{G}}^{(g)} \underline{\mathbf{B}} \tag{39}$$

are established which contain all rows of $\underline{\mathbf{B}}$ of (19), which are related to the data symbols $\underline{d}_n$, $\underline{d}_n \in \mathbb{G}_g$, assigned to group g, $g = 1 \ldots G$. The continuous-valued estimate $\widehat{\underline{\mathbf{d}}}_{\mathrm{G}}^{(g)}$ of $\underline{\mathbf{d}}_{\mathrm{G}}^{(g)}$ of (38) follows by

$$\widehat{\underline{\mathbf{d}}}_{\mathrm{G}}^{(g)} = \mathbf{S}_{\mathrm{G}}^{(g)} \widehat{\underline{\mathbf{d}}} \tag{40}$$

using the continuous-valued estimate $\widehat{\underline{\mathbf{d}}}$ of the total data vector $\underline{\mathbf{d}}$ of (2). If the transmission of the data symbols $\underline{d}_n$, $\underline{d}_n \in \mathbb{G}_g$, assigned to group g, $g = 1 \ldots G$, should be unbiased and interference free then, in analogy to (31), for the expectation

$$\underline{\mathbf{q}}_{\mathrm{G}}^{(g)} = \left(\underline{q}_{\mathrm{G},1}^{(g)} \cdots \underline{q}_{\mathrm{G},\|\mathbb{G}_g\|}^{(g)} \right)^{\mathrm{T}} = \mathop{\mathrm{E}}_{\underline{\mathbf{n}}} \left\{ \widehat{\underline{\mathbf{d}}}_{\mathrm{G}}^{(g)} \middle| \underline{\mathbf{d}}_{\mathrm{G}}^{(g)} \right\} \tag{41}$$

of the continuous-valued estimate $\widehat{\underline{\mathbf{d}}}_{\mathrm{G}}^{(g)}$ of (40) the necessary and sufficient condition

$$\underline{\mathbf{q}}_{\mathrm{G}}^{(g)} = \mathbf{S}_{\mathrm{G}}^{(g)} \underline{\mathbf{q}}, \;\; \underline{\mathbf{q}} \in \mathbb{V}_{\mathrm{q}}, \tag{42}$$

has to be fulfilled. Quite generally, each component $\underline{q}_{\mathrm{G},n}^{(g)}$ of $\underline{\mathbf{q}}_{\mathrm{G}}^{(g)}$ of (41), which represents a specific data symbol $\underline{d}_{n'}$, $\underline{d}_{n'} \in \mathbb{G}_g$, comes about as the sum of an interference component $\underline{i}_{\mathrm{G},n}^{(g)}$ resulting from the transmission of other data symbols and a component $\underline{\Delta}_{\mathrm{G},n}^{(g)}$ intended for the transmission of this data symbol, i.e.,

$$\underline{q}_{\mathrm{G},n}^{(g)} = \underline{i}_{\mathrm{G},n}^{(g)} + \underline{\Delta}_{\mathrm{G},n}^{(g)}, n = 1 \ldots \|\mathbb{G}_g\|. \tag{43}$$

If (42) should be fulfilled, $\underline{\Delta}_{\mathrm{G},n}^{(g)}$ of (43) can be interpreted as the correction component necessary to obtain $\underline{q}_{\mathrm{G},n}^{(g)}$ under the influence of the interference $\underline{i}_{\mathrm{G},n}^{(g)}$.

By stacking $\underline{i}_{\mathrm{G},n}^{(g)}$, $n = 1 \ldots \|\mathbb{G}_g\|$, and $\underline{\Delta}_{\mathrm{G},n}^{(g)}$, $n = 1 \ldots \|\mathbb{G}_g\|$, to the vectors

$$\underline{\mathbf{i}}_{\mathrm{G}}^{(g)} = \left(\underline{i}_{\mathrm{G},1}^{(g)} \ldots \underline{i}_{\mathrm{G},\|\mathbb{G}_g\|}^{(g)}\right)^{\mathrm{T}} \tag{44}$$

and

$$\underline{\boldsymbol{\Delta}}_{\mathrm{G}}^{(g)} = \left(\underline{\Delta}_{\mathrm{G},1}^{(g)} \ldots \underline{\Delta}_{\mathrm{G},\|\mathbb{G}_g\|}^{(g)}\right)^{\mathrm{T}}, \tag{45}$$

respectively, the $\|\mathbb{G}_g\|$ relations of (43) are combined to

$$\underline{\mathbf{q}}_{\mathrm{G}}^{(g)} = \underline{\mathbf{i}}_{\mathrm{G}}^{(g)} + \underline{\boldsymbol{\Delta}}_{\mathrm{G}}^{(g)}. \tag{46}$$

This representation allows to define the following strategy for transmit signal design: The group specific transmitted signals $\underline{\mathbf{t}}_{\mathrm{G}}^{(g)}$, $g = 1 \ldots G$, of (37) are generated one by another, starting with $\underline{\mathbf{t}}_{\mathrm{G}}^{(1)}$. This sorting order implies no lack of generality as any sorting order could be achieved by appropriately relabeling the groups g, $g = 1 \ldots G$. The group specific transmit signal $\underline{\mathbf{t}}_{\mathrm{G}}^{(g)}$ for a certain group g, $g = 1 \ldots G$, is designed in such a way that $\underline{\mathbf{t}}_{\mathrm{G}}^{(g)}$

- produces no interferences to all data symbols $\underline{d}_n$, $\underline{d}_n \in \mathbb{G}_g$, assigned to that group,
- produces no interferences to all data symbols $\underline{d}_n$, $\underline{d}_n \in \mathbb{G}_{g'}$, $g' < g$, of subsequently processed groups and
- may produce interferences to all data symbols $\underline{d}_n$, $\underline{d}_n \in \mathbb{G}_{g'}$, $g' > g$, of groups to be processed in the following.

As a consequence of this procedure, the interference $\underline{\mathbf{i}}_{\mathrm{G}}^{(g)}$ of (44) only results from the transmission of the group specific transmitted signals $\underline{\mathbf{t}}_{\mathrm{G}}^{(g')}$, $g' < g$, i.e., can be calculated to be (step 1)

$$\underline{\mathbf{i}}_{\mathrm{G}}^{(g)} = \underline{\mathbf{B}}_{\mathrm{G}}^{(g)} \sum_{g'=1}^{g-1} \underline{\mathbf{t}}_{\mathrm{G}}^{(g')}, g > 1. \tag{47}$$

After choosing for the considered group g, $g = 1 \ldots G$, a certain $\underline{\mathbf{q}}_{\mathrm{G}}^{(g)}$ of (46) (step 2) – this choice will be detailed in Subsection V-B – with $\underline{\mathbf{i}}_{\mathrm{G}}^{(g)}$ of (47) the correction component $\underline{\boldsymbol{\Delta}}_{\mathrm{G}}^{(g)}$ has to be adjusted (step 3) to be

$$\underline{\boldsymbol{\Delta}}_{\mathrm{G}}^{(g)} = \underline{\mathbf{q}}_{\mathrm{G}}^{(g)} - \underline{\mathbf{i}}_{\mathrm{G}}^{(g)}, \tag{48}$$

if (42) should be satisfied. (48) can be fulfilled by appropriately designing the group specific transmitted signal $\underline{\mathbf{t}}_{\mathrm{G}}^{(g)}$; at the same time the above listed constrains concerning interference avoidance have to be taken into account. It is desirable that for given $\underline{\boldsymbol{\Delta}}_{\mathrm{G}}^{(g)}$ the corresponding $\underline{\mathbf{t}}_{\mathrm{G}}^{(g)}$ should have the lowest possible transmitted energy. Therefore, in order to fulfill the above explained interference constrains, using the cumulative matrices

$$\underline{\mathbf{B}}_g = \left(\underline{\mathbf{B}}_{\mathrm{G}}^{(1)\,\mathrm{T}} \ldots \underline{\mathbf{B}}_{\mathrm{G}}^{(g)\,\mathrm{T}}\right)^{\mathrm{T}}, g = 1 \ldots G, \tag{49}$$

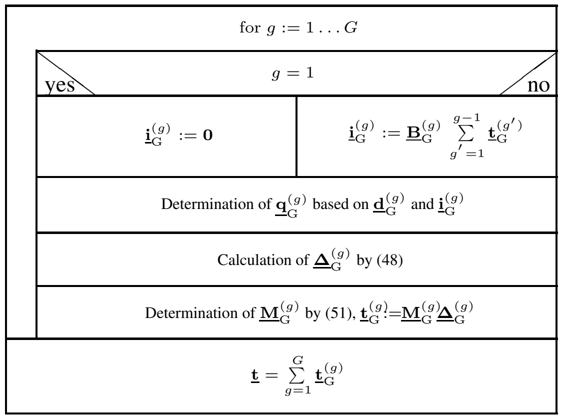

Fig. 5. Nassi-Shneiderman diagram describing the modulator operator $\mathcal{M}_{\mathrm{TxNZF}}\{\cdot\}$ for TxNZF, i.e., the generation of the transmitted signal $\underline{\mathbf{t}}$ in TxNZF

one obtains the optimum $\underline{\mathbf{t}}_{\mathrm{G}}^{(g)}$ by resorting to TxZF. Let us designate by $[\cdot]_i^j$ a matrix consisting of columns i to j of the matrix in brackets. Then the group specific transmitted signal $\underline{\mathbf{t}}_{\mathrm{G}}^{(g)}$ of group g can be calculated (step 4) as

$$\underline{\mathbf{t}}_{\mathrm{G}}^{(g)} = \underline{\mathbf{M}}_{\mathrm{G}}^{(g)} \underline{\boldsymbol{\Delta}}_{\mathrm{G}}^{(g)} \tag{50}$$

with

$$\underline{\mathbf{M}}_{\mathrm{G}}^{(g)} = \left[\underline{\mathbf{B}}_g{}^{\mathrm{H}} \left(\underline{\mathbf{B}}_g \underline{\mathbf{B}}_g{}^{\mathrm{H}}\right)^{-1}\right]_{\|\mathbb{G}_1 \cup \ldots \cup \mathbb{G}_g\|}^{\|\mathbb{G}_1 \cup \ldots \cup \mathbb{G}_{g-1}\|+1} \tag{51}$$

being the group specific modulator matrix. The efficient calculation of the matrix $\underline{\mathbf{M}}_{\mathrm{G}}^{(g)}$ of (51) can be performed by means of QR-decomposition and will be the topic of a further contribution. Repeating the steps 1 to 4 for all groups g, $g = 1 \ldots G$, G group specific transmitted signals $\underline{\mathbf{t}}_{\mathrm{G}}^{(g)}$ are determined. Then, based on (38) and (50) follows the total transmitted signal (step 5) by applying (37). Based on (37) the energy

$$T = \frac{1}{2} \underline{\mathbf{t}}^{\mathrm{H}} \underline{\mathbf{t}} = \sum_{g=1}^{G} \underbrace{\frac{1}{2} \underline{\mathbf{t}}_{\mathrm{G}}^{(g)\,\mathrm{H}} \underline{\mathbf{t}}_{\mathrm{G}}^{(g)}}_{T_{\mathrm{G}}^{(g)}} \tag{52}$$

of the total transmitted signal $\underline{\mathbf{t}}$ of (5) can be determined. Surprisingly, the energy T of the total transmitted signal is only the sum of the energies $T_{\mathrm{G}}^{(g)}$ of the group specific transmitted signals $\underline{\mathbf{t}}_{\mathrm{G}}^{(g)}$. This results from the fact that due to the design strategy followed in TxNZF the group specific transmitted signals $\underline{\mathbf{t}}_{\mathrm{G}}^{(g)}$ and $\underline{\mathbf{t}}_{\mathrm{G}}^{(g')}$ of two different groups g and g', $g \neq g'$, respectively, are orthogonal.

The entire algorithm constituted by the steps 1 to 5 form the mapping between the total data vector $\underline{\mathbf{d}}$ and the total transmitted signal $\underline{\mathbf{t}}$ in the case of TxNZF. Therefore, these steps describe the corresponding modulator operator $\mathcal{M}_{\mathrm{TxNZF}}\{\cdot\}$ of (6). $\mathcal{M}_{\mathrm{TxNZF}}\{\cdot\}$ is illustrated in a self explanatory comprehensive form by the Nassi-Shneiderman diagram [21] of Fig. 5.

B. *Choice of representatives* $\underline{\mathbf{q}}$

B.1 General

For $\underline{\mathbf{q}}_{\mathrm{G}}^{(g)}$ of (42) different realizations $\mathbf{S}_{\mathrm{G}}^{(g)}\underline{\mathbf{q}}$, $\underline{\mathbf{q}} \in \mathbb{V}_{\mathrm{q}}$, are allowed which represent the group specific data vector $\underline{\mathbf{d}}_{\mathrm{G}}^{(g)}$ to be transmitted. In the following two different strategies are presented to chose one of these realizations. The described strategies relay on evaluating $\underline{\mathbf{i}}_{\mathrm{G}}^{(g)}$ of (44) and $\underline{\mathbf{d}}_{\mathrm{G}}^{(g)}$ of (38) to find the best choice for $\underline{\mathbf{q}}_{\mathrm{G}}^{(g)}$.

B.2 Optimum choice

The transmitted energy T of (7) can be expressed by (52) for TxNZF, i.e., a sum of group specific transmitted energies $T_{\mathrm{G}}^{(g)}$. Therefore, if T of (7) should be minimized for the given partition of $\mathbb{G}$, each group specific transmitted energy $T_{\mathrm{G}}^{(g)}$, $g = 1\ldots G$, has to be minimized. This can be achieved by appropriately choosing $\underline{\mathbf{q}}_{\mathrm{G}}^{(g)}$. One obtains for the optimal choice

$$\underline{\mathbf{q}}_{\mathrm{G,opt}}^{(g)} = \arg \min_{\substack{\forall \underline{\mathbf{q}}_{\mathrm{G}} = \mathbf{S}_{\mathrm{G}}^{(g)}\underline{\mathbf{q}}, \\ \underline{\mathbf{q}} \in \mathbb{V}_{\mathrm{q}}}} \left\| \underline{\mathbf{M}}_{\mathrm{G}}^{(g)} \left(\underline{\mathbf{q}}_{\mathrm{G}} - \underline{\mathbf{i}}_{\mathrm{G}}^{(g)} \right) \right\|. \quad (53)$$

Again, as already mentioned for the optimum approach of Section IV, the minimization problem in (53) can only be solved by exhaustive search. However, its computational complexity is only exponential in $\|\mathbb{G}_g\|$ which is typically much smaller than that of the optimum approach, c.f. Section IV, making it, in contrast to the optimum approach of Section IV also feasible, if N_{t} is quite large. For the degenerated case of G equal to one, i.e., all data symbols are in one and the same group, TxNZF converges towards the optimum approach of Section IV.

B.3 Low-complexity suboptimum choice

If complexity reasons do not allow to determine $\underline{\mathbf{q}}_{\mathrm{G,opt}}^{(g)}$ of (53) one can resort to a symbol-by-symbol strategy which can be expressed as

$$\underline{q}_{\mathrm{G},n}^{(g)} = \arg \min_{\substack{\forall \underline{q} = [\mathbf{S}_{\mathrm{G}}^{(g)}]_n \underline{\mathbf{q}}, \\ \underline{\mathbf{q}} \in \mathbb{V}_{\mathrm{q}}}} \left\| \underline{q} - \underline{i}_{\mathrm{G},n}^{(g)} \right\|. \quad (54)$$

(54) means to take this representative $\underline{q}$ that has minimum distance to the interference $\underline{i}_{\mathrm{G},n}^{(g)}$. Performing (54) for all $\underline{d}_n$, $\underline{d}_n \in \mathbb{G}_g$, representatives $\underline{q}_{\mathrm{G},n'}^{(g)}$, $n' = 1\ldots\|\mathbb{G}_g\|$, for all data symbols $\underline{d}_n$, $\underline{d}_n \in \mathbb{G}_g$, can be determined. In contrast to (34) and (53) the minimization problem of (54) has a rather low complexity, which is linear in $\|\mathbb{G}_g\|$. However, (54) is only a very rough approximation of the optimum choice of (53). For G equal to N_{t} TxNZF degenerates to the well-known THP based strategy of Fischer et al. [13] or Erez et al. [14]. Therefore, THP can be interpreted as a special case of TxNZF; however this special case with lowest performance potential [17].

C. *Benefits and potentials of TxNZF*

As already explained in Subsection V-A, TxNZF may serve as a framework for several techniques for transmit signal design. It allows to almost freely balance computational complexity versus transmission performance. To influence this equilibrium in TxNZF one has several degrees of freedom, namely

- the number and sizes of groups,
- the assignment of data symbols $\underline{d}_n$, $n = 1\ldots N_{\mathrm{t}}$, to the groups,
- the design of the unconventional quantization scheme,
- the choice of representatives $\underline{q}_{\mathrm{G},n}^{(g)}$ out of $\mathbb{V}_{\mathrm{q},m}$.

TxNZF has a high potential with respect to the achievable transmission performance –, e.g. in terms of the necessary transmitted energy T of (7) to meet a required transmission quality, – as can be seen by the fact that even the optimum approach for transmit signal design introduced in Section IV is only a special case of TxNZF. The high potential of TxNZF mainly results from the friendly ratio between number of constrains to be fulfilled while designing the transmitted signal $\underline{\mathbf{t}}$ and the number of degrees of freedom available to do that. When designing the group specific transmitted signal $\underline{\mathbf{t}}_{\mathrm{G}}^{(g)}$ of group g, for each data symbol $\underline{d}_n$, $\underline{d}_n \in \mathbb{G}_g$, only interferences produced to $(\|\mathbb{G}_1 \cup \ldots \cup \mathbb{G}_G\| - 1)$ other data symbols $\underline{d}_{n'}$, $\underline{d}_{n'} \in \mathbb{G}_{g'}$, $g' \le g, n' \ne n$, have to be taken into account, which is for most groups g a much smaller number than $(N_{\mathrm{t}} - 1)$, the number of interference constrains per data symbol to obey in TxZF. The group specific transmitted signals $\underline{\mathbf{t}}_{\mathrm{G}}^{(g)}$, $g = 1\ldots G$, are generated based on TxZF. Therefore using the results of Subsection III-C for the transmit efficiency $\eta_{\mathrm{TxZF},n}$, each group specific transmitted signal $\underline{\mathbf{t}}_{\mathrm{G}}^{(g)}$ can be evaluated. With (29) one obtains for the average transmit efficiency of $\underline{\mathbf{t}}_{\mathrm{G}}^{(g)}$,

$$\overline{\eta}_{\mathrm{TxNZF}}^{(g)} = \frac{K_{\mathrm{B}}Q_{\mathrm{t}} - (\|\mathbb{G}_1 \cup \ldots \cup \mathbb{G}_g\| - 1)}{K_{\mathrm{B}}Q_{\mathrm{t}}} \ge \overline{\eta}_{\mathrm{TxZF}}. \quad (55)$$

(55) allows several conclusions:

- The average transmit efficiency $\overline{\eta}_{\mathrm{TxNZF}}^{(g)}$ is always larger than or at least equal to $\overline{\eta}_{\mathrm{TxZF}}$ of TxZF.
- Groups g which are processed first, i.e., which have low group indices g, are processed with transmit efficiencies $\overline{\eta}_{\mathrm{TxNZF}}^{(g)}$ of almost one.
- Groups g which are processed last, i.e., which have rather high group indices close to G are processed with lower transmit efficiencies $\overline{\eta}_{\mathrm{TxNZF}}^{(g)}$. However, $\overline{\eta}_{\mathrm{TxNZF}}^{(g)}$ is never smaller than $\overline{\eta}_{\mathrm{TxZF}}$.

These conclusions are a strong motivation to have a closer look at a rather usual situation in typical mobile radio systems, where the channel attenuations

$$\alpha^{(k)} = \left(\sum_{k_{\mathrm{M}}=1}^{K_{\mathrm{M}}} \sum_{k_{\mathrm{B}}=1}^{K_{\mathrm{B}}} \left\| \underline{\mathbf{h}}^{(k,k_{\mathrm{B}},k_{\mathrm{M}})} \right\|^2 \right)^{-1} \quad (56)$$

for the channels between the AP and the different MTs k, $k = 1\ldots K$, differ significantly from each other – sometimes by orders of magnitude –, which is usually the case due to shadowing and/or largely different distances between AP and MTs. Let us assume that the K MTs are labeled in such a way that $\alpha^{(k)}$ decreases with increasing k. Then a favorable choice for the partition of $\mathbb{G}$ would be to use G equal to K groups, where

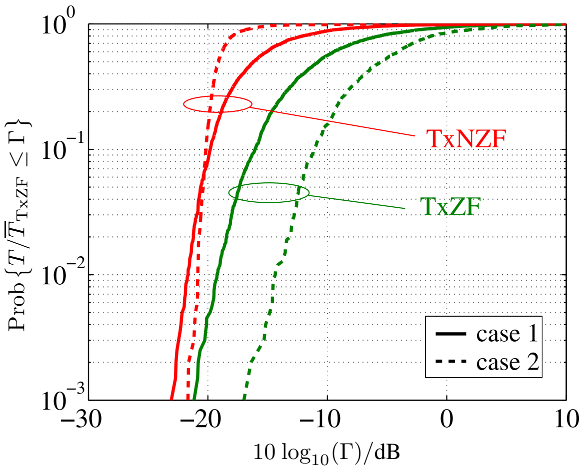

Fig. 6. Cummulative distribution functions of the normalized required transmitted energy $T/\overline{T}_{\mathrm{TxZF}}$ for case 1 and case 2

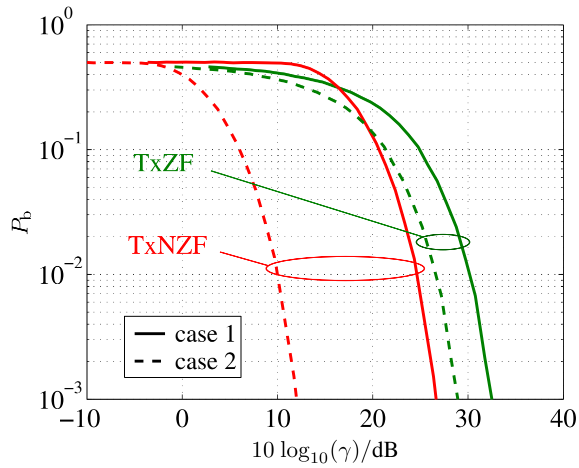

Fig. 7. Bit error rate P_{b} versus the pseudo SNR γ of (60) for case 1 and case 2

each group g, $g = 1 \ldots G$, corresponds to a single MT g and combines the data symbols $\underline{d}_n$, $n = (k-1)N \ldots kN$, of that MT g, i.e.,

$$\mathbb{G}_g = \left\{ \underline{d}_{(k-1)N+1} \cdots \underline{d}_{kN} \right\}. \tag{57}$$

Doing so, in TxNZF there is the tendency that the energies $T_{\mathrm{G}}^{(g)}$ of the group specific transmitted signals $\underline{\mathbf{t}}_{\mathrm{G}}^{(g)}$, $g = 1 \ldots G$, increase with decreasing g, due to the necessity to overcome the increasing channel attenuations. However, as explained above also the transmit efficiencies increase with decreasing g, so that the group specific transmitted signals $\underline{\mathbf{t}}_{\mathrm{G}}^{(g)}$ of basically high energies are endowed with high transmit efficiencies. This combination of originally high required transmitted energies and high transmit efficiencies is one of the keys to the aspired reduction of the required transmitted energy T typical of TxNZF.

VI. Simulation Results

In order to illustrate the advantage of TxNZF over TxZF with respect to the required transmit energy, comparative system simulations are performed for the partition $\mathbb{G}_g$ of (57). For the choice of the representatives $\underline{\mathbf{q}}_{\mathrm{G}}^{(g)}$ of (48) the low-complexity variant of TxNZF proposed in Subsection V-B.3 is chosen. The system parameters considered in the simulations are listed in Table I. A large number of statistically independent snapshots is evaluated according to the following side conditions:

- The $N(Q_{\mathrm{t}} + W - 1)$ elements of $\underline{\mathbf{D}}^{(k)}$ of (14) are derived from an orthonormal set of N binary sequences of dimension $Q_{\mathrm{t}} + W - 1$. The N rows of $\underline{\mathbf{D}}^{(k)}$ are obtained by scrambling the N sequences of this set by a random MT-specific scrambling code of dimension $Q_{\mathrm{t}} + W - 1$. The elements of this scrambling code have magnitude one.
- The $KK_{\mathrm{B}}W$ elements of the channel impulse responses $\underline{\mathbf{h}}^{(k,k_{\mathrm{B}},1)}$ are obtained by randomly generating independent bivariate Gaussian numbers with identical variance and expectation zero. However, in order to model the different channel attenuations $\alpha^{(k)}$ of (56) the generated channel impulse responses $\underline{\mathbf{h}}^{(k,k_{\mathrm{B}},1)}$ are normalized in such a way that

$$\left\| \underline{\mathbf{h}}^{(1,k_{\mathrm{B}},1)} \right\|^2 = 1, \; k_{\mathrm{B}} = 1 \ldots K_{\mathrm{B}}, \tag{58}$$

and for all k, $k = 2 \ldots K$,

$$10\log_{10}\left(\frac{\left\| \underline{\mathbf{h}}^{(k,k_{\mathrm{B}},1)} \right\|^2}{\left\| \underline{\mathbf{h}}^{(k-1,k_{\mathrm{B}},1)} \right\|^2} \right) = \begin{cases} 0 \text{ dB (case 1)}, \\ 3 \text{ dB (case 2)}, \end{cases} \tag{59}$$

hold.

The conventional and unconventional quantization schemes of Subsection II-C considered in the simulations for TxZF and TxNZF, respectively, are based on the Voronoi regions of the symbol constellation in QPSK modulation and the lattice structure based thereon, as e.g. described in [13].

The average required transmitted energy of TxZF obtained by averaging the transmitted energy T of (7) for TxZF over many snapshots characterized by randomly determined $\underline{\mathbf{h}}^{(k,k_{\mathrm{B}},1)}$ and $\underline{\mathbf{D}}^{(k)}$, see above, is termed $\overline{T}_{\mathrm{TxZF}}$. Fig. 6 shows for both cases of (59) the cumulative distribution functions of the ratio $T/\overline{T}_{\mathrm{TxZF}}$ for the schemes TxZF and TxNZF, respectively. As expected, TxNZF does with significantly lower transmitted energies than the TxZF. This superiority of TxNZF increases with increasing differences between consecutive channel attenuations $\alpha^{(k)}$, $k = 1 \ldots K$, of (56), because, when proceeding from MT k to MT $k+1$, see the explanation in Subsection V-C, the decrease of the transmit efficiency is more and more mitigated by an simultaneously decreasing channel attenuation.

TABLE I

System parameters for the simulations

M	N	Q_{t}	K	K_{B}	K_{M}	W
4	4	16	8	2	1	5

It is well known [13] that in the case of two consistently chosen conventional and unconventional quantization schemes – and this is the case considered here – which are subject to identical noise, the latter exhibits a somewhat larger error probability, because the demodulator output signals are more prone to land in a wrong decision region. To a certain degree this effect counteracts the energy advantage of TxNZF over TxZF illustrated in Fig. 6 and should therefore be studied. To this purpose the authors again consider the cases 1 and 2 of (59). We designate the average of the transmitted energy T as $\overline{T}$ and assume that the total received noise $\underline{\mathbf{n}}$ of (10) is Gaussian with covariance matrix $\underline{\mathbf{R}}_{\mathrm{n}}$ of (11) equal to $\sigma^2\mathbf{I}$. Then, the pseudo Signal-to-Noise-Ratio (SNR) which the authors define as the average ratio of the transmitted bit energy to σ^2, becomes

$$\gamma = \frac{\overline{T}/\left[\mathrm{ld}(M)KN\right]}{\sigma^2}. \tag{60}$$

In Fig. 7 the bit error rate P_{b} is shown versus γ of (60) for the cases 1 and 2 of (59). From these curves we can conclude the following:

- For sufficiently large values of γ of (60), TxNZF always outperforms TxZF.
- As in the case of the required transmitted energies, see Fig. 6, the superiority of TxNZF increases with increasing differences of consecutive channel attenuations $\alpha^{(k)}$ of (56).
- At low values of γ of (60) and low increments of the channel attenuations $\alpha^{(k)}$ of (56), TxZF may outperform TxNZF. However, this occurs only for values of P_{b} so large that they are of no practical interest.

The results presented above give a first impression of the potential performance gains of TxNZF compared to TxZF although only the suboptimum low-complexity variant of TxNZF introduced in Subsection V-B.3 has been considered in the simulations. Presently, extensive simulations of TxNZF are being performed by the authors to additionally analyze the potentials of TxNZF also for the optimum variant of Subsection V-B.2 especially in comparison with the non-practical optimum approach proposed by Peel et al. in [18] and generalized in this contribution in Section IV. Shortly the simulation results shall be presented in an extended paper. This contribution has the intention to initiate a critical discussion on TxNZF.

ACKNOWLEDGMENT

The authors gratefully appreciate the stimulating discussion and the fruitful exchange of ideas with Prof. P. W. Baier, and their co-workers at the Research Group for RF Communications at the University of Kaiserslautern (UKL). The support of individual parts of this work in the framework of the EU-IST-Project FLOWS (Flexible Convergence of Wireless Standards and Services), by DFG, by Siemens AG and by the supercomputer staff of the central computer facility (RHRK) of the UKL is highly acknowledged. Thanks are also extended to A. Bruhn and M. Cuntz for carefully typesetting the manuscript in LaTeX.

REFERENCES

[1] P. W. Baier, W. Qiu, H. Tröger, C. A. Jötten, and M. Meurer, "Modelling and optimization of receiver oriented multi-user MIMO downlinks for frequency selective channels," in *Proc. 10th International Conference on Telecommunications (ICT'03)*, Papeete, 2003, pp. 1547–1554.

[2] R. Esmailzadeh and M. Nakagawa, "Pre-RAKE diversity combining for direct sequence spread spectrum mobile communications systems," *IEICE Transactions on Communications*, vol. 76, pp. 1008–1015, 1993.

[3] A. Noll-Barreto and G. Fettweis, "Performance improvement in DS-spread spectrum CDMA systems using a pre- and a post-rake," in *Proc. 2000 International Zurich Seminar on Broadband Communications (IZS'2000)*, Zurich, 2000, pp. 39–46.

[4] B. Vojcic and J. Mee, "Transmitter precoding in synchronous multiuser communications," *IEEE Transactions on Communications*, vol. 46, pp. 1346–1355, 1998.

[5] M. Meurer, P. W. Baier, T. Weber, Y. Lu, and A. Papathanassiou, "Joint transmission: advantageous downlink concept for CDMA mobile radio systems using time division duplexing," *IEE ELECTRONICS LETTERS*, vol. 11, pp. 900–901, 2000.

[6] F. Kowalewski and P. Mangold, "Joint predistortion and transmit diversity," *Proc. IEEE Global Telecommunications Conference (GLOBECOM'00)*, pp. 245–249, 2000.

[7] M. Joham and W. Utschick, "Downlink processing for mitigation of intracell interference in DS-CDMA systems," *Proc. IEEE 6th International Symposium on Spread Spectrum Techniques & Applications (ISSSTA'00)*, pp. 15–19, 2000.

[8] P. W. Baier, M. Meurer, T. Weber, and H. Tröger, "Joint transmission (JT), an alternative rationale for the downlink of time division CDMA using multi-element transmit antennas," *Proc. IEEE 6th International Symposium on Spread Spectrum Techniques & Applications (ISSSTA'00)*, pp. 1–5, 2000.

[9] M. Joham, K. Kusume, M. H. Gzara, W. Utschick, and J. A. Nossek, "Transmit Wiener Filter for the Downlink of TDD DS-CDMA Systems," in *Proc. IEEE 7th International Symposium on Spread Spectrum Techniques & Applications (ISSSTA'02)*, Prague, 2002, pp. 9–13.

[10] P. W. Baier and M. Meurer, "Receiver orientation, an unconventional approach to mobile radio downlink design," in *Proc. European Conference on Wireless Technology (ECWT'03)*, Munich, 2003, pp. 11–14.

[11] T. Weber and M. Meurer, "Optimum joint transmission: Potentials and dualities," in *Proc. 6th International Symposium on Wireless Personal Multimedia Communications 2003 (WPMC'03)*, Yokosuka, 2003, vol. 1, pp. 79–83.

[12] R. Irmer, W. Rave, and G. Fettweis, "Minimum BER transmission for TDD-CDMA in frequency-selective channels," in *Proc. IEEE 14th International Symposium on Personal, Indoor and Mobile Radio Communications (PIMRC'03)*, Beijing, 2003, pp. 1260–1264.

[13] R. F. H. Fischer, C. Windpassinger, A. Lampe, and J. B. Huber, "Space-time transmission using Tomlinson-Harashima precoding," in *Proc. 4th ITG Conference on Source and Channel Coding (SCC'02)*, Berlin, 2002, pp. 139–147.

[14] U. Erez, S. Shamai, and R. Zamir, "Capacity and lattice-strategies for cancelling known interference," in *Proc. International Symposium on Information Theory and Its Applications (ISITA'00)*, Honolulu, 2000, pp. 681–684.

[15] M. Tomlinson, "New automatic equalizer employing modulo arithmetic," *IEE ELECTRONICS LETTERS*, vol. 7, pp. 138–139, 1971.

[16] H. Harashima and H. Miyakawa, "Matched-transmission technique for channels with intersymbol interference," *IEEE Transactions on Communications*, vol. COM-20, pp. 774–780, 1972.

[17] C. Windpassinger, R. F. H. Fischer, and J. B. Huber, "Lattice-reduction-aided broadcast precoding," in *Proc. 5th ITG Conference on Source and Channel Coding (SCC'04)*, Erlangen, 2004, pp. 403–408.

[18] C. B. Peel, B. M. Hochwald, and A. L. Swindlehurst, "A vector-perturbation technique for near-capacity multi-antenna multi-user communication," in *Proc. 41st Allerton Conference on Communication, Control, and Computing*, Allerton House, 2003.

[19] M. Abramowitz and I. Stegun, *Handbook of mathematical functions*, Dover, New York, 1965.

[20] T. Haustein, C. v. Helmolt, E. Jorswieck, V. Jungnickel, and V. Pohl, "Performance of MIMO systems with channel inversion," in *Proc. IEEE 55th Vehicular Technology Conference (VTC'02)*, Birmingham, 2002, pp. 35–39.

[21] I. Nassi and B. Shneiderman, "Flowchart techniques for structured programming," in *ACM SIGPLAN Notices*, 1973, vol. 8, pp. 12–26.

Kapitel 5

Suboptimale aufwandsgünstige Verfahren der gemeinsamen Sendesignalerzeugung bei unkonventionellen Empfängern

5.1 Vorbemerkung

Wie in Kapitel 4 erläutert, ist das optimale Verfahren der gemeinsamen Sendesignalerzeugung nach Kapitel 4 im allgemeinen sehr komplex. Daher beschäftigt sich dieses Kapitel mit aufwandsgünstigen suboptimalen Verfahren der gemeinsamen Sendesignalerzeugung bei unkonventionellen Empfängern.

In der Literatur [FTH01, Fis02, FWLH02b, FWLH02a, FWLH02c, HSB03, FW03, WF03, WVF03a, WVF03b, BHMW04, CM04d, JBU04, JBVU04, Joh04, NJU04, Win04] wurden in letzten vier Jahren suboptimale Verfahren der obigen Art vorgeschlagen, wobei diesen Verfahren meist ein heuristischer Ansatz zugrunde liegt und in fast allen Fällen, sei es aus Unwissenheit oder anderen Gründen, nicht einmal das optimale Verfahren der gemeinsamen Sendesignalerzeugung nach Kapitel 4 als Meßlatte herangezogen wird. Sämtliche obigen der Literatur entstammenden Vorschläge sind ausschließlich für spezielle unkonventionelle Empfänger gestaltet, die insbesondere Quantisierer verwenden, die auf dem in Abschnitt 1.3.3 eingeführten Lattice-Quantisierungsschema aufbauen. Es ist das Ziel dieses Kapitels, die gemachten Vorschläge zu verallgemeinern und ein aufwandsgünstiges Verfahren der gemeinsamen Sendesignalerzeugung für unkonventionelle Empfänger vorzustellen, das die zuvor genannten Vorschläge als Spezialfälle beinhaltet.

5.2 Verfahren der gemeinsamen Sendesignalerzeugung

Ausgehend von den Grundprinzipien, die dem aus Kapitel 4 bekannten optimalen Verfahren der gemeinsamen Sendesignalerzeugung für unkonventionelle Empfänger zugrunde liegen, wird in diesem Unterkapitel im Rahmen der Werke [MQBW04, WMZ04a] das aufwandsgünstige suboptimale Verfahren der gemeinsamen Sendesignalerzeugung

Tabelle 5.1. Wesentliche Unterschiede der Notationen nach Kapitel 1 und der Notation nach [MQBW04, WMZ04a]

dargestellte Größe	nach Kap. 1	nach $[\,\cdot\,]$	Bemerkung/ geltend für
Entscheidungsgebiet	$\mathbb{Q}_m$	$\mathbb{G}_m$	[MQBW04]
Repräsentant	$\underline{q}_{m,p}$	$\underline{g}_{m,p}$	[MQBW04]
Datensymbolalphabet	$\mathbb{V}_\mathrm{d}$	$\mathbb{D}$	[WMZ04a]
totales Sendesignal	$\underline{\mathbf{t}}$	$\underline{\mathbf{s}}$	[WMZ04a]
totales Empfangssignal	$\underline{\mathbf{r}}$	$\underline{\mathbf{e}}$	[WMZ04a]
wertekontinuierliche Schätzung von $\underline{\mathbf{d}}$	$\underline{\widehat{\mathbf{d}}}$	$\underline{\widehat{\mathbf{q}}}$	[WMZ04a]

„senderseitige nichtlineare Interferenzeliminierung (engl. transmit nonlinear zero forcing, TxNZF)“ vorgeschlagen. Dieses Verfahren basiert auf einer Gruppenbildung und erzeugt das totale Sendesignal $\underline{\mathbf{t}}$ in einer iterativen gruppenweisen Art. Wie sich herausstellt, sind die oben erwähnten, aus der Literatur [FTH01, Fis02, FWLH02b, FWLH02a, FWLH02c, HSB03, FW03, WF03, WVF03a, WVF03b, BHMW04, CM04d, JBU04, JBVU04, Joh04, NJU04, Win04] bekannten Verfahren Spezialfälle des vorgenannten Verfahrens, bei denen die Gruppengröße zu eins gewählt ist. Im einzelnen werden in [MQBW04, WMZ04a] die folgenden wichtigen Aspekte behandelt:

- Das auf Gruppenbildung basierende aufwandsgünstige Verfahren der gemeinsamen Sendesignalerzeugung wird mathematisch hergeleitet und beschrieben.
- Das Potential der Leistungssteigerung gegenüber Verfahren der gemeinsamen Sendesignalerzeugung für konventionelle Empfänger wird analytisch und durch Simulationen abgeschätzt.
- Eine wesentliche Motivation des Verfahrens TxNZF ist die Reduktion der senderseitigen Implementierungskomplexität. Daher wird für das Verfahren TxNZF in [WMZ04a] gezeigt, wie dieses auf Basis des mathematischen, aus der linearen Algebra entstammenden Kunstgriffes der QR-Zerlegung [HJ85, ZF86, ZF97, PTVF92] aufwandsgünstig implementiert werden kann.

Im Gegensatz zu der aus Kapitel 1 bekannten Notation werden in [MQBW04, WMZ04a] einige wenige Größen durch eine modifizierte Notation beschrieben. Tabelle 5.1 listet die wesentlichen Unterschiede in kompakter Form auf.

[MQBW04] Meurer, M.; Qiu, W., Baier, P.W., Weber, T.: *Transmit power reduction in CDMA mobile radio downlinks by nonlinear receiver oriented transmission combined with multiply connected quantization schemes.* Technische Mitteilung 15/04, Research Group for RF Communications, University of Kaiserslautern, 2004.

Transmit power reduction in CDMA mobile radio downlinks by nonlinear receiver oriented transmission combined with multiply connected quantization schemes

M. Meurer, W. Qiu, P.W. Baier, T. Weber
Research Group for RF Communications, University of Kaiserslautern
P.O. Box 3049, D-67653 Kaiserslautern, Germany
email: meurer@rhrk.uni-kl.de

Abstract—**For the downlink of TDD/CDMA mobile radio systems linear transmission schemes were recently proposed, which can be classified as receiver (Rx) oriented, because the receiver algorithms are a priori determined, whereas the transmitter (Tx) algorithms follow a posteriori. A main asset of these schemes is their low receiver complexity. In addition, they do without sacrificing downlink transmission resources to training signals for channel estimation, which is beneficial for capacity, and their combination with MIMO antenna structures is straightforward. In this paper a nonlinear modification of the mentioned linear Rx oriented schemes is presented with a view to reduce the required transmit power considerably, a feature mitigating intercell interference in cellular systems and, thereby, further enhancing capacity, and being also attractive with respect to the growing electro-phobia of the public. The crux of said modification consists in designing the transmit signal at the base station (BS) user-wise by a nonlinear approach, and in using multiply connected decision regions in the detectors of the mobile terminals (MT). The proposed scheme is particularly effective in the case of relatively large attenuation differences of the channels between the BS and the individual MTs. In practical systems such differences, due to shadowing and to largely different distances between the BS and the MTs, prevail.**

Keywords—**CDMA, multi-user MIMO downlinks, Rx orientation, precoding**

I. Introduction

For multi-user CDMA mobile radio downlinks, linear transmission schemes with modulators based on the rationales Transmit Matched Filter, Transmit Minimum Mean Square Error or Transmit Zero Forcing were proposed in [1], [2], [3]. For these schemes the acronyms TxMF, TxMMSE or TxZF, respectively, were coined [4]. They can be classified as receiver (Rx) oriented, because the Rx algorithms to be applied in the mobile terminals (MTs) are a priori determined, whereas the algorithms utilized in the transmitter (Tx) of the base station (BS) result a posteriori. As opposed to conventional, that is Tx oriented schemes, the main assets of Rx oriented schemes are their low receiver complexity and the fact that they do without sacrificing downlink transmission resources to training signals for channel estimation. In addition, the inclusion of MIMO antenna structures in Rx oriented schemes is straightforward [2], [3]. As a prerequisite of Rx orientation, the knowledge of the downlink channel impulse responses has to be available in the transmitter of the BS. This knowledge can be particularly easily gained in mobile radio systems applying Time Division Duplexing [2], [3].

In linear radio transmission systems each data symbol to be transmitted is represented by an individual transmitted signal termed here transmitted symbol signal. In order to produce at the receiver inputs the symbol energies necessary to offer the desired transmission quality, certain energies of the transmitted symbol signals have to be invested. In mobile radio applications these transmitted symbol energies should be as low as possible with a view to keep intercell interference low and, thereby, capacity high, and also with respect to the growing electro-phobia of the public. For the energy-wise characterization of the transmission from the BS to each MT, quantities termed energy efficiencies [2] are suited, which compare how efficiently transmitted symbol energies are transformed into received symbol energies in the system under consideration and in an optimum reference system. The transmitted symbol energies required for the support of a certain MT are inversely proportional to the corresponding energy efficiencies and proportional to the channel attenuation (in linear scale) from the BS to this MT. In practice, the channel attenuations are given by the environment and cannot be influenced by the system design. Therefore, a key to the reduction of the required transmitted symbol energies lies in enhancing the energy efficiencies.

The three linear schemes TxMF, TxMMSE and TxZF mentioned above differ from each other by the way in which the problems of intersymbol interference (ISI) and multiple access interference (MAI) are addressed when designing the transmitted signals [3], [4], [5]. ISI and MAI

- are totally neglected in the case of the TxMF,
- are admitted to a certain degree and beneficially balanced against the received noise in the case of the TxMMSE, and
- are strictly eliminated in the case of the TxZF.

Quite generally, the energy efficiencies decrease with increasing the degree of mitigation of mutual interferences in the form of ISI and MAI, because such an increase goes along with growing constraints on the design of the transmitted symbol signals. In the case of the TxMF the symbol signals are generated independently of each other, and, therefore, no such constraints exist. The TxMMSE and the TxZF imply such constraints, which are more stringent in the case of the TxZF than in the case of the TxMMSE. This means that, when proceeding from the TxMF over the TxMMSE to the TxZF, the energy efficiencies tend to go down. With the number K of MTs to be supported by the BS and the number N of data symbols to be transmitted to each MT, the total number of data symbols to be transmitted is KN. Therefore, in the case of the TxMMSE and the TxZF, the number of constraints to be considered when generating the KN symbol signals becomes $KN-1$. As a consequence, the energy efficiencies of the TxMMSE and the TxZF decrease with an increasing number K of supported MTs and an increasing number N of transmitted data symbols per MT. To summarize, there seems to be a rule telling us, the larger the energy efficiencies, the more distinct the impact of ISI and MAI. In the present paper we pursue the idea to overcome this rule, that is, we aim at enhancing the energy efficiencies without simultaneously putting up with an increased impact of ISI and MAI. The crux of the envisaged approach consists in

- reducing the above mentioned constraints when designing the symbol signals, and
- dealing with the simultaneously growing interference in an appropriate way.

Of course, in the case of the TxMF no such constraints exist. In the case of the TxMMSE and the TxZF the number of constraints shall be reduced by designing the transmitted symbol signals not as an entirety comprising KN symbol signals, but in groups with less than KN symbol signals. In addition, to tackle the problem of increased interference, ISI and MAI occurring in the data estimates are no longer considered as detrimental, but are exploited as contributions to the data estimates. Such an attitude towards interference is enabled – as an extension of ideas first presented in [6], [7], [8], [9], [10] – by resorting to multiply connected decision regions in the detectors of the receivers of the MTs. In the case of mobile radio downlinks utilizing the TxMMSE or the TxZF one obvious way to design the transmitted symbol signals in groups would rely on groups being constituted by subsets of the entirety of the K MTs. This approach will turn out particularly effective, if the channel attenuations from the BS to the individual MTs differ significantly, as it is usually the case in real world systems. It will become clear in the paper that the outlined generation of each transmitted symbol signal has to be performed under consideration of the data values carried by other symbol signals in a nonlinear way. The following considerations could be based on each of the three schemes TxMF, TxMMSE and TxZF with the result of slightly different performances of the obtained transmission schemes. However, for the sake of brevity, we restrict ourselves to the TxZF as a basis and term the corresponding downlink transmission scheme Transmit Nonlinear Zero Forcing (TxNZF).

In Section II the generic model of linear transmission systems introduced in [2], [3] is briefly recapitulated. The topic of Section III is the determination of the energy efficiencies. The nonlinear transmission scheme TxNZF is developed in Section IV. Section V presents simulation results, and Section VI summarizes the paper. As in [2], [3] the discrete time equivalent lowpass formalism is adopted, and complex vectors and matrices are represented by underlined bold face symbols.

II. Downlink system model

We consider a downlink situation where a BS supports K MTs numbered with $k=1\dots K$. The BS is equipped with K_{B} antennas, and each of the K MTs employs a single antenna. Fig. 1 illustrates this situation by a block diagram, which will be explained and mathematically described in what follows.

It is assumed that a sequence $(a_1^{(k)}\dots a_N^{(k)})$ of N message elements has to be transmitted from the BS to each MT k, $k=1\dots K$. For transmission the message element $a_n^{(k)}$ is represented by the complex transmit value $\underline{\Delta}_n^{(k)}$. The N transmit values intended for MT k are arranged in the MT specific transmit vector

$$\underline{\mathbf{\Delta}}^{(k)}=\left(\underline{\Delta}_1^{(k)}\dots\underline{\Delta}_N^{(k)}\right)^{\mathrm{T}}\in\mathbb{C}^{N\times 1}. \qquad (1)$$

The K MT specific transmit vectors $\underline{\mathbf{\Delta}}^{(k)}$ of (1) are stacked in the (total) transmit vector

$$\begin{aligned}\underline{\mathbf{\Delta}} &= \left(\underline{\mathbf{\Delta}}^{(1)\mathrm{T}}\dots\underline{\mathbf{\Delta}}^{(K)\mathrm{T}}\right)^{\mathrm{T}}\\ &= \left(\underline{\Delta}_1\dots\underline{\Delta}_n\dots\underline{\Delta}_{KN}\right)^{\mathrm{T}}\in\mathbb{C}^{(KN)\times 1}. \qquad (2)\end{aligned}$$

By linear modulation based on $\underline{\mathbf{\Delta}}$ of (2) and the K_{B} antenna specific modulator matrices

$$\underline{\mathbf{M}}^{(k_{\mathrm{B}})}\in\mathbb{C}^{Q_{\mathrm{t}}\times(KN)},\ k_{\mathrm{B}}=1\dots K_{\mathrm{B}}, \qquad (3)$$

K_{B} antenna specific transmitted signals

$$\begin{aligned}\underline{\mathbf{t}}^{(k_{\mathrm{B}})} &= \left(\underline{t}_1^{(k_{\mathrm{B}})}\dots\underline{t}_{Q_{\mathrm{t}}}^{(k_{\mathrm{B}})}\right)^{\mathrm{T}}\\ &= \underline{\mathbf{M}}^{(k_{\mathrm{B}})}\,\underline{\mathbf{\Delta}}\in\mathbb{C}^{Q_{\mathrm{t}}\times 1},\ k_{\mathrm{B}}=1\dots K_{\mathrm{B}}, \qquad (4)\end{aligned}$$

are generated. The K_{B} transmitted signals $\underline{\mathbf{t}}^{(k_{\mathrm{B}})}, k_{\mathrm{B}}=1\dots K_{\mathrm{B}}$, of (4) can be stacked in the signal

$$\begin{aligned}\underline{\mathbf{t}} &= \left(\underline{\mathbf{t}}^{(1)\mathrm{T}}\dots\underline{\mathbf{t}}^{(K_{\mathrm{B}})\mathrm{T}}\right)^{\mathrm{T}}\\ &= \underbrace{\left(\underline{\mathbf{M}}^{(1)\mathrm{T}}\dots\underline{\mathbf{M}}^{(K_{\mathrm{B}})\mathrm{T}}\right)^{\mathrm{T}}}_{\underline{\mathbf{M}}}\underline{\mathbf{\Delta}}=\underline{\mathbf{M}}\,\underline{\mathbf{\Delta}}\in\mathbb{C}^{(K_{\mathrm{B}}Q_{\mathrm{t}})\times 1} \qquad (5)\end{aligned}$$

termed (total) transmitted signal. $\underline{\mathbf{M}}$ in (5) is termed (total) modulator matrix and has the dimension $(K_{\mathrm{B}}Q_{\mathrm{t}})\times(KN)$.

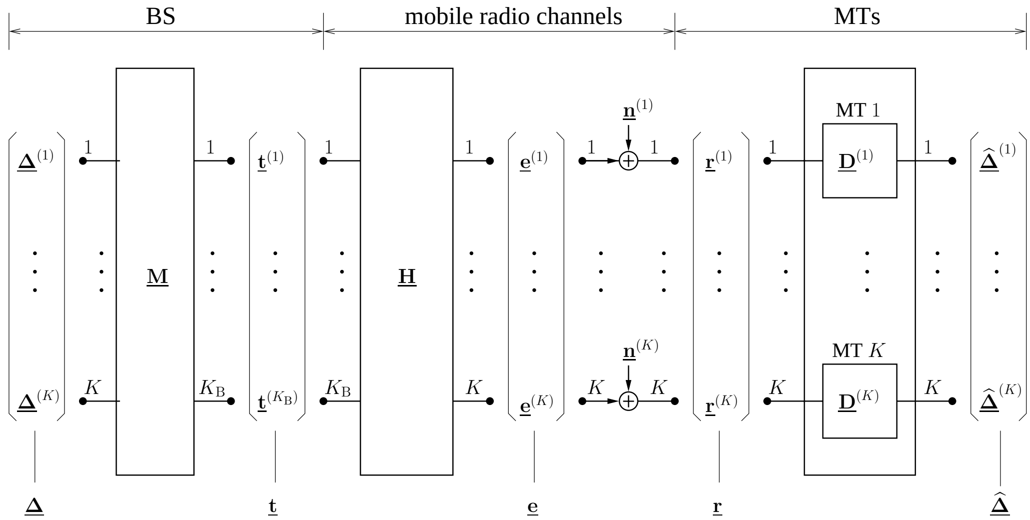

Fig. 1. Downlink system model

The frequency selective radio channel between the BS antenna k_B and the antenna of MT k is characterized by the channel impulse response [2]

$$\underline{\mathbf{h}}^{(k,k_\mathrm{B})} = \left(\underline{h}_1^{(k,k_\mathrm{B})} \ldots \underline{h}_W^{(k,k_\mathrm{B})}\right)^\mathrm{T} \in \mathbb{C}^{W\times 1}. \quad (6)$$

With $\underline{\mathbf{h}}^{(k,k_\mathrm{B})}$ of (6) and Q_t, see (3), the KK_B MT and antenna specific channel matrices

$$\begin{aligned}\underline{\mathbf{H}}^{(k,k_\mathrm{B})} &= \left(\underline{H}_{i,\,j}^{(k,k_\mathrm{B})}\right) \in \mathbb{C}^{(Q_\mathrm{t}+W-1)\times Q_\mathrm{t}},\\ &\quad i = 1\ldots Q_\mathrm{t}+W-1,\ j=1\ldots Q_\mathrm{t},\\ \underline{H}_{i,\,j}^{(k,k_\mathrm{B})} &= \begin{cases}\underline{h}_{i-j+1}^{(k,k_\mathrm{B})} & 1\le i-j+1\le W,\\ 0 & \text{else},\end{cases}\\ &\quad k=1\ldots K,\ k_\mathrm{B}=1\ldots K_\mathrm{B}, \quad (7)\end{aligned}$$

are established. With the KK_B matrices $\underline{\mathbf{H}}^{(k,k_\mathrm{B})}$ of (7) we form the K MT specific channel matrices

$$\underline{\mathbf{H}}^{(k)}=\left(\underline{\mathbf{H}}^{(k,1)}\ldots\underline{\mathbf{H}}^{(k,K_\mathrm{B})}\right)\in\mathbb{C}^{(Q_\mathrm{t}+W-1)\times(K_\mathrm{B}Q_\mathrm{t})},\quad k=1\ldots K, \quad (8)$$

and the total channel matrix

$$\underline{\mathbf{H}} = \left(\underline{\mathbf{H}}^{(1)^\mathrm{T}}\ldots\underline{\mathbf{H}}^{(K)^\mathrm{T}}\right)^\mathrm{T} \in \mathbb{C}^{[K(Q_\mathrm{t}+W-1)]\times(K_\mathrm{B}Q_\mathrm{t})}. \quad (9)$$

With $\underline{\mathbf{H}}^{(k)}$ of (8) the transmitted signal $\underline{\mathbf{t}}$ of (5) leads to the noisefree received signal

$$\underline{\mathbf{e}}^{(k)} = \left(\underline{e}_1^{(k)}\ldots\underline{e}_{Q_\mathrm{t}+W-1}^{(k)}\right)^\mathrm{T} = \underline{\mathbf{H}}^{(k)}\underline{\mathbf{t}} \in \mathbb{C}^{(Q_\mathrm{t}+W-1)\times 1} \quad (10)$$

of MT k, $k=1\ldots K$. With $\underline{\mathbf{H}}$ of (9) these signals can be stacked in the total noisefree received signal

$$\underline{\mathbf{e}} = \left(\underline{\mathbf{e}}^{(1)^\mathrm{T}}\ldots\underline{\mathbf{e}}^{(K)^\mathrm{T}}\right)^\mathrm{T} = \underline{\mathbf{H}}\,\underline{\mathbf{t}} \in \mathbb{C}^{[K(Q_\mathrm{t}+W-1)]\times 1}. \quad (11)$$

Finally, with (5) follows from (11)

$$\underline{\mathbf{e}} = \underline{\mathbf{H}}\,\underline{\mathbf{t}} = \underline{\mathbf{H}}\,\underline{\mathbf{M}}\,\underline{\mathbf{\Delta}}. \quad (12)$$

If $\underline{\mathbf{e}}^{(k)}$ of (10) is corrupted by an additive noise signal

$$\underline{\mathbf{n}}^{(k)} = \left(\underline{n}_1^{(k)}\ldots\underline{n}_{Q_\mathrm{t}+W-1}^{(k)}\right)^\mathrm{T} \in \mathbb{C}^{(Q_\mathrm{t}+W-1)\times 1}, \quad (13)$$

then we obtain for the noisy received signal of MT k

$$\begin{aligned}\underline{\mathbf{r}}^{(k)} &= \underline{\mathbf{e}}^{(k)} + \underline{\mathbf{n}}^{(k)}\\ &= \underline{\mathbf{H}}^{(k)}\underline{\mathbf{t}} + \underline{\mathbf{n}}^{(k)} \in \mathbb{C}^{(Q_\mathrm{t}+W-1)\times 1}, \quad (14)\end{aligned}$$

and for the total noisy received signal

$$\underline{\mathbf{r}} = \left(\underline{\mathbf{r}}^{(1)^\mathrm{T}}\ldots\underline{\mathbf{r}}^{(k)^\mathrm{T}}\right)^\mathrm{T} = \underline{\mathbf{e}} + \underline{\mathbf{n}} = \underline{\mathbf{H}}\,\underline{\mathbf{t}} + \underline{\mathbf{n}}, \quad (15)$$

where

$$\underline{\mathbf{n}} = \left(\underline{\mathbf{n}}^{(1)^\mathrm{T}}\ldots\underline{\mathbf{n}}^{(k)^\mathrm{T}}\right)^\mathrm{T} \quad (16)$$

denotes the total noise signal.

The detector of each MT k consist of a demodulator and a decision unit described which is detailed in Section IV. The demodulator of each MT k is described by a demodulator matrix

$$\underline{\mathbf{D}}^{(k)} \in \mathbb{C}^{N\times(Q_\mathrm{t}+W-1)} \quad (17)$$

[2], [3]. At the output of the demodulator of MT k we obtain the MT specific estimate

$$\underline{\widehat{\mathbf{\Delta}}}^{(k)} = \left(\underline{\widehat{\Delta}}_1^{(k)}\ldots\underline{\widehat{\Delta}}_N^{(k)}\right)^\mathrm{T} \quad (18)$$

of $\underline{\mathbf{\Delta}}^{(k)}$ of (1). If we stack the MT specific estimates $\hat{\underline{\mathbf{\Delta}}}^{(k)}$ of (18) in the total estimate

$$\hat{\underline{\mathbf{\Delta}}} = \left(\hat{\underline{\mathbf{\Delta}}}^{(1)\mathrm{T}} \ldots \hat{\underline{\mathbf{\Delta}}}^{(K)\mathrm{T}}\right)^{\mathrm{T}} \quad (19)$$

and the MT specific demodulator matrix $\underline{\mathbf{D}}^{(k)}$ of (17) in the total demodulator matrix

$$\underline{\mathbf{D}} = \mathrm{blockdiag}\left(\underline{\mathbf{D}}^{(1)} \ldots \underline{\mathbf{D}}^{(K)}\right) \in \mathbb{C}^{(KN)\times[K(Q_{\mathrm{t}}+W-1)]}, \quad (20)$$

then, with $\underline{\mathbf{r}}$ of (15),

$$\hat{\underline{\mathbf{\Delta}}} = \underline{\mathbf{D}}\,\underline{\mathbf{r}} = \underline{\mathbf{D}}\,\underline{\mathbf{H}}\,\underline{\mathbf{M}}\,\underline{\mathbf{\Delta}} + \underline{\mathbf{D}}\,\underline{\mathbf{n}} \quad (21)$$

holds. With $\underline{\mathbf{H}}$ of (9) and $\underline{\mathbf{D}}$ of (20) the modulator matrices of the TxMF and the TxZF are given by

$$\underline{\mathbf{M}} = \begin{cases} (\underline{\mathbf{D}}\,\underline{\mathbf{H}})^{\mathrm{H}}\left[\mathrm{diag}\left(\underline{\mathbf{D}}\,\underline{\mathbf{H}}\,(\underline{\mathbf{D}}\,\underline{\mathbf{H}})^{\mathrm{H}}\right)\right]^{-1} & (\mathrm{TxMF}), \\ (\underline{\mathbf{D}}\,\underline{\mathbf{H}})^{\mathrm{H}}\left[\left(\underline{\mathbf{D}}\,\underline{\mathbf{H}}\,(\underline{\mathbf{D}}\,\underline{\mathbf{H}})^{\mathrm{H}}\right)\right]^{-1} & (\mathrm{TxZF}), \end{cases} \quad (22)$$

[2], [3]. With the modulator matrices $\underline{\mathbf{M}}$ of (22) the contribution of the transmit value $\underline{\Delta}_n^{(k)}$ to the estimate $\hat{\underline{\Delta}}_n^{(k)}$ becomes equal to $\underline{\Delta}_n^{(k)}$ [2], [3].

For determining the modulator matrix $\underline{\mathbf{M}}$ of the TxMMSE, we assume that the components $\underline{n}_n^{(k)}$, $n = 1 \ldots N$, of the additive noise signals $\underline{\mathbf{n}}^{(k)}$, $k = 1 \ldots K$, of (13) are independent of each other and have the same variance σ^2, i.e.

$$\frac{1}{2}\mathrm{E}\left\{\underline{\mathbf{n}}\,\underline{\mathbf{n}}^{\mathrm{H}}\right\} = \frac{1}{2}\sigma^2 \mathbf{I}^{(K[Q_{\mathrm{t}}+W+1])} \quad (23)$$

holds. We further assume that all components $\underline{\Delta}_n^{(k)}$, $n = 1 \ldots N$, of $\underline{\mathbf{\Delta}}^{(k)}$ of (1) are independent and have the same variance σ_Δ^2. Then, with the energy

$$T = \frac{1}{2}\mathop{\mathrm{E}}_{\Delta}\left\{\underline{\mathbf{t}}^{\mathrm{H}}\underline{\mathbf{t}}\right\} \quad (24)$$

of $\underline{\mathbf{t}}$ of (5) and a real scalar κ the modulator matrix of the TxMMSE takes the form [3], [4], [5]

$$\underline{\mathbf{M}} = \kappa\,(\underline{\mathbf{D}}\,\underline{\mathbf{H}})^{\mathrm{H}}\left[\underline{\mathbf{D}}\,\underline{\mathbf{H}}\,(\underline{\mathbf{D}}\,\underline{\mathbf{H}})^{\mathrm{H}} + \frac{\sigma^2}{2T}\mathrm{trace}\left(\underline{\mathbf{D}}\,\underline{\mathbf{D}}^{\mathrm{H}}\right)\mathbf{I}^{(N)}\right]^{-1},$$
$$\text{s.t. } \tfrac{1}{2}\sigma_\Delta^2\,\mathrm{trace}\left\{\underline{\mathbf{M}}^{\mathrm{H}}\underline{\mathbf{M}}\right\} = T \qquad (\mathrm{TxMMSE}) \quad (25)$$

by proper choice of κ.

III. Energy efficiency

Let us designate the dominant singular value of the MT specific channel matrix $\underline{\mathbf{H}}^{(k)}$ of (8) as $\sqrt{\lambda^{(k)}}$. Then, as shown in [2], in the case of the TxZF being focused in what follows the energy efficiency of the transmit value $\underline{\Delta}_n^{(k)}$ becomes

$$\eta_n^{(k)} = \left(\left[\left(\underline{\mathbf{D}}\,\underline{\mathbf{H}}\,(\underline{\mathbf{D}}\,\underline{\mathbf{H}})\right)^{-1}\right]_{\nu,\nu} \cdot \lambda^{(k)}\right)^{-1},$$
$$\nu = (k-1)N + n. \quad (26)$$

In order to promote the understanding of the benefits of the scheme TxNZF to be developed in Section IV it would be convenient to make use of an average value of the KN values $\eta_n^{(k)}$ of (26). Such an average value $\overline{\eta}_{\mathrm{TxZF}}$ should be studied in the following. Basically, the energy efficiency $\eta_n^{(k)}$ of (26) is determined by two independent major effects. These two effects, which will be detailed in what follows, can be quantified by the two efficiencies

$$\eta_{\mathrm{a},n}^{(k)} = \frac{1}{\left[\left(\underline{\mathbf{D}}\,\underline{\mathbf{H}}\,(\underline{\mathbf{D}}\,\underline{\mathbf{H}})^{\mathrm{H}}\right)^{-1}\right]_{\nu,\nu} \cdot \left[\underline{\mathbf{D}}\,\underline{\mathbf{H}}\,(\underline{\mathbf{D}}\,\underline{\mathbf{H}})^{\mathrm{H}}\right]_{\nu,\nu}},$$
$$\nu = (k-1)N + n,\ 0 \le \eta_{\mathrm{a},n}^{(k)} \le 1, \quad (27)$$

and

$$\eta_{\mathrm{b},n}^{(k)} = \frac{\left[\underline{\mathbf{D}}\,\underline{\mathbf{H}}\,(\underline{\mathbf{D}}\,\underline{\mathbf{H}})^{\mathrm{H}}\right]_{\nu,\nu}}{\lambda^{(k)}},$$
$$\nu = (k-1)N + n,\ 0 \le \eta_{\mathrm{b},n}^{(k)} \le 1. \quad (28)$$

$\eta_{\mathrm{a},n}^{(k)}$ of (27) describes the price which has to be paid for avoiding MAI and ISI. As mentioned before, if MAI and ISI should be nulled, more or less stringent restrictions have to be obeyed while designing the transmitted symbol signals, which typically leads to an $\eta_{\mathrm{a},n}^{(k)}$ smaller than one.

$\eta_{\mathrm{b},n}^{(k)}$ of (28) only depends on the match between the demodulator matrix $\underline{\mathbf{D}}^{(k)}$ of MT k and the frequency selective radio channel between the BS antennas and the antenna of MT k and is therefore independent of $\eta_{\mathrm{a},n}^{(k)}$.

For $\eta_{\mathrm{b},n}^{(k)}$ equal to one, $\underline{\mathbf{D}}^{(k)}$ of MT k would be perfectly matched to the radio channel, if $\eta_{\mathrm{b},n}^{(k)}$ were zero, a complete mismatch would occur.

Setting out from (27) and (28), $\eta_n^{(k)}$ of (25) can be decomposed as

$$\eta_n^{(k)} = \eta_{\mathrm{a},n}^{(k)} \cdot \eta_{\mathrm{b},n}^{(k)}. \quad (29)$$

Based on (29) the average value

$$\eta_{\mathrm{TxZF}} = \mathop{\mathrm{E}}_{\underline{\mathbf{D}},\underline{\mathbf{H}}}\left\{\eta_n^{(k)}\right\} \quad (30)$$

of the KN values $\eta_n^{(k)}$ of (25) can be studied. For this purpose we assume the following:

- The $KK_{\mathrm{B}}W$ elements of the channel impulse responses $\underline{\mathbf{h}}^{(k,k_{\mathrm{B}})}$ of (6) are independent unbiased Gaussian random complex numbers with the same variance.
- The $N(Q_{\mathrm{t}} + w - 1)$ elements of $\underline{\mathbf{D}}^{(k)}$ of (17) are derived from an orthonormal set of N orthonormal binary sequences of dimension $Q_{\mathrm{t}} + W - 1$. The N rows of $\underline{\mathbf{D}}^{(k)}$ are obtained by scrambling the N sequences of this set by a common randomly generated scrambling code of dimension $Q_{\mathrm{t}} + W - 1$. The elements of this scrambling code have a fixed magnitude of one.

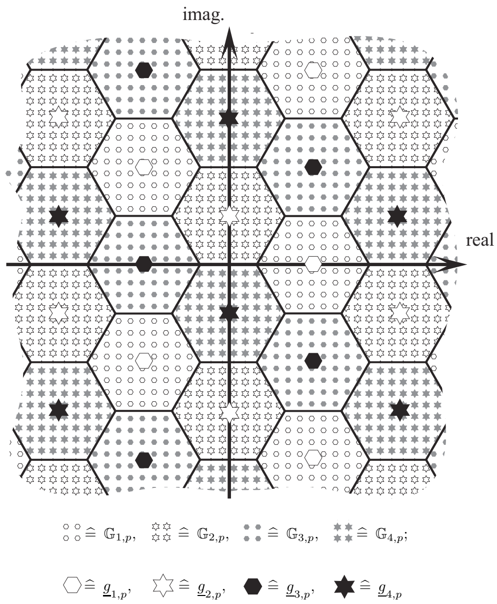

Fig. 2. Example of a quantization scheme with multiply connected decision regions $\mathbb{G}_m$ consisting of partial decision regions $\mathbb{G}_{m,p}$; $M = 4$

Based on results of the free probability theory [11] it can be shown that using

$$\eta_{\mathrm{a}} = \mathop{\mathrm{E}}_{\underline{\mathbf{D}},\underline{\mathbf{H}}}\left\{\eta_{\mathrm{a},n}^{(k)}\right\} \tag{31}$$

and

$$\eta_{\mathrm{b}} = \mathop{\mathrm{E}}_{\underline{\mathbf{D}},\underline{\mathbf{H}}}\left\{\eta_{\mathrm{b},n}^{(k)}\right\} \tag{32}$$

the average energy efficiency η_{TxZF} of (30) can be expressed as

$$\eta_{\mathrm{TxZF}} = \eta_{\mathrm{a}} \cdot \eta_{\mathrm{b}}. \tag{33}$$

To obtain η_{a} of (31) and η_{b} of (32) simulations are carried out. Therefore a large set of matrices $\underline{\mathbf{D}}$ and $\underline{\mathbf{H}}$ are randomly generated according to the way described above, for which, the equations (27), (28), (31) and (32) are evaluated. As a result of these simulations a very accurate expression for η_{a} can be obtained which reads

$$\eta_{\mathrm{a}} = \frac{K_B Q_{\mathrm{t}} - NK + 1}{K_B Q_{\mathrm{t}} - N + 1}. \tag{34}$$

Obviously, η_{a}, i.e., the price which has to be paid for avoiding MAI and ISI, is a linear function of K and independent of the dimension W of the channel impulse responses $\underline{\mathbf{h}}^{(k,k_{\mathrm{B}})}$ of (6). A related result for the case of Q_{t}, N and W equal to one, which is based on asymptotic analysis of random matrices [12] can be found in [13], [14].

Concerning η_{b} the simulation results disclose that, generally, η_{b} is a non-trivial function $\eta_{\mathrm{b}}(W, Q_{\mathrm{t}}, K_{\mathrm{B}})$ of W, Q_{t} and K_{B}, i.e., η_{b} does neither depend on the number K of MTs to be supported nor on the number N of data symbols per MT. Therefore, for given parameters W, Q_{t} and $K_{\mathrm{B}}, \eta_{\mathrm{b}}$ of (33) can be regarded as a constant. Especially for W equal one – that is in the case of non-frequency selective fading – it can be shown by analysing (28) that η_{b} becomes one, i.e. η_{TxZF} of (33) is totally described by (34).

Let us designate the required received symbol energy as R and the attenuation of the channel between the BS and MT k as $\alpha^{(k)}$. Then, if TxZF is applied, with η_{TxZF} of (34) the required average transmitted energy can be approximated as

$$\begin{aligned} T_{\mathrm{TxZF}} &= \frac{RN}{\eta_{\mathrm{TxZF}}} \sum_{k=1}^{K} \alpha^{(k)} \\ &= \frac{K_{\mathrm{B}}Q_{\mathrm{t}} - N + 1}{K_{\mathrm{B}}Q_{\mathrm{t}} - NK + 1} \cdot \frac{RN}{\eta_{\mathrm{b}}(W, Q_{\mathrm{t}}, K_{\mathrm{B}})} \sum_{k=1}^{K} \alpha^{(k)}. \end{aligned} \tag{35}$$

If we now for example design the transmitted symbol signals MT-wise, then, based on (30), (33) and (34) for K equal to one, we would obtain for the average energy efficiency

$$\eta_{\mathrm{TxNZF}} = \eta_{\mathrm{b}}(W, Q_{\mathrm{t}}, K_{\mathrm{B}}) > \eta_{\mathrm{TxZF}}, \tag{36}$$

which would approximately lead to the reduced required average transmitted energy

$$\begin{aligned} T_{\mathrm{TxNZF}} &= \frac{RN}{\eta_{\mathrm{TxNZF}}} \sum_{k=1}^{K} \alpha^{(k)} \\ &= \frac{RN}{\eta_{\mathrm{b}}(W, Q_{\mathrm{t}}, K_{\mathrm{B}})} \cdot \sum_{k=1}^{K} \alpha^{(k)} < T_{\mathrm{TxZF}}. \end{aligned} \tag{37}$$

IV. Proposed Downlink transmission scheme TxNZF

A. Multiply connected decision regions

We assume that the realizations of the message elements $a_n^{(k)}$ to be transmitted from the BS to the MTs are taken from a message element set $\{\mathcal{G}_1 \ldots \mathcal{G}_M\}$ of cardinality M. The decision devices in the MTs, see Section II, can be characterized by a complete pavement of the complex plane by M non-overlapping decision regions $\mathbb{G}_m$, $m = 1 \ldots M$, with each of these regions enclosing a specific representative $\underline{g}_m$, $m = 1 \ldots M$, [15]. It is aspired that in the noiseless case a message element $a_n^{(k)}$ of realization $\mathcal{G}_m$ would lead to the representative $\underline{g}_m$ at the demodulator output. Conventionally, the decision regions $\mathbb{G}_m$ are simply connected. An essential aspect of what follows is the utilization of P-fold connected decision regions [8]

$$\mathbb{G}_m = \mathbb{G}_{m,1} \cup \ldots \cup \mathbb{G}_{m,p} \cup \ldots \cup \mathbb{G}_{m,P} \tag{38}$$

with each partial decision region $\mathbb{G}_{m,p}$ containing its own representative $\underline{g}_{m,p}$. Fig. 2 shows an example with multiply connected decision regions for the case M equal to four.

Let us now assume that the message element $\underline{a}_n^{(k)}$ has the realization $\mathcal{G}_m$. Then, in the noiseless case, the demodulator should deliver one of the P values $\underline{g}_{m,p}$, $p \in \{1 \ldots P\}$. Quite generally, this value comes about as the sum of an interference component $\underline{i}_n^{(k)}$ resulting from the transmission of other message elements $\underline{a}_{n'}^{(k')}$, $k' \neq k \vee n' \neq n$, and a component being equal to the corresponding transmit value $\underline{\Delta}_n^{(k)}$ of (1). We then can write

$$\underline{\Delta}_n^{(k)} = \underline{g}_{m,p} - \underline{i}_n^{(k)} \tag{39}$$

and term $\underline{\Delta}_n^{(k)}$ as the correction component necessary to obtain $\underline{g}_{m,p}$ under the influence of the interference $\underline{i}_n^{(k)}$. In conventional TxZF the interference components $\underline{i}_n^{(k)}$ are a priori nulled [1], [2], whereas in the following considerations such components are deliberately conceded. As will be shown below, they depend on the realizations of the transmit message elements $\underline{a}_n^{(k)}$ and influence the choice of the correction components $\underline{\Delta}_n^{(k)}$. This way of generating $\underline{\Delta}_n^{(k)}$ constitutes the nonlinear feature of the proposed scheme TxNZF.

In the case of the P-fold connected decision regions provided in TxNZF, for a given value $\underline{i}_n^{(k)}$ of the interference and a given realization $\mathcal{G}_m$ of $\underline{a}_n^{(k)}$, according to (39), P options for $\underline{\Delta}_n^{(k)}$ exist, of which, with a view to radiate minimum energy for $\underline{a}_n^{(k)}$, the one with the smallest magnitude $|\underline{\Delta}_n^{(k)}|$ should be chosen, that is

$$\underline{a}_n^{(k)} = \mathcal{G}_m \quad \Rightarrow \quad \underline{\Delta}_n^{(k)} = \underline{g}_{m,p'} - \underline{i}_n^{(k)}, \tag{40}$$
$$p' = \arg \min_{p \in \{1 \ldots P\}} \left\{ \left| \underline{i}_n^{(k)} - \underline{g}_{m,p} \right|^2 \right\}.$$

The quantities $\underline{\Delta}_n^{(k)}, n = 1 \ldots N$, constitute the vector $\underline{\mathbf{\Delta}}^{(k)}$ of (1), and the quantities $\underline{i}_n^{(k)}$ can be stacked in the vector

$$\underline{\mathbf{i}}^{(k)} = \left(\underline{i}_1^{(k)} \ldots \underline{i}_n^{(k)} \ldots \underline{i}_N^{(k)} \right)^{\mathrm{T}}. \tag{41}$$

B. Construction of the transmit signal of TxNZF

In Section II we introduced the MT specific matrices $\underline{\mathbf{H}}^{(k)}$ and $\underline{\mathbf{D}}^{(k)}$, $k = 1 \ldots K$, of the channel and the demodulator, respectively. These matrices are now stacked in the matrices

$$\underline{\mathbf{H}}_k = \left(\underline{\mathbf{H}}^{(1)\mathrm{T}} \ldots \underline{\mathbf{H}}^{(k)\mathrm{T}} \right)^{\mathrm{T}} \tag{42}$$

and

$$\underline{\mathbf{D}}_k = \mathrm{blockdiag} \left(\underline{\mathbf{D}}^{(1)} \ldots \underline{\mathbf{D}}^{(k)} \right), \tag{43}$$

which we term cumulative matrices. Let us designate by $[\,\cdot\,]_i^j$ a matrix consisting of columns i to j of the matrix in brackets. Then, in TxNZF we a posteriori determine the MT specific modulator matrices

$$\underline{\mathbf{M}}^{(k)} = \left[(\underline{\mathbf{D}}_k \underline{\mathbf{H}}_k)^{\mathrm{H}} \left[\underline{\mathbf{D}}_k \underline{\mathbf{H}}_k \, (\underline{\mathbf{D}}_k \underline{\mathbf{H}}_k)^{\mathrm{H}} \right]^{-1} \right]_{(k-1)N+1}^{kN}, \quad k = 1 \ldots K, \tag{44}$$

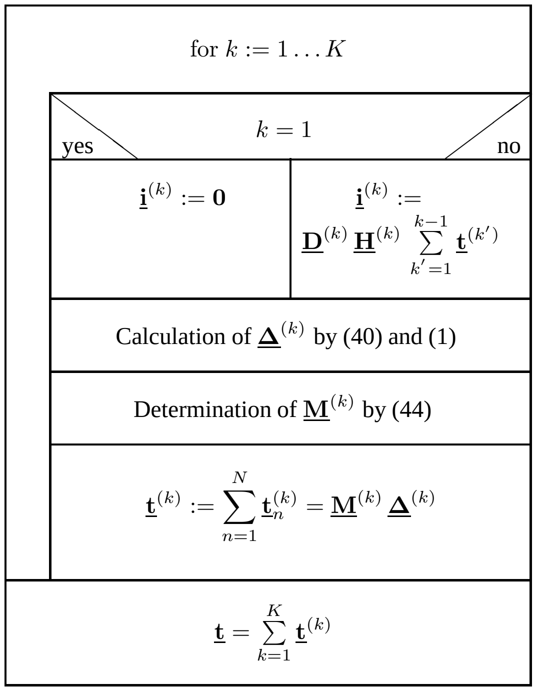

Fig. 3. Nassi-Shneiderman diagram describing the generation of the transmit signal $\underline{\mathbf{t}}$ in TxNZF

with $\underline{\mathbf{H}}_k$ of (42) and $\underline{\mathbf{D}}_k$ of (43). The basis of this way of determining the matrices $\underline{\mathbf{M}}^{(k)}$ is a modified version of the algorithm TxZF of (22).

In conventional TxZF to each transmit message element $\underline{a}_n^{(k)}$ corresponds a transmitted symbol signal $\underline{\mathbf{t}}_n^{(k)}$ [1], [2]. This situation shall be maintained in the case of TxNZF. The transmitted symbol signals yield the K MT specific transmit signals $\underline{\mathbf{t}}^{(k)}$, $k = 1 \ldots K$, and the total transmit signal

$$\underline{\mathbf{t}} = \sum_{k=1}^{K} \underbrace{\sum_{n=1}^{N} \underline{\mathbf{t}}_n^{(k)}}_{\underline{\mathbf{t}}^{(k)}} = \sum_{k=1}^{K} \underline{\mathbf{t}}^{(k)}. \tag{45}$$

In conventional TxZF the transmitted symbol signals $\underline{\mathbf{t}}_n^{(k)}$ are designed to have minimum energies under the side condition that ISI and intracell MAI are nulled [2], [3]. In TxNZF the MT specific transmit signals $\underline{\mathbf{t}}^{(k)}$ and the total transmit signal $\underline{\mathbf{t}}$ are determined by the MT-wise algorithm illustrated in a self-explanatory way by the Nassi-Shneiderman diagram [16] of Fig. 3. In this algorithm we assume that the mobile terminals MT k, $k = 1 \ldots K$, are arranged in the order of decreasing channel attenuations $\alpha^{(k)}$.

C. Benefits of TxNZF

As mentioned in Section I, with the total number KN of transmit message elements the zero forcing condition

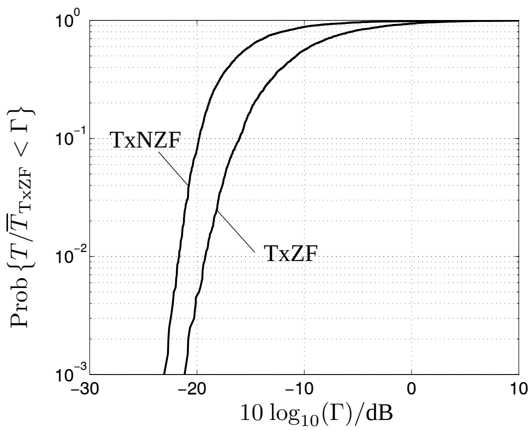

Fig. 4. Cumulative distribution functions of the required total transmit energy ratio $T/\overline{T}_{\mathrm{TxZF}}$, case 1

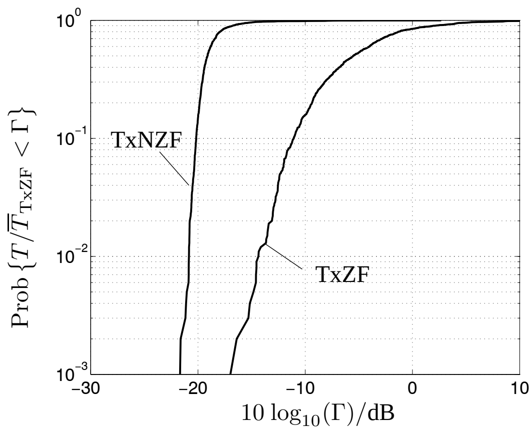

Fig. 5. Cumulative distribution functions of the required total transmit energy ratio $T/\overline{T}_{\mathrm{TxZF}}$, case 2

of the TxZF leads to $KN-1$ constraints on each transmitted symbol signal $\underline{\mathbf{t}}_n^{(k)}$, and the larger the number of such constraints, the smaller the energy efficiency, c.f. (34). In TxNZF, see Fig. 3, the transmitted symbol signals $\underline{\mathbf{t}}_n^{(k)}$, $n=1\ldots N$, for a certain MT k are constructed in such a way that, by zero forcing, ISI within the transmission for MT k as well as MAI to the MT $1\ldots(k-1)$ are avoided. However, MAI to the MTs $(k+1)\ldots K$ is allowed. Therefore, the number of constraints on the transmitted symbol signals $\underline{\mathbf{t}}_n^{(k)}$, $n=1\ldots N$, for MT k is $kN-1$. Consequently, the energy efficiencies of the transmitted symbol signals $\underline{\mathbf{t}}_n^{(k)}$ are highest for the MT with lowest value k.

As mentioned above, the MTs are arranged in the order of decreasing channel attenuation $\alpha^{(k)}$. Therefore, both in conventional TxZF and in TxNZF there is the tendency that the energies of the transmitted symbol signals $\underline{\mathbf{t}}_n^{(k)}$, $n=1\ldots N$, increase with decreasing k. However, in TxNZF also the energy efficiencies increase with decreasing k so that the transmitted symbol signals of basically high energy are endowed with high energy efficiencies. This combination of originally high required transmit energies and high energy efficiencies leads to the aspired reduction of the required transmit energies typical of TxNZF. This energy reduction is particularly distinct thanks to the utilization of multiply connected decision regions $\mathbb{G}_m$, $m=1\ldots M$, and the energy minimizing generation of the correction components $\underline{\mathbf{\Delta}}_n^{(k)}$, see (40).

V. Simulation results

Simulations of the transmission scheme TxNZF developed in Section IV are performed for the system parameters of Table I. A large number of snapshots is considered, in which the channel impulse responses $\underline{\mathbf{h}}^{(k,k_{\mathrm{B}})}$ of (6) and the demodulator matrices $\underline{\mathbf{D}}^{(k)}$ of (17) are basically generated as described in Section III. However, in order to model the different channel attenuations $\alpha^{(k)}$ the generated channel impulse responses $\underline{\mathbf{h}}^{(k,k_{\mathrm{B}})}$ are normalized in such a way that

$$\left\|\underline{\mathbf{h}}^{(1,k_{\mathrm{B}})}\right\|^2 = 1,\ k_{\mathrm{B}} = 1\ldots K_{\mathrm{B}}, \tag{46}$$

and

$$10\,\log_{10}\left(\frac{\left\|\underline{\mathbf{h}}^{(k,k_{\mathrm{B}})}\right\|^2}{\left\|\underline{\mathbf{h}}^{(k-1,k_{\mathrm{B}})}\right\|^2}\right) = \begin{cases} 0\ \mathrm{dB} & (\text{case } 1),\\ 3\ \mathrm{dB} & (\text{case } 2),\\ 6\ \mathrm{dB} & (\text{case } 3),\end{cases} \quad k = 2\ldots K, \tag{47}$$

hold. The considered multiply connected quantization scheme is a quadratic scheme as mentioned for instance in [10]. Figs. 4 to 6 show for the three cases of (47) the cumulative distribution functions of the ratio $T/\overline{T}_{\mathrm{TxZF}}$ of the required total transmitted energy T of (24) for the conventional TxZF and the novel TxNZF, respectively, and the average transmitted energy $\overline{T}_{\mathrm{TxZF}}$ for the conventional TxZF. Obviously, as expected, see (37), the scheme TxNZF is superior to the scheme TxZF with respect to the required transmitted energies. As also expected, this superiority of TxNZF increases with increasing differences of the channel attenuations.

It is well known that the application of multiply connected instead of simply connected decision regions

TABLE I
System parameters for the simulations

M	N	Q_{t}	K_{B}	K	W
4	4	16	2	8	5

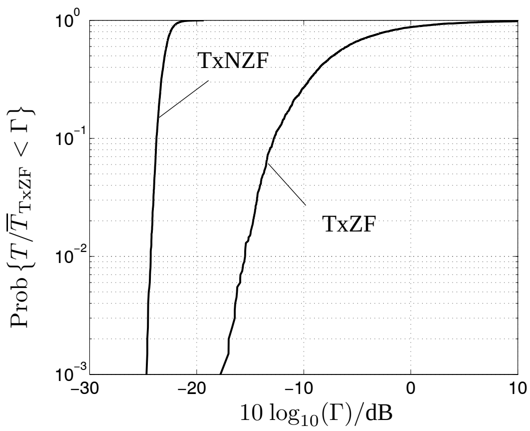

Fig. 6. Cumulative distribution functions of the required total transmit energy ratio $T/\overline{T}_{\mathrm{TxZF}}$, case 3

goes along with a slight increase of the symbol error probabilities. However, this disadvantage of TxNZF is inferior as compared to the significant transmit energy reductions offered by this scheme.

VI. Summary

The recently proposed linear Rx oriented transmission schemes for CDMA mobile radio downlinks excel by low receiver complexity, and they work without sacrificing downlink transmission resources for training signals, which is beneficial for capacity. These schemes can be modified in a nonlinear way by constructing the transmit signals MT-wise and by using multiply connected decision regions in the detectors of the MTs. The nonlinear Rx oriented transmission schemes obtained in this way require significantly less transmit power than conventional linear schemes, a desirable feature with respect to intercell interference mitigation in cellular systems, and to the growing electro-phobia of the public.

Acknowledgment

The authors gratefully appreciate the fruitful exchange of ideas with Prof. Nossek's group at TU Munich. The support of individual parts of this work in the framework of the EU-IST-Project FLOWS (Flexible Convergence of Wireless Standards and Services), by DFG, by Siemens AG and by the supercomputer staff of the central computer facility (RHRK) of the University of Kaiserslautern is highly acknowledged. Thanks are also extended to A. Bruhn and M. Cuntz for carefully typesetting the manuscript in LaTeX.

References

[1] M. Meurer, P. W. Baier, T. Weber, Y. Lu, and A. Papathanassiou, "Joint transmission: advantageous downlink concept for CDMA mobile radio systems using time division duplexing," *IEE ELECTRONICS LETTERS*, vol. 11, pp. 900–901, 2000.

[2] P. W. Baier, W. Qiu, H. Tröger, C. A. Jötten, and M. Meurer, "Modelling and optimization of receiver oriented multi-user MIMO downlinks for frequency selective channels," in *Proc. 10th International Conference on Telecommunications (ICT'03)*, Papeete, 2003, pp. 1547–1554.

[3] P. W. Baier and M. Meurer, "Receiver orientation, an unconventional approach to mobile radio downlink design," in *Proc. European Conference on Wireless Technology (ECWT'03)*, Munich, 2003, pp. 11–14.

[4] M. Joham, K. Kusume, M. H. Gzara, W. Utschick, and J. A. Nossek, "Transmit Wiener Filter for the Downlink of TDD DS-CDMA Systems," in *Proc. IEEE 7th International Symposium on Spread Spectrum Techniques & Applications (ISSSTA'02)*, Prague, 2002, pp. 9–13.

[5] B.R. Vojcic and J.W. Mee, "Transmitter precoding in synchronous multiuser communications," *IEEE Transactions on Communications*, vol. 46, no. 10, pp. 1346–1355, October 1998.

[6] M. Tomlinson, "New automatic equalizer employing modulo arithmetic," *IEE ELECTRONICS LETTERS*, vol. 7, pp. 138–139, 1971.

[7] H. Harashima and H. Miyakawa, "Matched-transmission technique for channels with intersymbol interference," *IEEE Transactions on Communications*, vol. COM-20, pp. 774–780, 1972.

[8] M. V. Eyuboglu and G. D. Forney, Jr., "Trellis precoding: combined coding, precoding and shaping for intersymbol interference channels," *IEEE Transactions on Information Theory*, vol. 38, pp. 301–314, 1992.

[9] Wei Yu and J. M. Cioffi, "Trellis precoding for the broadcast channel," in *Proc. IEEE Global Telecommunications Conference (GLOBECOM'01)*, San Antonio, 2002, pp. 1344–1348.

[10] R.F.H. Fischer, *Precoding and Signal Shaping for Digital Transmission*, John Wiley & Sons, New York, 2002.

[11] D. V. Voiculescu, K. J. Dykema, and A. Nica, "Limit laws for random matrices and free products," *Inventiones Mathematicae*, vol. 104, pp. 201–220, 1991.

[12] M. L. Mehta, *Random matrices*, Academic Press, San Diego, 1991.

[13] E. Jorswieck, G. Wunder, V. Jungnickel, and T. Haustein, "Inverse eigenvalue statistics for rayleigh and rician MIMO channels," *IEE Professional Network on Antennas and Propagation*, pp. 3/1–3/6, 2001.

[14] T. Haustein, C. von Helmolt, E. Jorswieck, V. Jungnickel, and V. Pohl, "Performance of MIMO systems with channel inversion," in *Proc. IEEE 55th Vehicular Technology Conference (VTC'02)*, Birmingham, 2002, pp. 35–39.

[15] A. J. Viterbi and J. K. Omura, *Principles of Digital Communication and Coding*, McGraw-Hill, New York, 1979.

[16] I. Nassi and B. Shneiderman, "Flowchart techniques for structured programming," in *ACM SIGPLAN Notices*, 1973, vol. 8, pp. 12–26.

[WMZ04a] Weber, T.; Meurer, M.; Zirwas, W.: "Low Complexity Energy Efficient Joint Transmission for OFDM Multiuser Downlinks". *Proc. IEEE 15th International Symposium on Personal, Indoor and Mobile Radio Communications (PIMRC'04)*, Barcelona, 2004.

Low Complexity Energy Efficient Joint Transmission for OFDM Multiuser Downlinks

Tobias Weber, Michael Meurer, Wolfgang Zirwas
Tobias Weber and Michael Meurer are with the Research Group for RF Communications, University of Kaiserslautern, D–67653 Kaiserslautern, Germany, Email: tweber@rhrk.uni-kl.de,
Wolfgang Zirwas is with Siemens AG, Information & Communication Mobile Networks, D–81730 Munich, Germany

***Abstract*— A specially favorable concept for interference reduction in future mobile radio systems consists in the application of joint detection in the uplink and joint transmission in the downlink. Concerning joint detection both optimum nonlinear and low complexity suboptimum linear signal processing algorithms are well known. This is not the case for joint transmission, where up to now most research work focuses on linear signal processing algorithms, which are dual to the ones applied for joint detection. In the present paper a novel signal processing algorithm for joint transmission, termed transmit nonlinear zero forcing, is presented. The main characteristic is the application of an unconventional multiply connected quantization scheme, which allows to improve the energy efficiency, i.e., for data symbols to be transmitted over channels with high attenuations without introducing excessive interferences. Especially in scenarios with large gain differences of the channels between the access point and individual mobile terminals said improved energy efficiencies allow a significant reduction of the required transmitted powers, a feature mitigating intercell interference in cellular systems and thereby enhancing system capacity. In practical systems such gain differences, due to shadowing and largely different distances between the access point and the mobile terminals, prevail.**

I. Introduction

The basic idea of joint transmission (JT) is to design the transmitted signals in such a way that interferences in the received data symbols are a-priori avoided. For doing so, knowledge about the receivers and the channels is required on the transmitter side. In the following it is assumed that the receivers consist of a linear filter followed by a quantizer. Both the filter impulse responses and the quantization schemes are assumed to be a-priori known on the transmitter side. Furthermore perfect channel knowledge is assumed to be available on the transmitter side. In practical systems said channel knowledge could be obtained by channel estimation in the uplink if time division duplexing is used.

Up to now investigations focused on linear signal processing algorithms for JT in combination with conventional, i.e., simply connected quantization schemes [1], [2], [3], [4]. It was only recently that nonlinear JT algorithms, which exploit the discrete nature of the modulation alphabet, attained attraction. First investigations focused on nonlinear transmitter side signal processing in combination with conventional simply connected quantization schemes on the receiver side [5], [6]. However, nonlinear transmitter side signal processing alone can not combat the problem of large required transmitted energies for interference compensation. This problem can only be avoided by going to unconventional multiply connected quantization schemes. The novel transmit nonlinear zero forcing (TxNZF) exploits multiply connected quantization schemes for transmitted energy reduction. Similar transmission schemes were published in [7], [8], [9].

In the following a mobile radio system without spreading where each mobile terminal (MT) k, $k = 1 \dots K$, receives a single data symbol and is equipped with a single receive antenna and where the access point (AP) has multiple transmit antennas k_A, $k_\mathrm{A} = 1 \dots K_\mathrm{A}$, is considered. In order to enable multiple access interference reduction by linear transmission techniques, the number of antennas at the AP must be at least as large as the number of MTs

$$K_\mathrm{A} \geq K. \tag{1}$$

The radio channel between the antennas $k_\mathrm{A} = 1 \dots K_\mathrm{A}$ of the AP and the entirety of all antennas $k = 1 \dots K$ of the MTs constitutes a MIMO channel. In the following for simplicity only flat fading MIMO channels are considered. This is no restriction as any frequency selective channel can be converted into multiple parallel flat fading channels, e.g., by the use of OFDM [10], without any performance loss. An exemplary mobile radio system concept which fulfills the above made assumptions is the JOINT concept for beyond 3G mobile radio systems presented in [11], [12]. In the present paper $[\cdot]_{k,k}$ denotes the k-th diagonal element of a matrix, $[\cdot]_k$ denotes the k-th element of a vector, and $[\cdot]_{y_2,x_2}^{y_1,x_1}$ yields the submatrix bounded by the rows y_1 and y_2 and columns x_1 and x_2.

II. System Model

The data symbol to be transmitted for MT k is denoted by $\underline{d}^{(k)}$. For simplicity it is assumed that the data symbols are QPSK modulated in the following, i.e., each data symbol contains two bits:

$$\begin{aligned} \underline{d}^{(k)} \quad &\in \quad \mathbb{D}_\mathrm{QPSK} = \{+1+\mathrm{j}, +1-\mathrm{j}, -1+\mathrm{j}, -1-\mathrm{j}\}, \\ & \quad\;\; k = 1 \dots K. \end{aligned} \tag{2}$$

In the following it is assumed that the data symbols $\underline{d}^{(k)}$, $k = 1 \dots K$, are uncorrelated. The energy of the data symbol $\underline{d}^{(k)}$ is

$$E_\mathrm{d} = \frac{1}{2}\mathrm{E}\left\{\left|\underline{d}^{(k)}\right|^2\right\} = 1. \tag{3}$$

All K data symbols of the different MTs are compiled in the data vector

$$\underline{\mathbf{d}} = \left(\underline{d}^{(1)} \dots \underline{d}^{(K)}\right)^\mathrm{T}. \tag{4}$$

On the transmitter side transmitted signals for K_A inputs to the mobile radio channel are generated. The transmitted signal for input k_A, which corresponds to transmit antenna

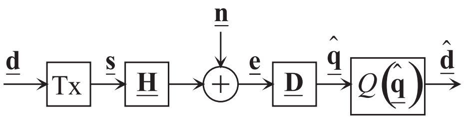

Fig. 1. System model

$k_{\rm A}$, is characterized by the complex value $\underline{s}^{(k_{\rm A})}$, which may be thought of as a sample of the signal in the equivalent lowpass domain or a complex amplitude [13]. From all $K_{\rm A}$ transmitted signals the transmitted vector

$$\underline{\mathbf{s}} = \left(\underline{s}^{(1)} \dots \underline{s}^{(K_{\rm A})}\right)^{\rm T} \tag{5}$$

is formed. The energy of the transmitted vector $\underline{\mathbf{s}}$ may depend on the data vector $\underline{\mathbf{d}}$ to be transmitted. In the following only the average transmitted energy

$$T = \frac{1}{2}{\rm E}\left\{\underline{\mathbf{s}}^{\rm H}\underline{\mathbf{s}}\right\} \tag{6}$$

is considered. In general the elements $\underline{s}^{(k_{\rm A})}$, $k_{\rm A} = 1 \dots K_{\rm A}$, of the transmitted vector $\underline{\mathbf{s}}$ are generated depending on all data symbols $\underline{d}^{(k)}$, $k = 1 \dots K$, of the data vector $\underline{\mathbf{d}}$.

The received signal of MT k is also characterized by a complex value $\underline{e}^{(k)}$. From all K received signals the received vector

$$\underline{\mathbf{e}} = \left(\underline{e}^{(1)} \dots \underline{e}^{(K)}\right)^{\rm T} \tag{7}$$

is formed.

The received signals $\underline{e}^{(k)}$, $k = 1 \dots K$, are linear functions of the transmitted signals $\underline{s}^{(k_{\rm A})}$, $k_{\rm A} = 1 \dots K_{\rm A}$, plus some noise $\underline{n}^{(k_{\rm A})}$, $k_{\rm A} = 1 \dots K_{\rm A}$. With the channel matrix $\underline{\mathbf{H}}$ describing the linear MIMO channel and the noise vector

$$\underline{\mathbf{n}} = \left(\underline{n}^{(1)} \dots \underline{n}^{(K_{\rm A})}\right)^{\rm T} \tag{8}$$

follows

$$\underline{\mathbf{e}} = \underline{\mathbf{H}} \cdot \underline{\mathbf{s}} + \underline{\mathbf{n}}, \tag{9}$$

see Fig. 1. For simplicity it is assumed in the following that the elements $\underline{n}^{(k_{\rm A})}$, $k_{\rm A} = 1 \dots K_{\rm A}$ of the noise vector $\underline{\mathbf{n}}$ are uncorrelated, Gaussian distributed with variance σ^2 of real and imaginary part [13].

On the receiver side, discrete valued estimates $\hat{\underline{d}}^{(k)}$ of the transmitted data symbols $\underline{d}^{(k)}$, $k = 1 \dots K$, are obtained in a two step procedure. First of all continuous valued estimates $\hat{\underline{q}}^{(k)}$, $k = 1 \dots K$, compiled in the vector

$$\hat{\underline{\mathbf{q}}} = \left(\hat{\underline{q}}^{(1)} \dots \hat{\underline{q}}^{(K)}\right)^{\rm T} \tag{10}$$

are obtained as a linear function of the received vector $\underline{\mathbf{e}}$ characterized by the demodulator matrix $\underline{\mathbf{D}}$:

$$\hat{\underline{\mathbf{q}}} = \underline{\mathbf{D}} \cdot \underline{\mathbf{e}}. \tag{11}$$

In practical systems the estimate $\hat{\underline{q}}^{(k)}$ has to be determined from the corresponding received signal $\underline{e}^{(k)}$ of MT k alone due to the spatial separation of the MTs. In the following it is assumed that the demodulator matrix $\underline{\mathbf{D}}$ is equal to the identity matrix

$$\underline{\mathbf{D}} = \mathbf{I}. \tag{12}$$

In a second step the discrete valued estimates $\hat{\underline{d}}^{(k)}$ are obtained by quantization of the continuous valued estimates $\hat{\underline{q}}^{(k)}$, $k = 1 \dots K$. Here again each discrete valued estimate $\hat{\underline{q}}^{(k)}$ is a function of the corresponding continuous valued estimate $\hat{\underline{d}}^{(k)}$ alone.

Concerning the quantizer in general multiple representatives $\underline{q}_{m,p^{(m)}}$, $p^{(m)} = 1 \dots P^{(m)}$, exist for each possible data symbol value

$$\underline{d}_m \in \mathbb{D},\ m = 1 \dots M = \|\mathbb{D}\|\,. \tag{13}$$

The Voronoi regions $\mathbb{Q}_{m,p^{(m)}}$ of the representatives $\underline{q}_{m,p^{(m)}}$, $m = 1 \dots M$, $p^{(m)} = 1 \dots P^{(m)}$, are termed partial decision regions in the following. In general each decision region $\mathbb{Q}_m$, $m = 1 \dots M$, consists of multiple partial decision regions $\mathbb{Q}_{m,p^{(m)}}$:

$$\mathbb{Q}_m = \bigcup_{p^{(m)}=1}^{P^{(m)}} \mathbb{Q}_{m,p^{(m)}} \tag{14}$$

The operation of the quantizer can be characterized by the quantization function

$$\underline{Q}\left(\hat{\underline{q}}^{(k)}\right) = \hat{\underline{d}}^{(k)} \in \mathbb{D}, \tag{15}$$

which assigns to an observed value $\hat{\underline{q}}^{(k)} \in \mathbb{C}$ a specific value $\hat{\underline{d}}^{(k)}$ out of $\mathbb{D}$ in the following two steps:

1) Determine the index m of the decision region $\mathbb{Q}_m$, in which $\hat{\underline{q}}^{(k)}$ lies.
2) Give out the value $\underline{d}_m$ as the decided value $\hat{\underline{d}}^{(k)}$.

The notation $\underline{Q}\left(\hat{\underline{\mathbf{q}}}\right)$ in Fig. 1 means that the quantization function $\underline{Q}\left(\hat{\underline{q}}^{(k)}\right)$ of (15) is applied to each of the K components of the vector $\hat{\underline{\mathbf{q}}}$.

We term a quantization scheme, in which

- the decision regions $\mathbb{Q}_m$, $m = 1 \dots M$, are simply connected, that is $P^{(m)} = 1$, $m = 1 \dots M$, and
- the representative $\underline{q}_{m,1}$ is equal to the corresponding data symbol value $\underline{d}_m$

conventional. Otherwise, we designate the quantization scheme as unconventional. Besides the conventional quantization scheme for QPSK modulation defined by (2) a regular unconventional quantization scheme will be considered in the paper. With the integer numbers $n_{\rm r} \in \mathbb{Z}$ and $n_{\rm i} \in \mathbb{Z}$

$$\underline{q}_{m,p^{(m)}} = \underline{d}_m + n_{\rm r} \cdot 4 + {\rm j} \cdot n_{\rm i} \cdot 4, \tag{16}$$

holds for the infinitely many representatives $\underline{q}_{m,p^{(m)}}$, $p^{(m)} = 1 \dots P^{(m)}$, of the data symbol value $\underline{d}_m \in \mathbb{D}_{\rm QPSK}$ in the considered regular unconventional quantization scheme. For this regular quantization scheme the quantization function of (15) reads

$$Q\left(\underline{\hat{q}}^{(k)}\right) = \operatorname{sign}\left(\left(\operatorname{Re}\left\{\underline{\hat{q}}^{(k)} + 2\right\}\right) \bmod 4 - 2\right) \\ +\mathrm{j}\operatorname{sign}\left(\left(\operatorname{Im}\left\{\underline{\hat{q}}^{(k)} + 2\right\}\right) \bmod 4 - 2\right). \quad (17)$$

III. Linear multiuser transmission

A. Generalized linear data transmission

For linear data transmission conventional quantizers are employed at the receiver side. Consequently, the transmitter should be designed in such a way, that the continuous valued data estimates $\underline{\hat{q}}^{(k)}$ are as close as possible to the true data symbols $\underline{d}^{(k)}$, $k = 1\ldots K$. For this linear transmitters, characterized by a modulator matrix $\underline{\mathbf{M}}$ may be used. For the transmitted vector

$$\underline{\mathbf{s}} = \underline{\mathbf{M}} \cdot \underline{\mathbf{d}} \quad (18)$$

holds. With (3) the average transmitted energy of (6) reads

$$T = \operatorname{trace}\left\{\underline{\mathbf{M}}^{\mathrm{H}}\underline{\mathbf{M}}\right\} E_{\mathrm{d}}. \quad (19)$$

In the case of linear data transmission the transmitted vector $\underline{\mathbf{s}}$ is the superposition of partial transmitted vectors

$$\underline{\mathbf{s}}^{(k)} = [\underline{\mathbf{M}}]^{1,k}_{K_{\mathrm{A}},k}\, \underline{d}^{(k)},\ k = 1\ldots K, \quad (20)$$

each one containing the information on a specific data symbol $\underline{d}^{(k)}$. For the transmitted vector

$$\underline{\mathbf{s}} = \sum_{k=1}^{K} \underline{\mathbf{s}}^{(k)} \quad (21)$$

follows. The column vector $[\underline{\mathbf{M}}]^{1,k}_{K_{\mathrm{A}},k}$ is termed transmitted signature for the data symbol $\underline{d}^{(k)}$ in the following, i.e., the modulator matrix $\underline{\mathbf{M}}$ is made up from the transmitted signatures of all data symbols $\underline{d}^{(k)}$, $k = 1\ldots K$. The average partial transmitted energy $T^{(k)}$ for a specific data symbol $\underline{d}^{(k)}$ can be calculated as follows:

$$T^{(k)} = \frac{1}{2}\mathrm{E}\left\{\underline{\mathbf{s}}^{(k)\,\mathrm{H}}\underline{\mathbf{s}}^{(k)}\right\} = [\underline{\mathbf{M}}]^{1,k\ \mathrm{H}}_{K_{\mathrm{A}},k}\,[\underline{\mathbf{M}}]^{1,k}_{K_{\mathrm{A}},k} \cdot E_{\mathrm{d}}. \quad (22)$$

B. Transmit matched filtering (TxMF)

The idea behind TxMF is the minimization of the average partial transmitted energy $T^{(k)}_{\mathrm{MF}}$ of (22) required for the transmission of a certain data symbol $\underline{d}^{(k)}$ if interferences are neglected, i.e., each transmitted signature is optimized separately. From this rationale the modulator matrix

$$\underline{\mathbf{M}}_{\mathrm{MF}} = \underline{\mathbf{H}}^{\mathrm{H}} \cdot \left(\operatorname{diag}\left(\underline{\mathbf{H}}\,\underline{\mathbf{H}}^{\mathrm{H}}\right)\right)^{-1} \quad (23)$$

follows. If multiple data symbols are transmitted in parallel the partial transmitted vector $\underline{\mathbf{s}}^{(k)}$, $k = 1\ldots K$, of (20) obtained by TxMF may cause quite strong interferences $[\underline{\mathbf{H}}]^{k',1}_{k',K_{\mathrm{A}}} \cdot [\underline{\mathbf{M}}_{\mathrm{MF}}]^{1,k}_{K_{\mathrm{A}},k} \cdot \underline{d}^{(k)}$ to other data symbols $k' \neq k$.

C. Transmit zero forcing (TxZF)

TxZF totally eliminates interferences, i.e.,

$$\underline{\mathbf{H}} \cdot \underline{\mathbf{M}}_{\mathrm{ZF}} = \mathbf{I} \quad (24)$$

holds. Remaining degrees of freedom in the choice of $\underline{\mathbf{M}}_{\mathrm{ZF}}$ are exploited for a minimization of the required average transmitted energy T_{ZF} of (22). From this rationale the modulator matrix

$$\underline{\mathbf{M}}_{\mathrm{ZF}} = \underline{\mathbf{H}}^{\mathrm{H}}\left(\underline{\mathbf{H}}\,\underline{\mathbf{H}}^{\mathrm{H}}\right)^{-1} \quad (25)$$

is obtained. Alternately, using the QR-decomposition [14], [15]

$$\underline{\mathbf{H}} = \underline{\mathbf{R}} \cdot \underline{\mathbf{Q}} \quad (26)$$

with the square lower triangular matrix $\underline{\mathbf{R}}$ the modulator matrix could be calculated as

$$\underline{\mathbf{M}}_{\mathrm{ZF}} = \underline{\mathbf{Q}}^{\mathrm{H}}\underline{\mathbf{R}}^{-1}. \quad (27)$$

The price to be paid for the elimination of interferences is an increase of the average transmitted energy T_{ZF} as compared to TxMF. The energy efficiency $\epsilon^{(k)}_{\mathrm{ZF}}$ for a certain data symbol $\underline{d}^{(k)}$ is defined as the ratio of the average partial transmitted energy $T^{(k)}_{\mathrm{MF}}$ required by TxMF and the average partial transmitted energy $T^{(k)}_{\mathrm{ZF}}$ of TxZF:

$$\epsilon^{(k)}_{\mathrm{ZF}} = \frac{T^{(k)}_{\mathrm{MF}}}{T^{(k)}_{\mathrm{ZF}}} = \frac{1}{\left[\left(\underline{\mathbf{R}}\,\underline{\mathbf{R}}^{\mathrm{H}}\right)^{-1}\right]_{k,k} \cdot \left[\underline{\mathbf{R}}\,\underline{\mathbf{R}}^{\mathrm{H}}\right]_{k,k}}. \quad (28)$$

The energy efficiency $\epsilon^{(k)}_{\mathrm{ZF}}$ takes values from 0 to 1, with 1 being the optimum.

D. Partial transmit zero forcing (TxPZF)

In TxPZF forcing the elimination of interference to certain data symbols is sacrificed for the reduction of the required transmitted energy. Without loss of generality the partial transmitted vector $\underline{\mathbf{s}}^{(k)}$ for data symbol $\underline{d}^{(k)}$ is considered in the following. Interferences to preceding data symbols $\underline{d}^{(k')}$, $k' = 1\ldots k-1$, should be eliminated whereas interferences to subsequent data symbols $\underline{d}^{(k')}$, $k' = k+1\ldots K$, are allowed. Exploiting the remaining degrees of freedom for energy minimization the transmitted signature

$$[\underline{\mathbf{M}}_{\mathrm{PZF}}]^{1,k}_{K_{\mathrm{A}},k} = \left[[\underline{\mathbf{H}}]^{1,1\ \mathrm{H}}_{k,K_{\mathrm{A}}}\left([\underline{\mathbf{H}}]^{1,1}_{k,K_{\mathrm{A}}}\,[\underline{\mathbf{H}}]^{1,1\ \mathrm{H}}_{k,K_{\mathrm{A}}}\right)^{-1}\right]^{1,k}_{K_{\mathrm{A}},k} \quad (29)$$

for data symbol $\underline{d}^{(k)}$ is obtained. The computational complexity required for computing the modulator matrix $\underline{\mathbf{M}}_{\mathrm{PZF}}$ could be reduced using the QR-decomposition of (26)

$$\underline{\mathbf{M}}_{\mathrm{PZF}} = \underline{\mathbf{Q}}^{\mathrm{H}}\left(\operatorname{diag}\left(\underline{\mathbf{R}}\right)\right)^{-1}. \quad (30)$$

The energy efficiency of TxPZF reads

$$\epsilon^{(k)}_{\mathrm{PZF}} = \frac{T^{(k)}_{\mathrm{MF}}}{T^{(k)}_{\mathrm{PZF}}} = \frac{[\underline{\mathbf{R}}]_{k,k}\left[\underline{\mathbf{R}}^{\mathrm{H}}\right]_{k,k}}{\left[\underline{\mathbf{R}}\,\underline{\mathbf{R}}^{\mathrm{H}}\right]_{k,k}}. \quad (31)$$

and is always larger than or equal to the energy efficiency $\epsilon_{\mathrm{ZF}}^{(k)}$ of TxZF of (28). In general the energy efficiency $\epsilon_{\mathrm{PZF}}^{(k)}$ of TxPZF becomes larger if less interference is eliminated, i.e., for smaller values of k.

IV. Transmit nonlinear zero forcing (TxNZF)

The dilemma of linear transmission in combination with conventional quantizers is that it is not possible to simultaneously

- eliminate interferences and to
- obtain high energy efficiencies $\epsilon^{(k)}$, $k = 1 \dots K$.

In [5], [6] it is shown that even nonlinear transmission techniques cannot overcome this dilemma.

The crux of our new approach TxNZF consists in using an unconventional quantizer, which requires only slight modifications of the receivers. Thanks to this unconventional quantizer it is not necessary to totally eliminate interferences in order to render them harmless anymore. The goal is to design the transmitter in such a way that the continuous valued estimates $\underline{\hat{q}}^{(k)}$, $k = 1 \dots K$, are as close as possible to one of the representatives of the data symbol values to be transmitted, i.e., there exists the additional degree of freedom to chose one of the representatives. Preferably the representatives are chosen in such a way that the average transmitted energy T is minimized [16]. In general this optimization is a very complex task. In the following a suboptimum, low complexity algorithm for the selection of the representatives which leads to a good overall performance is presented.

The partial transmitted vectors $\underline{\mathbf{s}}^{(k)}$ for the data symbols $\underline{d}^{(k)}$, $k = 1 \dots K$, are designed one after the other in TxNZF, starting with the partial transmitted vector $\underline{\mathbf{s}}^{(1)}$ for the first data symbol $\underline{d}^{(1)}$. This is no restriction since the MTs can be numbered in any desired order. In the following the design of the partial transmitted vector $\underline{\mathbf{s}}^{(k)}$ for one specific data symbol $\underline{d}^{(k)}$, taking the value $\underline{d}_m$, is described in detail. First of all the interference $\underline{i}^{(k)}$ resulting from the partial transmitted vectors $\underline{\mathbf{s}}^{(k')}$ of the preceding data symbols $\underline{d}^{(k')}$, $k' = 1 \dots k-1$, is calculated

$$\underline{i}^{(k)} = \left[\underline{\mathbf{H}} \cdot \sum_{k'=1}^{k-1} \underline{\mathbf{s}}^{(k')}\right]_k . \tag{32}$$

We introduce the difference signal

$$\underline{\Delta}^{(k)} = \underline{q}_{m,p^{(m)}} - \underline{i}^{(k)}. \tag{33}$$

Preferably, the representative $\underline{q}_{m,p^{(m)}}$ for which the difference signal energy $\frac{1}{2}\left|\underline{\Delta}^{(k)}\right|^2$ is minimum is chosen. Finally, following the idea of TxPZF, the partial transmitted vector $\underline{\mathbf{s}}^{(k)}$ is designed in such a way that no new interferences to the previous data symbols $\underline{d}^{(k')}$, $k' = 1 \dots k-1$, are introduced. In contrast to TxZF interferences to subsequent data symbols $\underline{d}^{(k')}$, $k' = k+1 \dots K$, are allowed, leading to an improved energy efficiency $\epsilon_{\mathrm{PZF}}^{(k)}$ for the considered data symbol $\underline{d}^{(k)}$ especially for the first data symbols with small values of k. With (29) and (33) follows

$$\underline{\mathbf{s}}^{(k)} = [\underline{\mathbf{M}}_{\mathrm{PZF}}]_{K_{\mathrm{A}},k}^{1,k} \cdot \underline{\Delta}^{(k)}. \tag{34}$$

QR-decomposition $\underline{\mathbf{H}} = \underline{\mathbf{R}}\underline{\mathbf{Q}}$

$\underline{\mathbf{M}}_{\mathrm{PZF}} = \underline{\mathbf{Q}}^{\mathrm{H}} \left(\mathrm{diag}\left(\underline{\mathbf{R}}\right)\right)^{-1}$

$\underline{\mathbf{s}} = \mathbf{0}$

for $k = 1 \dots K$

- $\underline{i}^{(k)} = [\underline{\mathbf{H}}\,\underline{\mathbf{s}}]_k$
- $\underline{q}^{(k)} = \underset{\text{all representatives } \underline{q} \text{ for } \underline{d}^{(k)}}{\arg\min} \left\{\frac{1}{2}\left|\underline{q} - \underline{i}^{(k)}\right|^2\right\}$
- $\underline{\Delta}^{(k)} = \underline{q}^{(k)} - \underline{i}^{(k)}$
- $\underline{\mathbf{s}} = \underline{\mathbf{s}} + [\underline{\mathbf{M}}_{\mathrm{PZF}}]_{K_{\mathrm{A}},k}^{1,k} \cdot \underline{\Delta}^{(k)}$

Fig. 2. Signal processing algorithm for TxNZF

The Nassi Shneiderman diagram shown in Fig. 2 summarizes the signal processing algorithm applied in TxNZF.

TxNZF is particularly beneficial if the MTs are numbered in the order of increasing channel gain

$$g^{(k)} = \left[\underline{\mathbf{H}}\,\underline{\mathbf{H}}^{\mathrm{H}}\right]_{k,k} . \tag{35}$$

Then the partial transmitted vectors $\underline{\mathbf{s}}^{(k)}$ of the MTs with the lowest channel gains are designed first. This way especially the energy efficiencies $\epsilon_{\mathrm{PZF}}^{(k)}$ for MTs with low channel gains $g^{(k)}$ are improved as compared to TxZF and consequently the partial average transmitted energies $T^{(k)}$ for those MTs can be significantly reduced. As the partial average transmitted energies $T^{(k)}$ for MTs with low channel gains $g^{(k)}$ have dominant influence on the average transmitted energy T, also the average transmitted energy T is reduced considerably.

V. Illustrative example

To illustrate the benefits of TxNZF a simple scenario containing

$$K = 2 \tag{36}$$

MTs and an AP with

$$K_{\mathrm{A}} = 2 \tag{37}$$

antennas is considered. The unconventional quantization scheme of (16) is used. For this regular quantization scheme

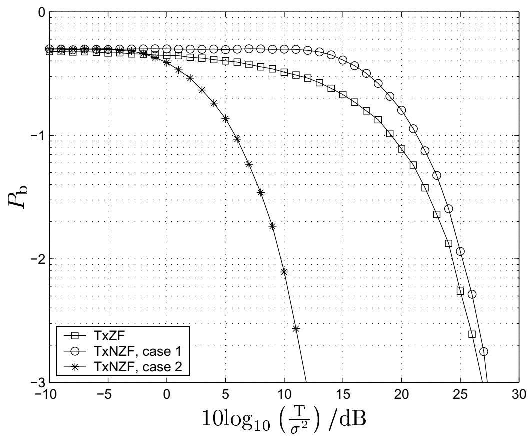

Fig. 3. Average bit error probability P_b as a function of T/σ^2

the calculation of the difference signal $\underline{\Delta}^{(k)}$ can be simplified as follows:

$$\underline{\Delta}^{(k)} = \text{round}\left\{\left(\underline{i}^{(k)} - \underline{d}^{(k)}\right)\Big/4\right\}\cdot 4 + \underline{d}^{(k)} - \underline{i}^{(k)}. \quad (38)$$

For the flat fading MIMO channel two cases are considered:

1) A channel with the second MT having the lower channel gain $g^{(k)}$:

$$\underline{\mathbf{H}} = \begin{pmatrix} 10 & 10 \\ 1 & 0.8 \end{pmatrix} \quad (39)$$

2) A channel with the first MT having the lower channel gain $g^{(k)}$:

$$\underline{\mathbf{H}} = \begin{pmatrix} 1 & 0.8 \\ 10 & 10 \end{pmatrix} \quad (40)$$

Fig. 3 shows the average bit error probability P_b as a function of the ratio of the average transmitted energy T and the variance σ^2 of the noise at the receiver input for TxZF and TxNZF. As can be seen from Fig. 3 TxNZF does not offer any performance advantages over TxZF if the second MT has a lower channel gain, as in this case practically always the representatives

$$\underline{q}^{(k)} = \underline{d}^{(k)} \quad (41)$$

are chosen. In this case the unconventional quantizer in the receiver even approximately doubles the bit error probability P_b as the partial decision regions $\mathbb{Q}_{m,p^{(m)}}$ are smaller than the decision regions in a conventional quantizer. Finally in Fig. 3 the case of correct ordering of the MTs is considered. Tremendous performance gains by TxNZF as compared to TxZF can be observed.

VI. Conclusion

The novel JT scheme TxNZF described in Section IV offers significant performance gains as compared to TxZF if

- the gains of the channels to different MTs are significantly different, and
- the MTs are correctly ordered.

The first condition is usually fulfilled in typical mobile radio scenarios whereas the latter condition can always be fulfilled by proper design of the signal processing. TxNZF requires the use of unconventional quantization schemes on the receiver side. The complexity of TxNZF is comparable to the one of TxZF.

Acknowledgment

The authors gratefully appreciate the stimulating discussions and the fruitful exchange of ideas with Prof. P.W. Baier and their co-workers at the Research Group for RF Communications at the Technical University of Kaiserslautern. The support of individual parts of this work in the framework of the EU-IST-Project FLOWS (Flexible Convergence of Wireless Standards and Services), by DFG and by Siemens AG is highly acknowledged.

References

[1] M. Joham, K. Kusume, M. H. Gzara, W. Utschick, and J. A. Nossek, “Transmit Wiener filter for the downlink of TDD DS-CDMA systems,” in *Proc. IEEE 7th International Symposium on Spread Spectrum Techniques & Applications (ISSSTA'02)*, vol. 1, Prague, Sept. 2002, pp. 9–13.
[2] M. Joham and W. Utschick, “Downlink processing for mitigation of intracell interference in DS-CDMA systems,” in *Proc. IEEE 6th International Symposium on Spread Spectrum Techniques & Applications (ISSSTA'00)*, vol. 1, Parsippany, Sept. 2000, pp. 15–19.
[3] F. Kowalewski and P. Mangold, “Joint predistortion and transmit diversity,” in *Proc. IEEE Global Telecommunications Conference (GLOBECOM'00)*, vol. 1, San Francisco, Nov. 2000, pp. 245–249.
[4] M. Meurer, P. W. Baier, T. Weber, Y. Lu, and A. Papathanassiou, “Joint transmission: advantageous downlink concept for CDMA mobile radio systems using time division duplexing,” *IEE Electronics Letters*, vol. 36, no. 10, pp. 900–901, May 2000.
[5] T. Weber and M. Meurer, “Optimum joint transmission: Potentials and dualities,” in *Proc. 6th International Symposium on Wireless Personal Multimedia Communications (WPMC'03)*, vol. 1, Yokosuka, Oct. 2003, pp. 79–83.
[6] R. Irmer, R. Habendorf, W. Rave, and G. Fettweis, “Nonlinear multiuser transmission using multiple antennas for TD-CDMA,” in *Proc. 6th International Symposium on Wireless Personal Multimedia Communications (WPMC'03)*, vol. 3, Yokosuka, Oct. 2003, pp. 251–255.
[7] M. Tomlinson, “New automatic equalizer employing modulo arithmetic,” *IEE Electronics Letters*, vol. 7, no. 5, pp. 138–139, 1971.
[8] H. Harashima and H. Miyakawa, “Matched-transmission technique for channels with intersymbol interference,” *IEEE Transactions on Communications*, vol. 20, pp. 774–780, 1972.
[9] R. F. H. Fischer, *Precoding and Signal Shaping for Digital Transmission*. New York: John Wiley & Sons, 2002.
[10] R. D. J. van Nee and R. Prasad, *OFDM for Wireless Multimedia Communications*. Boston: Artech House, 2000.
[11] T. Weber, A. Sklavos, Y. Liu, and M. Weckerle, “The air interface concept JOINT for beyond 3G mobile radio networks,” in *Proc. 15th International Conference on Wireless Communications (WIRELESS 2003)*, vol. 1, Calgary, July 2003, pp. 25–33.
[12] T. Weber, I. Maniatis, A. Sklavos, and Y. Liu, “Joint transmission and detection integrated network (JOINT), a generic proposal for beyond 3G systems,” in *Proc. 9th International Conference on Telecommunications (ICT'02)*, vol. 3, Beijing, June 2002, pp. 479–483.
[13] J. G. Proakis, *Digital Communications*, 3rd ed. New York: McGraw-Hill, 1995.
[14] W. H. Press, S. A. Teukolsky, W. T. Vetterling, and B. P. Flannery, *Numerical Recipes in C*, 2nd ed. New York: Cambridge University Press, 1992.
[15] R. A. Horn and C. R. Johnson, *Matrix Analysis*. Cambridge: Cambridge University Press, 1985.
[16] C. B. Peel, B. M. Hochwald, and A. L. Swindlehurst, “A vector-perturbation technique for near-capacity multi-antenna multi-user communication,” in *Proc. of 41th Annual Allerton Conference on Communications, Control and Computing*, Oct. 2003.

5.3 Analyse der Übertragungsqualität

Dieses Unterkapitel beschäftigt sich mit der Analyse der Leistungsfähigkeit des im vorherigen Unterkapitel 5.2 eingeführten aufwandsgünstigen suboptimalen Verfahrens der gemeinsamen Sendesignalerzeugung TxNZF. Im Rahmen von [QMBW04] wird die Leistungsfähigkeit dieses Verfahrens anhand von

- Bitfehlerwahrscheinlichkeiten und
- Verteilungsfunktionen (engl. cumulative distribution functions) der zum Erzielen einer vorgegebenen Übertragungsqualität notwendigen totalen Sendeenergie T nach (1.30)

für exemplarische Szenarien bewertet.

Im Gegensatz zu der aus Unterkapitel 1.3 bekannten Notation werden in [QMBW04] einige wenige Größen durch eine modifizierte Notation beschrieben. Tabelle 5.2 listet die wesentlichen Unterschiede in kompakter Form auf.

Tabelle 5.2. Wesentliche Unterschiede der Notationen nach Unterkapitel 1.3 und der Notation nach [QMBW04]

dargestellte Größe	Formelzeichen nach Unterkap. 1.3	Formelzeichen nach [QMBW04]
Entscheidungsgebiet	$\mathbb{Q}_m$	$\mathbb{G}_m$
Repräsentant	$\underline{q}_{m,p}$	$\underline{g}_{m,p}$

[QMBW04] Qiu, W.; Meurer, M.; Baier, P. W.; Weber, T.: "Power efficient CDMA broadcast system doing without any channel knowledge at the receivers, a non-obvious modification of THP". *Proc. IEEE joint conference (APCC/MDMC'04) of 10th Asia-Pacific Conference on Communications (APCC2004) and 5th International Symposium on Multi-Dimensional Mobile Communications (MDMC2004)*, Peking, 2004, S. 793–799.

Power efficient CDMA broadcast system doing without any channel knowledge at the receivers, a non-obvious modification of THP

W. Qiu, M. Meurer, P.W. Baier, T. Weber
Research Group for RF Communications, University of Kaiserslautern,
P.O. Box 3049,D-67653 Kaiserslautern, Germany
email: wqiu@rhrk.uni-kl.de

Abstract— **For CDMA broadcast transmission recently the linear receiver oriented scheme Transmit Zero Forcing (TxZF) was proposed, in which the receiver algorithms are a priori determined, whereas the transmitter algorithms follow a posteriori. A main asset of this scheme is its low receiver complexity. In addition, it does without sacrificing downlink transmission resources to training signals for channel estimation, which is beneficial for capacity, and its combination with MIMO antenna structures is straightforward. In this paper a nonlinear modification of the scheme TxZF termed Transmit Non-linear Zero Forcing (TxNZF) is presented with a view to reduce the required transmit power considerably, a feature mitigating intercell interference in cellular systems and, thereby, further enhancing capacity, and being also attractive with respect to the growing electro-phobia of the public. The crux of TxNZF consists in using multiply connected decision regions in the detectors of the receivers and in advantageously selecting the partial decision regions from the possible set of such regions depending on the messages to be transmitted. TxNZF is particularly effective in the case of relatively large attenuation differences of the channels between the transmitter and the individual receivers. The envisaged practical application of the scheme TxNZF are CDMA mobile radio downlinks. In such systems due to shadowing and to largely different distances between the base station and the mobile terminals, large attenuation differences prevail. The ideas presented in this paper are related to the well known concept of Tomlinson-Harashima Precoding (THP).**

Keywords— **CDMA broadcast systems, multi-user MIMO downlinks, receiver orientation, precoding**

I. Introduction

In [1–3] the linear scheme Transmit Zero Forcing (TxZF) was proposed for CDMA broadcast systems with blockwise transmission, where the emphasis was on CDMA mobile radio downlinks consisting of a base station (BS) and a number of mobile terminals (MT). Without restricting the general applicability of the results of this paper, also here the focus will be on mobile radio downlinks. The scheme TxZF totally eliminates multiple access interference (MAI) and intersymbol interference (ISI). It can be considered as receiver (Rx) oriented [2], because the Rx algorithms to be applied in the MTs are $a\ priori$ given, whereas the algorithms utilized in the transmitter (Tx) of the BS result $a\ posteriori$. As a prerequisite of Rx orientation, the downlink channel impulse responses must be known in the BS transmitter, whereas the receivers in the MTs do without any channel knowledge [2]. The BS can gain the channel knowledge particularly easily in mobile radio systems separating uplink and downlink transmissions by Time Division Duplexing (TDD) [2]. As compared to conventional, that is Tx oriented schemes, the main assets of Rx orientation are a potentially very low receiver complexity and the fact that no downlink transmission resources have to be sacrificed to training signals for channel estimation. The inclusion of MIMO antenna structures in Rx oriented schemes would be straightforward [2]. Besides TxZF, other linear Rx oriented transmission schemes would be the Transmit Matched Filter (TxMF) and the Transmit Minimum Mean Square Error Modulator (TxMMSE) [3,4]. Basically, the following considerations could be based on any of the schemes TxZF, TxMF or TxMMSE, which in each case would lead to somewhat different system performances, but would result in the same principal findings. Here, for the sake of brevity, we restrict ourselves to the TxZF.

Let us assume that we have in total K MTs, and that, with the definition of a message as in [5], to each MT k, $k=1\dots K$, a block $(\mathrm{a}_1^{(k)}\dots\mathrm{a}_N^{(k)})$ of N messages have to be transmitted. Then, the total number of messages to be transmitted from the BS to the MTs is KN. The realizations of the messages $\mathrm{a}_n^{(k)}$ are taken from a realization set $\{\mathcal{G}_1\dots\mathcal{G}_M\}$ of cardinality M. The realizations $\mathcal{G}_m$, $m=1\dots M$, can be considered as general abstract objects and are not necessarily complex numbers in the sense of data symbols [5]. The detectors of the MTs can be characterized by a quantization scheme constituted by a complete tiling of the complex plain by M non-overlapping decision regions $\mathbb{G}_m$, $m=1\dots M$, with each of these regions enclosing a specific representative $\underline{g}_m$, $m=1\dots M$ [5]. Fig. 1 shows an example of such a quantization scheme for the case M equal to four. We require that in the noisefree case a transmitted message $\mathrm{a}_n^{(k)}$ of realization $\mathcal{G}_m$ would yield the signal value $\underline{g}_m$, that is the value of the correct representative of $\mathrm{a}_n^{(k)}$ at the demodulator output of MT k. This requirement is exactly fulfilled by jointly taking into account all KN messages $\mathrm{a}_n^{(k)}$ by TxZF [2]. The set of representatives $\underline{g}_m$ corresponding to a certain realization of the message set $\mathrm{a}_n^{(k)}$, $n=1\dots N$, $k=1\dots K$, is termed correct set of representatives of this message set.

In this paper we deal with the radiated energy required to support the K MTs. This energy should be as low as possible with a view to keep − in the case of cellular systems − intercell interference low and, thereby, capacity high, and also with respect to the growing electro-phobia of the public. Under the condition of totally avoiding MAI and ISI, TxZF minimizes this energy, that is for a given quantization scheme, given radio channels and given system parameters, see [2], there is no possibility to arrive at a transmit energy lower than the one required by TxZF unless MAI and/or ISI are allowed.

With a view to reduce the required transmit energy, it is well known under the designation Tomlinson-Harashima Precoding (THP) [6,7] that, instead of using **q**uantization schemes with **s**imply connected decision region (QS) as the one shown

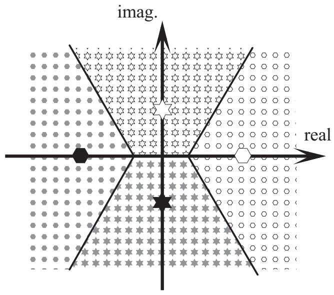

$\circ\circ \widehat{=} \mathbb{G}_1$, $\widehat{=} \mathbb{G}_2$, $\widehat{=} \mathbb{G}_3$, $\widehat{=} \mathbb{G}_4$;

$\widehat{=} \underline{g}_1$, $\widehat{=} \underline{g}_2$, $\widehat{=} \underline{g}_3$, $\widehat{=} \underline{g}_4$

Fig. 1. Example of a quantization scheme with simply connected decision regions $\mathbb{G}_m$; $M = 4$

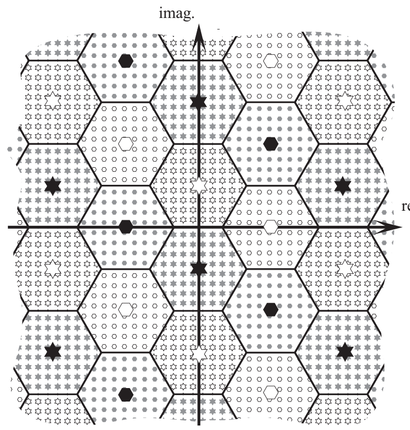

$\widehat{=} \mathbb{G}_{1,p}$, $\widehat{=} \mathbb{G}_{2,p}$, $\widehat{=} \mathbb{G}_{3,p}$, $\widehat{=} \mathbb{G}_{4,p}$;

$\widehat{=} \underline{g}_{1,p}$, $\widehat{=} \underline{g}_{2,p}$, $\widehat{=} \underline{g}_{3,p}$, $\widehat{=} \underline{g}_{4,p}$

Fig. 2. Example of a quantization scheme with multiply connected decision regions $\mathbb{G}_m$ each consisting of partial decision regions $\mathbb{G}_{m,p}$; $M = 4$

in Fig. 1, modulo quantization schemes , or more generally, **q**uantization schemes with **m**ultiply connected decision regions (QM)

$$\mathbb{G}_m = \mathbb{G}_{m,1} \cup \ldots \cup \mathbb{G}_{m,p} \cup \ldots \cup \mathbb{G}_{m,P} \tag{1}$$

may be used, where each decision region $\mathbb{G}_m$ consists of P partial decision region $\mathbb{G}_{m,p}$. Each partial decision region $\mathbb{G}_{m,p}$ contains its own representative $\underline{g}_{m,p}$. The idea of QM is adopted in what follows. Fig. 2 shows an example of such a QM, again for the case M equal to four. If now a message $\mathrm{a}_n^{(k)}$ takes on the realization $\mathcal{G}_m$, then, in the noisefree case, the corresponding demodulator should deliver any one of the P values $\underline{g}_{m,p}$, $p \in \{1 \ldots P\}$, what again can be achieved by jointly treating all KN messages $\mathrm{a}_n^{(k)}$ by TxZF. For a certain set of realizations of the KN messages $\mathrm{a}_n^{(k)}$ we now have P^{KN} options of correct sets of representatives instead of only one as in the case of a QS. In general, for each of these options, the required transmit energy is different. In order to minimize the transmit energy, the option entailing the lowest transmit energy would be optimum and should be chosen. Unfortunately, a straightforward procedure to perform this selection is not yet known, even though first steps into this direction have been undertaken [8]. An alternative would be the exhaustive search through all P^{KN} options, which, however, would be prohibitively expensive. In this paper we propose a low cost iterative procedure to choose the correct set of representatives in the case of QMs. This procedure does not yield the optimum correct set of representatives, but it, nevertheless, allows a significant transmit energy reduction as compared to TxZF utilizing a QS. With respect to the well known application of TxZF, the proposed procedure is linear; however, a non-linear feature is introduced when selecting the correct set of representatives. The proposed scheme is termed Transmit Non-linear Zero Forcing (TxNZF) by the authors in order to take into account both its being based on TxZF and its non-linear feature.

In Section IV it will become evident that the main ideas of TxNZF are the MT-wise generation of the radiated signals and the application of QMs. Basically, these ideas are not new [6, 7, 9–13]. However, their specific way of utilization followed in this paper is novel. In particular, in the mentioned literature the radiated signals are generated message-wise and not MT-wise, and channel knowledge is not only required in the BS, but at least to a certain degree also in the receivers of the MTs [9, 11, 12]. Also, in the published schemes [11, 12], the transmit energies are limited, which may result in different QoSs for different MTs and, thus, to an unfair resource allocation. Further, in the case of frequency selective channels, the literature [11–13] covers only schemes for the case of continuous transmission, even though, as mentioned above, in the case of Rx orientation the favorite duplexing scheme should be TDD, which would imply a block-wise transmission as considered in this paper. Finally, the authors believe that their illustrative way of explaining the transmit energy reduction enabled by TxNZF by not only stressing mathematical arguments would be helpful to the reader to grasp the basic conception of advantageously utilizing QMs.

The paper is structured as follows. After this introduction a brief review of TxZF is given in Section II. In order to well understand the concept of TxNZF, in Section III a quantity is introduced which describes how efficiently the invested transmit energy is used in the system. Then, Section IV presents the proposed scheme TxNZF in verbal description and in mathematical form. The energy-wise advantageous behavior of TxNZF is demonstrated by simulation results in Section V. Finally, Section VI concludes the paper. As in [2], the time discrete equivalent lowpass formalism is adopted, and complex vectors and matrices are represented by underlined bold face symbols.

II. Brief review of TxZF

In the considered downlinks the BS is equipped with K_B antennas, and each of the K MTs employs a single antenna. Fig. 3

illustrates this situation by a block diagram, which is described in detail in [2] and, therefore, will be only briefly treated in what follows. For convenience, quantities helpful to understand this paper and/or occurring in the system of Fig. 3 are listed and explained in Table I.

Let us assume that the message $\mathrm{a}_n^{(k)}$ has the realization $\mathcal{G}_m$ and that TxZF is employed. Then, at the transmitter input of the system of Fig. 3, $\mathrm{a}_n^{(k)}$ has to be mapped on a complex input value

$$\underline{\Delta}_n^{(k)} \in \left(\underline{g}_{m,1} \dots \underline{g}_{m,P}\right). \tag{2}$$

By (2), depending on P, both QSs and QMs are covered. Again, the crux of minimizing the transmit energy in the case of a QM would consist in the proper selection of a correct representative from the set in (2) for each message $\mathrm{a}_n^{(k)}$, which then via (2) would yield the proper input value $\underline{\Delta}_n^{(k)}$. The N input values for MT k are arranged in the MT specific input vector

$$\underline{\mathbf{\Delta}}^{(k)} = \left(\underline{\Delta}_1^{(k)} \dots \underline{\Delta}_N^{(k)}\right)^{\mathrm{T}}. \tag{3}$$

The K MT specific input vectors $\underline{\mathbf{\Delta}}^{(k)}$ of (3) are stacked in the total input vector

$$\underline{\mathbf{\Delta}} = \left(\underline{\mathbf{\Delta}}^{(1)\mathrm{T}} \dots \underline{\mathbf{\Delta}}^{(K)\mathrm{T}}\right)^{\mathrm{T}} = \left(\underline{\Delta}_1 \dots \underline{\Delta}_n \dots \underline{\Delta}_{KN}\right)^{\mathrm{T}}. \tag{4}$$

With $\underline{\mathbf{D}}$, $\underline{\mathbf{r}}$, $\underline{\mathbf{H}}$, $\underline{\mathbf{M}}$ and $\underline{\mathbf{n}}$ explained in Table I, feeding $\underline{\mathbf{\Delta}}$ of (4) into the BS input leads to

$$\underline{\mathbf{D}}\,\underline{\mathbf{r}} = \underline{\mathbf{D}}\,\underline{\mathbf{H}}\,\underline{\mathbf{M}}\,\underline{\mathbf{\Delta}} + \underline{\mathbf{D}}\,\underline{\mathbf{n}} \tag{5}$$

at the outputs of the MT demodulators [2]. In the case of the TxZF featured here, the total modulator matrix results *aposteriori* from the total demodulator matrix $\underline{\mathbf{D}}$ and the total channel matrix $\underline{\mathbf{H}}$ according to

$$\underline{\mathbf{M}} = \left(\underline{\mathbf{D}}\,\underline{\mathbf{H}}\right)^{\mathrm{H}} \left[\left(\underline{\mathbf{D}}\,\underline{\mathbf{H}}\left(\underline{\mathbf{D}}\,\underline{\mathbf{H}}\right)^{\mathrm{H}}\right)\right]^{-1} \tag{6}$$

[2]. Then, we obtain from (5) at the outputs of the MT demodulators

$$\underline{\mathbf{D}}\,\underline{\mathbf{r}} = \underline{\mathbf{\Delta}} + \underline{\mathbf{D}}\,\underline{\mathbf{n}}, \tag{7}$$

that is, see (2), the selected correct representatives are reached. Due to the linear character of TxZF, each input value $\underline{\Delta}_n^{(k)}$ has no other effect than generating a correct representative for the message $\mathrm{a}_n^{(k)}$ at the corresponding demodulator output, and in particular has no impact on the demodulator outputs for other messages $\mathrm{a}_{n'}^{(k')}$, $(k' \neq k) \cup (n \neq n')$.

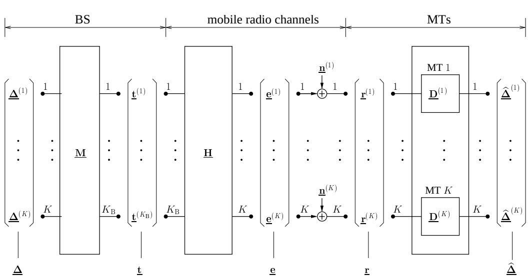

Fig. 3. Downlink system model [2]

TABLE I
QUANTITIES IN THE SYSTEM MODEL OF FIG. 3 [2]

quantities	designations
Q_{t}	temporal spreading factor
$\underline{\mathbf{M}} \in \mathbb{C}^{Q_{\mathrm{t}} \times (KN)}$	total modulator matrix
$\underline{\mathbf{t}}^{(k_{\mathrm{B}})} = \left(\underline{t}_1^{(k_{\mathrm{B}})} \dots \underline{t}_{Q_{\mathrm{t}}}^{(k_{\mathrm{B}})}\right)^{\mathrm{T}}$	antenna specific Tx signal
$\underline{\mathbf{t}} = \left(\underline{\mathbf{t}}^{(1)\mathrm{T}} \dots \underline{\mathbf{t}}^{(K_{\mathrm{B}})\mathrm{T}}\right)^{\mathrm{T}}$	total Tx signal
W	number of channel taps
$\underline{\mathbf{h}}^{(k,k_{\mathrm{B}})} = \left(\underline{h}_1^{(k,k_{\mathrm{B}})} \dots \underline{h}_W^{(k,k_{\mathrm{B}})}\right)^{\mathrm{T}}$	channel impulse response
$\underline{\mathbf{H}}^{(k,k_{\mathrm{B}})} \in \mathbb{C}^{(Q_{\mathrm{t}}+W-1)\times Q_{\mathrm{t}}}$	MT and Tx antenna specific channel matrix
$\underline{\mathbf{H}}^{(k)} = \left(\underline{\mathbf{H}}^{(k,1)} \dots \underline{\mathbf{H}}^{(k,K_{\mathrm{B}})}\right)$	MT specific channel matrix
$\underline{\mathbf{H}} = \left(\underline{\mathbf{H}}^{(1)\mathrm{T}} \dots \underline{\mathbf{H}}^{(K)\mathrm{T}}\right)^{\mathrm{T}}$	total channel matrix
$\underline{\mathbf{e}}^{(k)} = \underline{\mathbf{H}}^{(k)}\underline{\mathbf{t}}$	MT specific undisturbed Rx signal
$\underline{\mathbf{e}} = \left(\underline{\mathbf{e}}^{(1)\mathrm{T}} \dots \underline{\mathbf{e}}^{(K)\mathrm{T}}\right)^{\mathrm{T}}$	total undisturbed Rx signal
$\underline{\mathbf{n}}^{(k)}$	received MT specific noise signal
$\underline{\mathbf{n}} = \left(\underline{\mathbf{n}}^{(1)\mathrm{T}} \dots \underline{\mathbf{n}}^{(K)\mathrm{T}}\right)^{\mathrm{T}}$	total received noise signal
$\underline{\mathbf{r}}^{(k)} = \underline{\mathbf{e}}^{(k)} + \underline{\mathbf{n}}^{(k)}$	MT specific disturbed Rx signal
$\underline{\mathbf{r}} = \left(\underline{\mathbf{r}}^{(1)\mathrm{T}} \dots \underline{\mathbf{r}}^{(K)\mathrm{T}}\right)$	total disturbed Rx signal
$\underline{\mathbf{D}}^{(k)} \in \mathbb{C}^{N\times(Q_{\mathrm{t}}+W-1)}$	MT specific demodulator matrix
$\underline{\mathbf{D}} = \mathrm{blockdiag}\left(\underline{\mathbf{D}}^{(1)} \dots \underline{\mathbf{D}}^{(K)}\right)$	total demodulator matrix

III. ENERGY EFFICIENCY OF TXZF

In TxZF to each message $\underline{a}_n^{(k)}$ and, consequently, to each input value $\underline{\Delta}_n^{(k)}$ of (2) an energy efficiency can be assigned [2], which quantifies the percentage to which the energy radiated for the transmission of $\mathrm{a}_n^{(k)}$ is transformed into useful energy at MT k. As shown in [2],

$$0 \leq \eta_n^{(k)} \leq 1 \tag{8}$$

holds. The closer $\eta_n^{(k)}$ to one, the lower the energy to be radiated for the transmission of $\mathrm{a}_n^{(k)}$.

If we have in total K MTs, then, in the case of usual TxZF, all these MTs are jointly supported [2]. However, it would also be possible to jointly support only a subset of $K_{\mathrm{ZF}} < K$ MTs by TxZF. In this paper, it would be desirable to have informations on the dependency of $\eta_n^{(k)}$ of (8) on the parameters K_{ZF}, N, W, Q_{t} and K_{B}. In order to obtain such informations, the authors studied the average value

$$\eta = \mathop{\mathrm{E}}_{\underline{\mathbf{D}},\underline{\mathbf{H}}}\left\{\eta_n^{(k)}\right\} \tag{9}$$

of the $K_{\mathrm{ZF}}N$ energy efficiencies $\eta_n^{(k)}$ for a large number of different matrices $\underline{\mathbf{D}}$ and $\underline{\mathbf{H}}$, which were randomly chosen according to the following scheme:

- The $N(Q_\mathrm{t}+W-1)$ elements of $\underline{\mathbf{D}}^{(k)}$, see Table I, are derived from an orthonormal set of N binary sequences of dimension $Q_\mathrm{t}+W-1$. The N rows of $\underline{\mathbf{D}}^{(k)}$ are obtained by scrambling the N sequences of this set by a random MT-specific scrambling code of dimension $Q_\mathrm{t}+W-1$. The elements of this scrambling code have magnitude one.
- The $K_\mathrm{ZF}K_\mathrm{B}W$ elements of the channel impulse responses $\underline{\mathbf{h}}^{(k,k_\mathrm{B})}$, see Table I, are randomly picked independent bivariate Gaussian numbers with identical variance and expectation zero.

Based on results of free probability theory [14] it can be shown that η of (9) can be approximated by [15]

$$\eta = \frac{K_B Q_\mathrm{t} - N K_\mathrm{ZF} + 1}{K_B Q_\mathrm{t} - N + 1} \cdot \eta_\mathrm{b}(W, Q_\mathrm{t}, K_\mathrm{B}) \qquad (10)$$

with a non-trivial function $\eta_\mathrm{b}(W, Q_\mathrm{t}, K_\mathrm{B})$ of W, Q_t and K_B. Specifically, this function neither depends on K_ZF nor N. The derivation of (10) will be treated in [15]. According to (10), for given values of K_B, Q_t, N and W, η attains its maximum $\eta_\mathrm{b}(W, Q_\mathrm{t}, K_\mathrm{B})$ for K_ZF equal to one and decreases monotonously with an increasing number K_ZF of MTs to be jointly supported by TxZF.

IV. Proposed transmission scheme TxNZF

A. Illustrative explanation

In this subsection the proposed scheme TxNZF for advantageously selecting the correct representatives of the messages $\mathrm{a}_n^{(k)}$ in Rx oriented CDMA systems with QM is explained in an illustrative way.

In mobile radio communications the attenuations of the channels between the BS and the individual MTs may differ significantly. With the channel impulse responses $\underline{\mathbf{h}}^{(k,k_\mathrm{B})}$, see Table I, we introduce the quantity

$$\alpha^{(k)} = \left(\sum_{k_\mathrm{B}=1}^{K_\mathrm{B}} \left\| \underline{\mathbf{h}}^{(k,k_\mathrm{B})} \right\|^2 \right)^{-1} \qquad (11)$$

as a measure of the attenuation of the channel between the BS and MT k. In what follows we assume that the K MTs are ordered in such a way that

$$\alpha^{(1)} > \alpha^{(2)} > \ldots > \alpha^{(K)} \qquad (12)$$

holds.

In TxNZF first the support of MT 1 is considered. For the messages $\mathrm{a}_n^{(1)}$, $n = 1 \ldots N$, the representatives closest to the origin are chosen, an obvious choice with respect to low transmit energy. In order to generate signal values equal to these representatives at the demodulator output of MT 1, TxZF with consideration of solely the messages $\mathrm{a}_n^{(1)}$, $n = 1 \ldots N$, and under neglection of the existence of MTs $2 \ldots K$ is performed. This gives for each message $\mathrm{a}_n^{(1)}$ an input value $\underline{\delta}_n^{(1)}$ to be fed into the BS transmitter. When supporting MT 1 in this way, the average energy efficiency $\eta^{(1)}$ for this MT follows from (10) by setting K_ZF equal to one, which means that $\eta^{(1)}$ attains the largest possible value $\eta_\mathrm{b}(W, Q_\mathrm{t}, K_\mathrm{B})$. With respect to achieving low transmit energy, this maximization of especially $\eta^{(1)}$ is particularly rewarding, because the communication with MT 1 suffers from the highest channel attenuation, see (12).

Next the support of MT 2 is considered, for which the messages $\mathrm{a}_n^{(2)}$, $n = 1 \ldots N$, have to be transmitted. When supporting MT 1 by TxZF the existence of MTs $2 \ldots K$ was neglected. Therefore, the support of MT 1 causes interference values $\underline{i}_n^{(2)}$, $n = 1 \ldots N$, at the demodulator output of MT 2. Now, by TxZF under consideration of both MT 1 and MT 2 a transmit signal is generated for the support of MT 2 which is not visible at the demodulator output of MT 1 and which complements each interference value $\underline{i}_n^{(2)}$, $n = 1 \ldots N$, by a value $\underline{\delta}_n^{(2)}$, $n = 1 \ldots N$, in such a way that the closest correct representative of $\mathrm{a}_n^{(2)}$, $n = 1 \ldots N$, is reached at the demodulator output of MT 2. In order to achieve this complementing effect, the values $\underline{\delta}_n^{(2)}$ have to be fed as input value into the BS transmitter. Also here, choosing the closest correct representative of $\mathrm{a}_n^{(2)}$, $n = 1 \ldots N$, – closest now not to the origin but to the interference value $\underline{i}_n^{(2)}$, $n = 1 \ldots N$, – helps to keep the transmit energy low. When supporting MT 2 by TxZF under the condition not causing a signal at the demodulator output of MT 1, now K_ZF in (10) has to be set equal to two, which results in an average energy efficiency $\eta^{(2)}$ for MT 2 smaller than $\eta^{(1)}$ valid for MT 1. However, the impact of this efficiency decay experienced by MT 2 is mitigated because the required energy tends to be smaller for the support of MT 2 than for the support of MT 1 due to $\alpha^{(2)} < \alpha^{(1)}$.

When supporting MT 3, interference values $\underline{i}_n^{(3)}$, $n = 1 \ldots N$, caused at the demodulator output of MT 3 by supporting MTs 1 and 2 are compensated by values $\underline{\delta}_n^{(3)}$, $n = 1 \ldots N$, with a view to reach the closest correct representatives of the messages $\mathrm{a}_n^{(3)}$, $n = 1 \ldots N$. Again, we have an efficiency decay as compared to MTs 1 and 2, which, however, is counteracted by the fact that $\alpha^{(3)}$ is smaller than $\alpha^{(1)}$ and $\alpha^{(2)}$.

The procedure described for the case of MTs 1 to 3 is continued in an analogue way until all K MTs are considered.

As mentioned at the end of Section II, each of the input values $\underline{\Delta}_n^{(k)}$ of (3) is exclusively responsible for achieving the correct representative of the corresponding message $\mathrm{a}_n^{(k)}$ at the demodulator output of MT k. As opposed to this, in TxNZF the message value $\underline{\delta}_n^{(k)}$ contributes to reaching the correct representative at the outputs of the demodulators of MTs $(k+1) \ldots K$. In order to express this difference between $\underline{\Delta}_n^{(k)}$ and $\underline{\delta}_n^{(k)}$, the latter quantities are termed complementing values in the following.

B. Mathematical description

The interference values $\underline{i}_n^{(k)}$, $n = 1 \ldots N$, caused at the demodulator output of MT k by the support of MTs $1 \ldots (k-1)$ are stacked in the interference vector

$$\underline{\mathbf{i}}^{(k)} = \left(\underline{i}_1^{(k)} \ldots \underline{i}_N^{(k)} \right)^\mathrm{T}. \qquad (13)$$

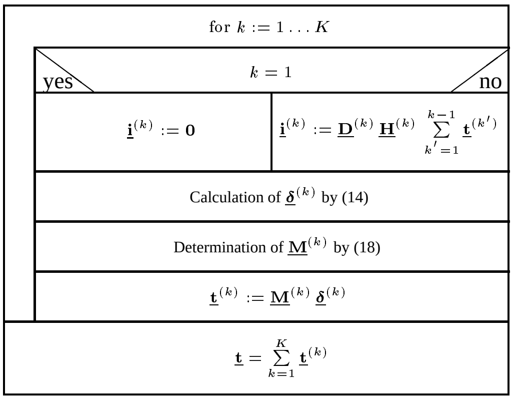

Fig. 4. Nassi-Shneiderman diagram [16] describing the generation of the transmit signal $\underline{\mathbf{t}}$ in TxNZF

According to the verbal description in Subsection IV-A, the complementing values $\underline{\delta}_n^{(k)}$, $n = 1 \dots N$, for MT k are determined as follows:

$$\mathrm{a}_n^{(k)} = \mathcal{G}_m \quad \Rightarrow \quad \underline{\Delta}_n^{(k)} = \underline{g}_{m,p'} - \underline{i}_n^{(k)}, \tag{14}$$
$$p' = \arg \min_{p \in \{1 \dots P\}} \left\{ \left| \underline{i}_n^{(k)} - \underline{g}_{m,p} \right|^2 \right\}.$$

These values are stacked in the MT specific complementing vector

$$\underline{\boldsymbol{\delta}}^{(k)} = \left(\underline{\delta}_1^{(k)} \dots \underline{\delta}_N^{(k)} \right)^{\mathrm{T}}. \tag{15}$$

In order to generate the complementing vector $\underline{\boldsymbol{\delta}}^{(k)}$ at the demodulator output of MT k without causing interference at the demodulator outputs of MTs $1 \dots (k-1)$, we proceed as follows:

In Table I we introduced the MT specific matrices $\underline{\mathbf{H}}^{(k)}$ and $\underline{\mathbf{D}}^{(k)}$, $k = 1 \dots K$, of the channels and the demodulators, respectively. These matrices are now stacked in the matrices

$$\underline{\mathbf{H}}_k = \left(\underline{\mathbf{H}}^{(1)^{\mathrm{T}}} \dots \underline{\mathbf{H}}^{(k)^{\mathrm{T}}} \right)^{\mathrm{T}} \tag{16}$$

and

$$\underline{\mathbf{D}}_k = \mathrm{blockdiag}\left(\underline{\mathbf{D}}^{(1)} \dots \underline{\mathbf{D}}^{(k)} \right), \tag{17}$$

which we term cumulative matrices. Let us designate by $[\,\cdot\,]_i^j$ a matrix consisting of columns i to j of the matrix in brackets. Then, in TxNZF we $aposteriori$ determine the MT specific modulator matrices

$$\underline{\mathbf{M}}^{(k)} = \left[(\underline{\mathbf{D}}_k \underline{\mathbf{H}}_k)^{\mathrm{H}} \left[\underline{\mathbf{D}}_k \underline{\mathbf{H}}_k \, (\underline{\mathbf{D}}_k \underline{\mathbf{H}}_k)^{\mathrm{H}} \right]^{-1} \right]_{(k-1)N+1}^{kN}, \quad k = 1 \dots K, \tag{18}$$

Now, in order to produce $\underline{\boldsymbol{\delta}}^{(k)}$ at the demodulator output of MT k, we transmit the signal

$$\underline{\mathbf{t}}^{(k)} = \underline{\mathbf{M}}^{(k)} \, \underline{\boldsymbol{\delta}}^{(k)}. \tag{19}$$

The algorithm to determine the MT specific transmit signals $\underline{\mathbf{t}}^{(k)}$ of (19) and the total transmit signal

$$\underline{\mathbf{t}} = \sum_{k=1}^{K} \underline{\mathbf{t}}^{(k)} \tag{20}$$

is illustrated in a self-explanatory way by the Nassi-Shneiderman diagram [16] of Fig. 4. In another paper presently in preparation the efficient implementation of this algorithm based on the QR-decomposition will be presented.

V. Simulation results

In order to illustrate the advantage of TxNZF over TxZF with respect to the required transmit energy, comparative system simulations are performed. The system parameters considered in these simulations are listed in Table II. A large number of snapshots is evaluated, in which the channel impulse responses $\underline{\mathbf{h}}^{(k,k_{\mathrm{B}})}$ and demodulator matrices $\underline{\mathbf{D}}^{(k)}$, see Table I, are randomly generated as described in Section III. However, in order to model the different channel attenuations $\alpha^{(k)}$ of (11) and (12), the generated channel impulse responses $\underline{\mathbf{h}}^{(k,k_{\mathrm{B}})}$ are normalized in such a way that

$$\left\| \underline{\mathbf{h}}^{(1,k_{\mathrm{B}})} \right\|^2 = 1, \; k_{\mathrm{B}} = 1 \dots K_{\mathrm{B}}, \tag{21}$$

and

$$10 \log_{10} \left(\frac{\left\| \underline{\mathbf{h}}^{(k,k_{\mathrm{B}})} \right\|^2}{\left\| \underline{\mathbf{h}}^{(k-1,k_{\mathrm{B}})} \right\|^2} \right) = \begin{cases} 0\ \mathrm{dB} & (\text{case } 1), \\ 3\ \mathrm{dB} & (\text{case } 2), \\ 6\ \mathrm{dB} & (\text{case } 3), \end{cases} \quad k = 2 \dots K, \tag{22}$$

hold.

The QM considered in the simulations is a quadratic moduloscheme as for instance described in [10], and for the sake of comparability the considered QS corresponds to the modulation scheme QPSK. The QM and the QS are made consistent in the sense that the four representatives of the QM closest to the origin and the four representatives of the QS are chosen identical.

With the total transmit signal $\underline{\mathbf{t}}$ which is obtained as described in Section IV in the case of TxNZF and as described in [2] in the case of TxZF, the required transmit energy becomes

$$T = \frac{1}{2} \underline{\mathbf{t}}^{\mathrm{H}} \underline{\mathbf{t}}. \tag{23}$$

TABLE II
System parameters for the simulations

M	N	Q_{t}	K_{B}	K	W
4	4	16	2	8	5

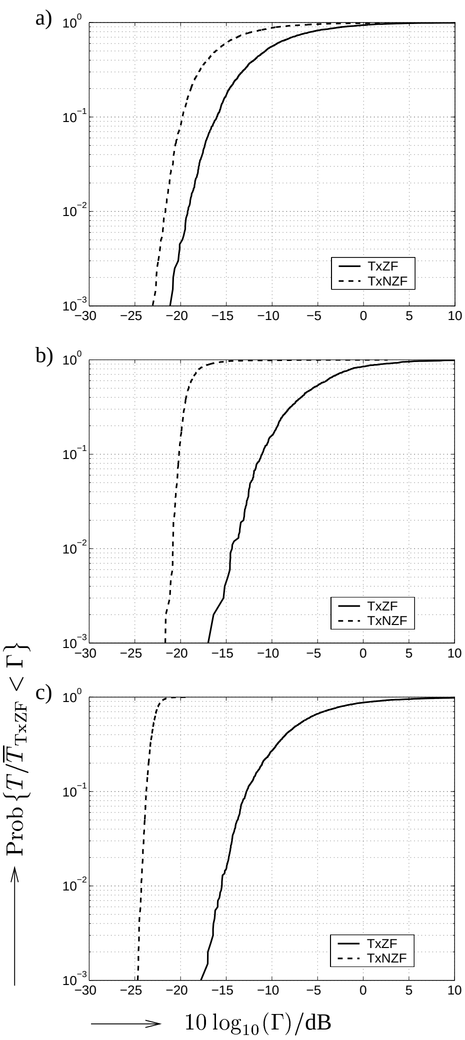

Fig. 5. Cumulative distribution functions of the normalized required transmit energy $T/\overline{T}_{\mathrm{TxZF}}$,
a) case 1; b) case 2; c) case 3

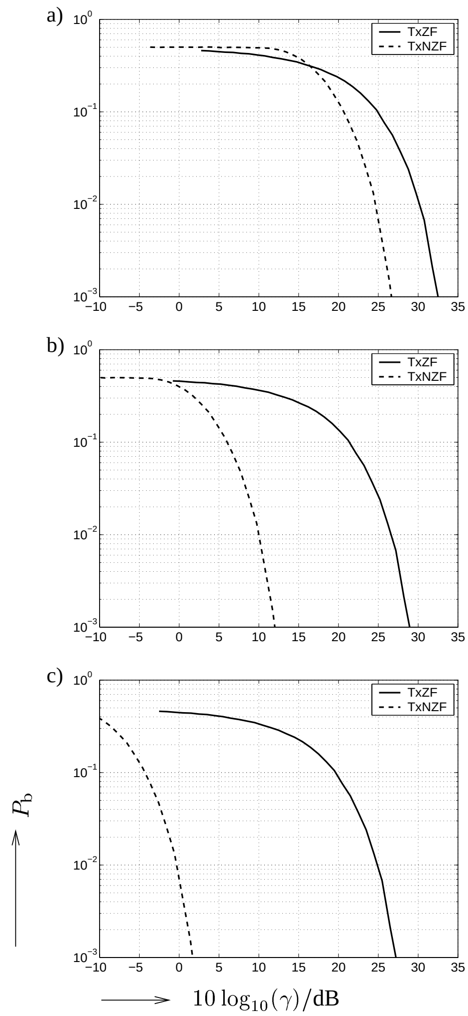

Fig. 6. Bit error rate P_{b} vesus the pseudo SNR γ of (24),
a) case 1; b) case 2; c) case 3

The average required transmit energy of TxZF obtained by averaging over many snapshots characterized by randomly determined $\underline{\mathbf{h}}^{(k,k_{\mathrm{B}})}$ and $\underline{\mathbf{D}}^{(k)}$, see above, is termed $\overline{T}_{\mathrm{TxZF}}$. Figs. 5a to c show for the three cases of (22) the cumulative distribution functions of the ratio $T/\overline{T}_{\mathrm{TxZF}}$ for the schemes TxZF and TxNZF, respectively. As expected, the TxNZF does with significantly lower transmit energies than the TxZF. This superiority of TxNZF increases with increasing differences between consecutive channel attenuations $\alpha^{(k)}$, $k = 1\ldots K$, of (11) and (12), because, when proceeding from MT k to MT $k+1$, see the explanation in Subsection IV-A, the decrease of the energy efficiency is more and more mitigated by an simultaneously decreasing channel attenuation.

It is well known [17] that in the case of two consistently chosen schemes QS and QM subject to identical noise, the latter exhibits a somewhat larger error probability, because the demodulator output signals are more prone to land in a wrong decision region. To a certain degree this effect counteracts the energy advantage of TxNZF over TxZF illustrated in Fig. 5a to c and should be studied. To this purpose the authors again consider the cases 1 to 3 of (22). We designate the average of the transmit energy T as $\overline{T}$ and assume that the total received noise $\underline{\mathbf{n}}$, see Table I, is white and Gaussian with variance σ^2 and zero expectation [2]. Then, the pseudo SNR which the authors define as the average ratio of the transmitted bit energy to σ^2, becomes

$$\gamma = \frac{\overline{T}/[\mathrm{ld}(M)KN]}{\sigma^2}. \tag{24}$$

In Figs. 6a to c, the bit error rate P_b is shown versus γ of (24) for the cases 1 to 3 of (22). From these curves we can conclude the following:

- For sufficiently large values of γ of (24), TxNZF always outperforms TxZF.
- As in the case of the required transmit energies, see Figs. 5a to c, the superiority of TxNZF increases with increasing differences of consecutive channel attenuations $\alpha^{(k)}$ of (11) and (12).
- As becoming apparent by Fig. 6a, at low values of γ of (24) and low increments of the channel attenuations $\alpha^{(k)}$ of (11) and (12), TxZF may outperform TxNZF. However, this occurs only for values of P_b so large that they are of no practical interest.

VI. Summary

The recently proposed linear Rx oriented transmission scheme TxZF for CDMA broadcast transmission excels by low receiver complexity, and it works without sacrificing transmission resources to training signals, which is beneficial for capacity. TxZF can be modified in a nonlinear way, which leads to the Rx oriented CDMA broadcast concept TxNZF. The crux of this scheme consists in using quantizers with multiply connected decision regions in the detectors of the receivers and in, depending on the messages to be transmitted, beneficially selecting the partial decision regions. TxNZF requires significantly less transmit energy than conventional linear TxZF, and, therefore, is attractive with respect to intercell interference mitigation in cellular systems, and to the growing electro-phobia of the public.

Acknowledgment

The support of individual parts of this work in the framework of the EU-IST-Project FLOWS (Flexible Convergence of Wireless Standards and Services), by DFG and by Siemens AG is highly acknowledged.

References

[1] M. Meurer, P. W. Baier, T. Weber, Y. Lu, and A. Papathanassiou, "Joint transmission: advantageous downlink concept for CDMA mobile radio systems using time division duplexing," *IEE ELECTRONICS LETTERS*, vol. 11, pp. 900–901, 2000.

[2] P. W. Baier, W. Qiu, H. Tröger, C. A. Jötten, and M. Meurer, "Modelling and optimization of receiver oriented multi-user MIMO downlinks for frequency selective channels," in *Proc. 10th International Conference on Telecommunications (ICT'03)*, Papeete, 2003, pp. 1547–1554.

[3] P. W. Baier and M. Meurer, "Receiver orientation, an unconventional approach to mobile radio downlink design," in *Proc. European Conference on Wireless Technology (ECWT'03)*, Munich, 2003, pp. 11–14.

[4] M. Joham, K. Kusume, M. H. Gzara, W. Utschick, and J. A. Nossek, "Transmit Wiener Filter for the Downlink of TDD DS-CDMA Systems," in *Proc. IEEE 7th International Symposium on Spread Spectrum Techniques & Applications (ISSSTA'02)*, Prague, 2002, pp. 9–13.

[5] A. J. Viterbi and J. K. Omura, *Principles of Digital Communication and Coding*, McGraw-Hill, New York, 1979.

[6] M. Tomlinson, "New automatic equalizer employing modulo arithmetic," *IEE ELECTRONICS LETTERS*, vol. 7, pp. 138–139, 1971.

[7] H. Harashima and H. Miyakawa, "Matched-transmission technique for channels with intersymbol interference," *IEEE Transactions on Communications*, vol. COM-20, pp. 774–780, 1972.

[8] C.B. Peel, B.M. Hochwald, and A.L. Swindlehurst, "A Vector-Perturbation Technique for Near-Capacity Multi-Antenna Multi-User Communication," in *Proc. 41st Allerton Conference on Communication, Control, and Computing*, Allerton House, Oct. 2003.

[9] G. Ginis and J.M. Cioffi, "A Multi-user Precoding Scheme achieving Crosstalk Cancellation with Application to DSL Systems," in *Proc. 34th The Asilomar Conference on Signals, Systems, and Computers*, Oct. 2000, pp. 1627–1631.

[10] R.F.H. Fischer, *Precoding and Signal Shaping for Digital Transmission*, John Wiley & Sons, New York, 2002.

[11] R.F.H. Fischer, C. Windpassinger, A. Lampe, and J.B. Huber, "Spatio-Time Transmission using Tomlinson-Harashima Precoding," in *Proc. 4th International ITG Conference on Source and Channel Coding (SCC'02)*, Jan. 2002, pp. 139–147.

[12] R.F.H. Fischer, C. Windpassinger, A. Lampe, and J.B. Huber, "MIMO Precoding for Decentralized Receivers," in *Proc. IEEE International Symposium on Information Theory (ISIT'02)*, 2002, p. 496.

[13] M. Joham, J. Brehmer, and W. Utschick, "MMSE Approaches to Multiuser Spatio-Temporal Tomlinson-Harashima Precoding," in *Proc. 5th International ITG Conference on Source and Channel Coding (SCC'04)*, Jan. 2004, pp. 387–394.

[14] D. V. Voiculescu, K. J. Dykema, and A. Nica, "Limit laws for random matrices and free products," *Inventiones Mathematicae*, vol. 104, pp. 201–220, 1991.

[15] M. Meurer, T. Weber, and W. Qiu, "Transmit non-linear zero forcing: energy eficient receiver oriented transmission in MIMO CDMA mobile radio downlinks," submitted to IEEE 8th International Symposium on Spread Spectrum Techniques & Applications, 2004 (ISSSTA'04).

[16] I. Nassi and B. Shneiderman, "Flowchart techniques for structured programming," in *ACM SIGPLAN Notices*, 1973, vol. 8, pp. 12–26.

[17] J.H. Conway and N.J.A Sloane, "A Lower Bound on the Average Error of Vector Quantizers," *IEEE Transactions on Information Theory*, vol. IT-31, no. 1, pp. 106–109, 1985.

Kapitel 6
Problem der Verfügbarkeit akkurater senderseitiger Kanalzustandsinformation

6.1 Vorbemerkung

Sämtliche im Rahmen dieser Schrift betrachteten Verfahren der gemeinsamen Sendesignalerzeugung basieren auf dem senderseitigen Vorliegen von Kanalzustandsinformation (engl. transmitted sided channel state information, TxCSI). Diese Information ist typischerweise auf Seiten der Basisstation nicht a priori vorhanden, sondern muß durch geeignete Maßnahmen verfügbar gemacht werden. Dieses Kapitel beschäftigt sich daher mit dem zur Verfügung Stellen derartiger Information. Prinzipiell lassen sich dabei verschiedene Herangehensweisen unterscheiden, die im folgenden Unterkapitel 6.2 im Grundsätzlichen beleuchtet werden.

Bei allen Vorgehensweisen des Bereitstellens von Kanalzustandsinformation sind die Zeitpunkte des Erfassens der Kanalzustandsinformation und des Nutzens dieser Information zur gemeinsamen Sendesignalerzeugung typischerweise nicht gleich. Bei zeitvarianten Mobilfunkkanälen ist daher ein Verwenden von mehr oder weniger veralteter Kanalzustandsinformation zur gemeinsamen Sendesignalerzeugung, das heißt für den Zeitpunkt des Sendens fehlerhafter Kanalzustandsinformation, nicht vermeidbar. Daher sind weitere Ziele dieses Kapitels

- den durch Zeitvarianz entstehenden Fehler der verfügbaren Kanalzustandsinformation abzuschätzen und
- die Auswirkungen dieser inakkuraten Kanalzustandsinformation auf die Leistungsfähigkeit empfängerorientierter Funkkommunikation zu bewerten.

Die Gliederung dieses Kapitels richtet sich nach den zuvor genannten Zielen.

6.2 Prinzipien des Bereitstellens senderseitiger Kanalzustandsinformation

6.2.1 Kanalreziprozitätsbasiertes Gewinnen von Kanalzustandsinformation

In zellularen Mobilfunksystemen ist typischerweise, wie bereits in Abschnitt 1.1.1 erläutert, eine Duplexübertragung realisiert. Dieses kann genutzt werden, um die für die Abwärtsstreckenübertragung benötigte Kanalzustandsinformation mit Hilfe der Aufwärtsstreckenübertragung zu gewinnen. Ein derartiges Vorgehen setzt voraus, daß die Mobilfunkkanäle, die in beiden Übertragungsrichtungen genutzt werden, reziprok sind [Par92]. Dies ist, wie bereits in Kapitel 1 angerissen, unter gewissen im folgenden noch genauer beleuchteten Nebenbedingungen genau dann gegeben, wenn zur Organisation der Aufwärtsstrecken- und Abwärtsstreckenübertragung [Web02]

- das Zeitduplexverfahren (engl. time division duplex, TDD) eingesetzt wird oder

- das Frequenzduplexverfahren (engl. frequency division duplex, FDD) eingesetzt wird und die Differenz der Mittenfrequenzen der für die beiden Übertragungsrichtungen verwendeten Frequenzbänder deutlich kleiner als die Kohärenzbandbreiten der wirksamen Mobilfunkkanäle ist.

Ist einer der beiden oben dargelegten Fälle gegeben, so kann die angesprochene Kanalzustandsinformation in Form der totalen Kanalmatrix $\underline{\mathbf{H}}$ nach (1.5), die für eine Abwärtsstreckenübertragung gemäß Empfängerorientierung benötigt wird, am Ort der Basisstation durch Schätzen während der Aufwärtsstreckenübertragung verfügbar gemacht werden. Erfolgt die Aufwärtsstreckenübertragung gemäß Senderorientierung — und dies ist, wie bereits in Unterkapitel 1.2 erläutert, der Vorschlag des Verfassers —, so ist die Kenntnis dieser totalen Kanalmatrix $\underline{\mathbf{H}}$ ohnehin für die mit Senderorientierung einhergehende an der Basisstation durchgeführte Empfangssignalverarbeitung nötig und daher auch für die Abwärtsstreckenübertragung verfügbar.

Typischerweise sind die Zeitpunkte T_{est} des Schätzens der Kanalzustandsinformation in der Aufwärtsstrecke und T_{use} des Nutzens dieser Information zum gemeinsamen Sendesignalerzeugen nicht gleich. Bei zeitvarianten Mobilfunkkanälen ist daher die in der Aufwärtsstrecke geschätzte totale Kanalmatrix $\underline{\mathbf{H}}(T_{\text{est}})$ im allgemeinen nicht identisch mit der für die Abwärtsstrecke geltenden totalen Kanalmatrix $\underline{\mathbf{H}}(T_{\text{use}})$. Folglicherweise, ist ein Verwenden von mehr oder weniger veralteter Kanalzustandsinformation zur gemeinsamen Sendesignalerzeugung nicht vermeidbar, was im allgemeinen mit einer Degradation der Leistungsfähigkeit empfängerorientierter Funkkommunikation einher geht. Im folgenden Abschnitt 6.2.3 wird daher auf das Problem der Zeitvarianz im Detail eingegangen und der aus der Zeitvarianz folgende Fehler

$$\underline{\mathbf{E}}(T_{\text{est}}, T_{\text{use}}) = \underline{\mathbf{H}}(T_{\text{est}}) - \underline{\mathbf{H}}(T_{\text{use}}) \tag{6.1}$$

der zur Abwärtsstreckenübertragung verwendeten Kanalzustandsinformation quantitativ abgeschätzt.

6.2.2 Rücksignalisieren empfängerseitig gewonnener Kanalzustandsinformation

Ist ein auf Kanalreziprozität basierendes Bereitstellen der für die Abwärtsstreckenübertragung benötigten Kanalzustandsinformation nicht möglich, so kann nach dem oben geschilderten Prinzip keine Kanalzustandsinformation über die Mobilfunkkanäle in der MIMO-Abwärtsstrecke in Form der totalen Kanalmatrix $\underline{\mathbf{H}}$ nach (1.5) verfügbar gemacht werden. Dies ist beispielsweise dann gegeben, wenn das Frequenzduplexverfahren eingesetzt wird und die für Abwärtsstrecken- und Aufwärtsstreckenübertragung verwendeten Frequenzbänder frequenzmäßig voneinander um mehr als die Kohärenzbandbreite mindestens eines der wirksamen Mobilfunkkanäle separiert sind. Die zum Schätzen der benötigten Kanalzustandsinformation verwendbaren Beobachtungen der Mobilfunkkanäle können dann lediglich an den Orten der Empfänger, also den Mobilstationen, gemacht werden und müssen somit auf eine geschickte Art und Weise an den Sender, das heißt die Basisstation, rücksignalisiert werden.

Das Hauptproblem bei der beschriebenen Vorgehensweise besteht darin, daß typischerweise die zum Rücksignalisieren dieser Information von einer Mobilstation zur Basisstation zur Verfügung stehenden Kapazitäten in der Aufwärtsstrecke stark begrenzt sind [JBM+02]. Die folgenden beiden Veröffentlichungen [JBMW02b, JBM+02] beschäftigen sich daher mit dem Problem, des ressourceneffizienten akkuraten Rücksignalisierens von Kanalzustandsinformation. Ressourceneffizient heißt dabei, daß die Kapazitäten, die in der Aufwärtsstrecke benötigt werden, um die Kanalzustandsinformation mit einer geforderten Genauigkeit zurückzusignalisieren, möglichst gering sind.

Auch im Falle des Bereitstellens von Kanalzustandsinformation durch das oben geschriebene Rücksignalisieren sind die Zeitpunkte T_{est} des Schätzens der Kanalzustandsinformation an den Mobilstationen und T_{use} des Nutzens dieser Information zum gemeinsamen Sendesignalerzeugen an der Basisstation nicht gleich. Das bedeutet, daß auch beim Bereitstellen von Kanalzustandsinformation durch Rücksignalisieren das im vorherigen Abschnitt 6.2.1 erläuterte und sich in (6.1) manifestierende Problem der Zeitvarianz auftritt. Für eine Analyse dieses Problems sei der interessierte Leser daher auf die detaillierte Analyse in Abschnitt 6.2.3 verwiesen.

[JBMW02b] Jötten, C. A.; Baier, P. W.; Meurer, M.; Weber, T.: "Subspace related signalling of feedback information for low rank MIMO channels". *Frequenz*, Bd. 56, 2002, S. 146–145.

Frequenz
56 (2002)
7-8

Subspace Related Signalling of Feedback Information for Low Rank MIMO Channels

Unterraum-basiertes Rücksignalisieren von Kanalzustandsinformation für niederrangige MIMO-Kanäle

Abstract
In recent years radio communications systems, which utilize antenna arrangements consisting of several transmit and receive antennas, have inspired theorists and are now on the verge of practical application, for instance in future mobile radio systems. In order to fully benefit of the potential offered by such MIMO (Multiple Input Multiple Output) systems, the knowledge of the radio channels should be available and considered in the signal processing algorithms both at the transmitter and the receiver. At the receiver this knowledge can be gained by state of the art training sequence based, semi-blind or blind channel estimation. However, at the transmitter the channel knowledge is not readily available and has to be obtained for instance by signalling the channel information gained at the receiver back to the transmitter. Unfortunately, this back signalling consumes transmission resources. In the paper a cost efficient signalling concept for this purpose is proposed, which relies on subspace methods.

Übersicht
In den vergangenen Jahren fanden Funkübertragungssysteme, die sender- und empfängerseitig Antennenkonfigurationen mit mehreren Einzelantennen verwenden (engl. MIMO, Multiple Input Multiple Output), das Interesse der Theoretiker, und inzwischen denkt man an die praktische Anwendung solcher Konfigurationen, z. B. in künftigen Mobilfunksystemen. Um das Potential des MIMO-Konzepts voll ausschöpfen zu können, sollte die Kenntnis der Funkkanäle sowohl im Sender als auch im Empfänger verfügbar sein und in die Signalverarbeitungsalgorithmen einbezogen werden. Am Empfänger kann die Kanalkenntnis durch trainingssequenzbasierte, halbblinde oder blinde Kanalschätzverfahren gemäß dem Stand der Technik gewonnen werden. Dagegen ist die Kanalkenntnis am Sender nicht ohne weiteres verfügbar und muß z. B. dadurch bereitgestellt werden, daß die vom Empfänger gewonnene Kanalinformation vom Empfänger zum Sender zurücksignalisiert wird. Diese Rücksignalisierung beansprucht allerdings Übertragungsressourcen. In dem Beitrag wird ein aufwandsgünstiges Konzept zur Rücksignalisierung der Kanalinformation vorgeschlagen, das auf Unterraumverfahren beruht.

By Christoph Arnold Jötten*,
Paul Walter Baier*,
Michael Meurer*
and Tobias Weber*

Für die Dokumentation
MIMO / Kanaleigenschaften / Antennensysteme / Mobilkommunikation / Unterraumverfahren

1. Introduction

Fig. 1a shows an antenna arrangement consisting of K_B transmit antennas and K_M receive antennas. For such arrangements the attribute MIMO (Multiple Input Multiple Output) has been coined [1, 2]. In order to optimize the performance of radio transmission systems utilizing MIMO antenna arrangements, the signal processing algorithms employed at the transmitter and receiver should take into consideration the properties of the $K_\mathrm{B}K_\mathrm{M}$ radio channels between the inputs of the K_B transmit antennas and the outputs of the K_M receive antennas. As a prerequisite of such a consideration the channel impulse responses should be known both at the transmitter and the receiver [3]. At the receiver this knowledge can be obtained by state of the art channel estimation techniques relying on transmitted training signals [4], where in the case of multi-antennas at the transmitter for each transmit antenna an antenna specific training signal has to be provided [5]. At the transmitter the channel information is not immediately available except for the case of duplex transmission systems applying TDD (Time Division Duplex) [6], where the same channel impulse responses, due to the reciprocity theorem, are valid for both the uplink and the downlink. In all other cases the channel information gained at the receiver has to be signalled back to the transmitter. Due to the time variance of mobile radio scenarios a single transmission of channel information is not sufficient. Rather this information has to be updated more or less frequently. The required rate of these updates grows with decreasing coherence time [7] of the mobile radio channels. The back signalling of channel information requires transmission resources, and it would be desirable to develop cost efficient concepts for representing and signalling this information. In this paper such a concept will be proposed. The concept relies on the observation that the basic structural properties of mobile radio scenarios as e. g. the propagation directions of the relevant waves vary – in the sense of slow fading – rather slowly with time, whereas other phenomena as e. g. the superposition of partial waves exhibit – in the sense of fast fading – more rapid fluctuations. As the crux of the proposed concept the total channel information is split up into a partial information I_slow representing said basic structural properties on the one side and a partial information I_fast representing said rapid phenomena on the other side. I_slow can be determined and signalled back at a low rate, whereas I_fast requires frequent updates. In the paper, first the representation of the total channel information by I_slow and I_fast is treated. Then, signalling back I_fast is considered during time periods, in which I_slow can be assumed to be unaltered.

The situations to be considered in the paper are visualized by scenarios of the type shown in **Fig. 2**. It is assumed that in these scenarios the possible receiver locations are restricted to a fraction of the total service area termed observation domain, and that the receiver randomly takes each position within this domain with a certain probability. For a given observation environment the basic structural properties of the total service area (I_slow) are determined by the shape and the location of an observation do-

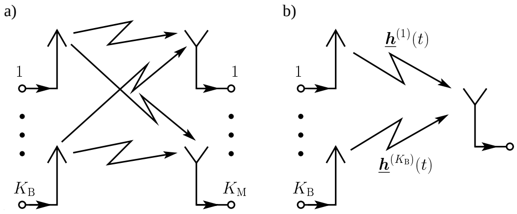

Fig 1: Antenna arrangements: a) MIMO, b) MISO

* Research Group for RF Communications, University of Kaiserslautern

Frequenz 56 (2002) 7-8

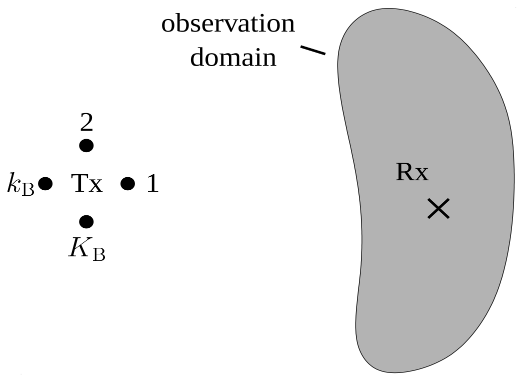

Fig. 2: Scenario with observation domain. Tx: Transmitter with K_B antenna elements; Rx: Receiver

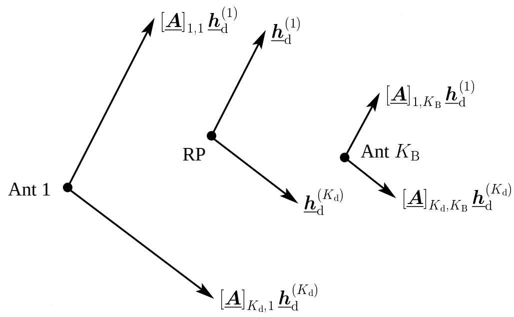

Fig. 3: Transmit side of the considered MISO antenna arrangement

main and by the probability with which the receiver appears at each location. These properties remain unaltered as long as the receiver stays within the observation domain. The rapid fluctuations of the channel information represented by I_fast take place by the movements of the receiver within the observation domain. The larger the observation domain relative to the total service area, the larger the information content of I_fast.

The channel information characterizing the MIMO arrangement of Fig. 1a is equivalent to the channel information of K_M MISO (Multiple Input Single Output) arrangements of the type shown in **Fig. 1b**. In order to provide the transmitter with the channel information of the MIMO arrangement of Fig. 1a, simply the channel information of K_M MISO arrangements must be determined at the receiver and signalled back to the transmitter. Therefore, the following considerations, which are performed in the discrete time equivalent lowpass domain [7], can be restricted to the MISO arrangement of Fig. 1b. Such an arrangement can be characterized by K_B time variant Tx antenna specific channel impulse responses [8]. It should be emphasized that these antenna specific channel impulse responses are generally determined by a multitude of scatterers both within and outside the observation domain. If it is assumed that the receiver takes all random positions within the observation domain, the entirety of the K_B channel impulse responses can be considered as a sample function of a multi-dimensional wide sense stationary ergodic process.

In the succeeding Sections 2–4 a simplified scenario is considered which is characterized as follows:

- A number of

$$K_\mathrm{d} \le K_\mathrm{B} \tag{1}$$

directions of departure (DODs) common to all K_B transmit antennas and termed relevant DODs lead – via scatterers in the propagation environment – from the transmitter to the receiver [8].
- The K_d relevant DODs are only subject to slow fading, that is they vary slowly with time.
- The channel impulse responses valid for each of the K_d relevant DODs exhibit – in the sense of fast fading – fast time variance.

2. Cost efficient representation of channel impulse responses

Let us assume that a reference point (RP) is placed in the neighborhood of the K_B transmit antennas, see **Fig. 3**. Only waves launched by the transmitter into the K_d relevant DODs introduced can generate output signals at the receive antenna. To each of these relevant DODs a directional channel impulse response [8]

$$\underline{\boldsymbol{h}}_\mathrm{d}^{(k_\mathrm{d})} = \left(\underline{h}_{\mathrm{d},1}^{(k_\mathrm{d})} \ldots \underline{h}_{\mathrm{d},W}^{(k_\mathrm{d})}\right)^T, \qquad k_\mathrm{d} = 1\ldots K_\mathrm{d}, \tag{2}$$

of dimension W can be assigned, which would be valid for the channel between the input of a virtual omni antenna placed at RP and the output of the receive antenna of the MISO arrangement of Fig. 1b. In compliance with the conditions formulated before it is assumed that the elements $\underline{h}_{\mathrm{d},w}^{(k_\mathrm{d})}$ of $\underline{\boldsymbol{h}}_\mathrm{d}^{(k_\mathrm{d})}$ of (2) are subject to fast fading. The K_d directional channel impulse responses $\underline{\boldsymbol{h}}_\mathrm{d}^{(k_\mathrm{d})}$ of (2) can be arranged in a matrix

$$\underline{\boldsymbol{H}}_\mathrm{d} = \left(\underline{\boldsymbol{h}}_\mathrm{d}^{(1)} \ldots \underline{\boldsymbol{h}}_\mathrm{d}^{(K_\mathrm{d})}\right) \tag{3}$$

of dimension $W \times K_\mathrm{d}$ termed directional channel matrix.

As shown in [8] a matrix $\underline{\boldsymbol{A}}$ of dimension $K_\mathrm{d} \times K_\mathrm{B}$ termed steering matrix can be introduced, which is determined by the K_d relevant DODs and by the geometrical arrangement as well as the radiation patterns of the K_B transmit antennas. For a given arrangement of transmit antennas, $\underline{\boldsymbol{A}}$ remains unaltered as long as the K_d relevant DODs remain the same. The directional channel impulse response valid for transmit antenna K_B and DOD K_d can be expressed as the product of $\underline{\boldsymbol{h}}_\mathrm{d}^{(k_\mathrm{d})}$ of (2) and the element $[\underline{\boldsymbol{A}}]_{k_\mathrm{d},k_\mathrm{B}}$ of the matrix $\underline{\boldsymbol{A}}$, see Fig. 3. The channel impulse response between the input of the transmit antenna K_B and the output of the receive antenna of the MISO arrangement of Fig. 1b can be described by a vector

$$\underline{\boldsymbol{h}}^{(k_\mathrm{B})} = \left(\underline{h}_1^{(k_\mathrm{B})} \ldots \underline{h}_W^{(k_\mathrm{B})}\right)^T, \qquad k_\mathrm{B} = 1\ldots K_\mathrm{B}, \tag{4}$$

of dimension W termed antenna specific channel impulse response. The K_B antenna specific channel impulse responses of (4) can be compiled to form the spatial channel matrix

$$\underline{\boldsymbol{H}} = \left(\underline{\boldsymbol{h}}^{(1)} \ldots \underline{\boldsymbol{h}}^{(K_\mathrm{B})}\right) \tag{5}$$

of dimension $W \times K_\mathrm{B}$.

With $\underline{\boldsymbol{A}}$ the spatial channel matrix $\underline{\boldsymbol{H}}$ of (5) can be expressed by the directional channel matrix $\underline{\boldsymbol{H}}_\mathrm{d}$ of (3) as follows [8]:

$$\underline{\boldsymbol{H}} = \underline{\boldsymbol{H}}_\mathrm{d}\underline{\boldsymbol{A}}. \tag{6}$$

Due to the fact that $\underline{\boldsymbol{A}}$ is of the size $K_\mathrm{d} \times K_\mathrm{B}$,

$$R_\mathrm{A} = \mathrm{rank}\left\{\underline{\boldsymbol{A}}\right\} \le \min\left(K_\mathrm{d}, K_\mathrm{B}\right) \tag{7}$$

holds for the rank R_A of $\underline{\boldsymbol{A}}$. (7) together with (6) yields for the rank R_H of $\underline{\boldsymbol{H}}$

$$R_\mathrm{H} = \mathrm{rank}\left\{\underline{\boldsymbol{H}}\right\} \le \min\left(W, K_\mathrm{d}, K_\mathrm{B}\right). \tag{8}$$

With (7) and (8) also the relation

Frequenz 56 (2002) 7-8

$$R_\mathrm{H} \le R_\mathrm{A} \tag{9}$$

holds. On account of (8) an infinite number of pairs ($\underline{\boldsymbol{U}}$, $\underline{\boldsymbol{G}}$) of $R_\mathrm{A} \times K_\mathrm{B}$ matrices

$$\underline{\boldsymbol{U}} = \left(\underline{\boldsymbol{u}}^{(1)^T} \ldots \underline{\boldsymbol{u}}^{(R_\mathrm{A})^T}\right)^T \tag{10}$$

consisting of R_A orthogonal rows $\underline{\boldsymbol{u}}^{(\ell)}$, $\ell = 1 \ldots R_\mathrm{A}$, and $W \times \mathrm{R_A}$ matrices $\underline{\boldsymbol{G}}$ exist, which allow to express $\underline{\boldsymbol{H}}$ of (5) as

$$\underline{\boldsymbol{H}} = \underline{\boldsymbol{G}}\underline{\boldsymbol{U}} \tag{11}$$

The subspaces spanned by the rows of $\underline{\boldsymbol{A}}$ and by the rows of $\underline{\boldsymbol{U}}$ of (10) are identical, and the rows of $\underline{\boldsymbol{H}}$ of (5) lie in this subspace. This implies that all matrices $\underline{\boldsymbol{H}}$ of (5) which can occur under the influence of fast fading for a given set of K_d relevant DODs can be expressed via (11) by a fixed matrix $\underline{\boldsymbol{U}}$ of (10) and a matrix $\underline{\boldsymbol{G}}$ which only depends on the momentary configuration of $\underline{\boldsymbol{H}}$.

Now a specific choice of the matrices $\underline{\boldsymbol{U}}$ and $\underline{\boldsymbol{G}}$ is introduced. As mentioned above, the rows of $\underline{\boldsymbol{H}}$ of (5) are situated in the space spanned by the rows of $\underline{\boldsymbol{U}}$ of (10). Therefore, determining the covariance matrix $\underline{\boldsymbol{H}}^{*T}\underline{\boldsymbol{H}}$ of $\underline{\boldsymbol{H}}$ for a sufficiently large number of successive samples of $\underline{\boldsymbol{H}}$ and averaging yields an average covariance matrix $\overline{\underline{\boldsymbol{H}}^{*T}\underline{\boldsymbol{H}}}$, the rows of which span the same space as the rows of $\underline{\boldsymbol{U}}$ of (10). In order to determine the specific $\underline{\boldsymbol{U}}$ mentioned above the matrix $\overline{\underline{\boldsymbol{H}}^{*T}\underline{\boldsymbol{H}}}$ is subject to eigenvalue decomposition. Then, the rows of $\underline{\boldsymbol{U}}$ can be obtained as the complex conjugate transposed eigenvectors corresponding to the non-vanishing eigenvalues of the matrix $\overline{\underline{\boldsymbol{H}}^{*T}\underline{\boldsymbol{H}}}$ [9]. The number of these non-vanishing eigenvalues is equal to the rank R_A of $\underline{\boldsymbol{A}}$, see (7).

3. Signalling the channel information back to the transmitter

Let us assume that, due to fast fading, updates of the channel information are required at the transmitter at a rate of $1/T_\mathrm{fast}$. Because $\underline{\boldsymbol{H}}$ of (5) has $K_\mathrm{B}W$ elements, this updating, if performed in a straightforward manner, would require a transmission rate of

$$R_\mathrm{H} = K_\mathrm{B} W / T_\mathrm{fast} \tag{12}$$

complex numbers per time unit. Instead of signalling the information on $\underline{\boldsymbol{H}}$ back to the transmitter, alternatively the information on $\underline{\boldsymbol{U}}$ and $\underline{\boldsymbol{G}}$ could be signalled back, see (11). Let us now assume that, due to slow fading, the K_d relevant DODs change at a rate of only $1/T_\mathrm{slow}$, which means that the matrix $\underline{\boldsymbol{U}}$ of (10) should be updated at the transmitter at this rate. This updating would require a signalling rate of

$$R_\mathrm{U} = R_\mathrm{A} K_\mathrm{B} / T_\mathrm{slow} \tag{13}$$

complex numbers per time unit. Now, the crux of the proposed cost efficient back signalling concept consists in signalling $\underline{\boldsymbol{U}}$ of (10) at the rate $1/T_\mathrm{slow}$ and $\underline{\boldsymbol{G}}$ of (11) at the rate $1/T_\mathrm{fast}$. Because $\underline{\boldsymbol{G}}$ has $R_\mathrm{A} W$ elements, the rate required for the signalling of $\underline{\boldsymbol{G}}$ is

$$R_\mathrm{G} = R_\mathrm{A} W / T_\mathrm{fast}\,. \tag{14}$$

With R_H of (12), R_U of (13) and R_G of (14) the reduction of the transmission rate offered by the proposed scheme can be quantified as

$$r = \frac{R_\mathrm{U} + R_\mathrm{G}}{R_\mathrm{H}} = \frac{R_\mathrm{A} K_\mathrm{B}/T_\mathrm{slow} + R_\mathrm{A} W/T_\mathrm{fast}}{K_\mathrm{B} W/T_\mathrm{fast}}$$
$$= R_\mathrm{A}\left(\frac{1}{W}\frac{T_\mathrm{fast}}{T_\mathrm{slow}} + \frac{1}{K_\mathrm{B}}\right). \tag{15}$$

It is desirable that r of (15) becomes as small as possible. According to (15), r decreases with increasing values of W, T_slow and K_B, and it grows with increasing values of R_A and T_fast. As an example, let us consider the case

$$K_\mathrm{d} = R_\mathrm{A} = 2, \quad W = 10, \quad T_\mathrm{fast} = 1\,\mathrm{ms},$$
$$T_\mathrm{slow} = 1\,\mathrm{s}, \quad K_\mathrm{B} = 8. \tag{16}$$

With these values we obtain from (15)

$$r = 0.25, \tag{17}$$

which means a significant reduction of the resources required for signalling the channel information back to the transmitter.

4. MISO antenna structure with weighting network

In the foregoing sections the MISO arrangement of Fig. 1b was considered as a subset of the MIMO arrangement of Fig. 1a. In some applications as for instance in the downlink of mobile radio systems the utilized antenna arrangement is of the type MISO and not of the type MIMO. Such a situation will be considered in this section. An obvious concept how to utilize MISO arrangements in practical transmission systems is illustrated in **Fig. 4**. In this concept the K_B transmit antennas are fed from a common feeding input via a weighting network characterized by the weight vector

$$\underline{\boldsymbol{w}} = \left(\underline{w}_1 \ldots \underline{w}_{K_\mathrm{B}}\right)^T \tag{18}$$

of dimension K_B. With $\underline{\boldsymbol{H}}$ of (5) and $\underline{\boldsymbol{w}}$ of (18) the channel between the input and the output of the MISO structure of Fig. 3 has the impulse response

$$\underline{\boldsymbol{h}} = \underline{\boldsymbol{H}}\underline{\boldsymbol{w}}. \tag{19}$$

According to (11) the rows of $\underline{\boldsymbol{H}}$ of (5) are linear combinations of the orthonormal rows $\underline{\boldsymbol{u}}^{(\ell)}$, $\ell = 1 \ldots R_\mathrm{A}$, of $\underline{\boldsymbol{U}}$ of (10). With a vector $\underline{\boldsymbol{G}}$ of dimension R_A and a vector $\underline{\boldsymbol{w}}_\mathrm{orth}$ of dimension K_B and being orthogonal to the space spanned by the rows of $\underline{\boldsymbol{U}}$, any conceivable weight vector $\underline{\boldsymbol{w}}$ to be utilized at the transmitter can be written – by a proper choice of $\underline{\boldsymbol{G}}$ and $\underline{\boldsymbol{w}}_\mathrm{orth}$ – as the sum

$$\underline{\boldsymbol{w}} = \underline{\boldsymbol{U}}^{*T}\,\underline{\boldsymbol{g}} + \underline{\boldsymbol{w}}_\mathrm{orth}\,. \tag{20}$$

$\underline{\boldsymbol{w}}_\mathrm{orth}$ does not contribute to $\underline{\boldsymbol{h}}$ of (19) and represents transmitted signal components which have no impact on the received signal. In order to avoid the radiation of energy, which does not arrive at

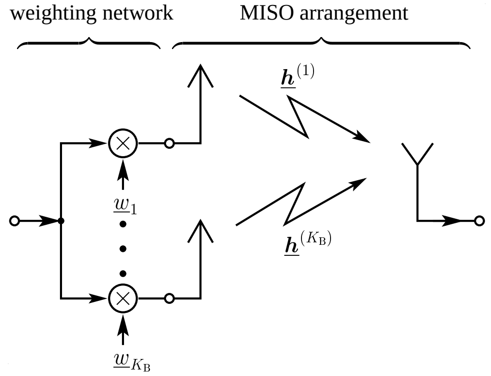

Fig. 4: Combination of weighting network and MISO antenna arrangement

the receiver, $\underline{\boldsymbol{w}}_{\text{orth}}$ should be zero. Then, the substitution of $\underline{\boldsymbol{H}}$ of (11) and $\underline{\boldsymbol{w}}$ of (20) into (19) yields

$$\underline{\boldsymbol{h}} = \underbrace{\underline{\boldsymbol{G}}\underline{\boldsymbol{U}}\underline{\boldsymbol{U}}^{*T}\underline{\boldsymbol{g}}}_{\underline{\boldsymbol{G}}\underline{\boldsymbol{g}}} + \underbrace{\underline{\boldsymbol{G}}\underline{\boldsymbol{U}}\underline{\boldsymbol{w}}_{\text{orth}}}_{\mathbf{0}} = \underline{\boldsymbol{G}}\underline{\boldsymbol{g}}. \tag{21}$$

Let us now consider the task to generate a certain $\underline{\boldsymbol{h}}$ by properly choosing the weight vector $\underline{\boldsymbol{w}}$ at the transmitter. If $W \le \mathrm{R}_{\mathrm{A}}$ holds, an infinite number of vectors $\underline{\boldsymbol{g}}$ can be found, which, when substituted into (21), result in any demanded channel impulse response $\underline{\boldsymbol{h}} \in \mathbb{C}^W$. The vector $\underline{\boldsymbol{g}}$ which leads to the desired $\underline{\boldsymbol{h}}$ under the side condition of minimum transmit energy is given by [9]

$$\underline{\boldsymbol{g}} = \underline{\boldsymbol{G}}^{*T}\left(\underline{\boldsymbol{G}}\underline{\boldsymbol{G}}^{*T}\right)^{-1}\underline{\boldsymbol{h}}. \tag{22}$$

If $W > R_{\mathrm{A}}$ holds, a vector $\underline{\boldsymbol{g}}$ to enforce a demanded channel impulse response $\underline{\boldsymbol{h}} \in \mathbb{C}^W$ generally does not exist. In this case a vector $\underline{\boldsymbol{G}}$ resulting in an impulse response $\tilde{\underline{\boldsymbol{h}}}$ which, in the Gaussian sense, best matches the demanded impulse response $\underline{\boldsymbol{h}}$ can be found as [9]

$$\underline{\boldsymbol{g}} = \left(\underline{\boldsymbol{G}}^{*T}\underline{\boldsymbol{G}}\right)^{-1}\underline{\boldsymbol{G}}^{*T}\underline{\boldsymbol{h}}. \tag{23}$$

The vector $\underline{\boldsymbol{g}}$ is generated at the receiver and then signalled back to the transmitter. Then, at the transmitter $\underline{\boldsymbol{w}}$ can be determined by substituting $\underline{\boldsymbol{g}}$ into (20). Because $\underline{\boldsymbol{g}}$ consists of only R_{A} complex numbers, this back signalling is very cost efficient.

Instead of choosing $\underline{\boldsymbol{w}}$ in such a way that a specific desired $\underline{\boldsymbol{h}}$ of (19) is achieved, one can also choose a vector $\underline{\boldsymbol{w}}$ by which the energy $\underline{\boldsymbol{h}}^{*T}\underline{\boldsymbol{h}}$ of $\underline{\boldsymbol{h}}$ relative to the transmitted energy $\underline{\boldsymbol{w}}^{*T}\underline{\boldsymbol{w}}$ is maximized, see also [10]. From (20) and (21) follow

$$\underline{\boldsymbol{w}}^{*T}\underline{\boldsymbol{w}} = \underline{\boldsymbol{g}}^{*T}\underline{\boldsymbol{U}}\underline{\boldsymbol{U}}^{*T}\underline{\boldsymbol{g}} = \underline{\boldsymbol{g}}^{*T}\underline{\boldsymbol{g}}, \tag{24}$$

where vanishing $\underline{\boldsymbol{w}}_{\text{orth}}$ is assumed, and

$$\underline{\boldsymbol{h}}^{*T}\underline{\boldsymbol{h}} = \underline{\boldsymbol{g}}^{*T}\underline{\boldsymbol{G}}^{*T}\underline{\boldsymbol{G}}\underline{\boldsymbol{g}}, \tag{25}$$

respectively. From (24) and (25) we obtain

$$\underline{\boldsymbol{g}} = \arg\max_{\underline{\boldsymbol{g}} \in \boldsymbol{C}^{K_{\mathrm{M}}}}\left[\frac{\underline{\boldsymbol{g}}^{*T}\underline{\boldsymbol{G}}^{*T}\underline{\boldsymbol{G}}\underline{\boldsymbol{g}}}{\underline{\boldsymbol{g}}^{*T}\underline{\boldsymbol{g}}}\right] \tag{26}$$

The vector $\underline{\boldsymbol{g}}$ which fulfills (26) is the eigenvector corresponding to the largest eigenvalue of the matrix $\underline{\boldsymbol{G}}^{*T}\underline{\boldsymbol{G}}$ [9]. This vector has to be determined at the receiver and signalled back to the transmitter. There it can be substituted into (20) in order to obtain the required $\underline{\boldsymbol{w}}$.

5. Summary

A cost efficient concept for signalling the channel information from the output to the input of MIMO systems is presented. This concept is based on subspace methods. It is applicable, whenever few and slowly varying directions of departure lead from the transmitter to the receiver.

The authors are indebted to Deutsche Forschungsgemeinschaft (DFG) for sponsoring part of this work within "DFG Schwerpunktprogramm Adaptivität in heterogenen Kommunikationsnetzen mit drahtlosem Zugang (AKOM)". They gratefully appreciate the stimulating discussions and the fruitful exchange of ideas with their colleagues at the Research Group for RF Communications, University of Kaiserslautern, and Siemens AG. Furthermore, they express their thanks for the invaluable support by the supercomputing staff at the Central Computer Facility of the University of Kaiserlautern (RHRK).

References

[1] Telatar, E: Capacity of multi antenna gaussian channels. European Transactions on Telecommunications (ETT), vol. 10 (1999) pp. 585–595.

[2] Foschini. G. J.; Gans, M. J.: On limits of wireless communications in a fading environment when using multiple antennas. Wireless Personal Communications, vol. 6 (1998) pp. 311–335.

[3] Spencer, Q. H.; Swindlehurst, A. L.: Some results on channel capacity when using multiple antennas. Proc. IEEE 52th Vehicular Technology Conference (VTC '00 – Fall), Boston, 2000, vol. 2, pp. 681–688.

[4] Steiner, B.; Baier, P. W.: Low cost channel estimation in the uplink receiver of CDMA mobile radio systems. FREQUENZ, vol. 47, no. 11-12 (1993) pp. 292–298.

[5] 3rd Generation Partnership Project (3GPP). Technical specification group (TSG) RAN WG4, spreading and modulation (FDD). Technical Specification TS 25.213 Version 3.1.0, 3GPP, 1999.

[6] Technical specification of IMT-2000 CDMA TDD (TD-SCDMA). China Wireless Telecommunications Standard (CWTS). Published in internet under the URL: http://www.cwts.org, 1999.

[7] Proakis, J. G.: Digital Communications, New York: McGraw-Hill, 1995.

[8] Jötten, C. A.; Baier, P. W.; Meurer, M.: Transmit array processing in CDMA downlinks utilizing the duplexing scheme FDD. inProc. 8th International Conference on Telecommunications (ICT '01), Bucharest, 2001, pp. 419–424.

[9] Haykin, S.: Adaptive Filter Theory, Prentice-Hall, Upper Saddle River, 1996.

[10] Brunner, C.; Hammerschmidt, J. S.; Nossek, J. A.: Downlink Eigenbeamforming in WCDMA. in Proc. VDE/ITG European Wireless Conference, Dresden, 2000, pp. 195–200.

Dipl.-Ing. C. A. Jötten
Prof. Dr.-Ing. habil. P. W. Baier
Dipl.-Ing. M. Meurer
Dr.-Ing. T. Weber
Lehrstuhl für hochfrequente Signalübertragung und -verarbeitung
Fachbereich Elektrotechnik und Informationstechnik
Universität Kaiserslautern
Erwin Schrödiger Strasse 11
D-67653 Kaiserslautern
Fax: +49 (0)6 31 / 2 05 36 12
e-mail: joetten@rhrk.uni-kl.de

(Received on April 18, 2002)

[JBM+02] Jötten, C. A.; Baier, P. W.; Meurer, M.; Weber, T.; Haardt, M.: "Efficient representation and feedback signaling of channel state information in frequency division duplexing MIMO systems". *Proc. of 5th International Symposium on Wireless Personal Multimedia Communications (WPMC'02)*, Honolulu, 2002, S. 444–448.

Efficient Representation and Feedback Signaling of Channel State Information in Frequency Division Duplexing MIMO Systems

C.A. Jötten, P.W. Baier, M. Meurer, T. Weber
Research Group for RF Communications
University of Kaiserslautern
P.O. Box 3049, D–67653 Kaiserslautern, Germany
joetten@rhrk.uni-kl.de

M. Haardt
Communications Research Laboratory
Ilmenau University of Technology
P.O. Box 100565, D–98684 Ilmenau, Germany
martin.haardt@tu-ilmenau.de

Abstract
In order to fully benefit from the potential offered by the application of Multiple-Input-Multiple-Output (MIMO) configurations in mobile radio systems, the knowledge of the radio channels should be available and considered in the signal processing algorithms both at the transmitter and the receiver. At the receiver this knowledge can be gained by state of the art training sequence based, semi–blind or blind channel estimation. However, at the transmitter the channel knowledge is not readily available and has to be imparted from the receiver by signaling the relevant information back to the transmitter, which ties up transmission resources. Therefore, a cost efficient signaling concept for this purpose is proposed, which relies on subspace methods. A quantitative example is discussed to show how this concept can be applied and how it performs in different scenarios.

INTRODUCTION
In order to optimize the performance of radio transmission systems utilizing Multiple-Input-Multiple-Output (MIMO) antenna arrangements, see Figure 1a, the signal processing algorithms employed at the transmitter and receiver should take into consideration the properties of the $K_{\mathrm{B}}K_{\mathrm{M}}$ radio channels between the inputs of the K_{B} transmit antennas and the outputs of the K_{M} receive antennas [1, 2]. The potential for performance improvement depends on the grade of channel knowledge at the transmitter [3]. Knowledge of the spatial correlation properties of the DL channels allows to increase the capacity compared to the case where no channel knowledge is available at the transmitter [4]. If the exact channel impulse responses are known at the transmitter the performance can be enhanced further. At the receiver channel knowledge can be obtained by state of the art channel estimation techniques, e.g., relying on transmitted training signals [5], where in the case of multiple antennas at the transmitter for each transmit antenna an antenna specific training signal has to be provided [6]. At the transmitter the channel information is not immediately available except for the case of duplex transmission systems applying TDD (Time Division Duplex) [7], where, due to the reciprocity theorem, the same channel impulse responses are valid for both transmission and reception. In all other cases the channel information gained at the receiver has to be signaled back to the transmitter. Due to the time variance of mobile radio scenarios a single re-transmission of the channel information is not sufficient. Rather this information has to be updated more or less frequently. The required rate of these updates grows with decreasing coherence time [8] of the mobile radio channels. The back signaling of the channel information requires transmission resources, and it would be desirable to develop cost efficient concepts for representing and signaling this information. In this paper such a concept will be proposed. This concept relies on the observation that the basic structural properties of mobile radio scenarios as, e.g., the propagation directions of the relevant waves vary - in the sense of slow fading - rather slowly with time, whereas other phenomena as, e.g., the superposition of partial waves exhibit - in the sense of fast fading - more rapid fluctuations. The basic idea of the proposed concept is to split up the total channel information into a long term information I_{slow} representing said basic structural properties on the one hand and a short term information I_{fast} representing said rapid phenomena on the other hand [9]. I_{slow} can be determined and signaled back at a low rate, whereas I_{fast} requires frequent updates. In the paper, first the representation of the total channel information by I_{slow} and I_{fast} is treated. Then, signaling back I_{fast} is considered during time periods, in which I_{slow} can be assumed to be unaltered.

REPRESENTATION OF SPATIAL CHANNELS
The MIMO arrangement of Figure 1a can be considered as a set of K_{M} parallel Multiple-Input-Single-Output (MISO) arrangements of the type shown in Figure 1b. In order to provide the transmitter with the channel information of the MIMO arrangement of Figure 1a, simply the channel information of K_{M} MISO arrangements could be determined

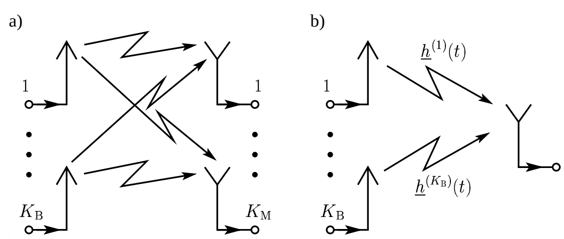

Figure 1. Antenna arrangements: a) MIMO, b) MISO

at the receiver and then be signaled back to the transmitter. Therefore, the following considerations, which are performed in the discrete time equivalent lowpass domain [8], can be restricted to the MISO arrangement of Figure 1b. Let us now assume that the considered mobile radio channels are non frequency selective and that the spatial channel impulse response of Figure 1b is described by the vector

$$\underline{\mathbf{h}}_{\mathrm{s}}(t) = \left(\underline{h}^{(1)}(t)\ldots\underline{h}^{(k_{\mathrm{B}})}(t)\right)^{\mathrm{T}} \in \mathbb{C}^{K_{\mathrm{B}}}. \tag{1}$$

During time periods where the basic structural properties of the considered mobile radio scenarios remain approximately unaltered the spatial covariance matrix

$$\underline{\mathbf{R}} = \mathrm{E}\left\{\underline{\mathbf{h}}_{\mathrm{s}}(t)\underline{\mathbf{h}}_{\mathrm{s}}^{\mathrm{H}}(t)\right\} \in \mathbb{C}^{K_{\mathrm{B}}\times K_{\mathrm{B}}} \tag{2}$$

can be derived by temporal averaging. Thus, $\underline{\mathbf{R}}$ of (2) represents the long term information I_{slow}.
Eigenvalue decomposition [10] of $\underline{\mathbf{R}}$ of (2) yields the orthonormal unitary $K_{\mathrm{B}}\times K_{\mathrm{B}}$ matrix $\underline{\mathbf{U}}$ termed eigenvector matrix, the columns of which are the unit norm eigenvectors of $\underline{\mathbf{R}}$, and the real eigenvalue matrix

$$\mathbf{\Lambda} = \mathrm{diag}\left(\lambda_1\ldots\lambda_{K_{\mathrm{B}}}\right) \in \mathbb{C}^{K_{\mathrm{B}}\times K_{\mathrm{B}}}, \tag{3}$$

where the eigenvalues are arranged in descending order, i.e.,

$$\lambda_1 \geq \lambda_2 \geq \cdots \geq \lambda_{K_{\mathrm{B}}}. \tag{4}$$

The sorted representation of eigenvalues according to (4) is termed eigenvalue profile throughout the paper.
Now, $\underline{\mathbf{R}}$ of (2) can be displayed as

$$\underline{\mathbf{R}} = \underline{\mathbf{U}}\mathbf{\Lambda}\underline{\mathbf{U}}^{\mathrm{H}}. \tag{5}$$

As $\underline{\mathbf{R}}$ of (2), the matrices $\underline{\mathbf{U}}$ and $\mathbf{\Lambda}$ of (5) represent the long term information I_{slow}. Throughout the paper it is assumed that these matrices are known at the transmitter. Efficient schemes for tracking and feedback of $\underline{\mathbf{U}}$ are proposed and discussed , e.g., in [11].
Now, with a vector

$$\underline{\mathbf{x}}(t) = \left(\underline{x}_1(t)\ldots\underline{x}_{K_{\mathrm{B}}}(t)\right)^{\mathrm{T}} \in \mathbb{C}^{K_{\mathrm{B}}} \tag{6}$$

each realization of $\underline{\mathbf{h}}_{\mathrm{s}}(t)$ of (1) can be expressed as a linear combination of the columns of $\underline{\mathbf{U}}$ of (5) as

$$\underline{\mathbf{h}}_{\mathrm{s}}(t) = \underline{\mathbf{U}}\,\underline{\mathbf{x}}(t). \tag{7}$$

If $\underline{\mathbf{h}}_{\mathrm{s}}(t)$ is known, $\underline{\mathbf{x}}(t)$ can be determined directly by inversion of (7). From (7) it becomes obvious that the rapid fluctuations of $\underline{\mathbf{h}}_{\mathrm{s}}(t)$ are directly reflected in the vector $\underline{\mathbf{x}}(t)$. Thus, $\underline{\mathbf{x}}(t)$ represents the short term information I_{fast}.

FEEDBACK OF CHANNEL STATE INFORMATION

Each realization of $\underline{\mathbf{h}}_{\mathrm{s}}(t)$ of (1) can be directly expressed by its K_{B} components $\underline{h}^{(k_{\mathrm{B}})}(t)$, $k_{\mathrm{B}}=1\ldots K_{\mathrm{B}}$. As an alternative to this trivial approach, if $\underline{\mathbf{U}}$ of (5) is known at the receiver and the transmitter, the K_{B} components $\underline{x}_{k_{\mathrm{B}}}(t)$, $k_{\mathrm{B}}=1\ldots K_{\mathrm{B}}$, of $\underline{\mathbf{x}}(t)$ of (6) can serve to represent $\underline{\mathbf{h}}_{\mathrm{s}}(t)$ of (1), see (7). Signaling of the K_{B} components $\underline{h}^{(k_{\mathrm{B}})}(t)$, $k_{\mathrm{B}}=1\ldots K_{\mathrm{B}}$, would mean that the total channel information $I_{\text{slow}}+I_{\text{fast}}$ is transmitted, whereas signaling of the K_{B} components $\underline{x}_{k_{\mathrm{B}}}(t)$, $k_{\mathrm{B}}=1\ldots K_{\mathrm{B}}$, would restrict the transmission to I_{fast}. Obviously, signaling $\underline{\mathbf{x}}(t)$ of (7) instead of signaling directly $\underline{\mathbf{h}}_{\mathrm{s}}(t)$ of (1) tends to be more cost efficient. However, the question to be treated in what follows is, how much transmission capacity could be saved by signaling only I_{fast} instead of $I_{\text{slow}}+I_{\text{fast}}$.
Substitution of (7) into (2) yields

$$\underline{\mathbf{R}} = \underline{\mathbf{U}}\,\mathrm{E}\left\{\underline{\mathbf{x}}(t)\underline{\mathbf{x}}^{\mathrm{H}}(t)\right\}\underline{\mathbf{U}}^{\mathrm{H}}. \tag{8}$$

The comparison of (5) and (8) shows that the components $\underline{x}_{k_{\mathrm{B}}}(t)$ of $\underline{\mathbf{x}}(t)$ are uncorrelated with each other and that the variances of the real and imaginary parts of the component $\underline{x}_{k_{\mathrm{B}}}(t)$ of $\underline{\mathbf{x}}(t)$ in (7) are [10]

$$\sigma^2_{\mathrm{x},k_{\mathrm{B}}} = \frac{1}{2}\mathrm{E}\left\{\underline{x}^*_{k_{\mathrm{B}}}(t)\underline{x}_{k_{\mathrm{B}}}(t)\right\} = \lambda_{k_{\mathrm{B}}}/2, \tag{9}$$

and for the sum of these variances follows

$$\sum_{k_{\mathrm{B}}=1}^{K_{\mathrm{B}}}\sigma^2_{\mathrm{x},k_{\mathrm{B}}} = \frac{1}{2}\sum_{k_{\mathrm{B}}=1}^{K_{\mathrm{B}}}\lambda_{k_{\mathrm{B}}}. \tag{10}$$

For the sum of the K_{B} variances $\sigma^2_{\mathrm{h},k_{\mathrm{B}}}$, $k_{\mathrm{B}}=1\ldots K_{\mathrm{B}}$, of the real and imaginary parts of the components $\underline{h}_{\mathrm{s}}^{(k_{\mathrm{B}})}$ of the vector $\underline{\mathbf{h}}_{\mathrm{s}}(t)$ of (1) holds

$$\begin{aligned}\sum_{k_{\mathrm{B}}=1}^{K_{\mathrm{B}}}\sigma^2_{\mathrm{h},k_{\mathrm{B}}} &= \frac{1}{2}\mathrm{E}\left\{\underline{\mathbf{x}}^{\mathrm{H}}(t)\underline{\mathbf{U}}^{\mathrm{H}}\underline{\mathbf{U}}\,\underline{\mathbf{x}}(t)\right\}\\ &= \frac{1}{2}\sum_{k_{\mathrm{B}}=1}^{K_{\mathrm{B}}}\lambda_{k_{\mathrm{B}}}.\end{aligned} \tag{11}$$

Therefore, both in the case of signaling the vector $\underline{\mathbf{x}}(t)$ of (7) and of directly signaling the vector $\underline{\mathbf{h}}_{\mathrm{s}}(t)$ of (1), K_{B} complex quantities or $2K_{\mathrm{B}}$ real quantities have to be transmitted, where the sum of the K_{B} variances $\sigma^2_{\mathrm{x},k_{\mathrm{B}}}$ on the one side and of the K_{B} variances $\sigma^2_{\mathrm{h},k_{\mathrm{B}}}$ on the other side is the same in both cases. A difference between the two cases can be observed in the following respect: The variances $\sigma^2_{\mathrm{x},k_{\mathrm{B}}}$ tend to decrease with increasing k_{B}, whereas the variances $\sigma^2_{h,k_{\mathrm{B}}}$ do usually not show this tendency. Before signaling back the channel information to the transmitter, the component values $\underline{x}_{k_{\mathrm{B}}}(t)$ of $\underline{\mathbf{x}}(t)$ from (7) and $\underline{h}^{(K_{\mathrm{B}})}(t)$ of $\underline{\mathbf{h}}_{\mathrm{s}}(t)$ from (1) have to be quantized. Let us assume that $b_{k_{\mathrm{B}}}$ bits are provided for quantizing each the real part and imaginary part of the component $\underline{x}_{k_{\mathrm{B}}}(t)$ of $\underline{\mathbf{x}}(t)$ in (7) or for quantizing the real part and imaginary part of the component $\underline{h}^{(k_{\mathrm{B}})}(t)$ of $\underline{\mathbf{h}}_{\mathrm{s}}(t)$ from (1), respectively. Let us further assume that the total number of bits available for quantizing the real and imaginary parts each has the fixed value

$$B = \sum_{k_{\mathrm{B}}=1}^{K_{\mathrm{B}}} b_{k_{\mathrm{B}}}. \tag{12}$$

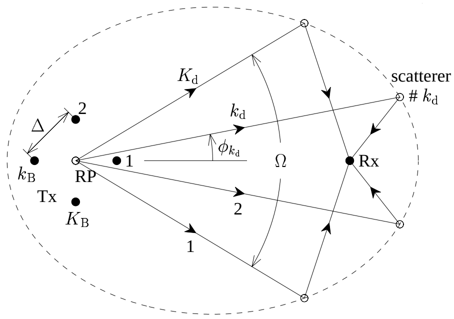

Figure 2. Considered scenario

If a continuous valued real quantity of variance σ^2 is quantized with b bits, this entails a quantization error which can be written as $\sigma^2 f(b)$. The function $f(b)$ depends on the shape of the probability density function of the quantity to be coded and on the chosen quantization scheme [12]. In what follows $f(b)$ shall be chosen in an optimum way [12] which means that the quantization error is minimized for the given probability density function of the quantity to be quantized and for the given number b of bits.

Let us now assume that $\underline{\mathbf{h}}_\mathrm{s}(t)$ is approximated by substituting a quantized version $\widehat{\underline{\mathbf{x}}}(t)$ of $\underline{\mathbf{x}}(t)$ into (7), where the real and imaginary parts of the component $\underline{x}_{k_\mathrm{B}}(t)$ are quantized with b_{k_B} bits each, and where the optimum quantization scheme is used. Then under consideration of (9) the mean relative quantization error of the spatial channel impulse response given by the vector $\underline{\mathbf{h}}_\mathrm{s}(t)$ of (1) becomes

$$\varepsilon_\mathrm{x} = \frac{\mathrm{E}\left\{\left|\underline{\mathbf{h}}_\mathrm{s}(t) - \underline{\mathbf{U}}\,\widehat{\underline{\mathbf{x}}}(t)\right|^2\right\}}{\mathrm{E}\left\{\left|\underline{\mathbf{h}}_\mathrm{s}(t)\right|^2\right\}} = \frac{\sum\limits_{k_\mathrm{B}=1}^{K_\mathrm{B}} \lambda_{k_\mathrm{B}} f(b_{k_\mathrm{B}})}{\sum\limits_{k_\mathrm{B}=1}^{K_\mathrm{B}} \lambda_{k_\mathrm{B}}}. \quad (13)$$

Under consideration of the constraint (12) the achievable minimum of ε_x of (13) is given by

$$\varepsilon_\mathrm{x,min} = \frac{1}{\sum\limits_{k_\mathrm{B}=1}^{K_\mathrm{B}} \lambda_{k_\mathrm{B}}} \min_{\substack{b_{k_\mathrm{B}} \\ \forall k_\mathrm{B}\in\{1...K_\mathrm{B}\}}} \left[\sum_{k_\mathrm{B}=1}^{K_\mathrm{B}} \lambda_{k_\mathrm{B}} f(b_{k_\mathrm{B}})\right]. \quad (14)$$

If, instead of signaling the components $\underline{x}_{k_\mathrm{B}}(t)$ of the vector $\underline{\mathbf{x}}(t)$ of (7), the components $\underline{h}^{(k_\mathrm{B})}$ of the vector $\underline{\mathbf{h}}_{\mathrm{s},k_\mathrm{B}}$ of (1) would be directly transmitted, then the minimum achievable mean quantization error of the total channel impulse response would become, subject to the constraint (12),

$$\varepsilon_\mathrm{h,min} = \frac{1}{\sum\limits_{k_\mathrm{B}=1}^{K_\mathrm{B}} \sigma^2_{\mathrm{h},k_\mathrm{B}}} \min_{\substack{b_{k_\mathrm{B}} \\ \forall k_\mathrm{B}\in\{1...K_\mathrm{B}\}}} \left[\sum_{k_\mathrm{B}=1}^{K_\mathrm{B}} \sigma^2_{\mathrm{h},k_\mathrm{B}} f(b_{k_\mathrm{B}})\right]. \quad (15)$$

For given B of (12), depending on the values $\varepsilon_\mathrm{x,min}$ of (14) and $\varepsilon_\mathrm{h,min}$ of (15), the benefit of signaling only I_fast instead of $I_\mathrm{slow} + I_\mathrm{fast}$ strongly depends on the considered scenario.

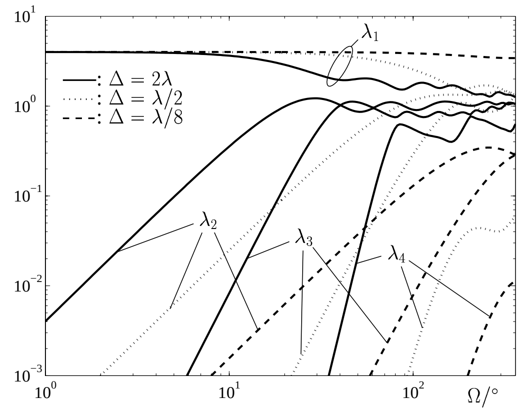

Figure 3. Eigenvalue profile versus DOD spread Ω

EXAMPLE

In order to illustrate the theoretical considerations performed in the previous sections a specific scenario is quantitatively investigated in the present section. The considered scenario is depicted in Figure 2. $K_\mathrm{B} = 4$ transmit antennas are arranged in a uniform circular array. The spacing between adjacent antennas is Δ, see Figure 2. The channel coefficients $\underline{h}^{(k_\mathrm{B})}(t)$, $k_\mathrm{B}=1...K_\mathrm{B}$, characterizing the channels from the K_B transmit antennas to the receive antenna are constituted by K_d independent scatterers, see Figure 2. As seen from the transmitter, these scatterers are distributed in such a way that for a given direction of departure (DOD) spread Ω, see Figure 2, they appear under the DODs

$$\phi_{k_\mathrm{d}} = \Omega\,\left(-\frac{1}{2} + \frac{k_\mathrm{d}-1}{K_\mathrm{d}-1}\right), \quad k_\mathrm{d}=1...K_\mathrm{d}. \quad (16)$$

For a fictitious omni antenna placed at the reference point (RP), see Figure 2, each of the K_d scatterers delivers a contribution $\underline{h}_\mathrm{d}^{(k_\mathrm{d})}(t)$, $k_\mathrm{d} = 1\ldots K_\mathrm{d}$, to the channel coefficient $\underline{h}^{(k_\mathrm{B})}(t)$ characterizing the channel between the input of said omni antenna at RP and the output of the receive antenna. The K_d quantities $\underline{h}_\mathrm{d}^{(k_\mathrm{d})}(t)$ are assumed to be independent complex Gaussian with the variance σ^2 of their real and imaginary parts, i.e.,

$$\mathrm{E}\left\{\left|\underline{h}_\mathrm{d}^{(k_\mathrm{d})}(t)\right|^2\right\} = 2\sigma^2,\ k_\mathrm{d}=1...K_\mathrm{d}. \quad (17)$$

From the independence of the K_d quantities $\underline{h}_\mathrm{d}^{(k_\mathrm{d})}(t)$ follows

$$\mathrm{E}\left\{\left|\underline{h}_\mathrm{s}^{(k_\mathrm{B})}(t)\right|^2\right\} = 2\sigma^2_{\mathrm{h},k_\mathrm{B}} = K_\mathrm{d} 2\sigma^2,\ k_\mathrm{B}=1...K_\mathrm{B}, \quad (18)$$

for the K_B variances of the antenna specific channel impulse responses $\underline{h}_\mathrm{s}^{(k_\mathrm{B})}(t)$, $k_\mathrm{B}=1...K_\mathrm{B}$, cf. (11). With the array steering vectors [13] $\underline{\mathbf{a}}^{(k_\mathrm{d})}$, $k_\mathrm{d}=1...K_\mathrm{d}$, relevant for the DODs ϕ_{k_d}, $k_\mathrm{d}=1...K_\mathrm{d}$, the spatial impulse response $\underline{\mathbf{h}}_\mathrm{s}(t)$

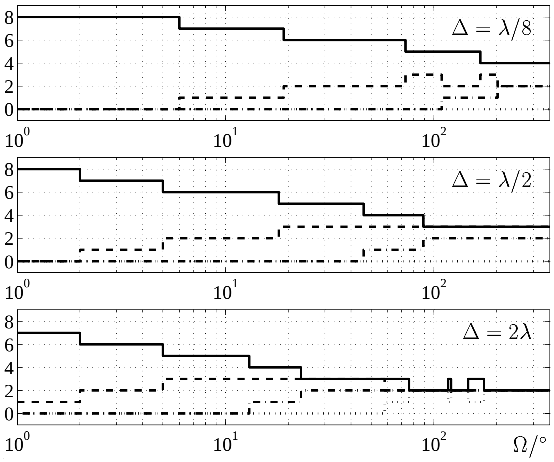

Figure 4. Bit numbers b_{k_B}, $k_\mathrm{B} = 1\ldots4$, versus DOD spread Ω for the antenna spacings $\Delta = \lambda/8$, $\lambda/2$, 2λ. b_1: —, b_2: ---, b_3: -·-, b_4: ······ .

can be expressed as

$$\underline{\mathbf{h}}_\mathrm{s}(t) = \sum_{k_\mathrm{d}=1}^{K_\mathrm{d}} \underline{\mathbf{a}}^{(k_\mathrm{d})} \underline{h}_\mathrm{d}^{(k_\mathrm{d})}(t). \quad (19)$$

For the expectation of the respective spatial covariance matrix follows with (19)

$$\underline{\mathbf{R}} = \mathrm{E}\left\{\underline{\mathbf{h}}_\mathrm{s}(t)\underline{\mathbf{h}}_\mathrm{s}^\mathrm{H}(t)\right\} = \mathrm{E}\left\{\sum_{k_\mathrm{d}=1}^{K_\mathrm{d}} 2\sigma^2 \underline{\mathbf{a}}^{(k_\mathrm{d})} \underline{\mathbf{a}}^{(k_\mathrm{d})\mathrm{H}}\right\}. \quad (20)$$

In Figure 3 for the observed antenna arrangement and different antenna spacings Δ the eigenvalue profiles, cf. (4), are depicted versus the DOD spread Ω, that is, each graph in Figure 3 represents the evolution of a certain eigenvalue λ_{k_B}, $k_\mathrm{B} = 1\ldots K_\mathrm{B}$, when the antenna spacing Δ is fixed and the DOD spread Ω takes values in the range $\Omega/^\circ \in [1, 360]$. For small DOD spreads Ω the eigenvalue λ_1 is dominant, whereas the other $K_\mathrm{B}-1$ eigenvalues are negligibly small. λ_1 decreases with increasing DOD spread Ω, whereas the lower eigenvalues λ_{k_B}, $k_\mathrm{B} = 2\ldots K_\mathrm{B}$, increase. This behavior can be quantified by the decrease of the eigenvalue spread $\lambda_1/\lambda_{K_\mathrm{B}}$ [10] with increasing DOD spread Ω and it is visualized in Figure 5, where the reciprocal of the eigenvalue spread, that is, the ratio $\lambda_{K_\mathrm{B}}/\lambda_1$, is depicted versus the DOD spread Ω for different antenna spacings Δ. In general the ratio $\lambda_{K_\mathrm{B}}/\lambda_1$ becomes larger if the DOD spread Ω or the antenna spacing Δ is increased. For fixed antenna spacings Δ and for small DOD spreads Ω the ratio $\lambda_{K_\mathrm{B}}/\lambda_1$ increases approximately linearly with Ω. For larger DOD spreads $\Omega \to 360^\circ$ the ratio $\lambda_{K_\mathrm{B}}/\lambda_1$ converges to an upper bound, with this bound depending on the antenna spacing Δ. The smaller the antenna spacing Δ, the larger the DOD spread Ω, for which the ratio $\lambda_{K_\mathrm{B}}/\lambda_1$ converges, and the lower the upper bound.

Now a total number of $2B$ equal to sixteen bits is utilized for quantizing either the components of the vector $\underline{\mathbf{x}}(t)$ in (7) or the components of the vector $\underline{\mathbf{h}}_\mathrm{s}(t)$ from (1). In Figure 4 the bit numbers b_{k_B} allocated according (14) for the representation of the components $\underline{x}_{k_\mathrm{B}}$, $k_\mathrm{B} = 1\ldots4$, are depicted versus the DOD spread Ω for the analyzed antenna spacings Δ. In Table 1 the bit numbers b_{k_B}, $k_\mathrm{B} = 1\ldots4$, are listed for significant DOD spreads Ω where the bit allocation changes. In Figure 6 the mean relative quantization error $\varepsilon_\mathrm{x,min}$ of (14) is depicted versus the DOD spread Ω, cf. (16), for different antenna spacings Δ. As a reference also the mean relative quantization error $\varepsilon_\mathrm{h,min}$ of (15) is depicted. Due to the fact that the variance σ^2 depends neither on the DOD spread Ω nor on the antenna spacing Δ, $\varepsilon_\mathrm{h,min}$ is identical for all DOD spreads $\Omega/^\circ \in [1, 360]$ and all considered antenna spacings Δ; in our example $\varepsilon_\mathrm{h,min}$ takes the value -9.3dB. For all considered antenna spacings Δ, $\varepsilon_\mathrm{x,min}$ increases with growing DOD spread Ω. As to be expected, in all cases $\varepsilon_\mathrm{x,min}$ is lower than or equal to $\varepsilon_\mathrm{h,min}$. A comparison of the mean relative quantization errors $\varepsilon_\mathrm{x,min}$ of Figure 6 with the respective ratios λ_1/λ_4 in Figure 5 shows that the error $\varepsilon_\mathrm{x,min}$ increases linearly with Ω as long as the respective ratio λ_1/λ_4 increases with Ω. Only in the case $\Delta = 2\lambda$ and $\Omega > 75^\circ$ the error $\varepsilon_\mathrm{x,min}$ becomes as large as the error $\varepsilon_\mathrm{h,min}$.

SUMMARY AND OUTLOOK

A cost efficient concept for signaling the channel information from the output to the input of MIMO systems is presented. A quantitative example has been given to show how the concept can be applied and how it performs in different scenarios. The example shows, that in most of the con-

Table 1. Bit numbers b_{k_B}, $k_\mathrm{B} = 1\ldots4$, for certain DOD spreads Ω and different antenna spacings Δ.

$\Delta = \lambda/8$

$\Omega/^\circ$	b_1	b_2	b_3	b_4
1	8	0	0	0
6	7	1	0	0
19	6	2	0	0
73	5	3	0	0
109	5	2	1	0
167	4	3	1	0
202	4	2	2	0

$\Delta = \lambda/2$

$\Omega/^\circ$	b_1	b_2	b_3	b_4
1	8	0	0	0
2	7	1	0	0
5	6	2	0	0
18	5	3	0	0
46	4	3	1	0
89	3	3	2	0

$\Delta = 2\lambda$

$\Omega/^\circ$	b_1	b_2	b_3	b_4
1	7	1	0	0
2	6	2	0	0
5	5	3	0	0
13	4	3	1	0
23	3	3	2	0
58	3	2	2	1
76	2	2	2	2
117	3	2	2	1
121	2	2	2	2
146	3	2	2	1
174	2	2	2	2

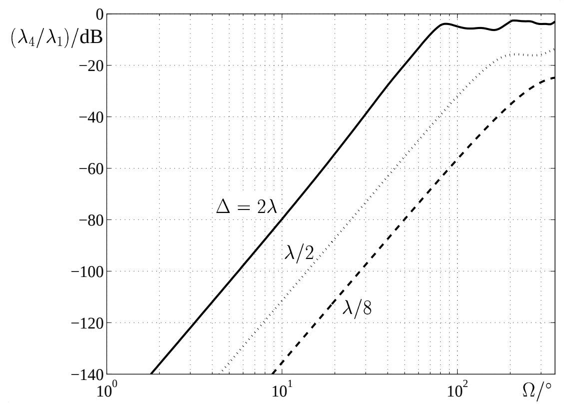

Figure 5. Reciprocal ratio of the eigenvalue spread versus DOD spread Ω for different antenna spacings Δ

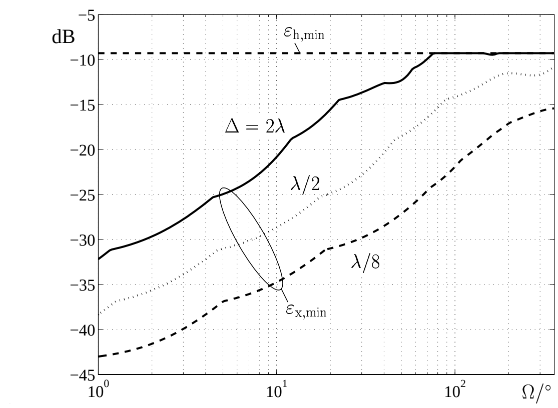

Figure 6. Quantization error $\varepsilon_{\min}$ versus DOD spread Ω for different antenna spacings Δ

sidered scenarios the quantization error for a given feedback rate could be significantly decreased by the application of the proposed method. In the case that the conjugate of the reconstructed spatial channel impulse response is used to steer a Tx weighting network the introduced signaling concept can be interpreted as a downlink Eigenbeamformer with quantized combination of Eigenbeams [14]. The proposed concept can be straightforwardly extended for the case of frequency selective channels [9]. Due to the fact that a prerequisite for the proposed scheme is the knowledge of the slowly varying channel properties at both the receiver and the transmitter, further research should be performed with respect to the efficient signaling of the slowly varying channel properties.

ACKNOWLEDGMENT

The authors are indebted to Deutsche Forschungsgemeinschaft (DFG) and Siemens AG for sponsoring part of this work.

REFERENCES

[1] E. Telatar, "Capacity of multi antenna gaussian channels," *European Transactions on Telecommunications (ETT)*, vol. 10, pp. 585–595, 1999.

[2] G. J. Foschini and M. J. Gans, "On limits of wireless communications in a fading environment when using multiple antennas," *Wireless Personal Communications*, vol. 6, pp. 311–335, 1998.

[3] S. A. Jafar and A. Goldsmith, "On optimality of beamforming for multiple antenna systems with imperfect feedback," in *Proc. International Symposium on Information Theory*, Washington D.C., 2001.

[4] E. Visotsky and U. Madhow, "Space–time transmit precoding with imperfect feedback," *IEEE Transactions on Information Theory*, vol. 47, pp. 2632–2639, 2001.

[5] B. Steiner and P. W. Baier, "Low cost channel estimation in the uplink receiver of CDMA mobile radio systems," *Frequenz*, vol. 47, no. 11–12, pp. 292–298, 1993.

[6] "3rd generation partnership project (3GPP); technical specification group (TSG) RAN WG4, spreading and modulation (FDD)," Technical Specification TS 25.213, V. 3.1.0, 3GPP, 1999.

[7] Technical specification of IMT-2000 CDMA TDD (TD-SCDMA), "China Wireless Telecommunications Standard (CWTS)," URL: http://www.cwts.org, 1999.

[8] J. G. Proakis, *Digital Communications*, McGraw-Hill, New York, 3. edition, 1995.

[9] C. A. Jötten, P. W. Baier, M. Meurer, and T. Weber, "Cost efficient representation and signaling of channel information in MIMO systems," in *Proc. IEEE 56th Vehicular Technology Conference (VTC'02 Fall)*, Vancouver, 2002.

[10] S. Haykin, *Adaptive Filter Theory*, Prentice-Hall, Upper Saddle River, 1996.

[11] W. Utschick, "Tracking of signal subspace projectors," *IEEE Transactions on Signal Processing*, vol. 50, pp. 769–778, 2002.

[12] S. P. Lloyd, "Least squares quantization in PCM," *IEEE Transactions on Information Theory*, vol. 28, pp. 129–137, 1982.

[13] L. C. Godara, "Applications of antenna arrays to mobile communications, part II: Beam-forming and direction-of-arrival considerations," *Proceedings of the IEEE*, vol. 85, no. 8, pp. 1195–1245, 1997.

[14] M. Haardt, C. F. Mecklenbräuker, M. Vollmer, and P. Slania, "Smart antennas for UTRA TDD," *European Transactions on Telecommunications (ETT)*, vol. 12, pp. 393–406, 2001.

6.2.3 Problem der Zeitvarianz

Sind die zwischen Basisstation und Mobilstationen wirksamen Mobilfunkkanäle zeitvariant, so ist die totale Kanalmatrix $\underline{\mathbf{H}}$ nach (1.5) im allgemeinen eine von der Zeit t abhängige Matrix $\underline{\mathbf{H}}(t)$, siehe auch Abschnitt 1.1.2, mit den zeitvarianten Elementen

$$\underline{h}_{i,j}(t) = \Big[\underline{\mathbf{H}}(t)\Big]_{i,j}, \forall i, j. \tag{6.2}$$

Wird fälschlicherweise die für einen Zeitpunkt T_{est} gültige totale Kanalmatrix $\underline{\mathbf{H}}(T_{\mathrm{est}})$ für die gemeinsame Sendesignalerzeugung und Abwärtsstreckenübertragung zum Zeitpunkt T_{use} eingesetzt, so ergibt sich der in (6.1) eingeführte Fehler $\underline{\mathbf{E}}(T_{\mathrm{est}}, T_{\mathrm{use}})$ der an der Basisstation verwendeten Kanalzustandsinformation mit den Elementen

$$\underline{e}_{i,j}(T_{\mathrm{est}}, T_{\mathrm{use}}) = \Big[\underline{\mathbf{E}}(T_{\mathrm{est}}, T_{\mathrm{use}})\Big]_{i,j}, \forall i, j. \tag{6.3}$$

Durch Kombinieren von (6.2), (6.3) und (6.1) ergibt sich somit der von T_{est} und T_{use} abhängige Fehler

$$\underline{e}_{i,j}(T_{\mathrm{est}}, T_{\mathrm{use}}) = \underline{h}_{i,j}(T_{\mathrm{est}}) - \underline{h}_{i,j}(T_{\mathrm{use}}) \tag{6.4}$$

eines jeden Elements $\underline{h}_{i,j}(T_{\mathrm{use}})$ der für die Abwärtsstreckenübertragung gültigen totalen Kanalmatrix $\underline{\mathbf{H}}(T_{\mathrm{use}})$.

In den folgenden Betrachtungen soll ausschließlich ein Element $\underline{h}_{i,j}(t)$ der totalen Kanalmatrix $\underline{\mathbf{H}}(t)$ und das zugehörige Element $\underline{e}_{i,j}(T_{\mathrm{est}}, T_{\mathrm{use}})$ der Fehlermatrix $\underline{\mathbf{E}}(T_{\mathrm{est}}, T_{\mathrm{use}})$ auf einmal betrachtet werden. Daher wird im folgenden der Übersichtlichkeit halber auf die Verwendung der Indizes „i, j“ verzichtet.

Im folgenden soll des weiteren angenommen werden, daß die zwischen Basisstation und Mobilstationen wirksamen zeitvarianten Mobilfunkkanäle hinreichend genau durch das wohl bekannte WSSUS-Kanalmodell (engl. wide sense stationary uncorrelated scattering channel model, WSSUS channel model) [Bel63, Pro95] beschrieben werden können. Dann gilt, daß jedes Element $\underline{h}(t)$ von $\underline{\mathbf{H}}(t)$ als schwach stationäre Zufallsgröße betrachtet werden kann. Betrachtet man den auf die beschriebene Zeitvarianz zurückgehenden Fehler $\underline{e}(T_{\mathrm{est}}, T_{\mathrm{use}})$ nach (6.4), so hat dies die Konsequenz, daß infolge der schwachen Stationarität von $\underline{h}(t)$ der Erwartungswert

$$\mathrm{E}\left\{\underline{e}(T_{\mathrm{est}}, T_{\mathrm{use}})\right\} = \mathrm{E}\left\{\underline{h}(T_{\mathrm{est}})\right\} - \mathrm{E}\left\{\underline{h}(T_{\mathrm{use}})\right\} = 0 \tag{6.5}$$

identisch null wird. Vereinfachend ausgedrückt bedeutet dies, daß im Mittel der aus der Zeitvarianz folgende Fehler $\underline{e}(T_{\mathrm{est}}, T_{\mathrm{use}})$ nach (6.4) eines jeden Elements $\underline{h}(T_{\mathrm{use}})$ der für die Abwärtsstreckenübertragung gültigen totalen Kanalmatrix $\underline{\mathbf{H}}(T_{\mathrm{use}})$ verschwindet. Leider gilt dies ausschließlich im Mittel, so daß eine genauere Bewertung des Fehlers

$\underline{e}(T_{\mathrm{est}}, T_{\mathrm{use}})$ nach (6.4) nötig wird. Als kompaktes Maß der Bewertung eignet sich die Varianz

$$\begin{aligned}\sigma_{\mathrm{h}}^2(T_{\mathrm{est}}, T_{\mathrm{use}}) &= \mathrm{E}\left\{|\underline{e}(T_{\mathrm{est}}, T_{\mathrm{use}})|^2\right\} \\ &= \mathrm{E}\left\{|\underline{h}(T_{\mathrm{est}})|^2\right\} + \mathrm{E}\left\{|\underline{h}(T_{\mathrm{use}})|^2\right\} - 2\mathrm{Re}\left\{\mathrm{E}\left\{\underline{h}^*(T_{\mathrm{est}})\underline{h}(T_{\mathrm{use}})\right\}\right\}\end{aligned} \tag{6.6}$$

des Fehlers $\underline{e}(T_{\mathrm{est}}, T_{\mathrm{use}})$ nach (6.4). Infolge der bereits angesprochenen Stationarität lassen sich die beiden ersten in (6.6) eingehenden Summanden durch die mittlere Kanalenergie

$$E_{\mathrm{h}} = \mathrm{E}\left\{|\underline{h}(T_{\mathrm{est}})|^2\right\} = \mathrm{E}\left\{|\underline{h}(T_{\mathrm{use}})|^2\right\} \tag{6.7}$$

beschreiben. Des weiteren folgt mit der WSSUS-Kanäle beschreibenden Zeitkorrelationsfunktion (engl. spaced-time correlation function) [Bel63]

$$\underline{\rho}_{\mathrm{F}}(0, \Delta t) = \frac{1}{2}\mathrm{E}\left\{\underline{h}^*(t)\underline{h}(t+\Delta t)\right\} \tag{6.8}$$

und der Eigenschaft der Stationarität von $\underline{h}(t)$ für die in (6.6) eingehenden Summanden

$$\mathrm{E}\left\{\underline{h}^*(T_{\mathrm{est}})\underline{h}(T_{\mathrm{use}})\right\} = 2\underline{\rho}_{\mathrm{F}}\Big(0,\ \underbrace{T_{\mathrm{use}} - T_{\mathrm{est}}}_{=T_{\mathrm{tot}}}\Big) \tag{6.9}$$

und

$$E_{\mathrm{h}} = 2\underline{\rho}_{\mathrm{F}}\Big(0, 0\Big). \tag{6.10}$$

In (6.9) bezeichnet T_{tot} die Differenz zwischen dem Zeitpunkt T_{use} der Verwendung der Kanalzustandsinformation zur Abwärtsstreckenübertragung und dem Zeitpunkt T_{est} der Bereitstellung der Kanalzustandsinformation. Diese Differenz T_{tot} wird im folgenden als Totzeit bezeichnet. Unter der Annahme, daß die zeitliche Veränderung von $\underline{h}(t)$ einem Jakes-Doppler-Spektrum [Pro95] mit dem minimalen Wert $S_{\mathrm{c,min}}$ entspricht — und dies ist im Bereich der Analyse von Mobilfunksystemen als hinreichend gute Approximation anerkannt und in Realität in typischen Mobilfunkszenarien näherungsweise gegeben — so lassen sich mit der maximalen Geschwindigkeit der Mobilstationen v, der Mittenfrequenz f_0 des zur Abwärtsstreckenübertragung eingesetzten Frequenzbandes und der Ausbreitungsgeschwindigkeit c_0 der Funkwellen die maximale Dopplerfrequenz

$$f_{\mathrm{d,max}} = \frac{v f_0}{c_0} \tag{6.11}$$

und die Zeitkorrelationsfunktion

$$\underline{\rho}_{\mathrm{F}}\Big(0, \Delta t\Big) = S_{\mathrm{c,min}}\, f_{\mathrm{d,max}}\, \pi \mathrm{J}_0\Big(2\pi \Delta t f_{\mathrm{d,max}}\Big) \tag{6.12}$$

nach (6.8) angeben. In (6.12) bezeichnet $\mathrm{J}_0(\cdot)$ die Besselfunktion erster Art und nullter Ordnung [BS79]. Mit Hilfe der Umkehrfunktion $\mathrm{J}_0^{-1}(\cdot)$ dieser Besselfunktion läßt sich die Korrelationsdauer

$$T_{\mathrm{cor}} = \mathrm{J}_0^{-1}\Big(\frac{1}{2}\Big)\frac{1}{2\pi f_{\mathrm{d,max}}} \tag{6.13}$$

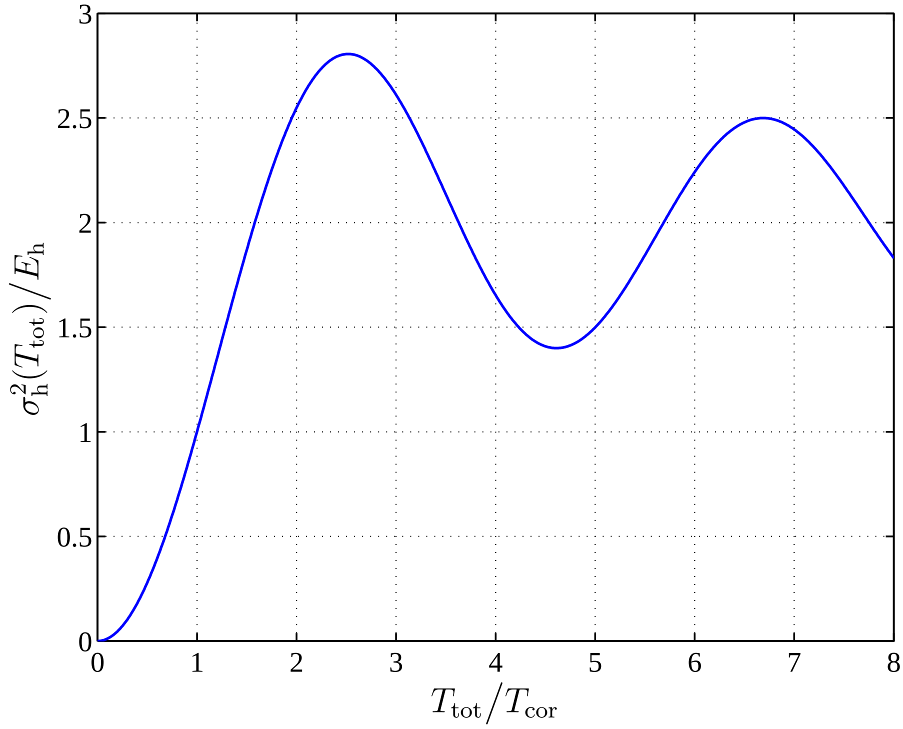

Bild 6.1. Normierte Varianz $\sigma_{\mathrm{h}}^2/E_{\mathrm{h}}$ des Fehlers $\underline{e}(T_{\mathrm{est}}, T_{\mathrm{use}})$ nach (6.4) infolge von Zeitvarianz als Funktion der normierten Totzeit $T_{\mathrm{tot}}/T_{\mathrm{cor}}$

als Funktion der maximalen Dopplerfrequenz $f_{\mathrm{d,max}}$ nach (6.11) bestimmen. Durch Einsetzen von (6.7), (6.9), (6.10), (6.12) und (6.13) in (6.6) erhält man schließlich die normierte Varianz

$$\frac{\sigma_{\mathrm{h}}^2\left(T_{\mathrm{tot}}\right)}{E_{\mathrm{h}}} = 2\left(1-\mathrm{J}_0\left(2\pi T_{\mathrm{tot}} f_{\mathrm{d,max}}\right)\right) = 2\left(1-\mathrm{J}_0\left(\frac{T_{\mathrm{tot}}}{T_{\mathrm{cor}}}\,\mathrm{J}_0^{-1}\left(\frac{1}{2}\right)\right)\right) \quad (6.14)$$

des Fehlers $\underline{e}(T_{\mathrm{est}}, T_{\mathrm{use}})$ nach (6.4) infolge von Zeitvarianz als Funktion der normierten Totzeit $T_{\mathrm{tot}}/T_{\mathrm{cor}}$. Der Zusammenhang nach (6.14) ist in Bild 6.1 graphisch verdeutlicht. Dabei wird deutlich, daß ausschließlich für Totzeiten T_{tot}, die signifikant kleiner als die Korrelationsdauer T_{cor} des Mobilfunkkanals sind, akzeptable Fehler $\underline{e}(T_{\mathrm{est}}, T_{\mathrm{use}})$ nach (6.4) zu erwarten sind. Anschaulich ist somit klar, daß das Einsatzgebiet von Empfängerorientierung in der Abwärtsstrecke zellularer Mobilfunksysteme massiv durch die Variationsgeschwindigkeit der in der Abwärtsstrecke wirksamen Mobilfunkkanäle begrenzt ist. Praktisch bedeutet dies, daß bei gegebener Totzeit T_{tot} — und diese hängt ausschließlich vom Entwurf des Mobilfunksystems ab — und gegebener Mittenfrequenz f_0 des zur Abwärtsstreckenübertragung eingesetzten Frequenzbandes die Geschwindigkeiten v der Mobilstationen limitiert sind. Die für die Geschwindigkeiten geltenden sich in Bild 6.1 manifestierenden weichen Grenzen lassen sich durch geeignete Verfahren wie beispielsweise Kanalprädiktionsverfahren [DH-

JU03, Win04, CM04a, CM03, Lay00] nach oben verschieben, sind jedoch prinzipiell stets vorhanden und unumgänglich.

6.3 Konsequenzen imperfekter senderseitiger Kanalzustandsinformation

Als Essenz der Betrachtungen des vorherigen Unterkapitels 6.2 ist klar, daß in Mobilfunksystemen die zur gemeinsamen Sendesignalerzeugung benötige Kanalzustandsinformation in Form der totalen Kanalmatrix $\underline{\mathbf{H}}$ in der Praxis nie genau, sondern lediglich in Form einer mehr oder weniger genauen Schätzung $\widehat{\underline{\mathbf{H}}}$ vorliegt. Die Ursachen für die sich zwischen $\widehat{\underline{\mathbf{H}}}$ und $\underline{\mathbf{H}}$ ergebenden Unterschiede sind dabei vorrangig

- die begrenzte Genauigkeit der durch Verfahren des Kanalschätzens erzielbaren Kanalschätzungen, wenn die zum Kanalschätzen eingesetzten Empfangssignale Störungen, wie beispielsweise Rauschen, unterworfen sind und

- die zeitliche Separierung der Zeitpunkte T_{est} des Ermittelns der Kanalzustandsinformation und T_{use} des Verwendens derselben im Falle zeitvarianter Mobilfunkkanäle, siehe auch Abschnitt 6.2.3.

Derartige imperfekte Kanalzustandsinformation hat grundsätzlich zur Folge, daß die Leistungsfähigkeit empfängerorientierter Funkkommunikation beeinträchtigt wird [KM00, WLMM03, HvHJ$^+$02, DHJU03, JN98, CM04a, CM04c, CM03, Skl04, RIF02, IHRF04a]. Die folgenden Veröffentlichungen [MW04a, MW04b, WSM04, WM04a] haben daher zum Ziel, derartige Beeinträchtigungen quantitativ zu bewerten. Zu diesem Zweck werden sowohl analytische wie auch numerische Untersuchungen angestellt.

Im Gegensatz zu dem aus Tabelle 1.2 bekannten Systemmodell werden in [WSM04, WM04a] einige wenige Größen durch eine modifizierte Notation beschrieben. Tabelle 6.1 listet die wesentlichen Unterschiede in kompakter Form auf.

Tabelle 6.1. Wesentliche Unterschiede der Notationen nach Tabelle 1.2 und der Notation nach [WSM04, WM04a]

dargestellte Größe	Formelzeichen nach Tab. 1.2	Formelzeichen nach [WSM04, WM04a]
totales Empfangssignal	$\underline{\mathbf{r}}$	$\underline{\mathbf{e}}$
totales Sendesignal	$\underline{\mathbf{t}}$	$\underline{\mathbf{s}}$

[MW04a] Meurer, M.; Weber, T.: “Imperfect channel knowledge: An insurmountable barrier in Rx oriented multi-user MIMO transmission?”. *Proc. 5th International ITG Conference on Source and Channel Coding 2004 (SCC’2004)*, Erlangen, 2004, S. 371–380.

Imperfect channel knowledge: An insurmountable barrier in Rx oriented multi-user MIMO transmission ?

Michael Meurer, Tobias Weber
Research Group for RF Communications, University of Kaiserslautern,
P.O. Box 3049, D–67653 Kaiserslautern, Germany,phone/fax: +49 631 205 2084/3612, e–mail: meurer@rhrk.uni-kl.de

Abstract

In conventional transmission schemes the transmitter algorithms are a priori given, whereas the algorithms to be used by the receivers have to be a posteriori adapted. Such schemes can be termed transmitter (Tx) oriented. The opposite to Tx orientation would be receiver (Rx) orientation, in which the receiver algorithms are a priori given, and the transmitter algorithms have to be a posteriori adapted under consideration of channel knowledge. A question still open concerns the impact of imperfect channel knowledge on the transmission quality of Rx oriented data transmission, especially if radio transmission systems with multi-antennas both at the transmitter and receiver are considered. In the paper this question is analytically studied. To that purpose closed form expressions for signal-to-noise-plus-interference-ratios and bit error probabilities are derived which show a good match to simulation results.

1 Introduction

In conventional transmission schemes the transmitter algorithms are *a priori* given and made known to the receivers, whereas the algorithms to be used by the receivers have to be *a posteriori* adapted, possibly under consideration of channel information. For this approach, where the transmitter (Tx) is the master and the receivers (Rx) are the slaves, the authors have coined the term Tx orientation [1]. The opposite to Tx orientation is Rx orientation, in which the receiver algorithms are *a priori* given and made known to the transmitter, and the transmitter algorithms, again possibly under consideration of channel information, have to be *a posteriori* adapted correspondingly. It was only recently that the rationale Rx orientation was clearly formulated and started to attract some attention [2], [3], [4], [5], although this approach offers some quite interesting advantages [1]. The most important advantage might be that the *a priori* determined receiver algorithms can be chosen with a view to arrive at particularly simple receiver structures. Therefore, if we consider, as an important example of radio transmission, mobile radio systems, the quasi natural choice in the downlink (DL) would be Rx orientation, because this leads to low cost receivers at the mobile terminals (MTs) [3]. Both Tx orientation and Rx orientation have in common that at the receivers or at the transmitter, respectively, channel knowledge has to be used. This channel knowledge is *a priori* not available but has to be made available at the receivers or at the transmitter, respectively, by channel estimation [6], [7]. By this procedure in general only imperfect channel knowledge can be made available for further signal processing. For Tx oriented data transmission the impact of such imperfections onto the performance of the data transmission has been well-studied [6], [7]. However, for Rx oriented data transmission this impact is still an open question, which is still not satisfactorily answered. In [8] a special SISO (single input single output) system is considered and it is shown by few simulations which impact imperfect channel measurements have onto the transmission quality in the considered special scenario. The focus of [9] still lies on a special SISO system but, in contrast to [8], the impact of out-dated channel knowledge onto the transmission quality is discussed. Out-dated channel knowledge is a severe problem if the mobile radio channels are time-variant and the time elapsing between channel estimation and data transmission is not sufficiently small compared to the coherence time of the mobile radio channels. In [10] these simulation based insights are extended to MISO (multi input single output) systems, still focusing on the same special scenario. In all three contributions [8], [9] and [10] no generally valid analysis is presented which allows to apply the obtained simulation results to a large variety of scenarios. A somewhat more general view on MIMO (multiple input multiple output) configurations, where Rx oriented data transmission is applied, is presented in [11] and [12]. These contributions focus on the fact that imperfect channel knowledge may go back to a feedback scheme which only allows to track slowly varying channel properties. A more basic information theoretic perspective of the same topic for MIMO systems is given in [13]. However, in none of the three contributions [11], [12], [13] other kinds of channel knowledge imperfections than those due to feedback restrictions are considered. Especially, an analytical performance evaluation of Rx oriented transmission is not available. Therefore, in this paper the authors give a first fundamental –, i.e., we do not focus on the reason of imperfect channel knowledge like out-dated channel estimation but on the fact itself – analytical answer to the question raised above. The focus of the analysis lies on linear Rx oriented transmission based on the Transmit Zero Forcer (TxZF) [1], [5], [14].

The investigations are performed in the time discrete equivalent low pass domain under utilization of the vector-matrix representation for signals and system components [1], [15].

2 Generic model of linear MIMO transmission systems

We consider a situation, where an access point (AP) supports K MTs k, $k=1\ldots K$. The AP is equipped with K_B transmit antennas, and each of the K MTs employs K_M receive antennas. Therefore, each link between the AP and one of the K MTs constitutes a MIMO structure, and the total system is a multi-user MIMO structure. We further assume that the radio channel between the AP and each MT k, $k=1\ldots K$, is a flat blockfading MIMO channel. N data symbols $\underline{d}_n^{(k)}$, $n=1\ldots N$, have to be transmitted from the AP to each MT k, $k=1\ldots K$. The N data symbols $\underline{d}_n^{(k)}$, $n=1\ldots N$, intended for MT k are arranged in the MT specific data vector

$$\underline{\mathbf{d}}^{(k)} = \left(\underline{d}_1^{(k)} \ldots \underline{d}_N^{(k)}\right)^\mathrm{T} \tag{1}$$

of dimension N. The K MT specific data vectors $\underline{\mathbf{d}}^{(k)}$, $k=1\ldots K$, of (1) are stacked to the total data vector

$$\underline{\mathbf{d}} = \left(\underline{\mathbf{d}}^{(1)\mathrm{T}} \ldots \underline{\mathbf{d}}^{(K)\mathrm{T}}\right)^\mathrm{T} = \left(\underline{d}_1 \ldots \underline{d}_{N_\mathrm{t}}\right)^\mathrm{T} \tag{2}$$

of dimension

$$N_\mathrm{t} = KN. \tag{3}$$

The elements $\underline{d}_n$, $n=1\ldots N_\mathrm{t}$, of $\underline{\mathbf{d}}$ of (2) are taken from a finite symbol alphabet $\mathbb{V}$. $\underline{\mathbf{d}}$ of (2) is assumed to be wide sense stationary with zero mean and the covariance matrix

$$\underline{\mathbf{R}}_\mathrm{d} = \mathop{\mathrm{E}}_{\underline{\mathbf{d}}}\left\{\underline{\mathbf{d}}\,\underline{\mathbf{d}}^\mathrm{H}\right\} = E_\mathrm{d}\mathbf{I}^{(N_\mathrm{t})}. \tag{4}$$

By modulation a transmit signal

$$\underline{\mathbf{t}} = \left(\underline{t}_1 \ldots \underline{t}_{K_\mathrm{B}}\right)^\mathrm{T} \tag{5}$$

of dimension K_B is generated. As we assume linear processing at the transmitter, the modulation process can be described by a $K_\mathrm{B} \times N$-matrix $\underline{\mathbf{M}}$, i.e.,

$$\underline{\mathbf{t}} = \underline{\mathbf{M}}\,\underline{\mathbf{d}}. \tag{6}$$

$\underline{\mathbf{M}}$ in (6) is termed modulator matrix [3]. Via (6) the N_t components of $\underline{\mathbf{d}}$ of (2) are mapped onto the K_B components of $\underline{\mathbf{t}}$.

The MIMO channel between the AP and MT k is assumed to be linear. Therefore, the MT specific noise-free received signal $\underline{\mathbf{e}}^{(k)}$ at the MT k of dimension K_M is a linear function of the transmit signal $\underline{\mathbf{t}}$, i.e., with the MT specific channel matrix $\underline{\mathbf{H}}^{(k)}$ of dimension $K_\mathrm{M} \times K_\mathrm{B}$

$$\underline{\mathbf{e}}^{(k)} = \underline{\mathbf{H}}^{(k)}\underline{\mathbf{t}} \tag{7}$$

holds. The K MT specific noise-free received signals $\underline{\mathbf{e}}^{(k)}$, $k=1\ldots K$, are stacked to the total noise-free received signal

$$\underline{\mathbf{e}} = \left(\underline{\mathbf{e}}^{(1)\mathrm{T}} \ldots \underline{\mathbf{e}}^{(K)\mathrm{T}}\right)^\mathrm{T} \tag{8}$$

of dimension KK_M. Taking the noise $\underline{\mathbf{n}}^{(k)}$ at the input of MT k into account, one obtains

$$\underline{\mathbf{r}}^{(k)} = \underline{\mathbf{e}}^{(k)} + \underline{\mathbf{n}}^{(k)} = \underline{\mathbf{H}}^{(k)}\underline{\mathbf{t}} + \underline{\mathbf{n}}^{(k)} \tag{9}$$

for the MT specific received signal and

$$\begin{aligned}\underline{\mathbf{r}} &= \left(\underline{\mathbf{r}}^{(1)\mathrm{T}} \ldots \underline{\mathbf{r}}^{(K)\mathrm{T}}\right)^\mathrm{T} \\ &= \underbrace{\left(\underline{\mathbf{H}}^{(1)\mathrm{T}} \ldots \underline{\mathbf{H}}^{(K)\mathrm{T}}\right)^\mathrm{T}}_{\underline{\mathbf{H}}}\underline{\mathbf{t}} + \underbrace{\left(\underline{\mathbf{n}}^{(1)\mathrm{T}} \ldots \underline{\mathbf{n}}^{(K)\mathrm{T}}\right)^\mathrm{T}}_{\underline{\mathbf{n}}}\end{aligned} \tag{10}$$

for the total received signal [3]. Substituting (6) in (10) yields

$$\underline{\mathbf{r}} = \underline{\mathbf{H}}\,\underline{\mathbf{M}}\,\underline{\mathbf{d}} + \underline{\mathbf{n}}. \tag{11}$$

$\underline{\mathbf{H}}$ in (11) is termed (total) channel matrix. $\underline{\mathbf{n}}$ of (10) and (11), which is termed (total) noise signal, is assumed to be Gaussian, wide sense stationary with zero mean, independent of $\underline{\mathbf{d}}$ of (2), and to have the covariance matrix

$$\underline{\mathbf{R}}_\mathrm{n} = \mathop{\mathrm{E}}_{\underline{\mathbf{n}}}\left\{\underline{\mathbf{n}}\,\underline{\mathbf{n}}^\mathrm{H}\right\}. \tag{12}$$

At MT k the received signal $\underline{\mathbf{r}}^{(k)}$ of this MT, see (9), is fed to a MT specific demodulator in order to obtain a value-continuous estimate $\widehat{\underline{\mathbf{d}}}^{(k)}$ of $\underline{\mathbf{d}}^{(k)}$ of (1). The estimate $\widehat{\underline{\mathbf{d}}}^{(k)}$ is fed to a decision unit to map the value-continuous estimates $\widehat{\underline{d}}_n^{(k)}$ of the data symbols $\underline{d}_n^{(k)}$, $n=1\ldots N$, onto valid elements of the symbol alphabet $\mathbb{V}$.

In the case of linear demodulation considered in this paper, the demodulation process performed at MT k is described by a MT specific demodulator matrix $\underline{\mathbf{D}}^{(k)}$ of dimension $N \times K_\mathrm{M}$ as follows [1]:

$$\widehat{\underline{\mathbf{d}}}^{(k)} = \left(\widehat{\underline{d}}_1^{(k)} \ldots \widehat{\underline{d}}_N^{(k)}\right)^\mathrm{T} = \underline{\mathbf{D}}^{(k)}\underline{\mathbf{r}}^{(k)}. \tag{13}$$

By properly stacking the K equations (13), we obtain with (2) and (10)

$$\begin{aligned}\widehat{\underline{\mathbf{d}}} &= \left(\widehat{\underline{\mathbf{d}}}^{(1)\mathrm{T}} \ldots \widehat{\underline{\mathbf{d}}}^{(K)\mathrm{T}}\right)^\mathrm{T} = \left(\widehat{\underline{d}}_1 \ldots \widehat{\underline{d}}_{N_\mathrm{t}}\right)^\mathrm{T} \\ &= \underbrace{\mathrm{blockdiag}\left(\underline{\mathbf{D}}^{(1)} \ldots \underline{\mathbf{D}}^{(K)}\right)}_{\underline{\mathbf{D}}}\underline{\mathbf{r}}.\end{aligned} \tag{14}$$

$\underline{\mathbf{D}}$ of (14) has the dimension $N_\mathrm{t} \times KK_\mathrm{M}$ and is termed (total) demodulator matrix. Substituting (11) in (14) yields

$$\widehat{\underline{\mathbf{d}}} = \underline{\mathbf{D}}\,\underline{\mathbf{H}}\,\underline{\mathbf{M}}\,\underline{\mathbf{d}} + \underline{\mathbf{D}}\,\underline{\mathbf{n}}. \tag{15}$$

$\underline{\mathbf{D}}\,\underline{\mathbf{H}}\,\underline{\mathbf{M}}$ of (15) is a square matrix of dimension $N_\mathrm{t} \times N_\mathrm{t}$, where generally all elements of $\underline{\mathbf{D}}\,\underline{\mathbf{H}}\,\underline{\mathbf{M}}$ are non-zero, i.e., each data symbol $\underline{d}_n$, $n=1\ldots N_\mathrm{t}$, influences all estimates $\widehat{\underline{d}}_{n'}$, $n'=1\ldots N_\mathrm{t}$. The data transmission is unbiased if and only if the diagonal elements of $\underline{\mathbf{D}}\,\underline{\mathbf{H}}\,\underline{\mathbf{M}}$ are equal to one.

In what follows, $[\cdot]_{n,n}$ designates the n-th diagonal element of a square matrix in brackets, and $[\cdot]_n$ stands for the n-th row of a matrix in brackets or the n-th element of a column vector in brackets. According to (4) and (6) the mean radiated energy invested for the data symbol $\underline{d}_n$ becomes

$$T_n = \left\| \left[\underline{\mathbf{M}}^{\mathrm{T}} \right]_n \right\|^2 E_{\mathrm{d}} = \left[\underline{\mathbf{M}}^{\mathrm{H}} \underline{\mathbf{M}} \right]_{n,n} E_{\mathrm{d}}. \quad (16)$$

By averaging over all N_{t} data symbols $\underline{d}_n$, $n=1\ldots N_{\mathrm{t}}$, we obtain the mean radiated energy

$$T = \frac{1}{N_{\mathrm{t}}} \sum_{n=1}^{N_{\mathrm{t}}} T_n = \frac{E_{\mathrm{d}}}{N_{\mathrm{t}}} \mathrm{trace} \left\{ \underline{\mathbf{M}}^{\mathrm{H}} \, \underline{\mathbf{M}} \right\} \quad (17)$$

per data symbol. The estimate $\widehat{\underline{d}}_n$ of the transmitted data symbol $\underline{d}_n$ consists of the sum of a useful part

$$\underline{d}_{\mathrm{use},n} = \mathop{\mathrm{E}}_{\underline{\mathbf{d}},\underline{\mathbf{n}}} \left\{ \widehat{\underline{d}}_n \middle| \underline{d}_n \right\} = [\underline{\mathbf{D}}\,\underline{\mathbf{H}}\,\underline{\mathbf{M}}]_{n,n} \underline{d}_n, \quad (18)$$

of an interference part

$$\underline{d}_{\mathrm{int},n} = \left[\overline{\mathrm{diag}} \left(\underline{\mathbf{D}}\,\underline{\mathbf{H}}\,\underline{\mathbf{M}} \right) \underline{\mathbf{d}} \right]_n, \quad (19)$$

and of a noise part

$$\underline{d}_{\mathrm{noise},n} = [\underline{\mathbf{D}}\,\underline{\mathbf{n}}]_n, \quad (20)$$

see also [15]. In (19) and (20) the terms in brackets are column vectors. To evaluate the impact of the interference part $\underline{d}_{\mathrm{int},n}$ of (19) and of the noise part $\underline{d}_{\mathrm{noise},n}$ of (20) on the data estimate $\widehat{\underline{d}}_n$, the estimation error

$$\begin{aligned} \underline{\boldsymbol{\varepsilon}} &= \widehat{\underline{\mathbf{d}}} - \left(\underline{d}_{\mathrm{use},1} \ldots \underline{d}_{\mathrm{use},N_{\mathrm{t}}} \right)^{\mathrm{T}} = \widehat{\underline{\mathbf{d}}} - \mathrm{diag} \left(\underline{\mathbf{D}}\,\underline{\mathbf{H}}\,\underline{\mathbf{M}} \right) \underline{\mathbf{d}} \\ &= \overline{\mathrm{diag}} \left(\underline{\mathbf{D}}\,\underline{\mathbf{H}}\,\underline{\mathbf{M}} \right) \underline{\mathbf{d}} + \underline{\mathbf{D}}\,\underline{\mathbf{n}} \end{aligned} \quad (21)$$

is considered. $\underline{\mathbf{d}}$ of (2) and $\underline{\mathbf{n}}$ of (10) are random vectors with the above explained statistical properties, c.f. (4) and (12). Therefore, $\underline{\boldsymbol{\varepsilon}}$ of (21) is also a random vector. Setting out from (4) and (12), $\underline{\boldsymbol{\varepsilon}}$ has zero-mean and the covariance matrix

$$\begin{aligned} &\underline{\mathbf{R}}_{\varepsilon} = \mathop{\mathrm{E}}_{\underline{\mathbf{d}},\underline{\mathbf{n}}} \left\{ \underline{\boldsymbol{\varepsilon}}\,\underline{\boldsymbol{\varepsilon}}^{\mathrm{H}} \right\} \\ &= \underbrace{\left[\overline{\mathrm{diag}} \left(\underline{\mathbf{D}}\,\underline{\mathbf{H}}\,\underline{\mathbf{M}} \right) \left(\overline{\mathrm{diag}} \left(\underline{\mathbf{D}}\,\underline{\mathbf{H}}\,\underline{\mathbf{M}} \right) \right)^{\mathrm{H}} \right] E_{\mathrm{d}}}_{\text{interference}} + \underbrace{\underline{\mathbf{D}}\,\underline{\mathbf{R}}_{\mathrm{n}}\,\underline{\mathbf{D}}^{\mathrm{H}}}_{\text{noise}}. \end{aligned} \quad (22)$$

A quality measure for the estimates $\widehat{\underline{d}}_n$ of (13) are the signal-to-noise-plus-interference-ratios (SNIR) $\gamma_{\mathrm{o},n}$ which are based on $\underline{\mathbf{R}}_{\varepsilon}$ of (22) [15]. With (4), (12), (18), (19), (20) and (22) we obtain

$$\begin{aligned} \gamma_{\mathrm{o},n} &= \frac{\mathop{\mathrm{E}}_{\underline{\mathbf{d}},\underline{\mathbf{n}}} \left\{ \left| \underline{d}_{\mathrm{use},n} \right|^2 \right\}}{\mathop{\mathrm{E}}_{\underline{\mathbf{d}},\underline{\mathbf{n}}} \left\{ \left| \underline{d}_{\mathrm{noise},n} \right|^2 \right\} + \mathop{\mathrm{E}}_{\underline{\mathbf{d}},\underline{\mathbf{n}}} \left\{ \left| \underline{d}_{\mathrm{int},n} \right|^2 \right\}} = \frac{\left| [\underline{\mathbf{D}}\,\underline{\mathbf{H}}\,\underline{\mathbf{M}}]_{n,n} \right|^2 E_{\mathrm{d}}}{[\underline{\mathbf{R}}_{\varepsilon}]_{n,n}} \\ &= \frac{\left| [\underline{\mathbf{D}}\,\underline{\mathbf{H}}\,\underline{\mathbf{M}}]_{n,n} \right|^2 E_{\mathrm{d}}}{\left[\underline{\mathbf{D}}\,\underline{\mathbf{R}}_{\mathrm{n}}\,\underline{\mathbf{D}}^{\mathrm{H}} \right]_{n,n} + \left\| \left[\overline{\mathrm{diag}} \left(\underline{\mathbf{D}}\,\underline{\mathbf{H}}\,\underline{\mathbf{M}} \right) \right]_n \right\|^2 E_{\mathrm{d}}}. \end{aligned} \quad (23)$$

3 Receiver oriented transmission

3.1 Fundamentals

As already mentioned in Section 1, in Rx oriented transmission the receiver algorithms, i.e., the MT specific demodulator mactrices $\underline{\mathbf{D}}^{(k)}$, $k=1\ldots K$, of (13) and, therefore, the total demodulator matrix $\underline{\mathbf{D}}$ of (14) are *a priori* chosen. On the other hand, the transmitter algorithms, i.e., the modulator matrix $\underline{\mathbf{M}}$ of (6), is *a posteriori* adapted under consideration of these demodulator matrices and channel information, here represented by the channel matrix $\underline{\mathbf{H}}$ of (10). Approaches meanwhile quite well known to determine $\underline{\mathbf{M}}$ based on the knowledge of $\underline{\mathbf{H}}$ and $\underline{\mathbf{D}}$ are the Transmit Matched Filter (TxMF) [1], [5] – also known as pre-rake [16], [17] – and the Transmit Zero Forcer (TxZF) [1], [2], [5]. Other options for Rx orientation are various kinds of Transmit Minimum Mean Square Error Modulators (TxMMSE) as, e.g., published in [5]. In the present paper only the TxZF should be considered, because this choice for the modulator $\underline{\mathbf{M}}$ is especially favorable if high Signal-to-Noise-Ratios (SNRs) at the input of the MTs are considered and results in a lower complexity than the TxMMSE [5].

3.2 Performance analysis of the Transmit Zero Forcer

For the TxZF the modulator matrix is *a posteriori* determined as follows [1]:

$$\underline{\mathbf{M}} = (\underline{\mathbf{D}}\,\underline{\mathbf{H}})^{\mathrm{H}} \underbrace{\left[\underline{\mathbf{D}}\,\underline{\mathbf{H}} \left(\underline{\mathbf{D}}\,\underline{\mathbf{H}} \right)^{\mathrm{H}} \right]}_{\underline{\mathbf{R}}_{\mathrm{B}}}^{-1}. \quad (24)$$

If $\underline{\mathbf{M}}$ is chosen according to (24) the data transmission is unbiased, i.e.,

$$[\underline{\mathbf{D}}\,\underline{\mathbf{H}}\,\underline{\mathbf{M}}]_{n,n} = 1, \forall n, n=1\ldots N_{\mathrm{t}}, \quad (25)$$

holds. Setting out from (24) and still having in mind that we assume that both $\underline{\mathbf{H}}$ and $\underline{\mathbf{D}}$ are perfectly known at the transmitter, the basic behaviour of Rx oriented data transmission using TxZF can be studied by taking a two-step procedure: In a first step, the quality of the data estimate $\widehat{\underline{\mathbf{d}}}$ of (14) described by the covariance matrix $\underline{\mathbf{R}}_{\varepsilon}$ of (22) of the estimation error $\underline{\boldsymbol{\varepsilon}}$ of (21) has to be studied. In a second step the mean symbol specific transmit energies T_n, $n = 1\ldots N_{\mathrm{t}}$, of (16) have to be considered. With (24), (22) yields

$$\underline{\mathbf{R}}_{\varepsilon} = \underline{\mathbf{D}}\,\underline{\mathbf{R}}_{\mathrm{n}} \underline{\mathbf{D}}^{\mathrm{H}}, \quad (26)$$

i.e., the interference term in (22) vanishes. Substituting (25) and (26) in (23), the SNIR $\gamma_{\mathrm{o},n}$ obtained, if TxZF is applied, reads

$$\gamma_{\mathrm{o},n} = \frac{E_{\mathrm{d}}}{\left[\underline{\mathbf{D}}\,\underline{\mathbf{R}}_{\mathrm{n}}\,\underline{\mathbf{D}}^{\mathrm{H}} \right]_{n,n}}. \quad (27)$$

(27) allows the following conclusions:

- Changes of the channel matrix $\underline{\mathbf{H}}$ have no influence on $\gamma_{\mathrm{o},n}$ of (27) as long as (24) is fulfilled and $\underline{\mathbf{D}}$, E_d and $\underline{\mathbf{R}}_\mathrm{n}$ are kept constant.
- $\gamma_{\mathrm{o},n}$ is proportional to E_d.
- Noise is the only performance limiting effect.
- Scaling the n-th row of the demodulator matrix $\underline{\mathbf{D}}$ by a factor β results in multiplying $\gamma_{\mathrm{o},n}$ by a factor of $1/\beta^2$.
- For fixed $\underline{\mathbf{D}}$, E_d, $\underline{\mathbf{R}}_\mathrm{n}$ and under the requirement of unbiased data transmission, c.f. (25), the TxZF maximizes $\gamma_{\mathrm{o},n}$, $n = 1 \ldots N_\mathrm{t}$. The reason for this behaviour is that the TxZF totally eliminates interference [1].

Reflecting the observations made above, one may get the impression that TxZF always shows an optimum behaviour with respect to $\gamma_{\mathrm{o},n}$ of (27) and the constrains mentioned in the last of the above items. This conclusion is correct. However, the price to be paid to achieve this goal has to be kept in mind: the mean symbol specific transmit energies T_n, $n = 1 \ldots N_\mathrm{t}$, of (16) may get very large. Therefore, in the following these mean symbol specific transmit energies T_n, $n=1 \ldots N_\mathrm{t}$, are studied to clarify the influence of $\underline{\mathbf{D}}$ and $\underline{\mathbf{H}}$ on T_n. Substituting (24) in (16) yields [3]

$$T_n = \left[\underline{\mathbf{R}}_\mathrm{B}^{-1}\right]_{n,n} E_\mathrm{d}, n=1 \ldots N_\mathrm{t}. \tag{28}$$

One observes that the mean symbol specific transmit energies T_n, $n = 1 \ldots N_\mathrm{t}$, depend on the scaling of $\underline{\mathbf{H}}$ and $\underline{\mathbf{D}}$. If, e.g., the absolute values of all components of $\underline{\mathbf{H}}$ or, equivalently, all components in the n-th row of $\underline{\mathbf{D}}$ are scaled by a factor β, then T_n is multiplied by $1/\beta^2$. Therefore, even if $\gamma_{\mathrm{o},n}$ of (27) does not depend on $\underline{\mathbf{H}}$, T_n of (28) massively changes if $\underline{\mathbf{H}}$ is changed. Consequently, to fairly assess the quality of the data estimate $\widehat{\underline{\mathbf{d}}}$ in a Rx oriented data transmission system E_d in (27) has to be expressed as a function of T_n leading to

$$\gamma_{\mathrm{o},n} = \frac{T_n}{\left[\underline{\mathbf{R}}_\mathrm{B}^{-1}\right]_{n,n} \left[\underline{\mathbf{D}}\,\underline{\mathbf{R}}_\mathrm{n}\,\underline{\mathbf{D}}^\mathrm{H}\right]_{n,n}}. \tag{29}$$

The above theory is valid under the implicit understanding that the matrices to be inverted in (24), (28) and (29) are non-singular. This condition is usually fulfilled, if K_B is not smaller than N_t and the considered system is reasonably designed.

In the special case of QPSK symbol modulation the above described observation allows to find a closed analytical expression for the bit error probability of the two bits being carried by data symbol $\underline{d}_n$. As shown above, in the case of the TxZF the only disturbing component of $\widehat{\underline{d}}_n$ is $\underline{d}_{\mathrm{noise},n}$. $\underline{d}_{\mathrm{noise},n}$ satisfies a Gaussian distribution. Therefore, the bit error probability of the two bits combined in data symbol $\underline{d}_n$ becomes [18]

$$P_{\mathrm{b},n} = \frac{1}{2}\mathrm{erfc}\left(\sqrt{\frac{T_n}{2\left[\underline{\mathbf{R}}_\mathrm{B}^{-1}\right]_{n,n} \left[\underline{\mathbf{D}}\,\underline{\mathbf{R}}_\mathrm{n}\,\underline{\mathbf{D}}^\mathrm{H}\right]_{n,n}}}\right). \tag{30}$$

It should be stressed that the conventional way of assessing the performance of communication systems based on the bit error probability $P_{\mathrm{b},n}$, $n=1 \ldots N_\mathrm{t}$, as a function of the ratio of received energy per bit and noise power spectral density is not suitable when considering Rx oriented data transmission. This is true, because, when studying Rx oriented data transmission, not only the performance degrading impact of noise but also the invested mean symbol specific transmit energies T_n, $n=1 \ldots N_\mathrm{t}$, have to be taken into account. Therefore, $P_{\mathrm{b},n}$ is considered as a function of T_n in (30). (30) allows a tradeoff between the invested mean symbol specific transmit energy T_n of (28) and the resulting bit error probability $P_{\mathrm{b},n}$. In the special case of white additive Gaussian noise, i.e., if

$$\underline{\mathbf{R}}_\mathrm{n} = \sigma^2 \mathbf{I}^{(KK_\mathrm{M})} \tag{31}$$

holds, a fair evalution of Rx oriented data transmission systems can be done by analyzing the bit error probability $P_{\mathrm{b},n}$ as a function of the ratio

$$\gamma_{\mathrm{i},n} = \frac{T_n}{\sigma^2} \tag{32}$$

of the mean symbol specific transmit energy T_n, $n = 1 \ldots N_\mathrm{t}$, and the noise variance σ^2. $\gamma_{\mathrm{i},n}$ of (32) is termed pseudo-SNR of data symbol $\underline{d}_n$, $n = 1 \ldots N_\mathrm{t}$. With $\gamma_{\mathrm{i},n}$ of (32) for the SNIR $\gamma_{\mathrm{o},n}$ of (29) follows

$$\gamma_{\mathrm{o},n} = \frac{\gamma_{\mathrm{i},n}}{\left[\underline{\mathbf{R}}_\mathrm{B}^{-1}\right]_{n,n} \left[\underline{\mathbf{D}}\,\underline{\mathbf{D}}^\mathrm{H}\right]_{n,n}}, \tag{33}$$

which allows to further simplify (30) to

$$P_{\mathrm{b},n} = \frac{1}{2}\mathrm{erfc}\left(\sqrt{\frac{\gamma_{\mathrm{i},n}}{2\left[\underline{\mathbf{R}}_\mathrm{B}^{-1}\right]_{n,n} \left[\underline{\mathbf{D}}\,\underline{\mathbf{D}}^\mathrm{H}\right]_{n,n}}}\right) \tag{34}$$

4 Influence of imperfect channel knowledge on the transmission performance

4.1 Model and assumptions

In Section 3 the basics of Rx oriented data transmission are recapitulated with special emphasis on the TxZF. Up to now, it was assumed that the transmitter has perfect knowledge of the demodulator matrix $\underline{\mathbf{D}}$ and of the channel matrix $\underline{\mathbf{H}}$, while *a posteriori* adapting the modulator matrix $\underline{\mathbf{M}}$. Unfortunately, in real-world data transmission systems channel knowledge is not *a priori* available but has to be obtained by channel estimation algorithms [6], [7]. As a consequence of this, usually not $\underline{\mathbf{H}}$ but a more or less accurate estimate $\widehat{\underline{\mathbf{H}}}$ of $\underline{\mathbf{H}}$ is available at the transmitter. In this section the performance degradation is analyzed which results by using $\widehat{\underline{\mathbf{H}}}$ instead of $\underline{\mathbf{H}}$ when *a posteriori* adjusting $\underline{\mathbf{M}}$ in the transmitter.

Generally, the channel matrix estimate $\widehat{\underline{\mathbf{H}}}$ can be considered as the sum of the true channel matrix $\underline{\mathbf{H}}$ and the channel estimation error matrix

$$\underline{\mathbf{E}} = \left(\underline{E}_{i,j}\right), i = 1\ldots KK_{\mathrm{M}}, j = 1\ldots K_{\mathrm{B}}, \tag{35}$$

that is

$$\widehat{\underline{\mathbf{H}}} = \underline{\mathbf{H}} + \underline{\mathbf{E}}. \tag{36}$$

As the transmitter does not know the channel estimation error matrix $\underline{\mathbf{E}}$, the elements $\underline{E}_{i,j}$ of $\underline{\mathbf{E}}$ can only be treated as random variables. In the following it is assumed that these random variables $\underline{E}_{i,j}$

- are uncorrelated,
- have zero mean,
- have uncorrelated, identically distributed real and imaginary parts,
- are independent of $\underline{\mathbf{n}}$ and $\underline{\mathbf{d}}$, and
- are identically distributed.

Then, the second order statistical properties of the elements $\underline{E}_{i,j}$ of $\underline{\mathbf{E}}$ are totally described by the variance

$$\underset{\underline{\mathbf{E}}}{\mathrm{E}}\left\{\underline{E}_{i,j}\underline{E}_{i,j}^{*}\right\} = \sigma_{\mathrm{h}}^{2}, i = 1\ldots KK_{\mathrm{M}}, j = 1\ldots K_{\mathrm{B}}, \tag{37}$$

of the channel estimation errors $\underline{E}_{i,j}$. The above mentioned requirements are usually fulfilled, especially if pilot-aided joint channel estimation [7] is applied. Besides, in this situation, if the noise effective during channel estimation is Gaussian, the real and imaginary parts of $\underline{E}_{i,j}$ satisfy the same Gaussian probability distribution. In the following considerations this assumption will not be generally made, but only when explicitly stated.

4.2 Analytical performance evaluation

If $\widehat{\underline{\mathbf{H}}}$ of (36) is used to *a posteriori* adapt $\underline{\mathbf{M}}$ of (6), (24) has to be rewritten as

$$\widetilde{\underline{\mathbf{M}}} = \left(\underline{\mathbf{D}}\left(\underline{\mathbf{H}}+\underline{\mathbf{E}}\right)\right)^{\mathrm{H}}\left(\underline{\mathbf{D}}\left(\underline{\mathbf{H}}+\underline{\mathbf{E}}\right)\left(\underline{\mathbf{H}}+\underline{\mathbf{E}}\right)^{\mathrm{H}}\underline{\mathbf{D}}^{\mathrm{H}}\right)^{-1}. \tag{38}$$

The tilde used in (38) and other equations in the following indicates that the respective quantity goes back to the imperfect estimate $\widehat{\underline{\mathbf{H}}}$ of the channel matrix $\underline{\mathbf{H}}$. $\widetilde{\underline{\mathbf{M}}}$ of (38) can generally be represented by an infinite Taylor series around the development point

$$\underline{\mathbf{E}}_0 = \mathbf{0}. \tag{39}$$

Then,

$$\widetilde{\underline{\mathbf{M}}} = \left(\underline{\mathbf{D}}\,\underline{\mathbf{H}}\right)^{\mathrm{H}}\underline{\mathbf{R}}_{\mathrm{B}}^{-1} + \sum_{i=1}^{KK_{\mathrm{M}}}\sum_{j=1}^{K_{\mathrm{B}}}\left[\left.\frac{\partial\widetilde{\underline{\mathbf{M}}}}{\partial\mathrm{Re}\left\{\underline{E}_{i,j}\right\}}\right|_{\underline{\mathbf{E}}=\mathbf{0}}\mathrm{Re}\left\{\underline{E}_{i,j}\right\} + \left.\frac{\partial\widetilde{\underline{\mathbf{M}}}}{\partial\mathrm{Im}\left\{\underline{E}_{i,j}\right\}}\right|_{\underline{\mathbf{E}}=\mathbf{0}}\mathrm{Im}\left\{\underline{E}_{i,j}\right\}\right] + \mathcal{O}(\underline{\mathbf{E}}^{2}) \tag{40}$$

holds, where $\mathcal{O}(\underline{\mathbf{E}}^{2})$ denotes higher-order elements of the Taylor series. If we consider small channel estimation errors – and this has to be the case, because we are focusing on high SNRs at the input of the MTs and low bit error probabilities $P_{\mathrm{b},n}$ of (30), which can only be achieved if the channel estimation errors are small compared to the elements of $\underline{\mathbf{H}}$ –, i.e., if σ_{h}^{2} is small compared to the components of $\underline{\mathbf{H}}$, $\widetilde{\underline{\mathbf{M}}}$ can be well approximated by (40), even if the Taylor series is truncated after the linear terms, i.e.,

$$\widetilde{\underline{\mathbf{M}}} \approx \left(\underline{\mathbf{D}}\,\underline{\mathbf{H}}\right)^{\mathrm{H}}\underline{\mathbf{R}}_{\mathrm{B}}^{-1} + \sum_{i=1}^{KK_{\mathrm{M}}}\sum_{j=1}^{K_{\mathrm{B}}}\left[\left.\frac{\partial\widetilde{\underline{\mathbf{M}}}}{\partial\mathrm{Re}\left\{\underline{E}_{i,j}\right\}}\right|_{\underline{\mathbf{E}}=\mathbf{0}}\mathrm{Re}\left\{\underline{E}_{i,j}\right\} + \left.\frac{\partial\widetilde{\underline{\mathbf{M}}}}{\partial\mathrm{Im}\left\{\underline{E}_{i,j}\right\}}\right|_{\underline{\mathbf{E}}=\mathbf{0}}\mathrm{Im}\left\{\underline{E}_{i,j}\right\}\right]. \tag{41}$$

The calculation of the derivatives in (41) can be found in Appendix I. Using the results obtained there, (41) can be rewritten as

$$\widetilde{\underline{\mathbf{M}}} = \left(\underline{\mathbf{D}}\,\underline{\mathbf{H}}\right)^{\mathrm{H}}\underline{\mathbf{R}}_{\mathrm{B}}^{-1} + \underline{\mathbf{E}}^{\mathrm{H}}\underline{\mathbf{D}}^{\mathrm{H}}\underline{\mathbf{R}}_{\mathrm{B}}^{-1} - \left(\underline{\mathbf{D}}\,\underline{\mathbf{H}}\right)^{\mathrm{H}}\underline{\mathbf{R}}_{\mathrm{B}}^{-1}\left(\underline{\mathbf{D}}\,\underline{\mathbf{E}}\,\underline{\mathbf{H}}^{\mathrm{H}}\underline{\mathbf{D}}^{\mathrm{H}} + \underline{\mathbf{D}}\,\underline{\mathbf{H}}\,\underline{\mathbf{E}}^{\mathrm{H}}\underline{\mathbf{D}}^{\mathrm{H}}\right)\underline{\mathbf{R}}_{\mathrm{B}}^{-1}. \tag{42}$$

Using $\widetilde{\underline{\mathbf{M}}}$ of (42), the performance of the Rx oriented data transmission based on TxZF is studied in the following, in a way analog to the procedure in Subsection 3.2. With $\widetilde{\underline{\mathbf{M}}}$ of (42) one can calculate the estimate

$$\widetilde{\widehat{\underline{\mathbf{d}}}} = \underline{\mathbf{d}} - \underline{\mathbf{D}}\,\underline{\mathbf{E}}\,\underline{\mathbf{H}}^{\mathrm{H}}\,\underline{\mathbf{D}}^{\mathrm{H}}\underline{\mathbf{R}}_{\mathrm{B}}^{-1}\underline{\mathbf{d}} + \underline{\mathbf{D}}\,\underline{\mathbf{n}} \tag{43}$$

of (15), but now taking the imperfect channel knowledge into account. If $\underline{\mathbf{E}}$ and $\underline{\mathbf{n}}$ change randomly, but the data symbol $\underline{d}_n$ is fixed, then the estimate $\widetilde{\widehat{\underline{d}}}_n$ also changes randomly. (43) allows the conclusion that in this situation

$$\underset{\underline{\mathbf{E}},\underline{\mathbf{n}}}{\mathrm{E}}\left\{\widetilde{\widehat{\underline{d}}}_n\middle|\underline{d}_n\right\} = \underline{d}_n \tag{44}$$

holds. This means that even if the channel matrix $\underline{\mathbf{H}}$ is not perfectly known, the estimate $\widetilde{\widehat{\underline{d}}}_n$ of $\underline{d}_n$ is still unbiased, see the consideration in Subsection 3.2. Setting out from (43) and (44) the estimation error

$$\widetilde{\underline{\boldsymbol{\varepsilon}}} = \widetilde{\widehat{\underline{\mathbf{d}}}} - \underline{\mathbf{d}} = -\underline{\mathbf{D}}\,\underline{\mathbf{E}}\,\underline{\mathbf{H}}^{\mathrm{H}}\underline{\mathbf{D}}^{\mathrm{H}}\underline{\mathbf{R}}_{\mathrm{B}}^{-1}\underline{\mathbf{d}} + \underline{\mathbf{D}}\,\underline{\mathbf{n}}. \tag{45}$$

of (21) is recalculated. $\widetilde{\underline{\boldsymbol{\varepsilon}}}$ of (45) describes the estimation error, if

- not $\underline{\mathbf{H}}$ but $\widehat{\underline{\mathbf{H}}}$ is used at the transmitter and
- the noise $\underline{\mathbf{n}}$ is present at the input of the MTs.

With $\widetilde{\underline{\boldsymbol{\varepsilon}}}$ of (45)

$$\widetilde{\underline{\mathbf{R}}}_{\varepsilon} = \underbrace{\underline{\mathbf{D}}\,\underline{\mathbf{R}}_{\mathrm{n}}\underline{\mathbf{D}}^{\mathrm{H}}}_{\widetilde{\underline{\mathbf{R}}}_{\varepsilon,\mathrm{n}}} + \underbrace{\underline{\mathbf{D}}\,\underline{\mathbf{D}}^{\mathrm{H}}\cdot\sigma_{\mathrm{h}}^{2}E_{\mathrm{d}}\mathrm{trace}\left\{\underline{\mathbf{R}}_{\mathrm{B}}^{-1}\right\}}_{\widetilde{\underline{\mathbf{R}}}_{\varepsilon,\mathrm{i}}}. \tag{46}$$

follows for the covariance matrix $\widetilde{\underline{\mathbf{R}}}_{\varepsilon}$ of (22). The proof of (46) can be found in Appendix II. The result in (46) allows several conlusions:

- The estimation errors due to noise and imperfect channel knowledge are uncorrelated. Therefore, the covariance matrix $\widetilde{\underline{\mathbf{R}}}_{\varepsilon}$ is a superpostition of a partial matrix $\widetilde{\underline{\mathbf{R}}}_{\varepsilon,\mathrm{n}}$ related to noise and a partial matrix $\widetilde{\underline{\mathbf{R}}}_{\varepsilon,\mathrm{i}}$ related to imperfect channel knowledge.
- The partial matrix $\widetilde{\underline{\mathbf{R}}}_{\varepsilon,\mathrm{n}}$ is identical to $\underline{\mathbf{R}}_{\varepsilon}$ of (26) obtained in Section 3 for the case of perfect channel knowledge.

- The structure of the partial matrix $\widetilde{\underline{\mathbf{R}}}_{\varepsilon,\mathrm{i}}$ is only determined by the structure of the demodulator matrix $\underline{\mathbf{D}}$ of (14).
- $\widetilde{\underline{\mathbf{R}}}_{\varepsilon,\mathrm{i}}$ is proportional to σ_{h}^2 of (37) and E_{d} of (4). Therefore, the lower the accuracy of $\widehat{\underline{\mathbf{H}}}$, the larger the absolute values of the elements of $\widetilde{\underline{\mathbf{R}}}_{\varepsilon,\mathrm{i}}$.
- The scaling of $\widetilde{\underline{\mathbf{R}}}_{\varepsilon,\mathrm{i}}$ not only depends on the statistical properties of the channel estimation error matrix $\underline{\mathbf{E}}$, but also on the channel under consideration itself.

To describe the quality of the obtained estimate $\widetilde{\widehat{\underline{\mathbf{d}}}}$ of (43) in a concise form, one can resort to the SNIR $\widetilde{\gamma}_{\mathrm{o},n}$ of (23). Using (44) and (46), (23) yields

$$\widetilde{\gamma}_{\mathrm{o},n} = \frac{E_{\mathrm{d}}}{\left[\underline{\mathbf{D}}\,\underline{\mathbf{R}}_{\mathrm{n}}\,\underline{\mathbf{D}}^{\mathrm{H}}\right]_{n,n} + \left[\underline{\mathbf{D}}\,\underline{\mathbf{D}}^{\mathrm{H}}\right]_{n,n} \cdot \sigma_{\mathrm{h}}^2 E_{\mathrm{d}} \mathrm{trace}\left\{\underline{\mathbf{R}}_{\mathrm{B}}^{-1}\right\}}. \tag{47}$$

In analogy to the procedure in Subsection 3.2, the mean symbol specific transmit energies T_n, $n=1\dots N_{\mathrm{t}}$, of (16) are studied in the following. Having in mind that we are now considering the case of imperfect channel knowledge, where an additional random quantity $\underline{\mathbf{E}}$ comes into the play, the definition of the mean symbol specific transmit energy T_n, $n=1\dots N_{\mathrm{t}}$, of (16) has to be thought about again: $\widetilde{\underline{\mathbf{M}}}$ is a function of $\underline{\mathbf{E}}$. Therefore, according to (16), T_n would also be a function of $\underline{\mathbf{E}}$ and, consequently, a random variable with a certain distribution. In the following we are only interested in the expectation

$$\widetilde{T}_n = E_{\mathrm{d}} \underset{\underline{\mathbf{E}}}{\mathrm{E}}\left\{\left[\widetilde{\underline{\mathbf{M}}}^{\mathrm{H}}\widetilde{\underline{\mathbf{M}}}\right]_{n,n}\right\} = E_{\mathrm{d}}\left[\underset{\underline{\mathbf{E}}}{\mathrm{E}}\left\{\widetilde{\underline{\mathbf{M}}}^{\mathrm{H}}\widetilde{\underline{\mathbf{M}}}\right\}\right]_{n,n} \tag{48}$$

of this random variable which, for reasons of simplicity, is referred to as mean symbol transmit energy $\widetilde{T}_n$ in the following. Using $\widetilde{\underline{\mathbf{M}}}$ of (42) and the definition of $\widetilde{T}_n$ of (48) one obtains after some calculations detailed in Appendix III

$$\begin{aligned}\widetilde{T}_n = {} & \left[\underline{\mathbf{R}}_{\mathrm{B}}^{-1}\right]_{n,n}\left[1+\sigma_{\mathrm{h}}^2 \mathrm{trace}\left\{\underline{\mathbf{R}}_{\mathrm{B}}^{-1}\underline{\mathbf{D}}\,\underline{\mathbf{D}}^{\mathrm{H}}\right\}\right] E_{\mathrm{d}} \\ & + \left[\underline{\mathbf{R}}_{\mathrm{B}}^{-1}\underline{\mathbf{D}}\,\underline{\mathbf{D}}^{\mathrm{H}}\underline{\mathbf{R}}_{\mathrm{B}}^{-1}\right]_{n,n} \cdot \sigma_{\mathrm{h}}^2 (K_{\mathrm{B}}-N_{\mathrm{t}}) E_{\mathrm{d}}. \end{aligned} \tag{49}$$

Comparing T_n of (28) and $\widetilde{T}_n$ of (49) the ratio

$$\begin{aligned}\widetilde{T}_n/T_n = {} & 1+\sigma_{\mathrm{h}}^2 \mathrm{trace}\left\{\underline{\mathbf{R}}_{\mathrm{B}}^{-1}\underline{\mathbf{D}}\,\underline{\mathbf{D}}^{\mathrm{H}}\right\} \\ & + \frac{\left[\underline{\mathbf{R}}_{\mathrm{B}}^{-1}\underline{\mathbf{D}}\,\underline{\mathbf{D}}^{\mathrm{H}}\underline{\mathbf{R}}_{\mathrm{B}}^{-1}\right]_{n,n}}{\left[\underline{\mathbf{R}}_{\mathrm{B}}^{-1}\right]_{n,n}} \cdot \sigma_{\mathrm{h}}^2 (K_{\mathrm{B}}-N_{\mathrm{t}}) \end{aligned} \tag{50}$$

can be introduced, which describes the extent to which the mean symbol specific transmit energy T_n is influenced, when coming from the case of perfect channel knownledge to the case of imperfect channel knowledge at the transmitter. (50) allows some quite interesting conclusions:

- $\widetilde{T}_n/T_n$ is always larger than or equal to one. Therefore, – if the assumptions for $\underline{\mathbf{E}}$ made in Subsection 4.1 hold and if unbiased TxZF based data transmission is considered – in the case of imperfect channel knowledge always higher mean symbol specific transmit energies $\widetilde{T}_n$, $n=1\dots N_{\mathrm{t}}$, are needed than in the case of perfect channel knowledge.
- The relative increase $\widetilde{T}_n/T_n-1$ is proportional to the variance σ_{h}^2 of the elements of the channel estimation error matrix $\underline{\mathbf{E}}$ of (35).
- The considered channel matrix $\underline{\mathbf{H}}$ and the chosen demodulator matrix $\underline{\mathbf{D}}$ have an influence on the relative increase $\widetilde{T}_n/T_n-1$.

A question still open is the interdependence between the mean symbol specific transmit energy $\widetilde{T}_n$ of (49) and the quality of the estimate $\widetilde{\widehat{\underline{\mathbf{d}}}}$ of (43). To describe this quality, the SNIR $\widetilde{\gamma}_{\mathrm{o},n}$ of (47) is an appropriate measure. Using (49) to substitute E_{d} in (47), the SNIR $\widetilde{\gamma}_{\mathrm{o},n}$ of (47) reads

$$\begin{aligned}\widetilde{\gamma}_{\mathrm{o},n} = {} & \widetilde{T}_n \Big/ \Bigg(\left[\underline{\mathbf{D}}\,\underline{\mathbf{R}}_{\mathrm{n}}\,\underline{\mathbf{D}}^{\mathrm{H}}\right]_{n,n}\Bigg(\left[\underline{\mathbf{R}}_{\mathrm{B}}^{-1}\right]_{n,n} \\ & \cdot\left[1+\sigma_{\mathrm{h}}^2 \mathrm{trace}\left\{\underline{\mathbf{R}}_{\mathrm{B}}^{-1}\underline{\mathbf{D}}\,\underline{\mathbf{D}}^{\mathrm{H}}\right\}\right] + \left[\underline{\mathbf{R}}_{\mathrm{B}}^{-1}\underline{\mathbf{D}}\,\underline{\mathbf{D}}^{\mathrm{H}}\underline{\mathbf{R}}_{\mathrm{B}}^{-1}\right]_{n,n} \\ & \cdot\sigma_{\mathrm{h}}^2 (K_{\mathrm{B}}-N_{\mathrm{t}})\Bigg) + \left[\underline{\mathbf{D}}\,\underline{\mathbf{D}}^{\mathrm{H}}\right]_{n,n}\sigma_{\mathrm{h}}^2 \widetilde{T}_n \mathrm{trace}\left\{\underline{\mathbf{R}}_{\mathrm{B}}^{-1}\right\}\Bigg). \end{aligned} \tag{51}$$

(51) shows an important difference to $\gamma_{\mathrm{o},n}$ of (27) obtained for the case of perfect channel knowledge: even if $\widetilde{T}_n$ is very large – or mathematically speaking if $\widetilde{T}_n$ goes towards infinity –, $\widetilde{\gamma}_{\mathrm{o},n}$ of (51) is limited by the upper bound

$$\widetilde{\gamma}_{\mathrm{o},n}^{\infty} = \lim_{\widetilde{T}_n\to\infty}\widetilde{\gamma}_{\mathrm{o},n} = \frac{1}{\left[\underline{\mathbf{D}}\,\underline{\mathbf{D}}^{\mathrm{H}}\right]_{n,n}\sigma_{\mathrm{h}}^2 \mathrm{trace}\left\{\underline{\mathbf{R}}_{\mathrm{B}}^{-1}\right\}}. \tag{52}$$

$\widetilde{\gamma}_{\mathrm{o},n}^{\infty}$ of (52) depends on the variance σ_{h}^2 of the elements $\underline{E}_{i,j}$ of $\underline{\mathbf{E}}$ – and, therefore, the quality of the estimate $\widehat{\underline{\mathbf{H}}}$ of the channel matrix $\underline{\mathbf{H}}$ –, on the channel matrix $\underline{\mathbf{H}}$ itself and on the demodulator matrix $\underline{\mathbf{D}}$. If we further assume that the elements $\underline{E}_{i,j}$ of $\underline{\mathbf{E}}$ satisfy a Gaussian probability distribution – and this is the case if joint channel estimation in the sense of Subsection 4.1 is applied to obtain $\widehat{\underline{\mathbf{H}}}$ –, then based on (51) the bit error probability can be analyzed in a closed form. For reasons of simplicity we consider again the case of QPSK symbol modulation introduced in Subsection 3.2. With the above mentioned assumptions the elements of the estimation error $\widetilde{\underline{\boldsymbol{\varepsilon}}}$ of (45) satisfy a Gaussian probability distribution. Consequently, the bit error probability $\widetilde{P}_{\mathrm{b},n}$ of the bits carried by the data symbol $\underline{d}_n$, $n=1\dots N_{\mathrm{t}}$, can be immediately calculated using (51) to be

$$\widetilde{P}_{\mathrm{b},n} = \frac{1}{2}\mathrm{erfc}\left(\sqrt{\frac{\widetilde{\gamma}_{\mathrm{o},n}}{2}}\right). \tag{53}$$

With the observation that $\widetilde{\gamma}_{\mathrm{o},n}$ is limited by the upper bound $\widetilde{\gamma}_{\mathrm{o},n}^{\infty}$ of (52), $\widetilde{P}_{\mathrm{b},n}$ is lower bounded by the minimum bit error probability

$$\widetilde{P}_{\mathrm{b},n}^{\infty} = \lim_{\widetilde{T}_n\to\infty}\widetilde{P}_{\mathrm{b},n} = \frac{1}{2}\mathrm{erfc}\left(\sqrt{\frac{1}{2\left[\underline{\mathbf{D}}\,\underline{\mathbf{D}}^{\mathrm{H}}\right]_{n,n}\sigma_{\mathrm{h}}^2 \mathrm{trace}\left\{\underline{\mathbf{R}}_{\mathrm{B}}^{-1}\right\}}}\right). \tag{54}$$

For high $\widetilde{T}_n$, $\widetilde{P}_{\mathrm{b},n}$ converges towards the lower bound $\widetilde{P}_{\mathrm{b},n}^{\infty}$ of (54) resulting in an error-floor. This observation is well known and understood for Tx oriented data transmission [6], [7], but still not analytically studied for Rx oriented data transmission. (53) and (54) are the first available analytical answers to this question raised in Section 1.

For the special case of white Gaussian noise $\underline{\mathbf{n}}$, which is already considered in Subsection 3.2, c.f. (31), and with the pseudo-SNR

$$\widetilde{\gamma}_{\mathrm{i},n} = \frac{\widetilde{T}_n}{\sigma^2}, \tag{55}$$

which is related to $\gamma_{\mathrm{i},n}$ of (32), but which takes the mean symbol specific transmit energy $\widetilde{T}_n$ of (48) into account, $\widetilde{P}_{\mathrm{b},n}$ of (53) reads

$$\widetilde{P}_{\mathrm{b},n} = \frac{1}{2}\mathrm{erfc}\Bigg(\bigg(\widetilde{\gamma}_{\mathrm{i},n} \Big/ \Big(2\left[\underline{\mathbf{D}}\,\underline{\mathbf{D}}^{\mathrm{H}}\right]_{n,n}\Big(\left[\underline{\mathbf{R}}_{\mathrm{B}}^{-1}\right]_{n,n} \cdot \left[1+\sigma_{\mathrm{h}}^2\,\mathrm{trace}\left\{\underline{\mathbf{R}}_{\mathrm{B}}^{-1}\underline{\mathbf{D}}\,\underline{\mathbf{D}}^{\mathrm{H}}\right\}\right] + \left[\underline{\mathbf{R}}_{\mathrm{B}}^{-1}\underline{\mathbf{D}}\,\underline{\mathbf{D}}^{\mathrm{H}}\underline{\mathbf{R}}_{\mathrm{B}}^{-1}\right]_{n,n} \cdot \sigma_{\mathrm{h}}^2(K_{\mathrm{B}}-N_{\mathrm{t}})\Big) + 2\left[\underline{\mathbf{D}}\,\underline{\mathbf{D}}^{\mathrm{H}}\right]_{n,n}\sigma_{\mathrm{h}}^2\widetilde{\gamma}_{\mathrm{i},n}\,\mathrm{trace}\left\{\underline{\mathbf{R}}_{\mathrm{B}}^{-1}\right\}\Big)\bigg)^{\frac{1}{2}}\Bigg). \tag{56}$$

Comparing (34) and (56) the degradation due to the imperfect knowledge of $\underline{\mathbf{H}}$ at the transmitter can be quantified: To achieve a certain bit error probability

$$P_{\mathrm{b},n} = \widetilde{P}_{\mathrm{b},n} \tag{57}$$

in a situation with a fixed channel matrix $\underline{\mathbf{H}}$ and fixed demodulator matrix $\underline{\mathbf{D}}$, on the one hand in the case of perfect channel knowledge and, on the other hand, in the case of imperfect channel knowledge, respectively, in general different pseudo-SNRs $\gamma_{\mathrm{i},n}$ and $\widetilde{\gamma}_{\mathrm{i},n}$, respectively, are required. By equating (34) and (56) it follows that in both cases the same bit error probability is obtained if

$$\widetilde{\gamma}_{\mathrm{i},n} = \Bigg(\left[\underline{\mathbf{R}}_{\mathrm{B}}^{-1}\right]_{n,n}\left[1+\sigma_{\mathrm{h}}^2\,\mathrm{trace}\left\{\underline{\mathbf{R}}_{\mathrm{B}}^{-1}\underline{\mathbf{D}}\,\underline{\mathbf{D}}^{\mathrm{H}}\right\}\right] + \left[\underline{\mathbf{R}}_{\mathrm{B}}^{-1}\underline{\mathbf{D}}\,\underline{\mathbf{D}}^{\mathrm{H}}\underline{\mathbf{R}}_{\mathrm{B}}^{-1}\right]_{n,n}\sigma_{\mathrm{h}}^2(K_{\mathrm{B}}-N_{\mathrm{t}})\Bigg)\gamma_{\mathrm{i},n} \Bigg/ \Bigg(\left[\underline{\mathbf{R}}_{\mathrm{B}}^{-1}\right]_{n,n} - \sigma_{\mathrm{h}}^2\gamma_{\mathrm{i},n}\,\mathrm{trace}\left\{\underline{\mathbf{R}}_{\mathrm{B}}^{-1}\right\}\Bigg) \tag{58}$$

is chosen. (58) allows several conclusions:

- $\widetilde{\gamma}_{\mathrm{i},n}$ of (58) is always larger than $\gamma_{\mathrm{i},n}$. Therefore, as expected, imperfect channel knowledge can only lead to a degraded transmission quality or, equivalently, to an increased necessary pseudo-SNR $\widetilde{\gamma}_{\mathrm{i},n}$.
- Only if the denominator in (58) is positive, i.e., if

$$\frac{\left[\underline{\mathbf{R}}_{\mathrm{B}}^{-1}\right]_{n,n}}{\mathrm{trace}\left\{\underline{\mathbf{R}}_{\mathrm{B}}^{-1}\right\}} > \sigma_{\mathrm{h}}^2\gamma_{\mathrm{i},n} \tag{59}$$

holds, a pseudo-SNR $\widetilde{\gamma}_{\mathrm{i},n}$ can be found which leads in the case of imperfect channel knowledge to the same bit error probability as the pseudo-SNR $\gamma_{\mathrm{i},n}$ in the case of perfectly known channel matrix $\underline{\mathbf{H}}$.

The relation (58) can be considered as one of the central results of this paper. Because – setting out from an Rx oriented transmission system where perfect channel knowledge is available and a certain $\gamma_{\mathrm{i},n}$ is utilized – this relation directly allows to calculate which increased $\widetilde{\gamma}_{\mathrm{i},n}$ has to be invested to achieve the same transmission performance. Therefore, (58) quantifies the price to be paid due to the imperfect channel knowledge – and this is the answer to one of the central questions posed in this contribution.

5 Exemplary numerical results

In Section 4 basic relations between the performance of TxZF based Rx oriented transmission and imperfect channel knowledge at the transmitter have been worked out. These results are quite general and – as long as the assumptions described in Section 4 hold – are valid for all kinds of channels. In the further study these analytical results should be briefly illustrated and validated by some simulations. Therefore in the following a very simple exemplary scenario is considered. We look at the situation, where we have K_{B} equal to N_{t} transmit antennas at the AP, in total N_{t} data symbols are transmitted and altogether the K MTs are equipped with N_{t} receive antennas. The demodulator matrix $\underline{\mathbf{D}}$ is chosen to be the identity matrix. The total noise signal $\underline{\mathbf{n}}$ of (10) over all receive antennas of the K MTs is assumed to be white with the covariance matrix

$$\underline{\mathbf{R}}_{\mathrm{n}} = \sigma^2\mathbf{I}^{(N_{\mathrm{t}})} \tag{60}$$

of (12). The channel matrix $\underline{\mathbf{H}}$ is chosen according to the very simple parametric ρ-model introduced in [7] for basic

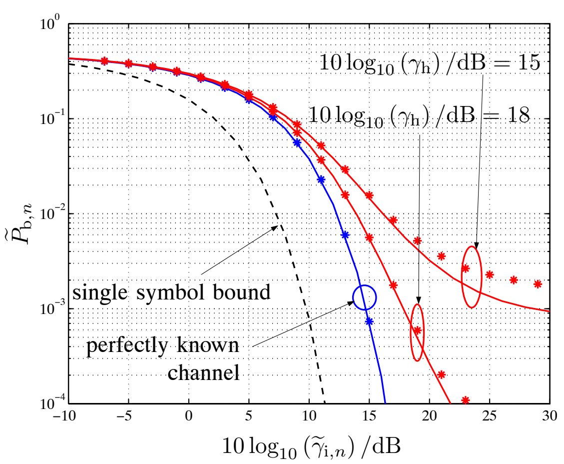

Fig. 1. $\widetilde{P}_{\mathrm{b},n}$ versus $\widetilde{\gamma}_{\mathrm{i},n}$ for $N_{\mathrm{t}} = 4$ and $x = 0.4$; comparison between simulation results ($*$) and analytical results (—)

studies, i.e.,

$$\underline{\mathbf{H}} = \frac{1}{\sqrt{1+(N_\mathrm{t}-1)x^2}} \begin{pmatrix} 1 & x & \dots & x \\ x & \ddots & \ddots & \vdots \\ \vdots & \ddots & \ddots & x \\ x & \dots & x & 1 \end{pmatrix}, x \in [-1 \dots 1[. \tag{61}$$

It is well known that $\underline{\mathbf{H}}$ of (61) massively differs from channel matrices describing real-world channels. However, the authors have the opinion that using such a simple model, which allows to analyze both channels with severe cross-talk –, i.e., $|x|$ is close to one – and without cross-talk –, i.e., x equal to zero – is favorable for basic studies. To describe the quality of the estimate $\underline{\widehat{\mathbf{H}}}$ of (36) the average signal-to-noise-ratio

$$\gamma_\mathrm{h} = \frac{1}{N_\mathrm{t}\sigma_\mathrm{h}^2} \tag{62}$$

of the individual elements of $\underline{\widehat{\mathbf{H}}}$ is introduced. Fig. 1 shows the analytical results for the bit error probability $\widetilde{P}_{\mathrm{b},n}$ of (56) and results obtained by simulation based on (38).

As can be seen from Fig. 1 the simulation results match quite well with the analytical results using the Taylor approximation. Although the above described example is quite simple, it can be expected that – as long as the assumptions described in Section 4 hold – this observation can be verified in more complex scenarios. It will be the topic of an additional paper to clarify this aspect.

Appendix I
Linear Taylor expansion of $\widetilde{\underline{\mathbf{M}}}$

In the following for $\underline{\mathbf{E}}$ equal to $\mathbf{0}$ the derivatives $\partial\widetilde{\underline{\mathbf{M}}}/\partial\mathrm{Re}\left\{\underline{E}_{i,j}\right\}$ and $\partial\widetilde{\underline{\mathbf{M}}}/\partial\mathrm{Im}\left\{\underline{E}_{i,j}\right\}$ contributing to (40) and (41) are derived. With (38) one obtains

$$\left.\frac{\partial\widetilde{\underline{\mathbf{M}}}}{\partial\mathrm{Re}\left\{\underline{E}_{i,j}\right\}}\right|_{\underline{\mathbf{E}}=\mathbf{0}} = \left.\frac{\partial\left((\underline{\mathbf{D}}(\underline{\mathbf{H}}+\underline{\mathbf{E}}))^\mathrm{H}\right)}{\partial\mathrm{Re}\left\{\underline{E}_{i,j}\right\}}\right|_{\underline{\mathbf{E}}=\mathbf{0}} \underline{\mathbf{R}}_\mathrm{B}^{-1}$$
$$+ (\underline{\mathbf{D}}\,\underline{\mathbf{H}})^\mathrm{H} \left.\frac{\partial\left(\left(\underline{\mathbf{D}}(\underline{\mathbf{H}}+\underline{\mathbf{E}})(\underline{\mathbf{H}}+\underline{\mathbf{E}})^\mathrm{H}\underline{\mathbf{D}}^\mathrm{H}\right)^{-1}\right)}{\partial\mathrm{Re}\left\{\underline{E}_{i,j}\right\}}\right|_{\underline{\mathbf{E}}=\mathbf{0}}. \tag{63}$$

Using the notation

$$\mathbf{1}_{i,j} = (\alpha_{\mu,\nu}), \mu = 1\dots KK_\mathrm{M}, \nu = 1\dots K_\mathrm{B}, \tag{64}$$

with

$$\alpha_{\mu,\nu} = \begin{cases} 1 & \mu = i \wedge \nu = j, \\ 0 & \text{else}, \end{cases} \tag{65}$$

the first term in (63) reads

$$\left.\frac{\partial\left((\underline{\mathbf{D}}(\underline{\mathbf{H}}+\underline{\mathbf{E}}))^\mathrm{H}\right)}{\partial\mathrm{Re}\left\{\underline{E}_{i,j}\right\}}\right|_{\underline{\mathbf{E}}=\mathbf{0}} = \mathbf{1}_{i,j}^\mathrm{H}\underline{\mathbf{D}}^\mathrm{H}. \tag{66}$$

Using the relation [19]

$$\frac{\partial\left(\underline{\mathbf{A}}^{-1}\right)}{\partial z} = -\underline{\mathbf{A}}^{-1}\frac{\partial\underline{\mathbf{A}}}{\partial z}\underline{\mathbf{A}}^{-1}, \tag{67}$$

where $\underline{\mathbf{A}}$ is a full-rank square matrix and z a real-valued scalar, the second derivative in (63) is simplified to

$$\left.\frac{\partial\left(\left(\underline{\mathbf{D}}(\underline{\mathbf{H}}+\underline{\mathbf{E}})(\underline{\mathbf{H}}+\underline{\mathbf{E}})^\mathrm{H}\underline{\mathbf{D}}^\mathrm{H}\right)^{-1}\right)}{\partial\mathrm{Re}\left\{\underline{E}_{i,j}\right\}}\right|_{\underline{\mathbf{E}}=\mathbf{0}}$$
$$= -\underline{\mathbf{R}}_\mathrm{B}^{-1}\left(\underline{\mathbf{D}}\,\mathbf{1}_{i,j}\,\underline{\mathbf{H}}^\mathrm{H}\underline{\mathbf{D}}^\mathrm{H} + \underline{\mathbf{D}}\,\underline{\mathbf{H}}\,\mathbf{1}_{i,j}^\mathrm{H}\underline{\mathbf{D}}^\mathrm{H}\right)\underline{\mathbf{R}}_\mathrm{B}^{-1}. \tag{68}$$

Substituting (66) and (68) in (63) one obtains

$$\left.\frac{\partial\widetilde{\underline{\mathbf{M}}}}{\partial\mathrm{Re}\left\{\underline{E}_{i,j}\right\}}\right|_{\underline{\mathbf{E}}=\mathbf{0}} = \mathbf{1}_{i,j}^\mathrm{H}\underline{\mathbf{D}}^\mathrm{H}\underline{\mathbf{R}}_\mathrm{B}^{-1} - (\underline{\mathbf{D}}\,\underline{\mathbf{H}})^\mathrm{H}\,\underline{\mathbf{R}}_\mathrm{B}^{-1}$$
$$\left(\underline{\mathbf{D}}\,\mathbf{1}_{i,j}\,\underline{\mathbf{H}}^\mathrm{H}\underline{\mathbf{D}}^\mathrm{H} + \underline{\mathbf{D}}\,\underline{\mathbf{H}}\,\mathbf{1}_{i,j}^\mathrm{H}\underline{\mathbf{D}}^\mathrm{H}\right)\underline{\mathbf{R}}_\mathrm{B}^{-1}. \tag{69}$$

In analogy to (69) the derivative

$$\left.\frac{\partial\widetilde{\underline{\mathbf{M}}}}{\partial\mathrm{Im}\left\{\underline{E}_{i,j}\right\}}\right|_{\underline{\mathbf{E}}=\mathbf{0}} = -\mathrm{j}\mathbf{1}_{i,j}^\mathrm{H}\underline{\mathbf{D}}^\mathrm{H}\underline{\mathbf{R}}_\mathrm{B}^{-1} - \mathrm{j}\,(\underline{\mathbf{D}}\,\underline{\mathbf{H}})^\mathrm{H}\,\underline{\mathbf{R}}_\mathrm{B}^{-1}$$
$$\left(\underline{\mathbf{D}}\,\mathbf{1}_{i,j}\,\underline{\mathbf{H}}^\mathrm{H}\underline{\mathbf{D}}^\mathrm{H} - \underline{\mathbf{D}}\,\underline{\mathbf{H}}\,\mathbf{1}_{i,j}^\mathrm{H}\underline{\mathbf{D}}^\mathrm{H}\right)\underline{\mathbf{R}}_\mathrm{B}^{-1} \tag{70}$$

can be calculated. Substituting (69) and (70) in (41) yields

$$\begin{aligned}\widetilde{\underline{\mathbf{M}}} \approx\ & (\underline{\mathbf{D}}\,\underline{\mathbf{H}})^\mathrm{H}\,\underline{\mathbf{R}}_\mathrm{B}^{-1} + \sum_{\forall i,j}\mathbf{1}_{i,j}^\mathrm{H}\underline{E}_{i,j}^*\underline{\mathbf{D}}^\mathrm{H}\underline{\mathbf{R}}_\mathrm{B}^{-1} \\ & - (\underline{\mathbf{D}}\,\underline{\mathbf{H}})^\mathrm{H}\,\underline{\mathbf{R}}_\mathrm{B}^{-1}\Big(\underline{\mathbf{D}}\sum_{\forall i,j}\mathbf{1}_{i,j}\underline{E}_{i,j}\underline{\mathbf{H}}^\mathrm{H}\underline{\mathbf{D}}^\mathrm{H} \\ & + \underline{\mathbf{D}}\,\underline{\mathbf{H}}\sum_{\forall i,j}\mathbf{1}_{i,j}^\mathrm{H}\underline{E}_{i,j}^*\underline{\mathbf{D}}^\mathrm{H}\Big)\underline{\mathbf{R}}_\mathrm{B}^{-1},\end{aligned} \tag{71}$$

which is simplified to the desired result of (42).

Appendix II
Covariance matrix $\widetilde{\underline{\mathbf{R}}}_\varepsilon$ of $\widetilde{\underline{\boldsymbol{\varepsilon}}}$

Setting out from (45) the covariance matrix $\widetilde{\underline{\mathbf{R}}}_\varepsilon$ of (22) reads

$$\begin{aligned}\widetilde{\underline{\mathbf{R}}}_\varepsilon =\ & \mathop{\mathrm{E}}_{\underline{\mathbf{d}},\underline{\mathbf{E}},\underline{\mathbf{n}}}\left\{\underline{\mathbf{D}}\,\underline{\mathbf{E}}\,\underline{\mathbf{H}}^\mathrm{H}\underline{\mathbf{D}}^\mathrm{H}\underline{\mathbf{R}}_\mathrm{B}^{-1}\underline{\mathbf{d}}\,\underline{\mathbf{d}}^\mathrm{H}\underline{\mathbf{R}}_\mathrm{B}^{-1}\underline{\mathbf{D}}\,\underline{\mathbf{H}}\,\underline{\mathbf{E}}^\mathrm{H}\underline{\mathbf{D}}^\mathrm{H}\right\} \\ & + \mathop{\mathrm{E}}_{\underline{\mathbf{d}},\underline{\mathbf{E}},\underline{\mathbf{n}}}\left\{\underline{\mathbf{D}}\,\underline{\mathbf{n}}\,\underline{\mathbf{n}}^\mathrm{H}\underline{\mathbf{D}}^\mathrm{H}\right\} = \underline{\mathbf{D}}\,\underline{\mathbf{R}}_\mathrm{n}\underline{\mathbf{D}}^\mathrm{H} \\ & + \underline{\mathbf{D}}\mathop{\mathrm{E}}_{\underline{\mathbf{E}}}\left\{\underline{\mathbf{E}}\,\underline{\mathbf{H}}^\mathrm{H}\underline{\mathbf{D}}^\mathrm{H}\underline{\mathbf{R}}_\mathrm{B}^{-1}\underline{\mathbf{R}}_\mathrm{d}\underline{\mathbf{R}}_\mathrm{B}^{-1}\underline{\mathbf{D}}\,\underline{\mathbf{H}}\,\underline{\mathbf{E}}^\mathrm{H}\right\}\underline{\mathbf{D}}^\mathrm{H}.\end{aligned} \tag{72}$$

Using the relation

$$\mathop{\mathrm{E}}_{\underline{\mathbf{E}}}\left\{\underline{\mathbf{E}}^\mathrm{H}\underline{\mathbf{A}}\,\underline{\mathbf{E}}\right\} = \sigma_\mathrm{h}^2\mathrm{trace}\left\{\underline{\mathbf{A}}\right\}\cdot\mathbf{I}^{(K_\mathrm{B})}, \tag{73}$$

where $\underline{\mathbf{A}}$ is a square matrix, (72) can be simplified to

$$\widetilde{\underline{\mathbf{R}}}_\varepsilon = \underline{\mathbf{D}}\,\underline{\mathbf{R}}_\mathrm{n}\underline{\mathbf{D}}^\mathrm{H} + \underline{\mathbf{D}}\,\underline{\mathbf{D}}^\mathrm{H}\cdot\sigma_\mathrm{h}^2\mathrm{trace}\left\{\underline{\mathbf{H}}^\mathrm{H}\underline{\mathbf{D}}^\mathrm{H}\underline{\mathbf{R}}_\mathrm{B}^{-1}\underline{\mathbf{R}}_\mathrm{d}\underline{\mathbf{R}}_\mathrm{B}^{-1}\underline{\mathbf{D}}\,\underline{\mathbf{H}}\right\}. \tag{74}$$

With

$$\mathrm{trace}\left\{\underline{\mathbf{A}}\,\underline{\mathbf{B}}\,\underline{\mathbf{C}}\right\} = \mathrm{trace}\left\{\underline{\mathbf{B}}\,\underline{\mathbf{C}}\,\underline{\mathbf{A}}\right\} \tag{75}$$

[19], (74) yields

$$\widetilde{\underline{\mathbf{R}}}_{\varepsilon} = \underline{\mathbf{D}}\,\underline{\mathbf{R}}_{\mathrm{n}}\underline{\mathbf{D}}^{\mathrm{H}} + \underline{\mathbf{D}}\,\underline{\mathbf{D}}^{\mathrm{H}} \cdot \sigma_{\mathrm{h}}^{2}\mathrm{trace}\left\{\underline{\mathbf{R}}_{\mathrm{B}}^{-1}\underline{\mathbf{R}}_{\mathrm{d}}\right\}. \quad (76)$$

By substituting (4) in (76), one obtains (46).

APPENDIX III
TRANSMIT ENERGY $\widetilde{T}_n$

By substituting $\widetilde{\underline{\mathbf{M}}}$ of (42) in (48) and considering that

$$\underset{\underline{\mathbf{E}}}{\mathrm{E}}\left\{\underline{\mathbf{E}}\,\underline{\mathbf{A}}\,\underline{\mathbf{E}}\right\} = \underset{\underline{\mathbf{E}}}{\mathrm{E}}\left\{\underline{\mathbf{E}}^{\mathrm{H}}\,\underline{\mathbf{A}}\,\underline{\mathbf{E}}^{\mathrm{H}}\right\} = \mathbf{0} \quad (77)$$

the expectation in (48) can be rewritten as

$$\begin{aligned}\underset{\underline{\mathbf{E}}}{\mathrm{E}}\left\{\widetilde{\underline{\mathbf{M}}}^{\mathrm{H}}\widetilde{\underline{\mathbf{M}}}\right\} &= \underline{\mathbf{R}}_{\mathrm{B}}^{-1} + \underset{\underline{\mathbf{E}}}{\mathrm{E}}\left\{\underline{\mathbf{R}}_{\mathrm{B}}^{-1}\underline{\mathbf{D}}\,\underline{\mathbf{E}}\,\underline{\mathbf{E}}^{\mathrm{H}}\underline{\mathbf{D}}^{\mathrm{H}}\underline{\mathbf{R}}_{\mathrm{B}}^{-1}\right\}\\ &+\underset{\underline{\mathbf{E}}}{\mathrm{E}}\left\{\underline{\mathbf{R}}_{\mathrm{B}}^{-1}\underline{\mathbf{D}}\,\underline{\mathbf{H}}\,\underline{\mathbf{E}}^{\mathrm{H}}\underline{\mathbf{D}}^{\mathrm{H}}\underline{\mathbf{R}}_{\mathrm{B}}^{-1}\underline{\mathbf{D}}\,\underline{\mathbf{E}}\,\underline{\mathbf{H}}^{\mathrm{H}}\underline{\mathbf{D}}^{\mathrm{H}}\underline{\mathbf{R}}_{\mathrm{B}}^{-1}\right\}\\ &-\underset{\underline{\mathbf{E}}}{\mathrm{E}}\left\{\underline{\mathbf{R}}_{\mathrm{B}}^{-1}\underline{\mathbf{D}}\,\underline{\mathbf{E}}\,\underline{\mathbf{H}}^{\mathrm{H}}\underline{\mathbf{D}}^{\mathrm{H}}\underline{\mathbf{R}}_{\mathrm{B}}^{-1}\underline{\mathbf{D}}\,\underline{\mathbf{H}}\,\underline{\mathbf{E}}^{\mathrm{H}}\underline{\mathbf{D}}^{\mathrm{H}}\underline{\mathbf{R}}_{\mathrm{B}}^{-1}\right\}. \quad (78)\end{aligned}$$

Using (73) the expectation operations in (78) can be evaluated, leading to

$$\begin{aligned}\underset{\underline{\mathbf{E}}}{\mathrm{E}}\left\{\widetilde{\underline{\mathbf{M}}}^{\mathrm{H}}\widetilde{\underline{\mathbf{M}}}\right\} &= \underline{\mathbf{R}}_{\mathrm{B}}^{-1} + \underline{\mathbf{R}}_{\mathrm{B}}^{-1}\underline{\mathbf{D}}\,\underline{\mathbf{D}}^{\mathrm{H}}\underline{\mathbf{R}}_{\mathrm{B}}^{-1}\cdot\sigma_{\mathrm{h}}^{2}K_{\mathrm{B}}\\ &+\underline{\mathbf{R}}_{\mathrm{B}}^{-1}\cdot\sigma_{\mathrm{h}}^{2}\mathrm{trace}\left\{\underline{\mathbf{D}}^{\mathrm{H}}\underline{\mathbf{R}}_{\mathrm{B}}^{-1}\underline{\mathbf{D}}\right\}\\ &-\underline{\mathbf{R}}_{\mathrm{B}}^{-1}\underline{\mathbf{D}}\,\underline{\mathbf{D}}^{\mathrm{H}}\underline{\mathbf{R}}_{\mathrm{B}}^{-1}\cdot\sigma_{\mathrm{h}}^{2}\mathrm{trace}\left\{\underline{\mathbf{H}}^{\mathrm{H}}\underline{\mathbf{D}}^{\mathrm{H}}\underline{\mathbf{R}}_{\mathrm{B}}^{-1}\underline{\mathbf{D}}\,\underline{\mathbf{H}}\right\}. \quad (79)\end{aligned}$$

Applying (75) and simplifying (79) one obtains

$$\begin{aligned}\underset{\underline{\mathbf{E}}}{\mathrm{E}}\left\{\widetilde{\underline{\mathbf{M}}}^{\mathrm{H}}\widetilde{\underline{\mathbf{M}}}\right\} &= \underline{\mathbf{R}}_{\mathrm{B}}^{-1}\left[1+\sigma_{\mathrm{h}}^{2}\mathrm{trace}\left\{\underline{\mathbf{R}}_{\mathrm{B}}^{-1}\underline{\mathbf{D}}\,\underline{\mathbf{D}}^{\mathrm{H}}\right\}\right]\\ &+\underline{\mathbf{R}}_{\mathrm{B}}^{-1}\underline{\mathbf{D}}\,\underline{\mathbf{D}}^{\mathrm{H}}\underline{\mathbf{R}}_{\mathrm{B}}^{-1}\cdot\sigma_{\mathrm{h}}^{2}(K_{\mathrm{B}}-N_{\mathrm{t}}). \quad (80)\end{aligned}$$

Considering the diagonal elements of (80), (49) follows.

Acknowledgment

The authors gratefully appreciate the fruitful exchange of ideas with Prof. P.W. Baier, and their colleagues at the Research Group for RF Communications, University of Kaiserslautern, and with M. Joham from Prof. Nossek's group at TU Munich. The support of individual parts of this work in the framework of the EU-IST-Project FLOWS (Flexible Convergence of Wireless Standards and Services), by DFG, by Siemens AG and by the super-computer staff of the central computer facility (RHRK) of the University of Kaiserslautern is highly acknowledged. Thanks are also extended to the anonymous reviewers for their valuable comments.

References

[1] P. W. Baier, W. Qiu, H. Tröger, C. A. Jötten, and M. Meurer, "Modelling and optimization of receiver oriented multi-user MIMO downlinks for frequency selective channels," *Proc. 10th International Conference on Telecommunications (ICT'03)*, vol. 2, Papeete, 2003, pp. 1547–1554.

[2] M. Meurer, P. W. Baier, T. Weber, Y. Lu, and A. Papathanassiou, "Joint transmission: advantageous downlink concept for CDMA mobile radio systems using time division duplexing," *IEE Electronics Letters*, vol. 11, no. 10, pp. 900–901, 2000.

[3] P. W. Baier, M. Meurer, T. Weber, and H. Tröger, "Joint transmission (JT), an alternative rationale for the downlink of time division CDMA using multi-element transmit antennas," *Proc. IEEE 6th International Symposium on Spread Spectrum Techniques & Applications (ISSSTA'00)*, vol. 1, Parsippany, 2000, pp. 1–5.

[4] H. Tröger, T. Weber, M. Meurer, and P. W. Baier, "Performance assessment of Joint Transmission (JT) multi-user downlinks with multi-element transmit antennas," *European Transactions on Telecommunications*, vol. 12, no. 5, pp. 407–416, 2001.

[5] M. Joham, K. Kusume, M. H. Gzara, W. Utschick, and J. A. Nossek, "Transmit Wiener filter for the downlink of TDD DS-CDMA systems," *Proc. IEEE 7th International Symposium on Spread Spectrum Techniques & Applications (ISSSTA'02)*, vol. 1, Prague, 2002, pp. 9–13.

[6] B. Steiner and P. W. Baier, "Low cost channel estimation in the uplink receiver of CDMA mobile radio systems," *Frequenz*, vol. 47, no. 11–12, pp. 292–298, 1993.

[7] T. Weber and I. Maniatis, "Channel knowledge: a crucial prerequisite for MIMO transmission ?" *COST 273 TD(03)083*, Paris, 2003.

[8] B. R. Vojcic and W. M. Jang, "Transmitter precoding in synchronous multiuser communications," *IEEE Transactions on Communications*, vol. 46, no. 10, pp. 1346–1355, 1998.

[9] F. Kowalewski and P. Mangold, "Joint predistortion and transmit diversity," *Proc. IEEE Global Telecommunications Conference (GLOBECOM'00)*, vol. 1, San Francisco, 2000, pp. 245–249.

[10] F. Dietrich, R. Hunger, M. Joham, and W. Utschick, "Linear precoding over time-varying channels in TDD systems," *Proc. IEEE International Conference on Acoustics, Speech, and Signal Processing (ICASSP'03)*, vol. 5, Hong Kong, 2003, pp. 117–120.

[11] R. Fischer, C. Windpassinger, A. Lampe, and J. Huber, "Tomlinson-Harashima precoding in space-time transmission for low-rate backward channel," *Proc. 2002 International Zurich Seminar on Broadband Communications (IZS'2002)*, Zurich, 2002.

[12] M. Joham, K. Kusume, W. Utschick, and J. Nossek, "Transmit matched filter and transmit wiener filter for the downlink of FDD DS-CDMA systems," *Proc. IEEE 13th International Symposium on Personal, Indoor and Mobile Radio Communications (PIMRC'02)*, vol. 5, Lisbon, Sept. 2002, pp. 2312–2316.

[13] E. Visotsky and U. Madhow, "Space-time transmit precoding with imperfect feedback," *IEEE Transactions on Information Theory*, vol. 47, no. 6, pp. 2632–2639, 2001.

[14] F. Wathan, R. Irmer, and G. Fettweis, "On transmitter-based interference mitigation in TDD-downlink with frequency-selective fading channel environment," *Proc. 8th Asia-Pacific Conference on Communications (APCC'02)*, Bandung, 2002, pp. 125–128.

[15] A. Klein, *Multi-user detection of CDMA signals – algorithms and their application to cellular mobile radio*, no. 423 in Fortschrittberichte VDI, Reihe 10. Düsseldorf: VDI-Verlag, 1996.

[16] R. Esmailzadeh and M. Nakagawa, "Pre-RAKE diversity combining for direct sequence spread spectrum mobile communications systems," *IEICE Transactions on Communications*, vol. 76, no. 8, pp. 1008–1015, Aug. 1993.

[17] A. Noll-Barreto and G. Fettweis, "Performance improvement in DS-spread spectrum CDMA systems using a pre- and a post-rake," *Proc. 2000 International Zurich Seminar on Broadband Communications (IZS'2000)*, Zurich, 2000, pp. 39–46.

[18] T. Weber, A. Sklavos, Y. Liu, and M. Weckerle, "The air interface concept JOINT for beyond 3G mobile radio networks," *Proc. 15th International Conference on Wireless Communications*, Calgary, July 2003, pp. 25–33.

[19] H. Lütkepohl, *Handbook of matrices*. New York: John Wiley & Sons, 1996.

[MW04b] Meurer, M.; Weber, T.: "On the impact of imperfect channel knowledge on transmit zero forcing based receiver oriented multi-user MIMO transmission". Accepted for publication in *IEEE Transactions on Wireless Communications*, 2004.

On the impact of imperfect channel knowledge on transmit zero forcing based receiver oriented multi-user MIMO transmission

Michael Meurer, Tobias Weber

Abstract

In conventional transmission schemes the transmitter algorithms are a priori given, whereas the algorithms to be used by the receivers have to be a posteriori adapted. Such schemes can be termed transmitter (Tx) oriented. The opposite to Tx orientation would be receiver (Rx) orientation, in which the receiver algorithms are a priori given, and the transmitter algorithms have to be a posteriori adapted under consideration of channel knowledge. A question still open concerns the impact of imperfect channel knowledge on the transmission quality of Rx oriented data transmission, especially if radio transmission systems with multi-antennas both at the transmitter and receiver are considered. In the paper, after the introduction of adequate models for such MIMO (Multiple Input Multiple Output) systems, this question is analytically studied. To that purpose closed form expressions for signal-to-noise-plus-interference-ratios and bit error probabilities are derived which show a good match to simulation results.

Index Terms

Receiver orientation, imperfect channel state information, transmit zero-forcing, MIMO

The material in the paper was presented in part at the 5th ITG Conference on Source and Channel Coding, Erlangen, Jan. 2004.

M. Meurer and T. Weber are with the Research Group for RF Communications, University of Kaiserslautern, Germany.

Contact via email: meurer@rhrk.uni-kl.de

I. INTRODUCTION

In conventional transmission schemes the transmitter (Tx) algorithms are *a priori* given and made known to the receivers (Rx), whereas the algorithms to be used by the receivers are *a posteriori* adapted, possibly under consideration of channel information. For this approach the authors have coined the term Tx orientation [1]. The opposite to Tx orientation is Rx orientation, in which the receiver algorithms are *a priori* given and made known to the transmitter, and the transmitter algorithms, again possibly under consideration of channel information, are *a posteriori* adapted correspondingly. It was not before the 1990s that the first ideas of Rx orientation came up [2]–[7]. It took another couple of years to clearly formulate this rationale in 2000 [8]. From then on it attracted broader attention so that a systematical study could begin. This late perception of Rx orientation is astonishing, because this approach offers some quite interesting advantages [1]:

- The *a priori* determined receiver algorithms can be chosen with the aim to obtain particularly simple receiver structures. Therefore, if we consider mobile radio systems, the quasi natural choice in the downlink (DL) would be Rx orientation, because this leads to low cost receivers at the mobile terminals (MTs) [8].
- Channel information is only required at the transmitter, i.e., if we focus on the downlink of a mobile radio system, at the access point (AP). Therefore, no downlink transmission resources have to be sacrificed for training signals, and no channel estimators are required at the MTs.

Both Tx orientation and Rx orientation have in common that at the receivers or at the transmitter, respectively, channel knowledge has to be used. This channel knowledge is *a priori* not available but has to be made available at the receivers or at the transmitter, respectively, by channel estimation [9], [10]. By this procedure in general only imperfect channel knowledge can be made available for further signal processing. For Tx oriented data transmission the impact of such imperfections onto the performance of the data transmission has been well-studied [9], [10]. However, for Rx oriented data transmission this impact is still an open question, which is still not satisfactorily answered. In [3] a special SISO (single input single output) system is considered and it is shown by few simulations which impact imperfect channel measurements have onto the transmission quality in the considered special scenario. The focus of [6] still lies on a special SISO system but, in contrast to [3], the impact of out-dated channel knowledge onto the transmission quality is discussed. Out-dated channel knowledge is a severe problem if the mobile radio channels are time-variant and the time elapsing between channel estimation and data transmission is not sufficiently small compared to the coherence time of the mobile radio channels. In [11] these simulation based insights are extended to MISO (multi input single output) systems, still focusing on the same special scenario. In all three contributions [3], [6] and [11] no generally valid analysis is presented which allows to apply the obtained simulation results to a large variety of scenarios. A somewhat more general view on MIMO (multiple input multiple output) configurations, where Rx oriented data transmission is applied, is presented in [12], [13] and [14]. These contributions, especially [13] and [14], focus on the fact that imperfect channel knowledge may go back to a feedback scheme which only allows to track slowly varying channel properties. A more basic information theoretic perspective of the same topic for MIMO systems is given in [15]. However, in none of the three contributions [13]–[15] other kinds of channel knowledge imperfections than those due to feedback restrictions are considered. Especially, an analytical performance evaluation of Rx oriented transmission is not available. Therefore, in [16] the authors of this contribution gave a first brief analytical answer to the question raised above. In this paper these insights are deepened and extended aiming at a more fundamental view, i.e., we do not focus on the reason of imperfect channel knowledge like out-dated channel estimation but on the fact itself. The focus of the analysis lies on linear Rx oriented transmission based on the Transmit Zero Forcer (TxZF) [1], [14], [17].

The paper is organized as follows: In Section II a generic model of linear MIMO transmission systems is developed. The topic of Section III is the detailed description of the rationale Rx orientation with special emphasis on the linear algorithm TxZF [1]. The crux of this paper is concentrated in Section IV, where the influence of imperfect channel knowledge on the performance of the linear algorithm introduced in Section III is scrutinized. Section V illustrates and deepens the insights of Section IV for an exemplary scenario. The investigations are performed in the time discrete equivalent low pass domain under utilization of a vector-matrix representation [1]. Consequently, signals and system components are represented by complex vectors or matrices, respectively, which are printed in bold face. In the analysis, $[\cdot]_{n\times m}$ designates the element in the n-th row and m-th column of the matrix in brackets, $[\cdot]_n$ stands for the n-th row of the matrix or the n-th element of the vector in brackets and $\|\cdot\|$ denotes the Euclidean norm. Moreover, the operation $\overline{\mathrm{diag}}(\cdot)$ yields a copy of a square matrix with the diagonal elements being set to zero.

II. Generic model Of linear MIMO transmission systems

We consider a situation, where an AP supports K MTs k, $k=1\dots K$. The AP is equipped with K_B transmit antennas, and each of the K MTs employs K_M receive antennas. Therefore, each link between the AP and one of the K MTs constitutes a MIMO structure, and the total system is a multi-user MIMO broadcast structure. We further assume that the radio channel between the AP and each MT k, $k=1\dots K$, is a flat blockfading MIMO channel. N data symbols $\underline{d}_n^{(k)}$, $n=1\dots N$, taken from a finite symbol alphabet $\mathbb{V}$ have to be transmitted from the AP to each MT k, $k=1\dots K$. These N data symbols are arranged in the MT specific data vector

$$\underline{\mathbf{d}}^{(k)}=\left(\underline{d}_1^{(k)}\dots\underline{d}_N^{(k)}\right)^{\mathrm{T}}\in\mathbb{V}^N. \tag{1}$$

The K MT specific data vectors $\underline{\mathbf{d}}^{(k)}$, $k=1\dots K$, of (1) are stacked to the total data vector

$$\underline{\mathbf{d}}=\left(\underline{\mathbf{d}}^{(1)\mathrm{T}}\dots\underline{\mathbf{d}}^{(K)\mathrm{T}}\right)^{\mathrm{T}}=\left(\underline{d}_1\dots\underline{d}_{N_\mathrm{t}}\right)^{\mathrm{T}}\in\mathbb{V}^{N_\mathrm{t}},N_\mathrm{t}=KN. \tag{2}$$

$\underline{\mathbf{d}}$ of (2) is assumed to be wide sense stationary with zero mean and the covariance matrix

$$\underline{\mathbf{R}}_\mathrm{d}=\mathop{\mathrm{E}}_{\underline{\mathbf{d}}}\left\{\underline{\mathbf{d}}\,\underline{\mathbf{d}}^{\mathrm{H}}\right\}=E_\mathrm{d}\mathbf{I}^{(N_\mathrm{t})}. \tag{3}$$

By linear modulation based on $\underline{\mathbf{d}}$ of (2) a transmit signal $\underline{\mathbf{t}}$ of dimension K_B is generated. The modulation process is described by a $K_\mathrm{B}\times N_\mathrm{t}$-matrix $\underline{\mathbf{M}}$ termed modulator matrix [8], i.e.,

$$\underline{\mathbf{t}}=\underline{\mathbf{M}}\,\underline{\mathbf{d}}. \tag{4}$$

The MIMO channel between the AP and MT k, $k=1\dots K$, is assumed to be linear. Therefore, the MT specific noise-free received signal $\underline{\mathbf{e}}^{(k)}$ at the MT k, $k=1\dots K$, of dimension K_M is a linear function of the transmit signal $\underline{\mathbf{t}}$, i.e., with the MT specific channel matrix $\underline{\mathbf{H}}^{(k)}\in\mathbb{C}^{K_\mathrm{M}\times K_\mathrm{B}}$

$$\underline{\mathbf{e}}^{(k)}=\underline{\mathbf{H}}^{(k)}\underline{\mathbf{t}} \tag{5}$$

holds. Taking the noise $\underline{\mathbf{n}}^{(k)}$ at the input of MT k, $k=1\dots K$, into account, one obtains

$$\underline{\mathbf{r}}^{(k)}=\underline{\mathbf{e}}^{(k)}+\underline{\mathbf{n}}^{(k)}=\underline{\mathbf{H}}^{(k)}\underline{\mathbf{t}}+\underline{\mathbf{n}}^{(k)} \tag{6}$$

for the MT specific received signal and

$$\underline{\mathbf{r}} = \left(\underline{\mathbf{r}}^{(1)\mathrm{T}} \ldots \underline{\mathbf{r}}^{(K)\mathrm{T}}\right)^{\mathrm{T}} = \underbrace{\left(\underline{\mathbf{H}}^{(1)\mathrm{T}} \ldots \underline{\mathbf{H}}^{(K)\mathrm{T}}\right)^{\mathrm{T}}}_{\underline{\mathbf{H}}} \underline{\mathbf{t}} + \underbrace{\left(\underline{\mathbf{n}}^{(1)\mathrm{T}} \ldots \underline{\mathbf{n}}^{(K)\mathrm{T}}\right)^{\mathrm{T}}}_{\underline{\mathbf{n}}} \in \mathbb{C}^{KK_{\mathrm{M}}} \tag{7}$$

for the total received signal [8]. Substituting (4) in (7) yields

$$\underline{\mathbf{r}} = \underline{\mathbf{H}}\,\underline{\mathbf{M}}\,\underline{\mathbf{d}} + \underline{\mathbf{n}}. \tag{8}$$

$\underline{\mathbf{H}}$ in (8) is termed (total) channel matrix. $\underline{\mathbf{n}}$ of (7) and (8), which is termed (total) noise signal, is assumed to be Gaussian, wide sense stationary with zero mean, independent of $\underline{\mathbf{d}}$ of (2), and to have the covariance matrix

$$\underline{\mathbf{R}}_{\mathrm{n}} = \mathop{\mathrm{E}}_{\underline{\mathbf{n}}}\left\{\underline{\mathbf{n}}\,\underline{\mathbf{n}}^{\mathrm{H}}\right\}. \tag{9}$$

At MT k, $k = 1 \ldots K$, the received signal $\underline{\mathbf{r}}^{(k)}$ of this MT, see (6), is fed to a MT specific demodulator in order to obtain a value-continuous estimate $\widehat{\underline{\mathbf{d}}}^{(k)}$ of $\underline{\mathbf{d}}^{(k)}$ of (1). The estimate $\widehat{\underline{\mathbf{d}}}^{(k)}$ is fed to a decision unit to map the value-continuous estimates $\widehat{\underline{d}}_n^{(k)}$ of the data symbols $\underline{d}_n^{(k)}$, $n = 1 \ldots N$, onto valid elements of the symbol alphabet $\mathbb{V}$. In the case of linear demodulation considered in this paper, the demodulation process performed at MT k, $k = 1 \ldots K$, is described by a MT specific demodulator matrix $\underline{\mathbf{D}}^{(k)}$ of dimension $N \times K_{\mathrm{M}}$ as follows [1]:

$$\widehat{\underline{\mathbf{d}}}^{(k)} = \left(\widehat{\underline{d}}_1^{(k)} \ldots \widehat{\underline{d}}_N^{(k)}\right)^{\mathrm{T}} = \underline{\mathbf{D}}^{(k)} \underline{\mathbf{r}}^{(k)}. \tag{10}$$

By properly stacking the K equations (10), we obtain with (2) and (7)

$$\widehat{\underline{\mathbf{d}}} = \left(\widehat{\underline{\mathbf{d}}}^{(1)\mathrm{T}} \ldots \widehat{\underline{\mathbf{d}}}^{(K)\mathrm{T}}\right)^{\mathrm{T}} = \left(\widehat{\underline{d}}_1 \ldots \widehat{\underline{d}}_{N_{\mathrm{t}}}\right)^{\mathrm{T}} = \underbrace{\mathrm{blockdiag}\left(\underline{\mathbf{D}}^{(1)} \ldots \underline{\mathbf{D}}^{(K)}\right)}_{\underline{\mathbf{D}}} \underline{\mathbf{r}}. \tag{11}$$

$\underline{\mathbf{D}}$ of (11) has the dimension $N_{\mathrm{t}} \times KK_{\mathrm{M}}$ and is termed (total) demodulator matrix. Substituting (8) in (11) yields

$$\widehat{\underline{\mathbf{d}}} = \underline{\mathbf{D}}\,\underline{\mathbf{H}}\,\underline{\mathbf{M}}\,\underline{\mathbf{d}} + \underline{\mathbf{D}}\,\underline{\mathbf{n}}. \tag{12}$$

The system model described above is summarized in Fig. 1. A brief recapitulation of the most important quantities can be found in Table I.

According to (3) and (4) the mean radiated energy invested for the data symbol $\underline{d}_n$, $n = 1 \ldots N_{\mathrm{t}}$, becomes

$$T_n = \left\|\left[\underline{\mathbf{M}}^{\mathrm{T}}\right]_n\right\|^2 E_{\mathrm{d}} = \left[\underline{\mathbf{M}}^{\mathrm{H}}\underline{\mathbf{M}}\right]_{n,n} E_{\mathrm{d}}. \tag{13}$$

By averaging over all N_t data symbols $\underline{d}_n$, $n=1\dots N_\mathrm{t}$, we obtain the mean radiated energy

$$T = \frac{1}{N_\mathrm{t}}\sum_{n=1}^{N_\mathrm{t}} T_n = \frac{E_\mathrm{d}}{N_\mathrm{t}}\mathrm{trace}\left\{\underline{\mathbf{M}}^\mathrm{H}\,\underline{\mathbf{M}}\right\} \tag{14}$$

per data symbol. The estimate $\widehat{\underline{d}}_n$ of the transmitted data symbol $\underline{d}_n$ consists of the sum of a useful part

$$\underline{d}_{\mathrm{use},n} = \mathop{\mathrm{E}}_{\underline{\mathbf{d}},\underline{\mathbf{n}}}\left\{\widehat{\underline{d}}_n \middle| \underline{d}_n\right\} = \left[\underline{\mathbf{D}}\,\underline{\mathbf{H}}\,\underline{\mathbf{M}}\right]_{n,n}\underline{d}_n, \tag{15}$$

of an interference part

$$\underline{d}_{\mathrm{int},n} = \left[\,\overline{\mathrm{diag}}\left(\underline{\mathbf{D}}\,\underline{\mathbf{H}}\,\underline{\mathbf{M}}\right)\underline{\mathbf{d}}\right]_n, \tag{16}$$

and of a noise part

$$\underline{d}_{\mathrm{noise},n} = \left[\underline{\mathbf{D}}\,\underline{\mathbf{n}}\right]_n, \tag{17}$$

see also [16]. In (16) and (17) the terms in brackets are column vectors. To evaluate the impact of the interference part $\underline{d}_{\mathrm{int},n}$ of (16) and of the noise part $\underline{d}_{\mathrm{noise},n}$ of (17) on the data estimate $\widehat{\underline{d}}_n$, the estimation error

$$\underline{\boldsymbol{\varepsilon}} = \widehat{\underline{\mathbf{d}}} - \left(\underline{d}_{\mathrm{use},1}\dots\underline{d}_{\mathrm{use},N_\mathrm{t}}\right)^\mathrm{T} = \widehat{\underline{\mathbf{d}}} - \mathrm{diag}\left(\underline{\mathbf{D}}\,\underline{\mathbf{H}}\,\underline{\mathbf{M}}\right)\underline{\mathbf{d}} = \overline{\mathrm{diag}}\left(\underline{\mathbf{D}}\,\underline{\mathbf{H}}\,\underline{\mathbf{M}}\right)\underline{\mathbf{d}} + \underline{\mathbf{D}}\,\underline{\mathbf{n}} \tag{18}$$

is considered. $\underline{\mathbf{d}}$ of (2) and $\underline{\mathbf{n}}$ of (7) are random vectors with the above explained statistical properties, c.f. (3) and (9). Therefore, $\underline{\boldsymbol{\varepsilon}}$ of (18) is also a random vector. Setting out from (3) and (9), $\underline{\boldsymbol{\varepsilon}}$ has zero-mean and the covariance matrix

$$\underline{\mathbf{R}}_\varepsilon = \mathop{\mathrm{E}}_{\underline{\mathbf{d}},\underline{\mathbf{n}}}\left\{\underline{\boldsymbol{\varepsilon}}\,\underline{\boldsymbol{\varepsilon}}^\mathrm{H}\right\} = \underbrace{\left[\overline{\mathrm{diag}}\left(\underline{\mathbf{D}}\,\underline{\mathbf{H}}\,\underline{\mathbf{M}}\right)\left(\overline{\mathrm{diag}}\left(\underline{\mathbf{D}}\,\underline{\mathbf{H}}\,\underline{\mathbf{M}}\right)\right)^\mathrm{H}\right]E_\mathrm{d}}_{\text{interference}} + \underbrace{\underline{\mathbf{D}}\,\underline{\mathbf{R}}_\mathrm{n}\,\underline{\mathbf{D}}^\mathrm{H}}_{\text{noise}}. \tag{19}$$

A concise and obvious quality measure for the estimates $\widehat{\underline{d}}_n$ of (10) are the signal-to-noise-plus-interference-ratios (SNIR) $\gamma_{\mathrm{o},n}$ which are based on $\underline{\mathbf{R}}_\varepsilon$ of (19) [16]. With (3), (9), (15), (16), (17) and (19) we obtain [16]

$$\gamma_{\mathrm{o},n} = \frac{\mathop{\mathrm{E}}_{\underline{\mathbf{d}},\underline{\mathbf{n}}}\left\{\left|\underline{d}_{\mathrm{use},n}\right|^2\right\}}{\mathop{\mathrm{E}}_{\underline{\mathbf{d}},\underline{\mathbf{n}}}\left\{\left|\underline{d}_{\mathrm{noise},n}\right|^2\right\} + \mathop{\mathrm{E}}_{\underline{\mathbf{d}},\underline{\mathbf{n}}}\left\{\left|\underline{d}_{\mathrm{int},n}\right|^2\right\}} = \frac{\left|\left[\underline{\mathbf{D}}\,\underline{\mathbf{H}}\,\underline{\mathbf{M}}\right]_{n,n}\right|^2 E_\mathrm{d}}{\left[\underline{\mathbf{R}}_\varepsilon\right]_{n,n}} = \frac{\left|\left[\underline{\mathbf{D}}\,\underline{\mathbf{H}}\,\underline{\mathbf{M}}\right]_{n,n}\right|^2 E_\mathrm{d}}{\left[\underline{\mathbf{D}}\,\underline{\mathbf{R}}_\mathrm{n}\,\underline{\mathbf{D}}^\mathrm{H}\right]_{n,n} + \left\|\left[\,\overline{\mathrm{diag}}\left(\underline{\mathbf{D}}\,\underline{\mathbf{H}}\,\underline{\mathbf{M}}\right)\right]_n\right\|^2 E_\mathrm{d}}. \tag{20}$$

III. Receiver oriented transmission

A. Fundamentals

As already mentioned in Section I, in Rx oriented transmission the receiver algorithms, i.e., the MT specific demodulator mactrices $\underline{\mathbf{D}}^{(k)}$, $k=1\dots K$, of (10) and, therefore, the total demodulator matrix $\underline{\mathbf{D}}$ of (11) are *a priori* chosen. On the other hand, the transmitter algorithms, i.e., the modulator matrix $\underline{\mathbf{M}}$ of (4), is *a posteriori* adapted under consideration of these demodulator matrices and channel information, here represented by the channel matrix $\underline{\mathbf{H}}$ of (7). Approaches meanwhile quite well known to adjust $\underline{\mathbf{M}}$ based on $\underline{\mathbf{H}}$ and $\underline{\mathbf{D}}$ are the Transmit Matched Filter (TxMF) [1], [14] – also known as pre-rake [2], [5] – and the Transmit Zero Forcer (TxZF) [1], [4], [14]. Other options for Rx orientation are various kinds of Transmit Minimum Mean Square Error Modulators (TxMMSE) as, e.g., published in [14]. In this paper only the TxZF is considered, because this choice for adjusting $\underline{\mathbf{M}}$ is especially favorable if high signal-to-noise-ratios (SNRs) at the input of the MTs are considered and results in a lower complexity than the TxMMSE [14].

B. Performance analysis of the Transmit Zero Forcer

For the TxZF the modulator matrix is *a posteriori* determined as follows [8], [1]:

$$\underline{\mathbf{M}} = (\underline{\mathbf{D}}\,\underline{\mathbf{H}})^{\mathrm{H}} \underbrace{\left[\underline{\mathbf{D}}\,\underline{\mathbf{H}}\,(\underline{\mathbf{D}}\,\underline{\mathbf{H}})^{\mathrm{H}}\right]}_{\underline{\mathbf{R}}_{\mathrm{B}}}{}^{-1}. \tag{21}$$

If $\underline{\mathbf{M}}$ is chosen according to (21) the data transmission is unbiased, i.e., all diagonal elements of $\underline{\mathbf{D}}\,\underline{\mathbf{H}}\,\underline{\mathbf{M}}$ are equal to one. Setting out from (21) and still having in mind that we assume that both $\underline{\mathbf{H}}$ and $\underline{\mathbf{D}}$ are perfectly known at the transmitter, the basic behaviour of TXZF based data transmission can be studied by taking a two-step procedure: In a first step, the quality of the data estimate $\widehat{\underline{\mathbf{d}}}$ of (11) described by the covariance matrix $\underline{\mathbf{R}}_{\varepsilon}$ of (19) of the estimation error $\underline{\boldsymbol{\varepsilon}}$ of (18) has to be studied. In a second step the mean symbol specific transmit energies T_n, $n=1\ldots N_{\mathrm{t}}$, of (13) have to be considered. With (21), (19) yields

$$\underline{\mathbf{R}}_{\varepsilon} = \underline{\mathbf{D}}\,\underline{\mathbf{R}}_{\mathrm{n}}\underline{\mathbf{D}}^{\mathrm{H}}, \tag{22}$$

i.e., the interference term in (19) vanishes. Substituting (21) and (22) in (20), the SNIR $\gamma_{\mathrm{o},n}$ obtained, if TxZF is applied, reads

$$\gamma_{\mathrm{o},n} = \frac{E_{\mathrm{d}}}{\left[\underline{\mathbf{D}}\,\underline{\mathbf{R}}_{\mathrm{n}}\,\underline{\mathbf{D}}^{\mathrm{H}}\right]_{n,n}}. \tag{23}$$

(23) allows the following conclusions:

- Changes of the channel matrix $\underline{\mathbf{H}}$ have no influence on $\gamma_{\mathrm{o},n}$ of (23) as long as (21) is fulfilled and $\underline{\mathbf{D}}$, E_{d} and $\underline{\mathbf{R}}_{\mathrm{n}}$ are kept constant, because noise is the only performance limiting effect.

- $\gamma_{\text{o},n}$ is proportional to E_d.
- Scaling the n-th row of the demodulator matrix $\underline{\mathbf{D}}$ by a factor β results in multiplying $\gamma_{\text{o},n}$ by a factor of $1/\beta^2$.
- For fixed $\underline{\mathbf{D}}$, E_d, $\underline{\mathbf{R}}_\text{n}$ and under the requirement of unbiased data transmission, TxZF maximizes $\gamma_{\text{o},n}$. The reason for this behaviour is that the TxZF totally eliminates interference [1].

Reflecting the observations made above, one may get the impression that TxZF always shows an optimum behaviour with respect to $\gamma_{\text{o},n}$ of (23) and the constraints mentioned in the last of the above items. This conclusion is correct. However, the price to be paid to achieve this goal has to be kept in mind: the mean symbol specific transmit energies T_n, $n=1\dots N_\text{t}$, of (13) may get very large. Therefore, in the following these mean symbol specific transmit energies T_n, $n=1\dots N_\text{t}$, are studied to clarify the influence of $\underline{\mathbf{D}}$ and $\underline{\mathbf{H}}$ on T_n. Substituting (21) in (13) yields [8]

$$T_n = \left[\underline{\mathbf{R}}_\text{B}^{-1}\right]_{n,n} E_\text{d}, n=1\dots N_\text{t}. \tag{24}$$

One observes that the mean symbol specific transmit energies T_n, $n=1\dots N_\text{t}$, depend on the scaling of $\underline{\mathbf{H}}$ and $\underline{\mathbf{D}}$. Therefore, even if $\gamma_{\text{o},n}$ of (23) does not depend on $\underline{\mathbf{H}}$, T_n of (24) massively changes if $\underline{\mathbf{H}}$ is changed. Consequently, to fairly assess the quality of the data estimate $\widehat{\underline{\mathbf{d}}}$ in a Rx oriented data transmission system E_d in (23) has to be expressed as a function of T_n leading to

$$\gamma_{\text{o},n} = \frac{T_n}{\left[\underline{\mathbf{R}}_\text{B}^{-1}\right]_{n,n}\left[\underline{\mathbf{D}}\,\underline{\mathbf{R}}_\text{n}\,\underline{\mathbf{D}}^\text{H}\right]_{n,n}}. \tag{25}$$

In the special case of QPSK symbol modulation the above described observation allows to find a closed analytical expression for the bit error probability of the two bits being carried by data symbol $\underline{d}_n$. As shown above, in the case of the TxZF the only disturbing component of $\widehat{\underline{d}}_n$ is $\underline{d}_{\text{noise},n}$. $\underline{d}_{\text{noise},n}$ satisfies a Gaussian distribution. Therefore, the bit error probability of the two bits combined in data symbol $\underline{d}_n$, $n=1\dots N_\text{t}$, becomes [18]

$$P_{\text{b},n} = \frac{1}{2}\text{erfc}\left(\sqrt{\frac{T_n}{2\left[\underline{\mathbf{R}}_\text{B}^{-1}\right]_{n,n}\left[\underline{\mathbf{D}}\,\underline{\mathbf{R}}_\text{n}\,\underline{\mathbf{D}}^\text{H}\right]_{n,n}}}\right). \tag{26}$$

(26) allows a tradeoff between the invested mean symbol specific transmit energy T_n of (24) and the resulting bit error probability $P_{\text{b},n}$. In the special case of white additive Gaussian noise, i.e., if

$\underline{\mathbf{R}}_{\mathrm{n}}$ is equal to $\sigma^2\mathbf{I}^{(KK_{\mathrm{M}})}$, a fair evaluation of Rx oriented data transmission systems can be done by analyzing the bit error probability $P_{\mathrm{b},n}$ as a function of the ratio

$$\gamma_{\mathrm{i},n} = \frac{T_n}{\sigma^2}, n=1\ldots N_{\mathrm{t}}, \tag{27}$$

of the mean symbol specific transmit energy T_n and the noise variance σ^2. $\gamma_{\mathrm{i},n}$ of (27) is termed pseudo-SNR (PSNR) of data symbol $\underline{d}_n$. With $\gamma_{\mathrm{i},n}$ of (27) for the SNIR $\gamma_{\mathrm{o},n}$ of (25) follows

$$\gamma_{\mathrm{o},n} = \frac{\gamma_{\mathrm{i},n}}{\left[\underline{\mathbf{R}}_{\mathrm{B}}^{-1}\right]_{n,n}\left[\underline{\mathbf{D}}\,\underline{\mathbf{D}}^{\mathrm{H}}\right]_{n,n}}, \tag{28}$$

which allows to further simplify (26) to

$$P_{\mathrm{b},n} = \frac{1}{2}\mathrm{erfc}\left(\sqrt{\frac{\gamma_{\mathrm{i},n}}{2\left[\underline{\mathbf{R}}_{\mathrm{B}}^{-1}\right]_{n,n}\left[\underline{\mathbf{D}}\,\underline{\mathbf{D}}^{\mathrm{H}}\right]_{n,n}}}\right) \tag{29}$$

IV. Influence of imperfect channel knowledge on the transmission performance: the general case

A. Model and assumptions

In Section III it was assumed that the transmitter has perfect knowledge of the demodulator matrix $\underline{\mathbf{D}}$ and of the channel matrix $\underline{\mathbf{H}}$, while *a posteriori* adapting the modulator matrix $\underline{\mathbf{M}}$. Unfortunately, in real-world data transmission systems channel knowledge is not *a priori* available but has to be obtained by channel estimation [9], [10]. As a consequence, usually not $\underline{\mathbf{H}}$ but a more or less accurate estimate $\widehat{\underline{\mathbf{H}}}$ of $\underline{\mathbf{H}}$ is available at the transmitter. In this section the performance degradation is analyzed which results by using $\widehat{\underline{\mathbf{H}}}$ instead of $\underline{\mathbf{H}}$ when *a posteriori* adjusting $\underline{\mathbf{M}}$ in the transmitter.

Generally, the channel matrix estimate $\widehat{\underline{\mathbf{H}}}$ can be considered as the sum

$$\widehat{\underline{\mathbf{H}}} = \underline{\mathbf{H}} + \underline{\mathbf{E}} \tag{30}$$

of the true channel matrix $\underline{\mathbf{H}}$ and the channel estimation error matrix

$$\underline{\mathbf{E}} = \left(\underline{E}_{i,j}\right), i = 1\ldots KK_{\mathrm{M}}, j = 1\ldots K_{\mathrm{B}}. \tag{31}$$

As the transmitter does not know $\underline{\mathbf{E}}$, the elements $\underline{E}_{i,j}$ of $\underline{\mathbf{E}}$ can only be treated as random variables. In the following it is assumed that these random variables $\underline{E}_{i,j}$

- are uncorrelated and identically distributed with zero mean,
- have uncorrelated, identically distributed real and imaginary parts and
- are independent of $\underline{\mathbf{n}}$ and $\underline{\mathbf{d}}$.

Then, the second order statistical properties of $\underline{E}_{i,j}$ are totally described by their variance

$$\underset{\underline{\mathbf{E}}}{\mathrm{E}}\left\{\underline{E}_{i,j}\underline{E}_{i,j}^{*}\right\} = \sigma_{\mathrm{h}}^{2}, i = 1\ldots KK_{\mathrm{M}}, j = 1\ldots K_{\mathrm{B}}. \tag{32}$$

The above mentioned requirements are usually fulfilled, especially if pilot-aided joint channel estimation [9], [10] is applied. Besides, in this situation, if the noise effective during channel estimation is Gaussian, the real and imaginary parts of $\underline{E}_{i,j}$ satisfy the same Gaussian probability distribution. In the following considerations this assumption will not be generally made, but only when explicitly stated.

B. Analytical performance evaluation

If $\widehat{\underline{\mathbf{H}}}$ of (30) is used to *a posteriori* adapt $\underline{\mathbf{M}}$ of (4), (21) has to be rewritten as

$$\widetilde{\underline{\mathbf{M}}} = \Big(\underline{\mathbf{D}}\,(\underline{\mathbf{H}}+\underline{\mathbf{E}})\Big)^{\mathrm{H}}\Big(\underline{\mathbf{D}}\,(\underline{\mathbf{H}}+\underline{\mathbf{E}})\,(\underline{\mathbf{H}}+\underline{\mathbf{E}})^{\mathrm{H}}\,\underline{\mathbf{D}}^{\mathrm{H}}\Big)^{-1}. \tag{33}$$

The tilde used in (33) and other equations in the following indicates that the respective quantity goes back to the imperfect estimate $\widehat{\underline{\mathbf{H}}}$ of the channel matrix $\underline{\mathbf{H}}$. $\widetilde{\underline{\mathbf{M}}}$ of (33) can generally be represented by an infinite Taylor series around the development point $\mathbf{0}$. Then,

$$\widetilde{\underline{\mathbf{M}}}=(\underline{\mathbf{D}}\,\underline{\mathbf{H}})^{\mathrm{H}}\,\underline{\mathbf{R}}_{\mathrm{B}}^{-1}+\sum_{i=1}^{KK_{\mathrm{M}}}\sum_{j=1}^{K_{\mathrm{B}}}\left[\left.\frac{\partial\widetilde{\underline{\mathbf{M}}}}{\partial\mathrm{Re}\left\{\underline{E}_{i,j}\right\}}\right|_{\underline{\mathbf{E}}=\mathbf{0}}\mathrm{Re}\left\{\underline{E}_{i,j}\right\}+\left.\frac{\partial\widetilde{\underline{\mathbf{M}}}}{\partial\mathrm{Im}\left\{\underline{E}_{i,j}\right\}}\right|_{\underline{\mathbf{E}}=\mathbf{0}}\mathrm{Im}\left\{\underline{E}_{i,j}\right\}\right]+\mathcal{O}(\underline{\mathbf{E}}^{2}) \tag{34}$$

holds, where $\mathcal{O}(\underline{\mathbf{E}}^{2})$ denotes higher-order elements of the Taylor series. If we consider small channel estimation errors – and this has to be the case, because we are focusing on high SNRs at the input of the MTs and low bit error probabilities $P_{\mathrm{b},n}$ of (26), which can only be achieved if the channel estimation errors are small compared to the elements of $\underline{\mathbf{H}}$ –, i.e., if σ_{h}^{2} is small compared to the components of $\underline{\mathbf{H}}$, $\widetilde{\underline{\mathbf{M}}}$ can be well approximated by (34), even if the Taylor series is truncated after the linear terms [16], i.e.,

$$\widetilde{\underline{\mathbf{M}}}\approx(\underline{\mathbf{D}}\,\underline{\mathbf{H}})^{\mathrm{H}}\,\underline{\mathbf{R}}_{\mathrm{B}}^{-1}+\sum_{i=1}^{KK_{\mathrm{M}}}\sum_{j=1}^{K_{\mathrm{B}}}\left[\left.\frac{\partial\widetilde{\underline{\mathbf{M}}}}{\partial\mathrm{Re}\left\{\underline{E}_{i,j}\right\}}\right|_{\underline{\mathbf{E}}=\mathbf{0}}\mathrm{Re}\left\{\underline{E}_{i,j}\right\}+\left.\frac{\partial\widetilde{\underline{\mathbf{M}}}}{\partial\mathrm{Im}\left\{\underline{E}_{i,j}\right\}}\right|_{\underline{\mathbf{E}}=\mathbf{0}}\mathrm{Im}\left\{\underline{E}_{i,j}\right\}\right]. \tag{35}$$

The calculation of the derivatives in (35) can be found in Appendix I. Using the results obtained therein, (35) can be rewritten as

$$\underline{\widetilde{\mathbf{M}}} = (\underline{\mathbf{D}}\,\underline{\mathbf{H}})^{\mathrm{H}}\,\underline{\mathbf{R}}_{\mathrm{B}}^{-1} + \underline{\mathbf{E}}^{\mathrm{H}}\underline{\mathbf{D}}^{\mathrm{H}}\underline{\mathbf{R}}_{\mathrm{B}}^{-1} - (\underline{\mathbf{D}}\,\underline{\mathbf{H}})^{\mathrm{H}}\,\underline{\mathbf{R}}_{\mathrm{B}}^{-1}\big(\underline{\mathbf{D}}\,\underline{\mathbf{E}}\,\underline{\mathbf{H}}^{\mathrm{H}}\underline{\mathbf{D}}^{\mathrm{H}} + \underline{\mathbf{D}}\,\underline{\mathbf{H}}\,\underline{\mathbf{E}}^{\mathrm{H}}\underline{\mathbf{D}}^{\mathrm{H}}\big)\,\underline{\mathbf{R}}_{\mathrm{B}}^{-1}. \tag{36}$$

Using $\underline{\widetilde{\mathbf{M}}}$ of (36), the performance of the Rx oriented data transmission based on TxZF is studied in the following, in a way analog to the procedure in Subsection III-B. With $\underline{\widetilde{\mathbf{M}}}$ of (36) one can calculate the estimate

$$\underline{\widetilde{\widehat{\mathbf{d}}}} = \underline{\mathbf{d}} - \underline{\mathbf{D}}\,\underline{\mathbf{E}}\,\underline{\mathbf{H}}^{\mathrm{H}}\,\underline{\mathbf{D}}^{\mathrm{H}}\underline{\mathbf{R}}_{\mathrm{B}}^{-1}\underline{\mathbf{d}} + \underline{\mathbf{D}}\,\underline{\mathbf{n}} \tag{37}$$

of (12), but now taking the imperfect channel knowledge into account. If $\underline{\mathbf{E}}$ and $\underline{\mathbf{n}}$ change randomly, but the data symbol $\underline{d}_n$ is fixed, then the estimate $\widetilde{\widehat{\underline{d}}}_n$ also changes randomly. (37) allows the conclusion that in this situation

$$\underset{\underline{\mathbf{E}},\underline{\mathbf{n}}}{\mathrm{E}}\left\{\widetilde{\widehat{\underline{d}}}_n \,\middle|\, \underline{d}_n\right\} = \underline{d}_n \tag{38}$$

holds. This means that even if the channel matrix $\underline{\mathbf{H}}$ is not perfectly known, the estimate $\widetilde{\widehat{\underline{d}}}_n$ of $\underline{d}_n$, $n=1\ldots N_{\mathrm{t}}$, is still unbiased, see the consideration in Subsection III-B. Setting out from (37) and (38) the estimation error

$$\underline{\widetilde{\boldsymbol{\varepsilon}}} = \underline{\widetilde{\widehat{\mathbf{d}}}} - \underline{\mathbf{d}} = -\underline{\mathbf{D}}\,\underline{\mathbf{E}}\,\underline{\mathbf{H}}^{\mathrm{H}}\underline{\mathbf{D}}^{\mathrm{H}}\underline{\mathbf{R}}_{\mathrm{B}}^{-1}\underline{\mathbf{d}} + \underline{\mathbf{D}}\,\underline{\mathbf{n}}. \tag{39}$$

of (18) is recalculated. $\underline{\widetilde{\boldsymbol{\varepsilon}}}$ of (39) describes the estimation error, if

- not $\underline{\mathbf{H}}$ but $\underline{\widehat{\mathbf{H}}}$ is used at the transmitter and
- the noise $\underline{\mathbf{n}}$ is present at the input of the MTs, see Fig. 1.

With $\underline{\widetilde{\boldsymbol{\varepsilon}}}$ of (39)

$$\underline{\widetilde{\mathbf{R}}}_{\varepsilon} = \underbrace{\underline{\mathbf{D}}\,\underline{\mathbf{R}}_{\mathrm{n}}\underline{\mathbf{D}}^{\mathrm{H}}}_{\underline{\widetilde{\mathbf{R}}}_{\varepsilon,\mathrm{n}}} + \underbrace{\underline{\mathbf{D}}\,\underline{\mathbf{D}}^{\mathrm{H}}\cdot\sigma_{\mathrm{h}}^2 E_{\mathrm{d}}\mathrm{trace}\left\{\underline{\mathbf{R}}_{\mathrm{B}}^{-1}\right\}}_{\underline{\widetilde{\mathbf{R}}}_{\varepsilon,\mathrm{i}}}. \tag{40}$$

follows for the covariance matrix $\underline{\widetilde{\mathbf{R}}}_{\varepsilon}$ of (19). The proof of (40) can be found in Appendix II. The result in (40) allows several conlusions:

- The estimation errors due to noise and imperfect channel knowledge are uncorrelated. Therefore, the covariance matrix $\underline{\widetilde{\mathbf{R}}}_{\varepsilon}$ is a superpostition of a partial matrix $\underline{\widetilde{\mathbf{R}}}_{\varepsilon,\mathrm{n}}$ related to noise and a partial matrix $\underline{\widetilde{\mathbf{R}}}_{\varepsilon,\mathrm{i}}$ related to imperfect channel knowledge.

- $\underline{\widetilde{\mathbf{R}}}_{\varepsilon,\mathrm{n}}$ is identical to $\underline{\mathbf{R}}_{\varepsilon}$ of (22) obtained in Section III for the case of perfect channel knowledge.
- The structure of the partial matrix $\underline{\widetilde{\mathbf{R}}}_{\varepsilon,\mathrm{i}}$ is only determined by the structure of $\underline{\mathbf{D}}$ of (11).
- $\underline{\widetilde{\mathbf{R}}}_{\varepsilon,\mathrm{i}}$ is proportional to σ_{h}^2 of (32) and E_{d} of (3). Therefore, the lower the accuracy of $\underline{\widehat{\mathbf{H}}}$, the larger the absolute values of the elements of $\underline{\widetilde{\mathbf{R}}}_{\varepsilon,\mathrm{i}}$.
- The scaling of $\underline{\widetilde{\mathbf{R}}}_{\varepsilon,\mathrm{i}}$ does not only depend on the statistical properties of the channel estimation error matrix $\underline{\mathbf{E}}$, but also on the channel under consideration itself.

To describe the quality of the obtained estimate $\underline{\widetilde{\widetilde{\mathbf{d}}}}$ of (37) in a concise form, one can resort to the SNIR $\widetilde{\gamma}_{\mathrm{o},n}$ of (20). Using (38) and (40), (20) yields

$$\widetilde{\gamma}_{\mathrm{o},n} = \frac{E_{\mathrm{d}}}{\left[\underline{\mathbf{D}}\,\underline{\mathbf{R}}_{\mathrm{n}}\,\underline{\mathbf{D}}^{\mathrm{H}}\right]_{n,n} + \left[\underline{\mathbf{D}}\,\underline{\mathbf{D}}^{\mathrm{H}}\right]_{n,n} \cdot \sigma_{\mathrm{h}}^2 E_{\mathrm{d}} \mathrm{trace}\left\{\underline{\mathbf{R}}_{\mathrm{B}}^{-1}\right\}}. \tag{41}$$

In analogy to the procedure in Subsection III-B, the mean symbol specific transmit energies T_n, $n=1\ldots N_{\mathrm{t}}$, of (13) are studied in the following. Having in mind that we are now considering the case of imperfect channel knowledge, where an additional random quantity $\underline{\mathbf{E}}$ comes into the play, the definition of the mean symbol specific transmit energy T_n, $n=1\ldots N_{\mathrm{t}}$, of (13) has to be thought about again: $\underline{\widetilde{\mathbf{M}}}$ is a function of $\underline{\mathbf{E}}$. Therefore, according to (13), T_n would also be a function of $\underline{\mathbf{E}}$ and, consequently, a random variable with a certain distribution. In the following we are only interested in the expectation

$$\widetilde{T}_n = E_{\mathrm{d}} \underset{\underline{\mathbf{E}}}{\mathrm{E}}\left\{\left[\underline{\widetilde{\mathbf{M}}}^{\mathrm{H}}\underline{\widetilde{\mathbf{M}}}\right]_{n,n}\right\} = E_{\mathrm{d}}\left[\underset{\underline{\mathbf{E}}}{\mathrm{E}}\left\{\underline{\widetilde{\mathbf{M}}}^{\mathrm{H}}\underline{\widetilde{\mathbf{M}}}\right\}\right]_{n,n} \tag{42}$$

with respect to $\underline{\mathbf{E}}$ of this random variable which, for reasons of simplicity, is referred to as mean symbol transmit energy $\widetilde{T}_n$ in the following. Using $\underline{\widetilde{\mathbf{M}}}$ of (36) and the definition of $\widetilde{T}_n$ of (42) one obtains after some calculations detailed in Appendix III

$$\widetilde{T}_n = \left[\underline{\mathbf{R}}_{\mathrm{B}}^{-1}\right]_{n,n}\left[1+\sigma_{\mathrm{h}}^2\mathrm{trace}\left\{\underline{\mathbf{R}}_{\mathrm{B}}^{-1}\underline{\mathbf{D}}\,\underline{\mathbf{D}}^{\mathrm{H}}\right\}\right]E_{\mathrm{d}} + \left[\underline{\mathbf{R}}_{\mathrm{B}}^{-1}\underline{\mathbf{D}}\,\underline{\mathbf{D}}^{\mathrm{H}}\underline{\mathbf{R}}_{\mathrm{B}}^{-1}\right]_{n,n} \cdot \sigma_{\mathrm{h}}^2 (K_{\mathrm{B}}-N_{\mathrm{t}})E_{\mathrm{d}}. \tag{43}$$

Comparing T_n of (24) and $\widetilde{T}_n$ of (43) the ratio

$$\widetilde{T}_n/T_n = 1+\sigma_{\mathrm{h}}^2\mathrm{trace}\left\{\underline{\mathbf{R}}_{\mathrm{B}}^{-1}\underline{\mathbf{D}}\,\underline{\mathbf{D}}^{\mathrm{H}}\right\} + \frac{\left[\underline{\mathbf{R}}_{\mathrm{B}}^{-1}\underline{\mathbf{D}}\,\underline{\mathbf{D}}^{\mathrm{H}}\underline{\mathbf{R}}_{\mathrm{B}}^{-1}\right]_{n,n}}{\left[\underline{\mathbf{R}}_{\mathrm{B}}^{-1}\right]_{n,n}} \cdot \sigma_{\mathrm{h}}^2 (K_{\mathrm{B}}-N_{\mathrm{t}}) \tag{44}$$

can be introduced, which describes the extent to which the mean symbol specific transmit energy T_n is influenced, when coming from the case of perfect channel knownledge to the case of imperfect channel knowledge at the transmitter. (44) allows some quite interesting conclusions:

- $\widetilde{T}_n/T_n$ is always larger than or equal to one. Therefore, – if the assumptions for $\underline{\mathbf{E}}$ made in Subsection IV-A hold and if unbiased TxZF based data transmission is considered – in the case of imperfect channel knowledge always higher mean symbol specific transmit energies $\widetilde{T}_n$, $n = 1 \dots N_\mathrm{t}$, are needed than in the case of perfect channel knowledge.
- The relative increase $\widetilde{T}_n/T_n - 1$ is proportional to the variance σ_h^2 of the elements of the channel estimation error matrix $\underline{\mathbf{E}}$ of (31) and, moreover, depends on the considered channel matrix $\underline{\mathbf{H}}$ and the chosen demodulator matrix $\underline{\mathbf{D}}$.

A question still open is the interdependence between the mean symbol specific transmit energy $\widetilde{T}_n$ of (43) and the quality of the estimate $\underline{\widetilde{\widetilde{\mathbf{d}}}}$ of (37). To describe this quality, the SNIR $\widetilde{\gamma}_{\mathrm{o},n}$ of (41) is an appropriate measure. Using (43) to substitute E_d in (41), the SNIR $\widetilde{\gamma}_{\mathrm{o},n}$ of (41) reads

$$\widetilde{\gamma}_{\mathrm{o},n} = \widetilde{T}_n \Big/ \Bigg(\left[\underline{\mathbf{D}}\,\underline{\mathbf{R}}_\mathrm{n}\,\underline{\mathbf{D}}^\mathrm{H}\right]_{n,n} \Big(\left[\underline{\mathbf{R}}_\mathrm{B}^{-1}\right]_{n,n} \cdot \left[1 + \sigma_\mathrm{h}^2 \mathrm{trace}\left\{\underline{\mathbf{R}}_\mathrm{B}^{-1}\underline{\mathbf{D}}\,\underline{\mathbf{D}}^\mathrm{H}\right\}\right] + \left[\underline{\mathbf{R}}_\mathrm{B}^{-1}\underline{\mathbf{D}}\,\underline{\mathbf{D}}^\mathrm{H}\underline{\mathbf{R}}_\mathrm{B}^{-1}\right]_{n,n} \cdot \sigma_\mathrm{h}^2 (K_\mathrm{B} - N_\mathrm{t}) \Big) + \left[\underline{\mathbf{D}}\,\underline{\mathbf{D}}^\mathrm{H}\right]_{n,n} \sigma_\mathrm{h}^2 \widetilde{T}_n \mathrm{trace}\left\{\underline{\mathbf{R}}_\mathrm{B}^{-1}\right\} \Bigg). \tag{45}$$

(45) shows an important difference to $\gamma_{\mathrm{o},n}$ of (23) obtained for the case of perfect channel knowledge: even if $\widetilde{T}_n$ is very large – or mathematically speaking if $\widetilde{T}_n$ goes towards infinity –, $\widetilde{\gamma}_{\mathrm{o},n}$ of (45) is limited by the upper bound

$$\widetilde{\gamma}_{\mathrm{o},n}^{\infty} = \lim_{\widetilde{T}_n \to \infty} \widetilde{\gamma}_{\mathrm{o},n} = \frac{1}{\left[\underline{\mathbf{D}}\,\underline{\mathbf{D}}^\mathrm{H}\right]_{n,n} \sigma_\mathrm{h}^2 \mathrm{trace}\left\{\underline{\mathbf{R}}_\mathrm{B}^{-1}\right\}}. \tag{46}$$

$\widetilde{\gamma}_{\mathrm{o},n}^{\infty}$ of (46) depends on the variance σ_h^2 of the elements $\underline{E}_{i,j}$ of $\underline{\mathbf{E}}$ – and, therefore, the quality of the estimate $\underline{\widehat{\mathbf{H}}}$ of the channel matrix $\underline{\mathbf{H}}$ –, on the channel matrix $\underline{\mathbf{H}}$ itself and on the demodulator matrix $\underline{\mathbf{D}}$. If we further assume that the elements $\underline{E}_{i,j}$ of $\underline{\mathbf{E}}$ satisfy a Gaussian probability distribution – and this is the case if joint channel estimation in the sense of Subsection IV-A is applied to obtain $\underline{\widehat{\mathbf{H}}}$ –, then based on (45) the bit error probability can be analyzed in a closed form. For reasons of simplicity we consider again the case of QPSK symbol modulation introduced in Subsection III-B. With the above mentioned assumptions the elements of the estimation error $\underline{\widetilde{\boldsymbol{\varepsilon}}}$ of (39) satisfy a Gaussian probability distribution. Consequently, the bit error probability $\widetilde{P}_{\mathrm{b},n}$ of the bits carried by the data symbol $\underline{d}_n$, $n = 1 \dots N_\mathrm{t}$, can be immediately calculated using (45) to be

$$\widetilde{P}_{\mathrm{b},n} = \frac{1}{2}\mathrm{erfc}\left(\sqrt{\frac{\widetilde{\gamma}_{\mathrm{o},n}}{2}}\right). \tag{47}$$

With the observation that $\widetilde{\gamma}_{\mathrm{o},n}$ is limited by the upper bound $\widetilde{\gamma}_{\mathrm{o},n}^{\infty}$ of (46), $\widetilde{P}_{\mathrm{b},n}$ is lower bounded by the minimum bit error probability

$$\widetilde{P}_{\mathrm{b},n}^{\infty}=\lim_{\widetilde{T}_n\to\infty}\widetilde{P}_{\mathrm{b},n}=\frac{1}{2}\mathrm{erfc}\left(\sqrt{\frac{1}{2\left[\underline{\mathbf{D}}\,\underline{\mathbf{D}}^{\mathrm{H}}\right]_{n,n}\sigma_{\mathrm{h}}^2\mathrm{trace}\left\{\underline{\mathbf{R}}_{\mathrm{B}}^{-1}\right\}}}\right). \tag{48}$$

For high $\widetilde{T}_n$, $\widetilde{P}_{\mathrm{b},n}$ converges towards the lower bound $\widetilde{P}_{\mathrm{b},n}^{\infty}$ of (48) resulting in an error-floor. This observation is well known and understood for Tx oriented data transmission [9], [10], but up to now still not analytically studied for Rx oriented data transmission. (47) and (48) are the first available analytical answers to this question raised in Section I.

For the special case of white Gaussian noise $\underline{\mathbf{n}}$, which is already considered in Subsection III-B and with the PSNR

$$\widetilde{\gamma}_{\mathrm{i},n}=\frac{\widetilde{T}_n}{\sigma^2}, \tag{49}$$

which is related to $\gamma_{\mathrm{i},n}$ of (27), but which takes the mean symbol specific transmit energy $\widetilde{T}_n$ of (42) into account, $\widetilde{P}_{\mathrm{b},n}$ of (47) reads

$$\begin{aligned}\widetilde{P}_{\mathrm{b},n}=\frac{1}{2}\mathrm{erfc}\Bigg(\Bigg(\widetilde{\gamma}_{\mathrm{i},n}\Bigg/\Bigg(2\left[\underline{\mathbf{D}}\,\underline{\mathbf{D}}^{\mathrm{H}}\right]_{n,n}\Big(\left[\underline{\mathbf{R}}_{\mathrm{B}}^{-1}\right]_{n,n}\cdot\left[1+\sigma_{\mathrm{h}}^2\mathrm{trace}\left\{\underline{\mathbf{R}}_{\mathrm{B}}^{-1}\underline{\mathbf{D}}\,\underline{\mathbf{D}}^{\mathrm{H}}\right\}\right]+\left[\underline{\mathbf{R}}_{\mathrm{B}}^{-1}\underline{\mathbf{D}}\,\underline{\mathbf{D}}^{\mathrm{H}}\underline{\mathbf{R}}_{\mathrm{B}}^{-1}\right]_{n,n}\\ \cdot\sigma_{\mathrm{h}}^2(K_{\mathrm{B}}-N_{\mathrm{t}})\Big)+2\left[\underline{\mathbf{D}}\,\underline{\mathbf{D}}^{\mathrm{H}}\right]_{n,n}\sigma_{\mathrm{h}}^2\widetilde{\gamma}_{\mathrm{i},n}\mathrm{trace}\left\{\underline{\mathbf{R}}_{\mathrm{B}}^{-1}\right\}\Bigg)\Bigg)^{\frac{1}{2}}\Bigg).\end{aligned} \tag{50}$$

Comparing (29) and (50) the degradation due to the imperfect knowledge of $\underline{\mathbf{H}}$ at the transmitter can be quantified: To achieve a certain bit error probability

$$P_{\mathrm{b},n}=\widetilde{P}_{\mathrm{b},n} \tag{51}$$

in a situation with a fixed channel matrix $\underline{\mathbf{H}}$ and fixed demodulator matrix $\underline{\mathbf{D}}$, on the one hand in the case of perfect channel knowledge and, on the other hand, in the case of imperfect channel knowledge, respectively, in general different PSNRs $\gamma_{\mathrm{i},n}$ and $\widetilde{\gamma}_{\mathrm{i},n}$, respectively, are required. By equating (29) and (50) it follows that in both cases the same bit error probability is obtained if

$$\begin{aligned}\widetilde{\gamma}_{\mathrm{i},n}=&\Big(\left[\underline{\mathbf{R}}_{\mathrm{B}}^{-1}\right]_{n,n}\left[1+\sigma_{\mathrm{h}}^2\mathrm{trace}\left\{\underline{\mathbf{R}}_{\mathrm{B}}^{-1}\underline{\mathbf{D}}\,\underline{\mathbf{D}}^{\mathrm{H}}\right\}\right]+\left[\underline{\mathbf{R}}_{\mathrm{B}}^{-1}\underline{\mathbf{D}}\,\underline{\mathbf{D}}^{\mathrm{H}}\underline{\mathbf{R}}_{\mathrm{B}}^{-1}\right]_{n,n}\sigma_{\mathrm{h}}^2(K_{\mathrm{B}}-N_{\mathrm{t}})\Big)\gamma_{\mathrm{i},n}\\ &\Big/\Big(\left[\underline{\mathbf{R}}_{\mathrm{B}}^{-1}\right]_{n,n}-\sigma_{\mathrm{h}}^2\gamma_{\mathrm{i},n}\mathrm{trace}\left\{\underline{\mathbf{R}}_{\mathrm{B}}^{-1}\right\}\Big)\end{aligned} \tag{52}$$

is chosen. (52) allows several conclusions:

- $\widetilde{\gamma}_{\mathrm{i},n}$ of (52) is always larger than $\gamma_{\mathrm{i},n}$. Therefore, as expected, imperfect channel knowledge only leads to a degraded transmission quality or, equivalently, to an increased necessary PSNR $\widetilde{\gamma}_{\mathrm{i},n}$.
- Only if the denominator in (52) is positive, i.e., if

$$\frac{\left[\underline{\mathbf{R}}_{\mathrm{B}}^{-1}\right]_{n,n}}{\operatorname{trace}\left\{\underline{\mathbf{R}}_{\mathrm{B}}^{-1}\right\}} > \sigma_{\mathrm{h}}^2 \gamma_{\mathrm{i},n} \tag{53}$$

  holds, a PSNR $\widetilde{\gamma}_{\mathrm{i},n}$ can be found which leads in the case of imperfect channel knowledge to the same bit error probability as the PSNR $\gamma_{\mathrm{i},n}$ in the case of perfectly known channel matrix $\underline{\mathbf{H}}$.

The relation (52) can be considered as one of the central results of this paper. Because – setting out from an Rx oriented transmission system where perfect channel knowledge is available and a certain $\gamma_{\mathrm{i},n}$ is utilized – this relation directly allows to calculate which increased $\widetilde{\gamma}_{\mathrm{i},n}$ has to be invested to achieve the same transmission performance. Therefore, (52) quantifies the price to be paid due to the imperfect channel knowledge – and this is the answer to one of the central questions posed in this contribution.

V. Influence of imperfect channel knowledge on the transmission performance: the special case

A. Model and assumptions

In Section IV basic relations between the performance of TxZF based Rx oriented transmission and imperfect channel knowledge at the transmitter have been worked out. These results are quite general and – as long as the assumptions described in Section IV hold – are valid for all kinds of channels. In the further study these analytical results should be briefly illustrated for an exemplary quite simple scenario and validated by some simulations. In the following, we look at the situation, where we have K_{B} equal to N_{t} transmit antennas at the AP, and in total N_{t} data symbols are transmitted. Altogether the K MTs introduced in Section II are equipped with N_{t} receive antennas. The demodulator matrices $\underline{\mathbf{D}}^{(k)}$ of the MTs k, $k = 1 \ldots K$, are chosen to be identity matrices, so that the total demodulator matrix $\underline{\mathbf{D}}$ also becomes the identity matrix of dimension $N_{\mathrm{t}} \times N_{\mathrm{t}}$. The total noise signal $\underline{\mathbf{n}}$ of (7) over all receive antennas of the K MTs is assumed to be white with the covariance matrix $\underline{\mathbf{R}}_{\mathrm{n}}$ introduced in Subsection III-B. To allow a fundamental analysis of the dominant effect when considering imperfect channel knowledge, the channel matrix $\underline{\mathbf{H}}$ is chosen according to the very simple parametric ρ-model introduced in [10] for basic studies, i.e.

$$\underline{\mathbf{H}} = \left(\underline{H}_{i,j}\right), \quad \underline{H}_{i,j} = \begin{cases} 1/\sqrt{1+(N_\mathrm{t}-1)x^2}, & i=j, \\ x/\sqrt{1+(N_\mathrm{t}-1)x^2}, & i \neq j, \end{cases}, x \in [-1 \dots 1[. \tag{54}$$

It is well known that $\underline{\mathbf{H}}$ of (54) massively differs from channel matrices describing real-world channels. However, the authors have the opinion that using such a simple model, which allows to analyze both channels with severe cross-talk –, i.e., $|x|$ is close to one – and without cross-talk –, i.e., x equal to zero – is favorable for basic studies. To describe the quality of the estimate $\widehat{\underline{\mathbf{H}}}$ of (30) the average signal-to-noise-ratio

$$\gamma_\mathrm{h} = \frac{1}{N_\mathrm{t}\sigma_\mathrm{h}^2} \tag{55}$$

of the individual elements of $\widehat{\underline{\mathbf{H}}}$ is introduced.

B. Analytical performance evaluation

Using the assumption for $\underline{\mathbf{D}}$ and $\underline{\mathbf{R}}_\mathrm{n}$ detailed above $\widetilde{\underline{\mathbf{R}}}_\varepsilon$ of (40) can be simplified to

$$\widetilde{\underline{\mathbf{R}}}_\varepsilon = \left(\sigma^2 + \sigma_\mathrm{h}^2 E_\mathrm{d} \mathrm{trace}\left\{\left(\underline{\mathbf{H}}\,\underline{\mathbf{H}}^\mathrm{H}\right)^{-1}\right\}\right)\mathbf{I}^{(N_\mathrm{t})}. \tag{56}$$

For the matrix product $\underline{\mathbf{H}}\,\underline{\mathbf{H}}^\mathrm{H}$ in (56) follows with (54)

$$\left[\underline{\mathbf{H}}\,\underline{\mathbf{H}}^\mathrm{H}\right]_{n,n'} = \begin{cases} 1, & n=n', \\ \rho, & n \neq n', \end{cases} \quad n,n' = 1 \dots N_\mathrm{t}, \rho = \frac{2x+(N_\mathrm{t}-2)x^2}{1+(N_\mathrm{t}-1)x^2}, 0 \leq \rho \leq 1, \tag{57}$$

where ρ is the cross-correlation coefficient between two different rows of $\underline{\mathbf{H}}$ of (54). The inverse of $\left(\underline{\mathbf{H}}\,\underline{\mathbf{H}}^\mathrm{H}\right)$ of (57) can be determined to be

$$\left[\left(\underline{\mathbf{H}}\,\underline{\mathbf{H}}^\mathrm{H}\right)^{-1}\right]_{n,n'} = \begin{cases} \overbrace{(1+(N_\mathrm{t}-2)\rho)/(1+(N_\mathrm{t}-2)\rho-(N_\mathrm{t}-1)\rho^2)}^{\xi}, & n=n', \\ -\rho/(1+(N_\mathrm{t}-2)\rho-(N_\mathrm{t}-1)\rho^2), & n \neq n'. \end{cases} \tag{58}$$

Substituting (55) and (58) in (56) yields for the covariance matrix

$$\widetilde{\underline{\mathbf{R}}}_\varepsilon = \left(\sigma^2 + \frac{1}{\gamma_\mathrm{h}} E_\mathrm{d} \frac{1+(N_\mathrm{t}-2)\rho}{1+(N_\mathrm{t}-2)\rho-(N_\mathrm{t}-1)\rho^2}\right)\mathbf{I}^{(N_\mathrm{t})} \tag{59}$$

of the estimation error $\widetilde{\underline{\boldsymbol{\varepsilon}}}$ of (39). Using (59) the SNIR $\widetilde{\gamma}_{\mathrm{o},n}$ at the output of the demodulator reads

$$\widetilde{\gamma}_{\mathrm{o},n} = \frac{E_\mathrm{d}}{\sigma^2 + \frac{1}{\gamma_\mathrm{h}} E_\mathrm{d} \frac{1+(N_\mathrm{t}-2)\rho}{1+(N_\mathrm{t}-2)\rho-(N_\mathrm{t}-1)\rho^2}}. \tag{60}$$

For the case that a fixed E_{d} is considered, (60) allows the following conclusions:

- Increasing γ_{h} and decreasing σ^2 leads to an increase of $\widetilde{\gamma}_{\mathrm{o},n}$.
- If the number N_{t} of data symbols is increased, $\widetilde{\gamma}_{\mathrm{o},n}$ decreases – which is due to the fact that one has to accept interference originating in an increasing number of data symbols if imperfect channel knowledge is considered – and asymptotically converges to the lower bound

$$\widetilde{\gamma}_{\mathrm{o},n}^{\mathrm{min}} = \lim_{N_{\mathrm{t}}\to\infty} \widetilde{\gamma}_{\mathrm{o},n} = \frac{E_{\mathrm{d}}}{\sigma^2 + \frac{1}{\gamma_{\mathrm{h}}}\frac{1}{1-\rho}E_{\mathrm{d}}}. \tag{61}$$

- Increasing $|\rho|$ results in a decrease of $\widetilde{\gamma}_{\mathrm{o},n}$.

As explained in detail in Section IV, $\widetilde{\gamma}_{\mathrm{o},n}$ of (60) can only be obtained by – compared to the case of perfect channel knowledge – an increased mean symbol specific transmit energy

$$\widetilde{T}_n = \xi E_{\mathrm{d}}\left(1 + \frac{1}{\gamma_{\mathrm{h}}}\xi\right). \tag{62}$$

For the factor $\widetilde{T}_n/T_n$ of (44) describing this increase,

$$\widetilde{T}_n/T_n = 1 + \frac{1}{\gamma_{\mathrm{h}}}\frac{1-(N_{\mathrm{t}}-2)\rho}{1+(N_{\mathrm{t}}-2)\rho-(N_{\mathrm{t}}-1)\rho^2} \tag{63}$$

holds. (63) implies the following consequences:

- $\widetilde{T}_n/T_n$ is – as already stated in Section IV – always larger than or equal to one.
- $\widetilde{T}_n/T_n$ decreases with increasing γ_{h}, i.e., the more accurate the estimate $\underline{\widehat{\mathbf{H}}}$ of $\underline{\mathbf{H}}$, the less transmit energy increase has to be accepted.
- For large N_{t} the ratio $\widetilde{T}_n/T_n$ of (63) increases, converging to the asymptotic upper limit

$$\lim_{N_{\mathrm{t}}\to\infty} \widetilde{T}_n/T_n = 1 + \frac{1}{\gamma_{\mathrm{h}}}\frac{1}{1-\rho}. \tag{64}$$

Using (49), (62) and ξ of (58) one obtains

$$\widetilde{\gamma}_{\mathrm{o},n} = \frac{\widetilde{\gamma}_{\mathrm{i},n}\gamma_{\mathrm{h}}}{\xi(\widetilde{\gamma}_{\mathrm{i},n}+\gamma_{\mathrm{h}})+\xi^2} \tag{65}$$

for the SNIR of (60) at the output of the demodulator, where ξ is chosen according to (58). For comparison,

$$\gamma_{\mathrm{o},n} = \frac{\gamma_{\mathrm{i},n}}{\xi} \tag{66}$$

would be the output SNIR if perfect channel knowledge would be available, c.f. (25). (65) discloses:

- If $\widetilde{\gamma}_{\mathrm{i},n}$ is very large, then $\widetilde{\gamma}_{\mathrm{o},n}$ converges to the upper limit γ_{h}/ξ.
- If γ_{h} increases, $\widetilde{\gamma}_{\mathrm{o},n}$ of (65) also increases, converging towards the upper limit $\widetilde{\gamma}_{\mathrm{i},n}/\xi$, c.f. (66).

On the other hand, comparing (65) and (66) allows us an interesting insight into Rx oriented transmission systems: We consider two Rx oriented transmission systems based on TxZF, where in the first system (system 1) perfect channel knowledge is available at the transmitter, and we achieve with a given $\gamma_{\mathrm{i},n}$ a certain $\gamma_{\mathrm{o},n}$. The second system (system 2) suffers from imperfect channel knowledge. Therefore, we achieve with a given $\widetilde{\gamma}_{\mathrm{i},n}$ a certain $\widetilde{\gamma}_{\mathrm{o},n}$. Then, if we want to achieve the same $\gamma_{\mathrm{o},n}$ and $\widetilde{\gamma}_{\mathrm{o},n}$ with both systems, we can express the necessary

$$\widetilde{\gamma}_{\mathrm{i},n} = \frac{\gamma_{\mathrm{i},n}(\gamma_{\mathrm{h}} + \xi)}{\gamma_{\mathrm{h}} - \gamma_{\mathrm{i},n}} \tag{67}$$

in system 2 as a function of $\gamma_{\mathrm{i},n}$ in system 1. A sufficiently high $\widetilde{\gamma}_{\mathrm{i},n}$ of (67) can only be found, if γ_{h} is larger than $\gamma_{\mathrm{i},n}$. Considering (67) from a different point of view, one can find

$$\gamma_{\mathrm{i},n} = \frac{\widetilde{\gamma}_{\mathrm{i},n}\gamma_{\mathrm{h}}}{\widetilde{\gamma}_{\mathrm{i},n} + \gamma_{\mathrm{h}} + \xi}. \tag{68}$$

$\gamma_{\mathrm{i},n}$ of (68) is this PSNR of system 1 which is equivalent – with respect to $\gamma_{\mathrm{o},n}$ and $\widetilde{\gamma}_{\mathrm{o},n}$, respectively – to $\widetilde{\gamma}_{\mathrm{i},n}$ in system 2. (68) is a quite interesting result, because for the considered case of small channel estimation errors, see Subsection IV-B, where γ_{h} is high compared to ξ, the equivalent PSNR $\gamma_{\mathrm{i},n}$ of (68) is the harmonic mean of the PSNR $\widetilde{\gamma}_{\mathrm{i},n}$ in the Rx oriented transmission system with imperfect channel knowledge at the transmitter and the SNR γ_{h} of the estimate $\underline{\widehat{\mathbf{H}}}$ of the channel matrix $\underline{\mathbf{H}}$. Fig.2 shows the relation of (68) for x equal to 0.4 and N_{t} equal to 4. One can observe that with increasing $\widetilde{\gamma}_{\mathrm{i},n}$ the equivalent $\gamma_{\mathrm{i},n}$ converges to an upper limit γ_{h}.

To complete the picture of the transmission quality in the exemplary Rx oriented data transmission system considered in this section, in the following an analysis of the bit error probability in the respective system is presented. The aim of this study is, on the one hand, to get an impression of the quality of the estimate $\underline{\widetilde{\widetilde{\mathbf{d}}}}$ of (37) in terms of bit error probabilities and, on the other hand, to allow an assessment of the accuracy of the analytical expressions presented in this paper by comparing analytically obtained results with simulation results. Considering again the case of QPSK symbol modulation introduced in Subsection III-B and also used in Subsection IV-B, the bit error probability of the two bits combined in data symbol $\underline{d}_n$, $n=1\ldots N_\mathrm{t}$, can be directly calculated based on (50), leading to

$$\widetilde{P}_{\mathrm{b},n} = \frac{1}{2}\mathrm{erfc}\left(\sqrt{\frac{1}{2}\frac{\widetilde{\gamma}_{\mathrm{i},n}\gamma_\mathrm{h}}{\xi(\widetilde{\gamma}_{\mathrm{i},n}+\gamma_\mathrm{h})+\xi^2}}\right). \tag{69}$$

Figs. 3 and 4 show $\widetilde{P}_{\mathrm{b},n}$ of (69) for N_t equal to 4 and x equal to 0.0 and 0.4, respectively. To get an impression of the accuracy of the analytical results derived in this contribution also simulation results are shown. These results follow from Monte-Carlo simulations comprising 100000 individual experiments. In each experiment

- $\underline{\widehat{\mathbf{H}}}$ is randomly generated according to (54) and (30),
- $\underline{\widetilde{\mathbf{M}}}$ is calculated according to (33), i.e., no Taylor approximation is made,
- $\underline{\mathbf{n}}$ and $\underline{\mathbf{d}}$ are randomly generated according to the models defined in Section III and
- the number of erroneously detected bits and totally transmitted bits is logged.

The analytical results are depicted in Figs. 3 and 4 by lines, where the markers represent the simulation results. Comparing the curves in Figs. 3 and 4, respectively, one observes that the Taylor based analysis presented in this contribution yields a good approximation of the performance of the Rx oriented transmission scheme under consideration. Although the above described example is quite simple, it can be expected that – as long as the assumptions described in Section IV hold – the observations made can be verified in more complex scenarios. It will be the topic of an additional paper to clarify this aspect.

APPENDIX I
DERIVATION OF THE LINEAR TAYLOR EXPANSION OF $\underline{\widetilde{\mathbf{M}}}$

In the following for $\underline{\mathbf{E}}$ equal to $\mathbf{0}$ the derivatives $\partial\underline{\widetilde{\mathbf{M}}}/\partial\mathrm{Re}\left\{\underline{E}_{i,j}\right\}$ and $\partial\underline{\widetilde{\mathbf{M}}}/\partial\mathrm{Im}\left\{\underline{E}_{i,j}\right\}$ contributing to (34) and (35) are derived. With (33) one obtains

$$\left.\frac{\partial\underline{\widetilde{\mathbf{M}}}}{\partial\mathrm{Re}\left\{\underline{E}_{i,j}\right\}}\right|_{\underline{\mathbf{E}}=\mathbf{0}} = \left.\frac{\partial\left(\left(\underline{\mathbf{D}}(\underline{\mathbf{H}}+\underline{\mathbf{E}})\right)^\mathrm{H}\right)}{\partial\mathrm{Re}\left\{\underline{E}_{i,j}\right\}}\right|_{\underline{\mathbf{E}}=\mathbf{0}} \underline{\mathbf{R}}_\mathrm{B}^{-1} + \left(\underline{\mathbf{D}}\,\underline{\mathbf{H}}\right)^\mathrm{H} \left.\frac{\partial\left(\left(\underline{\mathbf{D}}(\underline{\mathbf{H}}+\underline{\mathbf{E}})(\underline{\mathbf{H}}+\underline{\mathbf{E}})^\mathrm{H}\underline{\mathbf{D}}^\mathrm{H}\right)^{-1}\right)}{\partial\mathrm{Re}\left\{\underline{E}_{i,j}\right\}}\right|_{\underline{\mathbf{E}}=\mathbf{0}}. \tag{70}$$

Using the notation

$$\mathbf{1}_{i,j} = \left(\alpha_{\mu,\nu}\right), \mu = 1\ldots KK_\mathrm{M}, \nu = 1\ldots K_\mathrm{B}, \alpha_{\mu,\nu} = \begin{cases} 1 & \mu = i \wedge \nu = j, \\ 0 & \text{else,} \end{cases} \tag{71}$$

the first term in (70) reads

$$\left.\frac{\partial\left((\underline{\mathbf{D}}(\underline{\mathbf{H}}+\underline{\mathbf{E}}))^{\mathrm{H}}\right)}{\partial\mathrm{Re}\left\{\underline{E}_{i,j}\right\}}\right|_{\underline{\mathbf{E}}=\mathbf{0}} = \mathbf{1}_{i,j}^{\mathrm{H}}\underline{\mathbf{D}}^{\mathrm{H}}. \tag{72}$$

Using the relation [19]

$$\frac{\partial\left(\underline{\mathbf{A}}^{-1}\right)}{\partial z} = -\underline{\mathbf{A}}^{-1}\frac{\partial\underline{\mathbf{A}}}{\partial z}\underline{\mathbf{A}}^{-1}, \tag{73}$$

where $\underline{\mathbf{A}}$ is a full-rank square matrix and z a real-valued scalar, the second derivative in (70) is simplified to

$$\left.\frac{\partial\left(\left(\underline{\mathbf{D}}(\underline{\mathbf{H}}+\underline{\mathbf{E}})(\underline{\mathbf{H}}+\underline{\mathbf{E}})^{\mathrm{H}}\underline{\mathbf{D}}^{\mathrm{H}}\right)^{-1}\right)}{\partial\mathrm{Re}\left\{\underline{E}_{i,j}\right\}}\right|_{\underline{\mathbf{E}}=\mathbf{0}} = -\underline{\mathbf{R}}_{\mathrm{B}}^{-1}\left(\underline{\mathbf{D}}\,\mathbf{1}_{i,j}\,\underline{\mathbf{H}}^{\mathrm{H}}\underline{\mathbf{D}}^{\mathrm{H}}+\underline{\mathbf{D}}\,\underline{\mathbf{H}}\,\mathbf{1}_{i,j}^{\mathrm{H}}\underline{\mathbf{D}}^{\mathrm{H}}\right)\underline{\mathbf{R}}_{\mathrm{B}}^{-1}. \tag{74}$$

Substituting (72) and (74) in (70) one obtains

$$\left.\frac{\partial\widetilde{\underline{\mathbf{M}}}}{\partial\mathrm{Re}\left\{\underline{E}_{i,j}\right\}}\right|_{\underline{\mathbf{E}}=\mathbf{0}} = \mathbf{1}_{i,j}^{\mathrm{H}}\underline{\mathbf{D}}^{\mathrm{H}}\underline{\mathbf{R}}_{\mathrm{B}}^{-1}-(\underline{\mathbf{D}}\,\underline{\mathbf{H}})^{\mathrm{H}}\,\underline{\mathbf{R}}_{\mathrm{B}}^{-1}\left(\underline{\mathbf{D}}\,\mathbf{1}_{i,j}\,\underline{\mathbf{H}}^{\mathrm{H}}\underline{\mathbf{D}}^{\mathrm{H}}+\underline{\mathbf{D}}\,\underline{\mathbf{H}}\,\mathbf{1}_{i,j}^{\mathrm{H}}\underline{\mathbf{D}}^{\mathrm{H}}\right)\underline{\mathbf{R}}_{\mathrm{B}}^{-1}. \tag{75}$$

In analogy to (75) the derivative

$$\left.\frac{\partial\widetilde{\underline{\mathbf{M}}}}{\partial\mathrm{Im}\left\{\underline{E}_{i,j}\right\}}\right|_{\underline{\mathbf{E}}=\mathbf{0}} = -\mathrm{j}\mathbf{1}_{i,j}^{\mathrm{H}}\underline{\mathbf{D}}^{\mathrm{H}}\underline{\mathbf{R}}_{\mathrm{B}}^{-1}-\mathrm{j}\,(\underline{\mathbf{D}}\,\underline{\mathbf{H}})^{\mathrm{H}}\,\underline{\mathbf{R}}_{\mathrm{B}}^{-1}\left(\underline{\mathbf{D}}\,\mathbf{1}_{i,j}\,\underline{\mathbf{H}}^{\mathrm{H}}\underline{\mathbf{D}}^{\mathrm{H}}-\underline{\mathbf{D}}\,\underline{\mathbf{H}}\,\mathbf{1}_{i,j}^{\mathrm{H}}\underline{\mathbf{D}}^{\mathrm{H}}\right)\underline{\mathbf{R}}_{\mathrm{B}}^{-1} \tag{76}$$

can be calculated straight forward. Substituting (75) and (76) in (35) yields

$$\begin{aligned}\widetilde{\underline{\mathbf{M}}} \;\approx\;& (\underline{\mathbf{D}}\,\underline{\mathbf{H}})^{\mathrm{H}}\,\underline{\mathbf{R}}_{\mathrm{B}}^{-1}+\sum_{\forall i,j}\mathbf{1}_{i,j}^{\mathrm{H}}\underline{E}_{i,j}^{*}\underline{\mathbf{D}}^{\mathrm{H}}\underline{\mathbf{R}}_{\mathrm{B}}^{-1}-(\underline{\mathbf{D}}\,\underline{\mathbf{H}})^{\mathrm{H}}\,\underline{\mathbf{R}}_{\mathrm{B}}^{-1}\Big(\underline{\mathbf{D}}\sum_{\forall i,j}\mathbf{1}_{i,j}\underline{E}_{i,j}\underline{\mathbf{H}}^{\mathrm{H}}\underline{\mathbf{D}}^{\mathrm{H}}\\ &+\underline{\mathbf{D}}\,\underline{\mathbf{H}}\sum_{\forall i,j}\mathbf{1}_{i,j}^{\mathrm{H}}\underline{E}_{i,j}^{*}\underline{\mathbf{D}}^{\mathrm{H}}\Big)\underline{\mathbf{R}}_{\mathrm{B}}^{-1},\end{aligned} \tag{77}$$

which is simplified to the desired result of (36).

APPENDIX II

DETERMINATION OF THE COVARIANCE MATRIX $\widetilde{\underline{\mathbf{R}}}_{\varepsilon}$ OF $\widetilde{\underline{\boldsymbol{\varepsilon}}}$

Setting out from (39) the covariance matrix $\widetilde{\underline{\mathbf{R}}}_{\varepsilon}$ of (19) reads

$$\begin{aligned}\widetilde{\underline{\mathbf{R}}}_{\varepsilon} &= \underset{\underline{\mathbf{d}},\underline{\mathbf{E}},\underline{\mathbf{n}}}{\mathrm{E}}\left\{\underline{\mathbf{D}}\,\underline{\mathbf{E}}\,\underline{\mathbf{H}}^{\mathrm{H}}\underline{\mathbf{D}}^{\mathrm{H}}\underline{\mathbf{R}}_{\mathrm{B}}^{-1}\underline{\mathbf{d}}\,\underline{\mathbf{d}}^{\mathrm{H}}\underline{\mathbf{R}}_{\mathrm{B}}^{-1}\underline{\mathbf{D}}\,\underline{\mathbf{H}}\,\underline{\mathbf{E}}^{\mathrm{H}}\underline{\mathbf{D}}^{\mathrm{H}}\right\}+\underset{\underline{\mathbf{d}},\underline{\mathbf{E}},\underline{\mathbf{n}}}{\mathrm{E}}\left\{\underline{\mathbf{D}}\,\underline{\mathbf{n}}\,\underline{\mathbf{n}}^{\mathrm{H}}\underline{\mathbf{D}}^{\mathrm{H}}\right\}\\ &= \underline{\mathbf{D}}\,\underline{\mathbf{R}}_{\mathrm{n}}\underline{\mathbf{D}}^{\mathrm{H}}+\underline{\mathbf{D}}\,\underset{\underline{\mathbf{E}}}{\mathrm{E}}\left\{\underline{\mathbf{E}}\,\underline{\mathbf{H}}^{\mathrm{H}}\underline{\mathbf{D}}^{\mathrm{H}}\underline{\mathbf{R}}_{\mathrm{B}}^{-1}\underline{\mathbf{R}}_{\mathrm{d}}\underline{\mathbf{R}}_{\mathrm{B}}^{-1}\underline{\mathbf{D}}\,\underline{\mathbf{H}}\,\underline{\mathbf{E}}^{\mathrm{H}}\right\}\underline{\mathbf{D}}^{\mathrm{H}}.\end{aligned} \tag{78}$$

Using the relation

$$\underset{\underline{\mathbf{E}}}{\mathrm{E}}\left\{\underline{\mathbf{E}}^{\mathrm{H}}\underline{\mathbf{A}}\,\underline{\mathbf{E}}\right\} = \sigma_{\mathrm{h}}^{2}\mathrm{trace}\left\{\underline{\mathbf{A}}\right\}\cdot\mathbf{I}^{(K_{\mathrm{B}})}, \tag{79}$$

where $\underline{\mathbf{A}}$ is a square matrix, (78) can be simplified to

$$\underline{\widetilde{\mathbf{R}}}_{\varepsilon}=\underline{\mathbf{D}}\,\underline{\mathbf{R}}_{\mathrm{n}}\underline{\mathbf{D}}^{\mathrm{H}}+\underline{\mathbf{D}}\,\underline{\mathbf{D}}^{\mathrm{H}}\cdot\sigma_{\mathrm{h}}^{2}\mathrm{trace}\left\{\underline{\mathbf{H}}^{\mathrm{H}}\underline{\mathbf{D}}^{\mathrm{H}}\underline{\mathbf{R}}_{\mathrm{B}}^{-1}\underline{\mathbf{R}}_{\mathrm{d}}\underline{\mathbf{R}}_{\mathrm{B}}^{-1}\underline{\mathbf{D}}\,\underline{\mathbf{H}}\right\}. \tag{80}$$

With [19]

$$\mathrm{trace}\left\{\underline{\mathbf{A}}\,\underline{\mathbf{B}}\,\underline{\mathbf{C}}\right\}=\mathrm{trace}\left\{\underline{\mathbf{B}}\,\underline{\mathbf{C}}\,\underline{\mathbf{A}}\right\}, \tag{81}$$

(80) yields

$$\underline{\widetilde{\mathbf{R}}}_{\varepsilon}=\underline{\mathbf{D}}\,\underline{\mathbf{R}}_{\mathrm{n}}\underline{\mathbf{D}}^{\mathrm{H}}+\underline{\mathbf{D}}\,\underline{\mathbf{D}}^{\mathrm{H}}\cdot\sigma_{\mathrm{h}}^{2}\mathrm{trace}\left\{\underline{\mathbf{R}}_{\mathrm{B}}^{-1}\underline{\mathbf{R}}_{\mathrm{d}}\right\}. \tag{82}$$

By substituting (3) in (82), one obtains (40).

Appendix III

Derivation of the mean transmit energy $\widetilde{T}_n$

By substituting $\underline{\widetilde{\mathbf{M}}}$ of (36) in (42) and considering that

$$\mathop{\mathrm{E}}_{\underline{\mathbf{E}}}\left\{\underline{\mathbf{E}}\,\underline{\mathbf{A}}\,\underline{\mathbf{E}}\right\}=\mathop{\mathrm{E}}_{\underline{\mathbf{E}}}\left\{\underline{\mathbf{E}}^{\mathrm{H}}\,\underline{\mathbf{A}}\,\underline{\mathbf{E}}^{\mathrm{H}}\right\}=\mathbf{0}, \tag{83}$$

the expectation in (42) can be rewritten as

$$\begin{aligned}\mathop{\mathrm{E}}_{\underline{\mathbf{E}}}\left\{\underline{\widetilde{\mathbf{M}}}^{\mathrm{H}}\underline{\widetilde{\mathbf{M}}}\right\}=\underline{\mathbf{R}}_{\mathrm{B}}^{-1}&+\mathop{\mathrm{E}}_{\underline{\mathbf{E}}}\left\{\underline{\mathbf{R}}_{\mathrm{B}}^{-1}\underline{\mathbf{D}}\,\underline{\mathbf{E}}\,\underline{\mathbf{E}}^{\mathrm{H}}\underline{\mathbf{D}}^{\mathrm{H}}\underline{\mathbf{R}}_{\mathrm{B}}^{-1}\right\}+\mathop{\mathrm{E}}_{\underline{\mathbf{E}}}\left\{\underline{\mathbf{R}}_{\mathrm{B}}^{-1}\underline{\mathbf{D}}\,\underline{\mathbf{H}}\,\underline{\mathbf{E}}^{\mathrm{H}}\underline{\mathbf{D}}^{\mathrm{H}}\underline{\mathbf{R}}_{\mathrm{B}}^{-1}\underline{\mathbf{D}}\,\underline{\mathbf{E}}\,\underline{\mathbf{H}}^{\mathrm{H}}\underline{\mathbf{D}}^{\mathrm{H}}\underline{\mathbf{R}}_{\mathrm{B}}^{-1}\right\}\\&-\mathop{\mathrm{E}}_{\underline{\mathbf{E}}}\left\{\underline{\mathbf{R}}_{\mathrm{B}}^{-1}\underline{\mathbf{D}}\,\underline{\mathbf{E}}\,\underline{\mathbf{H}}^{\mathrm{H}}\underline{\mathbf{D}}^{\mathrm{H}}\underline{\mathbf{R}}_{\mathrm{B}}^{-1}\underline{\mathbf{D}}\,\underline{\mathbf{H}}\,\underline{\mathbf{E}}^{\mathrm{H}}\underline{\mathbf{D}}^{\mathrm{H}}\underline{\mathbf{R}}_{\mathrm{B}}^{-1}\right\}.\end{aligned} \tag{84}$$

Using (79) the expectation operations in (84) can be evaluated, leading to

$$\begin{aligned}\mathop{\mathrm{E}}_{\underline{\mathbf{E}}}\left\{\underline{\widetilde{\mathbf{M}}}^{\mathrm{H}}\underline{\widetilde{\mathbf{M}}}\right\}=\underline{\mathbf{R}}_{\mathrm{B}}^{-1}&+\underline{\mathbf{R}}_{\mathrm{B}}^{-1}\underline{\mathbf{D}}\,\underline{\mathbf{D}}^{\mathrm{H}}\underline{\mathbf{R}}_{\mathrm{B}}^{-1}\cdot\sigma_{\mathrm{h}}^{2}K_{\mathrm{B}}+\underline{\mathbf{R}}_{\mathrm{B}}^{-1}\cdot\sigma_{\mathrm{h}}^{2}\mathrm{trace}\left\{\underline{\mathbf{D}}^{\mathrm{H}}\underline{\mathbf{R}}_{\mathrm{B}}^{-1}\underline{\mathbf{D}}\right\}\\&-\underline{\mathbf{R}}_{\mathrm{B}}^{-1}\underline{\mathbf{D}}\,\underline{\mathbf{D}}^{\mathrm{H}}\underline{\mathbf{R}}_{\mathrm{B}}^{-1}\cdot\sigma_{\mathrm{h}}^{2}\mathrm{trace}\left\{\underline{\mathbf{H}}^{\mathrm{H}}\underline{\mathbf{D}}^{\mathrm{H}}\underline{\mathbf{R}}_{\mathrm{B}}^{-1}\underline{\mathbf{D}}\,\underline{\mathbf{H}}\right\}.\end{aligned} \tag{85}$$

Applying (81) and simplifying (85) one obtains

$$\mathop{\mathrm{E}}_{\underline{\mathbf{E}}}\left\{\underline{\widetilde{\mathbf{M}}}^{\mathrm{H}}\underline{\widetilde{\mathbf{M}}}\right\}=\underline{\mathbf{R}}_{\mathrm{B}}^{-1}\left[1+\sigma_{\mathrm{h}}^{2}\mathrm{trace}\left\{\underline{\mathbf{R}}_{\mathrm{B}}^{-1}\underline{\mathbf{D}}\,\underline{\mathbf{D}}^{\mathrm{H}}\right\}\right]+\underline{\mathbf{R}}_{\mathrm{B}}^{-1}\underline{\mathbf{D}}\,\underline{\mathbf{D}}^{\mathrm{H}}\underline{\mathbf{R}}_{\mathrm{B}}^{-1}\cdot\sigma_{\mathrm{h}}^{2}(K_{\mathrm{B}}-N_{\mathrm{t}}). \tag{86}$$

Considering the diagonal elements of (86), (43) follows.

Acknowledgment

The authors gratefully appreciate the fruitful exchange of ideas with Prof. P. W. Baier, and their colleagues at the Research Group for RF Communications, University of Kaiserslautern. The support of individual parts of this work in the framework of the EU-Project FLOWS (Flexible Convergence of Wireless Standards and Services), by Siemens AG and by DFG are highly acknowledged.

REFERENCES

[1] P. W. Baier, W. Qiu, H. Tröger, C. A. Jötten, and M. Meurer, “Modelling and optimization of receiver oriented multi-user MIMO downlinks for frequency selective channels,” in *Proc. 10th International Conference on Telecommunications (ICT’03)*, Papeete, 2003, pp. 1547–1554.

[2] R. Esmailzadeh and M. Nakagawa, “Pre-RAKE diversity combining for direct sequence spread spectrum mobile communications systems,” *IEICE Transactions on Communications*, vol. 76, no. 8, pp. 1008–1015, Aug. 1993.

[3] B. R. Vojcic and W. M. Jang, “Transmitter precoding in synchronous multiuser communications,” *IEEE Transactions on Communications*, vol. 46, no. 10, pp. 1346–1355, 1998.

[4] M. Meurer, P. W. Baier, T. Weber, Y. Lu, and A. Papathanassiou, “Joint transmission: advantageous downlink concept for CDMA mobile radio systems using time division duplexing,” *IEE Electronics Letters*, vol. 11, no. 10, pp. 900–901, 2000.

[5] A. Noll-Barreto and G. Fettweis, “Performance improvement in DS-spread spectrum CDMA systems using a pre- and a post-rake,” in *Proc. 2000 International Zurich Seminar on Broadband Communications (IZS’2000)*, Zurich, 2000, pp. 39–46.

[6] F. Kowalewski and P. Mangold, “Joint predistortion and transmit diversity,” in *Proc. IEEE Global Telecommunications Conference (GLOBECOM’00)*, San Francisco, 2000, pp. 245–249.

[7] M. Joham and W. Utschick, “Downlink processing for mitigation of intracell interference in DS-CDMA systems,” in *Proc. IEEE 6th International Symposium on Spread Spectrum Techniques & Applications (ISSSTA’00)*, Parsippany, 2000, pp. 15–19.

[8] P. W. Baier, M. Meurer, T. Weber, and H. Tröger, “Joint transmission (JT), an alternative rationale for the downlink of time division CDMA using multi-element transmit antennas,” in *Proc. IEEE 6th International Symposium on Spread Spectrum Techniques & Applications (ISSSTA’00)*, Parsippany, 2000, pp. 1–5.

[9] B. Steiner and P. W. Baier, “Low cost channel estimation in the uplink receiver of CDMA mobile radio systems,” *Frequenz*, vol. 47, no. 11–12, pp. 292–298, 1993.

[10] T. Weber and I. Maniatis, “Channel knowledge: a crucial prerequisite for MIMO transmission?” in *COST 273 TD(03)083*, Paris, 2003.

[11] F. Dietrich, R. Hunger, M. Joham, and W. Utschick, “Linear precoding over time-varying channels in TDD systems,” in *Proc. IEEE International Conference on Acoustics, Speech, and Signal Processing (ICASSP’03)*, Hong Kong, 2003, pp. 117–120.

[12] T. Haustein, C. von Helmolt, E. Jorswieck, V. Jungnickel, and V. Pohl, “Performance of MIMO systems with channel inversion,” in *Proc. IEEE 55th Vehicular Technology Conference (VTC’02)*, Birmingham, 2002, pp. 35–39.

[13] R. Fischer, C. Windpassinger, A. Lampe, and J. Huber, “Tomlinson-Harashima precoding in space-time transmission for low-rate backward channel,” in *Proc. 2002 International Zurich Seminar on Broadband Communications (IZS’2002)*, Zurich, 2002.

[14] M. Joham, K. Kusume, W. Utschick, and J. Nossek, “Transmit matched filter and transmit Wiener filter for the downlink of FDD DS-CDMA systems,” in *Proc. IEEE 13th International Symposium on Personal, Indoor and Mobile Radio Communications (PIMRC’02)*, Lisbon, Sept. 2002, pp. 2312–2316.

[15] E. Visotsky and U. Madhow, “Space-time transmit precoding with imperfect feedback,” *IEEE Transactions on Information Theory*, vol. 47, no. 6, pp. 2632–2639, 2001.

[16] M. Meurer and T. Weber, “Imperfect channel knowledge: An insurmountable barrier in rx oriented multi-user mimo transmission?” in *Proc. 5th ITG Conference on Source and Channel Coding (SCC’04)*, Erlangen, 2004, pp. 371–380.

[17] F. Wathan, R. Irmer, and G. Fettweis, “On transmitter-based interference mitigation in TDD-downlink with frequency-selective fading channel environment,” in *Proc. 8th Asia-Pacific Conference on Communications (APCC’02)*, Bandung, 2002, pp. 125–128.

[18] T. Weber, A. Sklavos, Y. Liu, and M. Weckerle, “The air interface concept JOINT for beyond 3G mobile radio networks,” in *Proc. 15th International Conference on Wireless Communications*, Calgary, July 2003, pp. 25–33.

[19] H. Lütkepohl, *Handbook of matrices*. New York: John Wiley & Sons, 1996.

TABLE I

DIMENSIONS OF THE VECTORS AND MATRICES USED IN THE STRUCTURE OF FIG. 1

vector or matrix, resp.	dimensions
$\underline{\mathbf{d}} = (\underline{d}_1 \dots \underline{d}_{N_\mathrm{t}})^\mathrm{T}$	$\mathbb{C}^{N_\mathrm{t} \times 1}$
$\underline{\mathbf{t}} = (\underline{t}_1 \dots \underline{t}_{K_\mathrm{B}})^\mathrm{T}$	$\mathbb{C}^{K_\mathrm{B} \times 1}$
$\underline{\mathbf{M}}$	$\mathbb{C}^{K_\mathrm{B} \times N_\mathrm{t}}$
$\underline{\mathbf{H}}$	$\mathbb{C}^{K K_\mathrm{M} \times K_\mathrm{B}}$
$\underline{\mathbf{e}}$	$\mathbb{C}^{K K_\mathrm{M} \times 1}$
$\underline{\mathbf{n}}$	$\mathbb{C}^{K K_\mathrm{M} \times 1}$
$\underline{\mathbf{r}}$	$\mathbb{C}^{K K_\mathrm{M} \times 1}$
$\underline{\mathbf{D}}$	$\mathbb{C}^{N_\mathrm{t} \times K K_\mathrm{M}}$
$\widehat{\underline{\mathbf{d}}}$	$\mathbb{C}^{N_\mathrm{t} \times 1}$

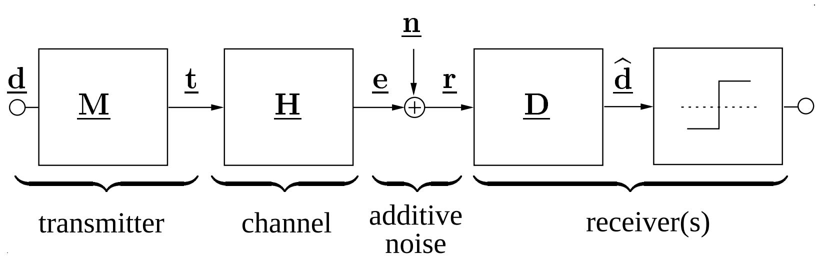

Fig. 1. Generic model of a linear multi-user MIMO transmission system with an additional decision unit

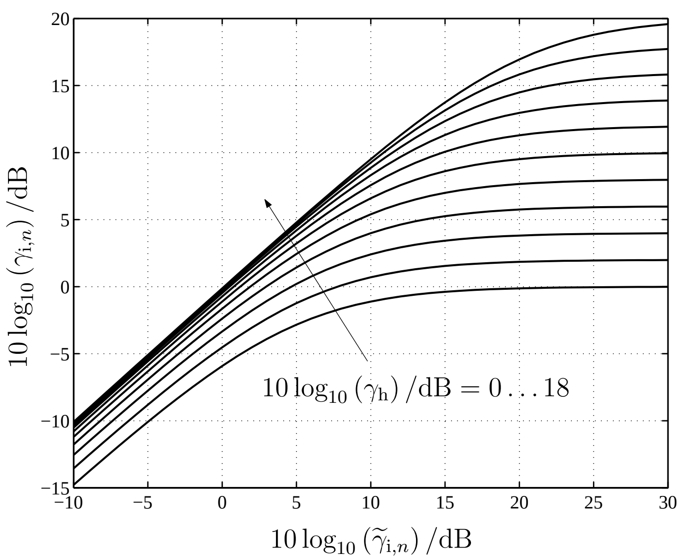

Fig. 2. Relation between $\widetilde{\gamma}_{\mathrm{i},n}$ of (49), γ_{h} of (55) and $\gamma_{\mathrm{i},n}$ of (68) for $N_{\mathrm{t}} = 4$ and $x = 0.4$

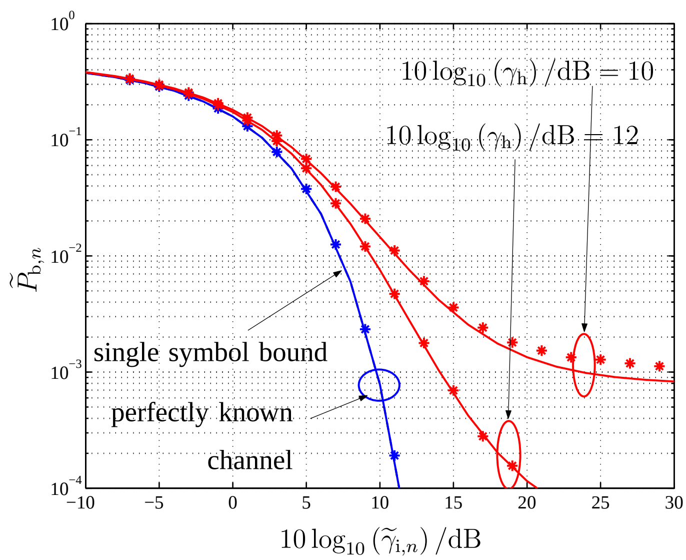

Fig. 3. $\widetilde{P}_{\mathrm{b},n}$ versus $\widetilde{\gamma}_{\mathrm{i},n}$ for $N_{\mathrm{t}} = 4$ and $x = 0$; comparison between simulation results $(\,*\,)$ and analytical results (—)

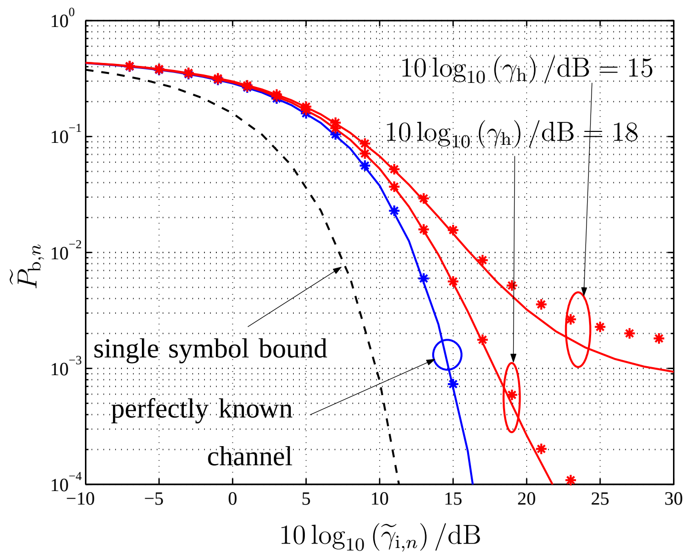

Fig. 4. $\widetilde{P}_{\mathrm{b},n}$ versus $\widetilde{\gamma}_{\mathrm{i},n}$ for $N_\mathrm{t} = 4$ and $x = 0.4$; comparison between simulation results $(*)$ and analytical results (—)

[WSM04] Weber, T.; Sklavos, A.; Meurer, M.: “Imperfect Channel State Information in MIMO-Transmission”. Submitted for publication in *IEEE Transactions on Communications*, 2004.

Imperfect Channel State Information in MIMO Transmission

Tobias Weber, *Member, IEEE,* Alexandros Sklavos, *Member, IEEE,* and Michael Meurer, *Member, IEEE*

Abstract

A specially favorable MIMO based concept for future mobile radio systems consists in the application of Joint Detection (JD) in the uplink and Joint Transmission (JT) in the downlink. By this, all the computational complex signal processing is shifted to the base station (BS) resulting in low complexity mobile stations (MSs). Both JD and JT require channel knowledge at the BS which, if time division duplexing is applied, can be obtained by training signal based channel estimation in the uplink. Unfortunately channel estimates are never perfect which leads to performance degradations if these channel estimates instead of perfect channel knowledge are used for JD or JT. Especially channel errors due to the time variance of the mobile radio channel are often considered to be a severe problem in the application of MIMO techniques in high mobility scenarios which requires closer investigation. In the present paper a novel analysis of the performance degradations of zero forcing JD and JT due to imperfect channel knowledge is presented. The analysis is based on linear Taylor approximation of the data estimation error due to imperfect channel knowledge.

Index Terms

MIMO, joint detection, joint transmission, imperfect channel state information.

T. Weber, A. Sklavos and M. Meurer are with the Research Group for RF Communications, University of Kaiserslautern, D-67653 Kaiserslautern, Germany, email: tweber@rhrk.uni-kl.de.

I. Introduction

Future demands for high spectral efficiencies in mobile radio systems can be met by MIMO systems. In the following a scenario containing a single BS and multiple MSs with a flat fading MIMO channel between BS and MSs is considered. This is no restriction since any frequency selective channel can be converted into parallel, flat fading channels by multicarrier transmission techniques like OFDM [1]. In the case of OFDM transmission the signals on a specific subcarrier are described by their complex amplitudes and the channels are described by their transfer functions. The number of antennas at the BS and the total number of antennas at all the considered MSs together are denoted by K_{B} and K_{M}, respectively. Consequently, the uplink channel can be described by a $K_{\mathrm{B}} \times K_{\mathrm{M}}$ channel matrix $\underline{\mathbf{H}}_{\mathrm{U}}$ and the downlink channel can be described by a $K_{\mathrm{M}} \times K_{\mathrm{B}}$ channel matrix $\underline{\mathbf{H}}_{\mathrm{D}}$. If the radio channel is reciprocal — and this is assumed in the following,

$$\underline{\mathbf{H}} = \underline{\mathbf{H}}_{\mathrm{U}} = \underline{\mathbf{H}}_{\mathrm{D}}^{\mathrm{T}} \tag{1}$$

holds. In the following it is assumed that the number K_{B} of antennas at the BS is larger than or equal to the number K_{M} of antennas at the MSs. The optimum MIMO transmission scheme would consist in singular value decomposition of the channel matrix $\underline{\mathbf{H}}$ and waterfilling [2]. From a practical point of view canonical transmission schemes based on singular value decomposition and bit loading might [3] not be desirable as

- they require cooperative signal processing for all receive antennas and all transmit antennas, respectively, which is not feasible in the case of multiple MTs,
- they require channel knowledge on both the transmitter and the receiver side, and
- the computational complexity of the singular value decomposition might be too high especially on the MSs side.

Consequently, suboptimum JD based data transmission in the uplink and JT based data transmission in the downlink, see Fig. 1, is an interesting alternative. In both cases of JD and of JT K data symbols, comprised in the data vector $\underline{\mathbf{d}}$, are transmitted in parallel. In the case of JD interferences due to cross couplings of the MIMO channel are removed on the receiver side [4].

For example the widely known BLAST system utilizes JD for MIMO transmission [5], [6]. In the case of JT interferences due to cross couplings of the MIMO channel are a priori avoided by an appropriate design of the transmitted signals [7]. The transmitted energies can be adjusted by scaling the data symbols with a real factor. Both JD and JT require channel knowledge in the form of the channel matrix $\underline{\mathbf{H}}_{\mathrm{U}}$ and $\underline{\mathbf{H}}_{\mathrm{D}}$, respectively. It was shown that concerning the signal processing and the performance with perfect channel knowledge linear JD and linear JT are dual to each other [8]. The case of imperfect channel state information in MIMO transmission has been already dealt with from an information theoretic point of view, e.g., in [9], [10], [11]. Recently, first results on the performance of linear JD and linear JT with imperfect channel knowledge were published [8], [12], [13]. Also system performance investigations of JD receivers including channel estimation were carried out, see, e.g., [14]. Concerning JT investigations up to now focused on the case that fading channel gains are compensated by properly adjusting the transmitted energies. Unfortunately, in the typical case of Rayleigh fading channels this may lead to quite high average transmitted energies [15]. From a practical point of view it is necessary to keep the transmitted energies constant, as it is already the case in JD. In the present paper the influence of imperfect channel state information on JT with constant transmitted energies is studied. Furthermore, the impact of imperfect channel knowledge on linear JD and linear JT is compared. For simplicity we concentrate our work on linear zero forcing JD [4] and linear zero forcing JT [16], [17], [18]. A similar analysis for other linear JD and JT techniques, e.g., MMSE processing, [4], [19], [20], will be possible. In the following we skip the attribute linear zero forcing.

In the paper, the equivalent lowpass representation of signals and channel transfer functions is chosen. Complex quantities are underlined, and vectors and matrices are printed in boldface. The element in the i-th row and j-th column of a matrix is denoted by $[.]_{i,j}$. The diag-operator returns a diagonal matrix with diagonal elements which are equal to the diagonal elements of the argument.

II. SYSTEM MODEL

The linear MIMO channel is described by the $K_{\mathrm{B}} \times K_{\mathrm{M}}$ channel matrix

$$\underline{\mathbf{H}} = \begin{pmatrix} \underline{H}^{(1,1)} & \dots & \underline{H}^{(1,K_{\mathrm{M}})} \\ \vdots & & \vdots \\ \underline{H}^{(K_{\mathrm{B}},1)} & \dots & \underline{H}^{(K_{\mathrm{B}},K_{\mathrm{M}})} \end{pmatrix}. \tag{2}$$

As already mentioned the case

$$K_{\mathrm{B}} \geq K_{\mathrm{M}} = K \tag{3}$$

is considered in the following. The K dimensional data vector to be transmitted is denoted by

$$\underline{\mathbf{d}} = \left(\underline{d}^{(1)} \dots \underline{d}^{(K)}\right)^{\mathrm{T}}. \tag{4}$$

The elements $\underline{d}^{(k)}$, $k = 1 \dots K$, of the data vector $\underline{\mathbf{d}}$ are assumed to be independent identically distributed with unit variance of real and imaginary part. For the covariance matrix follows

$$\underline{\mathbf{R}}_{\mathrm{d}} = \mathrm{E}\left\{\underline{\mathbf{d}}\,\underline{\mathbf{d}}^{*\mathrm{T}}\right\} = 2\mathbf{I}. \tag{5}$$

Concerning the signal-to-noise-plus-interference ratios (SNIRs) our investigations hold for any linear PSK modulation scheme. For bit error rate investigations QPSK modulation is assumed, i.e., the elements $\underline{d}^{(k)}$, $k = 1 \dots K$, of the data vector $\underline{\mathbf{d}}$ are taken from the alphabet $\{(1 + \mathrm{j}),\ (1 - \mathrm{j})\,(-1 + \mathrm{j}),\ (-1 - \mathrm{j})\}$. Similar analytical results could also be found for the case of BPSK modulation. In the following the transmitted energy per data symbol is denoted by E_{d}.

In the case of uplink transmission with the noise vector $\underline{\mathbf{n}}_{\mathrm{U}}$, the received vector reads

$$\underline{\mathbf{e}} = \underline{\mathbf{H}}_{\mathrm{U}} \cdot \sqrt{E_{\mathrm{d}}} \cdot \underline{\mathbf{d}} + \underline{\mathbf{n}}_{\mathrm{U}} = \sqrt{E_{\mathrm{d}}} \cdot \underline{\mathbf{H}} \cdot \underline{\mathbf{d}} + \underline{\mathbf{n}}_{\mathrm{U}}, \tag{6}$$

i.e., the data symbols are scaled by $\sqrt{E_{\mathrm{d}}}$ on the transmitter side. For simplicity it is assumed in the following that the elements of the noise vector $\underline{\mathbf{n}}_{\mathrm{U}}$ are uncorrelated, Gaussian distributed with variance σ^2 of real and imaginary part [21]. For the covariance matrix follows

$$\underline{\mathbf{R}}_{\mathrm{n,U}} = \mathrm{E}\left\{\underline{\mathbf{n}}_{\mathrm{U}}\underline{\mathbf{n}}_{\mathrm{U}}^{*\mathrm{T}}\right\} = 2\sigma^2\mathbf{I}. \tag{7}$$

Linear zero forcing JD [4] calculates an estimate $\underline{\hat{\mathbf{d}}}$ of the data vector $\underline{\mathbf{d}}$ which minimizes the error $\left\|\underline{\mathbf{e}} - \sqrt{E_\mathrm{d}} \cdot \underline{\mathbf{H}} \cdot \underline{\hat{\mathbf{d}}}\right\|^2$. This estimate can be easily calculated as

$$\underline{\hat{\mathbf{d}}} = \frac{1}{\sqrt{E_\mathrm{d}}} \left(\underline{\mathbf{H}}^{*\mathrm{T}} \underline{\mathbf{H}}\right)^{-1} \underline{\mathbf{H}}^{*\mathrm{T}} \underline{\mathbf{e}}. \tag{8}$$

In (8) perfect channel knowledge, i.e., perfect knowledge of the channel matrix $\underline{\mathbf{H}}$ in the receiver is assumed.

In the case of downlink transmission with the noise vector $\underline{\mathbf{n}}_\mathrm{D}$ and the transmitted vector $\underline{\mathbf{s}}$ and exploiting the fact that the channel is reciprocal (1) the data estimate reads

$$\underline{\hat{\mathbf{d}}} = \left(\frac{\mathrm{diag}\left(\left(\underline{\mathbf{H}}_\mathrm{D}\, \underline{\mathbf{H}}_\mathrm{D}^{*\mathrm{T}}\right)^{-1}\right)}{E_\mathrm{d}}\right)^{\frac{1}{2}} \cdot \left(\underline{\mathbf{H}}_\mathrm{D} \cdot \underline{\mathbf{s}} + \underline{\mathbf{n}}_\mathrm{D}\right) = \left(\frac{\mathrm{diag}\left(\left(\underline{\mathbf{H}}^\mathrm{T} \underline{\mathbf{H}}^*\right)^{-1}\right)}{E_\mathrm{d}}\right)^{\frac{1}{2}} \cdot \left(\underline{\mathbf{H}}^\mathrm{T} \underline{\mathbf{s}} + \underline{\mathbf{n}}_\mathrm{D}\right), \tag{9}$$

i.e., the data symbols are equal to the received complex amplitudes $\underline{\mathbf{H}}_\mathrm{D} \cdot \underline{\mathbf{s}} + \underline{\mathbf{n}}_\mathrm{D}$ scaled by the real diagonal matrix $\left(\frac{\mathrm{diag}\left(\left(\underline{\mathbf{H}}^\mathrm{T} \underline{\mathbf{H}}^*\right)^{-1}\right)}{E_\mathrm{d}}\right)^{\frac{1}{2}}$ on the receiver side. It should be mentioned that this scaling is of no practical relevance in the considered case of QPSK modulation and consequently channel knowledge is not really required on the receiver side in the considered case of reciprocal channels and known transmit and receive timing. Furthermore also in the case of higher order modulation the scaling factor could be easily estimated at the receiver. In the noise free case the estimate should be equal to the transmitted data vector $\underline{\mathbf{d}}$:

$$\underline{\mathbf{d}} = \left(\frac{\mathrm{diag}\left(\left(\underline{\mathbf{H}}^\mathrm{T} \underline{\mathbf{H}}^*\right)^{-1}\right)}{E_\mathrm{d}}\right)^{\frac{1}{2}} \cdot \underline{\mathbf{H}}^\mathrm{T} \underline{\mathbf{s}}. \tag{10}$$

Together with the requirement that the transmitted energy $\frac{1}{2}\left\|\underline{\mathbf{s}}\right\|^2$ should be as low as possible this leads to the JT transmitted vector

$$\underline{\mathbf{s}} = \underline{\mathbf{H}}^* \left(\underline{\mathbf{H}}^\mathrm{T} \underline{\mathbf{H}}^*\right)^{-1} \left(\frac{\mathrm{diag}\left(\left(\underline{\mathbf{H}}^\mathrm{T} \underline{\mathbf{H}}^*\right)^{-1}\right)}{E_\mathrm{d}}\right)^{-\frac{1}{2}} \underline{\mathbf{d}}. \tag{11}$$

As can be seen from (11) the scaling of the data symbols introduced in (9) leads to a transmitted energy

$$\left[\left(\frac{\mathrm{diag}\left(\left(\underline{\mathbf{H}}^\mathrm{T} \underline{\mathbf{H}}^*\right)^{-1}\right)}{E_\mathrm{d}}\right)^{-\frac{1}{2}} \left(\underline{\mathbf{H}}^\mathrm{T} \underline{\mathbf{H}}^*\right)^{-1} \cdot \left(\frac{\mathrm{diag}\left(\left(\underline{\mathbf{H}}^\mathrm{T} \underline{\mathbf{H}}^*\right)^{-1}\right)}{E_\mathrm{d}}\right)^{-\frac{1}{2}}\right]_{k,k} = E_\mathrm{d} \tag{12}$$

per data symbol. In both (9) and (11) perfect channel knowledge is assumed to be available. In the following analysis of JT it is assumed that the elements of the noise vector $\underline{\mathbf{n}}_{\mathrm{D}}$ are uncorrelated, Gaussian distributed with the variance σ^2 of real and imaginary part [21]. For the covariance matrix follows

$$\underline{\mathbf{R}}_{\mathrm{n,D}} = \mathrm{E}\left\{\underline{\mathbf{n}}_{\mathrm{D}}\underline{\mathbf{n}}_{\mathrm{D}}^{*\mathrm{T}}\right\} = 2\sigma^2\mathbf{I}. \tag{13}$$

The performance of both JD and JT are analyzed for the case of perfect channel knowledge, i.e., perfect knowledge of $\underline{\mathbf{H}}$, in the receiver and the transmitter, respectively, and the case of imperfect channel knowledge. In the case of imperfect channel knowledge the estimated channel matrix $\hat{\underline{\mathbf{H}}}$, which with the channel error matrix $\underline{\mathbf{E}}$ can be written as

$$\hat{\underline{\mathbf{H}}} = \underline{\mathbf{H}} + \underline{\mathbf{E}}, \tag{14}$$

is used for JD and JT. In the following it is assumed that the channel estimation errors, i.e., the elements of the channel error matrix $\underline{\mathbf{E}}$, are independent identically Gaussian distributed with a variance σ_{E}^2 of real and imaginary part. This assumption is justified by the analysis of the channel estimation errors presented in [8].

III. Performance of Joint Detection

A. Perfect Channel Knowledge

As can be seen from (8) JD in the case of perfect channel knowledge perfectly eliminates the multiple access interference at the price of enhancing the noise. The data estimation error

$$\hat{\underline{\mathbf{d}}} - \underline{\mathbf{d}} = \frac{1}{\sqrt{E_{\mathrm{d}}}}\left(\underline{\mathbf{H}}^{*\mathrm{T}}\underline{\mathbf{H}}\right)^{-1}\underline{\mathbf{H}}^{*\mathrm{T}}\underline{\mathbf{n}}_{\mathrm{U}} \tag{15}$$

consists of enhanced noise only. With (7) follows for the signal-to-noise ratio (SNR) of the data estimates $\hat{\underline{d}}^{(k)}$ [22], [4]

$$\gamma_{\mathrm{JD}}^{(k)} = \frac{E_{\mathrm{d}}}{\sigma^2\left[\left(\underline{\mathbf{H}}^{*\mathrm{T}}\underline{\mathbf{H}}\right)^{-1}\right]_{k,k}}. \tag{16}$$

With (16) and the assumption that the noise $\underline{\mathbf{n}}_{\mathrm{U}}$ is Gaussian distributed the bit error probability [4]

$$P_{\mathrm{b}}^{(k)} = \frac{1}{2}\mathrm{erfc}\left(\sqrt{\frac{\gamma_{\mathrm{JD}}^{(k)}}{2}}\right) = \frac{1}{2}\mathrm{erfc}\left(\sqrt{\frac{E_{\mathrm{d}}}{2\sigma^2\left[\left(\underline{\mathbf{H}}^{*\mathrm{T}}\underline{\mathbf{H}}\right)^{-1}\right]_{k,k}}}\right) \tag{17}$$

in the case of QPSK modulation is obtained.

B. Imperfect Channel Knowledge

The JD described in the previous Subsection III-A requires channel knowledge in the form of the channel matrix $\underline{\mathbf{H}}$. However, in reality only an imperfect estimate $\hat{\underline{\mathbf{H}}}$ of the channel matrix $\underline{\mathbf{H}}$ will be available. The estimate $\hat{\underline{\mathbf{H}}}$ is used for calculating the data estimate

$$\hat{\underline{\mathbf{d}}} = \frac{1}{\sqrt{E_{\mathrm{d}}}}\left(\hat{\underline{\mathbf{H}}}^{*\mathrm{T}}\hat{\underline{\mathbf{H}}}\right)^{-1}\hat{\underline{\mathbf{H}}}^{*\mathrm{T}}\underline{\mathbf{e}}. \tag{18}$$

With (14) this can be rewritten as

$$\hat{\underline{\mathbf{d}}} = \frac{1}{\sqrt{E_{\mathrm{d}}}}\left((\underline{\mathbf{H}}+\underline{\mathbf{E}})^{*\mathrm{T}}(\underline{\mathbf{H}}+\underline{\mathbf{E}})\right)^{-1}(\underline{\mathbf{H}}+\underline{\mathbf{E}})^{*\mathrm{T}}\underline{\mathbf{e}}. \tag{19}$$

For the data estimation error in the case of imperfect channel knowledge

$$\begin{aligned}\hat{\underline{\mathbf{d}}} - \underline{\mathbf{d}} \;&=\; -\underbrace{\left((\underline{\mathbf{H}}+\underline{\mathbf{E}})^{*\mathrm{T}}(\underline{\mathbf{H}}+\underline{\mathbf{E}})\right)^{-1}(\underline{\mathbf{H}}+\underline{\mathbf{E}})^{*\mathrm{T}}\underline{\mathbf{E}}}_{\underline{\mathbf{D}}_{\mathrm{U}}}\cdot\underline{\mathbf{d}} \\ &\quad+\frac{1}{\sqrt{E_{\mathrm{d}}}}\underbrace{\left((\underline{\mathbf{H}}+\underline{\mathbf{E}})^{*\mathrm{T}}(\underline{\mathbf{H}}+\underline{\mathbf{E}})\right)^{-1}(\underline{\mathbf{H}}+\underline{\mathbf{E}})^{*\mathrm{T}}}_{\underline{\mathbf{N}}_{\mathrm{U}}}\cdot\underline{\mathbf{n}}_{\mathrm{U}}\end{aligned} \tag{20}$$

follows. Thus, the data estimation error is a nonlinear not analytical function of the elements $[\underline{\mathbf{E}}]_{k_{\mathrm{B}},k_{\mathrm{M}}}$ of the channel error matrix $\underline{\mathbf{E}}$. For small channel estimation errors $[\underline{\mathbf{E}}]_{k_{\mathrm{B}},k_{\mathrm{M}}}$, $k_{\mathrm{B}} = 1\ldots K_{\mathrm{B}}$, $k_{\mathrm{M}} = 1\ldots K_{\mathrm{M}}$, i.e., a small variance σ_{E}^2, these nonlinear functions can be approximated by a Taylor series which is truncated after the linear terms, i.e.,

$$\begin{aligned}
&\hat{\underline{\mathbf{d}}} - \underline{\mathbf{d}} \approx \\
&\quad -\left[\sum_{k_\mathrm{B},k_\mathrm{M}} \left.\frac{\partial \underline{\mathbf{D}}_\mathrm{U}}{\partial \mathrm{Re}\left\{[\underline{\mathbf{E}}]_{k_\mathrm{B},k_\mathrm{M}}\right\}}\right|_{\underline{\mathbf{E}}=\mathbf{0}} \mathrm{Re}\left\{[\underline{\mathbf{E}}]_{k_\mathrm{B},k_\mathrm{M}}\right\} + \sum_{k_\mathrm{B},k_\mathrm{M}} \left.\frac{\partial \underline{\mathbf{D}}_\mathrm{U}}{\partial \mathrm{Im}\left\{[\underline{\mathbf{E}}]_{k_\mathrm{B},k_\mathrm{M}}\right\}}\right|_{\underline{\mathbf{E}}=\mathbf{0}} \mathrm{Im}\left\{[\underline{\mathbf{E}}]_{k_\mathrm{B},k_\mathrm{M}}\right\} \right] \cdot \underline{\mathbf{d}} \\
&\quad + \frac{1}{\sqrt{E_\mathrm{d}}} \left[\left(\underline{\mathbf{H}}^{*\mathrm{T}}\underline{\mathbf{H}}\right)^{-1} \underline{\mathbf{H}}^{*\mathrm{T}} \right. \\
&\quad \left. + \sum_{k_\mathrm{B},k_\mathrm{M}} \left.\frac{\partial \underline{\mathbf{N}}_\mathrm{U}}{\partial \mathrm{Re}\left\{[\underline{\mathbf{E}}]_{k_\mathrm{B},k_\mathrm{M}}\right\}}\right|_{\underline{\mathbf{E}}=\mathbf{0}} \mathrm{Re}\left\{[\underline{\mathbf{E}}]_{k_\mathrm{B},k_\mathrm{M}}\right\} + \sum_{k_\mathrm{B},k_\mathrm{M}} \left.\frac{\partial \underline{\mathbf{N}}_\mathrm{U}}{\partial\, \mathrm{Im}\left\{[\underline{\mathbf{E}}]_{k_\mathrm{B},k_\mathrm{M}}\right\}}\right|_{\underline{\mathbf{E}}=\mathbf{0}} \mathrm{Im}\left\{[\underline{\mathbf{E}}]_{k_\mathrm{B},k_\mathrm{M}}\right\} \right] \cdot \underline{\mathbf{n}}_\mathrm{U}.
\end{aligned} \tag{21}$$

After calculation of the derivatives in (21) and some simplifications the approximation

$$\begin{aligned}
\hat{\underline{\mathbf{d}}} - \underline{\mathbf{d}} &\approx -\left(\underline{\mathbf{H}}^{*\mathrm{T}}\underline{\mathbf{H}}\right)^{-1} \underline{\mathbf{H}}^{*\mathrm{T}} \underline{\mathbf{E}}\, \underline{\mathbf{d}} + \frac{1}{\sqrt{E_\mathrm{d}}} \left(\underline{\mathbf{H}}^{*\mathrm{T}}\underline{\mathbf{H}}\right)^{-1} \left(\underline{\mathbf{H}}^{*\mathrm{T}} + \underline{\mathbf{E}}^{*\mathrm{T}}\right) \underline{\mathbf{n}}_\mathrm{U} \\
&\quad - \frac{1}{\sqrt{E_\mathrm{d}}} \left(\underline{\mathbf{H}}^{*\mathrm{T}}\underline{\mathbf{H}}\right)^{-1} \left(\underline{\mathbf{H}}^{*\mathrm{T}}\underline{\mathbf{E}} + \underline{\mathbf{E}}^{*\mathrm{T}}\underline{\mathbf{H}}\right) \left(\underline{\mathbf{H}}^{*\mathrm{T}}\underline{\mathbf{H}}\right)^{-1} \underline{\mathbf{H}}^{*\mathrm{T}} \underline{\mathbf{n}}_\mathrm{U}
\end{aligned} \tag{22}$$

of the data estimation error for small channel estimation errors is found, see Appendix I. With (5) and (7) and the reasonable assumption that the data $\underline{\mathbf{d}}$, the noise $\underline{\mathbf{n}}_\mathrm{U}$, and the channel estimation error $\underline{\mathbf{E}}$ are statistically independent the covariance matrix of the data estimation error in the case of PSK modulation reads

$$\begin{aligned}
\underline{\mathbf{R}}_{\hat{\mathrm{d}}-\mathrm{d}} &\approx \frac{2\sigma^2}{E_\mathrm{d}} \left(\underline{\mathbf{H}}^{*\mathrm{T}}\underline{\mathbf{H}}\right)^{-1} \left[1 + \frac{2E_\mathrm{d} 2\sigma_\mathrm{E}^2 K_\mathrm{M}}{2\sigma^2} + 2\sigma_\mathrm{E}^2\, \mathrm{trace}\left\{\left(\underline{\mathbf{H}}^{*\mathrm{T}}\underline{\mathbf{H}}\right)^{-1}\right\}\right] \\
&\quad + \frac{2\sigma^2 2\sigma_\mathrm{E}^2}{E_\mathrm{d}} \left(K_\mathrm{B} - K_\mathrm{M}\right) \left(\underline{\mathbf{H}}^{*\mathrm{T}}\underline{\mathbf{H}}\right)^{-2},
\end{aligned} \tag{23}$$

see Appendix II. It must be said that the data estimation error of (22) contains contributions which are the product of Gaussian distributed channel estimation errors and Gaussian distributed noise and is thus not Gaussian distributed anymore. The SNIR

$$\begin{aligned}
\gamma_\mathrm{JD}^{(k)} &\approx E_\mathrm{d} \Big/ \left(\sigma^2 \left[\left(\underline{\mathbf{H}}^{*\mathrm{T}}\underline{\mathbf{H}}\right)^{-1}\right]_{k,k} \left[1 + \frac{2E_\mathrm{d} 2\sigma_\mathrm{E}^2 K_\mathrm{M}}{2\sigma^2} + 2\sigma_\mathrm{E}^2\, \mathrm{trace}\left\{\left(\underline{\mathbf{H}}^{*\mathrm{T}}\underline{\mathbf{H}}\right)^{-1}\right\}\right] \right. \\
&\quad \left. + \sigma^2 2\sigma_\mathrm{E}^2 \left(K_\mathrm{B} - K_\mathrm{M}\right) \left[\left(\underline{\mathbf{H}}^{*\mathrm{T}}\underline{\mathbf{H}}\right)^{-2}\right]_{k,k} \right)
\end{aligned} \tag{24}$$

describes the quality of the estimate $\hat{\underline{d}}^{(k)}$ in the case of imperfect channel knowledge. A good approximation

$$P_{\mathrm{b}}^{(k)} \approx \frac{1}{2}\mathrm{erfc}\left(\left(E_{\mathrm{d}} \Big/ \left(2\sigma^2 \left[\left(\underline{\mathbf{H}}^{*\mathrm{T}}\underline{\mathbf{H}}\right)^{-1}\right]_{k,k} \left(1 + \frac{2E_{\mathrm{d}}2\sigma_{\mathrm{E}}^2 K_{\mathrm{M}}}{2\sigma^2} + 2\sigma_{\mathrm{E}}^2 \,\mathrm{trace}\left\{\left(\underline{\mathbf{H}}^{*\mathrm{T}}\underline{\mathbf{H}}\right)^{-1}\right\}\right) + 2\sigma^2 2\sigma_{\mathrm{E}}^2 \left(K_{\mathrm{B}} - K_{\mathrm{M}}\right) \left[\left(\underline{\mathbf{H}}^{*\mathrm{T}}\underline{\mathbf{H}}\right)^{-2}\right]_{k,k}\right)\right)^{\frac{1}{2}}\right) \tag{25}$$

for the bit error probability in the case of QPSK modulation can be found based on the assumtion that the data estimation error is Gaussian distributed. This assumption is justified by the fact that the data estimation error contains many independent contributions. For large transmitted energies E_{d} the bit error probability converges towards the error floor

$$P_{\mathrm{b},\infty}^{(k)} = \lim_{T^{(k)}\to\infty} P_{\mathrm{b}}^{(k)} \approx \frac{1}{2}\mathrm{erfc}\left(\sqrt{\frac{1}{4\sigma_{\mathrm{E}}^2 K_{\mathrm{M}} \left[\left(\underline{\mathbf{H}}^{*\mathrm{T}}\underline{\mathbf{H}}\right)^{-1}\right]_{k,k}}}\right), \tag{26}$$

which is, for a given channel, in general different for the different data symbols $\underline{d}^{(k)}$, $k = 1 \ldots K$.

IV. Performance of Joint Transmission

A. Perfect Channel Knowledge

JT perfectly avoids interferences at the price of decreased received energies for given transmitted energies E_{d}. The data estimation error

$$\hat{\underline{\mathbf{d}}} - \underline{\mathbf{d}} = \left(\frac{\mathrm{diag}\left(\left(\underline{\mathbf{H}}_{\mathrm{D}}\,\underline{\mathbf{H}}_{\mathrm{D}}^{*\mathrm{T}}\right)^{-1}\right)}{E_{\mathrm{d}}}\right)^{\frac{1}{2}} \underline{\mathbf{n}}_{\mathrm{D}} \tag{27}$$

consists of noise only. With (13) follows for the SNR of the data estimates $\hat{\underline{d}}^{(k)}$

$$\gamma_{\mathrm{JT}}^{(k)} = \frac{E_{\mathrm{d}}}{\sigma^2 \left[\left(\underline{\mathbf{H}}^{\mathrm{T}}\underline{\mathbf{H}}^{*}\right)^{-1}\right]_{k,k}}. \tag{28}$$

This SNR obtained in the uplink with JT is identical to the SNR of (16) obtained in the downlink with JD. With the assumption that the noise $\underline{\mathbf{n}}_{\mathrm{D}}$ is Gaussian distributed the bit error probability

$$P_{\mathrm{b}}^{(k)} = \frac{1}{2}\mathrm{erfc}\left(\sqrt{\frac{\gamma_{\mathrm{JT}}^{(k)}}{2}}\right) = \frac{1}{2}\mathrm{erfc}\left(\sqrt{\frac{E_{\mathrm{d}}}{2\sigma^2 \left[\left(\underline{\mathbf{H}}^{\mathrm{T}}\underline{\mathbf{H}}^{*}\right)^{-1}\right]_{k,k}}}\right) \tag{29}$$

in the case of QPSK modulation is obtained. This is the same result as in the case of JD, i.e., the performance of the uplink with JD is equal to the performance of the downlink with JT for a given average transmitted energy E_{d} and a given variance σ^2 of the noise.

B. Imperfect Channel Knowledge

In reality an imperfect estimate $\hat{\underline{\mathbf{H}}}$ of the channel matrix $\underline{\mathbf{H}}$ will be used for calculating the transmitted vector

$$\underline{\mathbf{s}} = \hat{\underline{\mathbf{H}}}^{*} \left(\hat{\underline{\mathbf{H}}}^{\mathrm{T}} \hat{\underline{\mathbf{H}}}^{*} \right)^{(-1)} \left(\frac{\operatorname{diag}\left(\left(\hat{\underline{\mathbf{H}}}^{\mathrm{T}} \hat{\underline{\mathbf{H}}}^{*} \right)^{-1} \right)}{E_{\mathrm{d}}} \right)^{-\frac{1}{2}} \underline{\mathbf{d}}. \tag{30}$$

Concerning the receiver we assume that the real scaling factors used in the transmitter are perfectly known, i.e., the data estimate in the case of imperfect channel knowledge reads

$$\hat{\underline{\mathbf{d}}} = \left(\frac{\operatorname{diag}\left(\left(\hat{\underline{\mathbf{H}}}^{\mathrm{T}} \hat{\underline{\mathbf{H}}}^{*} \right)^{-1} \right)}{E_{\mathrm{d}}} \right)^{\frac{1}{2}} \left(\underline{\mathbf{H}}^{\mathrm{T}} \underline{\mathbf{s}} + \underline{\mathbf{n}}_{\mathrm{D}} \right). \tag{31}$$

This assumption is justified by the fact that in the considered case of QPSK modulation the scaling factors are irrelevant anyway and are used here only to simplify the theoretical calculations. If the scaling factors were not known they could be easily estimated. Using (14) the data estimation error in the case of imperfect channel knowledge reads

$$\begin{aligned}
\hat{\underline{\mathbf{d}}} - \underline{\mathbf{d}} = & - \left(\operatorname{diag}\left(\left((\underline{\mathbf{H}} + \underline{\mathbf{E}})^{\mathrm{T}} (\underline{\mathbf{H}} + \underline{\mathbf{E}})^{*} \right)^{-1} \right) \right)^{\frac{1}{2}} \underline{\mathbf{E}}^{\mathrm{T}} \\
& \cdot (\underline{\mathbf{H}} + \underline{\mathbf{E}})^{*} \left((\underline{\mathbf{H}} + \underline{\mathbf{E}})^{\mathrm{T}} (\underline{\mathbf{H}} + \underline{\mathbf{E}})^{*} \right)^{-1} \cdot \left(\operatorname{diag}\left(\left((\underline{\mathbf{H}} + \underline{\mathbf{E}})^{\mathrm{T}} (\underline{\mathbf{H}} + \underline{\mathbf{E}})^{*} \right)^{-1} \right) \right)^{-\frac{1}{2}} \cdot \underline{\mathbf{d}} \\
& + \frac{1}{\sqrt{E_{\mathrm{d}}}} \left(\operatorname{diag}\left(\left((\underline{\mathbf{H}} + \underline{\mathbf{E}})^{\mathrm{T}} (\underline{\mathbf{H}} + \underline{\mathbf{E}})^{*} \right)^{-1} \right) \right)^{\frac{1}{2}} \cdot \underline{\mathbf{n}}_{\mathrm{D}} \\
= & -\underline{\mathbf{D}}_{\mathrm{D}} \cdot \underline{\mathbf{d}} + \frac{1}{\sqrt{E_{\mathrm{d}}}} \underline{\mathbf{N}}_{\mathrm{D}} \cdot \underline{\mathbf{n}}_{\mathrm{D}}.
\end{aligned} \tag{32}$$

Here again the data estimation error is a nonlinear not analytical function of the elements $[\underline{\mathbf{E}}]_{k_{\mathrm{B}},k_{\mathrm{M}}}$ of the channel error matrix $\underline{\mathbf{E}}$. For small channel estimation errors $[\underline{\mathbf{E}}]_{k_{\mathrm{B}},k_{\mathrm{M}}}$, $k_{\mathrm{B}} = 1 \ldots K_{\mathrm{B}}$, $k_{\mathrm{M}} = 1 \ldots K_{\mathrm{M}}$, i.e., a small variance σ_{E}^2, these nonlinear functions are again approximated by a

Taylor series which is truncated after the linear terms. After calculation of the derivatives and some simplifications the approximation

$$\begin{aligned}\underline{\hat{\mathbf{d}}} - \underline{\mathbf{d}} \;\approx\; & -\left(\mathrm{diag}\left(\left(\underline{\mathbf{H}}^{\mathrm{T}}\underline{\mathbf{H}}^{*}\right)^{-1}\right)\right)^{\frac{1}{2}} \underline{\mathbf{E}}^{\mathrm{T}}\underline{\mathbf{H}}^{*}\left(\underline{\mathbf{H}}^{\mathrm{T}}\underline{\mathbf{H}}^{*}\right)^{-1} \cdot \left(\mathrm{diag}\left(\left(\underline{\mathbf{H}}^{\mathrm{T}}\underline{\mathbf{H}}^{*}\right)^{-1}\right)\right)^{-\frac{1}{2}} \underline{\mathbf{d}} \\ & + \frac{1}{\sqrt{E_{\mathrm{d}}}}\left(\mathrm{diag}\left(\left(\underline{\mathbf{H}}^{\mathrm{T}}\underline{\mathbf{H}}^{*}\right)^{-1}\right)\right)^{\frac{1}{2}} \underline{\mathbf{n}}_{\mathrm{D}} \\ & - \frac{1}{2\sqrt{E_{\mathrm{d}}}}\left(\mathrm{diag}\left(\left(\underline{\mathbf{H}}^{\mathrm{T}}\underline{\mathbf{H}}^{*}\right)^{-1}\right)\right)^{-\frac{1}{2}} \mathrm{diag}\Big(\left(\underline{\mathbf{H}}^{\mathrm{T}}\underline{\mathbf{H}}^{*}\right)^{-1} \\ & \cdot \left(\underline{\mathbf{H}}^{\mathrm{T}}\underline{\mathbf{E}}^{*} + \underline{\mathbf{E}}^{\mathrm{T}}\underline{\mathbf{H}}^{*}\right)\left(\underline{\mathbf{H}}^{\mathrm{T}}\underline{\mathbf{H}}^{*}\right)^{-1}\Big)\underline{\mathbf{n}}_{\mathrm{D}} \end{aligned} \tag{33}$$

of the data estimation error for small channel estimation errors is found, see Appendix III. With (5) and (13) and the reasonable assumption that the data $\underline{\mathbf{d}}$, the noise $\underline{\mathbf{n}}_{\mathrm{U}}$, and the channel estimation error $\underline{\mathbf{E}}$ are statistically independent the covariance matrix of the data estimation error in the case of PSK modulation reads

$$\underline{\mathbf{R}}_{\hat{\mathrm{d}}-\mathrm{d}} \approx 4\sigma_{\mathrm{E}}^{2} K_{\mathrm{M}} \mathrm{diag}\left(\left(\underline{\mathbf{H}}^{\mathrm{T}}\underline{\mathbf{H}}^{*}\right)^{-1}\right) + \frac{2\sigma^{2}}{E_{\mathrm{d}}}\mathrm{diag}\left(\left(\underline{\mathbf{H}}^{\mathrm{T}}\underline{\mathbf{H}}^{*}\right)^{-1}\right) + \frac{\sigma^{2} 2\sigma_{\mathrm{E}}^{2}}{E_{\mathrm{d}}}\mathrm{diag}\left(\left(\underline{\mathbf{H}}^{\mathrm{T}}\underline{\mathbf{H}}^{*}\right)^{-2}\right). \tag{34}$$

see Appendix IV. In contrast to the case of JD, see (23), the data estimation errors of different data symbols are always uncorrelated in the case of JT. The SNIR

$$\gamma_{\mathrm{JT}}^{(k)} \approx E_{\mathrm{d}} \Big/ \left(\sigma^{2}\left[\left(\underline{\mathbf{H}}^{\mathrm{T}}\underline{\mathbf{H}}^{*}\right)^{-1}\right]_{k,k}\left[1 + \frac{2E_{\mathrm{d}} 2\sigma_{\mathrm{E}}^{2} K_{\mathrm{M}}}{2\sigma^{2}}\right] + \sigma^{2}\sigma_{\mathrm{E}}^{2}\left[\left(\underline{\mathbf{H}}^{\mathrm{T}}\underline{\mathbf{H}}^{*}\right)^{-2}\right]_{k,k}\right) \tag{35}$$

describes the quality of the estimate $\underline{d}^{(k)}$ in the case of imperfect channel knowledge. Under the assumption that the data estimation error is Gaussian distributed the bit error probability

$$P_{\mathrm{b}}^{(k)} \approx \frac{1}{2}\mathrm{erfc}\left(\left(E_{\mathrm{d}} \Big/ \left(2\sigma^{2}\left[\left(\underline{\mathbf{H}}^{\mathrm{T}}\underline{\mathbf{H}}^{*}\right)^{-1}\right]_{k,k}\left[1 + \frac{2E_{\mathrm{d}} 2\sigma_{\mathrm{E}}^{2} K_{\mathrm{M}}}{2\sigma^{2}}\right] + 2\sigma^{2}\sigma_{\mathrm{E}}^{2}\left[\left(\underline{\mathbf{H}}^{\mathrm{T}}\underline{\mathbf{H}}^{*}\right)^{-2}\right]_{k,k}\right)\right)^{\frac{1}{2}}\right) \tag{36}$$

in the case of QPSK modulation is obtained. For large transmitted energies E_{d} the bit error probability converges towards the error floor

$$P_{\mathrm{b},\infty}^{(k)} = \lim_{T^{(k)}\to\infty} P_{\mathrm{b}}^{(k)} \approx \frac{1}{2}\mathrm{erfc}\left(\sqrt{\frac{1}{4\sigma_{\mathrm{E}}^{2} K_{\mathrm{M}}\left[\left(\underline{\mathbf{H}}^{*\mathrm{T}}\underline{\mathbf{H}}\right)^{-1}\right]_{k,k}}}\right), \tag{37}$$

which is identical to the one obtained for JD with imperfect channel knowledge, see (26).

V. Simulation Results

In order to visualize and verify the theoretical results of the previous Sections, simulation results of the average bit error probability $\overline{P}_{\mathrm{b}}$ in Rayleigh fading channels are presented in this Section. The simulations are based on the system model of Fig. 1. Linear zero forcing JD of (18) and linear zero forcing JT of (30) are employed.

In all simulations, the channel matrix $\underline{\mathbf{H}}$ is a random matrix of dimension $K_{\mathrm{B}} \times K_{\mathrm{M}}$. The elements of $\underline{\mathbf{H}}$ are independent identicaly Gaussian distributed complex random variables, with zero-mean real- and imaginary parts of variance σ_{H}^2. With the variance σ_{E}^2 of the channel estimation errors $[\underline{\mathbf{E}}]_{k_{\mathrm{B}},k_{\mathrm{M}}}$, the SNR

$$\gamma_{\mathrm{H}} = \sigma_{\mathrm{H}}^2/\sigma_{\mathrm{E}}^2 \tag{38}$$

of the imperfect channel estimates comprising the estimated channel matrix $\hat{\underline{\mathbf{H}}}$ is defined. Due to the fact that both the channel matrix $\underline{\mathbf{H}}$ and the estimated channel matrix $\hat{\underline{\mathbf{H}}}$ consist of independent and identically distributed elements, the performance of the system in terms of the average bit error probability $\overline{P}_{\mathrm{b}}^{(k)}$ is the same for all $k,\ k = 1 \ldots K$, thus the superscript k is redundant and omitted in what follows.

In Figs. 2 and 3 the average bit error probability $\overline{P}_{\mathrm{b}}$ of JD and JT with perfect and with imperfect channel knowledge in Rayleigh fading channels is plotted as a function of the SNR γ_{H} of the channel estimates of (38) for given $10\log_{10}\left(E_{\mathrm{d}}/\sigma^2\right) = 10\mathrm{dB}$ and $\sigma_{\mathrm{H}}^2 = 1/2$. As can be seen from Figs. 2 and 3, for given K and K_{B} JD and JT present the same average bit error probability $\overline{P}_{\mathrm{b}}$ for both perfect and imperfect channel knowledge. Thus it follows from Figs. 2 and 3 that the performance duality of JD and JT shown to hold for perfect channel knowledge [8] extends also to the case of imperfect channel knowledge. From Figs. 2 and 3 follows also that imperfect channel knowledge starts to have a significant impact on the average bit error probability $\overline{P}_{\mathrm{b}}$ of JD and JT already at an SNR γ_{H} of 20dB. Hence, JD and JT prove to be rather sensitive to the quality of the available channel state information. Finally, from Figs. 2 and 3 it is seen that for an SNR γ_{H} equal or less to $-10\mathrm{dB}$ an average bit error probability $\overline{P}_{\mathrm{b}}$

close to 0.5 results. This happens because a large variance σ_{E}^2 of the channel estimation error drives the SNIR $\gamma^{(k)}$ of (24) and of (35) to zero.

The average bit error probability $\overline{P}_{\mathrm{b}}$ of JD and JT as a function of E_{d}/σ^2 is illustrated in Figs. 4 to 7, with the SNR γ_{H} of (38) of the channel estimates as a parameter. An infinite SNR γ_{H} represents the case of JD and JT with perfect channel knowledge. In order to verify the theoretical findings of Sections III-B and IV-B, the average bit error probability $\overline{P}_{\mathrm{b}}$ of JD and JT obtained by averaging of (25) and of (36) over the random channel matrix $\underline{\mathbf{H}}$, respectively, is also plotted.

In Fig. 4 the single data symbol and single BS antenna case is depicted. As seen in Fig. 4, the average bit error probability $\overline{P}_{\mathrm{b}}$ of JD and JT, as obtained by averaging of (25) and of (36), respectively, matches the average bit error probability $\overline{P}_{\mathrm{b}}$ as obtained by simulations. Hence, the linear Taylor approximation of $\underline{\mathbf{D}}_{\mathrm{U}}$ and of $\underline{\mathbf{N}}_{\mathrm{U}}$ for the case of JD and of $\underline{\mathbf{D}}_{\mathrm{D}}$ and of $\underline{\mathbf{N}}_{\mathrm{D}}$ for the case of JT and the assumption of Gaussian distributed data estimation errors proves to be sufficiently precise.

It is expected from theory that JD and JT experience the same error floor $\overline{P}_{\mathrm{b},\infty}$ of the average bit error probability, see (26) and (37). However, according to the simulation result of Fig. 4, JD and JT with imperfect channel knowledge have not only equal error floors $\overline{P}_{\mathrm{b},\infty}$, but also equal average bit error probabilities $\overline{P}_{\mathrm{b}}$ in general. Thus, the performance equality between JD and JT not only in the case of perfect channel knowledge, but also in the case of imperfect channel knowledge is demonstrated.

For the case of $K = 2$ data symbols and $K_{\mathrm{B}} = 2$ antennas at the BS, Fig. 5 shows that the unavailability of perfect channel state information results in an error floor $\overline{P}_{\mathrm{b},\infty}$ of the average bit error probability $\overline{P}_{\mathrm{b}}$ which is higher than the single data symbol and single BS antenna case of Fig. 4.

An interesting equality exists in the average bit error probability of $\overline{P}_{\mathrm{b}}$ of JD and of JT between the cases depicted in Fig. 4 and Fig. 5 and if perfect channel knowledge is available. The aforementioned equality between the cases of $K_{\mathrm{B}} = K = 2$ and $K_{\mathrm{B}} = K = 4$ can be shown to hold in general if $K_{\mathrm{B}} = K_{\mathrm{M}} = K$ holds and if perfect channel state information is available. In particular, for fixed transmitted energy E_{d} and in the case that the transfer matrix $\underline{\mathbf{H}}$ is a random matrix, with the variance σ^2 of the real and imaginary parts of the noise, the SNR $\gamma^{(k)}$ of JD of (16) and of JT of (28), respectively, is a χ^2 distributed random variable with $2(K_{\mathrm{B}} - K + 1)$ degrees of freedom and mean value $2\frac{E_{\mathrm{d}}}{\sigma^2}\sigma_{\mathrm{H}}^2(K_{\mathrm{B}} - K + 1)$ [21], [23]. Thus, if $K_{\mathrm{B}} = K$ holds, the SNIR $\gamma^{(k)}$ of (16) and of (28) is a random variable following a χ^2 distribution with 2 degrees of freedom and mean value $2\sigma_{\mathrm{H}}^2$ independently of K, and hence the same average bit error probability $\overline{P}_{\mathrm{b}}$ results for all K.

Increasing the number K_{B} of antennas at the BS to 4, Fig. 6 shows that in the case of imperfect channel knowledge, lower error floors $\overline{P}_{\mathrm{b},\infty}$ in the average bit error probability $\overline{P}_{\mathrm{b}}$ are obtained for a given SNR γ_{H}, in comparison to Fig. 5. The lower error floors $\overline{P}_{\mathrm{b},\infty}$ are caused by the increased antenna gain of the system as compared to the case of Fig. 5. Finally, the comparison of Fig. 6 to Fig. 5 shows that the beneficial impact of the increased antenna gain on the average bit error probability $\overline{P}_{\mathrm{b}}$ of JD and JT increases for increasing SNR γ_{H}.

In Fig. 7 the case of $K = 3$ data symbols and $K_{\mathrm{B}} = 8$ antennas at the BS is depicted. As can be seen in Figs. 6 and 7, in the case of a high SNR γ_{H} of the channel estimates, e.g., if $10\log_{10}(\gamma_{\mathrm{H}}) = 10\mathrm{dB}$ holds, the error floor $\overline{P}_{\mathrm{b},\infty}$ for JT obtained by simulations does not match perfectly the error floor $\overline{P}_{\mathrm{b},\infty}$ predicted by (37). In particular, due to the truncation of the Taylor approximation of $\underline{\mathbf{D}}_{\mathrm{D}}$ and of $\underline{\mathbf{N}}_{\mathrm{D}}$ after the linear terms and the assumption of Gaussian distributed data estimation errors, the error floor $\overline{P}_{\mathrm{b},\infty}$ predicted by theory is slightly different from the error floor $\overline{P}_{\mathrm{b},\infty}$ obtained by simulations in the case of JT, proving to be rather optimistic.

Summarizing the simulation results of Figs. 2 to 7 follows that a rather high SNR γ_{H} is required by JD and JT in order not to observe any performance degradations due to imperfect channel state information. Furthermore, the linear Taylor approximation is sufficiently precise yielding an average bit error probability $\overline{P}_{\mathrm{b}}$ very close to the one obtained by simulations, except for the cases of low system loads K/K_{B} and high SNRs γ_{H} in which the Taylor approximation for the error floor $\overline{P}_{\mathrm{b},\infty}$ of JT proves to be slightly optimistic. Finally, an important conclusion is that the performance equality of JD and JT in the case of perfect channel knowledge can be generally extended to the case of imperfect channel knowledge.

VI. CONCLUSIONS

The influence of channel estimation errors on JD and JT is studied for the case that both JD and JT use constant transmitted energies. Analytical results based on linear Taylor approximation are presented and verified by simulations. Although in general different results on the influence of imperfect channel knowledge on JD and JT are obtained, measures of outstanding importance to practical applications, namely the energy of the emerging interferences and the resulting error floor, are identical for both JD and JT. It can be concluded that the sensitivities to channel estimation errors of JD and JT are comparable.

APPENDIX I
LINEAR TAYLOR EXPANSION OF $\underline{\mathbf{D}}_{\mathrm{U}}$ AND $\underline{\mathbf{N}}_{\mathrm{U}}$

In the following for $\underline{\mathbf{E}}$ equal to $\mathbf{0}$ the derivatives $\partial\underline{\mathbf{D}}_{\mathrm{U}} \Big/ \partial\mathrm{Re}\left\{[\underline{\mathbf{E}}]_{k_{\mathrm{B}},k_{\mathrm{M}}}\right\}$ and $\partial\underline{\mathbf{D}}_{\mathrm{U}} \Big/ \partial\mathrm{Im}\left\{[\underline{\mathbf{E}}]_{k_{\mathrm{B}},k_{\mathrm{M}}}\right\}$ contributing to (21) are derived. With (20) one obtains

$$\left.\frac{\partial\underline{\mathbf{D}}_{\mathrm{U}}}{\partial\mathrm{Re}\left\{[\underline{\mathbf{E}}]_{k_{\mathrm{B}},k_{\mathrm{M}}}\right\}}\right|_{\underline{\mathbf{E}}=\mathbf{0}} = \left(\underline{\mathbf{H}}^{*\mathrm{T}}\underline{\mathbf{H}}\right)^{-1}\underline{\mathbf{H}}^{*\mathrm{T}}\left.\frac{\partial\underline{\mathbf{E}}}{\partial\mathrm{Re}\left\{[\underline{\mathbf{E}}]_{k_{\mathrm{B}},k_{\mathrm{M}}}\right\}}\right|_{\underline{\mathbf{E}}=\mathbf{0}}. \tag{39}$$

Using the notation

$$\mathbf{1}_{k_{\mathrm{B}},k_{\mathrm{M}}} = \begin{array}{cl} \begin{pmatrix} 0 & \cdots & 0 & \cdots & 0 \\ \vdots & & \vdots & & \vdots \\ 0 & \cdots & 1 & \cdots & 0 \\ \vdots & & \vdots & & \vdots \\ 0 & \cdots & 0 & \cdots & 0 \end{pmatrix} & \leftarrow k_{\mathrm{B}}\text{th row} \\ \uparrow & \\ k_{\mathrm{M}}\text{th column} & \end{array} \tag{40}$$

(39) reads

$$\left.\frac{\partial \underline{\mathbf{D}}_{\mathrm{U}}}{\partial \mathrm{Re}\left\{[\underline{\mathbf{E}}]_{k_{\mathrm{B}},k_{\mathrm{M}}}\right\}}\right|_{\underline{\mathbf{E}}=\mathbf{0}} = \left(\underline{\mathbf{H}}^{*\mathrm{T}}\underline{\mathbf{H}}\right)^{-1}\underline{\mathbf{H}}^{*\mathrm{T}}\mathbf{1}_{k_{\mathrm{B}},k_{\mathrm{M}}}. \tag{41}$$

In analogy to (41) one obtains

$$\left.\frac{\partial \underline{\mathbf{D}}_{\mathrm{U}}}{\partial \mathrm{Im}\left\{[\underline{\mathbf{E}}]_{k_{\mathrm{B}},k_{\mathrm{M}}}\right\}}\right|_{\underline{\mathbf{E}}=\mathbf{0}} = \mathrm{j}\left(\underline{\mathbf{H}}^{*\mathrm{T}}\underline{\mathbf{H}}\right)^{-1}\underline{\mathbf{H}}^{*\mathrm{T}}\mathbf{1}_{k_{\mathrm{B}},k_{\mathrm{M}}}. \tag{42}$$

In the following next step for $\underline{\mathbf{E}}$ equal to $\mathbf{0}$ the derivatives $\partial\underline{\mathbf{N}}_{\mathrm{U}} \Big/ \partial\mathrm{Re}\left\{[\underline{\mathbf{E}}]_{k_{\mathrm{B}},k_{\mathrm{M}}}\right\}$ and $\partial\underline{\mathbf{N}}_{\mathrm{U}} \Big/ \partial\mathrm{Im}\left\{[\underline{\mathbf{E}}]_{k_{\mathrm{B}},k_{\mathrm{M}}}\right\}$ contributing to (21) are derived. With (20) one obtains

$$\begin{aligned} &\left.\frac{\partial \underline{\mathbf{N}}_{\mathrm{U}}}{\partial \mathrm{Re}\left\{[\underline{\mathbf{E}}]_{k_{\mathrm{B}},k_{\mathrm{M}}}\right\}}\right|_{\underline{\mathbf{E}}=\mathbf{0}} \\ &= \left(\underline{\mathbf{H}}^{*\mathrm{T}}\underline{\mathbf{H}}\right)^{-1}\left.\frac{\partial\left(\underline{\mathbf{H}}+\underline{\mathbf{E}}\right)^{*\mathrm{T}}}{\partial \mathrm{Re}\left\{[\underline{\mathbf{E}}]_{k_{\mathrm{B}},k_{\mathrm{M}}}\right\}}\right|_{\underline{\mathbf{E}}=\mathbf{0}} + \left.\frac{\partial\left(\left(\underline{\mathbf{H}}+\underline{\mathbf{E}}\right)^{*\mathrm{T}}\left(\underline{\mathbf{H}}+\underline{\mathbf{E}}\right)\right)^{-1}}{\partial \mathrm{Re}\left\{[\underline{\mathbf{E}}]_{k_{\mathrm{B}},k_{\mathrm{M}}}\right\}}\right|_{\underline{\mathbf{E}}=\mathbf{0}}\underline{\mathbf{H}}^{*\mathrm{T}}. \end{aligned} \tag{43}$$

Using the notation of (40) the first derivative in (43) reads

$$\left.\frac{\partial\left(\underline{\mathbf{H}}+\underline{\mathbf{E}}\right)^{*\mathrm{T}}}{\partial \mathrm{Re}\left\{[\underline{\mathbf{E}}]_{k_{\mathrm{B}},k_{\mathrm{M}}}\right\}}\right|_{\underline{\mathbf{E}}=\mathbf{0}} = \mathbf{1}^{*\mathrm{T}}_{k_{\mathrm{B}},k_{\mathrm{M}}}. \tag{44}$$

Using the relation [24]

$$\frac{\partial\left(\underline{\mathbf{A}}^{-1}\right)}{\partial z} = -\underline{\mathbf{A}}^{-1}\frac{\partial\underline{\mathbf{A}}}{\partial z}\underline{\mathbf{A}}^{-1}, \tag{45}$$

where $\underline{\mathbf{A}}$ is a full rank square matrix and z is a real valued scalar, the second derivative in (43) is simplified to

$$\begin{aligned} &\left.\frac{\partial\left(\left(\underline{\mathbf{H}}+\underline{\mathbf{E}}\right)^{*\mathrm{T}}\left(\underline{\mathbf{H}}+\underline{\mathbf{E}}\right)\right)^{-1}}{\partial \mathrm{Re}\left\{[\underline{\mathbf{E}}]_{k_{\mathrm{B}},k_{\mathrm{M}}}\right\}}\right|_{\underline{\mathbf{E}}=\mathbf{0}} \\ &= -\left(\underline{\mathbf{H}}^{*\mathrm{T}}\underline{\mathbf{H}}\right)^{-1}\left.\frac{\partial\left(\left(\underline{\mathbf{H}}+\underline{\mathbf{E}}\right)^{*\mathrm{T}}\left(\underline{\mathbf{H}}+\underline{\mathbf{E}}\right)\right)}{\partial \mathrm{Re}\left\{[\underline{\mathbf{E}}]_{k_{\mathrm{B}},k_{\mathrm{M}}}\right\}}\right|_{\underline{\mathbf{E}}=\mathbf{0}}\left(\underline{\mathbf{H}}^{*\mathrm{T}}\underline{\mathbf{H}}\right)^{-1} \\ &= -\left(\underline{\mathbf{H}}^{*\mathrm{T}}\underline{\mathbf{H}}\right)^{-1}\left(\underline{\mathbf{H}}^{*\mathrm{T}}\mathbf{1}_{k_{\mathrm{B}},k_{\mathrm{M}}} + \mathbf{1}^{*\mathrm{T}}_{k_{\mathrm{B}},k_{\mathrm{M}}}\underline{\mathbf{H}}\right)\left(\underline{\mathbf{H}}^{*\mathrm{T}}\underline{\mathbf{H}}\right)^{-1}. \end{aligned} \tag{46}$$

Substituting (44) and (46) in (43) one obtains

$$\begin{aligned} &\left.\frac{\partial \underline{\mathbf{N}}_{\mathrm{U}}}{\partial \mathrm{Re}\left\{[\underline{\mathbf{E}}]_{k_{\mathrm{B}},k_{\mathrm{M}}}\right\}}\right|_{\underline{\mathbf{E}}=\mathbf{0}} = \\ &\left(\underline{\mathbf{H}}^{*\mathrm{T}}\underline{\mathbf{H}}\right)^{-1}\mathbf{1}^{*\mathrm{T}}_{k_{\mathrm{B}},k_{\mathrm{M}}} - \left(\underline{\mathbf{H}}^{*\mathrm{T}}\underline{\mathbf{H}}\right)^{-1}\left(\underline{\mathbf{H}}^{*\mathrm{T}}\mathbf{1}_{k_{\mathrm{B}},k_{\mathrm{M}}} + \mathbf{1}^{*\mathrm{T}}_{k_{\mathrm{B}},k_{\mathrm{M}}}\underline{\mathbf{H}}\right)\left(\underline{\mathbf{H}}^{*\mathrm{T}}\underline{\mathbf{H}}\right)^{-1}\underline{\mathbf{H}}^{*\mathrm{T}}. \end{aligned} \tag{47}$$

In analogy to (47) one obtains

$$\left.\frac{\partial \underline{\mathbf{N}}_{\mathrm{U}}}{\partial \mathrm{Im}\left\{[\underline{\mathbf{E}}]_{k_{\mathrm{B}},k_{\mathrm{M}}}\right\}}\right|_{\underline{\mathbf{E}}=\mathbf{0}} = \\ -\mathrm{j}\left(\underline{\mathbf{H}}^{*\mathrm{T}}\underline{\mathbf{H}}\right)^{-1}\mathbf{1}^{*\mathrm{T}}_{k_{\mathrm{B}},k_{\mathrm{M}}} - \mathrm{j}\left(\underline{\mathbf{H}}^{*\mathrm{T}}\underline{\mathbf{H}}\right)^{-1}\left(\underline{\mathbf{H}}^{*\mathrm{T}}\mathbf{1}_{k_{\mathrm{B}},k_{\mathrm{M}}} - \mathbf{1}^{*\mathrm{T}}_{k_{\mathrm{B}},k_{\mathrm{M}}}\underline{\mathbf{H}}\right)\left(\underline{\mathbf{H}}^{*\mathrm{T}}\underline{\mathbf{H}}\right)^{-1}\underline{\mathbf{H}}^{*\mathrm{T}}. \quad (48)$$

Substituting (41), (42), (47) and (48) in (21) yields the desired result of (22).

Appendix II

Covariance Matrix $\underline{\mathbf{R}}_{\hat{\mathrm{d}}-\mathrm{d}}$ for JD

Setting out from (22), the covariance matrix $\underline{\mathbf{R}}_{\hat{\mathrm{d}}-\mathrm{d}}$ reads

$$\begin{aligned}\underline{\mathbf{R}}_{\hat{\mathrm{d}}-\mathrm{d}} &= \mathrm{E}\left\{\left(\hat{\underline{\mathbf{d}}}-\underline{\mathbf{d}}\right)\left(\hat{\underline{\mathbf{d}}}-\underline{\mathbf{d}}\right)^{*\mathrm{T}}\right\} \\ &\approx 4\sigma_{\mathrm{E}}^2 K_{\mathrm{M}}\left(\underline{\mathbf{H}}^{*\mathrm{T}}\underline{\mathbf{H}}\right)^{-1} + \frac{2\sigma^2}{E_{\mathrm{d}}}\left(\underline{\mathbf{H}}^{*\mathrm{T}}\underline{\mathbf{H}}\right)^{-1} + \frac{2\sigma^2 K_{\mathrm{B}}\,2\sigma_{\mathrm{E}}^2}{E_{\mathrm{d}}}\left(\underline{\mathbf{H}}^{*\mathrm{T}}\underline{\mathbf{H}}\right)^{-2} \\ &\quad -\frac{2\sigma^2}{E_{\mathrm{d}}}\mathrm{E}\Big\{\left(\underline{\mathbf{H}}^{*\mathrm{T}}\underline{\mathbf{H}}\right)^{-1}\cdot\underline{\mathbf{E}}^{*\mathrm{T}}\underline{\mathbf{H}}\left(\underline{\mathbf{H}}^{*\mathrm{T}}\underline{\mathbf{H}}\right)^{-1}\underline{\mathbf{H}}^{*\mathrm{T}}\underline{\mathbf{E}}\left(\underline{\mathbf{H}}^{*\mathrm{T}}\underline{\mathbf{H}}\right)^{-1}\Big\} \\ &\quad +\frac{2\sigma^2}{E_{\mathrm{d}}}\mathrm{E}\Big\{\left(\underline{\mathbf{H}}^{*\mathrm{T}}\underline{\mathbf{H}}\right)^{-1}\underline{\mathbf{H}}^{*\mathrm{T}}\underline{\mathbf{E}}\left(\underline{\mathbf{H}}^{*\mathrm{T}}\underline{\mathbf{H}}\right)^{-1}\underline{\mathbf{E}}^{*\mathrm{T}}\underline{\mathbf{H}}\left(\underline{\mathbf{H}}^{*\mathrm{T}}\underline{\mathbf{H}}\right)^{-1}\Big\}.\end{aligned} \quad (49)$$

Using the relation

$$\mathrm{E}\left\{\underline{\mathbf{E}}^{*\mathrm{T}}\underline{\mathbf{A}}\,\underline{\mathbf{E}}\right\} = 2\sigma_{\mathrm{E}}^2\,\mathrm{trace}\left\{\underline{\mathbf{A}}\right\}\mathbf{I}, \quad (50)$$

where $\underline{\mathbf{A}}$ is a square matrix, (49) can be simplified to

$$\begin{aligned}\underline{\mathbf{R}}_{\hat{\mathrm{d}}-\mathrm{d}} &\approx \frac{2\sigma^2}{E_{\mathrm{d}}}\left(\underline{\mathbf{H}}^{*\mathrm{T}}\underline{\mathbf{H}}\right)^{-1}\left[1+\frac{2\mathrm{E}_{\mathrm{d}}2\sigma_{\mathrm{E}}^2 K_{\mathrm{M}}}{2\sigma^2}+2\sigma_{\mathrm{E}}^2\mathrm{trace}\left\{\left(\underline{\mathbf{H}}^{*\mathrm{T}}\underline{\mathbf{H}}\right)^{-1}\right\}\right] \\ &\quad +\frac{2\sigma^2 2\sigma_{\mathrm{E}}^2}{E_{\mathrm{d}}}\left(\underline{\mathbf{H}}^{*\mathrm{T}}\underline{\mathbf{H}}\right)^{-2}\left(K_{\mathrm{B}}-K_{\mathrm{M}}\right).\end{aligned} \quad (51)$$

Appendix III

Linear Taylor Expansion of $\underline{\mathbf{D}}_{\mathrm{D}}$ and $\underline{\mathbf{N}}_{\mathrm{D}}$

In the following for $\underline{\mathbf{E}}$ equal to $\mathbf{0}$ the derivatives $\partial\underline{\mathbf{D}}_{\mathrm{D}} \Big/ \partial\mathrm{Re}\left\{[\underline{\mathbf{E}}]_{k_{\mathrm{B}},k_{\mathrm{M}}}\right\}$ and $\partial\underline{\mathbf{D}}_{\mathrm{D}} \Big/ \partial\mathrm{Im}\left\{[\underline{\mathbf{E}}]_{k_{\mathrm{B}},k_{\mathrm{M}}}\right\}$ contributing to

$$
\begin{aligned}
&\hat{\underline{\mathbf{d}}} - \underline{\mathbf{d}} \approx \\
&-\left[\sum_{k_{\mathrm{B}},k_{\mathrm{M}}} \left.\frac{\partial\underline{\mathbf{D}}_{\mathrm{D}}}{\partial\mathrm{Re}\left\{[\underline{\mathbf{E}}]_{k_{\mathrm{B}},k_{\mathrm{M}}}\right\}}\right|_{\underline{\mathbf{E}}=\mathbf{0}} \mathrm{Re}\left\{[\underline{\mathbf{E}}]_{k_{\mathrm{B}},k_{\mathrm{M}}}\right\} + \sum_{k_{\mathrm{B}},k_{\mathrm{M}}} \left.\frac{\partial\underline{\mathbf{D}}_{\mathrm{D}}}{\partial\mathrm{Im}\left\{[\underline{\mathbf{E}}]_{k_{\mathrm{B}},k_{\mathrm{M}}}\right\}}\right|_{\underline{\mathbf{E}}=\mathbf{0}} \mathrm{Im}\left\{[\underline{\mathbf{E}}]_{k_{\mathrm{B}},k_{\mathrm{M}}}\right\}\right] \cdot \underline{\mathbf{d}} \\
&+\frac{1}{\sqrt{E_{\mathrm{d}}}}\left[\left(\mathrm{diag}\left(\left(\underline{\mathbf{H}}^{\mathrm{T}}\underline{\mathbf{H}}^{*}\right)^{-1}\right)\right)^{\frac{1}{2}}\right. \\
&\left.+\sum_{k_{\mathrm{B}},k_{\mathrm{M}}} \left.\frac{\partial\underline{\mathbf{N}}_{\mathrm{D}}}{\partial\mathrm{Re}\left\{[\underline{\mathbf{E}}]_{k_{\mathrm{B}},k_{\mathrm{M}}}\right\}}\right|_{\underline{\mathbf{E}}=\mathbf{0}} \mathrm{Re}\left\{[\underline{\mathbf{E}}]_{k_{\mathrm{B}},k_{\mathrm{M}}}\right\} + \sum_{k_{\mathrm{B}},k_{\mathrm{M}}} \left.\frac{\partial\underline{\mathbf{N}}_{\mathrm{D}}}{\partial\,\mathrm{Im}\left\{[\underline{\mathbf{E}}]_{k_{\mathrm{B}},k_{\mathrm{M}}}\right\}}\right|_{\underline{\mathbf{E}}=\mathbf{0}} \mathrm{Im}\left\{[\underline{\mathbf{E}}]_{k_{\mathrm{B}},k_{\mathrm{M}}}\right\}\right] \cdot \underline{\mathbf{n}}_{\mathrm{D}}
\end{aligned}
\tag{52}
$$

are derived. With (32) and the notation of (40) one obtains

$$
\begin{aligned}
&\left.\frac{\partial\underline{\mathbf{D}}_{\mathrm{D}}}{\partial\mathrm{Re}\left\{[\underline{\mathbf{E}}]_{k_{\mathrm{B}},k_{\mathrm{M}}}\right\}}\right|_{\underline{\mathbf{E}}=\mathbf{0}} \\
&= \left(\mathrm{diag}\left(\left(\underline{\mathbf{H}}^{\mathrm{T}}\underline{\mathbf{H}}^{*}\right)^{-1}\right)\right)^{\frac{1}{2}} \mathbf{1}^{\mathrm{T}}_{k_{\mathrm{B}},k_{\mathrm{M}}}\underline{\mathbf{H}}^{*}\left(\underline{\mathbf{H}}^{\mathrm{T}}\underline{\mathbf{H}}^{*}\right)^{-1}\left(\mathrm{diag}\left(\left(\underline{\mathbf{H}}^{\mathrm{T}}\underline{\mathbf{H}}^{*}\right)^{-1}\right)\right)^{-\frac{1}{2}}.
\end{aligned}
\tag{53}
$$

In analogy to (53) one obtains

$$
\begin{aligned}
&\left.\frac{\partial\underline{\mathbf{D}}_{\mathrm{D}}}{\partial\mathrm{Im}\left\{[\underline{\mathbf{E}}]_{k_{\mathrm{B}},k_{\mathrm{M}}}\right\}}\right|_{\underline{\mathbf{E}}=\mathbf{0}} \\
&= \left(\mathrm{diag}\left(\left(\underline{\mathbf{H}}^{\mathrm{T}}\underline{\mathbf{H}}^{*}\right)^{-1}\right)\right)^{\frac{1}{2}} \mathbf{1}^{\mathrm{T}}_{k_{\mathrm{B}},k_{\mathrm{M}}}\underline{\mathbf{H}}^{*}\left(\underline{\mathbf{H}}^{\mathrm{T}}\underline{\mathbf{H}}^{*}\right)^{-1}\left(\mathrm{diag}\left(\left(\underline{\mathbf{H}}^{\mathrm{T}}\underline{\mathbf{H}}^{*}\right)^{-1}\right)\right)^{-\frac{1}{2}}.
\end{aligned}
\tag{54}
$$

In the following next step for $\underline{\mathbf{E}}$ equal to $\mathbf{0}$ the derivatives $\partial\underline{\mathbf{N}}_{\mathrm{D}} \Big/ \partial\mathrm{Re}\left\{[\underline{\mathbf{E}}]_{k_{\mathrm{B}},k_{\mathrm{M}}}\right\}$ and $\partial\underline{\mathbf{N}}_{\mathrm{D}} \Big/ \partial\mathrm{Im}\left\{[\underline{\mathbf{E}}]_{k_{\mathrm{B}},k_{\mathrm{M}}}\right\}$ contributing to (52) are derived. With (32) one obtains

$$
\begin{aligned}
&\left.\frac{\partial\underline{\mathbf{N}}_{\mathrm{D}}}{\partial\mathrm{Re}\left\{[\underline{\mathbf{E}}]_{k_{\mathrm{B}},k_{\mathrm{M}}}\right\}}\right|_{\underline{\mathbf{E}}=\mathbf{0}} = \\
&\qquad \frac{1}{2}\left(\mathrm{diag}\left(\left(\underline{\mathbf{H}}^{\mathrm{T}}\underline{\mathbf{H}}^{*}\right)^{-1}\right)\right)^{-\frac{1}{2}} \left.\frac{\partial\mathrm{diag}\left(\left((\underline{\mathbf{H}}+\underline{\mathbf{E}})^{\mathrm{T}}(\underline{\mathbf{H}}+\underline{\mathbf{E}})^{*}\right)^{-1}\right)}{\partial\mathrm{Re}\left\{[\underline{\mathbf{E}}]_{k_{\mathrm{B}},k_{\mathrm{M}}}\right\}}\right|_{\underline{\mathbf{E}}=\mathbf{0}}
\end{aligned}
$$

$$= \frac{1}{2}\left(\mathrm{diag}\left(\left(\underline{\mathbf{H}}^{\mathrm{T}}\underline{\mathbf{H}}^{*}\right)^{-1}\right)\right)^{-\frac{1}{2}} \mathrm{diag}\left(\left.\frac{\partial\left(\left(\underline{\mathbf{H}}+\underline{\mathbf{E}}\right)^{\mathrm{T}}\left(\underline{\mathbf{H}}+\underline{\mathbf{E}}\right)^{*}\right)^{-1}}{\partial\mathrm{Re}\left\{\left[\underline{\mathbf{E}}\right]_{k_{\mathrm{B}},k_{\mathrm{M}}}\right\}}\right|_{\underline{\mathbf{E}}=\mathbf{0}}\right). \tag{55}$$

In analogy to (46) one obtains for the derivative in the last line of (55)

$$\left.\frac{\partial\left(\left(\underline{\mathbf{H}}+\underline{\mathbf{E}}\right)^{\mathrm{T}}\left(\underline{\mathbf{H}}+\underline{\mathbf{E}}\right)^{*}\right)^{-1}}{\partial\mathrm{Re}\left\{\left[\underline{\mathbf{E}}\right]_{k_{\mathrm{B}},k_{\mathrm{M}}}\right\}}\right|_{\underline{\mathbf{E}}=\mathbf{0}} = -\left(\underline{\mathbf{H}}^{\mathrm{T}}\underline{\mathbf{H}}^{*}\right)^{-1}\cdot\left(\underline{\mathbf{H}}^{\mathrm{T}}\mathbf{1}^{*}_{k_{\mathrm{B}},k_{\mathrm{M}}}+\mathbf{1}^{\mathrm{T}}_{k_{\mathrm{B}},k_{\mathrm{M}}}\underline{\mathbf{H}}^{*}\right)\left(\underline{\mathbf{H}}^{\mathrm{T}}\underline{\mathbf{H}}^{*}\right)^{-1}. \tag{56}$$

Substituting this result in (55) yields the result

$$\left.\frac{\partial\underline{\mathbf{N}}_{\mathrm{D}}}{\partial\mathrm{Re}\left\{\left[\underline{\mathbf{E}}\right]_{k_{\mathrm{B}},k_{\mathrm{M}}}\right\}}\right|_{\underline{\mathbf{E}}=\mathbf{0}} = -\frac{1}{2}\left(\mathrm{diag}\left(\left(\underline{\mathbf{H}}^{\mathrm{T}}\underline{\mathbf{H}}^{*}\right)^{-1}\right)\right)^{-\frac{1}{2}} \cdot\mathrm{diag}\left(\left(\underline{\mathbf{H}}^{\mathrm{T}}\underline{\mathbf{H}}^{*}\right)^{-1}\cdot\left(\underline{\mathbf{H}}^{\mathrm{T}}\mathbf{1}^{*}_{k_{\mathrm{B}},k_{\mathrm{M}}}+\mathbf{1}^{\mathrm{T}}_{k_{\mathrm{B}},k_{\mathrm{M}}}\underline{\mathbf{H}}^{*}\right)\left(\underline{\mathbf{H}}^{\mathrm{T}}\underline{\mathbf{H}}^{*}\right)^{-1}\right). \tag{57}$$

In analogy to (57) one obtains

$$\left.\frac{\partial\underline{\mathbf{N}}_{\mathrm{D}}}{\partial\mathrm{Im}\left\{\left[\underline{\mathbf{E}}\right]_{k_{\mathrm{B}},k_{\mathrm{M}}}\right\}}\right|_{\underline{\mathbf{E}}=\mathbf{0}} = -\frac{1}{2}\left(\mathrm{diag}\left(\left(\underline{\mathbf{H}}^{\mathrm{T}}\underline{\mathbf{H}}^{*}\right)^{-1}\right)\right)^{-\frac{1}{2}} \cdot\mathrm{diag}\left(\left(\underline{\mathbf{H}}^{\mathrm{T}}\underline{\mathbf{H}}^{*}\right)^{-1}\cdot\left(-\underline{\mathbf{H}}^{\mathrm{T}}\mathbf{1}^{*}_{k_{\mathrm{B}},k_{\mathrm{M}}}+\mathbf{1}^{\mathrm{T}}_{k_{\mathrm{B}},k_{\mathrm{M}}}\underline{\mathbf{H}}^{*}\right)\left(\underline{\mathbf{H}}^{\mathrm{T}}\underline{\mathbf{H}}^{*}\right)^{-1}\right). \tag{58}$$

Substituting (53), (54), (57) and (58) in (52) yields the desired result of (33).

Appendix IV

Covariance Matrix $\underline{\mathbf{R}}_{\hat{\mathrm{d}}-\mathrm{d}}$ for JT

Setting out from (33), the covariance matrix $\underline{\mathbf{R}}_{\hat{\mathrm{d}}-\mathrm{d}}$ reads

$$\begin{aligned}\underline{\mathbf{R}}_{\hat{\mathrm{d}}-\mathrm{d}} &= \mathrm{E}\left\{\left(\hat{\underline{\mathbf{d}}}-\underline{\mathbf{d}}\right)\left(\hat{\underline{\mathbf{d}}}-\underline{\mathbf{d}}\right)^{*\mathrm{T}}\right\}\\ &\approx 2\mathrm{E}\Bigg\{\left(\mathrm{diag}\left(\left(\underline{\mathbf{H}}^{\mathrm{T}}\underline{\mathbf{H}}^{*}\right)^{-1}\right)\right)^{\frac{1}{2}}\underline{\mathbf{E}}^{\mathrm{T}}\underline{\mathbf{H}}^{*}\left(\underline{\mathbf{H}}^{\mathrm{T}}\underline{\mathbf{H}}^{*}\right)^{-1}\\ &\quad\cdot\left(\mathrm{diag}\left(\left(\underline{\mathbf{H}}^{\mathrm{T}}\underline{\mathbf{H}}^{*}\right)^{-1}\right)\right)^{-1}\left(\underline{\mathbf{H}}^{\mathrm{T}}\underline{\mathbf{H}}^{*}\right)^{-1}\underline{\mathbf{H}}^{\mathrm{T}}\underline{\mathbf{E}}^{*}\left(\mathrm{diag}\left(\left(\underline{\mathbf{H}}^{\mathrm{T}}\underline{\mathbf{H}}^{*}\right)^{-1}\right)\right)^{\frac{1}{2}}\Bigg\}\\ &\quad+\frac{2\sigma^{2}}{E_{\mathrm{d}}}\mathrm{diag}\left(\left(\underline{\mathbf{H}}^{\mathrm{T}}\underline{\mathbf{H}}^{*}\right)^{-1}\right)+\frac{\sigma^{2}}{E_{\mathrm{d}}}\mathrm{E}\Bigg\{\mathrm{diag}\left(\left(\underline{\mathbf{H}}^{\mathrm{T}}\underline{\mathbf{H}}^{*}\right)^{-1}\underline{\mathbf{H}}^{\mathrm{T}}\underline{\mathbf{E}}^{*}\left(\underline{\mathbf{H}}^{\mathrm{T}}\underline{\mathbf{H}}^{*}\right)^{-1}\right)\\ &\quad\cdot\mathrm{diag}\left(\left(\underline{\mathbf{H}}^{\mathrm{T}}\underline{\mathbf{H}}^{*}\right)^{-1}\underline{\mathbf{E}}^{\mathrm{T}}\underline{\mathbf{H}}^{*}\left(\underline{\mathbf{H}}^{\mathrm{T}}\underline{\mathbf{H}}^{*}\right)^{-1}\right)\Bigg\}\left(\mathrm{diag}\left(\left(\underline{\mathbf{H}}^{\mathrm{T}}\underline{\mathbf{H}}^{*}\right)^{-1}\right)\right)^{-1}.\end{aligned} \tag{59}$$

With $\left[\left(\underline{\mathbf{H}}^{\mathrm{T}}\underline{\mathbf{H}}^{*}\right)^{-1}\right]_k$ denoting the k-th row of the hermitian matrix $\left(\underline{\mathbf{H}}^{\mathrm{T}}\underline{\mathbf{H}}^{*}\right)^{-1}$, and (50) the k-th diagonal element of

$$\mathrm{E}\left\{\operatorname{diag}\left(\left(\underline{\mathbf{H}}^{\mathrm{T}}\underline{\mathbf{H}}^{*}\right)^{-1}\underline{\mathbf{H}}^{\mathrm{T}}\underline{\mathbf{E}}^{*}\left(\underline{\mathbf{H}}^{\mathrm{T}}\underline{\mathbf{H}}^{*}\right)^{-1}\right)\operatorname{diag}\left(\left(\underline{\mathbf{H}}^{\mathrm{T}}\underline{\mathbf{H}}^{*}\right)^{-1}\underline{\mathbf{E}}^{\mathrm{T}}\underline{\mathbf{H}}^{*}\left(\underline{\mathbf{H}}^{\mathrm{T}}\underline{\mathbf{H}}^{*}\right)^{-1}\right)\right\} \tag{60}$$

reads

$$\begin{aligned}
&\mathrm{E}\left\{\left[\left(\underline{\mathbf{H}}^{\mathrm{T}}\underline{\mathbf{H}}^{*}\right)^{-1}\right]_k\underline{\mathbf{H}}^{\mathrm{T}}\underline{\mathbf{E}}^{*}\left[\left(\underline{\mathbf{H}}^{\mathrm{T}}\underline{\mathbf{H}}^{*}\right)^{-1}\right]_k^{*\mathrm{T}}\left[\left(\underline{\mathbf{H}}^{\mathrm{T}}\underline{\mathbf{H}}^{*}\right)^{-1}\right]_k\underline{\mathbf{E}}^{\mathrm{T}}\underline{\mathbf{H}}^{*}\left[\left(\underline{\mathbf{H}}^{\mathrm{T}}\underline{\mathbf{H}}^{*}\right)^{-1}\right]_k^{*\mathrm{T}}\right\}\\
&= 2\sigma_{\mathrm{E}}^2\left[\left(\underline{\mathbf{H}}^{\mathrm{T}}\underline{\mathbf{H}}^{*}\right)^{-1}\right]_k\underline{\mathbf{H}}^{\mathrm{T}}\operatorname{trace}\left\{\left[\left(\underline{\mathbf{H}}^{\mathrm{T}}\underline{\mathbf{H}}^{*}\right)^{-1}\right]_k^{*\mathrm{T}}\left[\left(\underline{\mathbf{H}}^{\mathrm{T}}\underline{\mathbf{H}}^{*}\right)^{-1}\right]_k\right\}\underline{\mathbf{H}}^{*}\left[\left(\underline{\mathbf{H}}^{\mathrm{T}}\underline{\mathbf{H}}^{*}\right)^{-1}\right]_k^{*\mathrm{T}}\\
&= 2\sigma_{\mathrm{E}}^2\left[\left(\underline{\mathbf{H}}^{\mathrm{T}}\underline{\mathbf{H}}^{*}\right)^{-1}\right]_k\left[\left(\underline{\mathbf{H}}^{\mathrm{T}}\underline{\mathbf{H}}^{*}\right)^{-1}\right]_k^{*\mathrm{T}}\left[\left(\underline{\mathbf{H}}^{\mathrm{T}}\underline{\mathbf{H}}^{*}\right)^{-1}\right]_k\underline{\mathbf{H}}^{\mathrm{T}}\underline{\mathbf{H}}^{*}\left[\left(\underline{\mathbf{H}}^{\mathrm{T}}\underline{\mathbf{H}}^{*}\right)^{-1}\right]_k^{*\mathrm{T}}\\
&= 2\sigma_{\mathrm{E}}^2\left[\operatorname{diag}\left(\left(\underline{\mathbf{H}}^{\mathrm{T}}\underline{\mathbf{H}}^{*}\right)^{-2}\right)\right]_{k,k}\cdot\left[\operatorname{diag}\left(\left(\underline{\mathbf{H}}^{\mathrm{T}}\underline{\mathbf{H}}^{*}\right)^{-1}\right)\right]_{k,k}.
\end{aligned} \tag{61}$$

Using (50) and (61), (59) is simplified to

$$\begin{aligned}
\underline{\mathbf{R}}_{\hat{\mathrm{d}}-\mathrm{d}} \approx{}& 4\sigma_{\mathrm{E}}^2\operatorname{trace}\left\{\underline{\mathbf{H}}^{*}\left(\underline{\mathbf{H}}^{\mathrm{T}}\underline{\mathbf{H}}^{*}\right)^{-1}\left(\operatorname{diag}\left(\left(\underline{\mathbf{H}}^{\mathrm{T}}\underline{\mathbf{H}}^{*}\right)^{-1}\right)\right)^{-1}\left(\underline{\mathbf{H}}^{\mathrm{T}}\underline{\mathbf{H}}^{*}\right)^{-1}\underline{\mathbf{H}}^{\mathrm{T}}\right\}\\
&\cdot\operatorname{diag}\left(\left(\underline{\mathbf{H}}^{\mathrm{T}}\underline{\mathbf{H}}^{*}\right)^{-1}\right)+\frac{2\sigma^2}{E_{\mathrm{d}}}\operatorname{diag}\left(\left(\underline{\mathbf{H}}^{\mathrm{T}}\underline{\mathbf{H}}^{*}\right)^{-1}\right)+\frac{\sigma^2 2\sigma_{\mathrm{E}}^2}{E_{\mathrm{d}}}\operatorname{diag}\left(\left(\underline{\mathbf{H}}^{\mathrm{T}}\underline{\mathbf{H}}^{*}\right)^{-2}\right).
\end{aligned} \tag{62}$$

(62) can be further simplified to the desired result of (34).

ACKNOWLEDGMENTS

The authors gratefully appreciate the stimulating discussions and the fruitful exchange of ideas with Professor P.W. Baier and their co-workers at the Research Group for RF Communications at the University of Kaiserslautern. The support of individual parts of this work in the framework of the EU-IST-Project FLOWS (Flexible Convergence of Wireless Standards and Services), by DFG and by Siemens AG is highly acknowledged.

REFERENCES

[1] R. D. J. van Nee and R. Prasad, *OFDM for Wireless Multimedia Communications.* Boston: Artech House, 2000.
[2] E. Telatar, “Capacity of multi-antenna Gaussian channels,” *European Transactions on Telecommunications*, vol. 10, no. 6, pp. 585–595, 1999.
[3] G. Lebrun, T. Ying, and M. Faulkner, “MIMO transmission over a time-varying channel using SVD,” in *Proc. IEEE Global Telecommunications Conference (GLOBECOM’02)*, Taipei, Nov. 2002, pp. 414–418.
[4] S. Verdú, *Multiuser Detection.* Cambridge: Cambridge University Press, 1998.

[5] P. Wolniansky, G. Foschini, G. Golden, and R. Valenzuela, “V-BLAST: An architecture for realizing very high data rates over rich-scattering wireless channel,” in *Proc. URSI International Symposium on Signals Systems, and Electronics (ISSSE’98)*, Pisa, 1998, pp. 295–300.

[6] G. J. Foschini, “Layered space-time architecture for wireless communication in a fading environment when using multi-element antennas,” *The Bell System Technical Journal*, vol. 1, no. 2, pp. 41–59, 1996.

[7] R. F. H. Fischer, *Precoding and Signal Shaping for Digital Transmission*. New York: John Wiley & Sons, 2002.

[8] T. Weber and I. Maniatis, “Channel knowledge: A crucial prerequisite for MIMO transmission?” in *COST 273 TD(03)083*, Paris, 2003.

[9] E. Visotsky and U. Madhow, “Space-time transmit precoding with imperfect feedback,” *IEEE Transactions on Information Theory*, vol. 47, no. 6, pp. 2632–2639, 2001.

[10] S. A. Jafar, S. Vishwanath, and A. J. Goldsmith, “Channel capacity and beamforming for multiple transmit and receive antennas with covariance feedback,” in *Proc. IEEE International Conference on Communications (ICC’01)*, vol. 7, Burbank, California, 2001, pp. 2266–2270.

[11] S. Simon and A. Moustakas, “Optimizing MIMO antenna systems with channel covariance feedback,” *IEEE Journal on Selected Areas in Communications*, vol. 21, pp. 502–513, 2000.

[12] M. Meurer and T. Weber, “Imperfect channel knowledge: An insurmountable barrier in Rx oriented multi-user MIMO transmission?” in *Proc. 5th ITG Conference on Source and Channel Coding (SCC’04)*, Erlangen, 2004, pp. 371–379.

[13] T. Weber and M. Meurer, “Imperfect channel state information in MIMO-transmission,” in *Proc. IEEE 59th Vehicular Technology Conference (VTC’04-Spring)*, Milan, 2004.

[14] Z. Zvonar and M. Stajanovic, “Performance of multiuser diversity reception in nonselective rayleigh fading CDMA channels,” in *Global Telecommunications Conference, Communications Theory Mini-Conference Record*, Nov. 1994, pp. 171–175.

[15] V. Jungnickel, T. Haustein, E. Jorswieck, and C. Helmolt, “On linear pre-processing in multi-antenna systems,” in *Proc. IEEE Global Telecommunications Conference (GLOBECOM’02)*, Taipei, 2002, pp. 1012–1016.

[16] D. Gerlach and A. Paulraj, “Adaptive transmitting antenna arrays with feedback,” *IEEE Signal Processing Letters*, vol. 1, no. 10, pp. 150–152, Oct. 1994.

[17] M. Meurer, P. W. Baier, T. Weber, Y. Lu, and A. Papathanassiou, “Joint transmission: advantageous downlink concept for CDMA mobile radio systems using time division duplexing,” *IEE Electronics Letters*, vol. 36, no. 10, pp. 900–901, 2000.

[18] F. Kowalewski and P. Mangold, “Joint predistortion and transmit diversity,” in *Proc. IEEE Global Telecommunications Conference (GLOBECOM’00)*, San Francisco, 2000, pp. 245–249.

[19] R. L.-U. Choi and R. D. Murch, “New transmit schemes and simplified receivers for MIMO wireless communication systems,” *IEEE Transactions on Wireless Communications*, vol. 2, no. 6, pp. 1217–1230, Nov. 2003.

[20] ——, “A pre-BLAST-DFE technique for the downlink of frequency-selective fading MIMO channels,” *IEEE Transactions on Communications*, vol. 52, no. 5, pp. 737–743, May 2004.

[21] J. G. Proakis, *Digital Communications*, 3rd ed. New York: McGraw-Hill, 1995.

[22] A. Klein, *Multi-user detection of CDMA signals – algorithms and their application to cellular mobile radio*. Düsseldorf: Fortschrittberichte VDI, Reihe 10, 1996, no. 423.

[23] M. Meurer, T. Weber, and W. Qiu, “Transmit Nonlinear Zero Forcing: Energy efficient receiver oriented transmission in MIMO CDMA mobile radio downlinks,” in *Proc. IEEE 8th International Symposium on Spread Spectrum Techniques & Applications (ISSSTA’04)*, Sydney, 2004, accepted for publication.

[24] H. Lütkepohl, *Handbook of Matrices*. New York: John Wiley & Sons, 1996.

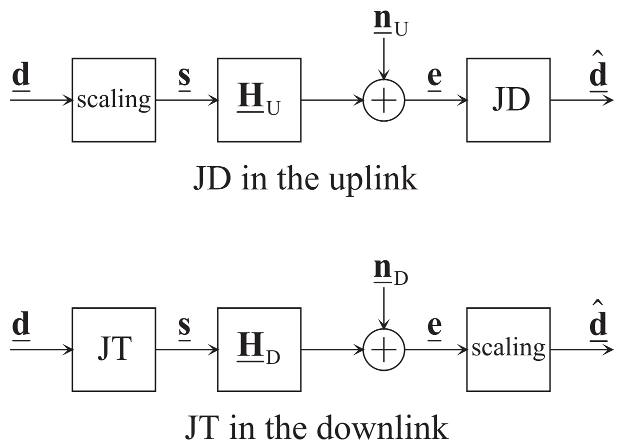

Fig. 1. Data transmission based on JD and JT

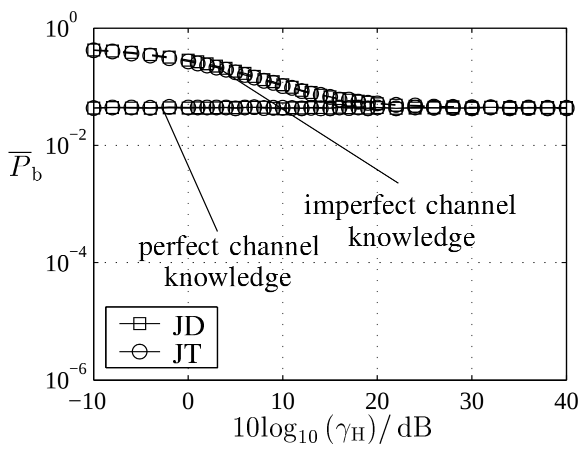

Fig. 2. Average average bit error probability $\overline{P}_{\mathrm{b}}$ of JD and JT with perfect and imperfect channel knowledge; Parameters: $\sigma_{\mathrm{H}}^2 = 1/2$, $10\log_{10}\left(E_{\mathrm{d}}/\sigma^2\right) = 10\mathrm{dB}$, $K = 2$, $K_{\mathrm{B}} = 2$.

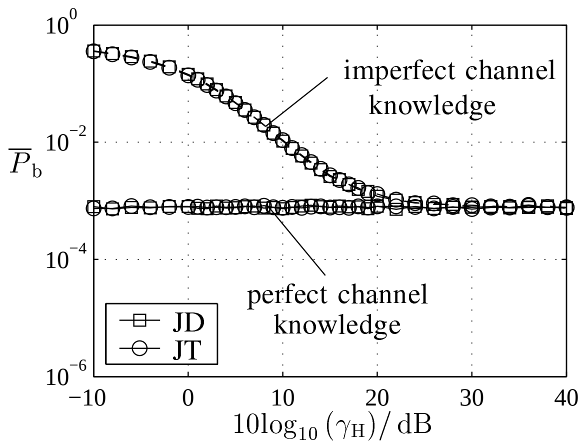

Fig. 3. Average average bit error probability $\overline{P}_\mathrm{b}$ of JD and JT with perfect and imperfect channel knowledge; Parameters: $\sigma_\mathrm{H}^2 = 1/2$, $10\log_{10}\left(E_\mathrm{d}/\sigma^2\right) = 10\mathrm{dB}$, $K = 2$, $K_\mathrm{B} = 4$.

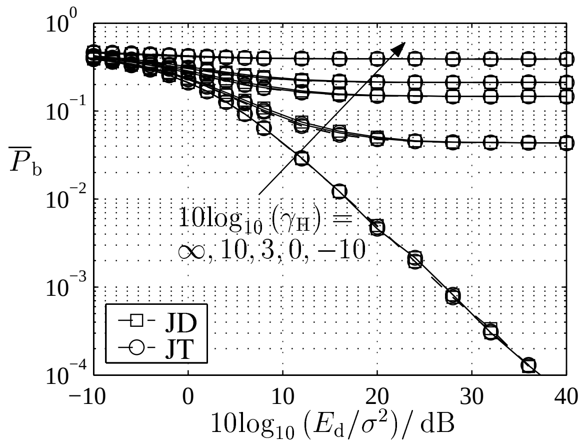

Fig. 4. Average bit error probability $\overline{P}_\mathrm{b}$ of JD and JT from theory (solid lines) and from simulation (dashed lines); Parameters: $K = 1$, $K_\mathrm{B} = 1$, QPSK modulation.

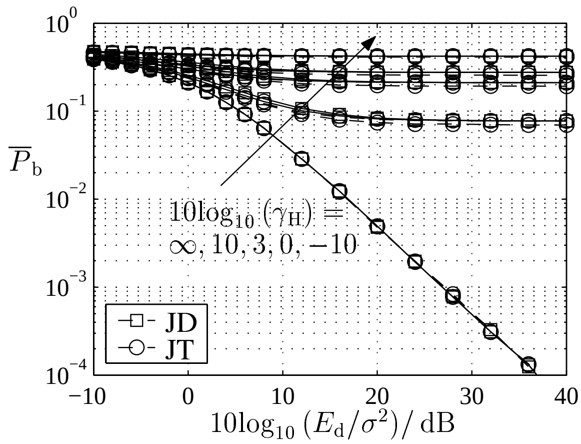

Fig. 5. Average bit error probability $\overline{P}_\mathrm{b}$ of JD and JT from theory (solid lines) and from simulation (dashed lines); Parameters: $K = 2$, $K_\mathrm{B} = 2$, QPSK modulation.

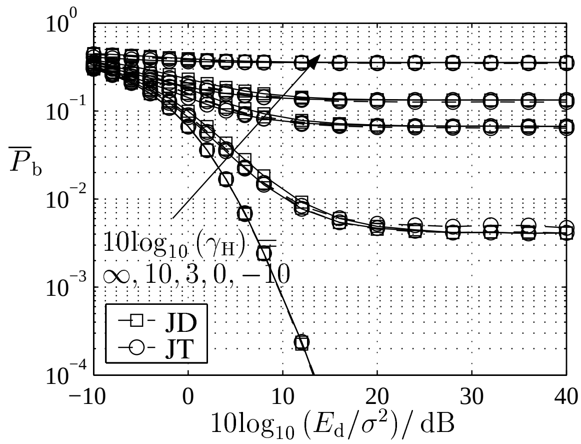

Fig. 6. Average bit error probability $\overline{P}_\mathrm{b}$ of JD and JT from theory (solid lines) and from simulation (dashed lines); Parameters: $K = 2$, $K_\mathrm{B} = 4$, QPSK modulation.

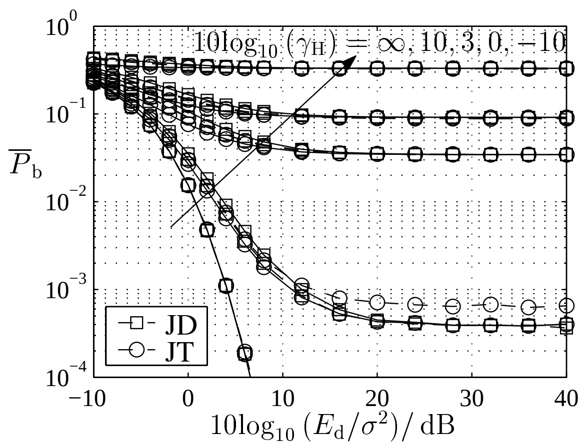

Fig. 7. Average bit error probability $\overline{P}_\mathrm{b}$ of JD and JT from theory (solid lines) and from simulation (dashed lines); Parameters: $K = 3$, $K_\mathrm{B} = 8$, QPSK modulation.

[WM04a] Weber, T.; Meurer, M.: “Imperfect channel state information in MIMO-transmission”. *Proc. IEEE 59th Vehicular Technology Conference (VTC'04-Spring)*, Mailand, 2004.

Imperfect Channel State Information in MIMO-Transmission

Tobias Weber, Michael Meurer
Research Group for RF Communications, University of Kaiserslautern,
D–67653 Kaiserslautern, Germany, Email: tweber@rhrk.uni-kl.de

***Abstract*— A specially favorable MIMO-based concept for future mobile radio systems consists in the application of Joint Detection (JD) in the uplink and Joint Transmission (JT) in the downlink. By this, all the computational complex signal processing is shifted to the base station (BS) resulting in low complexity mobile stations (MSs). Both JD and JT require channel knowledge at the BS which, if time division duplexing is applied, can be obtained by training signal based channel estimation in the uplink. Unfortunately channel estimates are never perfect which leads to performance degradations if these channel estimates instead of perfect channel knowledge are used for JD or JT. In the present paper a novel analytical analysis of these performance degradations is presented.**

I. Introduction

Future demands for high spectral efficiencies in mobile radio systems can be met by MIMO systems. In the following a scenario containing a single BS and a single MS with a flat fading MIMO channel between BS and MS is considered. The number of antennas at the BS and the number of antennas at the considered MS are denoted by K_{B} and K_{M}, respectively. Consequently, the uplink channel can be described by a $K_{\mathrm{B}} \times K_{\mathrm{M}}$ channel matrix $\underline{\mathbf{H}}_{\mathrm{U}}$ and the downlink channel can be described by a $K_{\mathrm{B}} \times K_{\mathrm{M}}$ channel matrix $\underline{\mathbf{H}}_{\mathrm{D}}$. If the radio channel is reciprocal – and this is assumed in the following –

$$\underline{\mathbf{H}} = \underline{\mathbf{H}}_{\mathrm{U}} = \underline{\mathbf{H}}_{\mathrm{D}}^{\mathrm{T}} \tag{1}$$

holds. In the following it is assumed that the number K_{B} of antennas at the BS is larger than or equal to the number K_{M} of antennas at the MS. The optimum MIMO transmission scheme for this MIMO-channel consists in singular value decomposition of the channel matrix $\underline{\mathbf{H}}$ and waterfilling [1]. From a practical point of view canonical transmission schemes based on singular value decomposition and bit loading [2], [3], [4] might not be desireable as

- they require channel knowledge on both the transmitter and the receiver side, and
- the computational complexity of the singular value decomposition might be to high especially on the MS side.

Consequently, suboptimum JD and JT based data transmission is an interesting alternative. In both cases of JD and of JT K data symbols, comprised in the data vector $\underline{\mathbf{d}}$, are transmitted in parallel. In the case of JD interferences due to cross couplings of the MIMO channel are removed on the receiver side [5]. For example the widely known BLAST system utilizes JD for MIMO-transmission [6], [7]. In the case of JT interferences due to cross couplings of the MIMO channel are a priori avoided by appropriate design of the transmitted signals [8]. Both JD and JT require channel knowledge in the form of the channel matrix $\underline{\mathbf{H}}_{\mathrm{U}}$ and $\underline{\mathbf{H}}_{\mathrm{D}}$, respectively. It was shown that concerning the signal processing and the performance with perfect channel knowledge linear JD and linear JT are dual to each other [9]. A still open question – which is answered in the present paper – concerns the influence of imperfect channel knowledge on the performance of linear JD and linear JT. For simplicity we concentrate our work on linear zero forcing JD [5] and linear zero forcing JT [10], [11]. In the following we skip the attribute linear zero forcing. In the paper the element in the i-th row and j-th column of a matrix is denoted by $[.]_{i,j}$.

II. System Model

The K dimensional data vector to be transmitted is denoted by

$$\underline{\mathbf{d}} = \left(\underline{d}^{(1)} \ldots \underline{d}^{(K)}\right)^{\mathrm{T}}. \tag{2}$$

The elements $\underline{d}^{(k)}$, $k = 1 \ldots K$, of the data vector $\underline{\mathbf{d}}$ are assumed to be independent identical distributed with a variance E_{d} of real and imaginary part. For the covariance matrix follows

$$\underline{\mathbf{R}}_{\mathrm{d}} = \mathrm{E}\left\{\underline{\mathbf{d}}\,\underline{\mathbf{d}}^{*\mathrm{T}}\right\} = 2E_{\mathrm{d}}\mathbf{I}. \tag{3}$$

For bit error rate investigations QPSK modulation is assumed, i.e., the elements $\underline{d}^{(k)}$, $k = 1 \ldots K$, of the data vector $\underline{\mathbf{d}}$ are taken from the alphabet

$$\underline{d}^{(k)}/\sqrt{E_{\mathrm{d}}} \in \{(1+\mathrm{j})\,,\ (1-\mathrm{j})\,(-1+\mathrm{j})\,,\ (-1-\mathrm{j})\}\,. \tag{4}$$

In the case of uplink transmission with the noise vector $\underline{\mathbf{n}}_{\mathrm{U}}$, the received vector reads

$$\underline{\mathbf{e}} = \underline{\mathbf{H}}_{\mathrm{U}} \cdot \underline{\mathbf{d}} + \underline{\mathbf{n}}_{\mathrm{U}} = \underline{\mathbf{H}} \cdot \underline{\mathbf{d}} + \underline{\mathbf{n}}_{\mathrm{U}}. \tag{5}$$

For simplicity it is assumed in the following that the elements of the noise vector $\underline{\mathbf{n}}_{\mathrm{U}}$ are uncorrelated, Gaussian distributed with variance σ^2 of real and imaginary part [12]. For the covariance matrix follows

$$\underline{\mathbf{R}}_{\mathrm{n,U}} = \mathrm{E}\left\{\underline{\mathbf{n}}_{\mathrm{U}}\underline{\mathbf{n}}_{\mathrm{U}}^{*\mathrm{T}}\right\} = 2\sigma^2\mathbf{I}. \tag{6}$$

Linear zero forcing JD calculates an estimate $\hat{\underline{\mathbf{d}}}$ of the data vector $\underline{\mathbf{d}}$ which minimizes the error $\left\|\underline{\mathbf{e}} - \underline{\mathbf{H}} \cdot \hat{\underline{\mathbf{d}}}\right\|^2$. This estimate can be easily calculated as

$$\hat{\underline{\mathbf{d}}} = \left(\underline{\mathbf{H}}^{*\mathrm{T}}\underline{\mathbf{H}}\right)^{-1}\underline{\mathbf{H}}^{*\mathrm{T}}\underline{\mathbf{e}}. \tag{7}$$

In (7) perfect channel knowledge, i.e., perfect knowledge of the channel matrix $\underline{\mathbf{H}}$ in the receiver is assumed.

In the case of downlink transmission with the noise vector $\underline{\mathbf{n}}_{\mathrm{D}}$ and the transmitted vector $\underline{\mathbf{s}}$ the data estimate reads

$$\hat{\underline{\mathbf{d}}} = \underline{\mathbf{H}}_{\mathrm{D}} \cdot \underline{\mathbf{s}} + \underline{\mathbf{n}}_{\mathrm{D}} = \underline{\mathbf{H}}^{\mathrm{T}} \cdot \underline{\mathbf{s}} + \underline{\mathbf{n}}_{\mathrm{D}}. \tag{8}$$

In the noise free case

$$\underline{\mathbf{n}}_{\mathrm{D}} = \mathbf{0} \tag{9}$$

this estimate should be equal to the transmitted data vector $\underline{\mathbf{d}}$:

$$\underline{\mathbf{d}} = \underline{\mathbf{H}}^{\mathrm{T}} \cdot \underline{\mathbf{s}}. \tag{10}$$

Together with the requirement that the transmitted energy $\frac{1}{2}\left\|\underline{\mathbf{s}}\right\|^2$ should be as low as possible this leads to the JT transmitted vector

$$\underline{\mathbf{s}} = \underline{\mathbf{H}}^{*}\left(\underline{\mathbf{H}}^{\mathrm{T}}\underline{\mathbf{H}}^{*}\right)^{-1}. \tag{11}$$

In (11) perfect channel knowledge is assumed to be available in the transmitter In the following analysis of JT it is assumed that the elements of the noise vector $\underline{\mathbf{n}}_{\mathrm{D}}$ are uncorrelated, Gaussian distributed with the variance σ^2 of real and imaginary part [12]. For the covariance matrix follows

$$\underline{\mathbf{R}}_{\mathrm{n,D}} = \mathrm{E}\left\{\underline{\mathbf{n}}_{\mathrm{D}}\underline{\mathbf{n}}_{\mathrm{D}}^{*\mathrm{T}}\right\} = 2\sigma^2\mathbf{I}. \tag{12}$$

The performance of both JD and JT are analyzed for the case of perfect channel knowledge, i.e., perfect knowledge of $\underline{\mathbf{H}}$, in the receiver and the transmitter, respectively, and the case of imperfect channel knowledge. In the case of imperfect channel knowledge the estimated channel matrix $\hat{\underline{\mathbf{H}}}$, which with the channel error matrix $\underline{\mathbf{E}}$ can be written as

$$\hat{\underline{\mathbf{H}}} = \left(\underline{\mathbf{H}} + \underline{\mathbf{E}}\right), \tag{13}$$

is used for JD and JT. In the following it is assumed that the channel estimation errors, i.e., the elements of the channel error matrix $\underline{\mathbf{E}}$, are independent identical Gaussian distributed with a variance σ_{h}^2 of real and imaginary part. This assumption is justified by the analysis of the channel estimation errors presented in [9].

III. Performance of Joint Detection

A. Perfect Channel Knowledge

As can be seen from (7) JD in the case of perfect channel knowledge perfectly eliminates the multiple access interference at the price of enhancing the noise. The data estimation error

$$\hat{\underline{\mathbf{d}}} - \underline{\mathbf{d}} = \left(\underline{\mathbf{H}}^{*\mathrm{T}}\underline{\mathbf{H}}\right)^{-1}\underline{\mathbf{H}}^{*\mathrm{T}}\underline{\mathbf{n}}_{\mathrm{U}} \tag{14}$$

consists of enhanced noise only. With (6) follows for the covariance matrix of the data estimation error

$$\underline{\mathbf{R}}_{\hat{\mathrm{d}}-\mathrm{d}} = 2\sigma^2\left(\underline{\mathbf{H}}^{*\mathrm{T}}\underline{\mathbf{H}}\right)^{-1}. \tag{15}$$

For the signal-to-noise ratio (SNR) of the data estimates $\hat{\underline{\mathbf{d}}}^{(k)}$ follows [13]

$$\gamma_{\mathrm{JD}}^{(k)} = \frac{E_{\mathrm{d}}}{\sigma^2\left[\left(\underline{\mathbf{H}}^{*\mathrm{T}}\underline{\mathbf{H}}\right)^{-1}\right]_{k,k}}. \tag{16}$$

In the case of JD the transmitted energies invested for the different data symbols $\underline{d}^{(k)}$ are the equal

$$T^{(k)} = E_{\mathrm{d}},\ k = 1\ldots K. \tag{17}$$

With (16) and the assumption that the noise $\underline{\mathbf{n}}_{\mathrm{U}}$ is Gaussian distributed the bit error probability

$$P_{\mathrm{b}}^{(k)} = \frac{1}{2}\mathrm{erfc}\left(\sqrt{\frac{T^{(k)}}{2\sigma^2\left[\left(\underline{\mathbf{H}}^{*\mathrm{T}}\underline{\mathbf{H}}\right)^{-1}\right]_{k,k}}}\right) \tag{18}$$

in the case of QPSK modulation is obtained.

B. Imperfect Channel Knowledge

The JD described in the previous Subsection III-A requires channel knowledge in the form of the channel matrix $\underline{\mathbf{H}}$. However, in reality only an imperfect estimate $\hat{\underline{\mathbf{H}}}$ of the channel matrix $\underline{\mathbf{H}}$ will be available. The estimate $\hat{\underline{\mathbf{H}}}$ is used for calculating the data estimate

$$\hat{\underline{\mathbf{d}}} = \left(\hat{\underline{\mathbf{H}}}^{*\mathrm{T}}\hat{\underline{\mathbf{H}}}\right)^{-1}\hat{\underline{\mathbf{H}}}^{*\mathrm{T}}\underline{\mathbf{e}}. \tag{19}$$

For the data estimation error in the case of imperfect channel knowledge

$$\begin{aligned}\hat{\underline{\mathbf{d}}} - \underline{\mathbf{d}} = {} & \underbrace{-\left(\left(\underline{\mathbf{H}}+\underline{\mathbf{E}}\right)^{*\mathrm{T}}\left(\underline{\mathbf{H}}+\underline{\mathbf{E}}\right)\right)^{-1}\left(\underline{\mathbf{H}}+\underline{\mathbf{E}}\right)^{*\mathrm{T}}\underline{\mathbf{E}}}_{\underline{\mathbf{D}}}\cdot\underline{\mathbf{d}} \\ & + \underbrace{\left(\left(\underline{\mathbf{H}}+\underline{\mathbf{E}}\right)^{*\mathrm{T}}\left(\underline{\mathbf{H}}+\underline{\mathbf{E}}\right)\right)^{-1}\left(\underline{\mathbf{H}}+\underline{\mathbf{E}}\right)^{*\mathrm{T}}}_{\underline{\mathbf{N}}}\cdot\underline{\mathbf{n}}_{\mathrm{U}}\end{aligned} \tag{20}$$

follows with (13). Thus, the data estimation error is a nonlinear function of the elements $[\underline{\mathbf{E}}]_{k_{\mathrm{B}},k_{\mathrm{M}}}$ of the channel error matrix $\underline{\mathbf{E}}$. For small channel estimation errors $[\underline{\mathbf{E}}]_{k_{\mathrm{B}},k_{\mathrm{M}}}$, $k_{\mathrm{B}} = 1\ldots K_{\mathrm{B}}$, $k_{\mathrm{M}} = 1\ldots K_{\mathrm{M}}$, i.e., a small variance σ_{h}^2, these nonlinear functions can be approximated by Taylor series which are truncated after the linear terms, i.e.,

$$\begin{aligned}&\hat{\underline{\mathbf{d}}} - \underline{\mathbf{d}} \approx \\ &\left[\sum_{k_{\mathrm{B}},k_{\mathrm{M}}} \left.\frac{\partial\underline{\mathbf{D}}}{\partial\mathrm{Re}\left\{[\underline{\mathbf{E}}]_{k_{\mathrm{B}},k_{\mathrm{M}}}\right\}}\right|_{\underline{\mathbf{E}}=\mathbf{0}} \mathrm{Re}\left\{[\underline{\mathbf{E}}]_{k_{\mathrm{B}},k_{\mathrm{M}}}\right\}\right. \\ &\left.+\sum_{k_{\mathrm{B}},k_{\mathrm{M}}} \left.\frac{\partial\underline{\mathbf{D}}}{\partial\mathrm{Im}\left\{[\underline{\mathbf{E}}]_{k_{\mathrm{B}},k_{\mathrm{M}}}\right\}}\right|_{\underline{\mathbf{E}}=\mathbf{0}} \mathrm{Im}\left\{[\underline{\mathbf{E}}]_{k_{\mathrm{B}},k_{\mathrm{M}}}\right\}\right]\cdot\underline{\mathbf{d}} \\ &+\left[\left(\underline{\mathbf{H}}^{*\mathrm{T}}\underline{\mathbf{H}}\right)^{-1}\underline{\mathbf{H}}^{*\mathrm{T}}\right. \\ &+\sum_{k_{\mathrm{B}},k_{\mathrm{M}}} \left.\frac{\partial\underline{\mathbf{N}}}{\partial\mathrm{Re}\left\{[\underline{\mathbf{E}}]_{k_{\mathrm{B}},k_{\mathrm{M}}}\right\}}\right|_{\underline{\mathbf{E}}=\mathbf{0}} \mathrm{Re}\left\{[\underline{\mathbf{E}}]_{k_{\mathrm{B}},k_{\mathrm{M}}}\right\} \\ &\left.+\sum_{k_{\mathrm{B}},k_{\mathrm{M}}} \left.\frac{\partial\underline{\mathbf{N}}}{\partial\,\mathrm{Im}\left\{[\underline{\mathbf{E}}]_{k_{\mathrm{B}},k_{\mathrm{M}}}\right\}}\right|_{\underline{\mathbf{E}}=\mathbf{0}} \mathrm{Im}\left\{[\underline{\mathbf{E}}]_{k_{\mathrm{B}},k_{\mathrm{M}}}\right\}\right]\cdot\underline{\mathbf{n}}_{\mathrm{U}}.\end{aligned} \tag{21}$$

After calculation of the derivatives in (21) and some simplifications the approximation

$$\begin{aligned}\underline{\hat{\mathbf{d}}}-\underline{\mathbf{d}} \approx & -\left(\underline{\mathbf{H}}^{*\mathrm{T}}\underline{\mathbf{H}}\right)^{-1}\underline{\mathbf{H}}^{*\mathrm{T}}\underline{\mathbf{E}}\,\underline{\mathbf{d}}+\left(\underline{\mathbf{H}}^{*\mathrm{T}}\underline{\mathbf{H}}\right)^{-1}\underline{\mathbf{H}}^{*\mathrm{T}}\underline{\mathbf{n}}_{\mathrm{U}} \\ & +\left(\underline{\mathbf{H}}^{*\mathrm{T}}\underline{\mathbf{H}}\right)^{-1}\underline{\mathbf{E}}^{*\mathrm{T}}\underline{\mathbf{n}}_{\mathrm{U}} \\ & -\left(\underline{\mathbf{H}}^{*\mathrm{T}}\underline{\mathbf{H}}\right)^{-1}\left(\underline{\mathbf{H}}^{*\mathrm{T}}\underline{\mathbf{E}}+\underline{\mathbf{E}}^{*\mathrm{T}}\underline{\mathbf{H}}\right) \\ & \cdot\left(\underline{\mathbf{H}}^{*\mathrm{T}}\underline{\mathbf{H}}\right)^{-1}\underline{\mathbf{H}}^{*\mathrm{T}}\underline{\mathbf{n}}_{\mathrm{U}}\end{aligned} \tag{22}$$

of the data estimation error for small channel estimation errors is found. With (3) and (6) and the reasonable assumption that the data $\underline{\mathbf{d}}$ and the noise $\underline{\mathbf{n}}_{\mathrm{U}}$ are statistically independent the covariance matrix of the data estimation error reads

$$\begin{aligned}\underline{\mathbf{R}}_{\hat{\mathrm{d}}-\mathrm{d}} \approx & \; 2\sigma^2\left(\underline{\mathbf{H}}^{*\mathrm{T}}\underline{\mathbf{H}}\right)^{-1}\left[1+\frac{2E_{\mathrm{d}}2\sigma_{\mathrm{h}}^2K_{\mathrm{M}}}{2\sigma^2}\right. \\ & \left.+2\sigma_{\mathrm{h}}^2\operatorname{trace}\left\{\left(\underline{\mathbf{H}}^{*\mathrm{T}}\underline{\mathbf{H}}\right)^{-1}\right\}\right] \\ & +2\sigma^2 2\sigma_{\mathrm{h}}^2\left(K_{\mathrm{B}}-K_{\mathrm{M}}\right)\left(\underline{\mathbf{H}}^{*\mathrm{T}}\underline{\mathbf{H}}\right)^{-2}.\end{aligned} \tag{23}$$

The signal-to-noise-plus-interference ratio (SNIR)

$$\begin{aligned}\gamma_{\mathrm{JD}}^{(k)} \approx & \; E_{\mathrm{d}}\Big/\left(\sigma^2\left[\left(\underline{\mathbf{H}}^{*\mathrm{T}}\underline{\mathbf{H}}\right)^{-1}\right]_{k,k}\left[1+\frac{2E_{\mathrm{d}}2\sigma_{\mathrm{h}}^2K_{\mathrm{M}}}{2\sigma^2}\right.\right. \\ & \left.+2\sigma_{\mathrm{h}}^2\operatorname{trace}\left\{\left(\underline{\mathbf{H}}^{*\mathrm{T}}\underline{\mathbf{H}}\right)^{-1}\right\}\right] \\ & \left.+\sigma^2 2\sigma_{\mathrm{h}}^2\left(K_{\mathrm{B}}-K_{\mathrm{M}}\right)\left[\left(\underline{\mathbf{H}}^{*\mathrm{T}}\underline{\mathbf{H}}\right)^{-2}\right]_{k,k}\right)\end{aligned} \tag{24}$$

describes the quality of the estimate $\underline{d}^{(k)}$ in the case of imperfect channel knowledge. Under the assumption that the noise $\underline{\mathbf{n}}_{\mathrm{U}}$ and the channel estimation errors $[\underline{\mathbf{E}}]_{k_{\mathrm{B}},k_{\mathrm{M}}}$, $k_{\mathrm{B}}=1\ldots K_{\mathrm{B}}$, $k_{\mathrm{M}}=1\ldots K_{\mathrm{M}}$, are Gaussian distributed and with (17) the bit error probability

$$\begin{aligned}P_{\mathrm{b}}^{(k)} \approx & \;\frac{1}{2}\operatorname{erfc}\left(\left(T^{(k)}\Big/\left(2\sigma^2\left[\left(\underline{\mathbf{H}}^{*\mathrm{T}}\underline{\mathbf{H}}\right)^{-1}\right]_{k,k}\right.\right.\right. \\ & \cdot\left(1+\frac{2T^{(k)}2\sigma_{\mathrm{h}}^2K_{\mathrm{M}}}{2\sigma^2}+2\sigma_{\mathrm{h}}^2\operatorname{trace}\left\{\left(\underline{\mathbf{H}}^{*\mathrm{T}}\underline{\mathbf{H}}\right)^{-1}\right\}\right) \\ & \left.\left.\left.+2\sigma^2 2\sigma_{\mathrm{h}}^2\left(K_{\mathrm{B}}-K_{\mathrm{M}}\right)\left[\left(\underline{\mathbf{H}}^{*\mathrm{T}}\underline{\mathbf{H}}\right)^{-2}\right]_{k,k}\right)\right)^{\frac{1}{2}}\right)\end{aligned} \tag{25}$$

in the case of QPSK modulation is obtained. For large transmitted energies $T^{(k)}$ the bit error probability converges towards the error floor

$$P_{\mathrm{b},\infty}^{(k)} \approx \frac{1}{2}\operatorname{erfc}\left(\sqrt{\frac{1}{4\sigma_{\mathrm{h}}^2K_{\mathrm{M}}\left[\left(\underline{\mathbf{H}}^{*\mathrm{T}}\underline{\mathbf{H}}\right)^{-1}\right]_{k,k}}}\right). \tag{26}$$

IV. Performance of Joint Transmission

A. Perfect Channel Knowledge

JT perfectly avoids interferences at the price of increased transmitted energies $T^{(k)}$, $k=1\ldots K$. The data estimation error

$$\underline{\hat{\mathbf{d}}}-\underline{\mathbf{d}}=\underline{\mathbf{n}}_{\mathrm{D}} \tag{27}$$

consists of noise only. With (12) follows for the covariance matrix of the data estimation error

$$\underline{\mathbf{R}}_{\hat{\mathrm{d}}-\mathrm{d}}=\mathrm{E}\left\{\left(\underline{\hat{\mathbf{d}}}-\underline{\mathbf{d}}\right)\left(\underline{\hat{\mathbf{d}}}-\underline{\mathbf{d}}\right)^{*\mathrm{T}}\right\}=2\sigma^2\mathbf{I}. \tag{28}$$

In the case of JT the transmitted vector $\underline{\mathbf{s}}$ is a superposition of partial transmitted signals for the individual data symbols $\underline{d}^{(k)}$, $k=1\ldots K$. The average transmitted energy invested for data symbol $\underline{d}^{(k)}$ reads

$$T^{(k)}=E_{\mathrm{d}}\left[\left(\underline{\mathbf{H}}^{\mathrm{T}}\underline{\mathbf{H}}^{*}\right)^{-1}\right]_{k,k}. \tag{29}$$

In general different average transmitted energies $T^{(k)}$, $k=1\ldots K$, will be used for the different data symbols $\underline{d}^{(k)}$, $k=1\ldots K$. Due to the correlations of the partial transmitted signals the total transmitted energy is only on the average the sum of the average transmitted energies $T^{(k)}$, $k=1\ldots K$. The average transmitted energy $T^{(k)}$ results in a received energy E_{d} per data symbol and the SNR

$$\gamma_{\mathrm{JT}}^{(k)}=\frac{E_{\mathrm{d}}}{\sigma^2}=\frac{T^{(k)}}{\sigma^2\left[\left(\underline{\mathbf{H}}^{\mathrm{T}}\underline{\mathbf{H}}^{*}\right)^{-1}\right]_{k,k}}. \tag{30}$$

With the assumption that the noise $\underline{\mathbf{n}}_{\mathrm{D}}$ is Gaussian distributed the bit error probability

$$P_{\mathrm{b}}^{(k)}=\frac{1}{2}\operatorname{erfc}\left(\sqrt{\frac{T^{(k)}}{2\sigma^2\left[\left(\underline{\mathbf{H}}^{\mathrm{T}}\underline{\mathbf{H}}^{*}\right)^{-1}\right]_{k,k}}}\right) \tag{31}$$

in the case of QPSK modulation is obtained. This is the same result in the case of JD, i.e., the performance of the uplink with JD is equal to the performance of the downlink with JT for a given average transmitted energy $T^{(k)}$ and a given variance σ^2 of the noise.

B. Imperfect Channel Knowledge

In reality an imperfect estimate $\underline{\hat{\mathbf{H}}}$ of the channel matrix W will be used for calculating the transmitted signal

$$\underline{\mathbf{s}}=\underbrace{\underline{\hat{\mathbf{H}}}^{*\mathrm{T}}\left(\underline{\hat{\mathbf{H}}}^{\mathrm{T}}\underline{\hat{\mathbf{H}}}^{*}\right)^{-1}}_{\underline{\mathbf{M}}}\cdot\underline{\mathbf{d}}. \tag{32}$$

Channel estimation errors influence JT in two ways:

- The energy of the transmitted vector $\underline{\mathbf{s}}$ calculated with the estimated channel matrix $\underline{\hat{\mathbf{H}}}$ will be different from the energy of the transmitted vector $\underline{\mathbf{s}}$ calculated with the true channel matrix $\underline{\mathbf{H}}$.

- Even in the noise free case the estimate $\hat{\underline{\mathbf{d}}}$ obtained in the receiver will be different from the true data vector $\underline{\mathbf{d}}$.

The matrix $\underline{\mathbf{M}}$ introduced in (32) is a nonlinear function of the elements $[\underline{\mathbf{E}}]_{k_\mathrm{B},k_\mathrm{M}}$ of the channel error matrix $\underline{\mathbf{E}}$. For small channel estimation errors $[\underline{\mathbf{E}}]_{k_\mathrm{B},k_\mathrm{M}}$, $k_\mathrm{B} = 1\ldots K_\mathrm{B}$, $k_\mathrm{M} = 1\ldots K_\mathrm{M}$, i.e., a small variance σ_h^2, these nonlinear functions can be approximated by Taylor series which are truncated after the linear terms, i.e.,

$$\begin{aligned}\underline{\mathbf{M}} \approx\ & \underline{\mathbf{H}}^* \left(\underline{\mathbf{H}}^\mathrm{T}\underline{\mathbf{H}}^*\right)^{-1} \\ & + \sum_{k_\mathrm{B},k_\mathrm{M}} \left.\frac{\partial \underline{\mathbf{M}}}{\partial \mathrm{Re}\left\{[\underline{\mathbf{E}}]_{k_\mathrm{B},k_\mathrm{M}}\right\}}\right|_{\underline{\mathbf{E}}=\mathbf{0}} \mathrm{Re}\left\{[\underline{\mathbf{E}}]_{k_\mathrm{B},k_\mathrm{M}}\right\} \\ & + \sum_{k_\mathrm{B},k_\mathrm{M}} \left.\frac{\partial \underline{\mathbf{M}}}{\partial \mathrm{Im}\left\{[\underline{\mathbf{E}}]_{k_\mathrm{B},k_\mathrm{M}}\right\}}\right|_{\underline{\mathbf{E}}=\mathbf{0}} \mathrm{Im}\left\{[\underline{\mathbf{E}}]_{k_\mathrm{B},k_\mathrm{M}}\right\}\end{aligned} \tag{33}$$

holds. After calculation of the derivatives and some simplifications the approximation

$$\begin{aligned}\underline{\mathbf{M}} \approx\ & \underline{\mathbf{H}}^* \left(\underline{\mathbf{H}}^\mathrm{T}\underline{\mathbf{H}}^*\right)^{-1} + \underline{\mathbf{E}}^* \left(\underline{\mathbf{H}}^\mathrm{T}\underline{\mathbf{H}}^*\right)^{-1} - \underline{\mathbf{H}}^* \\ & \cdot \left(\underline{\mathbf{H}}^\mathrm{T}\underline{\mathbf{H}}^*\right)^{-1} \left(\underline{\mathbf{H}}^\mathrm{T}\underline{\mathbf{E}}^* + \underline{\mathbf{E}}^\mathrm{T}\underline{\mathbf{H}}^*\right) \left(\underline{\mathbf{H}}^\mathrm{T}\underline{\mathbf{H}}^*\right)^{-1}\end{aligned} \tag{34}$$

is obtained. For the estimation error in the case of imperfect channel knowledge

$$\hat{\underline{\mathbf{d}}} - \underline{\mathbf{d}} \approx -\underline{\mathbf{E}}^\mathrm{T}\underline{\mathbf{H}}^* \left(\underline{\mathbf{H}}^\mathrm{T}\underline{\mathbf{H}}^*\right)^{-1} \underline{\mathbf{d}} + \underline{\mathbf{n}}_\mathrm{D} \tag{35}$$

is obtained. With (3) and (12) and the reasonable assumption that the data $\underline{\mathbf{d}}$ and noise $\underline{\mathbf{n}}_\mathrm{D}$ are statistically independent the covariance matrix of the data estimation error reads

$$\underline{\mathbf{R}}_{\hat{\mathrm{d}}-\mathrm{d}} \approx 2\sigma^2\,\mathbf{I} + 2E_\mathrm{d}2\sigma_\mathrm{h}^2\,\mathbf{I}\,\mathrm{trace}\left\{\left(\underline{\mathbf{H}}^\mathrm{T}\underline{\mathbf{H}}^*\right)^{-1}\right\}. \tag{36}$$

To describe the quality of the obtained estimate $\underline{\mathbf{d}}$ one can resort to the SNIR

$$\gamma_\mathrm{JT}^{(k)} \approx \frac{E_\mathrm{d}}{\sigma^2 + E_\mathrm{d}2\sigma_\mathrm{h}^2\,\mathrm{trace}\left\{\left(\underline{\mathbf{H}}^\mathrm{T}\underline{\mathbf{H}}^*\right)^{-1}\right\}}. \tag{37}$$

For a sound performance assessment also the average transmitted energy

$$T^{(k)} = E_\mathrm{d}\left[\mathrm{E}\left\{\underline{\mathbf{M}}^{*\mathrm{T}}\underline{\mathbf{M}}\right\}\right]_{k,k} \tag{38}$$

invested for data symbol $\underline{d}^{(k)}$, which is influenced by the channel estimation errors, has to be taken into consideration. Using (34) one obtains after some calculations

$$\begin{aligned}T^{(k)} \approx\ & \left[\left(\underline{\mathbf{H}}^\mathrm{T}\underline{\mathbf{H}}^*\right)^{-1}\right]_{k,k} E_\mathrm{d} \\ & \cdot \left(1 + 2\sigma_\mathrm{h}^2\,\mathrm{trace}\left\{\left(\underline{\mathbf{H}}^\mathrm{T}\underline{\mathbf{H}}^*\right)^{-1}\right\}\right) \\ & + \left[\left(\underline{\mathbf{H}}^\mathrm{T}\underline{\mathbf{H}}^*\right)^{-2}\right]_{k,k} E_\mathrm{d}2\sigma_\mathrm{h}^2\left(K_\mathrm{B} - K_\mathrm{M}\right).\end{aligned} \tag{39}$$

Comparing $T^{(k)}$ of (39) and $T^{(k)}$ of (29) one observes that the average transmitted energy invested for the data symbol $\underline{d}^{(k)}$ in the case of imperfect channel knowledge is always larger than in the case of perfect channel knowledge. With (37) and the assumption that the noise $\underline{\mathbf{n}}_\mathrm{D}$ and the channel estimation errors $[\underline{\mathbf{E}}]_{k_\mathrm{B},k_\mathrm{M}}$, $k_\mathrm{B} = 1\ldots K_\mathrm{B}$, $k_\mathrm{M} = 1\ldots K_\mathrm{M}$, are Gaussian distributed the bit error probability

$$\begin{aligned}P_\mathrm{b}^{(k)} \approx \frac{1}{2}\mathrm{erfc}\Bigg(\Bigg(T^{(k)} \Big/ \Bigg(2\sigma^2\Bigg(& \left[\left(\underline{\mathbf{H}}^\mathrm{T}\underline{\mathbf{H}}^*\right)^{-1}\right]_{k,k} \\ & \cdot\left(1 + 2\sigma_\mathrm{h}^2\,\mathrm{trace}\left\{\left(\underline{\mathbf{H}}^\mathrm{T}\underline{\mathbf{H}}^*\right)^{-1}\right\}\right) \\ & + \left[\left(\underline{\mathbf{H}}^\mathrm{T}\underline{\mathbf{H}}^*\right)^{-2}\right]_{k,k} 2\sigma_\mathrm{h}^2\left(K_\mathrm{B} - K_\mathrm{M}\right)\Bigg) \\ & + 2T^{(k)}2\sigma_\mathrm{h}^2\,\mathrm{trace}\left\{\left(\underline{\mathbf{H}}^\mathrm{T}\underline{\mathbf{H}}^*\right)^{-1}\right\}\Bigg)\Bigg)^{\frac{1}{2}}\Bigg)\end{aligned} \tag{40}$$

in the case of QPSK modulation is obtained. For large transmitted energies $T^{(k)}$ this bit error probability converges towards the error floor

$$P_{\mathrm{b},\infty}^{(k)} \approx \frac{1}{2}\mathrm{erfc}\left(\sqrt{\frac{1}{4\sigma_\mathrm{h}^2\,\mathrm{trace}\left\{\left(\underline{\mathbf{H}}^\mathrm{T}\underline{\mathbf{H}}^*\right)^{-1}\right\}}}\right). \tag{41}$$

The results obtained in this Subsection for JT with imperfect channel knowledge are clearly different from the results obtained in Subsection III-B for JD with imperfect channel knowledge. This result is unexpected as both JD and JT with perfect channel knowledge, see Subsection III-A and IV-A, are – with respect to the signal processing and the performance – dual to each other.

V. Illustrative Example

In order to visualize the theoretical results of the previous Sections an exemplary scenario with the channel matrix

$$\underline{\mathbf{H}} = \begin{pmatrix} 1 & 2 & 3 \\ 3 & 1 & 1 \\ 2 & 2 & 0 \end{pmatrix} \tag{42}$$

and a variance

$$\sigma_\mathrm{h}^2 = 0.09 \tag{43}$$

is considered. $K = 3$ data symbols $\underline{d}^{(k)}$, $k = 1,\ 2,\ 3$, are transmitted in parallel and for each data symbol results an individual bit error probability $P_\mathrm{b}^{(k)}$, $k = 1,\ 2,\ 3$. The bit error probabilities $P_\mathrm{b}^{(k)}$, $k = 1,\ 2,\ 3$, for JD and JT with perfect channel knowledge as a function of the ratio $T^{(k)}/\sigma^2$ are shown in Fig. 1. The lines are the theoretical results and the markers are the simulation results. As expected the theoretical results match with the simulation results. The bit error probabilities $P_\mathrm{b}^{(k)}$, $k = 1,\ 2,\ 3$, for JD with imperfect channel knowledge as a function of the ratio $T^{(k)}/\sigma^2$ are shown in Fig. 2. The dashed lines are the theoretical error floors. It can be seen that the theoretical results based on linear

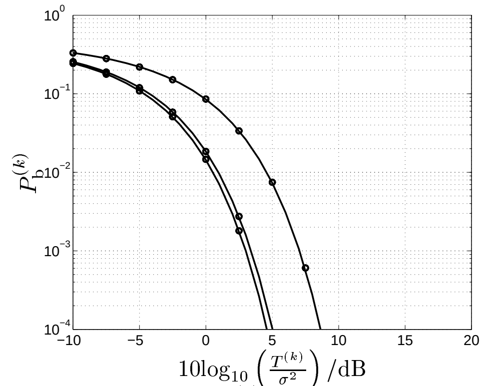

Fig. 1. Bit error probabilities $P_{\mathrm{b}}^{(k)}$ of JD and JT with perfect channel knowledge as a function of $\frac{T^{(k)}}{\sigma^2}$

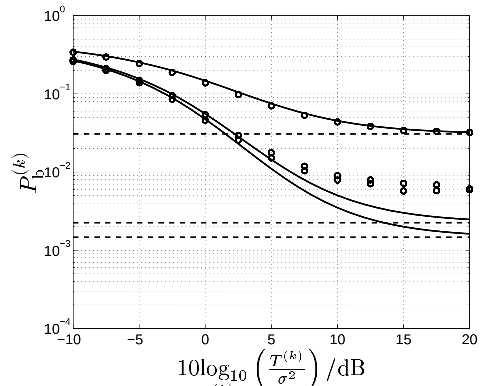

Fig. 2. Bit error probabilities $P_{\mathrm{b}}^{(k)}$ of JD with imperfect channel knowledge as a function of $\frac{T^{(k)}}{\sigma^2}$

Taylor approximation match quite well with the simulation results. The bit error probabilities $P_{\mathrm{b}}^{(k)}$, $k = 1,\ 2,\ 3$, for JT with imperfect channel knowledge as a function of the ratio $T^{(k)}/\sigma^2$ are shown in Fig. 3. Again the theoretical results based on linear Taylor approximation match quite well with the simulation results. In contrast to JD in the case of JT with imperfect channel knowledge the error floor ist the same for all data symbols $\underline{d}^{(k)}$, $k = 1,\ 2,\ 3$. By comparing Fig. 2 and Fig. 3 it can be clearly seen that the results for JD and JT are different for the case of imperfect channel knowledge.

VI. Conclusion

The influence of channel estimation errors on JD and JT is studied analytically. The analysis is based on linear Taylor approximation. It is shown that the influence of channel estimation errors on JD and JT is totally different although JD and JT with perfect channel knowledge are dual to each other.

Acknowledgment

The authors gratefully appreciate the stimulating discussions and the fruitful exchange of ideas with Professor P.W. Baier and their co-workers at the Research Group for RF Communications at the University of Kaiserslautern. The support of individual parts of this work in the framework of the EU-IST-Project FLOWS (Flexible Convergence of Wireless Standards and Services), by DFG and by Siemens AG is highly acknowledged.

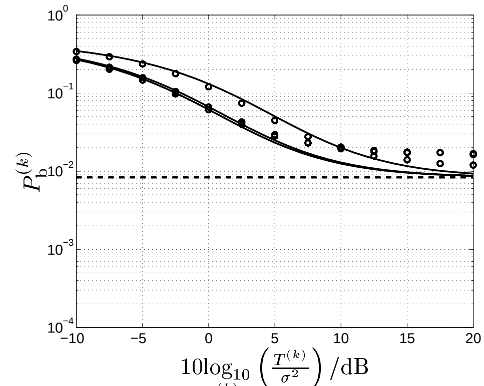

Fig. 3. Bit error probabilities $P_{\mathrm{b}}^{(k)}$ of JT with imperfect channel knowledge as a function of $\frac{T^{(k)}}{\sigma^2}$

References

[1] E. Telatar, "Capacity of multi-antenna Gaussian channels," *European Transactions on Telecommunications*, vol. 10, no. 6, pp. 585–595, 1999.

[2] D. Hughes-Hartogs, "Ensemble modem structure for imperfect transmission media," July 1987, United States Patent 4,679,227.

[3] ——, "Ensemble modem structure for imperfect transmission media," Mar. 1988, United States Patent 4,731,816.

[4] ——, "Ensemble modem structure for imperfect transmission media," May 1989, United States Patent 4,833,706.

[5] S. Verdú, *Multiuser Detection*. Cambridge: Cambridge University Press, 1998.

[6] P. Wolniansky, G. Foschini, G. Golden, and R. Valenzuela, "V-BLAST: An architecture for realizing very high data rates over rich-scattering wireless channel," in *Proc. URSI International Symposium on Signals Systems, and Electronics (ISSSE'98)*, Pisa, 1998, pp. 295–300.

[7] G. J. Foschini, "Layered space-time architecture for wireless communication in a fading environment when using multi-element antennas," *The Bell System Technical Journal*, vol. 1, no. 2, pp. 41–59, 1996.

[8] R. F. H. Fischer, *Precoding and Signal Shaping for Digital Transmission*. New York: John Wiley & Sons, 2002.

[9] T. Weber and I. Maniatis, "Channel knowledge: A crucial prerequisite for MIMO transmission?" in *COST 273 TD(03)083*, Paris, 2003.

[10] M. Meurer, P. W. Baier, T. Weber, Y. Lu, and A. Papathanassiou, "Joint transmission: advantageous downlink concept for CDMA mobile radio systems using time division duplexing," *IEE Electronics Letters*, vol. 36, no. 10, pp. 900–901, 2000.

[11] F. Kowalewski and P. Mangold, "Joint predistortion and transmit diversity," in *Proc. IEEE Global Telecommunications Conference (GLOBECOM'00)*, vol. 1, San Francisco, Nov. 2000, pp. 245–249.

[12] J. G. Proakis, *Digital Communications*, 3rd ed. New York: McGraw-Hill, 1995.

[13] A. Klein, *Multi-user detection of CDMA signals – algorithms and their application to cellular mobile radio*, Fortschrittberichte VDI, Reihe 10, no. 423. Düsseldorf: VDI-Verlag, 1996.

Kapitel 7
Ausblick und Potential für Weiterentwicklungen

7.1 Kanalorientierte Funkkommunikation

7.1.1 Vorbemerkung

Dieses Kapitel betrachtet mögliche Weiterentwicklungen des Grundkonzepts der Empfängerorientierung. Ein wesentlicher leistungsbegrenzender Faktor bei der Empfängerorientierung besteht in der von Kanalzustandsinformation unabhängigen A-priori-Wahl der Empfänger. Es gilt nämlich, daß aufgrund fehlender Kanalzustandsinformation an den Empfängern ein Adaptieren der Empfänger an die sich bietenden zeitlichen und räumlichen Eigenschaften der wirksamen relevanten Mobilfunkkanäle nicht möglich ist. Daher ist es denkbar, daß die empfängerseitige mobilfunkkanalunabhängige Signalverarbeitung ausschließlich solche Komponenten des totalen Empfangssignals $\underline{\mathbf{r}}$ auswertet, die, je nach Mobilfunkkanal, senderseitig nur schwer, das heißt mit großer totaler Sendeenergie T oder gar nicht beeinflußt werden können.

Optimale Verfahren der Funkkommunikation [FG98, Tel99] nutzen daher Kanalzustandsinformation sowohl auf der Senderseite als auch auf der Empfängerseite. Derartige optimale Verfahren sind jedoch bisher nur für Funkkommunikation der Grundarchitektur Punkt-zu-Punkt bekannt. Für Funkkommunikation der Grundarchitektur Punkt-zu-Mehrpunkt — diese ist, wie bereits mehrfach dargelegt, im Falle der Abwärtsstrecke eines zellularen Mobilfunksystems gegeben — sind jedoch solche optimalen Verfahren nach Kenntnis des Verfassers nicht bekannt.

In der Literatur [JVP98, YR94, IF02b, MTWB01b, MTWB01a, BQT+03, MT03, QTMJ03] wurden bereits suboptimale Verfahren vorgestellt, die das oben geschilderte Problem durch beidseitiges Nutzen von Kanalzustandsinformation umgehen. Da bei diesen Konzepten Kanalzustandsinformation auf beiden Seiten der Funkübertragung verwendet wird und sich sowohl die Senderverarbeitung, siehe auch Abschnitt 1.1.2, als auch die Empfängerverarbeitung, siehe auch Abschnitt 1.1.2, nach der Kanalzustandsinformation zu richten haben, charakterisiert man derartige Funkkommunikation mit dem Attribut kanalorientiert [BQT+03, BZT+03].

7.1.2 Exemplarische Verfahren der kanalorientierten Funkkommunikation

Ausgehend von der in den Kapitel 1 bis 6 behandelten empfängerorientierten Funkkommunikation sollen in diesem Abschnitt Wege aufgezeigt werden, das Grundkonzept der Empfängerorientierung in Richtung des Grundkonzepts der Kanalorientierung zu entwickeln, um so die im vorherigen Abschnitt 7.1.1 dargelegten Probleme der ungünstigen A-priori-Wahl der Empfänger zu umgehen.

In den folgenden Veröffentlichungen [MTWB01b, BQT^{+}03, QTMJ03] werden daher

- exemplarisch zwei prinzipielle Ausgestaltungsmöglichkeiten der kanalorientierten Funkkommunikation aufgezeigt, die unmittelbar auf der in den Kapitel 1 bis 6 behandelten empfängerorientierten Funkkommunikation aufbauen, und
- anhand geeigneter Gütekriterien dargelegt, welches Potential für Leistungssteigerungen durch das Verfolgen der beschriebenen kanalorientierten Konzepte der Funkkommunikation erschlossen wird.

Im Gegensatz zu dem aus Tabelle 1.2 bekannten Systemmodell werden in [MTWB01b] einige wenige Größen durch eine modifizierte Notation beschrieben. Tabelle 7.1 listet die wesentlichen Unterschiede in kompakter Form auf.

Tabelle 7.1. Wesentliche Unterschiede der Notationen nach Tabelle 1.2 und der Notation nach [MTWB01b]

dargestellte Größe	Formelzeichen nach Tab. 1.2	Formelzeichen nach [MTWB01b]
totales Sendesignal	$\underline{\mathbf{t}}$	$\underline{\mathbf{s}}$

[MTWB01b] Meurer, M.; Tröger, H.; Weber, T.; Baier, P. W.: "Synthesis of joint detection (JD) and joint transmission (JT) in CDMA downlinks". *IEE Electronics Letters*, Bd. 37, 2001, S. 919–920.

Synthesis of joint detection and joint transmission in CDMA downlinks

M. Meurer, H. Tröger, T. Weber and P.W. Baier

A non-obvious synthesis of two originally opposed concepts, joint detection and joint transmission, is presented for the duplexing scheme TDD. The proposal depends on minimising the energy of the transmitted signal while simultaneously maintaining the conventional JD receiver structure and the quality of the detected data.

Introduction: Joint detection (JD) is an advantageous detection scheme for time slotted CDMA systems, which leads to air-interface concepts known as JD-CDMA [1, 2]. TD-CDMA, the air interface for the TDD bands of UMTS and IMT-2000 [3], also uses JD as an option, which allows the total elimination of intracell multiple access interference and intersymbol interference. In many applications of TD-CDMA, such as web browsing, the downlink has to support much higher data rates than the uplink. Therefore, in TD-CDMA the downlink tends to be the bottleneck, and it would be desirable to enhance the performance of this link especially. We will show how such an enhancement can be achieved by a non-obvious and inexpensive combination of conventional JD-CDMA with the joint transmission (JT) scheme recently proposed in [4 – 6]. As a prerequisite of this combination, the channel impulse responses valid in the downlink have to be known at the BS. In the case of TDD systems this knowledge is at least approximately available from the uplink channel estimation. To keep the presentation as concise as possible, the reader is assumed to be familiar with the contents of [1 – 6] and with the notations introduced in those publications.

Conventional JD-CDMA: Let us consider a conventional JD-CDMA downlink where the base station (BS) supports K mobile stations (MSs) μ_k, $k = 1, ..., K$. The K partial data vectors $\mathbf{d}^{(k)}$ $k = 1, ..., K$, to be transmitted by the BS to the individual MSs μ_k, $k = 1, ..., K$, can be stacked to form the total data vector

$$\mathbf{d} = \left(\mathbf{d}^{(1)^T} \cdots \mathbf{d}^{(K)^T}\right)^T \qquad (1)$$

Generally, both the BS and the MSs dispose of more than one antenna. By means of a modulator matrix $\mathbf{M}$ which is *a priori* constituted by the CDMA codes used and (if multiple transmit antennas are employed at the BS) also by the antenna weights [2], the total transmit signal

$$\mathbf{s} = \mathbf{M}\,\mathbf{d} \qquad (2)$$

is generated. The channel impulse responses between the individual antennas of the BS and MS μ_k, $k = 1, ..., K$, can be represented by the partial channel matrix $\mathbf{H}^{(k)}$ [2]. Then, the desired signal impinging at MS μ_k is given by

$$\mathbf{e}^{(k)} = \mathbf{H}^{(k)}\mathbf{s} = \mathbf{H}^{(k)}\mathbf{M}\,\mathbf{d} \qquad (3)$$

where $\mathbf{s}$ in the middle term of eqn. 3 is substituted by eqn. 2 to obtain the right hand term of eqn. 3. At MS μ_k, with $\mathbf{e}^{(k)}$ of eqn. 3 and following the zero forcing algorithm to perform JD, the estimate

$$\hat{\mathbf{d}} = \left(\left(\mathbf{H}^{(k)}\mathbf{M}\right)^{*T}\mathbf{H}^{(k)}\mathbf{M}\right)^{-1}\left(\mathbf{H}^{(k)}\mathbf{M}\right)^{*T}\mathbf{e}^{(k)} \quad (4)$$

of $\mathbf{d}$ of eqn. 1 can be obtained [1, 2], where the matrix in brackets is *a posteriori* determined at MS μ_k. Of course, at MS μ_k, only the estimate

$$\hat{\mathbf{d}}^{(k)} = \underbrace{\left[\left(\left(\mathbf{H}^{(k)}\mathbf{M}\right)^{*T}\mathbf{H}^{(k)}\mathbf{M}\right)^{-1}\left(\mathbf{H}^{(k)}\mathbf{M}\right)^{*T}\right]_{kN}^{(k-1)N+1}}_{\mathbf{D}^{(k)}}\mathbf{e}^{(k)} \quad (5)$$

of the partial data vector $\mathbf{d}^{(k)}$ pertaining to MS μ_k is of interest, where $[\cdot]_i^j$ stands for a matrix $\mathbf{D}^{(k)}$ consisting of lines i to j of the matrix in brackets. Nevertheless, the matrix $((\mathbf{H}^{(k)}\mathbf{M})^{*T}\mathbf{H}^{(k)}\mathbf{M})^{-1} \cdot(\mathbf{H}^{(k)}\mathbf{M})^{*T}$, used unnecessarily in conventional JD, has the potential that, at MS μ_k, data of no use to this MS could be detected. This feature of conventional JD-CDMA can be considered as an unnecessary restriction when generating the transmit signal $\mathbf{s}$. Instead of generating $\mathbf{s}$ according to eqn. 2, which would have the effect that irrelevant data could also be detected by JD at MS μ_k, $\mathbf{s}$ should be generated solely by the data $\mathbf{d}^{(k)}$ of interest to this MS. This rationale would offer additional degrees of freedom when designing $\mathbf{s}$, which could, for instance, be exploited to minimise the required transmission energy and, consequently, the interference to MSs not belonging to the ensemble of the K MSs μ_k, $k = 1, ..., K$.

Table 1: System parameters

Number of MSs	$K = 2$
Spreading factor	$Q = 8$
Length of channel impulse responses	$W = 4$
Number of data symbols per MS	$N = 1$

Table 2: CDMA codes $\mathbf{c}^{(1)}$, $\mathbf{c}^{(2)}$ and channel impulse responses $\mathbf{h}^{(1)}$, $\mathbf{h}^{(2)}$

q	1	2	3	4	5	6	7	8
$\mathbf{c}^{(1)\mathrm{T}}$	–1	1	1	–1	1	1	–1	1
$\mathbf{c}^{(2)\mathrm{T}}$	–1	–1	1	1	1	–1	–1	–1

w	1	2	3	4
$\mathbf{h}^{(1)\mathrm{T}}$	0.3559–*j*0.3512	0.2681–*j*0.4220	0.3229–*j*0.3817	0.2885–*j*0.4083
$\mathbf{h}^{(2)\mathrm{T}}$	0.4289–*j*0.2569	–0.4996–*j*0.0204	0.4841+*j*0.1251	–0.3767–*j*0.3287

Enhancement of the JD-CDMA downlink by JT: As shown in [4 – 6], in the JT scheme, the demodulators at the MSs μ_k, $k = 1, ..., K$, are determined in the form of MS-specific (that is, partial) demodulator matrices. These matrices serve, together with the partial channel matrices $\mathbf{H}^{(k)}$ already explained above, as the inputs for determining a modulator matrix $\mathbf{M}$, which, in general, differs from the modulator matrix used in conventional JD-CDMA.

Now, as the crux of our new approach, the matrices $\mathbf{D}^{(k)}$ of eqn. 5 can be considered as the partial demodulator matrices of a transmission system using JT. As shown in [4 – 6] the partial demodulator matrices of a JT system can be stacked in a block-diagonal matrix, termed the total demodulator matrix. With the matrices $\mathbf{D}^{(k)}$ of eqn. 5 as the partial demodulator matrices, the total demodulator matrix

$$\mathbf{D} = \mathrm{blockdiag}\left(\mathbf{D}^{(1)}\cdots\mathbf{D}^{(K)}\right) \quad (6)$$

can be formed. The partial channel matrices $\mathbf{H}^{(k)}$ introduced above can be put together to form the total channel matrix [4 – 6]

$$\mathbf{H} = \left(\mathbf{H}^{(1)^T}\cdots\mathbf{H}^{(K)^T}\right)^T \quad (7)$$

According to the JT scheme, $\mathbf{D}$ of eqn. 6 and $\mathbf{H}$ of eqn. 7 are used to generate the JT modulation matrix [4 – 6]

$$\mathbf{M} = (\mathbf{D}\,\mathbf{H})^{*T}\left(\mathbf{D}\,\mathbf{H}(\mathbf{D}\,\mathbf{H})^{*T}\right)^{-1} \quad (8)$$

If the total transmit signal $\mathbf{s}$ of eqn. 2 is generated by the *a posteriori* determined modulator matrix $\mathbf{M}$ of eqn. 8, instead of the *a priori* determined modulator matrix of conventional JD-CDMA, then the total transmitted energy $\|\mathbf{s}\|^2/2$ is minimised [4 – 6].

Illustrative example: In what follows, two simple downlink systems utilising conventional JD-CDMA and the proposed combination of JD and JT are considered. Table 1 shows the basic parameters of these systems, and Table 2 shows the CDMA codes $\mathbf{c}^{(1)}$ and $\mathbf{c}^{(2)}$ used, as well as the channel impulse responses $\mathbf{h}^{(1)}$ and $\mathbf{h}^{(2)}$. Computer simulations of these two systems show the following required transmit energies:

$$\frac{\|\mathbf{s}\|^2}{2} = \begin{cases} 8.00 & \text{for conventional JD} \\ 1.76 & \text{for JD + JT} \end{cases} \quad (9)$$

These results clearly show that the proposed combination of JD and JT has the potential for considerable savings of required transmitted energy. In the considered example this saving amounted to approximately 6.5 dB.

25 April 2001
Electronics Letters Online No: 20010623
DOI: 10.1049/el:20010623

M. Meurer, H. Tröger, T. Weber and P.W. Baier (*Research Group for RF Communications, University of Kaiserslautern, PO Box 3049, D-67653 Kaiserslautern, Germany*)

E-mail: meurer@rhrk.uni-kl.de

References

1 KLEIN, A.: 'Multi-user detection of CDMA signals – algorithms and their application to cellular mobile radio'. Fortschrittberichte VDI, series 10, no. 423, VDI-Verlag, Düsseldorf, 1996

2 LU, Y., and BAIER, P.W.: 'Performance of adaptive antennas for the TD-CDMA downlink under special consideration of multi-directional channels and CDMA code pooling', *Int. J. Electron. Commun. (AEÜ)*, 2000, **54**, (5), pp. 249–258

3 Technical Specification Group Radio Access Network 3GPP: 'Spreading and modulation (TDD)', *3GPP*, 2000, **3.2.0**, (25.223)

4 MEURER, M., BAIER, P.W., WEBER, T., LU, Y., and PAPATHANASSIOU, A.: 'Joint transmission, an advantageous downlink concept for CDMA mobile radio systems using time division duplexing', *Electron. Lett.*, 2000, **36**, (10), pp. 900–901

5 MEURER, M., BAIER, P.W., LU, Y., PAPATHANASSIOU, A., and WEBER, T.: 'TD-CDMA downlink: optimum transmit signal design reduces receiver complexity and enhances system performance'. Proc. 7th Int. Conf. Telecommunications (ICT 2000), Acapulco, 2000, pp. 300–305

6 BAIER, P.W., MEURER, M., WEBER, T., and TRÖGER, H.: 'Joint transmission (JT), an alternative rationale for the downlink of time division CDMA using multi-element transmit antennas'. Proc. 6th Int. Symp. Spread Spectrum Techniques & Applications (ISSSTA 2000), Parsippany, 2000, pp. 1–5

[BQT+03] Baier, P. W.; Qiu, W.; Tröger, H.; Jötten, C. A.; Meurer, M.; Lehmann, G.: "Modelling and optimization of receiver oriented multi-user MIMO downlinks for frequency selective channels". *Proc. 10th International Conference on Telecommunications (ICT'03)*, Bd. 2, Papeete, 2003, S. 1547–1554.

Modelling and optimization of receiver oriented multi-user MIMO downlinks for frequency selective channels

P.W. Baier, W. Qiu, H. Tröger, C.A. Jötten, M. Meurer
Research Group for RF Communications, University of Kaiserslautern,
P.O. Box 3049, D–67653 Kaiserslautern, Germany
e–mail: baier@rhrk.uni-kl.de
G. Lehmann
SIEMENS AG, ICM N PG NM NE R2
Siemensdamm 62, D-13627 Berlin, Germany

Abstract— **The topic of the paper are mobile radio downlinks in which an access point (AP) supports a number of mobile terminals (MTs). As a special feature of the considered downlinks, both the AP and each MT are equipped with multi-antennas so that each of the partial downlinks from the AP to one of the MTs has a MIMO (Multiple Input Multiple Output) structure, and the total downlink is of the type multi-user MIMO. First a generic mathematical model for such downlinks is developed, which allows the inclusion of frequency selective channels. Then, based on this model, receiver oriented multi-user MIMO downlinks are introduced which are characterized by the fact that, in contrast to conventional downlinks, the algorithms to be utilized in the receivers are a priori determined, whereas the transmitter algorithms result a posteriori based on the receiver algorithms and on channel state information. The rationale behind receiver orientation implies the opportunity to transfer implementation complexity from the MTs to the AP and is especially suited for mobile radio systems utilizing the duplexing scheme TDD (Time Division Multiplexing). A favourable choice of the receiver algorithms is proposed, and the theoretical findings are completed by some illustrative simulation results.**

I. Introduction

In the paper mobile radio downlinks are considered in which an access point (AP) supports K mobile terminals (MTs). As a special feature of the considered downlinks, both the AP and each MT are equipped with multi-antennas so that each of the K partial downlinks from the AP to one of the K MTs has a MIMO (Multiple Input Multiple Output) structure, and the total system constitutes a multi-user MIMO downlink. As a further feature of the considerations, linear transmission is assumed. The first goal of the paper is the development of a generic model for linear multi-user MIMO downlinks, which also allows the inclusion of frequency selective channels.

Conventional transmission schemes are transmitter oriented, which means that the transmitter algorithms are *a priori* given, whereas the algorithms to be used at the receivers have to be *a posteriori* adapted under consideration of channel state information [1], [2]. In contrast to transmitter orientation, in receiver oriented systems the receiver algorithms are *a priori* given, and the transmitter algorithms, again under consideration of channel state information, have to be *a posteriori* adapted correspondingly. Recently, receiver oriented schemes have been proposed as promising approaches for mobile radio downlinks which utilize the duplexing scheme TDD [3] – [11]. In such applications the rationale receiver orientation may offer the following advantages [3] – [11]:

- The *a priori* determined receiver algorithms can be chosen with a view to arrive at particularly simple receiver structures. In this way, as compared to transmitter oriented systems, complexity can be transferred from the MTs to the AP.
- Channel information is only required at the AP. Therefore, no downlink transmission resources have to be sacrificed for training signals, and no channel estimators are required at the MTs.

To the authors knowledge, up to now linear receiver oriented multi-user MIMO downlinks are not considered in literature. Therefore, the second goal of the paper is the detailed description of such downlinks with special emphasis on concepts termed Transmit Zero Forcing (TxZF) [12]. In TxZF ISI (Intersymbol Interference) and MAI (Multiple Access Interference) are *a priori* avoided in the MTs, and simultaneously the required transmit energies are minimized [8], [9], [10], [11].

Further goals of the paper are the introduction of a performance criterion for multi-user MIMO downlinks and a proposal how to beneficially choose the receiver algorithms in the case of TxZF. The paper is completed by the presentation and discussion of some simulation results.

II. Multi-user MIMO downlink model

We consider a situation where an AP supports K MTs μ_k, $k = 1 \ldots K$. The AP is equipped with K_B transmit antennas, and each of the K MTs employs K_M receive antennas. Fig. 1 illustrates this situation by a transmission model, which will be explained and mathematically described in what follows.

It is assumed that N data symbols have to be transmitted from the AP to each MT μ_k, $k = 1 \ldots K$. The N data symbols intended for MT μ_k are arranged in the MT specific data vector

$$\underline{\boldsymbol{d}}^{(k)} = \left(\underline{d}_1^{(k)} \ldots \underline{d}_N^{(k)}\right)^\mathrm{T} \tag{1}$$

of dimension N. The K MT specific data vectors $\underline{\boldsymbol{d}}^{(k)}$ of (1) are stacked to the (total) data vector

$$\begin{aligned}\underline{\boldsymbol{d}} &= \left(\underline{\boldsymbol{d}}^{(1)\mathrm{T}} \ldots \underline{\boldsymbol{d}}^{(K)\mathrm{T}}\right)^\mathrm{T} \\ &= \left(\underline{d}_1 \ldots \underline{d}_n \ldots \underline{d}_{KN}\right)^\mathrm{T}\end{aligned} \tag{2}$$

of dimension KN. By linear modulation based on $\underline{\boldsymbol{d}}$ of (2) a transmit antenna specific transmit signal $\underline{\boldsymbol{t}}^{(k_\mathrm{B})}$, $k_\mathrm{B} =$

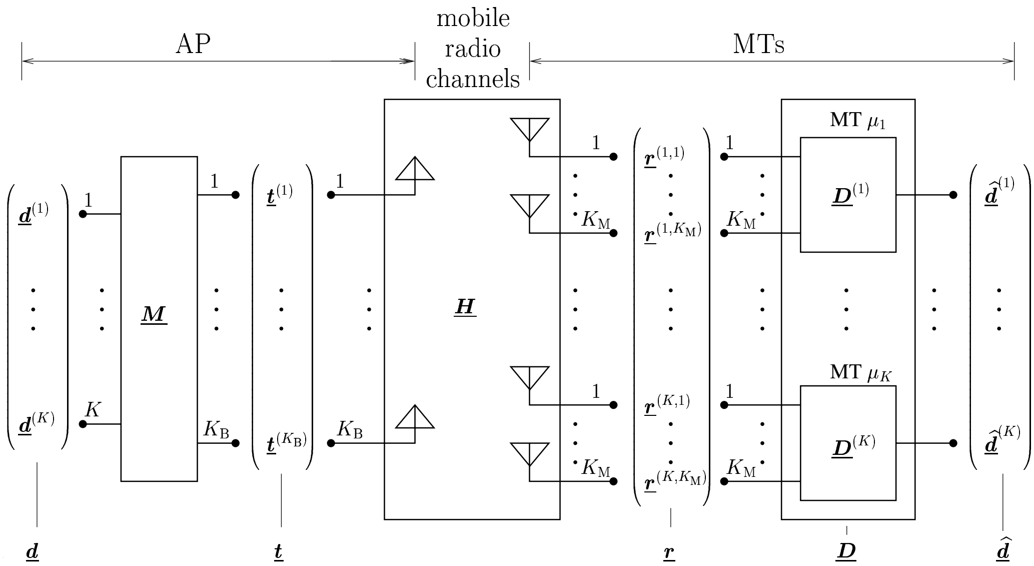

Fig. 1. Model of multi-user MIMO downlink

$1 \dots K_\mathrm{B}$, of dimension S is generated for each of the K_B transmit antennas. This linear modulation can be described by the K_B transmit antenna specific modulator matrices $\underline{\boldsymbol{M}}^{(k_\mathrm{B})}$, $k_\mathrm{B} = 1 \dots K_\mathrm{B}$, of dimension $S \times (KN)$ as follows:

$$\begin{aligned} \underline{\boldsymbol{t}}^{(k_\mathrm{B})} &= \left(\underline{t}_1^{(k_\mathrm{B})} \dots \underline{t}_S^{(k_\mathrm{B})}\right)^\mathrm{T} \\ &= \underline{\boldsymbol{M}}^{(k_\mathrm{B})}\, \underline{\boldsymbol{d}},\ k_\mathrm{B} = 1 \dots K_\mathrm{B}. \end{aligned} \tag{3}$$

The K_B equations of (3) can be stacked to form the equation

$$\begin{aligned} \underline{\boldsymbol{t}} &= \left(\underline{\boldsymbol{t}}^{(1)\mathrm{T}} \dots \underline{\boldsymbol{t}}^{(K_\mathrm{B})\mathrm{T}}\right)^\mathrm{T} \\ &= \underbrace{\left(\underline{\boldsymbol{M}}^{(1)\mathrm{T}} \dots \underline{\boldsymbol{M}}^{(K_\mathrm{B})\mathrm{T}}\right)^\mathrm{T}}_{\underline{\boldsymbol{M}}} \underline{\boldsymbol{d}} = \underline{\boldsymbol{M}}\, \underline{\boldsymbol{d}}. \end{aligned} \tag{4}$$

$\underline{\boldsymbol{t}}$ is termed (total) transmit signal and has the dimension $K_\mathrm{B}S$. $\underline{\boldsymbol{M}}$ in (4) is termed (total) modulator matrix and has the dimension $(K_\mathrm{B}S) \times (KN)$. Via (4) the KN components of $\underline{\boldsymbol{d}}$ of (2) are mapped on the $K_\mathrm{B}S$ components of $\underline{\boldsymbol{t}}$. In what follows we assume

$$K_\mathrm{B}S > KN, \tag{5}$$

that is the data symbols $\underline{d}_n$ of (2) are spread. This spreading consists of a spatial and spectral component quantified by K_B and S, respectively.

The frequency selective channel between the transmit antenna k_B of the AP and the receive antenna k_M of MT μ_k is characterized by the channel impulse response

$$\underline{\boldsymbol{h}}^{(k,k_\mathrm{B},k_\mathrm{M})} = \left(\underline{h}_1^{(k,k_\mathrm{B},k_\mathrm{M})} \dots \underline{h}_W^{(k,k_\mathrm{B},k_\mathrm{M})}\right)^\mathrm{T} \tag{6}$$

of dimension W. With this channel impulse response and the dimension S of $\underline{\boldsymbol{t}}^{(k_\mathrm{B})}$ of (3) the $(S+W-1) \times S$ channel convolution matrix

$$\begin{aligned} \underline{\boldsymbol{H}}^{(k,k_\mathrm{B},k_\mathrm{M})} &= \left(\underline{H}_{i,\,j}^{(k,k_\mathrm{B},k_\mathrm{M})}\right), \\ & \quad i = 1 \dots S+W-1,\ j = 1 \dots S, \\ \underline{H}_{i,\,j}^{(k,k_\mathrm{B},k_\mathrm{M})} &= \begin{cases} \underline{h}_{i-j+1}^{(k,k_\mathrm{B},k_\mathrm{M})} & 1 \le i-j+1 \le W, \\ 0 & \text{else}, \end{cases} \\ & \quad k = 1 \dots K,\ k_\mathrm{B} = 1 \dots K_\mathrm{B}, \\ & \quad k_\mathrm{M} = 1 \dots K_\mathrm{M}, \end{aligned} \tag{7}$$

is established. In total $KK_\mathrm{B}K_\mathrm{M}$ such matrices exist. With the K_B matrices $\underline{\boldsymbol{H}}^{(k,k_\mathrm{B},k_\mathrm{M})}$ obtained from (7) for $k_\mathrm{B} = 1 \dots K_\mathrm{B}$ and for given values k, k_M and with (4) the signal received by antenna k_M of MT μ_k can be expressed as

$$\begin{aligned} \underline{\boldsymbol{r}}^{(k,k_\mathrm{M})} &= \sum_{k_\mathrm{B}=1}^{K_\mathrm{B}} \underline{\boldsymbol{H}}^{(k,k_\mathrm{B},k_\mathrm{M})}\, \underline{\boldsymbol{t}}^{(k_\mathrm{B})} \\ &= \underbrace{\left(\underline{\boldsymbol{H}}^{(k,1,k_\mathrm{M})} \dots \underline{\boldsymbol{H}}^{(k,K_\mathrm{B},k_\mathrm{M})}\right)}_{\underline{\boldsymbol{H}}^{(k,k_\mathrm{M})}} \underline{\boldsymbol{t}} \\ &= \underline{\boldsymbol{H}}^{(k,k_\mathrm{M})}\, \underline{\boldsymbol{t}} = \underline{\boldsymbol{H}}^{(k,k_\mathrm{M})}\, \underline{\boldsymbol{M}}\, \underline{\boldsymbol{d}}. \end{aligned} \tag{8}$$

$\underline{\boldsymbol{r}}^{(k,k_\mathrm{M})}$ has the dimension $S + W - 1$. Stacking the K_M signals $\underline{\boldsymbol{r}}^{(k,k_\mathrm{M})}$, $k_\mathrm{M} = 1 \dots K_\mathrm{M}$, of (8) received by MT μ_k

yields the space-time receive signal

$$\begin{aligned}\underline{\boldsymbol{r}}^{(k)} &= \left(\underline{\boldsymbol{r}}^{(k,1)\,\mathrm{T}} \ldots \underline{\boldsymbol{r}}^{(k,K_\mathrm{M})\,\mathrm{T}}\right)^\mathrm{T} \\ &= \underbrace{\left(\underline{\boldsymbol{H}}^{(k,1)\,\mathrm{T}} \ldots \underline{\boldsymbol{H}}^{(k,K_\mathrm{M})\,\mathrm{T}}\right)^\mathrm{T}}_{\underline{\boldsymbol{H}}^{(k)}} \underline{\boldsymbol{t}} \\ &= \underline{\boldsymbol{H}}^{(k)}\, \underline{\boldsymbol{M}}\, \underline{\boldsymbol{d}} \end{aligned} \tag{9}$$

of MT μ_k. $\underline{\boldsymbol{r}}^{(k)}$ has the dimension $K_\mathrm{M}(S+W-1)$. $\underline{\boldsymbol{r}}^{(k)}$ and $\underline{\boldsymbol{H}}^{(k)}$ of (9) are termed MT specific receive signal and MT specific channel convolution matrix, respectively. The K signals $\underline{\boldsymbol{r}}^{(k)}$, $k = 1\ldots K$, of (9) can be arranged in a vector

$$\begin{aligned}\underline{\boldsymbol{r}} &= \left(\underline{\boldsymbol{r}}^{(1)\,\mathrm{T}} \ldots \underline{\boldsymbol{r}}^{(K)\,\mathrm{T}}\right)^\mathrm{T} \\ &= \underbrace{\left(\underline{\boldsymbol{H}}^{(1)\,\mathrm{T}} \ldots \underline{\boldsymbol{H}}^{(K)\,\mathrm{T}}\right)^\mathrm{T}}_{\underline{\boldsymbol{H}}} \underline{\boldsymbol{t}} \\ &= \underline{\boldsymbol{H}}\, \underline{\boldsymbol{M}}\, \underline{\boldsymbol{d}} \end{aligned} \tag{10}$$

of dimension $KK_\mathrm{M}(S+W-1)$. $\underline{\boldsymbol{r}}$ and $\underline{\boldsymbol{H}}$ of (10) are termed (total) receive signal and (total) channel convolution matrix, respectively. (10) describes the transmission model of Fig. 1 from the data input to receive antenna outputs.

At MT μ_k the receive signal $\underline{\boldsymbol{r}}^{(k)}$ of this MT, see (9), is fed to a demodulator in order to obtain an estimate $\hat{\underline{\boldsymbol{d}}}^{(k)}$ of $\underline{\boldsymbol{d}}^{(k)}$ of (1). In the case of linear demodulation considered in this paper the demodulation process performed at MT μ_k can be described by a MT specific demodulator matrix $\underline{\boldsymbol{D}}^{(k)}$ of dimension $N \times [K_\mathrm{M}(S+W-1)]$ as follows:

$$\hat{\underline{\boldsymbol{d}}}^{(k)} = \underline{\boldsymbol{D}}^{(k)}\, \underline{\boldsymbol{r}}^{(k)}. \tag{11}$$

By properly stacking the K equations (11) we can obtain with (2) and (10)

$$\begin{aligned}\hat{\underline{\boldsymbol{d}}} &= \mathrm{blockdiag}\left[\underline{\boldsymbol{D}}^{(1)} \ldots \underline{\boldsymbol{D}}^{(K)}\right] \underline{\boldsymbol{r}} \\ &= \underline{\boldsymbol{D}}\, \underline{\boldsymbol{r}}. \end{aligned} \tag{12}$$

$\underline{\boldsymbol{D}}$ of (12) has the dimension $(KN) \times [KK_\mathrm{M}(S+W-1)]$ and is termed (total) demodulator matrix. Substituting (10) in (12) yields

$$\hat{\underline{\boldsymbol{d}}} = \underline{\boldsymbol{D}}\, \underline{\boldsymbol{H}}\, \underline{\boldsymbol{M}}\, \underline{\boldsymbol{d}}, \tag{13}$$

which describes the model of Fig. 1 from the data input to the data output.

Up to now the noise free case is considered. If we now assume that $\underline{\boldsymbol{r}}$ of (10) is corrupted by an additive noise signal

$$\underline{\boldsymbol{n}} = \left(\underline{n}_1 \ldots \underline{n}_{KK_\mathrm{M}(S+W-1)}\right)^\mathrm{T} \tag{14}$$

of dimension $KK_\mathrm{M}(S+W-1)$, then we obtain instead of (13)

$$\hat{\underline{\boldsymbol{d}}} = \underline{\boldsymbol{D}}\left(\underline{\boldsymbol{H}}\, \underline{\boldsymbol{M}}\, \underline{\boldsymbol{d}} + \underline{\boldsymbol{n}}\right). \tag{15}$$

If we further assume stationary $\underline{\boldsymbol{d}}$ and $\underline{\boldsymbol{n}}$, we can determine from (15) the signal-to-noise-plus-interference ratio (SNIR) γ_n of the estimate $\hat{\underline{d}}_n$ of $\underline{d}_n$ in (2). Let us designate by $[\cdot]_i$ the component i of the column vector in brackets and by $[\cdot]_{i,i}$ the diagonal element i of the square matrix in brackets. Then, we obtain [1]

$$\gamma_n = \frac{\left|[\underline{\boldsymbol{D}}\, \underline{\boldsymbol{H}}\, \underline{\boldsymbol{M}}]_{n,n}\right|^2 \mathrm{E}\left\{|\underline{d}_n|^2\right\}}{\mathrm{E}\left\{|[\underline{\boldsymbol{D}}\, \underline{\boldsymbol{n}}]_n|^2\right\} + \mathrm{E}\left\{\left|\left[\overline{\mathrm{diag}}\left(\underline{\boldsymbol{D}}\, \underline{\boldsymbol{H}}\, \underline{\boldsymbol{M}}\right) \underline{\boldsymbol{d}}\right]_n\right|^2\right\}}. \tag{16}$$

III. Normalizations

It would be desirable that the transmission model introduced in Section II could be adjusted in the following respects:

- Pre-determining of the transmit energies E_n, $n = 1\ldots KN$, invested for the transmission of the data symbols $\underline{d}_n$, $n = 1\ldots KN$, see (2).
- Scaling of the attenuations of the channels from the AP to the individual MTs μ_k, $k = 1\ldots K$.
- Introduction of amplifiers in the individual MTs μ_k, $k = 1\ldots K$.

In this section it is shown how such adjustments could be achieved by utilizing normalized versions of the matrices $\underline{\boldsymbol{M}}$, $\underline{\boldsymbol{H}}$ and $\underline{\boldsymbol{D}}$ introduced in Section II. To this purpose the transmission model of Fig. 1 is concisely re-drawn as shown in Fig. 2. In this figure it is also indicated how the matrices $\underline{\boldsymbol{M}}$, $\underline{\boldsymbol{H}}$ and $\underline{\boldsymbol{D}}$ can be expressed by normalized matrices $\tilde{\underline{\boldsymbol{M}}}$, $\tilde{\underline{\boldsymbol{H}}}$ and $\tilde{\underline{\boldsymbol{D}}}$ and by real valued diagonal matrices $\boldsymbol{N}$, $\sqrt{\boldsymbol{E}}$, $\sqrt{\boldsymbol{\lambda}}$ and $\boldsymbol{X}$, respectively. According to Fig. 2

$$\underline{\boldsymbol{M}} = \tilde{\underline{\boldsymbol{M}}}\sqrt{\boldsymbol{E}}\,\boldsymbol{N}, \tag{17}$$

$$\underline{\boldsymbol{H}} = \sqrt{\boldsymbol{\lambda}}\,\tilde{\underline{\boldsymbol{H}}} \tag{18}$$

and

$$\underline{\boldsymbol{D}} = \boldsymbol{X}\,\tilde{\underline{\boldsymbol{D}}} \tag{19}$$

hold. With the elements $\underline{d}_n$, $n = 1\ldots KN$, of $\underline{\boldsymbol{d}}$ of (2) $\boldsymbol{N}$ in (17) is defined as the diagonal matrix

$$\boldsymbol{N} = \left(\sqrt{\mathrm{diag}\left(\underline{\boldsymbol{d}}\,\underline{\boldsymbol{d}}^\mathrm{H}\right)}\right)^{-1}. \tag{20}$$

$\boldsymbol{E}$ in (17) is constituted by the transmit energies E_n, $n = 1\ldots KN$:

$$\boldsymbol{E} = \mathrm{diag}\left(E_1 \ldots E_{KN}\right). \tag{21}$$

Both $\boldsymbol{N}$ and $\boldsymbol{E}$ have the dimension $(KN) \times (KN)$. The normalized modulator matrix $\tilde{\underline{\boldsymbol{M}}}$ in (17) shall fulfill

$$\mathrm{diag}\left(\tilde{\underline{\boldsymbol{M}}}^\mathrm{H}\, \tilde{\underline{\boldsymbol{M}}}\right) = \boldsymbol{I}^{(KN)}. \tag{22}$$

In order to obtain $\tilde{\underline{\boldsymbol{H}}}$ in (18), first the K normalized MT specific channel convolution matrices $\tilde{\underline{\boldsymbol{H}}}^{(k)}$, $k = 1\ldots K$, are introduced which are characterized by the fact that they

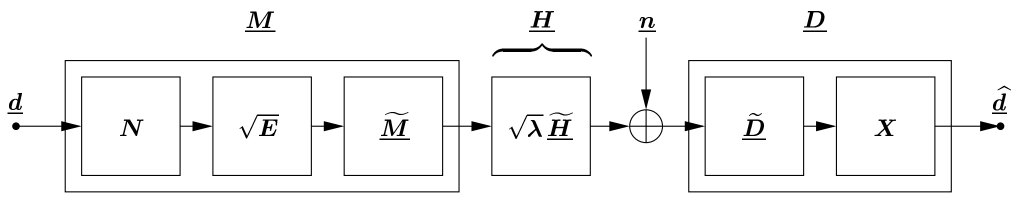

Fig. 2. Multi-user MIMO downlink with normalized matrices $\widetilde{\underline{\boldsymbol{M}}}$, $\widetilde{\underline{\boldsymbol{H}}}$ and $\tilde{\underline{\boldsymbol{D}}}$

allow to express $\underline{\boldsymbol{H}}^{(k)}$ of (9) by the largest eigenvalue $\lambda_1^{(k)}$ of $\underline{\boldsymbol{H}}^{(k)\mathrm{H}}\,\underline{\boldsymbol{H}}^{(k)}$ as

$$\underline{\boldsymbol{H}}^{(k)} = \sqrt{\lambda_1^{(k)}}\,\widetilde{\underline{\boldsymbol{H}}}^{(k)}. \tag{23}$$

By stacking the matrices $\widetilde{\underline{\boldsymbol{H}}}^{(k)}$ defined by (23) we obtain the normalized (total) channel convolution matrix

$$\widetilde{\underline{\boldsymbol{H}}} = \left(\widetilde{\underline{\boldsymbol{H}}}^{(1)^{\mathrm{T}}} \ldots \widetilde{\underline{\boldsymbol{H}}}^{(K)^{\mathrm{T}}}\right)^{\mathrm{T}}. \tag{24}$$

We now introduce the diagonal matrix

$$\sqrt{\boldsymbol{\lambda}} = \mathrm{diag}\left(\sqrt{\lambda_1^{(1)}}\boldsymbol{I} \ldots \sqrt{\lambda_1^{(K)}}\boldsymbol{I}\right), \tag{25}$$

where the unit matrix $\boldsymbol{I}$ in (25) has the dimension $[K_{\mathrm{M}}(S+W-1)] \times [K_{\mathrm{M}}(S+W-1)]$. Substitution of $\widetilde{\underline{\boldsymbol{H}}}$ of (24) and $\sqrt{\boldsymbol{\lambda}}$ of (25) in (18) yields $\underline{\boldsymbol{H}}$. Finally, the normalized demodulator matrix $\tilde{\underline{\boldsymbol{D}}}$ in (19) is chosen such that

$$\mathrm{diag}\left(\tilde{\underline{\boldsymbol{D}}}\,\tilde{\underline{\boldsymbol{D}}}^{\mathrm{H}}\right) = \boldsymbol{I}^{(KN)} \tag{26}$$

holds. The SNIRs γ_n of (16) are independent of the element values of the diagonal matrix $\boldsymbol{X}$ in (19). However, by proper choice of these elements it can be for instance achieved that the desired portions of the demodulator outputs are unbiased.

IV. Transmit Matched Filter and Transmit Zero Forcer

As already mentioned, in receiver oriented systems [3]–[11] the demodulator matrix $\underline{\boldsymbol{D}}$ introduced in (12) is *a priori* chosen; then, based on this choice and the knowledge of the channel convolution matrix $\underline{\boldsymbol{H}}$ of (10), the modulator matrix $\underline{\boldsymbol{M}}$ introduced in (4) is *a posteriori* determined. Two promising options for determining $\underline{\boldsymbol{M}}$ are the Transmit Matched Filter (TxMF) and the Transmit Zero Forcer (TxZF) [12], for which

$$\underline{\boldsymbol{M}} = \begin{cases} (\underline{\boldsymbol{D}}\,\underline{\boldsymbol{H}})^{\mathrm{H}} & \text{(TxMF)} \\ (\underline{\boldsymbol{D}}\,\underline{\boldsymbol{H}})^{\mathrm{H}}\left[(\underline{\boldsymbol{D}}\,\underline{\boldsymbol{H}})(\underline{\boldsymbol{D}}\,\underline{\boldsymbol{H}})^{\mathrm{H}}\right]^{-1} & \text{(TxZF)} \end{cases} \tag{27}$$

hold. In the case of the TxMF the transmitted symbol energies E_n, $n = 1\ldots KN$, see (21), are transformed into useful received energies at the MTs in an optimum way; however, ISI and MAI may occur. In the case of the TxZF, ISI

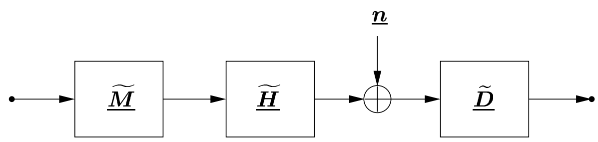

Fig. 3. Normalized multi-user MIMO downlink

and MAI are *a priori* avoided; however, for given transmit energies E_n the useful received energies are smaller than in the case of the TxMF. As a topic of further research, adequate compromises between TxMF and TxZF should be found, possibly based on a rationale similar to the one followed when deriving the MMSE (Minimum Mean Square Error) estimator in transmitter oriented systems. In this paper the focus is on TxZF.

In the case of the TxZF we obtain from (17), (18), (19) and (27) the normalized modulator matrix

$$\begin{aligned} \widetilde{\underline{\boldsymbol{M}}} &= \left(\tilde{\underline{\boldsymbol{D}}}\,\widetilde{\underline{\boldsymbol{H}}}\right)^{\mathrm{H}}\left[\left(\tilde{\underline{\boldsymbol{D}}}\,\widetilde{\underline{\boldsymbol{H}}}\right)\left(\tilde{\underline{\boldsymbol{D}}}\,\widetilde{\underline{\boldsymbol{H}}}\right)^{\mathrm{H}}\right]^{-1} \\ &\quad \cdot\left(\sqrt{\mathrm{diag}\left[\left(\tilde{\underline{\boldsymbol{D}}}\,\widetilde{\underline{\boldsymbol{H}}}(\tilde{\underline{\boldsymbol{D}}}\,\widetilde{\underline{\boldsymbol{H}}})^{\mathrm{H}}\right)^{-1}\right]}\right)^{-1}. \end{aligned} \tag{28}$$

Then, if unbiased data estimates $\widehat{\underline{d}}_n$, $n = 1\ldots KN$, would be required, $\boldsymbol{X}$ in (19) should be chosen as follows:

$$\begin{aligned} \boldsymbol{X} &= \boldsymbol{N}^{-1}\left(\sqrt{\boldsymbol{E}}\right)^{-1} \\ &\quad \cdot\mathrm{blockdiag}\left[\left(\sqrt{\lambda_1^{(1)}}\right)^{-1}\boldsymbol{I}^{(N)} \ldots \left(\sqrt{\lambda_1^{(K)}}\right)^{-1}\boldsymbol{I}^{(N)}\right] \\ &\quad \cdot\sqrt{\mathrm{diag}\left[\left(\tilde{\underline{\boldsymbol{D}}}\,\widetilde{\underline{\boldsymbol{H}}}(\tilde{\underline{\boldsymbol{D}}}\,\widetilde{\underline{\boldsymbol{H}}})^{\mathrm{H}}\right)^{-1}\right]}. \end{aligned} \tag{29}$$

V. Performance Assessment

Let us consider the transmission of a single data symbol $\underline{d}_n^{(k)}$, $n = 1\ldots N$, from the AP to MT μ_k. For this transmission the AP invests the energy $E_{(k-1)N+n}$, see (21). This transmitted energy leads to the useful received energy $R_{n,\,\mathrm{useful}}^{(k)}$ at MT μ_k. For comparison the same energy $E_{(k-1)N+n}$ could also be radiated by the AP in the form of a transmit signal which would, after having passed the

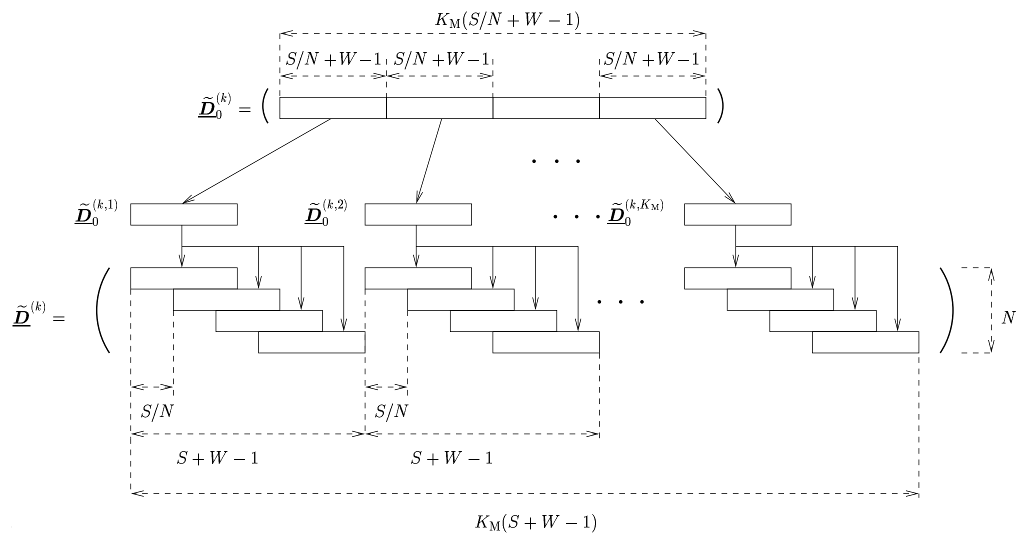

Fig. 4. Constitution of the K normalized MT specific demodulator matrices $\tilde{\underline{D}}^{(k)}$ based on the normalized MT specific demodulator matrices $\tilde{\underline{D}}_0^{(k)}$ for the single symbol/single MT case

channel from the AP to MT μ_k, produce maximum received energy $R_{\max}^{(k)}$ at MT μ_k. With the largest eigenvalue $\lambda_1^{(k)}$ of the matrix $\underline{\boldsymbol{H}}^{(k)\mathrm{H}}\underline{\boldsymbol{H}}^{(k)}$ we obtain

$$R_{\max}^{(k)} = \lambda_1^{(k)} E_{(k-1)N+1}. \tag{30}$$

Now, a quantity suitable to assess the performance of the transmission system related to the data symbol $\underline{d}_n^{(k)}$ would be the ratio

$$\eta_n^{(k)} = \frac{R_{n,\,\mathrm{useful}}^{(k)}}{R_{\max}^{(k)}}, \tag{31}$$

which is termed energy efficiency of the transmission system for this data symbol. For the values of the energy efficiency

$$0 \leq \eta_n^{(k)} \leq 1 \tag{32}$$

holds, and it is desirable that these values come as close to 1 as possible.

In order to determine the energy efficiencies $\eta_n^{(k)}$ of (31) it is sufficient to consider the normalized transmission model shown in Fig. 3. Let us designate by $[\cdot]_i$ the column i of the matrix in brackets. Then, in the system model of Fig. 3

$$\tilde{R}_{n,\,\mathrm{useful}}^{(k)} = \left| \left(\left[\tilde{\underline{\boldsymbol{D}}}^{\mathrm{T}}\right]_{(k-1)N+n} \right)^{\mathrm{T}} \widetilde{\underline{\boldsymbol{H}}}^{(k)} \left[\widetilde{\underline{\boldsymbol{M}}}\right]_{(k-1)N+n} \right|^2 \tag{33}$$

holds. Further, the largest eigenvalue of the matrix $\widetilde{\underline{\boldsymbol{H}}}^{(k)\mathrm{H}}\widetilde{\underline{\boldsymbol{H}}}^{(k)}$ and the transmitted energy are equal to 1. Therefore,

$$\tilde{R}_{\max}^{(k)} = 1 \tag{34}$$

is valid. Substitution of (33) and (34) into (31) yields

$$\eta_n^{(k)} = \tilde{R}_{n,\,\mathrm{useful}}^{(k)}. \tag{35}$$

In the case of the TxZF we obtain due to (28)

$$\begin{aligned} \eta_n^{(k)} &= \left| \left(\left[\tilde{\underline{\boldsymbol{D}}}^{\mathrm{T}}\right]_{\nu} \right)^{\mathrm{T}} \widetilde{\underline{\boldsymbol{H}}}^{(k)} \left[\widetilde{\underline{\boldsymbol{M}}}\right]_{\nu} \right|^2 \\ &= \left[\left(\mathrm{diag}\left[\left(\tilde{\underline{\boldsymbol{D}}}\,\widetilde{\underline{\boldsymbol{H}}} \left(\tilde{\underline{\boldsymbol{D}}}\,\widetilde{\underline{\boldsymbol{H}}} \right)^{\mathrm{H}} \right)^{-1} \right] \right)^{-1} \right]_{\nu,\nu}, \end{aligned} \tag{36}$$

where

$$\nu = (k-1)N + n. \tag{37}$$

VI. Beneficial choice of the demodulator matrix $\underline{\boldsymbol{D}}$

Let us consider the expression (36) for the energy efficiencies $\eta_n^{(k)}$ valid in the case of TxZF. According to this expression, for a given normalized channel convolution matrix $\widetilde{\underline{\boldsymbol{H}}}$ of (18) the values $\eta_n^{(k)}$ are determined by the chosen normalized demodulator matrix $\tilde{\underline{\boldsymbol{D}}}$ of (19). $\tilde{\underline{\boldsymbol{D}}}$ should be chosen in such a way that the values $\eta_n^{(k)}$ come as close to 1 as possible. Unfortunately, an analytical method for determining the optimum $\tilde{\underline{\boldsymbol{D}}}$ is not known yet. Therefore, an heuristic approach to arrive at a suitable matrix $\tilde{\underline{\boldsymbol{D}}}$ is proposed in what follows. This approach relies on

- first determining optimum demodulator matrices for the single symbol/single MT downlink, which is termed reference downlink, and then
- constituting $\tilde{\underline{\boldsymbol{D}}}$ for the multi-symbol/multi MT case based on these optimum matrices.

In the reference downlink N is equal to 1, and each of the K partial reference downlinks is considered without taking into account the other $K-1$ reference downlinks. The reference downlink is marked by the index "0". In the considered original TxZF downlink the dimension of the transmit signal is $K_\mathrm{B}S$, see (4). In the reference downlink we choose the dimension $K_\mathrm{B}S/N$ for the transmit signal $\underline{\boldsymbol{t}}_0^{(k)}$ in order to have the same symbol specific spatial-spectral spreading factor as in the original downlink. Then, the K normalized channel convolution matrices $\underline{\widetilde{\boldsymbol{H}}}_0^{(k)}$ have the dimension $[K_\mathrm{M}(S/N+W-1)]\times(K_\mathrm{B}S/N)$.

In the case of the reference downlink the transmit signal $\underline{\boldsymbol{t}}_0^{(k)}$ maximizing the energy transfer from the AP to MT μ_k is determined by the eigenvector $\underline{\boldsymbol{u}}_0^{(k)}$ of the matrix $\underline{\widetilde{\boldsymbol{H}}}_0^{(k)\mathrm{H}}\underline{\widetilde{\boldsymbol{H}}}_0^{(k)}$ corresponding to the largest eigenvalue $\lambda_{0,1}^{(k)}$ of this matrix - again the normalization is chosen such that $\lambda_{0,1}^{(k)}$ becomes equal to 1. $\underline{\boldsymbol{u}}_0^{(k)}$ can be termed space-time eigen-signature of the channel between the AP and MT μ_k. The corresponding normalized MT specific modulator matrix reads

$$\underline{\widetilde{\boldsymbol{M}}}_0^{(k)}=\underline{\boldsymbol{t}}_0^{(k)}=\frac{\underline{\boldsymbol{u}}_0^{(k)}}{\|\underline{\boldsymbol{u}}_0^{(k)}\|},\tag{38}$$

which leads to the received signal

$$\underline{\boldsymbol{r}}_0^{(k)}=\underline{\widetilde{\boldsymbol{H}}}_0^{(k)}\underline{\widetilde{\boldsymbol{M}}}_0^{(k)}=\underline{\widetilde{\boldsymbol{H}}}_0^{(k)}\frac{\underline{\boldsymbol{u}}_0^{(k)}}{\|\underline{\boldsymbol{u}}_0^{(k)}\|}.\tag{39}$$

Let us now choose $\underline{\widetilde{\boldsymbol{D}}}_0^{(k)}$ as the impulse response of a filter matched to $\underline{\boldsymbol{r}}_0^{(k)}$ of (39), that is

$$\begin{aligned}\underline{\widetilde{\boldsymbol{D}}}_0^{(k)} &= \left(\underline{\widetilde{\boldsymbol{H}}}_0^{(k)}\frac{\underline{\boldsymbol{u}}_0^{(k)}}{\|\underline{\boldsymbol{u}}_0^{(k)}\|}\right)^{\mathrm{H}}\\ &= \left(\underline{\widetilde{D}}_{0\,1}^{(k)}\ldots\underline{\widetilde{D}}_{0\,K_\mathrm{M}(S/N+W-1)}^{(k)}\right).\end{aligned}\tag{40}$$

Then, the energy efficiency of the reference downlink reaches the upper limit given in (32), that is

$$\eta_{0,\,n}^{(k)}=\underline{\widetilde{\boldsymbol{D}}}_0^{(k)}\underline{\boldsymbol{r}}_0^{(k)}=1.\tag{41}$$

Let us now consider the case that the AP communicates with all K MTs μ_k, $k=1\ldots K$, and that $N>1$ data symbols are transmitted to each MT with each of these data symbols being spectrally spread by a signature of dimension S/N. The authors propose to construct the normalized demodulator matrices $\underline{\widetilde{\boldsymbol{D}}}^{(k)}$ based on the normalized demodulator matrices $\underline{\widetilde{\boldsymbol{D}}}_0^{(k)}$ of (40). For MT μ_k, the N rows of the demodulator matrix $\underline{\widetilde{\boldsymbol{D}}}^{(k)}$ of (19) are obtained as shifted versions of $\underline{\widetilde{\boldsymbol{D}}}_0^{(k)}$ of (40) according to the scheme

$$\begin{aligned}\underline{\widetilde{\boldsymbol{D}}}^{(k)} &= \left(\underline{\widetilde{D}}_{i,j}^{(k)}\right),\\ & \quad i=1\ldots N,\ j=1\ldots[K_\mathrm{M}(S+W-1)],\\ \underline{\widetilde{D}}_{i,j}^{(k)} &= \begin{cases}\underline{\widetilde{D}}_{0\,p}^{(k)} & 1\le q\le S/N+W-1,\\ 0 & \text{else,}\end{cases}\end{aligned}\tag{42}$$

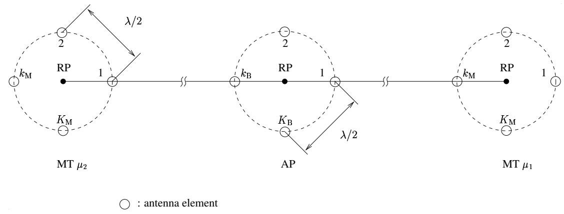

Fig. 5. Considered multi-user MIMO scenario with one AP and $K=2$ MTs

where

$$q = (j-1-(i-1)S/N)\bmod(S+W-1)+1,\tag{43}$$

and

$$\begin{aligned}p &= (j-1-(i-1)S/N)\bmod(S+W-1)+1\\ &\quad +(S/N+W-1)\cdot\left\lfloor\frac{j-1}{S+W-1}\right\rfloor.\end{aligned}\tag{44}$$

In (44) $\lfloor\cdot\rfloor$ denotes the integer part of the real-valued number in brackets. The structure of $\underline{\widetilde{\boldsymbol{D}}}^{(k)}$ of (42) to (44) is illustrated in Fig. 4.

The K transmit signals $\underline{\boldsymbol{t}}_0^{(k)}$, $k=1\ldots K$, of (38) and the demodulator matrices $\underline{\widetilde{\boldsymbol{D}}}_0^{(k)}$ of (40) derived for the single symbol/single MT case are optimum with respect to the energy transfer. It is expected that by generating the demodulator matrices $\underline{\widetilde{\boldsymbol{D}}}^{(k)}$ for the multi data symbol/multi user case based on the matrices $\underline{\widetilde{\boldsymbol{D}}}_0^{(k)}$ according to (42), (43) and (44), the optimality of the reference downlink may be conserved to a certain degree. It should be mentioned that by choosing $\underline{\widetilde{\boldsymbol{D}}}$ based on channel state information the rationale of pure receiver orientation is watered-down.

VII. Numerical results

In this section, a TxZF downlink utilizing the demodulator proposed in Section VI is evaluated by numerical analysis. The considered arrangement is illustrated in Fig. 5 [13]. At the AP K_B transmit antennas are placed on a circle around the reference point (RP). K equal to 2 MTs are supported by the AP and are point symmetrically situated relative to the AP in the far field of the transmit antennas. Each MT μ_k, $k=1,2$, has a circular array with K_M receive antennas around an RP. The distance between two adjacent antennas both at the transmitter and the receivers is one half of the carrier wavelength λ. The mobile radio channel between the AP and each MT μ_k, $k=1,2$, is assumed to be a single direction channel in the line-of-sight direction and is characterized by the channel impulse response

$$\underline{\boldsymbol{h}}^{(k)}=\left(\underline{h}_1^{(k)}\ldots\underline{h}_W^{(k)}\right)^{\mathrm{T}},\ k=1\ldots K,\tag{45}$$

between the RP of the AP and the RP of MT μ_k [14]. The channel impulse responses $\underline{\boldsymbol{h}}^{(k)}$, $k=1\ldots K$, of (45) are independently generated based on the 3GPP channel model

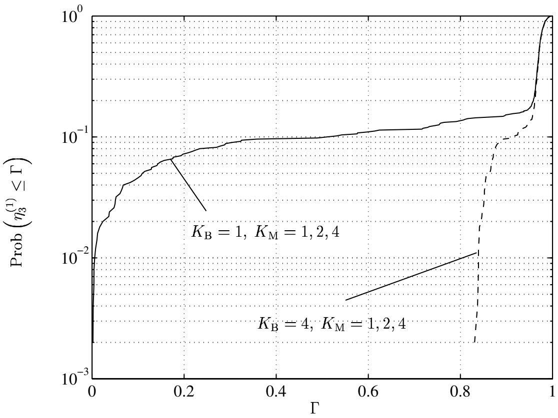

Fig. 6. CDF of energy efficiency $\eta_3^{(1)}$ of (36) of the third data symbol $\underline{d}_3^{(1)}$ of MT μ_1 for $N = 5$, $S = 80$ and $W = 4$; parameters: K_M and K_B

case 3 [15]. Based on $\underline{\boldsymbol{h}}^{(k)}$ of (45) and on the geometry of the configuration shown in Fig. 5 the channel impulse responses $\underline{\boldsymbol{h}}^{(k,k_\mathrm{B},k_\mathrm{M})}$ of (6) can be determined [16]. For the numerical analysis, N equal to five data symbols per MT are transmitted and S/N is chosen equal to 16. We study the performance of the central, that is the third data symbol $\underline{d}_3^{(1)}$ of MT μ_1, for a large number of snapshots. The channel impulse response $\boldsymbol{h}^{(k)}$ of (45) randomly varies from snapshot to snapshot. Fig. 6 shows the cumulative distribution function of the energy efficiency $\eta_3^{(1)}$ of (36) with K_B and K_M as parameters. In more than 80% of all cases the TxZF downlink utilizing the normalized demodulator matrix $\widetilde{\underline{\boldsymbol{D}}}^{(k)}$ of (42) to (44) proposed in Section VI performs near optimum, that is $\eta_3^{(1)}$ comes close to one. In about 20% of the cases the eigenvectors $\underline{\boldsymbol{u}}_0^{(1)}$ and $\underline{\boldsymbol{u}}_0^{(2)}$ of the MTs μ_1 and μ_2 introduced in Section VI are highly correlated. Then, a dramatic reduction of the values of $\eta_3^{(1)}$ can be observed, that is $\eta_3^{(1)} \ll 1$, see Fig. 6. The closer study of the effects leading to the form of the curves in Fig. 6 will be the topic of further research. In snapshots characterized by a high correlation between the two eigenvectors $\underline{\boldsymbol{u}}_0^{(k)}$, $k = 1, 2$, an opportunity to obtain values of $\eta_n^{(k)}$ of (36) closer to 1 may consist in choosing for the determination of $\widetilde{\underline{\boldsymbol{D}}}_0^{(k)}$ for one of the two MTs μ_k, $k = 1, 2$, the eigenvector corresponding to the second largest eigenvalue $\lambda_{0,2}^{(k)}$ of the matrix $\widetilde{\underline{\boldsymbol{H}}}_0^{(k)\mathrm{H}}\widetilde{\underline{\boldsymbol{H}}}_0^{(k)}$.

With an increasing number K_B of transmit antennas, the energy efficiency $\eta_3^{(1)}$ of (36) is improved. The number K_M of receive antennas at the MTs μ_k, $k = 1, 2$, has no impact on the energy efficiency $\eta_3^{(1)}$ in the case of the considered channel model of Fig. 5, because an increasing number K_M of receive antennas enhances the efficiency of the energy transfer in both the TxZF and the reference downlink to the same degree. Nevertheless, to achieve a certain transmission quality the required transmit energy decreases with increasing K_M and intercell MAI will decrease correspondingly.

VIII. Summary

Previous work on receiver oriented multi-user downlinks is extended by providing multi-antennas both at the AP and at the MTs. In this way multi-user MIMO downlinks are obtained. A system model for such downlinks is presented, and for assessing the system performance the criterion energy efficiency is proposed. Concerning the choice of the demodulator matrices an approach based on space-time eigensignatures of the mobile radio channels is proposed.

Acknowledgment

The authors gratefully appreciate the fruitful exchange of ideas within the Research Group for RF Communications, University of Kaiserslautern, and with Prof. Nossek's Group at TU Munich. The support of individual parts of this work in the framework of the IST-Project FLOWS (Flexible Convergence of Wireless Standards and Services) of the EU, Siemens AG and by the supercomputer staff of the central computer facility (RHRK) of the University of Kaiserslautern is highly acknowledged.

References

[1] A. Klein, *Multi-user detection of CDMA signals – algorithms and their application to cellular mobile radio*, Fortschrittberichte VDI, series 10, no. 423, VDI-Verlag, Düsseldorf, 1996.

[2] S. Verdu, *Multiuser Detection*, Cambridge University Press, 1998.

[3] B.R. Vojcic and J.W. Mee, "Transmitter precoding in synchronous multiuser communications", *IEEE Transactions on Communications*, vol. 46, no. 10, pp. 1346–1355, 1998.

[4] M. Brandt-Pearce and A. Dharap, "Transmitter-based multiuser interference rejection for the down-link of a wireless CDMA system in a multipath environment", *IEEE Journal on Selected Areas in Communications*, vol. 18, no. 3, pp. 407–417, 2000.

[5] M. Joham and W. Utschick, "Downlink processing for mitigation of intracell interference in DS-CDMA systems", *Proc. IEEE 6th International Symposium on Spread Spectrum Techniques & Applications (ISSSTA 2000), Parsippany*, pp. 15–19, 2000.

[6] K. Ban, M. Katayama, T. Yamazato and A. Ogawa, "Joint optimization of transmitter/receiver with multiple transmit/receive antennas in band-limited channels", *IEICE Transactions on Communications*, vol. E83-B, no. 8, pp. 1697–1704, 2000.

[7] F. Kowalewski and P. Mangold, "Joint predistortion and transmit diversity", *Proc. IEEE Global Telecommunications Conference (GLOBECOM'00)*, pp. 245–249, 2000.

[8] P.W. Baier, M. Meurer, T. Weber and H. Tröger, "Joint transmission (JT), an alternative rationale for the downlink of time division CDMA using multi-element transmit antennas", *Proc. IEEE 6th International Symposium on Spread Spectrum Techniques & Applications (ISSSTA 2000), Parsippany*, pp. 1–5, 2000.

[9] M. Meurer, P.W. Baier, Y. Lu, A. Papathanassiou and T. Weber, "TD-CDMA downlink: Optimum transmit signal design reduces receiver complexity and enhances system performance", *Proc. 7th International Conference on Telecommunications (ICT 2000), Acapulco*, pp. 300–305, 2000.

[10] M. Meurer, P.W. Baier, T. Weber, Y. Lu and A. Papathanassiou, "Joint transmission, an advantageous downlink concept for CDMA mobile radio systems using time division duplexing", *IEE ELECTRONICS LETTERS*, vol. 36, no. 10, pp. 900–901, 2000.

[11] M. Meurer, A. Papathanassiou, T. Weber and P.W. Baier, "A novel multiuser transmission scheme requiring no channel estimation and no equalization at the mobile stations for the downlink of TD–CDMA operating in the TDD mode", *Proc. IEEE 52th Vehicular Technology Conference (VTC 2000-Fall), Boston*, vol. 1, pp. 203–210, 2000.

[12] M. Joham, K. Kusume, M. H. Gzara, W. Utschick and J. A. Nossek, "Transmit Wiener Filter for the Downlink of TDD DS-CDMA Systems", *Proc. IEEE 6th International Symposium on Spread Spectrum Techniques & Applications (ISSSTA 2002), Prague*, pp. 9–13, 2002.

[13] H. Tröger, T. Weber, M. Meurer and P.W. Baier, "Performance assessment of Joint Transmission (JT) multi-user downlinks with multi-

element transmit antennas", *European Transactions on Telecommunications*, vol. 12, no. 5, pp. 407–416, 2001.

[14] A. Klein, W. Mohr and R. Thomas, "Direction-of-arrival of partial waves in wideband mobile radio channels for intelligent antenna concepts", *Proc. IEEE 46th Vehicular Technology Conference (VTC'96)*, pp. 849–853, 1996.

[15] "3rd generation partnership project (3GPP); technical specification group radio access network, UTRA (BS) TDD, radio transmission and reception", Technical Specification TS 25.105 Version 3.5.0, 3GPP, 2000.

[16] Y. Lu and P.W. Baier, "Performance of adaptive antennas for the TD-CDMA downlink under special consideration of multi-directional channels and CDMA code pooling", *International Journal of Electronics and Communications (AEÜ)*, vol. 54, no. 5, pp. 249–258, 2000.

[QTMJ03] Qiu, W.; Tröger, H.; Meurer, M.; Jötten, C. A.: "Performance analysis of a channel oriented concept for multi-user MIMO downlinks with frequency selective channels". *Proc. IEEE 57th Vehicular Technology Conference (VTC'03-Spring)*, Bd. 1, Jeju, 2003, S. 539–543.

Performance Analysis of a Channel Oriented Concept for Multi-User MIMO Downlinks with Frequency Selective Channels

Wei Qiu, Hendrik Tröger, Michael Meurer and Christoph A. Jötten
Research Group for RF Communications, University of Kaiserslautern,
P.O. Box 3049, D–67653 Kaiserslautern, Germany
e–mail: wqiu@rhrk.uni-kl.de

***Abstract*— Recently, receiver oriented transmission schemes have been proposed for multi-user MIMO (multiple input multiple output) mobile radio downlinks. In such systems the receiver algorithms are a priori chosen and the transmitter algorithms are a posteriori adapted under consideration of channel information and the receiver algorithms. This leads to the advantage of particularly simple receivers. A certain drawback of such schemes consists in a slight transmit energy increase as compared to conventional transmitter oriented systems. In order to overcome this drawback, in this paper a beneficial choice of the receiver algorithms based on space-time eigen-signatures is proposed for the receiver oriented transmission scheme Joint Transmission (JT). In this approach, not only the transmitter, but also the receivers exploit channel information, which leads to a channel oriented multi-user MIMO downlink. The analysis shows that the system performance strongly depends on the cross-correlation coefficients of the space-time eigen-signatures. Consequently, dependencies of these coefficients on the system performance are studied intensively. Analytical and numerical results show that the presented channel oriented multi-user MIMO downlink system performs near optimum with respect to the efficient use of the radiated transmit energy.**

I. Introduction

In the paper mobile radio downlinks are considered in which an access point (AP) supports K mobile terminals (MTs). Both the AP and each MT are equipped with multiple antennas so that each of the K partial downlinks from the AP to one of the K MTs has a MIMO structure, and the total system constitutes a multi-user MIMO downlink. Concerning such links, Joint Transmission (JT) [1] as one of the linear receiver oriented transmission schemes [2] is a promising approach, in which the receiver algorithms at the MTs are *a priori* chosen, whereas the algorithms to be used at the AP have to be *a posteriori* adapted under consideration of channel state information and the receiver algorithms. The favorable *a priori* choice of the receiver algorithms is an interesting task. Recently, an advantageous choice of the receiver algorithms based on space-time eigen-signatures was proposed for multi-user MIMO JT downlinks [2], [3]. In this approach, each MT exploits a part of the channel state information, which leads to a channel oriented multi-user MIMO downlink [3].

Numerical studies of the channel oriented multi-user MIMO JT downlink show that in most channel realizations the system performs near optimum with respect to the efficient use of the radiated transmit energy, but in other cases the system shows a considerable degradation [2]. Up to now, this phenomenon was not fully investigated. As shown in this paper, the system performance strongly depends on the cross-correlation coefficients of the space-time eigen-signatures. Therefore, in a first step the cross-correlation coefficients of the space-time eigen-signatures will be analyzed depending on the relevant system parameters, and in a second step the system performance will be evaluated.

Section II describes the system model of multi-user MIMO downlinks. Then, the beneficial choice of the receiver algorithms originally introduced in [3] is recapitulated in Section III in order to familiarize the reader with the contents of [3] to a degree which is sufficient to follow the reasoning of the paper. In Section IV an energy based criterion to evaluate the system performance is introduced. Then, the cross-correlation coefficients of space-time eigen-signatures are studied in Section V. Simulation results are given in Section VI. Section VII concludes the paper.

II. Receiver Oriented Multi-User MIMO Downlinks

We consider a situation where an AP supports K MTs μ_k, $k = 1 \ldots K$. The AP is equipped with K_B transmit antennas, and each of the K MTs employs K_M receive antennas. It is assumed that N data symbols $\underline{d}_n^{(k)}$, $n = 1 \ldots N$, which are arranged in a column vector $\underline{\boldsymbol{d}}^{(k)}$, have to be transmitted from the AP to each MT μ_k, $k = 1 \ldots K$. The K data vectors $\underline{\boldsymbol{d}}^{(k)}$, $k = 1 \ldots K$, are stacked to the total data vector

$$\underline{\boldsymbol{d}} \quad = \quad \left(\underline{\boldsymbol{d}}^{(1)\,\mathrm{T}} \ldots \underline{\boldsymbol{d}}^{(K)\,\mathrm{T}}\right)^{\mathrm{T}} \tag{1}$$

of dimension KN [2]. By linear modulation based on an $(K_\mathrm{B}S) \times (KN)$ matrix $\underline{\boldsymbol{M}}$ termed modulator matrix, $\underline{\boldsymbol{d}}$ of (1) is mapped on a $(K_\mathrm{B}S) \times 1$ spatially and spectrally spread transmit signal

$$\underline{\boldsymbol{t}} = \left(\underline{\boldsymbol{t}}^{(1)\,\mathrm{T}} \ldots \underline{\boldsymbol{t}}^{(K_\mathrm{B})\,\mathrm{T}}\right)^{\mathrm{T}} = \underline{\boldsymbol{M}}\,\underline{\boldsymbol{d}}, \tag{2}$$

where $\underline{\boldsymbol{t}}^{(k_\mathrm{B})}$ is the $S \times 1$ partial signal transmitted by transmit antenna k_B, $k_\mathrm{B} = 1 \ldots K_\mathrm{B}$ [2].

The frequency selective channel between the transmit antenna k_B of the AP and the receive antenna k_M of MT μ_k is characterized by the channel impulse response

$$\underline{\boldsymbol{h}}^{(k,k_\mathrm{B},k_\mathrm{M})} = \left(\underline{h}_1^{(k,k_\mathrm{B},k_\mathrm{M})} \ldots \underline{h}_W^{(k,k_\mathrm{B},k_\mathrm{M})}\right)^{\mathrm{T}} \tag{3}$$

of dimension W. With this channel impulse response and the dimension S of $\underline{\boldsymbol{t}}^{(k_\mathrm{B})}$ the $(S+W-1) \times S$ channel convolution matrix $\underline{\boldsymbol{H}}^{(k,k_\mathrm{B},k_\mathrm{M})}$ [2] is established. The signal received by antenna k_M of MT μ_k can be expressed as

$$\underline{\boldsymbol{r}}^{(k,k_\mathrm{M})} = \sum_{k_\mathrm{B}=1}^{K_\mathrm{B}} \underline{\boldsymbol{H}}^{(k,k_\mathrm{B},k_\mathrm{M})}\ \underline{\boldsymbol{t}}^{(k_\mathrm{B})}. \tag{4}$$

$\underline{\boldsymbol{r}}^{(k,k_{\rm M})}$ has the dimension $S+W-1$. Stacking the $K_{\rm M}$ signals $\underline{\boldsymbol{r}}^{(k,k_{\rm M})}$, $k_{\rm M}=1\dots K_{\rm M}$, of (4) received by MT μ_k yields the space-time receive signal

$$\begin{aligned}\underline{\boldsymbol{r}}^{(k)} &= \left(\underline{\boldsymbol{r}}^{(k,1)\,\rm T}\dots\underline{\boldsymbol{r}}^{(k,K_{\rm M})\,\rm T}\right)^{\rm T}\\ &= \underline{\boldsymbol{H}}^{(k)}\,\underline{\boldsymbol{t}} = \underline{\boldsymbol{H}}^{(k)}\,\underline{\boldsymbol{M}}\,\underline{\boldsymbol{d}}\end{aligned} \tag{5}$$

of MT μ_k. $\underline{\boldsymbol{r}}^{(k)}$ has the dimension $K_{\rm M}(S+W-1)$. The MT specific channel convolution matrix $\underline{\boldsymbol{H}}^{(k)}$ is a $K_{\rm M}\times K_{\rm B}$ block matrix, in which the block element $(k_{\rm M},\,k_{\rm B})$ is $\underline{\boldsymbol{H}}^{(k,\,k_{\rm B},\,k_{\rm M})}$. The K signals $\underline{\boldsymbol{r}}^{(k)}$, $k=1\dots K$, of (5) can be arranged in a vector

$$\begin{aligned}\underline{\boldsymbol{r}} &= \left(\underline{\boldsymbol{r}}^{(1)\,\rm T}\dots\underline{\boldsymbol{r}}^{(K)\,\rm T}\right)^{\rm T}\\ &= \underbrace{\left(\underline{\boldsymbol{H}}^{(1)\,\rm T}\dots\underline{\boldsymbol{H}}^{(K)\,\rm T}\right)^{\rm T}}_{\underline{\boldsymbol{H}}}\underline{\boldsymbol{t}} = \underline{\boldsymbol{H}}\,\underline{\boldsymbol{M}}\,\underline{\boldsymbol{d}}\end{aligned} \tag{6}$$

of dimension $KK_{\rm M}(S+W-1)$. $\underline{\boldsymbol{r}}$ and $\underline{\boldsymbol{H}}$ of (6) are termed total receive signal and total channel convolution matrix, respectively.

At MT μ_k the receive signal $\underline{\boldsymbol{r}}^{(k)}$ of this MT, see (5), is fed to a demodulator in order to obtain an estimate $\hat{\underline{\boldsymbol{d}}}^{(k)}$ of $\underline{\boldsymbol{d}}^{(k)}$. In the case of linear demodulation considered in this paper the demodulation process performed at MT μ_k can be described by a MT specific demodulator matrix $\underline{\boldsymbol{D}}^{(k)}$ of dimension $N\times[K_{\rm M}(S+W-1)]$ as follows:

$$\hat{\underline{\boldsymbol{d}}}^{(k)} = \underline{\boldsymbol{D}}^{(k)}\,\underline{\boldsymbol{r}}^{(k)}. \tag{7}$$

By properly stacking the K equations (7) we obtain with (1) and (6)

$$\hat{\underline{\boldsymbol{d}}} = \text{blockdiag}\left[\underline{\boldsymbol{D}}^{(1)}\dots\underline{\boldsymbol{D}}^{(K)}\right]\,\underline{\boldsymbol{r}} = \underline{\boldsymbol{D}}\,\underline{\boldsymbol{r}}. \tag{8}$$

$\underline{\boldsymbol{D}}$ of (8) has the dimension $(KN)\times[KK_{\rm M}(S+W-1)]$ and is termed total demodulator matrix. Substituting (6) in (8) yields

$$\hat{\underline{\boldsymbol{d}}} = \underline{\boldsymbol{D}}\,\underline{\boldsymbol{H}}\,\underline{\boldsymbol{M}}\,\underline{\boldsymbol{d}}, \tag{9}$$

which describes the transmission model from the data input at the AP to the data outputs at the MTs.

Up to now the noise free case was considered. If we now assume that $\underline{\boldsymbol{r}}$ of (6) is corrupted by an additive noise signal

$$\underline{\boldsymbol{n}} = \left(\underline{n}_1\dots\underline{n}_{KK_{\rm M}(S+W-1)}\right)^{\rm T} \tag{10}$$

of dimension $KK_{\rm M}(S+W-1)$, then we obtain instead of (9)

$$\hat{\underline{\boldsymbol{d}}} = \underline{\boldsymbol{D}}\left(\underline{\boldsymbol{H}}\,\underline{\boldsymbol{M}}\,\underline{\boldsymbol{d}} + \underline{\boldsymbol{n}}\right). \tag{11}$$

For the receiver oriented transmission scheme, the matrices $\underline{\boldsymbol{D}}^{(k)}$ of (7) are *a priori* determined at the MTs, which results in an *a priori* determined $\underline{\boldsymbol{D}}$ of (8), whereas $\underline{\boldsymbol{M}}$ has to be *a posteriori* adapted at the AP under consideration of $\underline{\boldsymbol{D}}$ and $\underline{\boldsymbol{H}}$. In this paper we focus on the JT technique presented in [2]. We introduce a diagonal matrix $\boldsymbol{E}$ in which the diagonal element $E_{(k-1)N+n}$ is the energy invested at the AP for the transmission of the data symbol $\underline{d}_n^{(k)}$. Then, we obtain the modulator matrix

$$\begin{aligned}\underline{\boldsymbol{M}} &= (\underline{\boldsymbol{D}}\,\underline{\boldsymbol{H}})^{\rm H}\left[(\underline{\boldsymbol{D}}\,\underline{\boldsymbol{H}})(\underline{\boldsymbol{D}}\,\underline{\boldsymbol{H}})^{\rm H}\right]^{-1}\\ &\quad\cdot\left\{\text{diag}\left[(\underline{\boldsymbol{D}}\,\underline{\boldsymbol{H}})\,(\underline{\boldsymbol{D}}\,\underline{\boldsymbol{H}})^{\rm H}\right]^{-1}\right\}^{-\frac{1}{2}}\sqrt{\boldsymbol{E}}.\end{aligned} \tag{12}$$

If $\underline{\boldsymbol{M}}$ is chosen according to (12), ISI (Intersymbol Interference) and MAI (Multiple Access Interference) are totally eliminated at the MTs [1].

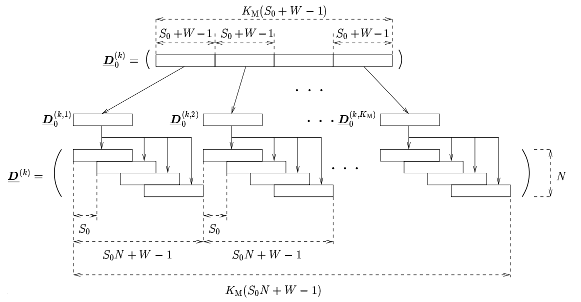

Fig. 1. Constitution of the K MT specific demodulator matrices $\underline{\boldsymbol{D}}^{(k)}$ based on the MT specific space-time eigen-signatures $\underline{\boldsymbol{v}}_0^{(k)}$

III. Beneficial Choice of the Demodulator Matrix – A Way to Channel Oriented Systems

Concerning the receiver oriented transmission system introduced in Section II, the question is how to save transmit energy while guaranteeing a certain SNR at the output of the MTs. In other words, if we invest the energy E for the transmission of one data symbol, then the received energy R_{useful} useful for the estimation of this data symbol should maximize the ratio R_{useful}/E, i.e. we aim at efficient energy transfer. Corresponding to the receiver oriented transmission system introduced in Section II, a suitable choice of $\underline{\boldsymbol{D}}$ might lead to an efficient energy transfer. Unfortunately, an analytical method for determining the optimum $\underline{\boldsymbol{D}}$ is not yet known. An heuristic approach to obtain a suitable $\underline{\boldsymbol{D}}$ originally proposed in [3] can be described as follows:

We first consider a single symbol/single MT downlink, termed reference downlink (RD), in which the AP communicates only with one of the K MTs, e.g. MT μ_k, and only a single data symbol is transmitted. The RD is marked by the index "0". In the RD, we choose the dimension $S_0 = S/N$ for the partial signal $\underline{\boldsymbol{t}}_0^{(k_{\rm B})}$, $k_{\rm B}=1\dots K_{\rm B}$. Therefore, the MT specific channel matrix $\underline{\boldsymbol{H}}_0^{(k)}$ of the RD has the dimension $[K_{\rm M}(S_0+W-1)]\times(K_{\rm M}S_0)$. The heuristic approach to determine $\underline{\boldsymbol{D}}^{(k)}$ is based on the principal eigenvector $\underline{\boldsymbol{v}}_0^{(k)}$ of the matrix $\underline{\boldsymbol{H}}_0^{(k)\,\rm H}\underline{\boldsymbol{H}}_0^{(k)}$, which is termed space-time eigen-signature in the following.

Fig. 1 illustrates the constitution of the MT specific demodulator matrix $\underline{\boldsymbol{D}}^{(k)}$, in which

$$\underline{\boldsymbol{D}}_0^{(k)} = \left(\underline{\boldsymbol{H}}_0^{(k)}\,\underline{\boldsymbol{v}}_0^{(k)}/\|\underline{\boldsymbol{H}}_0^{(k)}\underline{\boldsymbol{v}}_0^{(k)}\|\right)^{\rm H} \tag{13}$$

holds. As already indicated in (8), $\underline{\boldsymbol{D}}$ is a block diagonal matrix with the diagonal blocks $\underline{\boldsymbol{D}}^{(k)}$, $k = 1\ldots K$.

IV. Energy Efficiency

Let us consider the transmission of the data symbol $\underline{d}_n^{(k)}$ from the AP to MT μ_k. For this transmission the AP invests the energy $E_{(k-1)N+n}$, see (12). This transmitted energy leads to the useful received energy $R_{n,\,\mathrm{useful}}^{(k)}$ at MT μ_k. For comparison the same energy $E_{(k-1)N+n}$ could also be radiated by the AP in the form of a transmit signal which would, after having passed the channel from the AP to MT μ_k, produce maximum received energy $R_{\max}^{(k)}$ at MT μ_k. With the largest eigenvalue $\lambda_1^{(k)}$ of the matrix $\underline{\boldsymbol{H}}^{(k)\,\mathrm{H}}\underline{\boldsymbol{H}}^{(k)}$ we obtain [2]

$$R_{\max}^{(k)} = \lambda_1^{(k)} E_{(k-1)N+n}. \tag{14}$$

Now, a quantity suitable to assess the performance of the transmission system related to the data symbol $\underline{d}_n^{(k)}$ is the ratio [2]

$$\eta_n^{(k)} = \frac{R_{n,\,\mathrm{useful}}^{(k)}}{R_{\max}^{(k)}}, \tag{15}$$

which, by the authors, is termed energy efficiency of the transmission system for this data symbol. Let $[\cdot]_i$ and $[\cdot]_{i,\,i}$ designate the column i and the diagonal element i of the matrix in brackets, respectively. Then, concerning the receiver oriented system model of (11) and (12),

$$\begin{aligned}\eta_n^{(k)} &= \frac{1}{\lambda_1^{(k)} E_\nu}\left|\left(\left[\underline{\boldsymbol{D}}^{\mathrm{T}}\right]_\nu\right)^{\mathrm{T}} \underline{\boldsymbol{H}}^{(k)} \left[\underline{\boldsymbol{M}}\right]_\nu\right|^2 \\ &= \frac{1}{\lambda_1^{(k)}}\left[\left(\mathrm{diag}\left[\left(\underline{\boldsymbol{D}}\,\underline{\boldsymbol{H}}(\underline{\boldsymbol{D}}\,\underline{\boldsymbol{H}})^{\mathrm{H}}\right)^{-1}\right]\right)^{-1}\right]_{\nu,\nu}\end{aligned} \tag{16}$$

holds, where

$$\nu = (k-1)N + n \tag{17}$$

Due to the structure of $\underline{\boldsymbol{D}}^{(k)}$ shown in Fig. 1, when S_0 is chosen much larger than W, the ISI between successive transmitted data symbols can be neglected. This will also be shown by simulation results later. Therefore, for the performance analysis we only consider the situation where only a single data symbol is transmitted to each MT, i.e. $S_0 = S$ and $\underline{\boldsymbol{H}}^{(k)} = \underline{\boldsymbol{H}}_0^{(k)}$. Then, the demodulator matrix of MT μ_k has the form

$$\underline{\boldsymbol{D}}^{(k)} = \underline{\boldsymbol{D}}_0^{(k)} = \left(\underline{\boldsymbol{H}}_0^{(k)}\,\underline{\boldsymbol{v}}_0^{(k)}/\|\underline{\boldsymbol{H}}_0^{(k)}\underline{\boldsymbol{v}}_0^{(k)}\|\right)^{\mathrm{H}}. \tag{18}$$

Substituting (18) into (16) and noticing that $\underline{\boldsymbol{v}}_0^{(k)}$ is the principal eigenvector of the matrix $\underline{\boldsymbol{H}}_0^{(k)\,\mathrm{H}}\underline{\boldsymbol{H}}_0^{(k)}$, with the matrix

$$\underline{\boldsymbol{V}} = \left(\underline{\boldsymbol{v}}_0^{(1)}\ldots\underline{\boldsymbol{v}}_0^{(K)}\right), \tag{19}$$

we obtain

$$\eta^{(k)} = \left[\left(\mathrm{diag}\left[\left(\underline{\boldsymbol{V}}^{\mathrm{H}}\underline{\boldsymbol{V}}\right)^{-1}\right]\right)^{-1}\right]_{k,k}. \tag{20}$$

Obviously, the energy efficiency of the transmitted data symbol strongly depends on the cross-correlation coefficients $\underline{\rho}^{(k,k')}$ of the space-time eigen-signatures $\underline{\boldsymbol{v}}_0^{(k)}$ and $\underline{\boldsymbol{v}}_0^{(k')}$. In the case of $K = 2$, it can for instance be shown based on (20) that

$$\eta^{(1)} = \eta^{(2)} = 1 - \left|\underline{\rho}^{(1,2)}\right|^2 \tag{21}$$

holds. It can be observed that high cross-correlation coefficients $\underline{\rho}^{(k,k')}$ lead to a low energy efficiency. In the following the cross-correlation coefficients $\underline{\rho}^{(k,k')}$ will be studied for different MIMO channel models.

V. Cross-Correlation Coefficients of the Space-Time eigen-signatures

A. Line-of-Sight MIMO Channel

At both the AP and each MT a circular array is placed around a reference point (RP). The distance between two adjacent antennas is one half of the carrier wavelength λ. All the MTs are in the far field of the AP. The mobile radio channels between the AP and MT μ_k, $k = 1\ldots K$, are single direction channels in the Line-of-Sight (LOS) direction. Then, the channel impulse response $\underline{\boldsymbol{h}}^{(k,\,k_\mathrm{B},\,k_\mathrm{M})}$ of (3) can be expressed by the channel impulse response

$$\underline{\boldsymbol{h}}_\mathrm{R}^{(k)} = \left(\underline{h}_{\mathrm{R}\,1}^{(k)}\ldots\underline{h}_{\mathrm{R}\,W}^{(k)}\right)^{\mathrm{T}} \tag{22}$$

between the RP of the AP and the RP of MT μ_k multiplied by a steering factor $\underline{a}_{\mathrm{A}\,k_\mathrm{B}}^{(k)}$ [2] of the transmit antenna k_B for MT μ_k and a steering factor $\underline{a}_{\mathrm{M}\,k_\mathrm{M}}^{(k)}$ [2] of the receive antenna k_M at MT μ_k:

$$\underline{\boldsymbol{h}}^{(k,\,k_\mathrm{B},\,k_\mathrm{M})} = \underline{a}_{\mathrm{A}\,k_\mathrm{B}}^{(k)}\underline{a}_{\mathrm{M}\,k_\mathrm{M}}^{(k)}\underline{\boldsymbol{h}}_\mathrm{R}^{(k)}. \tag{23}$$

We denote the Kronecker product [4] with $\otimes$ in the following. Then, with the steering vectors

$$\underline{\boldsymbol{a}}_\mathrm{A}^{(k)} = \left(\underline{a}_{\mathrm{A}\,1}^{(k)}\ldots\underline{a}_{\mathrm{A}\,K_\mathrm{B}}^{(k)}\right)^{\mathrm{T}}, \tag{24}$$

$$\underline{\boldsymbol{a}}_\mathrm{M}^{(k)} = \left(\underline{a}_{\mathrm{M}\,1}^{(k)}\ldots\underline{a}_{\mathrm{M}\,K_\mathrm{M}}^{(k)}\right)^{\mathrm{T}} \tag{25}$$

and the $(S_0 + W - 1)\times S_0$ channel convolution matrix $\underline{\boldsymbol{H}}_\mathrm{R}^{(k)}$ [2] constituted by $\underline{\boldsymbol{h}}_\mathrm{R}^{(k)}$ of (22) the channel convolution matrix

$$\underline{\boldsymbol{H}}_0^{(k)} = \left(\underline{\boldsymbol{a}}_\mathrm{M}^{(k)}\otimes\underline{\boldsymbol{a}}_\mathrm{A}^{(k)\,\mathrm{T}}\right)\otimes\underline{\boldsymbol{H}}_\mathrm{R}^{(k)} \tag{26}$$

of the RD mentioned in Section III is obtained. Consequently [4],

$$\underline{\boldsymbol{H}}_0^{(k)\,\mathrm{H}}\underline{\boldsymbol{H}}_0^{(k)} = K_\mathrm{M}\left(\underline{\boldsymbol{a}}_\mathrm{A}^{(k)\,*}\underline{\boldsymbol{a}}_\mathrm{A}^{(k)\,\mathrm{T}}\right)\otimes\left(\underline{\boldsymbol{H}}_\mathrm{R}^{(k)\,\mathrm{H}}\underline{\boldsymbol{H}}_\mathrm{R}^{(k)}\right) \tag{27}$$

holds. The principal eigenvector $\underline{\boldsymbol{v}}_0^{(k)}$ of $\underline{\boldsymbol{H}}_0^{(k)\,\mathrm{H}}\underline{\boldsymbol{H}}_0^{(k)}$ is the Kronecker product of the principal eigenvector $\frac{1}{\sqrt{K_\mathrm{B}}}\underline{\boldsymbol{a}}_\mathrm{A}^{(k)\,*}$ of $\underline{\boldsymbol{a}}_\mathrm{A}^{(k)\,*}\underline{\boldsymbol{a}}_\mathrm{A}^{(k)\,\mathrm{T}}$ and the principal eigenvector $\underline{\boldsymbol{v}}_\mathrm{R}^{(k)}$ of $\underline{\boldsymbol{H}}_\mathrm{R}^{(k)\,\mathrm{H}}\underline{\boldsymbol{H}}_\mathrm{R}^{(k)}$. Then, the cross-correlation coefficient of the space-time eigen-signatures $\underline{\boldsymbol{v}}_0^{(k)}$ and $\underline{\boldsymbol{v}}_0^{(k')}$ becomes

$$\begin{aligned}\underline{\rho}^{(k,k')} &= \underline{\boldsymbol{v}}_0^{(k)\,\mathrm{H}}\underline{\boldsymbol{v}}_0^{(k')} \\ &= \frac{1}{K_\mathrm{B}}\left(\underline{\boldsymbol{a}}_\mathrm{A}^{(k)\,\mathrm{T}}\underline{\boldsymbol{a}}_\mathrm{A}^{(k')\,*}\right)\underbrace{\left(\underline{\boldsymbol{v}}_\mathrm{R}^{(k)\,\mathrm{H}}\underline{\boldsymbol{v}}_\mathrm{R}^{(k')}\right)}_{\underline{\rho}_\mathrm{R}^{(k,k')}},\end{aligned} \tag{28}$$

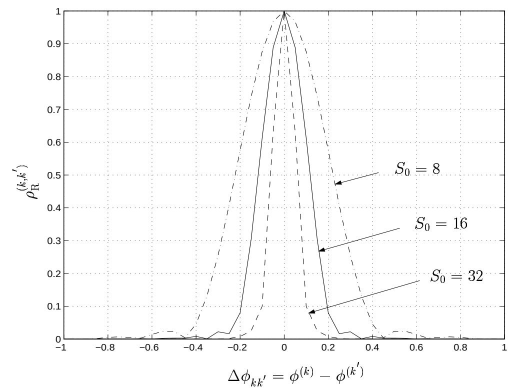

Fig. 2. Magnitude $\rho_{\mathrm{R}}^{(k,k')}$ of the cross-correlation coefficient $\underline{\rho}_{\mathrm{R}}^{(k,k')}$ versus $\Delta\phi_{k,k'} = \phi^{(k)} - \phi^{(k')}$

i.e. $\underline{\rho}^{(k,k')}$ depends on the geometrical properties of the transmit antenna array, the direction-of-departure to MT μ_k and $\mu_{k'}$ and the cross-correlation coefficient $\underline{\rho}_{\mathrm{R}}^{(k,k')}$. In the following, the cross-correlation coefficient $\underline{\rho}_{\mathrm{R}}^{(k,k')}$ of (28) can be studied for the very simple case that $\underline{\boldsymbol{h}}_{\mathrm{R}}^{(k)}$, $k = 1 \ldots K$, has only $W = 2$ elements. Then, the matrices $\underline{\boldsymbol{H}}_{\mathrm{R}}^{(k)\mathrm{H}} \underline{\boldsymbol{H}}_{\mathrm{R}}^{(k)}$, $k = 1 \ldots K$, are tridiagonal Hermitian Toeplitz matrices. With a normalization factor

$$\beta = \sqrt{\frac{2}{S_0 + 1}}, \tag{29}$$

the principal eigenvector of $\underline{\boldsymbol{H}}_{\mathrm{R}}^{(k)\mathrm{H}} \underline{\boldsymbol{H}}_{\mathrm{R}}^{(k)}$ becomes [5]

$$\underline{\boldsymbol{v}}_{\mathrm{R}}^{(k)} = \beta \left(\sin\left(\frac{\pi}{S_0 + 1}\right) \; \ldots \; \sin\left(\frac{S_0 \pi}{S_0 + 1}\right) e^{-\mathrm{j}(S_0 - 1)\phi^{(k)}} \right)^{\mathrm{T}} \tag{30}$$

and only depends on S_0 and the argument $\phi^{(k)} = \arg\{\underline{h}_{\mathrm{R},2}^{(k)*} \underline{h}_{\mathrm{R},1}^{(k)}\}$. Therefore, we obtain the cross-correlation coefficient

$$\underline{\rho}_{\mathrm{R}}^{(k,k')} = \frac{2}{S_0 + 1} \sum_{m=1}^{S_0} \sin^2\left(\frac{m\pi}{S_0 + 1}\right) e^{\mathrm{j}(m-1)(\phi^{(k)} - \phi^{(k')})}, \tag{31}$$

which is a periodic function of $\Delta\phi_{k,k'} = \phi^{(k)} - \phi^{(k')}$ with the period 2π. In the case of randomly time variant channels considered here, $\Delta\phi_{k,k'}$ is a random variable. Fig. 2 shows the magnitude $\rho_{\mathrm{R}}^{(k,k')}$ of the cross-correlation coefficient $\underline{\rho}_{\mathrm{R}}^{(k,k')}$ versus $\Delta\phi_{k,k'}$ in the region $(-\pi, +\pi)$ with S_0 as the parameter. The probability of large $\rho_{\mathrm{R}}^{(k,k')}$ depends on the width of the lobe of the curves in Fig. 2. This figure gives an impression of the probability of highly correlated $\underline{\boldsymbol{v}}_{\mathrm{R}}^{(k)}$ and $\underline{\boldsymbol{v}}_{\mathrm{R}}^{(k')}$. Obviously, $\rho_{\mathrm{R}}^{(k,k')}$ is large only in a small region around $\Delta\phi_{k,k'} = 0$, and this region gets smaller with increasing S_0. In other regions of $\Delta\phi_{k,k'}$ the cross-correlation coefficient is near to zero. Because

$$0 \leq \frac{1}{K_{\mathrm{B}}} \left| \underline{\boldsymbol{a}}_{\mathrm{A}}^{(k)\mathrm{T}} \underline{\boldsymbol{a}}_{\mathrm{A}}^{(k')*} \right| \leq 1 \tag{32}$$

is valid, we obtain with (28)

$$\rho^{(k,k')} \leq \rho_{\mathrm{R}}^{(k,k')}. \tag{33}$$

This means that with multiple transmit antennas the problem of highly correlated space-time eigen-signatures is mitigated. We can also observe from (28) that the fact that multiple receive antennas are employed at the MTs has no influence on the cross-correlation coefficients $\underline{\rho}^{(k,k')}$ of the space-time eigen-signatures.

B. *Semi-Correlated MIMO Channel*

Again, circular arrays are placed at both the AP and the MTs as described in Section V-A, and the MTs are in the far field of the AP. It is assumed that the K_{B} impulse responses of the channels from each of the K_{B} antennas of the AP to a certain MT antenna k_{M} are fully correlated, whereas the impulse responses of the channels to different MT antennas are uncorrelated. Such a situation may for instance occur if the antennas of the AP are relatively closely spaced and the MT antennas are far apart from each other. It is further assumed that all K_{M} antennas of a certain MT are reached under the same direction-of-departure from the AP. We assume the channel impulse response

$$\underline{\boldsymbol{h}}_{\mathrm{R}}^{(k,\,k_{\mathrm{M}})} = \left(\underline{h}_{\mathrm{R}\,1}^{(k,\,k_{\mathrm{M}})} \ldots \underline{h}_{\mathrm{R}\,W}^{(k,\,k_{\mathrm{M}})} \right)^{\mathrm{T}}, k_{\mathrm{M}} = 1 \ldots K_{\mathrm{M}}, \tag{34}$$

between the RP of the AP and receive antenna k_{M} of MT μ_k, $k = 1 \ldots K$. The channel impulse response $\underline{\boldsymbol{h}}^{(k,\,k_{\mathrm{B}},\,k_{\mathrm{M}})}$ of (3) can be simplified to

$$\underline{\boldsymbol{h}}^{(k,\,k_{\mathrm{B}},\,k_{\mathrm{M}})} = \underline{a}_{\mathrm{A}\,k_{\mathrm{B}}}^{(k)} \underline{\boldsymbol{h}}_{\mathrm{R}}^{(k,\,k_{\mathrm{M}})}. \tag{35}$$

$\underline{a}_{\mathrm{A}\,k_{\mathrm{B}}}^{(k)}$ is the steering factor of transmit antenna k_{B} for MT μ_k. With the $(S_0 + W - 1) \times S_0$ channel convolution matrices $\underline{\boldsymbol{H}}_{\mathrm{R}}^{(k,\,k_{\mathrm{M}})}$, $k_{\mathrm{M}} = 1 \ldots K_{\mathrm{M}}$, constituted by $\underline{\boldsymbol{h}}_{\mathrm{R}}^{(k,\,k_{\mathrm{M}})}$ of (34) , the channel convolution matrix $\underline{\boldsymbol{H}}_0^{(k)}$ of the RD can be written as

$$\underline{\boldsymbol{H}}_0^{(k)} = \underline{\boldsymbol{a}}_{\mathrm{A}}^{(k)\mathrm{T}} \otimes \left(\underline{\boldsymbol{H}}_{\mathrm{R}}^{(k,\,1)\mathrm{T}} \ldots \underline{\boldsymbol{H}}_{\mathrm{R}}^{(k,\,K_{\mathrm{M}})\mathrm{T}} \right)^{\mathrm{T}}. \tag{36}$$

Consequently,

$$\underline{\boldsymbol{H}}_0^{(k)\mathrm{H}} \underline{\boldsymbol{H}}_0^{(k)} = \left(\underline{\boldsymbol{a}}_{\mathrm{A}}^{(k)*} \underline{\boldsymbol{a}}_{\mathrm{A}}^{(k)\mathrm{T}} \right) \otimes \sum_{k_{\mathrm{M}}=1}^{K_{\mathrm{M}}} \underline{\boldsymbol{H}}_{\mathrm{R}}^{(k,\,k_{\mathrm{M}})\mathrm{H}} \underline{\boldsymbol{H}}_{\mathrm{R}}^{(k,\,k_{\mathrm{M}})}. \tag{37}$$

The principal eigenvector $\underline{\boldsymbol{v}}_0^{(k)}$ of $\underline{\boldsymbol{H}}_0^{(k)\mathrm{H}} \underline{\boldsymbol{H}}_0^{(k)}$ is the Kronecker product of the principal eigenvector $\frac{1}{\sqrt{K_{\mathrm{B}}}} \underline{\boldsymbol{a}}_{\mathrm{A}}^{(k)*}$ of $\underline{\boldsymbol{a}}_{\mathrm{A}}^{(k)*} \underline{\boldsymbol{a}}_{\mathrm{A}}^{(k)\mathrm{T}}$ and the principal eigenvector $\underline{\boldsymbol{v}}_{\mathrm{R}}^{(k)}$ of $\sum_{k_{\mathrm{M}}=1}^{K_{\mathrm{M}}} \underline{\boldsymbol{H}}_{\mathrm{R}}^{(k,\,k_{\mathrm{M}})\mathrm{H}} \underline{\boldsymbol{H}}_{\mathrm{R}}^{(k,\,k_{\mathrm{M}})}$. Analogously to the discussion in Section V-A, $\sum_{k_{\mathrm{M}}=1}^{K_{\mathrm{M}}} \underline{\boldsymbol{H}}_{\mathrm{R}}^{(k,\,k_{\mathrm{M}})\mathrm{H}} \underline{\boldsymbol{H}}_{\mathrm{R}}^{(k,\,k_{\mathrm{M}})}$, $k = 1 \ldots K$, if we again assume that W is equal to 2, are tridiagonal Hermitian Toeplitz matrices, and the situation of the cross-correlation coefficient is similar to that discussed in Section V-A. In most channel realizations, the space-time eigen-signatures are weakly correlated. Only in a few channel realizations, there exist highly correlated space-time eigen-signatures. The utilization of multiple receive antennas has no influence on the cross-correlation coefficients $\rho^{(k,k')}$ of the space-time eigen-signatures. The application of multiple transmit antennas will decrease the cross-correlation coefficients, and therefore, improve the system performance.

The study of the cross-correlation coefficients $\rho^{(k,k')}$ of the space-time eigen-signatures for the totally uncorrelated MIMO channel, where the channel impulse responses of different pairs of receive and transmit antennas are totally uncorrelated, will be the topic of further research.

VI. Simulation Results

In this section the presented channel oriented multi-user MIMO downlink is evaluated by simulation results for both the LOS MIMO channel and semi-correlated MIMO channel introduced in Section V. For the simulations, circular antenna arrays as described in Section V are considered. $K = 2$ MTs are randomly distributed on a circle around the AP in the far field of the transmit antennas. The channel impulse responses $\underline{\boldsymbol{h}}_{\mathrm{R}}^{(k)}$, $k = 1 \ldots K$, of (22) for the LOS MIMO channel and $\underline{\boldsymbol{h}}_{\mathrm{R}}^{(k,\,k_{\mathrm{M}})}$, $k = 1 \ldots K$, $k_{\mathrm{M}} = 1 \ldots K_{\mathrm{M}}$, of (34) for the semi-correlated MIMO channel are independently generated based on the 3GPP channel case 3 [6]. $N = 1$ or $N = 5$ data symbols per MT are transmitted, and S/N is chosen equal to 16. We study the central data symbol of MT μ_1 for a large number of snapshots. The related channel impulse responses vary from snapshot to snapshot. Figs. 3 and 4 show the cumulative distribution functions of the energy efficiency $\eta_n^{(1)}$ with K_{B} and K_{M} as parameters for the LOS MIMO channel and the semi-correlated MIMO channel, respectively. As analyzed in Section V, in most channel realizations the space-time eigen-signatures are weakly correlated. Therefore, the system performs near optimum, that is $\eta_n^{(1)}$ comes close to one. In other cases the space-time eigen-signatures are highly correlated. Then, a dramatic degradation can be observed, that is $\eta_n^{(1)} \ll 1$, see Figs. 3 and 4. With an increasing number K_{B} of transmit antennas the energy efficiency is improved. The utilization of multiple receive antennas has no influence on the energy efficiency.

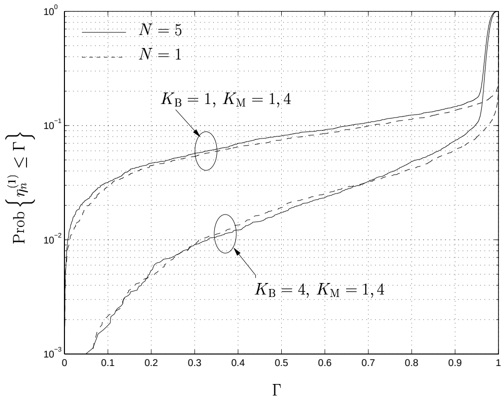

Fig. 3. Cumulative distribution functions of the energy efficiency $\eta_n^{(1)}$ of the central data symbol with K_{B} and K_{M} as parameters for the LOS MIMO channel.

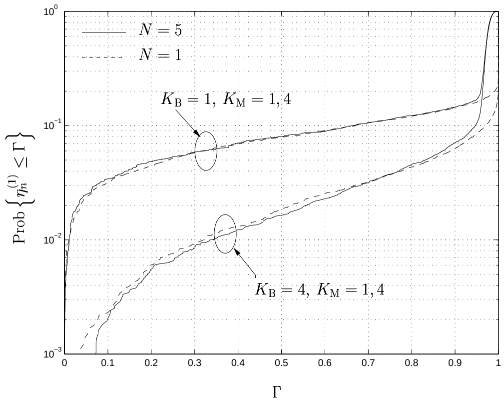

Fig. 4. Cumulative distribution functions of the energy efficiency $\eta_n^{(1)}$ of the central data symbol with K_{B} and K_{M} as parameters for the semi-correlated MIMO channel.

VII. Conclusions

In this paper we present a channel oriented multi-user MIMO downlink. To assess the system performance the criterion energy efficiency is proposed. The theoretical performance analysis shows that the energy efficiency of the presented system strongly depends on the cross-correlation coefficients of space-time eigen-signatures. Therefore, the behavior of these cross-correlation coefficients are studied for different MIMO channels. Simulation results justify the analysis.

Acknowledgment

The authors gratefully appreciate the fruitful exchange of ideas within the Research Group for RF Communications, University of Kaiserslautern, and especially with Prof. P.W. Baier. The support of parts of this work in the framework of the IST-Project FLOWS (Flexible Convergence of Wireless Standards and Services) of the EU, by Siemens AG and by the supercomputer staff of the central computer facility (RHRK) of the University of Kaiserslautern is highly acknowledged.

References

[1] P.W. Baier, M. Meurer, T. Weber, and H. Tröger, “Joint transmission (JT), an alternative rationale for the downlink of time division CDMA using multi-element transmit antennas,” *Proc. IEEE 6th International Symposium on Spread Spectrum Techniques & Applications (ISSSTA 2000),* Parsippany, pp. 1–5, 2000.

[2] P.W. Baier, W. Qiu, H. Tröger, C.A. Jötten, and M. Meurer, “Modelling and optimization of receiver oriented multi-user MIMO downlinks for frequency selective channels,” accepted for publication in *Proc. IEEE 10th International Conference on Telecommunications (ICT’03)*, Papeete, Tahiti, 2003.

[3] H. Tröger, W. Qiu, M. Meurer, and C.A. Jötten, “A channel oriented Joint Transmission scheme for MIMO multi-user downlinks,” *Proc. first COST 273 workshop,* Espoo, 2002.

[4] H. Lütkepohl, *Handbook of Matrices*. England: John Wiley & Sons, 1996.

[5] S. L. Marple, Jr., *Digital Spectral Analysis*. Englewood Cliffs: Prentice Hall, 1987.

[6] “3rd generation partnership project (3GPP); technical specification group radio access network, UTRA (BS) TDD, radio transmission and reception,” 3GPP, Technical Specification TS 25.105 Version 3.5.0, 2000.

7.2 Opportunistische Übertragung

In Mobilfunksystemen sind die Mobilfunkkanäle der K zu einer Referenzzelle gehörigen Mobilstationen typischerweise zeitvariant und variieren in guter Näherung unabhängig voneinander. Besteht die Möglichkeit der freien zeitlichen Organisation der Informationsübertragung der Basisstation an diese K Mobilstationen — und dies ist beispielsweise der Fall, wenn keine Dienste mit strikten Forderungen hinsichtlich der einzuhaltenden Übertragungsverzögerungen angeboten werden sollen —, so können weitere Erhöhungen der Leistungsfähigkeit der empfängerorientierten Funkkommunikation auf Basis des geschickten Ausnutzens dieser zeitlichen Veränderungen erzielt werden. Es ist nämlich möglich, eine Mobilstation k, $k = 1 \ldots K$, in einem gewissen Zeitintervall nur dann (gemäß Empfängerorientierung) zu versorgen, wenn der zwischen den Sendeantennen der Basisstation und den Empfangsantennen dieser Mobilstation k wirksame Mobilfunkkanal in diesem Zeitintervall eine gewisse Mindestqualität aufweist. Wird hingegen diese Mindestqualität für eine Mobilstation k, $k = 1 \ldots K$, im betrachteten Zeitintervall nicht erreicht, so wird diese Mobilstation k für diese Zeit von der Funkkommunikation ausgeschlossen. Sind die Mobilfunkkanäle der K zur Referenzzelle gehörigen Mobilstationen zeitvariant, so wechselt die Menge der Mobilstationen, deren Mobilfunkkanäle der genannten Mindestqualität genügen, mit der Zeit, so daß prinzipiell jede Mobilstation k, $k = 1 \ldots K$, der Referenzzelle früher oder später mit den für sie bestimmten Daten versorgt werden kann. Die beschriebene zeitliche Organisation der Funkübertragung wird als opportunistisches Übertragen (engl. opportunistic transmission) bezeichnet. Da in jedem der genannten Zeitintervalle prinzipiell ausschließlich solche Mobilstationen versorgt werden, deren Mobilfunkkanäle die geforderte Mindestqualität aufweisen oder überschreiten, ist opportunistische Übertragung sehr leistungseffizient.

Das Konzept der opportunistischen Übertragung betrifft ausschließlich die zeitliche Organisation der Übertragungen zwischen der Basisstation und den K Mobilstationen der Referenzzelle, wohingegen Empfängerorientierung die Organisation der gegebenenfalls gleichzeitigen Übertragung mehrerer Daten betrifft. Beide Konzepte sind daher hervorragend miteinander vereinbar und kombinierbar.

Die folgende Veröffentlichung [BM02] erläutert das Konzept der opportunistischen Übertragung im Detail.

[BM02] Baier, P. W.; Meurer, M.: "Air interface enhancements for 3G and beyond-3G mobile radio communications". *Proc. 9th International Conference on Telecommunications (ICT'02)*, Peking, 2002, S. 284–291.

Air interface enhancements for 3G and beyond-3G mobile radio communications

Paul Walter Baier and Michael Meurer
Research Group for RF Communications, University of Kaiserslautern
P.O. Box 3049, D–67653 Kaiserslautern, Germany
phone/fax:49 631 205 2075/3612, e–mail: baier@rhrk.uni-kl.de

Abstract— **In mobile radio communications, for a given system bandwidth the number of supported mobile terminals and the offered data rates per mobile terminal should be maximized. The enhancement of the air interfaces plays an important role when pursuing this goal. In the paper various possibilities of air interface enhancements suited for 3G and beyond-3G mobile radio systems are discussed. The considered approaches include advanced detection techniques, adaptive antennas, the rationale of opportunistic transmission, receiver and channel oriented transmission, and novel air interface architectures.**

I. Introduction

SINCE the early 1990s second generation (2G) mobile radio services have experienced an astounding extension and increase of acceptance in most parts of the world. In the meantime, third generation (3G) mobile radio systems are on the verge of becoming operational, and beyond-3G mobile radio systems are about captivating the interest of manufacturers, operators and standardization bodies [1]. For economical reasons it is a must in mobile radio communications that within the allotted frequency spectrum an amount of communication as high as possible is enabled, that is the number of supportable mobile terminals (MT) and the offered data rates per MT should be maximized under consideration of the required quality of service (QoS). In order to achieve this goal of high capacity, on the one side the resources of the physical layer constituted by the frequency bands and the transmit powers should be utilized as efficiently as possible based on a careful design of the air interface. On the other side organizational measures should be taken in order to make the best of the potentials offered by the air interface. This is the task of the higher system layers. A careful air interface design is important, because deficiencies introduced on the physical layer can hardly be compensated by measures on the higher layers. Therefore, without any doubt about the vital importance of the higher layers, the air interface deserves special attention, and continuous enhancements of the physical layer are highly rewarding both with respect to the presently operating 2G and the emerging 3G and beyond-3G mobile radio systems.

As the basic prerequisite of the observed rapid development of mobile radio communications, electromagnetic waves turned out to be an excellent carrier for information transmission as demonstrated for the first time as early as 1895 by Marconi. However, unfortunately, wireless electromagnetic communication suffers from an inherent disadvantage: It is usually unavoidable that signals of different connections intermingle with each other in a more or less harmful manner. Also mobile radio systems are affected by such signal corruptions, because in such systems a multitude of users simultaneously access the one and the same medium given by the propagation environment. In mobile radio communications these mutual disturbances are termed multiple access interference (MAI) and can be classified as follows:

- Interoperator interference (between links of different operators; caused by out-of-band radiation; can be controlled by sufficiently wide guard bands between operator spectra and appropriate transmit and receive filters).
- Intraoperator interference (between links of one and the same operator).
- Intercell interference (between links active in different cells of an operator; subclass of intraoperator interference; can be controlled by a sufficiently scarce frequency reuse, that is a sufficiently large cluster size of the cellular pattern; not present in the case of isolated cells).
- Intracell interference (between links active in one and the same cell of an operator; subclass of intraoperator interference; can be a priori avoided by applying the multiple access (MA) schemes FDMA or TDMA offering perfect signal separation; unavoidable when applying the MA scheme CDMA allowing only imperfect signal separation).

Coming back to the just mentioned signal separation, the MA schemes FDMA and TDMA can be considered perfect in the sense that the genuine orthogonality of FDMA and TDMA signals is not impaired by the frequency selectivity of the mobile radio channels. In contrast to that, even though orthogonal CDMA codes may be chosen at the transmitters, the received CDMA signals tend to be de-orthogonalized by the channels, which entails imperfect signal separation at the receivers. Despite of this disadvantage of the MA scheme CDMA it will play an important role in 3G and beyond-3G mobile radio systems due to its inherent frequency diversity and flexibility [2]. Bearing this in mind, in this paper special attention is paid to system concepts including CDMA. As a rule, in practice MA schemes will be employed which are constituted by advantageous combinations of FDMA, TDMA and CDMA [2], and which are termed hybrid MA schemes.

In addition to MAI, also different portions of the same signal may, after having passed through mobile radio channels with their frequency selectivity or, equivalently, multipath behaviour, disadvantageously interact. Such disturbances are known as intersymbol interference (ISI).

The QoS degrades with increasing MAI. If the desired QoS cannot be reached, then a straightforward measure would be to reduce MAI by cutting down the number of supported MTs, which means a capacity decrease. Alternatively, the impact of the incoming MAI could be mitigated, which would allow to keep the number of supported MTs. Considering the enhancement of mobile radio air interfaces with a view to high capacity, the reduction of the impact of MAI should be the dominant aspect. Therefore, in the paper various possibilities to mitigate or combat interference are discussed and evaluated, where the following areas will be identified as the most promising ones:

- Advanced detection techniques,
- Adaptive antennas,
- Opportunistic transmission,
- Receiver and channel oriented transmission,
- Novel air interface architectures.

As another field of air interface enhancements also briefly addressed in the paper, the required transmit powers should be kept as low as possible. This is important with respect to a high battery lifetime at the MTs and a low electromagnetic immission into the environment. The latter aspect is encountering an increasing attention by a critical public.

II. Advanced detection techniques

At the receivers of both the access points (AP) and the MTs of a mobile radio system a multitude of signals arrive simultaneously. Let us consider a receiver in a specific cell termed reference cell. Part of the signals impinging at this receiver originate in the reference cell and carry data transmitted for this receiver. These signals are termed signals of interest (SI) of the considered receiver in what follows. All other signals arriving at this receiver are termed signals of no interest (SnI). The SnIs can be classified depending on their origin

- in another mobile radio system (interoperator SnIs),
- in the considered mobile radio system (intraoperator SnIs),
- in cells other than the reference cell of the considered mobile radio system (intercell SnIs; subclass of intraoperator SnIs),
- in the reference cell (intracell SnIs; subclass of intraoperator SnIs).

For each individual SI at the considered receiver all other SIs and the received SnIs act as MAI. However, part of these interfering signals do not disturb and, therefore, are called irrelevant MAI signals. Such irrelevant MAI signals are SIs and intracell SnIs discernible from the considered SI by the perfectly separating MA schemes FDMA or TDMA. Disturbing MAI signals, that is relevant interfering signals, are SIs separated from the considered SI by the imperfectly separating MA scheme CDMA, co-channel intercell SnIs as well as interoperator SnIs being insufficiently separated by guard bands and filtering.

An important prerequisite for data detection is a sufficiently accurate knowledge of the impulse responses of the channels over which the considered signals have traveled. This knowledge has to be gained either on the basis of transmitted training signals a priori agreed upon by the transmitters and receivers [3], or by relying just on the data carrying transmit signals [4], an approach termed blind channel estimation. Channel estimation based on training signals can better cope with rapidly fluctuating channel properties than blind channel estimation, but consumes part of the transmission capacity for accommodating the training signals. Blind channel estimation requires rather long observation times during which the channel properties should not change, but works without sacrificing transmission capacity. In system design, a trade-off between the pros and cons of both methods has to be made, which, to the authors' impression, usually ends in favor of training signal based channel estimation. Despite its importance, channel estimation will be only cursorily touched in the paper.

The receiver has the task to detect the SIs in order to obtain the data carried by these signals with sufficiently good quality. This task is impaired by MAI, as already mentioned in Section I. As the simplest and straightforward approach to detecting a SI, no a priori knowledge whatsoever about the relevant MAI signals is taken into account, that is all these signals are virtually treated as noise. More advanced detection schemes utilize a priori information about at least some of the relevant MAI signals, which is in principle available for the signals originating in the own system. An important class of such schemes concern mobile radio systems employing the MA scheme CDMA and have the aim to combat the problem of imperfect signal separation typical of CDMA [5], [6]. Such schemes are also known as multi-user detection (MUD) schemes, where the most important a priori information to be utilized is, besides the knowledge of the channel impulse responses, the knowledge about the CDMA codes. As the crux of such schemes, at least some of the impinging CDMA signals, which may be intracell SIs or intracell SnIs, are subject to a common detection process which will be called Joint Detection (JD) in what follows. The CDMA signals included in JD no longer interfere with each other, that is their mutual interference is eliminated. Optimum JD schemes [6] have to take into account not only the knowledge of the CDMA codes of the jointly processed signals, but also other information as for instance the knowledge of the discrete valued data symbol alphabet and the applied FEC coding algorithms [7]. Unfortunately, such optimum JD schemes are prohibitively complex, because they work on a nonlinear basis. A rather low cost alternative would be linear JD schemes [5], by which continuous valued estimates of the discrete valued data are generated. However, as compared to the optimum nonlinear JD schemes, such linear schemes suffer from a significant performance degradation which manifests itself in an enhancement of the disturbing

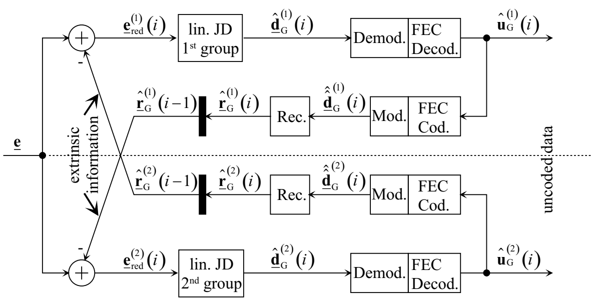

Fig. 1. Multi-Step JD (MSJD) [8]; i: iteration index; superscript: group number

effect of the relevant MAI signals excluded from JD and of the thermal noise. Basically, this degradation also called SNR degradation for reasons explained for instance in [5] growths with the number of CDMA signals included in linear JD. Therefore, increasing this number on the one side beneficially diminishes MAI by reducing the number of relevant interfering signals, but, on the other side, magnifies the impact of the residual relevant MAI plus thermal noise so that a compromise has to be found.

Presently an interesting research topic concerning air interface enhancement is the design of JD schemes, which take, with respect to complexity and performance, a favourable position between the expensive optimum and the low cost, but poorly performing linear JD schemes. An example of a promising scheme of this kind includes FEC decoding and is based on the iterative (turbo) principle, see Fig. 1. In [8] this scheme termed Multi-Step JD (MSJD) is described in detail. In the following paragraph it will be briefly explained. In the concept of Fig. 1, instead of one linear JD processor for all CDMA signals contained in the received signal $\underline{\mathbf{e}}$ and to be jointly processed, now two linear JD processors for a first and a second group each of them consisting of only one half of the received CDMA signals are implemented. After a first round of linear JD, demodulation and FEC decoding, the contributions of the first and second group to the received signal are reconstructed under consideration of the applied FEC coding and modulation schemes as well as the channel impulse responses, and the reconstructions are then mutually subtracted from the input signals of the two linear JD processors as shown in Fig. 1. In this way these linear JD processors are provided with input signals with a reduced MAI by the received CDMA signals of the other group contained in $\underline{\mathbf{e}}$. Therefore, in a second round of JD, demodulation and FEC decoding, improved data estimates can be obtained. The inclusion of FEC coding/decoding in this scheme has the effect of introducing additive a priori knowledge into the JD process. The described cycle can be gone through several times, and with each iteration the data estimates are further improved. The subtraction of the reconstructions can be regarded, in the sense of the iterative (turbo) principle, as an introduction of extrinsic information. It could be shown [8] that the described concept is superior to conventional linear JD both with respect to performance and complexity and comes quite close to the optimum JD.

Up to now the reduction of intracell MAI by advanced detection schemes was addressed in this section as a means to enhance the air interface. Concerning intercell MAI it can be often observed that, due to shadowing, most of the intercell MAI power traces back to only a few intercell SnIs, even though the number of potential intercell SnIs may be quite high [9]. For instance, in an exemplary cellular network with cluster size three and a number of eight simultaneously active CDMA signals per cell, on the average as much as 40% of the total intercell MAI power are caused by only four intercell SnIs [9]. Because the number of relevant intercell SnIs is so small, an obvious idea would be to include these few strong MAI signals into the JD process performed in the reference cell and thus eliminate a large portion of the intercell MAI. Such an approach requires the solution of two tasks at the receivers in the reference cell, namely, first, the identification of the strongest intercell SnIs, and, second, to consider these when performing JD. In [10] intercell MAI mitigation techniques based on this idea are investigated in detail. Fig. 2 shows the structure of a receiver following this rationale. This receiver consists of the blocks

- identification of the most relevant intercell SnIs,
- channel estimation, which delivers estimates of the impulse responses of the channels over which the intracell and intercell signals to be considered in the JD process of the reference cell have travelled,
- JD, which yields estimates of the data carried by the SIs under consideration of the strongest intercell SnIs.

In [10] quantitative results for the concept of Fig. 2 applied to a specific CDMA system are presented. These results show that this approach allows rather promising capacity

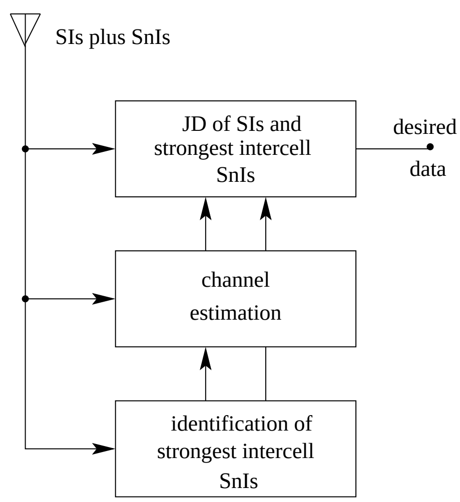

Fig. 2. Intercell MAI mitigation [10]

enhancements especially in the case of small cluster sizes, where intercell MAI has a greater impact than in the case of larger cluster sizes.

III. Adaptive antennas

Usually the radio channels encountered in mobile radio systems are more or less directional. This means that at each transmitter and receiver of a radio link in such a system only certain directions of departure (DODs) or directions of arrival (DOAs), respectively, are relevant for signal transport. In many cases the line of sight between transmitter and receiver is obstructed, and more than one DOD or DOA, respectively, or even a continuum of such directions contribute to each link. It is a well accepted fact that these directional properties of the mobile radio channels hold a high potential for enhancing the air interface performance [11]. As a first step to utilize this potential, sectorized antennas at the APs were introduced, which is nowadays a widely used technique in 2G mobile radio systems. However, more sophisticated and efficient approaches to exploit the directional properties of the mobile radio channels are likely to become important in the future. The key to such an exploitation is the use of adaptive antennas for both transmission and reception, where the attribute adaptive means that the antennas beneficially adjust themselves to time varying conditions like the channel properties and the MAI situation. An adaptive antenna consists of an array of non- or low-directional antenna elements plus an antenna signal processor. This processor has the task, in the case of the transmitter, to generate the feeding signals for the antenna elements or, in the case of the receiver, to evaluate the output signals of the antenna elements. The crux of applying such adaptive antennas consists

- at the transmitter in concentrating the radiated power to those receivers where it is desired and thereby simultaneously producing low powers of the SnIs impinging at other receivers, and
- at the receiver in enhancing the received SIs and in reducing the impact of the received SnIs.

Therefore, we can subsume that in both cases the powers of the SIs are enhanced and the powers of the SnIs are reduced.

In the case of adaptive receive antennas the processing of the output signals of the antenna elements may be integrated with the detection algorithms, which results in joint spatial-temporal signal processing [12]. Such approaches have the advantage that antenna signal processing and data detection can be jointly optimized. For detailed considerations of this topic see for instance in [13] and [14]. An example related to the application of a number of K_{B} receive antenna elements in a mobile radio system utilizing the MA scheme CDMA is given in Fig. 3 [15]. As a special feature of this concept, the spatial and temporal properties of the intercell SnIs contained in the total received signal $\underline{\mathbf{e}}$ and represented by $\underline{\mathbf{n}}$ are taken into account in the form of the spatial-temporal covariance matrix $\underline{\mathbf{R}}_{\mathrm{n}}$ of $\underline{\mathbf{n}}$. By this feature the system performance can be significantly enhanced in situations where $\underline{\mathbf{n}}$ mainly impinges from a few DOAs. For a detailed description of the concept of Fig. 3 the reader is referred to [15]. Here we describe this concept only briefly by addressing its major functional steps as follows:

- After channel estimation, JD of the SIs is performed under the assumption that the covariance matrix $\underline{\mathbf{R}}_{\mathrm{n}}$ is not yet known and is substituted by a unit matrix. This first step yields first estimates of the coded and uncoded data carried by the SIs.
- Approximate reconstruction of the received SIs based on the data estimates obtained in the first step.
- Subtraction of the reconstructed SIs gained in the second step from the total received signal $\underline{\mathbf{e}}$ in order to obtain an estimate of the received SnIs.
- Determination of an estimate of the covariance matrix $\underline{\mathbf{R}}_{\mathrm{n}}$ by evaluating the estimated SnIs.
- Once more performing channel estimation and JD, however, this time under consideration of the estimated covariance matrix $\underline{\mathbf{R}}_{\mathrm{n}}$. This second round of processing the total received signal $\underline{\mathbf{e}}$ leads to improved data estimates, which could be demonstrated by system simulations [15].

Approaches of joint spatial-temporal signal processing being, as shown above, feasible in the case of adaptive receive antennas, are not possible in the case of adaptive transmit antennas. Rather, spatial processing has to be performed at the transmitters, while temporal processing has to take place at the receivers. This leads to transmission models of the type shown in Fig. 4 for the example of a CDMA downlink, where an array of K_{B} antenna elements (AE) is

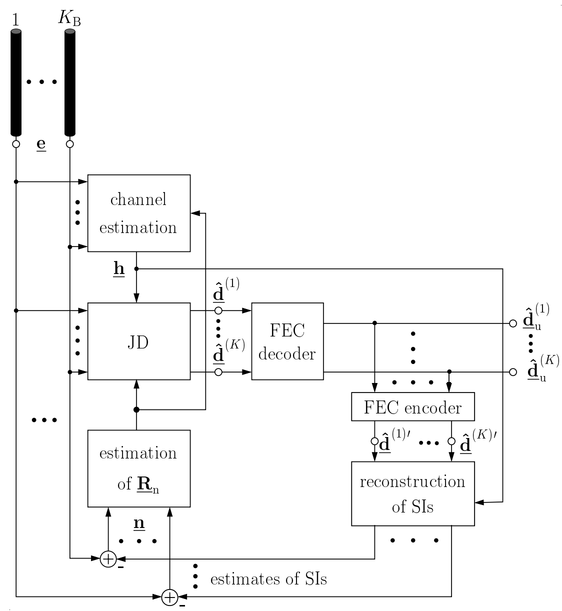

Fig. 3. Receiver concept incorporating joint spatial-temporal signal processing and exploitation of the SnI covariance matrix $\underline{\mathbf{R}}_{\mathrm{n}}$ [15]

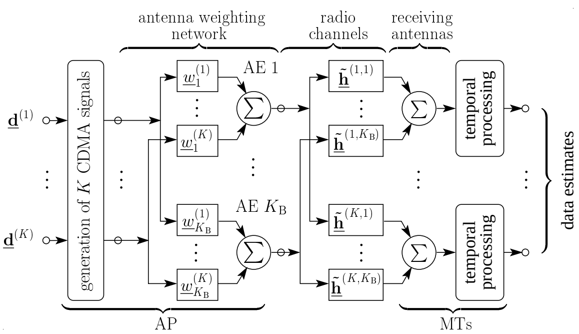

Fig. 4. Downlink transmission model with K_B antenna elements at the AP and K MTs

provided at the transmitter of the AP and single element antennas are used at the receivers of the K MTs. The spatial processing performed at the AP transmitter consists of nothing else but feeding weighted versions of the K different CDMA signals to the K_B antenna elements. The signals radiated by the antenna elements are then transmitted to each MT via K_B radio channels. At each MT the sum of K_B signals originating in the K transmitted CDMA signals appears at the output of the receive antenna. This signal is then processed in the time domain at the MT.

An important question when implementing schemes of the type shown in Fig. 4 is how the antenna weights should be chosen. There exist many options for this choice. One promising approach is based on the powers of the K radiated CDMA signals and of the SIs received at the MTs [16]. In this approach the antenna weights are chosen such that the power ratios of the SIs and the corresponding radiated signals are maximized for each receiver. In [16] it is shown that this approach can be implemented based on the knowledge of the channel impulse responses. As the key point of this approach, under consideration of the channel properties the transmit antenna array is utilized to minimize the radiated powers required to generate certain desired powers at the MT receivers. This reduces the MAI generated per served link and, thus, ultimately allows to increase the total system load in MAI limited systems, that is in systems where MAI significantly exceeds thermal noise and is, therefore, the dominant disturbance. As mentioned in Section II, linear JD has the potential to totally eliminate the mutual interference of the signals included into the JD process. However, the impact of the residual MAI signals is magnified. In the case of adaptive transmit antennas it can be achieved that the powers of the relevant intracell SnIs arriving at the receivers are kept small [16]. Therefore, by excluding these signals from JD, the SNR degradation explained in Section II significantly decreases, whereas the increase of interference power is only marginal. In [16] it is shown that this effect becomes remarkable for larger numbers of transmit antenna elements, and the implementation of a corresponding receiver concept is proposed.

As already mentioned above, the implementation of transmitter schemes of the type shown in Fig. 4 requires the knowledge of the channel impulse responses at the transmitter. Generally, this knowledge is not readily available. In the case of the duplexing scheme TDD (Time Division Duplex) the channel information obtained during reception, due to the reciprocity theorem, can be used as approximate channel information for adjusting the antenna weights for transmission as long as the successive transmit and receive intervals are sufficiently short as compared to the correlation time of the radio channels. However, in the case of applying the duplexing scheme FDD (Frequency Division Duplex), due to the frequency gap between the two transmission directions, only overall features of the channels like DODs can be extracted from reception with a view to be applied for transmission. This problem typical of FDD can be solved, by signaling the channel information obtained at the receivers to the transmitters [17]. This signaling should be performed without consuming much transmission capacity, a requirement which can be fulfilled by approaches as proposed in [17].

When considering adaptive transmit antennas in the foregoing paragraph, it was presumed that the receivers are equipped with single element antennas. In this respect each link between a transmitter and a receiver is of the type multiple-input-single-output (MISO). Since some years transmission links utilizing both at the transmitters and the receivers multi-element antennas are being investigated [18]. Such multiple-input-multiple-output (MIMO) structures allow, as compared to MISO structures, a further reduction of the impact of MAI. Up to now mainly single MIMO links have been intensively studied. With respect to mobile radio communications, in the future the application of MIMO structures in multi-link scenarios should be investigated. First steps in this direction are described for instance in [19].

As already mentioned above, usually mobile radio systems are designed to operate in the MAI limited mode, that is thermal noise plays an inferior role. In order to be in this mode the transmit powers have to be chosen so large that the receive powers are well above the thermal noise threshold. Now, for a given receive power the required transmit power can be reduced by using adaptive instead of single element antennas at the transmitters and/or the receivers. Therefore, such antennas also enhance the air interfaces with respect to the demand that the transmit powers should be kept as small as possible.

In addition to MAI considered up to now, another kind of interference is ISI as mentioned in Section I. Interestingly, also the impact of ISI can be mitigated by the use of adaptive antennas at the receiver. As shown in [20], such antennas have the potential to separate portions of the desired signals which have traveled over paths of different delays from the transmitter to the receiver, if these portions differ in their DOAs at the receiver. After having performed this separation, said signal components can be combined in such a way that their delay differences are compensated [20] and the impact of ISI is mitigated.

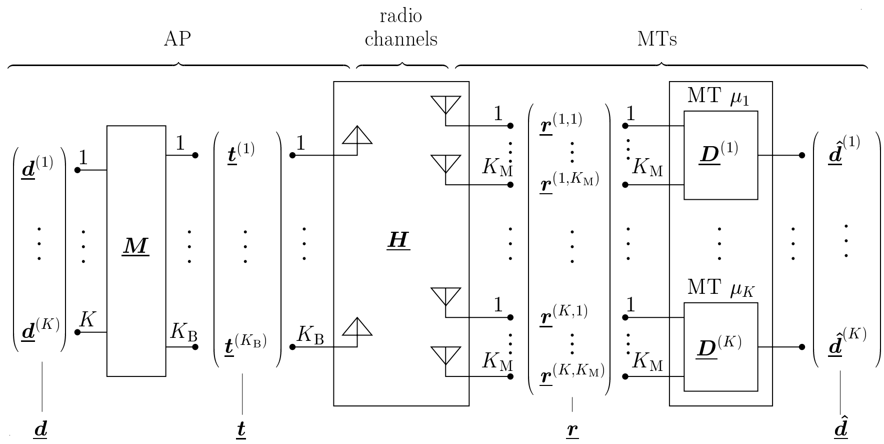

Fig. 5. Channel oriented multi-link MIMO air interface [21]

IV. Opportunistic transmission

Let us consider a certain transmission link in a mobile radio system. Due to the mobility of the MTs and the changing composition of the active user ensemble the quality of this link is time variant with respect to the MAI situation observed at the receiver and the propagation conditions of the radio channel, which are for instance given by its momentary transfer function. Roughly speaking, the link quality may vary between good and bad at a rate corresponding to the correlation time of the radio channel. The link is expected to transport, within its bandwidth B, a certain data rate R with a required QoS. Conventionally, one tries to maintain this QoS despite of the fluctuating link quality by adjusting the transmit power depending on that quality, that is the power is chosen high at times when the link quality is bad and vice versa. When following this rationale, the average transmit power tends to become rather high, because even at times when the link quality is bad the required data rate R and QoS are enforced by transmitting with high power. This leads to a rather high average transmit power, which, in its turn, aggravates MAI with the consequence of a decreasing air interface capacity.

A totally different rationale consists in adapting the load and mode of utilization of the link to the actual link quality, that is to take the opportunity to transmit with high data rates at those frequencies within the link bandwidth B and at those times, for which the link quality is good and vice versa with a view to maintain the desired QoS and to achieve a maximum average data rate R. Transmission with an average data rate R means that over a time period T an amount RT of information will be transported by the link within the link bandwidth B. With the average transmit power P, the transmit energy available for this transmission is PT. The product TB and the energy PT can be considered as the transmission resource of the link. In the time-frequency plane the product TB can be represented by a rectangle of width T and height B. Now, this rectangle can be divided up into bins of width ΔT and height ΔB. Let us assume that different bins are characterized by different link qualities. Now, following an opportunistic transmission rationale means that

- in the bins of higher link quality a larger portion ΔE of the transmit energy PT is invested than in the bins of lower link quality in such a way that the transmission capacities of the individual bins given by ΔT, ΔB and the bin specific ΔE add up to a maximum total capacity of the resource, and that
- the FEC coding and modulation schemes are chosen in such a way that the capacity of each bin is exploited to the largest possible extent, which means that also the average data rate R is maximized.

Opportunistic data transmission is prone to produce larger latency times than conventional transmission. Therefore, this type of transmission would be better suited for packetized data transmission than for telephony. The application of opportunistic data transmission requires the availability of link quality information at the transmitter. This information could for instance be obtained by a signaling channel from the receiver to the transmitter, an approach similar to that applied when performing closed loop power control. As a final remark, the assignment of partial transmit powers to different frequency bands by the waterfilling method [22] in order to maximize the total transmission capacity can be regarded as an early example of opportunistic transmission.

V. Receiver and channel oriented transmission

Conventional radio transmission systems can be characterized as follows:

- The algorithms employed at the transmitters as for instance FEC coding, modulation and antenna beam forming are a priori determined.
- The algorithms utilized at the receivers for processing the received signals are a posteriori chosen in such a way that, under consideration of the algorithms applied at the transmitters, of the properties of the radio channels and of the received disturbing signals, the quality of the

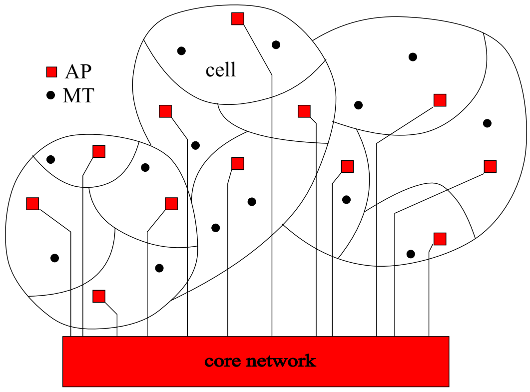

Fig. 6. Conventional cellular mobile radio air interface

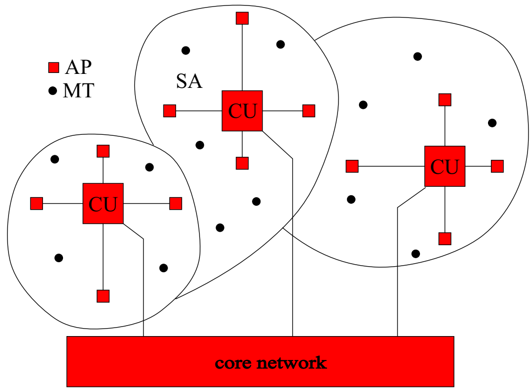

Fig. 7. Service area (SA) based air interface

detected data is optimized. Such an optimization could mean for instance in the case of a CDMA mobile radio system that intracell MAI and ISI are eliminated.

The described rationale of conventional transmission systems can be considered to be transmitter oriented, because the transmitter algorithms predestine the receiver algorithms. This rationale offers the advantage that the transmitters can be designed with a view to make them inexpensive. However, when generating the transmit signals according to this rationale, the channel properties are not taken into account. This may have the consequence that the transmitted signals may not be especially well suited to pass over the radio channels. For instance, these signals may have spectral minima at frequencies where the channel transfer functions have maxima and vice versa. Such a situation of mismatch between transmit signals and radio channels would demand rather large transmit powers in order to obtain the required receive powers, which is undesirable with respect to the requirement of generating low MAI. Therefore, it would be desirable to find more favorable alternatives to such transmitter oriented systems. Such alternatives could be receiver oriented systems on the one side and channel oriented systems on the other side.

In the case of receiver oriented systems

- the algorithms employed at the receivers for signal detection are a priori determined, and
- the algorithms utilized at the transmitters for signal generation are – under consideration of the channel properties – a posteriori chosen in such a way that a quality as good as possible of the data detected at the receiver is achieved.

Such receiver oriented systems offer the advantages that one can choose a priori receivers of low complexity, and that the channel properties can be taken into account when a posteriori determining the transmit signals. In this way an eventual mismatch between the transmit signals and the radio channels can be mitigated. An examples of a receiver oriented transmission scheme is the air interface concept Joint Transmission (JT) as described in [23]. JT is designed for the downlink of CDMA mobile radio systems. It allows very low cost receivers at the MTs at which, nevertheless, MAI and ISI are totally eliminated. As a disadvantage of receiver oriented systems, there may occur a mismatch between the radio channels and the a priori determined receiver algorithms. Such a mismatch would again require undesirably high transmit powers.

In the case of channel oriented systems both the algorithms utilized at the transmitters and at the receivers are a posteriori determined in such a way that the properties of the radio channels are taken into consideration with the goal to achieve a good transmission quality with the lowest possible transmit powers. As one idea to design such systems, the eigenfunctions of the radio channels are taken into consideration when determining the algorithms to be applied at the transmitters and the receivers. Fig. 5 shows the application of this idea to the downlink of a mobile radio system in which an AP supports K MTs. The AP is equipped with an array of K_{B} antenna elements, and each of the K MTs has an array of K_{M} antenna elements. Consequently, each link from the AP to a MT has a MIMO structure. The properties of the mobile radio channels are represented by the matrix $\underline{\mathbf{H}}$, the modulation to be performed at the AP by the matrix $\underline{\mathbf{M}}$ and the detection to be performed at each of the K MTs by the matrices $\underline{\mathbf{D}}^{(k)}$, $k = 1 \ldots K$. In [21] it is shown that the matrices $\underline{\mathbf{M}}$ and $\underline{\mathbf{D}}^{(k)}$, $k = 1 \ldots K$, can be derived from $\underline{\mathbf{H}}$ in such a way that intracell MAI and ISI are avoided at the receivers, and that the transmit power is minimized.

VI. Novel air interface architectures

As mentioned in Section I, it is a vital issue in mobile radio communications to maximize the amount of communication which can be supported within the given system bandwidth. A straightforward way to meet this demand would consist in diminishing the cell sizes and installing more APs. However, this approach is problematic, because the deployment of APs is critically observed by the public and the costs of AP installation cannot be neglected when it comes to the profitability of the system. As alternatives, non-conventional approaches to enhance the air interface capacity mainly by reducing the required transmit powers and, thereby, MAI should be taken into account. Examples of such approaches are multi-hop networks, ad-hoc networks and service area (SA) concepts.

In cellular mobile radio networks the MTs are rather densely scattered across the served environment, whereas the density of the APs is rather scarce. As the basic idea behind multi-hop systems, it is provided that, in addition to the direct communication between MTs and APs, also an indirect communication between MTs and APs via other MTs is possible. By such an option, in which certain MTs perform the function of relay stations, the total transmit power required per served MT may be reduced. In the case of ad-hoc networks a suitably located MT within an ensemble of MTs momentarily takes a function similar to that of an AP, which has a beneficial effect comparable to the above mentioned increase of the number of APs. Also service area (SA) concepts [24] are alternatives to conventional cellular systems and will be treated in some more detail in what follows.

Fig. 6 shows the air interface concept of a conventional cellular mobile radio system. In each cell we have an AP which supports the MTs of this cell and which is connected to a core network. As already explained in this paper, various possibilities exist to mitigate the impact of MAI, but, still, intercell MAI is a major problem. An efficient way to combat intercell MAI is enabled by the air interface concept of Fig. 7 [24]. In this concept a number of APs is connected to a central unit (CU), and a number of the original cells is integrated to a SA. As formerly the APs, now the CUs are connected to the core network. The MTs of each SA are jointly supported by all APs of this SA in such a way that in the downlink the transmit signals radiated by the APs of the SA are jointly generated in the corresponding CU, and that in the uplink the signals received by the APs of the SA from its MTs are jointly processed in the corresponding CU. In this way intercell MAI to be originally observed between the cells which now form a single SA is eliminated, and only inter SA MAI remains.

VII. Acknowledgement

The authors gratefully acknowledge the support by their co-workers and colleagues, respectively, at the research group for RF Communications, and by DFG and Siemens AG.

References

[1] *IEEE Communications Magazine*, vol. 40, pp. 108–138, 2002.

[2] P. W. Baier, "A critical review of CDMA", in *Proc. IEEE 46th Vehicular Technology Conference (VTC'96)*, Atlanta, 1996, vol. 1, pp. 6–10.

[3] B. Steiner and P. W. Baier, "Low cost channel estimation in the uplink receiver of CDMA mobile radio systems", *Frequenz*, vol. 47, no. 11–12, pp. 292–298, 1993.

[4] L. Tong and S. Perreau, "Multichannel blind identification: From subspace to maximum likelihood methods", *Proceedings of the IEEE*, vol. 86, 1998.

[5] A. Klein, *Multi-user detection of CDMA signals – algorithms and their application to cellular mobile radio*, Fortschrittberichte VDI, Reihe 10, no. 423, VDI-Verlag, Düsseldorf, 1996.

[6] S. Verdú, *Multiuser Detection*, Cambridge University Press, Cambridge, 1998.

[7] H. V. Poor, "Turbo multiuser detection: An overview", in *Proc. IEEE 6th International Symposium on Spread Spectrum Techniques & Applications (ISSSTA'2000)*, Parsippany, 2000, pp. 583–587.

[8] T. Weber, J. Oster, M. Weckerle and P. W. Baier, "Turbo multi–user detection for TD–CDMA", *International Journal of Electronics and Communications (AEÜ)*, vol. 56, no. 2, pp. 120–130, 2002.

[9] A. Steil, *Spektrale Effizienz digitaler CDMA–Mobilfunksysteme mit gemeinsamer Detektion*, Fortschrittberichte VDI, Reihe 10, no. 437, VDI-Verlag, Düsseldorf, 1996.

[10] C.-C. Wu, J. Oster, P. W. Baier, P. M. Grant and G. Ritter, "Intercell interference cancellation for TD–CDMA mobile systems", *IEE ELECTRONICS LETTERS*, vol. 36, no. 23, pp. 1960–1961, 2000.

[11] P. W. Baier, J. J. Blanz and R. M. Schmalenberger, "Fundamentals of smart antennas for mobile radio applications", in *Wireless communications – TDMA versus CDMA*, S. G. Glisic and P. A. Leppänen, Eds., Kluwer, Dordrecht, 1997, pp. 345–376.

[12] R. Kohno, "Spatial and temporal filtering for co–channel interference in CDMA", in *Proc. IEEE 3rd International Symposium on Spread Spectrum Techniques & Applications (ISSSTA'94)*, Oulu, 1994, pp. 51–60.

[13] J. Blanz, A. Klein, M. M. Naßhan and A. Steil, "Performance of a cellular hybrid C/TDMA mobile radio system applying joint detection and coherent receiver antenna diversity", *IEEE Journal on Selected Areas in Communications*, vol. 12, no. 4, pp. 568–579, 1994.

[14] A. Papathanassiou, I. Fourió, J. J. Blanz and P. W. Baier, "Smart antennas with two-dimensional array configurations for performance enhancement of a Joint Detection CDMA mobile radio system", *Wireless Personal Communications*, vol. 11, no. 1, pp. 98–108, 1999.

[15] M. Weckerle, "Turbo methods for exploiting spatial and temporal covariance matrices in the TD–CDMA uplink with multi-element antennas", in *Proc. 4th European Personal Mobile Communications Conference (EPMCC'2001)*, Vienna, 2001, no. 29.1.

[16] Y. Lu and P. W. Baier, "Performance of adaptive antennas for the TD-CDMA downlink under special consideration of multi-directional channels and CDMA code pooling", *International Journal of Electronics and Communications (AEÜ)*, vol. 54, no. 5, pp. 249–258, 2000.

[17] E. Visotsky and U. Madhow, "Space-time transmit precoding with imperfect feedback", *IEEE Transactions on Information Theory*, vol. 47, no. 6, pp. 2632–2639, 2001.

[18] G. J. Foschini, "Layered space-time architecture for wireless communication in a fading environment when using multi-element antennas", *The Bell System Technical Journal*, pp. 41–59, 1996.

[19] R. D. Kai-Kit Wong Murch, R. S.-K. Cheng and K. B. Letaief, "Optimizing the spectral efficiency of multiuser MIMO smart antenna systems", in *Proc. IEEE Wireless Communications and Networking Conference (WCNC'2000)*, Chicago, 2000, vol. 1, pp. 426–430.

[20] J. J. Blanz, P. W. Baier and P. Jung, "A flexible configurable statistical channel model for mobile radio systems with directional diversity", in *ITG-Fachbericht, Mobile Kommunikation*, B. Walke, Ed., VDE, Berlin, 1995, vol. 135, pp. 93–100.

[21] W. Qiu, H. Tröger and M. Meurer, "System model of Joint Transmission (JT) in multi-user MIMO transmission systems", in *COST 273 TD(02)008*, Guildford, 2002.

[22] J. L. Holsinger, *Digital communication over fixed time-continous channels with memory – with special application to telephone channels*, Technical Report no. 366, M.I.T Lincoln Lab., 1964.

[23] M. Meurer, P. W. Baier, T. Weber, Y. Lu and A. Papathanassiou, "Joint transmission, an advantageous downlink concept for CDMA mobile radio systems using time division duplexing", *IEE ELECTRONICS LETTERS*, vol. 36, no. 10, pp. 900–901, 2000.

[24] A. Sklavos, T. Weber, E. Costa, H. Haas and E. Schulz, "Joint Detection in multi-antenna and multi-user OFDM systems", in *Multi-Carrier Spread Spectrum & Related Topics*, K. Fazel and S. Kaiser, Eds., Kluwer, Dordrecht, 2002, pp. 191–198.

Kapitel 8
Zusammenfassung

8.1 Deutsch

In heutigen Mobilfunksystemen wird ausschließlich senderorientierte Funkkommunikation eingesetzt. Bei senderorientierter Funkkommunikation beginnt der Systementwurf mit dem Sender. Dies bedeutet, daß man a priori die senderseitig verwendeten Algorithmen der Sendesignalerzeugung auswählt und in Abhängigkeit davon a posteriori den im Empfänger zum Datenschätzen verwendeten Algorithmus gegebenenfalls unter Einbeziehen von Kanalzustandsinformation festlegt. Dies ist nötig, um beispielsweise einen möglichst großen Anteil der senderseitig investierten Energie empfängerseitig auszunutzen, das heißt energieeffizient zu sein, und dabei gleichzeitig das Entstehen schädlicher Interferenzsignale zu vermeiden oder zu begrenzen. Im Falle der Senderorientierung kann man senderseitig sehr einfache Algorithmen wählen und implementieren, wobei dieser Vorteil typischerweise durch eine ungleich höher Implementierungskomplexität der a posteriori festzulegenden empfängerseitigen Algorithmen aufgewogen werden muß. Betrachtet man die wirtschaftlich bedeutenden zellularen Mobilfunksysteme, so ist eine derartige Funkkommunikation in der Aufwärtsstrecke vorteilhaft, denn in der Aufwärtsstrecke sind die Endgeräte der mobilen Teilnehmer, die Mobilstationen, die einfachen Sender, wohingegen die ortsfesten Basisstationen die Empfänger sind — und dort kann typischerweise eine größere Komplexität in Kauf genommen werden. In der Abwärtsstrecke derartiger Mobilfunksysteme hingegen, sind die Basisstationen die einfachen Sender, wohingegen die Mobilstationen die aufwendigen Empfänger sind. Dies ist nicht vorteilhaft, da in praktischen Mobilfunksystemen Gewicht, Volumen, Energieverbrauch und Kosten der Endgerätehardware und damit der Mobilstationen mit der Implementierungskomplexität steigen.

Wie der Verfasser in der vorliegenden Schrift vorschlägt, läßt sich dieses Problem jedoch umgehen, denn die Funkkommunikation in Mobilfunksystemen kann auch in neuartiger Weise empfängerorientiert gestaltet werden. Empfängerorientierte Funkkommunikation ist dadurch gekennzeichnet, daß der Systementwurf auf der Empfängerseite beginnt. In diesem Fall werden die empfängerseitig verwendeten Algorithmen des Datenschätzens a priori festgelegt, und die senderseitig einzusetzenden Algorithmen der Sendesignalerzeugung ergeben sich dann daraus a posteriori durch Adaption wiederum gegebenenfalls unter Einbeziehen von Kanalzustandsinformation. Durch

Empfängerorientierung kann man empfängerseitig sehr einfache Algorithmen wählen und implementieren, muß dafür jedoch eine höhere Implementierungskomplexität auf der Senderseite tolerieren. Angesichts der erwähnten Komplexitätscharakteristika von Sender- beziehungsweise Empfängerorientierung schlägt der Verfasser daher für künftige Mobilfunksysteme vor, Empfängerorientierung in der Abwärtsstrecke und Senderorientierung in der Aufwärtsstrecke einzusetzen. Dies ist insbesondere deshalb vorteilhaft, da Empfängerorientierung in der Abwärtsstrecke neben anderen noch die folgenden weiteren Vorteile gegenüber herkömmlicher Senderorientierung aufweist:

- Die Leistung der von den Basisstationen abgestrahlten Signale kann reduziert werden. Dies erlaubt performanzhemmende systeminherente Störeinflüsse, die als Interzellinterferenz bezeichnet werden, zu reduzieren und ist im übrigen auch wünschenswert im Hinblick auf die zunehmende Elektrophobie der Bevölkerung.
- Kanalzustandsinformation wird empfängerseitig nicht benötigt, so daß auf das Senden resourcenbindender Trainingssignale verzichtet und anstelle dessen das Sende von Nutzdaten ermöglicht werden kann.
- Empfängerseitig ist kein Kanalschätzer vorzusehen, was des weiteren der Implementierungskomplexität des Empfängers zu gute kommt.

Mobilfunksysteme lassen sich demzufolge durch Einsetzen des Grundkonzepts der Empfängerorientierung maßgeblich aufwerten. Dieses ist eine klare Motivation die Grundzüge, das Potential und die Ausgestaltungen dieses Grundkonzepts in der Mobilkommunikation in dieser Schrift eingehend zu studieren.

Zur Klärung dieser Punkte im Kontext von Mobilkommunikation ist es entscheidend, die Frage der Wahl der Empfänger und die der Adaption der Sender zu beantworten. Die Frage nach der Adaption der Sender ist dabei gleichbedeutend mit der Frage nach der im allgemeinen auf Basis aller Daten erfolgenden gemeinsamen Sendesignalerzeugung. Nach der Einführung eines geeigneten allgemeinen Modells der Abwärtsstreckenübertragung eines zellularen Mobilfunksystems, das auch erst in jüngster Vergangenheit vorgeschlagene Mehrantennenkonfigurationen an den Basisstationen und Mobilstationen einschließt, wird hinsichtlich der A-priori-Wahl der Empfänger herausgestellt, daß, im Hinblick auf die bereits oben angesprochene möglichst geringe Implementierungskomplexität die Ausgestaltung der empfängerseitigen Signalverarbeitung als serielle Verkettung einer linearen Signalverarbeitung und eines nichtlinearen Quantisierers vorteilhaft ist. Die Prinzipien, die bei der Wahl sowohl der linearen Signalverarbeitung als auch des nichtlinearen Quantisierer gelten, werden im folgenden herausgearbeitet. Als Ergebnis dieser Betrachtungen stellt sich heraus, daß ein Gestalten der empfängerseitigen linearen Signalverarbeitung gemäß Codemultiplex hinsichtlich der ausnutzbaren Frequenz-, Zeit- und Raumdiversität vorteilhaft ist, jedoch leistungsfähige Verfahren der gemeinsamen Sendesignalerzeugung voraussetzt, die die Entstehung schädlicher Interferenzsignale verhindern. Des weiteren wird klar, daß sich die nichtlinearen Quantisierer sinnvollerweise in die Klasse der konventionellen und die der unkonventionellen Quantisierer unterteilen lassen; gleiches gilt für die diese Quantisierer verwendenden Empfänger. Konventionelle Quantisierer basieren auf einfach zusammenhängenden Entscheidungsgebieten, wobei jedes Entscheidungsgebiet eindeutig einer möglichen Ausprägung eines übertragenen Nachrichtenelements zugeordnet ist. Demgegenüber weisen unkonventionelle Quantisierer mehrfach zusammenhängende Entscheidungsgebiete auf, die sich jeweils aus mehreren Teilentscheidungsgebieten zusammensetzen. Das Vorhandensein mehrerer Teilentscheidungsgebiete pro Entscheidungsgebiet und damit pro Ausprägung eines übertragenen Nachrichtenelements stellt einen bei unkonventionellen Quantisierern verfügbaren zusätzlichen Freiheitsgrad dar, der bei der gemeinsamen Sendesignalerzeugung vorteilhaft genutzt werden kann, um die angesprochene Leistung der von den Basisstationen abgestrahlten Signale zu reduzieren.

Ein Schwerpunkt der vorliegenden Schrift ist das Studium von Verfahren der gemeinsamen Sendesignalerzeugung. Diese werden daher systematisch gegliedert und erarbeitet. Es stellt sich heraus, daß Verfahren der gemeinsamen Sendesignalerzeugung prinzipiell unterteilt werden können in solche Verfahren für konventionelle Empfänger und solche für unkonventionelle Empfänger. Hinsichtlich Verfahren der erstgenannten Art wird herausgearbeitet, wie eine optimale gemeinsame Sendesignalerzeugung zu erfolgen hat, die unter gewissen Nebenbedingungen eine optimale Übertragungsqualität im Sinne minimaler Übertragungsfehlerwahrscheinlichkeit erzielt. Eine derartige gemeinsame Sendesignalerzeugung ist im allgemeinen recht aufwendig, so daß im Folgeverlauf die suboptimalen linearen Verfahren der gemeinsamen Sendesignalerzeugung Transmit Matched Filter (TxMF), Transmit Zero-Forcing (TxZF) und Transmit Minimum-Mean-Square-Error (TxMMSE) vorgeschlagen werden, die jeweils einen mehr oder weniger guten Kompromiß zwischen Implementierungskomplexität, Interferenzunterdrückung und Robustheit hinsichtlich Rauschens aufweisen. Der Verfasser schlägt vor, die Leistungsfähigkeit derartiger suboptimaler Verfahren unter anderem durch die bei gegebener Zeitdauer abgestrahlte totale Energie der Sendesignale, die totale Sendeenergie, — denn diese ist nicht nur im technischen, sondern auch im gesellschaftlichen Sinn ein wichtiger Aspekt, — und das Kriterium der Sendeeffizienz zu bewerten. Sendeeffizienz beurteilt das Zusammenspiel aus Interferenzunterdrückung einerseits und energieeffizienter Übertragung andererseits. Es stellt sich durch analytische und numerische Betrachtungen heraus, daß beide Größen vorrangig von zwei Einflußfaktoren bestimmt werden: der Anzahl der Freiheitsgrade bei der gemeinsamen Sendesignalerzeugung — und das ist die Anzahl der zu bestimmenden Abtastwerte aller Sendesignale — und der Anzahl der dabei einzuhaltenden Restriktionen. Da die Anzahl der Restriktionen bei der Forderung einer möglichst geringen wechselseitigen Interferenz nicht beeinflußbar ist, schlägt der Verfasser daher zum Erhöhen der Leistungsfähigkeit der empfängerorientierten Funkkommunikation vor, die Anzahl der Freiheitsgrade zu erhöhen, was sich vorzugsweise durch Verfolgen des Prinzips der unkonventionellen Empfänger umsetzen läßt. Es wird gezeigt, wie unter gewissen Nebenbedingungen eine hinsichtlich der Übertragungsfehlerwahrscheinlichkeiten optimale gemeinsame Sendesignalerzeugung prinzipiell erfolgen muß, und welche erheblichen Performanzgewinne im Sinne der totalen Sendeenergie und der Sendeeffizienz möglich werden. Diese optimale Vorgehensweise ist sehr aufwendig, so daß darüber hinaus aufwandsgünstige suboptimale hochperformante Alternativen der gemeinsamen Sendesignalerzeugung für unkonventionelle Empfänger vorgeschlagen und betrachtet werden.

Die gemeinsame Sendesignalerzeugung setzt senderseitiges Vorliegen von Kanalzustandsinformation voraus. Daher werden die prinzipiellen Möglichkeiten des zur Verfügung Stellens dieser Information behandelt, wobei dabei das Bereitstellen dieser Information auf Basis gegebenenfalls vorliegender Kanalreziprozität im Falle von Duplexübertragung favorisiert wird. Dabei wird die in der Aufwärtsstrecke gewonnene Kanalzustandsinformation zur gemeinsamen Sendesignalerzeugung in der Abwärtsstrecke genutzt. Ist die dabei genutzte Kanalzustandsinformation nicht exakt, so hat dieses prinzipiell eine Degradation der Leistungsfähigkeit der empfängerorientierten Funkkommunikation zur Folge. Analytische und/oder numerische Betrachtungen erlauben, die Degradation zu quantifizieren. Es stellt sich heraus, daß diese Degradation vergleichbar mit der von konventionellen senderorientierten Funkkommunikationssystemen bekannten ist. Eine Betrachtung möglicher Weiterentwicklungen des Grundprinzips der Empfängerorientierung komplettieren die in dieser Schrift angestellten Betrachtungen.

Die Ergebnisse dieser Schrift belegen, daß Empfängerorientierung ein interessanter Kandidat für die Organisation der Abwärtsstreckenübertragung künftiger Mobilfunksysteme ist. Darüber hinaus wird klar, welche grundsätzlichen Prinzipien und Effekte bei der empfängerorientierten Funkkommunikation wirksam sind und durch welche Vorgehensweisen bei der Gestaltung derartiger Funkkommunikation die Einflüsse der verschiedenen Effekte gegeneinander ausbalanciert werden können. Für den Systemdesigner morgiger Mobilfunksysteme steht mit dieser Schrift daher ein wertvolles Nachschlagewerk zur Verfügung, daß dabei unterstützt, die genannten prinzipiellen Vorteile von Empfängerorientierung in Funktechnologien der Praxis umzumünzen.

8.2 English

Nowadays mobile radio systems only use transmitter oriented radio transmission. In the case of transmitter orientation the system design starts from the transmitter. That means that the transmitter-sided algorithms for transmission signal generation are a priori chosen, whereas, depending on that choice, the algorithms used at the receivers for data estimation are determined a posteriori possibly under consideration of channel state information. This a posteriori determination has for instance the aim to use as much of the energy invested at the transmitter as possible for receiver-sided data estimation, that is, to be energy efficient, and, at the same time, to avoid or limit the occurrence of harmful interference. In case of transmitter orientation the transmitter-sided algorithms can be chosen to be very simple, however, this advantage will come typically at the cost of a much higher implementation complexity of the a posteriori determined receiver-sided algorithms. With reference to the economically important cellular mobile radio systems, such a radio transmission is advantageous in the uplink. Because in the uplink, the terminals of the mobile users, the mobile stations, are the simple transmitters, whereas the fixed base stations are the receivers — and, typically, a higher complexity can be accepted there. However, in the downlink of such mobile radio systems, the base stations are the simple transmitters, whereas the mobile stations have to act as complex receivers. This is not beneficial, since in practical mobile radio systems, weight, volume, energy consumption and the cost of terminal hardware and, therefore, of the mobile stations, increase with implementation complexity.

As proposed by the author of this thesis, this drawback can be circumvented, as the radio transmission in mobile radio systems can alternatively be designed in a novel receiver oriented way. Receiver oriented radio transmission is characterized by the fact that the system design starts from the receiver side. In this case the algorithms used at the receiver side for data estimation are a priori chosen, and the algorithms utilized at the transmitter for transmission signal generation follow a posteriori by adaption, possibly again under consideration of channel state information. Receiver orientation allows the use of simple algorithms at the receiver side, but a higher implementation complexity at the transmitter side has to be accepted. In regard to the complexity features of both transmitter orientation and receiver orientation mentioned above, the author proposes the use of receiver orientation in the downlink and transmitter orientation in the uplink of future mobile radio systems. This is favorable since receiver orientation has, besides others, the following advantages when compared to transmitter orientation:

- The power of the signals radiated by the base stations can be reduced. This allows to reduce system inherent disturbing influences, which are termed intercell interference and which degrade the performance of the mobile radio system, and, moreover, is desirable with respect to the growing electro-phobia of the public.

- Channel state information is not necessary at the receiver side, which allows to do without resource consuming training signals.

- No channel estimator is needed at the receiver side which further reduces the implementation complexity of the receivers.

Thus, mobile radio systems can be significantly enhanced by the utilization of receiver orientation. This is a clear motivation for deeply studying the basics, potentials and the embodiment of this rationale in mobile communications within this thesis.

To clarify these aspects in the context of mobile communications, it is important, to consider the choice of the receivers as well as the adaption of the transmitter. The question concerning the adaption of the transmitter is equivalent to the question of joint transmission signal generation based on the entirety of all data. After introducing a suitable general model of the downlink transmission in a cellular mobile radio system, which also includes multi-antenna configurations at the base stations and at the mobile stations, it is pointed out that, concerning the a priori choice of the receiver in connection with the low implementation complexity mentioned afore, the design of the receiver-sided signal processing as a serial concatenation of a linear signal processing and a nonlinear quantizer is favorable. The principles, underlying the choice of the linear signal processing as well as the nonlinear quantizer are elaborated. As a result it becomes apparent that the design of the receiver-sided linear signal processing according to code multiplex is advantageous in terms of frequency diversity, time diversity and space diversity but, requires powerful techniques for joint transmission signal generation, which avoid the occurrence of harmful interference. Moreover, it becomes evident that nonlinear quantizers can be divided into the class of conventional and unconventional quantizers; the same applies to receivers utilizing such quantizers. Conventional quantizers rely on simply connected decision regions, where each decision region is uniquely assigned to a single possible value of a data message element. In contrast, unconventional quantizers are based on multiply connected decision regions, which are composed of several partial decision regions. The availability of multiple partial decision regions per decision region and, therefore, per value of the transmitted data message element in the case of unconventional quantization constitutes a degree of freedom, which can be utilized beneficially for joint transmission signal generation in order to reduce said powers of the radiated signals.

A focal point of this thesis is the elaboration of techniques for joint transmission signal generation. Therefore, theses techniques are systematically classified and elaborated. It turns out that techniques for joint transmission signal generation can be divided into techniques for conventional receivers and techniques for unconventional receivers. Concerning the former mentioned techniques it is shown, in which way an optimum transmission signal generation can be established, which under certain constraints achieves optimum transmission quality in terms of minimum transmission error probabilities. Such an optimum transmission signal generation is typically very complex, which is the motivation for certain suboptimum linear techniques for transmission signal generation, which are considered in the following. Especially the techniques transmit matched filter (TxMF), transmit zero-forcing (TxZF) and transmit minimum mean square error (TxMMSE) are proposed, which provide a more or less satisfying compromise between implementation complexity, interference suppression and robustness against noise. The author proposes to quantify the performance of such techniques by, among others, the total energy of the transmission signals, which are radiated by the base station during a certain time interval — this total transmit energy is an important aspect not only due to technical but also social reasons —, and by the criterion transmit efficiency. The transmit efficiency evaluates the interaction between interference suppression on the one hand and energy efficient transmission on the other hand. By means of analytical and numerical considerations it is shown that both quantities are primarily determined by two factors: the number of degrees of freedom for transmission signal generation — that is the number of samples of the transmitted signals to be determined — and the number of restrictions to be satisfied thereby. Since the number of restrictions can hardly be influenced if interference suppression is required, the author proposes to increase the performance of receiver oriented transmission by increasing the number of degrees of freedom, which, in particular, can be accomplished by using unconventional receivers. It is shown, how, with respect to certain constraints and a minimum probability of transmission errors, an optimum transmission signal generation has to be carried out and which significant performance improvements in terms of total transmit energy and transmit efficiency are achievable. This optimum transmission signal generation is typically of high complexity, and, therefore, suboptimum less complex techniques for transmission signal generation for unconventional receivers are considered which still guarantee a high transmission performance.

Joint transmission signal generation requires transmitter-sided channel state information. Therefore, the basic principles of providing such information are presented, whereby the provision of such information based on channel reciprocity in the case of duplex transmission is favored. In this case, the channel state information obtained in the uplink is used for joint transmission signal generation in the downlink. If the channel state information is not accurate, then this will lead in principle to a degradation of the performance of receiver oriented transmission. Analytical and/or numerical considerations allow to quantify theses degradations. It turns out that the mentioned degradations are comparable to those known from the conventional transmitter orientation. An outline of further possible developments on the subject of the basic principle receiver orientation completes the considerations within in this thesis.

The results of this thesis prove that receiver orientation is an attractive choice for the organization of the downlink transmission in future mobile radio systems. Moreover, it becomes clear, which basic principles and effects govern the receiver oriented radio transmission and which techniques for designing such radio transmission enable the best balance of the mentioned effects. Thus, this thesis may act as a valuable reference for system designers of tomorrow's mobile radio systems, which encourages the transformation of the basic advantages of receiver orientation worked out into practical radio technology.

Literatur

[Aar03] Aarts, E.: IC design challenges for Ambient Intelligence. *DATE 2003, Keynote Speech*, 2003.

[Aei73] Aein, J. M.: Power balancing in systems employing frequency reuse. *COMSAT Technical Review*, Bd. 3, 1973, S. 277–299.

[AF92] Abdulrahman, M.; Falconer, D.: Cyclostationary crosstalk suppression by decision feedback equalization on digital subscriber loops. *IEEE Journal on Selected Areas in Communications*, Bd. 10, 1992, S. 640–649.

[AFHS04] Airy, M.; Forenza, A.; Heath, Jr., R. W.; Shakkottai, S.: Practical costa precoding for the multiple antenna broadcast channel. *Proc. IEEE Global Telecommunications Conference (GLOBECOM'04)*, Bd. 6, Dallas, 2004, S. 3942 – 3946.

[AGR98] Alexander, P. D.; Grant, A. J.; Reed, M. C.: Iterative detection in code-division multiple-access with error control coding. *European Transactions on Telecommunications*, Bd. 9, 1998, S. 419–425.

[AMVW91] Anderson, S.; Millnert, M.; Viberg, M.; Wahlberg, B.: An adaptive array for mobile communication systems. *IEEE Transactions on Vehicular Technology*, Bd. 40, 1991, S. 230–236.

[AN82] Alavi, H.; Nettleton, R. W.: Downstream power control for a spread spectrum cellular mobile radio system. *Proc. IEEE Global Telecommunications Conference (GLOBECOM'82)*, Miami, 1982, S. 84–88.

[App76] Applebaum, S. P.: Adaptive arrays. *IEEE Transactions on Antennas and Propagation*, Bd. 24, 1976, S. 585–598.

[ARAS99] Alexander, P. D.; Reed, M. C.; Asenstorfer, J. A.; Schlegel, C. B.: Iterative multiuser interference reduction: Turbo CDMA. *IEEE Transactions on Communications*, Bd. 47, 1999, S. 1008–1014.

[ARS97] Alexander, P. D.; Rasmussen, L. K.; Schlegel, C. B.: A linear receiver for coded multiuser CDMA. *IEEE Transactions on Communications*, Bd. 45, 1997, S. 605–610.

[AS97] Adachi, F.; Sawahashi, M.: Wideband multi-rate DS-CDMA for next generation mobile communications systems. *Proc. Wireless Communications Conference (WCC'97)*, Boulder, 1997, S. 57–62.

[ASA97] Andoh, H.; Sawahashi, M.; Adachi, F.: Channel estimation using time multiplexed pilot symbols for coherent rake combining for DS-CDMA mobile radio. *Proc. IEEE 8th International Symposium on Personal, Indoor and Mobile Radio Communications (PIMRC'97)*, Bd. 3, Helsinki, 1997, S. 954–957.

[Asc84] Aschoff, V.: *Geschichte der Nachrichtentechnik*. Berlin: Springer-Verlag, 1984.

[ASF94] Abdulrahman, M.; Sheikh, A. U. H.; Falconer, D. D.: Decision feedback equalization for CDMA in indoor wireless communications. *IEEE Journal on Selected Areas in Communications*, Bd. 12, 1994, S. 698–706.

[ASS98] Adachi, F.; Sawahashi, M.; Suda, H.: Wideband DS-CDMA for next-generation mobile communications systems. *IEEE Communications Magazine*, Bd. 36, 1998, S. 56–69.

[BA94] Bonsley, S.; Azhang, B.: Subspace-based estimation of multipath channel parameters for CDMA communication systems. *Proc. IEEE Global Telecommunications Conference (GLOBECOM'94)*, 1994, S. 154–158.

[Bai86] Baier, A.: *Digitale signalangepaßte Filter und Korrelatoren zur Detektion von Bandpaßsignalen*. Fortschrittberichte VDI, Reihe 10, Nr. 74. Düsseldorf: VDI-Verlag, 1986.

[BDT95] Bossert, M.; Donder, A.; Trushkin, A.: Channel estimation and equalization in orthogonal frequency division multiplexing systems. *Proc. of ITG Fachtagung Mobile Kommunikation*, Neu-Ulm, 1995.

[Bel63] Bello, P. A.: Characterization of randomly time-variant linear channels. *IEEE Transactions on Communications Systems*, Bd. 11, 1963, S. 360–393.

[BF99] Barreto, A. N.; Fettweis, G.: On the downlink capacity of TDD CDMA using a Pre-Rake. *Proc. IEEE Global Telecommunications Conference (GLOBECOM'99)*, Bd. 1a, Rio de Janeiro, 1999, S. 117–121.

[BFKM93] Baier, P. W.; Felhauer, T.; Klein, A.; Mämmelä, A.: Survey of linear block estimation algorithms for the detection of spread spectrum signals transmitted over frequency selective channels. *IEICE Transactions on Communications*, Bd. 76, 1993, S. 825–834.

[BHMW04] Berenguer, I.; Host-Madsen, A.; Wang, X.: Multiuser TH-precoding for CDMA over multipath channels. *IEEE Transactions on Communications*, 2004. in press.

[BJK91] Baier, P. W.; Jung, P.; Klein, A.: CDMA – ein günstiges Vielfachzugriffsverfahren für frequenzselektive und zeitvariante Mobilfunkkanäle. *Nachrichtentechnik Elektronik*, Bd. 41, 1991, S. 223–227.

[BJM+04] Baier, P. W.; Jötten, C. A.; Meurer, M.; Weber, T.; Weckerle, M.; Tröger, H.; Lu, Y.; Oster, J.: Recent progress in time slotted CDMA. Ma, J.-G. (Hrsg.): *Third Generation Communication Systems*. Kap. 5, S. 121–164. Berlin: Springer-Verlag, 2004.

[BJW01a] Baier, P. W.; Jötten, C.; Weber, T.: Recent progress of time slotted CDMA. *Proc. International Symposium on Telecommunications (IST 2001)*, Teheran, 2001, S. 250–259.

[BJW01b] Baier, P. W.; Jötten, C. A.; Weber, T.: Review of TD-CDMA. *Proc. 3rd International Workshop on Commercial Radio Sensors and Communications Techniques (CRSCT 2001)*, Linz, 2001, S. 11–20.

[Bla98] Blanz, J. J.: *Empfangsantennendiversität in CDMA-Mobilfunksystemen mit gemeinsamer Detektion der Teilnehmersignale.* Fortschrittberichte VDI, Reihe 10, Nr. 535. Düsseldorf: VDI-Verlag, 1998.

[BM02] Baier, P. W.; Meurer, M.: Air interface enhancements for 3G and beyond-3G mobile radio communications. *Proc. 9th International Conference on Telecommunications (ICT'02)*, Peking, 2002, S. 284–291.

[BM03] Baier, P. W.; Meurer, M.: Receiver orientation, an unconventional approach to mobile radio downlink design. *Proc. European Conference on Wireless Technology (ECWT'03)*, München, 2003, S. 11–14.

[BM04] Baier, P. W.; Meurer, M.: Advanced CDMA transmission concepts for 3G and 4G mobile radio communications. *Proc. IEEE 8th International Symposium on Spread Spectrum Techniques & Applications (ISSSTA'04)*, Sydney, 2004, S. 601–608.

[BMWT00] Baier, P. W.; Meurer, M.; Weber, T.; Tröger, H.: Joint transmission (JT), an alternative rationale for the downlink of time division CDMA using multi-element transmit antennas. *Proc. IEEE 6th International Symposium on Spread Spectrum Techniques & Applications (ISSSTA'00)*, Bd. 1, Parsippany, 2000, S. 1–5.

[BNK00] Borran, M.; Nasiri-Kenari, M.: An efficient detection technique for synchronous CDMA communication systems based on the expectation maximization algorithm. *IEEE Transactions on Vehicular Technology*, Bd. 49, 2000, S. 1663–1668.

[Bos92] Bossert, M.: *Kanalcodierung.* Stuttgart: B. G. Teubner, 1992.

[BPD00] Brandt-Pearce, M.; Dharap, A.: Transmitter-based multiuser interference rejection for the down-link of a wireless CDMA system in a multipath environment. *IEEE Journal on Selected Areas in Communications*, Bd. 18, 2000, S. 407–417.

[BQT+03] Baier, P. W.; Qiu, W.; Tröger, H.; Jötten, C. A.; Meurer, M.; Lehmann, G.: Modelling and optimization of receiver oriented multi-user MIMO downlinks for frequency selective channels. *Proc. 10th International Conference on Telecommunications (ICT'03)*, Bd. 2, Papeete, 2003, S. 1547–1554.

[Bra97] Bravo, A.: Limited linear cancellation of multiuser interference in DS/CDMA asynchronous systems. *IEEE Transactions on Communications*, Bd. 45, 1997, S. 1435–1443.

[BS79] Bronstein, I. N.; Semendjajew, K. A.: *Taschenbuch der Mathematik.* Leipzig: B. G. Teubner, 1979.

[BTT02] Biglieri, E.; Taricco, G.; Tulino, A.: Decoding space-time codes with BLAST architectures. *IEEE Transactions on Signal Processing*, Bd. 50, 2002, S. 2547–2552.

[Bur05] Burnet, C.: Mitigation of adverse nonlinear satellite channel effects. *Seminar of the Research Group for RF Communications*, Kaiserslautern, Jan., 2005.

[BZT+03] Burr, A.; Zacharov, Y.; Tröger, H.; Qiu, W.; Meurer, M.; Stimming, C.; Vanaev, A.; Tauböck, G.; Shen, J.; Mai, H.: *Selected MIMO Techniques and their Performance*. Technische Mitteilung D14, European Union IST Project IST-2001-32125 FLOWS, 2003. http://www.flows-ist.org.

[Cal88] Calhoun, G.: *Digital cellular radio*. Norwood: Artech House, 1988.

[CL02] Cohen, A. S.; Lapidoth, A.: Generalized Writing on Dirty Paper. *Proc. International Symposium on Information Theory (ISIT'02)*, Lausanne, 2002, S. 227–233.

[CLM01] Choi, R. L.-U.; Letaief, K. B.; Murch, R. D.: MISO CDMA transmission with simplified receiver for wireless communication handsets. *IEEE Transactions on Communications*, Bd. 49, 2001, S. 888–898.

[CM02a] Choi, R. L.-U.; Murch, R. D.: Some Results on Channel Capacity when using Multiple Antennas. *IST Mobile & Wireless Telecommunications Summit 2002*, Thessaloniki, 2002.

[CM02b] Choi, R. L.-U.; Murch, R. D.: Transmit MMSE pre-rake preprocessing with simplified receivers for the downlinks of MISO TDD-CDMA systems. *Proc. IEEE Global Telecommunications Conference (GLOBECOM'02)*, Bd. 1, Taipei, 2002, S. 429–433.

[CM03] Choi, L.-U.; Murch, R. D.: New transmit schemes and simplified receivers for MIMO wireless communication systems. *IEEE Transactions on Wireless Communications*, Bd. 2, 2003, S. 1217–1230.

[CM04a] Choi, L.-U.; Murch, R. D.: A transmit MIMO scheme with frequency domain pre-equalization for wireless frequency selective channels. *IEEE Transactions on Wireless Communications*, Bd. 3, 2004, S. 929–938.

[CM04b] Choi, L.-U.; Murch, R. D.: A transmit preprocessing technique for multiuser MIMO systems using a decomposition approach. *IEEE Transactions on Wireless Communications*, Bd. 3, 2004, S. 20–24.

[CM04c] Choi, L.-U.; Murch, R. D.: Transmit-preprocessing techniques with simplified receivers for the downlink of MISO TDD-CDMA systems. *IEEE Transactions on Vehicular Technology*, Bd. 53, 2004, S. 285–295.

[CM04d] Choi, R. L.-U.; Murch, R. D.: A Pre-BLAST-DFE technique for the downlink of frequency-selective fading MIMO channels. *IEEE Transactions on Communications*, Bd. 52, 2004, S. 737–743.

[CML03] Choi, L.-U.; Murch, R. D.; Letaief, K. B.: MIMO CDMA antenna system for SINR enhancement. *IEEE Transactions on Wireless Communications*, Bd. 2, 2003, S. 240–249.

[CMO99] Chaudhury, P.; Mohr, W.; Onoe, S.: The 3GPP proposal for IMT-2000. *IEEE Communications Magazine*, Bd. 37, 1999, S. 72–81.

[Cos83] Costa, M. H. M.: Writing on Dirty Paper. *IEEE Transactions on Information Theory*, Bd. 29, 1983, S. 439–441.

[Cov72] Cover, T. M.: Broadcast Channels. *IEEE Transactions on Information Theory*, Bd. 18, 1972, S. 2–14.

[Cov98] Cover, T. M.: Comments on broadcast channels. *IEEE Transactions on Information Theory*, Bd. 44, 1998, S. 2524–2530.

[CRFLL00] Chizhik, D.; Rashid-Farrokhi, F.; Ling, J.; Lozano, A.: Effect of antenna separation on the capacity of BLAST in correlated channels. *IEEE Communications Letters*, Bd. 4, 2000, S. 337–339.

[CS82] Conway, J.; Sloane, N.: Voronoi regions of lattices, second moments of polytopes, and quantization. *IEEE Transactions on Information Theory*, Bd. 28, 1982, S. 211–226.

[CS88] Conway, J.; Sloane, N.: *Sphere packings, lattices and groups*. New York, Berlin: Springer-Verlag, 1988.

[CT91] Cover, T. M.; Thomas, J. A.: *Elements of Information Theory*. John Wiley & Sons, 1991.

[CWKS97] Crow, B. P.; Widjaja, I.; Kim, J. G.; Sakai, P. T.: IEEE 802.11 wireless local area networks. *IEEE Communications Magazine*, Bd. 35, 1997, S. 116–126.

[DAI96] Dasilva, J. S.; Arroyo, B.; Ikonomou, D.: European third-generation mobile systems. *IEEE Communications Magazine*, Bd. 34, 1996, S. 68–83.

[DB96] David, K.; Benkner, T.: *Digitale Mobilfunksysteme*. Stuttgart: B. G. Teubner, 1996.

[DGNS98] Dahlman, E.; Gudmundson, B.; Nilsson, M.; Sköld, J.: UMTS/IMT-2000 based on wideband CDMA. *IEEE Communications Magazine*, Bd. 36, 1998, S. 70–80.

[DH92] Duel-Hallen, A.: Equalizers for multiple input/multiple output channels and PAM systems with cyclostationary input sequences. *IEEE Journal on Selected Areas in Communications*, Bd. 10, 1992, S. 630–639.

[DH93] Duel-Hallen, A.: Decorrelating decision-feedback multiuser detector for synchronous code-division multiple-access channel. *IEEE Transactions on Communications*, Bd. 41, 1993, S. 285–290.

[DH95] Duel-Hallen, A.: A family of multiuser decision-feedback detectors for asynchronous code-division multiple-access channels. *IEEE Transactions on Communications*, Bd. 43, 1995, S. 421–434.

[DHHZ95] Duel-Hallen, A.; Holtzman, J.; Zvonar, Z.: Multiuser detection for CDMA systems. *IEEE Personal Communications*, Bd. 2, 1995, S. 46–58.

[DHJU03] Dietrich, F.; Hunger, R.; Joham, M.; Utschick, W.: Linear precoding over time-varying channels in TDD systems. *Proc. IEEE International Conference on Acoustics, Speech, and Signal Processing (ICASSP'03)*, Bd. 5, Hong Kong, 2003, S. 117–120.

[EF86] Effelsberg, W.; Fleischmann, A.: Das ISO-Referenzmodell für offene Systeme und seine sieben Schichten. *Informatik-Spektrum*, Bd. 9, 1986, S. 280–299.

[EGC80] El Gamal, A.; Cover, T.: Multiple user information theory. *Proceedings of the IEEE*, Bd. 68, 1980, S. 1466–1483.

[EGH81] El Gamal, A.; Heegard, C.: The capacity of computer memory with defects and noise. *Proc. International Symposium on Information Theory (ISIT'81)*, 1981, S. 107.

[EGH83] El Gamal, A.; Heegard, C.: On the capacity of computer memory with defects. *IEEE Transactions on Information Theory*, Bd. 29, 1983, S. 731–739.

[EMSW02] Eklund, C.; Marks, R. B.; Stanwood, K. L.; Wang, S.: IEEE standard 802.16: A technical overview of the WirelessMAN air interface for broadband wireless access. *IEEE Communications Magazine*, Bd. 40, 2002, S. 98–107.

[EN93] Esmailzadeh, R.; Nakagawa, M.: Pre-RAKE diversity combining for direct sequence spread spectrum mobile communications systems. *IEICE Transactions on Communications*, Bd. 76, 1993, S. 1008–1015.

[ESN93] Esmailzadeh, R.; Sourour, E.; Nakagawa, M.: Pre-rake diversity combing in time division duplex CDMA mobile communication. *Proc. IEEE International Conference on Communications (ICC'93)*, Genf, 1993, S. 463–467.

[ESN95] Esmailzadeh, R.; Sourour, E.; Nakagawa, M.: Pre-RAKE diversity combining in time division duplex CDMA mobile communications. *Proc. IEEE 6th International Symposium on Personal, Indoor and Mobile Radio Communications (PIMRC'95)*, Bd. 2, Toronto, 1995, S. 431–435.

[FG98] Foschini, G.; Gans, M.: On Limits of Wireless Communications in a Fading Environment when using Multiple Antennas. *Wireless Personal Communications*, Bd. 6, 1998, S. 311–335.

[FGVW99] Foschini, G. J.; Golden, G. D.; Valenzuela, R. A.; Wolniansky, P. W.: Simplified processing for high spectral efficiency wireless communication employing multi-element arrays. *IEEE Transactions on Information Theory*, Bd. 17, 1999, S. 1841–1852.

[Fis97] Fischer, R.: *Mehrkanal- und Mehrträgerverfahren für die schnelle digitale Übertragung im Ortsanschlußleitungsnetz.* Bd. 2 der Reihe *Berichte aus der Kommunikations- und Informationstechnik.* Aachen: Shaker-Verlag, 1997.

[Fis02] Fischer, R. F. H.: *Precoding and Signal Shaping for Digital Transmission.* New York: John Wiley & Sons, 2002.

[Fos96] Foschini, G. J.: Layered space-time architecture for wireless communication in a fading environment when using multi-element antennas. *The Bell System Technical Journal*, Bd. 1, 1996, S. 41–59.

[Fri96] Friedrichs, B.: *Kanalcodierung: Grundlagen und Anwendungen in modernen Kommunikationssystemen.* Berlin: Springer-Verlag, 1996.

[FST+96] Fukasawa, A.; Sato, T.; Takizawa, Y.; Kato, T.; Kawabe, M.; Fisher, R. R.: Wideband CDMA system for personal radio communications. *IEEE Communications Magazine*, Bd. 34, 1996, S. 116–123.

[FSW03] Fischer, R. F.; Stierstorfer, C.; Windpassinger, C.: Precoding and signal shaping for transmission over MIMO channels. *Proc. 2003 Canadian Workshop on Information Theory*, Waterloo, 2003, S. 83–87.

[FTH01] Fischer, R. F. H.; Tzschoppe, R.; Huber, J. B.: Signal shaping for reduction of peak-power and dynamic range in precoding schemes. *Proc. IEEE Global Telecommunications Conference (GLOBECOM'01)*, Bd. 2, San Antonio, 2001, S. 1344–1348.

[Fuh97] Fuhl, J.: *Smart Antennas for Second and Third Generation Mobile Communications Systems.* Dissertation, Institut für Nachrichtentechnik und Hochfrequenztechnik, Technische Universität Wien, 1997.

[FW03] Fischer, R. F. H.; Windpassinger, C. A.: Improved MIMO precoding for decentralized receivers resembling concepts from lattice reduction. *Proc. IEEE Global Telecommunications Conference (GLOBECOM'03)*, San Francisco, 2003.

[FWLH02a] Fischer, R. F. H.; Windpassinger, C.; Lampe, A.; Huber, J. B.: MIMO precoding for decentralized receivers. *Proc. 2002 IEEE International Symposium on Information Theory (ISIT'2002)*, Lausanne, 2002, S. 496.

[FWLH02b] Fischer, R. F. H.; Windpassinger, C.; Lampe, A.; Huber, J. B.: Space-time transmission using Tomlinson-Harashima precoding. *Proc. 4th International ITG Conference on Source and Channel Coding 2004 (SCC'2002)*, Berlin, 2002, S. 139–147.

[FWLH02c] Fischer, R. F. H.; Windpassinger, C.; Lampe, A.; Huber, J. B.: Tomlinson-Harashima precoding in space-time transmission for low-rate backward channel. *Proc. IEEE International Zurich Seminar on Broadband Communications (IZS'02)*, Zürich, 2002.

[Gab76] Gabriel, W. F.: Adaptive arrays — an introduction. *Proceedings of the IEEE*, Bd. 64, 1976, S. 239–273.

[GC01] Georgoulis, S.; Cruickshank, D. G. M.: Pre-equalization, transmitter precoding and joint transmission techniques for time division duplex CDMA. *Proc. International Conference on 3G Mobile Communications Technologies*, London, 2001, S. 257–261.

[GC02] Georgouilis, S.; Cruickshank, D.: Transmitter based inverse filters for MAI and ISI mitigation in a TDD/CDMA downlink. *Proc. IEEE 56th Vehicular Technology Conference (VTC'02-Fall)*, Vancouver, 2002.

[Geo03] Georgoulis, S. L.: *Transmitter Based Techniques for ISI and MAI Mitigation in CDMA-TDD Downlink*. Dissertation, The University of Edinburgh, 2003.

[GFVW99] Golden, G. D.; Foschini, C. J.; Valenzuela, R. A.; Wolniansky, P. W.: Detection algorithm and initial laboratory results using V-BLAST space-time communication architecture. *IEE Electronics Letters*, Bd. 35, 1999, S. 14–16.

[Gib99] Gibson, J. D. (Hrsg.): *The Mobile Communications Handbook*. 2 Auflage. Heidelberg: Springer-Verlag, 1999.

[GKV98] Gerthsen, C.; Kneser, H. O.; Vogel, H.: *Physik*. 16 Auflage. Berlin: Springer-Verlag, 1998.

[God97a] Godara, L. C.: Applications of antenna arrays to mobile communications, part I: Performance improvement, feasibility, and system considerations. *Proceedings of the IEEE*, Bd. 85, 1997, S. 1031–1060.

[God97b] Godara, L. C.: Applications of antenna arrays to mobile communications, part II: Beam-forming and direction-of-arrival considerations. *Proceedings of the IEEE*, Bd. 85, 1997, S. 1195–1245.

[GR91] Grohong, R.; Rusack, S.: Undersampling techniques simplify digital radio. *Electronic Design*, Bd. 5, 1991, S. 67–78.

[GVG94] Grandhi, S. A.; Vijayan, R.; Goodman, D. J.: Distributed power control in cellular radio systems. *IEEE Transactions on Communications*, Bd. 42, 1994, S. 226–228.

[GVGZ93] Grandhi, S. A.; Vijayan, R.; Goodman, D. J.; Zander, J.: Centralized power control in cellular radio systems. *IEEE Transactions on Vehicular Technology*, Bd. 42, 1993, S. 466–468.

[GW96] Garg, V. K.; Wilkes, J. E.: *Wireless and Personal Communications Systems*. Upper Saddle River: Prentice Hall, 1996.

[GZ94] Grandhi, S. A.; Zander, J.: Constrained power control in cellular radio systems. *Proc. IEEE 44th Vehicular Technology Conference (VTC'94)*, Bd. 2, Stockholm, 1994, S. 824–828.

[Hag96] Hagenauer, J.: Forward error correcting for CDMA systems. *Proc. IEEE 4th International Symposium on Spread Spectrum Techniques & Applications (ISSSTA'96)*, Bd. 2, Mainz, 1996, S. 566–569.

[Hay85] Haykin, S. (Hrsg.): *Array Signal Processing*. Englewood Cliffs: Prentice Hall, 1985.

[HJ85] Horn, R. A.; Johnson, C. R.: *Matrix analysis*. Cambridge: Cambridge University Press, 1985.

[HM72] Harashima, H.; Miyakawa, H.: Matched-transmission technique for channels with intersymbol interference. *IEEE Transactions on Communications*, Bd. 20, 1972, S. 774–780.

[HMC99] Host-Madsen, A.; Cho, K.-S.: MMSE/PIC multiuser detection for DS/CDMA systems with inter- and intra-cell interference. *IEEE Transactions on Communications*, Bd. 47, 1999, S. 291–299.

[HNP+99] Hardell, L.; Nasman, A.; Pahlson, A.; Hallquist, A.; Mild, K. H.: Use of cellular telephones and the risk for brain tumors: a case-control study. *International Journal of Oncology*, Bd. 15, 1999, S. 113–116.

[HS87] Hermanns, J.; Strunz, G.: Das Funktelefon-Netz C der Deutschen Bundespost. *Der Fernmelde-Ingenieur*, Bd. 12, 1987, S. 2–36.

[HS96] Hafeez, A.; Stark, W. E.: Combined decision-feedback multiuser detection / soft-decision decoding for CDMA channels. *Proc. IEEE 46th Vehicular Technology Conference (VTC'96)*, Bd. 1, Atlanta, 1996, S. 382–386.

[HSB03] Haustein, T.; Schubert, M.; Boche, H.: On power reduction strategies for the multi-user downlink with decentralized receivers. *Proc. IEEE 57th Vehicular Technology Conference (VTC'03-Spring)*, Bd. 2, Jeju, 2003, S. 1007–1011.

[HT00] Holma, H.; Toskala, A. (Hrsg.): *WCDMA For UMTS*. Chichester: John Wiley & Sons, 2000.

[Huf79] Huff, D. L.: Advanced mobile phone service: The developmental system. *The Bell System Technical Journal*, Bd. 58, 1979, S. 249–269.

[Hug00] Hughes, B. L.: Differential space-time modulation. *IEEE Transactions on Information Theory*, Bd. 46, 2000, S. 2567–2578.

[HvHJ+02] Haustein, T.; von Helmolt, C.; Jorswieck, E.; Jungnickel, V.; Pohl, V.: Performance of MIMO systems with channel inversion. *Proc. IEEE 55th Vehicular Technology Conference (VTC'02)*, Birmingham, 2002, S. 35–39.

[HWL97] He, B.; Wang, M. Z.; Li, K. C.: A new distributed power balancing algorithm for CDMA cellular systems. *Proc. IEEE International Symposium on Circuits and Systems ISCAS'97*, Bd. 3, Hong Kong, 1997, S. 1768–1771.

[ID96] Inacio, C.; Denise, O.: The DSP decision: fixed point or floating. *IEEE Spectrum*, Bd. 33, 1996, S. 72–74.

[IEE01] Human exposure to radio frequency and microwave radiation from portable and mobile telephones and other wireless communication devices – a comar technical information statement. *IEEE Engineering in Medicine and Biology Magazine*, Bd. 20, 2001, S. 128–131.

[IF02a] Irmer, R.; Fettweis, G.: MISO concepts for frequency-selective channels. *Proc. IEEE International Zurich Seminar on Broadband Communications (IZS'02)*, Zürich, 2002, S. 40/1–40/6.

[IF02b] Irmer, R.; Fettweis, G.: Combined Transmitter and Receiver Optimization for Multiple-Antenna Frequency-Selective Channels. *Proc. 5th International Symposium on Wireless Personal Multimedia Communications (WPMC'02)*, Honolulu, 2002, S. 412–416.

[IGF04] Irmer, R.; Gaur, J.; Fettwies, G.: Linear multiuser transmission for CDMA with reduced computational complexity. *Proc. IEEE 59th Vehicular Technology Conference (VTC'04-Spring)*, Mailand, 2004.

[IHRF03] Irmer, R.; Habendorf, R.; Rave, W.; Fettweis, G.: Nonlinear multiuser transmission using multiple antennas for TDD-CDMA. *Proc. 6th International Symposium on Wireless Personal Multimedia Communications (WPMC'03)*, Bd. 3, Yokosuka, 2003, S. 251–255.

[IHRF04a] Irmer, R.; Habendorf, R.; Rave, W.; Fettweis, G.: Nonlinear chip-level multiuser tranmission for TDD-CDMA with frequency-selective MIMO channels. *Proc. 5th International ITG Conference on Source and Channel Coding 2004 (SCC'2004)*, Erlangen, 2004, S. 363–370.

[IHRF04b] Irmer, R.; Habendorf, R.; Rave, W.; Fettweis, G.: Overloaded TDD-CDMA cells with multiuser transmission. *Proc. ITG Workshop on Smart Antennas (WSA'04)*, München, 2004.

[INBF01] Irmer, R.; Noll-Barreto, A.; Fettweis, G.: Transmitter precoding for spread-spectrum signals in frequency-selective fading channels. *Proc. 3G Wireless 2001*, San Francisco, 2001, S. 939–944.

[IRF03a] Irmer, R.; Rave, W.; Fettweis, G.: Minimum BER multiuser transmission for spread-spectrum systems in frequency-selective channels. Fazel, K.; Kaiser, S. (Hrsg.): *Multi-Carrier Spread-Spectrum & Related Topics*. Boston: Kluwer Academic Publishers, 2003. Proc. 4th International Workshop on Multi-Carrier Spread Spectrum (MC-SS 2003), Oberpfaffenhofen.

[IRF03b] Irmer, R.; Rave, W.; Fettweis, G.: Minimum BER transmission for TDD-CDMA in frequency-selective channels. *Proc. IEEE 14th International Symposium on Personal, Indoor and Mobile Radio Communications (PIMRC'03)*, Peking, 2003, S. 1260–1264.

[JA97] Juntti, M.; Aazhang, B.: Finite memory-length linear multiuser detection for asynchronous CDMA communications. *IEEE Transactions on Communications*, Bd. 45, 1997, S. 611–622.

[Jar01] Jarosch, A.: *Verfahren zur robusten Demodulation in der Abwärtsstrecke von UMTS mit breitbandigem Codevielfachzugriff*. Dissertation, ETH No. 14078, Swiss Federal Institute of Technology, 2001.

[Jax02] Jax, P.: *Enhancement of Bandlimited Speech Signals: Algorithms and Theoretical Bounds*. Bd. 15 der Reihe *Aachener Beiträge zu digitalen Nachrichtensystemen*. Aachen: Shaker-Verlag, 2002.

[JBM01] Jötten, C. A.; Baier, P. W.; Meurer, M.: Transmit array processing in CDMA downlinks utilizing the duplexing scheme FDD. *Proc. 8th International Conference on Telecommunications (ICT'01)*, Bukarest, 2001, S. 419–424.

[JBM+02] Jötten, C. A.; Baier, P. W.; Meurer, M.; Weber, T.; Haardt, M.: Efficient representation and feedback signaling of channel state information in frequency division duplexing MIMO systems. *Proc. 5th International Symposium on Wireless Personal Multimedia Communications (WPMC'02)*, Honolulu, 2002, S. 444–448.

[JBMW02a] Jötten, C. A.; Baier, P. W.; Meurer, M.; Weber, T.: Cost efficient representation and signaling of channel information in MIMO systems. *Proc. IEEE 56th Vehicular Technology Conference (VTC'02-Fall)*, Bd. 1, Vancouver, 2002, S. 175–179.

[JBMW02b] Jötten, C. A.; Baier, P. W.; Meurer, M.; Weber, T.: Subspace related signalling of feedback information for low rank MIMO channels. *Frequenz*, Bd. 56, 2002, S. 146–145.

[JBU04] Joham, M.; Brehmer, J.; Utschick, W.: MMSE Approaches to Multiuser Spatio-Temporal Tomlinson-Harashima Precoding. *Proc. 5th International ITG Conference on Source and Channel Coding 2004 (SCC'2004)*, 2004, S. 387–394.

[JBVU04] Joham, M.; Brehmer, J.; Voulgarelis, A.; Utschick, W.: Multiuser spatio-temporal Tomlinson-Harashima precoding for frequency selective vector channels. *Proceedings of the International ITG Workshop on Smart Antennas*, Munich, Germany, 2004.

[JD01] Jarosch, A.; Dahlhaus, D.: Linear space-time diversity receivers for the downlink of UMTS with WCDMA. *European Transactions on Telecommunications*, Bd. 12, 2001, S. 379–391.

[JHJvH02] Jungnickel, V.; Haustein, T.; Jorswieck, E.; von Helmolt, C.: On linear pre-processing in multi-antenna systems. *Proc. IEEE Global Telecommunications Conference (GLOBECOM'02)*, Bd. 1, Taipei, 2002, S. 1012–1016.

[JIB+03] Joham, M.; Irmer, R.; Berger, S.; Fettweis, G.; Utschick, W.: Linear precoding approaches for the TDD DS-CDMA downlink. *Proc. 6th International Symposium on Wireless Personal Multimedia Communications (WPMC'03)*, Bd. 3, Yokosuka, 2003, S. 323–327.

[JKG+02] Joham, M.; Kusume, K.; Gzara, M. H.; Utschick, W.; Nossek, J. A.: Transmit Wiener filter for the downlink of TDD DS-CDMA systems. *Proc. IEEE 7th International Symposium on Spread Spectrum Techniques & Applications (ISSSTA'02)*, Bd. 1, Prag, 2002, S. 9–13.

[JKUN02] Joham, M.; Kusume, K.; Utschick, W.; Nossek, J. A.: Transmit Matched Filter and Transmit Wiener Filter for the Downlink of FDD DS-CDMA Systems. *Proc. IEEE 13th International Symposium on Personal, Indoor and Mobile Radio Communications (PIMRC'02)*, Bd. 5, Lissabon, 2002, S. 2312–2316.

[JMB01] Jötten, C. A.; Meurer, M.; Baier, P. W.: Comparison of transmit array algorithms for CDMA downlinks operating in the FDD mode. *Proc. IEEE 12th International Symposium on Personal, Indoor and Mobile Radio Communications (PIMRC'01)*, San Diego, 2001, S. E16–E21.

[JMT02] Jötten, C. A.; Meurer, M.; Tröger, H.: Transmit array processing for CD-MA downlinks operating in mixed service environments. *Proc. IEEE 7th International Symposium on Spread Spectrum Techniques & Applications (ISSSTA'02)*, Bd. 2, Prag, 2002, S. 555–560.

[JN98] Joeng, I.; Nakagawa, M.: A novel multipath transmission diversity scheme in TDD-CDMA systems. *IEICE Transactions on Communications*, Bd. E81-B, 1998, S. 1409–1416.

[Joh04] Joham, M.: *Optimization of Linear and Nonlinear Transmit Signal Processing.* Berichte aus dem Lehrstuhl für Netzwerktheorie und Signalverarbeitung der Technischen Universität München. Aachen: Shaker-Verlag, 2004.

[Jöt03] Jötten, C. A.: *Ein Beitrag zur räumlichen Sendesignalvorverarbeitung in der Abwärtsstrecke frequenzduplexbasierter Mobilfunksysteme mit Code-Vielfachzugriff.* Dissertation, Lehrstuhl für hochfrequente Signalübertragung und -verarbeitung, Technische Universität Kaiserslautern, 2003.

[JU00] Joham, M.; Utschick, W.: Downlink processing for mitigation of intracell interference in DS-CDMA systems. *Proc. IEEE 6th International Symposium on Spread Spectrum Techniques & Applications (ISSSTA'00)*, Bd. 1, Parsippany, 2000, S. 15–19.

[JU01] Joham, M.; Utschick, W.: Symbol rate processing for the downlink of DS-CDMA systems. *IEEE Journal on Selected Areas in Communications*, Bd. 19, 2001, S. 61–68.

[JUN99] Joham, M.; Utschick, W.; Nossek, J. A.: A symbol rate multi-user downlink beamforming approach for WCDMA. *Proc. IEEE 10th International Symposium on Personal, Indoor and Mobile Radio Communications (PIMRC'99)*, Osaka, 1999, S. 228–232.

[JUN01] Joham, M.; Utschick, W.; Nossek, J. A.: On the equivalence of prerake and transmit matched filter. *Proc. 10th Aachen Symposium an Signal Theory (ASST'2001)*, Aachen, 2001, S. 313–318.

[JVP98] Jang, W. M.; Vojcic, B. R.; Pickholtz, R. L.: Joint Transmitter-Receiver Optimization in Synchronous Multiuser Communications over Multipath Channels. *IEEE Transactions on Communications*, Bd. 46, 1998, S. 269–278.

[JWJH01] Jorswieck, E.; Wunder, G.; Jungnickel, V.; Haustein, T.: Inverse eigenvalue statistics for Rayleigh and Rician MIMO channels. *IEE Professional Network on Antennas and Propagation*, 2001, S. 3/1–3/6.

[Kam84] Kammerlander, K.: C900 – an advanced mobile radio telephone system with optimum frequency utilization. *IEEE Journal on Selected Areas in Communications*, Bd. 2, 1984, S. 589–597.

[Kam85] Kammerlander, K.: Eigenschaften des zellularen Mobilfunksystems C450/900. *Telecom Report*, Bd. 8, 1985, S. 85–90.

[Kar99] Karimi, H. R.: Efficient multi-rate multi-user detection for the asynchronous WCDMA uplink. *Proc. IEEE 50th Vehicular Technology Conference (VTC'99-Fall)*, Bd. 1, Amsterdam, 1999, S. 593–597.

[KBF05] Karp, T.; Bauer, C.; Fliege, N. J.: Optimal one-tap equalization for DMT transceivers with insufficient guard interval. *Proc. IEEE International Conference on Acoustics, Speech, and Signal Processing (ICASSP'05)*, Philadelphia, 2005. accepted for publication.

[KBL97] Kuster, N.; Balzano, Q.; Lin, J.: *Mobile Communications Safety.* London, UK: Chapman & Hall, 1997.

[KIHP90] Kohno, R.; Imai, H.; Hatori, M.; Pasupathy, S.: An adaptive canceller of cochannel interference for spread-spectrum multiple-access communication networks in a power line. *IEEE Journal on Selected Areas in Communications*, Bd. 8, 1990, S. 691–699.

[KKKB94] Klein, A.; Kawas Kaleh, G.; Baier, P. W.: Equalizers for multi-user detection in code division multiple access mobile radio systems. *Proc. IEEE 44th Vehicular Technology Conference (VTC'94)*, Bd. 2, Stockholm, 1994, S. 762–766.

[KKKB96] Klein, A.; Kawas Kaleh, G.; Baier, P. W.: Zero forcing and minimum mean-square-error equalization for multiuser detection in code-division multiple-access channels. *IEEE Transactions on Vehicular Technology*, Bd. 45, 1996, S. 276–287.

[KKLN98] Knisely, D. N.; Kumar, S.; Laha, S.; Nanda, S.: Evolution of wireless data services: IS-95 to cdma2000. *IEEE Communications Magazine*, Bd. 36, 1998, S. 140–149.

[Kle96] Klein, A.: *Multi-user detection of CDMA signals – algorithms and their application to cellular mobile radio.* Fortschrittberichte VDI, Reihe 10, Nr. 423. Düsseldorf: VDI-Verlag, 1996.

[KM00] Kowalewski, F.; Mangold, P.: Joint predistortion and transmit diversity. *Proc. IEEE Global Telecommunications Conference (GLOBECOM'00)*, Bd. 1, San Francisco, 2000, S. 245–249.

[KMGW03] Kienle, F.; Michel, H.; Gilbert, F.; Wehn, N.: Efficient MAP-algorithm implementation on programmable architectures. *Kleinheubacher Berichte*, Bd. 46, Kleinheubach, 2003.

[Koh94] Kohno, R.: Spatial and temporal filtering for co–channel interference in CDMA. *Proc. IEEE 3rd International Symposium on Spread Spectrum Techniques & Applications (ISSSTA'94)*, Oulu, 1994, S. 51–60.

[KS01] Kammeyer, K.-D.; Schmidt, H.: OFDM: An old idea solves new problems. *Proc. 11th International Symposium on Theoretical Electrical Engineering (ISTET 2001)*, Linz, 2001, S. K1–K9.

[KSS99] Karimi, H. R.; Sandell, M.; Salz, J.: Comparison between transmitter and receiver array processing to achieve interference nulling and diversity. *Proc. IEEE 10th International Symposium on Personal, Indoor and Mobile Radio Communications (PIMRC'99)*, Bd. 3, Osaka, 1999, S. 997–1001.

[KTF04] Karp, T.; Trautmann, S.; Fliege, N. J.: Zero-forcing frequency-domain equalization for generalized DMT transceivers with insufficient guard interval. *EURASIP Journal on Applied Signal Processing*, Bd. 10, 2004, S. 1446–1459.

[KV96] Krim, H.; Viberg, M.: Two decades of array signal processing research. *IEEE Signal Processing Magazine*, Bd. 13, 1996, S. 67–94.

[KW04] Kienle, F.; Wehn, N.: Efficient hardware realization of IRA code decoders. *Proc. IEEE Workshop on Signal Processing Systems (SIPS 2004)*, Austin, Texas, 2004, S. 286–291.

[Lay00] Layer, F.: Prediction of inbuilding multipath radio channels for future radio services. *Frequenz*, Bd. 54, 2000, S. 165–170.

[LB00] Lu, Y.; Baier, P.: Performance of adaptive antennas for the TD-CDMA downlink under special consideration of multi-directional channels and CDMA code pooling. *International Journal of Electronics and Communications (AEÜ)*, Bd. 54, 2000, S. 249–258.

[LBM01] Lu, Y.; Baier, P. W.; Meurer, M.: SNIR optimization for the TD-CDMA downlink with CDMA code pooling and adaptive transmit antennas. *Proc. 11th International Symposium on Theoretical Electrical Engineering (ISTET 2001)*, Linz, 2001.

[Lee90] Lee, W. C. Y.: *Mobile Cellular Telecommunications Systems*. New York: McGraw-Hill, 1990.

[LL86] Lange, K.; Löcherer, K.-H.: *Taschenbuch der Hochfrequenztechnik*. Berlin: Springer-Verlag, 1986.

[Llo82] Lloyd, S. P.: Least squares quantization in PCM. *IEEE Transactions on Information Theory*, Bd. 28, 1982, S. 129–137.

[LLS95] Lee, T.-H.; Lin, J.-C.; Su, Y. T.: Downlink power control algorithms for cellular radio systems. *IEEE Transactions on Vehicular Technology*, Bd. 44, 1995, S. 89–94.

[LMTB01] Lu, Y.; Meurer, M.; Tröger, H.; Baier, P. W.: Downlink considerations for Time-Slotted CDMA. *Proc. ITG Diskussionssitzung: Systeme mit intelligenten Antennen*, Illmenau, 2001, S. 147–155.

[Lor85] Lorenz, R. W.: Zeit- und Frequenzabhängigkeit der Übertragungsfunktion eines Funkkanals bei Mehrwegeausbreitung mit besonderer Berücksichtigung des Mobilfunkkanals. *Der Fernmelde-Ingenieur*, Bd. 4, 1985, S. 2–45.

[LR99] Liberti, J. C.; Rappaport, T. S.: *Smart Antennas for Wireless Communications: IS-95 and Third Generation CDMA Applications*. Upper Saddle River: Prentice Hall, 1999.

[LSF03] Lampe, L. H.-J.; Schober, R.; Fischer, R.: Coded differential space-time modulation for flat fading channels. *IEEE Transactions on Wireless Communications*, Bd. 2, 2003, S. 582 – 590.

[LTM01] Lu, Y.; Tröger, H.; Meurer, M.: TD-CDMA-Abwärtsstrecke mit adaptiven Sendeantennen. *Proc. DFG-Kolloquium: Adaptivität in heterogenen Kommunikationsnetzen mit drahtlosem Zugang*, Kaiserslautern, 2001, S. 25–29.

[Lu02] Lu, Y.: *Contributions to the application of adaptive antennas and CDMA code pooling in the TD-CDMA downlink*. Dissertation, Lehrstuhl für hochfrequente Signalübertragung und -verarbeitung, Universität Kaiserslautern, 2002.

[Lük79] Lüke, H. D.: *Signalübertragung*. 2 Auflage. Berlin: Springer–Verlag, 1979.

[Lük99] Lüke, H. D.: The Origins of the Sampling Theorem. *IEEE Communications Magazine*, Bd. 37, 1999, S. 106–108.

[LV89] Lupas, R.; Verdú, S.: Linear multiuser detectors for synchronous code-division multiple-access channels. *IEEE Transactions on Information Theory*, Bd. 35, 1989, S. 123–136.

[LV90] Lupas, R.; Verdú, S.: Near-far resistance of multiuser detectors in asynchronous channels. *IEEE Transactions on Communications*, Bd. 38, 1990, S. 496–508.

[LW04] Litz, L.; Wehn, N.: Research center 'Ambient Intelligence' at the University of Kaiserslautern. *Proc. VDE-Kongress 2004*, Berlin, 2004, S. 19–24.

[Max60] Max, J.: Quantizing for minimum distortion. *IRE Transactions on Information Theory*, Bd. IT–6, 1960, S. 7–12.

[MBL+00] Meurer, M.; Baier, P. W.; Lu, Y.; Papathanassiou, A.; Weber, T.: TD-CDMA downlink: Optimum transmit signal design reduces receiver complexity and enhances system performance. *Proc. 7th International Conference on Telecommunications (ICT'00)*, Bd. 1, Acapulco, 2000, S. 300–305.

[MBQ04] Meurer, M.; Baier, P. W.; Qiu, W.: Receiver Orientation versus Transmitter Orientation in Linear MIMO Transmission Systems. *EURASIP Journal on Applied Signal Processing*, Bd. 9, 2004, S. 1191–1198.

[MBW+00] Meurer, M.; Baier, P. W.; Weber, T.; Lu, Y.; Papathanassiou, A.: Joint transmission: advantageous downlink concept for CDMA mobile radio systems using time division duplexing. *IEE Electronics Letters*, Bd. 36, 2000, S. 900–901.

[MD79] Mac Donald, V. H.: The cellular concept. *The Bell System Technical Journal*, Bd. 58, 1979, S. 15–41.

[MDCM95] Moulines, E.; Duhamel, P.; Cardoso, J.; Mayrargue, S.: Subspace methods for blind identification of multichannel FIR filters. *IEEE Transactions on Signal Processing*, Bd. 43, 1995, S. 516–525.

[Meu00] Meurer, M.: A joint A/D conversion scheme for multi antenna software radios based on Code Division Multiplex. *Proc. 1st Karlsruhe Workshop on Software Radios*, Karlsruhe, 2000, S. 7–12.

[Meu03] Meurer, M.: *Gemeinsame Empfangssignalverarbeitung in CDMA-Mobilfunksystemen mit infiniter oder quasiinfiniter Datenübertragung.* Dissertation, Lehrstuhl für hochfrequente Signalübertragung und -verarbeitung, Universität Kaiserslautern, 2003.

[Meu04a] Meurer, M.: An analytical view on receiver oriented multi-user MIMO transmission over dispersive Rayleigh fading channels. *IEEE Transactions on Communications*, 2004. Submitted for publication.

[Meu04b] Meurer, M.: On the transmit efficiency of multi-user MIMO transmission utilizing transmit zero-forcing. *IEEE Transactions on Wireless Communications*, 2004. Submitted for publication.

[MFP97] Masoomzadeh-Fard, A.; Pasupathy, S.: Combined equalization and differential detection using precoding. *IEEE Transactions on Communications*, Bd. 45, 1997, S. 274–278.

[MG62] Meinke, H.; Gundlach, F. W.: *Taschenbuch der Hochfrequenztechnik: Grundlagen.* Bd. 1. 2. Auflage. Berlin: Springer-Verlag, 1962.

[MG86] Meinke, H.; Gundlach, F. W.: *Taschenbuch der Hochfrequenztechnik: Komponenten.* Bd. 2. 4. Auflage. Berlin: Springer-Verlag, 1986.

[MGS98a] Montalbano, G.; Ghauri, I.; Slock, D. T. M.: Spatio-temporal array processing for CDMA/SDMA downlink transmission. *Proc. 32th Asilomar Conference on Signals, Systems and Computers*, Bd. 2, Pacific Grove, 1998, S. 1337–1341.

[MGS98b] Montalbano, G.; Ghauri, I.; Slock, D. T. M.: Spatio-temporal array processing for matched filter bound optimization in SDMA downlink transmission. *Proc. URSI International Symposium on Signals, Systems, and Electronics (ISSSE'98)*, Pisa, 1998, S. 416–421.

[MJWT01] Meurer, M.; Jötten, C. A.; Weber, T.; Tröger, H.: A novel approach to multi user detection for high-data-rate applications in CDMA downlinks. *Proc. 13th International Conference on Wireless Communications (WIRELESS 2001)*, Bd. 1, Calgary, 2001, S. 74–83.

[ML01] Maeng, S.; Lee, B. G.: Extended window decorrelating detector for asynchronous CDMA channels and its performance analysis. *IEEE Transactions on Communications*, Bd. 49, 2001, S. 35–40.

[ML02] Murch, R. D.; Letaief, K. B.: Antenna Systems for Broadband Wireless Access. *IEEE Communications Magazine*, Bd. 40, 2002, S. 76–83.

[MLW+02] Meurer, M.; Lu, Y.; Weber, T.; Jötten, C. A.; Baier, P. W.: Blind channel estimation for time-slotted code division multiple access mobile radio systems. *Proc. IEEE 7th International Symposium on Spread Spectrum Techniques & Applications (ISSSTA'02)*, Bd. 1, Prag, 2002, S. 49–53.

[MM80] Monzingo, R. A.; Miller, T. W.: *Introduction to Adaptive Arrays.* New York: John Wiley & Sons, 1980.

[Moh98] Moher, M.: An iterative multiuser decoder for near-capacity communications. *IEEE Transactions on Communications*, Bd. 46, 1998, S. 870–880.

[MPGF01] Morgado, A.; Pinho, P.; Gameiro, A.; Fernandes, J.: Pre-equalization technique for interference cancellation in the UMTS-TDD downlink channel. *Proc. IEEE 54th Vehicular Technology Conference (VTC'01-Fall)*, Bd. 1, Atlantic City, 2001.

[MQBW04] Meurer, M.; Qiu, W.; Baier, P.; Weber, T.: *Transmit power reduction in CDMA mobile radio downlinks by nonlinear receiver oriented transmission combined with multiply connected quantization schemes.* Technische Mitteilung 15/04, Research Group for RF Communications, University of Kaiserslautern, 2004.

[MQS+04] Meurer, M.; Qiu, W.; Stimming, C.; Tauböck, G.; White, G.; Burr, A.: *Outline Design for Terminal Baseband Processing and Implementation Complexity.* Technische Mitteilung D18, European Union IST Project IST-2001-32125 FLOWS, 2004. http://www.flows-ist.org.

[MQW03] Meurer, M.; Qiu, W.; Weber, T.: An advanced approach to joint transmission: Design of energy efficient transmit signals by transmit nonlinear zero forcing. *Proc. Dresden Workshop on "Senderseitige Signalverarbeitung im Mobilfunk"*, Dresden, 2003.

[MR00] Meurer, M.; Raulefs, R.: Enhancement of multichannel A/D conversion by a code division multiplex approach. *Proc. IEEE 6th International Symposium on Spread Spectrum Techniques & Applications (ISSSTA'00)*, Bd. 2, Parsippany, 2000, S. 641–646.

[MSN97] Matsutani, H.; Sanada, Y.; Nakagawa, M.: A forward link intracell orthogonalization techique using multicarrier pre-decorrelation for CDMA wireless local communication system. *Proc. IEEE 8th International Symposium on Personal, Indoor and Mobile Radio Communications (PIMRC'97)*, Bd. 1, Helsinki, 1997, S. 125–129.

[MT03] Meurer, M.; Tröger, H.: Channel oriented multi-user MIMO downlinks in frequency selective channels. *Proc. DFG-Kolloqium: Adaptivität in heterogenen Kommunikationsnetzen mit drahtlosem Zugang*, Hamburg, 2003.

[MTJ02] Meurer, M.; Tröger, H.; Jötten, C. A.: A novel generalized optimization criterion for transmit signal design in joint transmission (JT) multiuser downlinks. *Proc. 9th International Conference on Telecommunications (ICT'02)*, Bd. 1, Peking, 2002, S. 26–31.

[MTWB01a] Meurer, M.; Tröger, H.; Weber, T.; Baier, P. W.: Synthesis of joint detection (JD) and joint transmission (JT) in CDMA. *COST 273 TD(01)003*, Brüssel, 2001.

[MTWB01b] Meurer, M.; Tröger, H.; Weber, T.; Baier, P. W.: Synthesis of joint detection (JD) and joint transmission (JT) in CDMA downlinks. *IEE Electronics Letters*, Bd. 37, 2001, S. 919–920.

[MW03a] Meurer, M.; Weber, T.: Generalized data estimate refinement techniques for iterative multiuser detection in TD-CDMA including higher order modulation. *Proc. 10th International Conference on Telecommunications (ICT'03)*, Bd. 1, Papeete, 2003, S. 781–787.

[MW03b] Meurer, M.; Weber, T.: The soft symbol: soft quantization and higher-order modulation, a contradiction? *Proc. 2. Diskussionssitzung der ITG-Fachgruppe Angewandte Informationstheorie*, Dresden, 2003, S. 86–91.

[MW04a] Meurer, M.; Weber, T.: Imperfect channel knowledge: An insurmountable barrier in Rx oriented multi-user MIMO transmission? *Proc. 5th International ITG Conference on Source and Channel Coding 2004 (SCC'2004)*, Erlangen, 2004, S. 371–380.

[MW04b] Meurer, M.; Weber, T.: On the impact of imperfect channel knowledge on transmit zero forcing based receiver oriented multi-user MIMO transmission. *IEEE Transactions on Wireless Communications*, 2004. accepted for publication.

[MWQ04a] Meurer, M.; Weber, T.; Qiu, W.: A random matrix approach to performance evaluation of receiver-oriented transmission. *Proc. 4. Diskussionssitzung der ITG-Fachgruppe Angewandte Informationstheorie*, Kiel, 2004.

[MWQ04b] Meurer, M.; Weber, T.; Qiu, W.: Transmit Nonlinear Zero Forcing: Energy efficient receiver oriented transmission in MIMO CDMA mobile radio downlinks. *Proc. IEEE 8th International Symposium on Spread Spectrum Techniques & Applications (ISSSTA'04)*, Sydney, 2004, S. 260–269.

[MWSL02] Maniatis, I.; Weber, T.; Sklavos, A.; Liu, Y.: Pilots for joint channel estimation in multi-user OFDM mobile radio systems. *Proc. IEEE 7th International Symposium on Spread Spectrum Techniques & Applications (ISSSTA'02)*, Bd. 1, Prag, 2002, S. 44–48.

[NA83] Nettleton, R. W.; Alavi, H.: Power control for a spread spectrum cellular mobile radio system. *Proc. IEEE Vehicular Technology Conference (VTC'83)*, Toronto, 1983, S. 242–246.

[Naß95] Naßhan, M. M.: *Realitätsnahe Modellierung und Simulation nachrichtentechnischer Systeme, gezeigt am Beispiel eines CDMA-Mobilfunksystems.* Fortschrittberichte VDI, Reihe 10, Nr. 384. Düsseldorf: VDI-Verlag, 1995.

[NB02] Noll Barreto, A.: *Signal Pre-Processing in the Downlink of Spread-Spectrum Communications Systems*. Fortschrittberichte VDI, Reihe 10, Nr. 687. Düsseldorf: VDI-Verlag, 2002.

[NBF00] Noll-Barreto, A.; Fettweis, G.: Performance improvement in DS-spread spectrum CDMA systems using a pre- and a post-rake. *Proc. IEEE International Zurich Seminar on Broadband Communications (IZS'00)*, Zürich, 2000, S. 39–46.

[NJU04] Nossek, J. A.; Joham, M.; Utschick, W.: Transmit Processing in MIMO Wireless Systems. *Proc. 6th CAS Symposium on Emerging Technologies*, Bd. I, 2004, S. I–18–I–23.

[ntz00a] Europäische Vergabeverfahren von UMTS-Lizenzen kritisiert. *Nachrichtentechnische Zeitschrift*, Bd. 5, 2000, S. 16.

[ntz00b] UMTS-Versteigerungsverfahren erzielte 99,3682 Mrd. DM. *Nachrichtentechnische Zeitschrift*, Bd. 10, 2000, S. 16.

[OP98] Ojanperä, T.; Prasad, R.: An overview of air interface multiple access for IMT-2000/UMTS. *IEEE Communications Magazine*, Bd. 36, 1998, S. 82–95.

[OPM98] O'Leary, S.; Priestly, D.; McSparron, N.: Mobile broadcasting of DVB-T signals. *IEEE Transactions on Broadcasting*, Bd. 44, 1998, S. 346 – 352.

[Pad94] Padovani, R.: Reverse link performance of IS-95 based cellular systems. *IEEE Personal Communications*, Bd. 1, 1994, S. 28–34.

[Pap00] Papathanassiou, A.: *Adaptive antennas for mobile radio systems using Time Division CDMA and joint detection*. Dissertation, Lehrstuhl für hochfrequente Signalübertragung und -verarbeitung, Universität Kaiserslautern, 2000.

[Par92] Parsons, J. D.: *The Mobile Radio Propagation Channel*. London: Pentech Press, 1992.

[Pät99] Pätzold, M.: *Mobilfunkkanäle*. Braunschweig: Vieweg, 1999.

[PF94] Petersen, B.; Falconer, D.: Suppression of adjacent-channel, cochannel, and intersymbol interference by equalizers and linear combiners. *IEEE Transactions on Communications*, Bd. 42, 1994, S. 3109–3118.

[PHS03] Peel, C. B.; Hochwald, B. M.; Swindlehurst, A. L.: A vector-perturbation technique for near-capacity multi-antenna multi-user communication. *Proc. 41st Allerton Conference on Communication, Control, and Computing*, Allerton House, 2003.

[PMWB00] Papathanassiou, A.; Meurer, M.; Weber, T.; Baier, P. W.: A novel multiuser transmission scheme requiring no channel estimation and no equalization at the mobile stations for the downlink of TD-CDMA operating in the TDD mode. *Proc. IEEE 52nd Vehicular Technology Conference (VTC'00-Fall)*, Bd. 1, Boston, 2000, S. 203–210.

[Poo00] Poor, H. V.: Turbo multiuser detection: An overview. *Proc. IEEE 6th International Symposium on Spread Spectrum Techniques & Applications (ISSSTA'00)*, Bd. 2, Parsippany, 2000, S. 583–587.

[Pro95] Proakis, J. G.: *Digital Communications.* 3. Auflage. New York: McGraw-Hill, 1995.

[PTVF92] Press, W. H.; Teukolsky, S. A.; Vetterling, W. T.; Flannery, B. P.: *Numerical Recipes in C.* 2. Auflage. New York: Cambridge University Press, 1992.

[Qiu05] Qiu, W.: *Transmit power reduction in MIMO multi-user mobile radio downlinks by the rationale receiver orientation.* Dissertation, Lehrstuhl für hochfrequente Signalübertragung und -verarbeitung, Technische Universität Kaiserslautern, 2005.

[QMB+04] Qiu, W.; Meurer, M.; Burr, A.; White, G.; Stimming, C.; Tauböck, G.: Performance of MIMO systems. *Proc. FLOWS Workshop*, Redhill, 2004.

[QMBW04] Qiu, W.; Meurer, M.; Baier, P. W.; Weber, T.: Power efficient CDMA broadcast system doing without any channel knowledge at the receivers, a non-obvious modification of THP. *Proc. IEEE joint conference (APCC/MDMC'04) of 10th Asia-Pacific Conference on Communications (APCC2004) and 5th International Symposium on Multi-Dimensional Mobile Communications (MDMC2004)*, Peking, 2004, S. 793–799.

[QMWB05] Qiu, W.; Meurer, M.; Weber, T.; Baier, P. W.: Ein CDMA-basiertes Systemkonzept zur leistungssparenden nichtlinearen empfängerorientierten Übertragung in Mobilfunkabwärtstrecken. *Proc. DFG-Kolloqium: Adaptivität in heterogenen Kommunikationsnetzen mit drahtlosem Zugang*, Karlsruhe, 2005.

[QTM02] Qiu, W.; Tröger, H.; Meurer, M.: System model of joint transmission (JT) in multi-user MIMO transmission systems. *COST 273 TD(02)008*, London, 2002.

[QTMJ03] Qiu, W.; Tröger, H.; Meurer, M.; Jötten, C. A.: Performance analysis of a channel oriented concept for multi-user MIMO downlinks with frequency selective channels. *Proc. IEEE 57th Vehicular Technology Conference (VTC'03-Spring)*, Bd. 1, Jeju, 2003, S. 539–543.

[Rab00] Rabaey, J. M.: Silicon platforms for the next generation wireless systems - What role does reconfigurable hardware play? Hartenstein, R. W.; Grünbacher, H. (Hrsg.): *Field-Programmable Logic and Applications, The Roadmap to Reconfigurable Computing, Proc. 10th International Workshop (FPL'2000), Villach*, Bd. 1896 der Reihe *Lecture Notes in Computer Science*, 2000, S. 277–285.

[Rab01] Rabaey, J. M.: Silicon architectures for wireless systems. *Proc. Hotchips 2001, Tutorial*, Palo Alto, 2001.

[Rap98] Rappaport, T. S. (Hrsg.): *Smart Antennas.* Hoes Lane: Institute of Electrical and Electronics Engineers, 1998.

[Rei98] Reimers, U.: Digital video broadcasting. *IEEE Communications Magazine*, Bd. 36, 1998, S. 104 – 110.

[RF96] Reinhardt, M.; Frey, T.: Turbo-equalisation for symbol-spread block transmission system. *IEE Electronics Letters*, Bd. 32, 1996, S. 2321–2323.

[RIF02] Ringel, U.; Irmer, R.; Fettweis, G.: Transmit diversity for frequency-selective channels in UMTS-TDD. *Proc. IEEE 7th International Symposium on Spread Spectrum Techniques & Applications (ISSSTA'02)*, Bd. 2, Prag, 2002, S. 802–806.

[Roh95] Rohling, H.: *Einführung in die Informations- und Codierungstheorie.* Stuttgart: B. G. Teubner, 1995.

[RSAA98] Reed, M. C.; Schlegel, C. B.; Alexander, P. D.; Asenstorfer, J. A.: Iterative multiuser detection for CDMA with FEC: Near-single-user performance. *IEEE Transactions on Communications*, Bd. 46, 1998, S. 1693–1699.

[Rup93] Rupprecht, W.: *Signale und Übertragungssysteme.* Berlin: Springer-Verlag, 1993.

[RV94] Rapajic, P. B.; Vucetic, B. S.: Adaptive receiver structures for asynchronous CDMA systems. *IEEE Journal on Selected Areas in Communications*, Bd. 12, 1994, S. 685–697.

[RV95] Rapajic, P. B.; Vucetic, B. S.: Linear adaptive transmitter-receiver structures for asynchronous CDMA. *European Transactions on Telecommunications*, Bd. 6, 1995, S. 21–28.

[SB93] Steiner, B.; Baier, P. W.: Low cost channel estimation in the uplink receiver of CDMA mobile radio systems. *Frequenz*, Bd. 47, 1993, S. 292–298.

[Sch79] Schneider, K. S.: Optimum detection for code division multiplexed signals. *IEEE Transactions on Aerospace and Electronic Systems*, Bd. 15, 1979, S. 181–185.

[Sch80] Schneider, K. S.: Crosstalk resistant receiver for M-ary multiplexed communications. *IEEE Transactions on Aerospace and Electronic Systems*, Bd. 16, 1980, S. 426–433.

[Sch97] Schaller, R.: Moore's law: past, present and future. *IEEE Spectrum*, Bd. 34, 1997, S. 52 – 59.

[Sch99] Schlee, J.: *Ein Hardware-Demonstrator zur Konzeptverifikation eines JD-CDMA-Mobilfunksystems.* Dissertation, Lehrstuhl für hochfrequente Signalübertragung und -verarbeitung, Universität Kaiserslautern, 1999.

[SG91] Salmasi, A.; Gilhousen, K. S.: On the system design aspects of code division multiple access CDMA applied to digital cellular and personal communications networks. *Proc. IEEE 41st Vehicular Technology Conference (VTC'91)*, St. Louis, 1991, S. 57–62.

[Sha48] Shannon, C. E.: A mathematical theory of communication. *The Bell System Technical Journal*, Bd. 27, 1948, S. 379–423, 623–656.

[SJ67] Stein, S.; Jones, J. J.: *Modern Communication Principles.* New York: McGraw-Hill, 1967.

[SJ94] Steiner, B.; Jung, P.: Optimum and suboptimum channel estimation for the uplink of CDMA mobile radio systems with joint detection. *European Transactions on Telecommunications and Related Technologies*, Bd. 5, 1994, S. 39–50.

[Skl04] Sklavos, A.: *Service Area Based OFDM Air Interface for Beyond 3G Mobile Radio Systems.* Dissertation, Lehrstuhl für hochfrequente Signalübertragung und -verarbeitung, Technische Universität Kaiserslautern, 2004.

[SL04a] Schober, R.; Lampe, L.: Differentially-coherent parallel interference cancellation for DS-CDMA. *IEEE Transactions on Wireless Communications*, 2004. accepted for publication.

[SL04b] Schober, R.; Lampe, L.: Noncoherent receivers for multi-chip differentially encoded DS-CDMA. *IEEE Transactions on Wireless Communications*, Bd. 3, 2004, S. 2129 – 2140.

[SMWB01] Sklavos, A.; Maniatis, I.; Weber, T.; Baier, P. W.: Joint channel estimation in multi-user OFDM systems. *Proc. 6th International OFDM-Workshop (InOWo'01)*, Hamburg, 2001, S. 3–1–3–4.

[SOSL88] Simon, M. K.; Omura, J. K.; Scholtz, R. A.; Levitt, B. K.: *Spread spectrum communications.* Bd. 1–3. Rockville: Computer Science Press, 1988.

[SP99] Sampath, H.; Paulraj, J. A.: Joint Transmit and Receive Optimization for High Data Rate Wireless Communication Using Multiple Antennas. *Proc. of the 33th Asilomar Conference on Signals, Systems & Computers*, Bd. 1, Pacific Grove, 1999, S. 215–219.

[SRAX96] Schlegel, C.; Roy, S.; Alexander, P. D.; Xiang, Z.-J.: Multiuser projection receivers. *IEEE Journal on Selected Areas in Communications*, Bd. 14, 1996, S. 1610–1618.

[SS01] Shi, Z.; Schlegel, C.: Joint iterative decoding of serially concatenated error control coded CDMA. *IEEE Journal on Selected Areas in Communications*, Bd. 19, 2001, S. 1646–1653.

[SSB+02] Scaglione, A.; Stoica, P.; Barbarossa, S.; Giannakis, G. B.; Sampath, H.: Optimal Designs for Space-Time Linear Precoders and Decoders. *IEEE Transactions on Signal Processing*, Bd. 50, 2002, S. 1051–1064.

[SSH04] Spencer, Q. H.; Swindlehurst, A. L.; Haardt, M.: Zero-forcing methods for downlink spatial multiplexing in multiuser MIMO channels. *IEEE Transactions on Signal Processing*, Bd. 52, 2004, S. 461–471.

[SSP01] Sampath, H.; Stoica, P.; Paulraj, A.: Generalized linear precoder and decoder design for MIMO channels using the weighted MMSE criterion. *IEEE Transactions on Communications*, Bd. 49, 2001, S. 2198–2206.

[Ste92] Steele, R.: *Mobile Radio Communications*. London: Pentech Press, 1992.

[Ste95] Steiner, B.: *Ein Beitrag zur Mobilfunk-Kanalschätzung unter besonderer Berücksichtigung synchroner CDMA-Mobilfunksysteme mit Joint Detection*. Fortschrittberichte VDI, Reihe 10, Nr. 337. Düsseldorf: VDI-Verlag, 1995.

[Ste96] Steil, A.: *Spektrale Effizienz digitaler CDMA–Mobilfunksysteme mit gemeinsamer Detektion*. Fortschrittberichte VDI, Reihe 10, Nr. 437. Düsseldorf: VDI-Verlag, 1996.

[SW96] Sung, C. W.; Wong, W. S.: A cooperative algorithm for asynchronous distributed power control in cellular systems. *Proc. IEEE Global Telecommunications Conference (GLOBECOM'96)*, Bd. 3, London, 1996, S. 1979–1983.

[SWBC02] Sklavos, A.; Weber, T.; Baier, P. W.; Costa, E.: Beyond 3G radio interface JOINT: Optimum uplink data detection when applying OFDM. *Proc. 7th International OFDM-Workshop (InOWo'02)*, Hamburg, 2002, S. 11–15.

[SWM01] Sklavos, A.; Weber, T.; Maniatis, I.: Interference suppression in multi-user OFDM systems by antenna diversity and joint detection. *COST 273 TD(01)020*, Bologna, 2001.

[SWWM04] Schulz, E.; Weckerle, M.; Weber, T.; Meurer, M.: The OFDM based beyond 3G air interface JOINT featuring interference reduction by joint detection and joint transmission. *Proc. 8th WWRF Meeting*, Peking, 2004, S. 1–11.

[Tan92] Tanenbaum, A. S.: *Computer-Netzwerke*. 2. Auflage. Attenkirchen: Wolfram's Fachverlag, 1992.

[TAS95] Tidestav, C.; Ahlen, A.; Sternad, M.: Narrowband and broadband multiuser detection using a multivariable DFE. *Proc. IEEE 6th International Symposium on Personal, Indoor and Mobile Radio Communications (PIMRC'95)*, Bd. 2, Toronto, 1995, S. 732–736.

[TC94] Tang, Z.; Cheng, S.: Interference cancellation for DS-CDMA systems over flat fading channels through pre-decorrelating. *Proc. IEEE 5th International Symposium on Personal, Indoor and Mobile Radio Communications (PIMRC'94)*, Bd. 2, Den Haag, 1994, S. 435–438.

[Tel99] Telatar, I. E.: Capacity of multi-antenna Gaussian channels. *European Transactions on Telecommunications*, Bd. 10, 1999, S. 585–595.

[TJ00] Tarokh, V.; Jafarkhani, H.: A differential detection scheme for transmit diversity. *IEEE Journal on Selected Areas in Communications*, Bd. 18, 2000, S. 1169–1174.

[TMW00] Tröger, H.; Meurer, M.; Weber, T.: Adaptive antennas for the TD-CDMA downlink utilizing the novel concept joint transmission. *ITG Diskussionssitzung Antennen für mobile Systeme 2000*, Starnberg, 2000, S. 37–40.

[Tom71] Tomlinson, M.: New automatic equalizer employing modulo arithmetic. *IEE Electronics Letters*, Bd. 7, 1971, S. 138–139.

[TQMJ02] Tröger, H.; Qiu, W.; Meurer, M.; Jötten, C. A.: A channel oriented Joint Transmission scheme for MIMO multi-user downlinks. *Proc. of the 1st COST 273 Workshop on "Opportunities of the Multi-dimensional Propagation Channel"*, Espoo, 2002.

[TR00] Tan, P. H.; Rasmussen, L. K.: Linear interference cancellation in CDMA based on iterative techniques for linear equation systems. *IEEE Transactions on Communications*, Bd. 48, 2000, S. 2099–2108.

[Trö03] Tröger, H.: *Empfängerorientierte Mehrteilnehmer-Übertragungsverfahren für die Abwärtsstrecke zellularer Mobilfunksysteme*. Dissertation, Lehrstuhl für hochfrequente Signalübertragung und -verarbeitung, Universität Kaiserslautern, 2003.

[TVP96] Talwar, S.; Viberg, M.; Paulraj, A.: Blind separation of synchronous co-channel digital signals using an antenna array — part I: Algorithms. *IEEE Transactions on Signal Processing*, Bd. 44, 1996, S. 1184–1197.

[TWL+02] Tao, X.; Wang, S.; Li, Y.; Liu, B.; Zhang, P.: Pre-distortion based joint transmission. *Proc. IEEE 55th Vehicular Technology Conference (VTC'02)*, Birmingham, 2002, S. 493–496.

[TWMB01a] Tröger, H.; Weber, T.; Meurer, M.; Baier, P. W.: A novel performance evaluation technique for joint transmission multiuser downlinks with multi-element transmit antennas. *Proc. COST 262 Workshop Multiuser Detection in Spread Spectrum Communications*, Schloß Reisensburg / Ulm, 2001, S. 121–125.

[TWMB01b] Tröger, H.; Weber, T.; Meurer, M.; Baier, P. W.: Performance assessment of joint transmission (JT) multi-user downlinks with multi-element transmit antennas. *European Transactions on Telecommunications*, Bd. 12, 2001, S. 407–415.

[UY01] Ulukus, S.; Yates, R. D.: Signature Sequence Optimization in Asynchronous CDMA Systems. *Proc. IEEE International Conference on Communications (ICC'01)*, Helsinki, 2001, S. 545–549.

[VA89] Varanasi, M.; Aazhang, B.: Probability of error comparison of linear and iterative multiuser detectors. *Advances in Communications and Signal Processing, Lecture Notes in Control and Information Sciences*, 1989, S. 15–26.

[VA90] Varanasi, M. K.; Aazhang, B.: Multistage detection in asynchronous code-division multiple-access communications. *IEEE Transactions on Communications*, Bd. 38, 1990, S. 509–519.

[VA91] Varanasi, M. K.; Aazhang, B.: Near-optimum detection synchronous code-division multiple-access systems. *IEEE Transactions on Communications*, Bd. 39, 1991, S. 725–736.

[Ver86] Verdú, S.: Optimum multiuser asymptotic efficiency. *IEEE Transactions on Communications*, Bd. 34, 1986, S. 890–897.

[Ver88] Verdú, S.: Recent progress in multiuser detection. *Proc. International Conference on Advances in Communications and Control Systems*, Bd. 1, 1988, S. 66–77.

[Ver93] Verdú, S.: Multiuser detection. Poor, H. V.; Thomas, J. B. (Hrsg.): *Advances in Statistical Signal Processing: Signal Detection*, Greenwich, 1993, S. 369–410.

[Ver98] Verdú, S.: *Multiuser Detection*. Cambridge: Cambridge University Press, 1998.

[VHH98] Vary, P.; Heute, U.; Hess, W.: *Digitale Sprachsignalverarbeitung*. Stuttgart: B. G. Teubner, 1998.

[Vit95] Viterbi, A. J.: *CDMA: Principles of Spread Spectrum Communication*. Reading: Addison-Wesley, 1995.

[VJ98] Vojcic, B. R.; Jang, W. M.: Transmitter precoding in synchronous multiuser communications. *IEEE Transactions on Communications*, Bd. 46, 1998, S. 1346–1355.

[vNP00] van Nee, R. D. J.; Prasad, R.: *OFDM for Wireless Multimedia Communications*. Boston: Artech House, 2000.

[VW98] Valenti, M. C.; Woerner, B. D.: Iterative multiuser detection for convolutionally coded asynchronous DS-CDMA. *Proc. IEEE 9th International Symposium on Personal, Indoor and Mobile Radio Communications (PIMRC'98)*, Bd. 1, Boston, 1998, S. 213–217.

[Wal98a] Walke, B.: *Mobilfunknetze und ihre Protokolle: Bündelfunk, schnurlose Telefonsysteme, W-ATM, HIPERLAN, Satellitenfunk, UPT*. Bd. 2. Stuttgart: B. G. Teubner, 1998.

[Wal98b] Walke, B.: *Mobilfunknetze und ihre Protokolle: Grundlagen, GSM, UMTS und andere zellulare Mobilfunknetze*. Bd. 1. Stuttgart: B. G. Teubner, 1998.

[WBOW00] Weber, T.; Baier, P. W.; Oster, J.; Weckerle, M.: Performance enhancement of time division CDMA (TD-CDMA) by multi-step joint detection. *Proc. 7th International Conference on Telecommunications (ICT'00)*, Bd. 2, Acapulco, 2000, S. 1038–1044.

[WCS03] Wang, S.; Caffery, J. J.; Shen, H.: Linear multiuser precoding for synchronous CDMA. *Proc. IEEE Wireless Communications and Networking Conference (WCNC'2003)*, Bd. 4, 2003, S. 403–407.

[WDH94] Wu, H.; Duel-Hallen, A.: Performance of multiuser decision-feedback detectors for flat fading synchronous CDMA channels. *Proc. 28th Conference on Information Sciences and Systems*, 1994, S. 133–138.

[Web00] Weber, T.: *Signalverarbeitungskonzepte für Mobilfunksysteme der dritten Generation, gezeigt am Beispiel eines JD-CDMA-Mobilfunksystems.* Dissertation, Lehrstuhl für hochfrequente Signalübertragung und -verarbeitung, Universität Kaiserslautern, 2000.

[Web02] Weber, T.: *Interferenzreduktion in CDMA-Mobilfunksystemen — ein aktuelles Problem und Wege zu seiner Lösung.* Habilitationsschrift, Lehrstuhl für hochfrequente Signalübertragung und -verarbeitung, Universität Kaiserslautern, 2002.

[Wec02] Weckerle, M.: *Utilization of Correlation Matrices in Adaptive Array Processors for Time Slotted CDMA Uplinks.* Dissertation, Lehrstuhl für hochfrequente Signalübertragung und -verarbeitung, Universität Kaiserslautern, 2002.

[Wei94] Wei, L.-F.: Generalized square and hexagonal constellations for intersymbol-interference channels with generalized Tomlinson-Harashima precoders. *IEEE Transactions on Communications*, Bd. 42, 1994, S. 2713–2721.

[Wer94] Werner, M.: Multistage joint detection with decision feedback for CDMA mobile radio applications. *Proc. IEEE 5th International Symposium on Personal, Indoor and Mobile Radio Communications (PIMRC'94)*, Bd. 1, Den Haag, 1994, S. 178–183.

[Wes02] Wesołowski, K.: *Mobile Communication Systems.* New York: John Wiley & Sons, 2002.

[WES04] Wiesel, A.; Eldar, Y.; Shamai, S.: Multiusers precoders for fixed receivers. *Proc. IEEE International Zurich Seminar on Broadband Communications (IZS'04)*, 2004.

[WF03] Windpassinger, C.; Fischer, Robert, F. H.: Low-complexity near-maximum-likelihood detection and precoding for MIMO systems using lattice reduction. *Proc. IEEE Information Theory Workshop*, Paris, 2003, S. 345–348.

[WFGV98] Wolniansky, P.; Foschini, G. J.; Golden, G. D.; Valenzuela, R. A.: V-BLAST: An architecture for realizing very high data rates over the rich-scattering wireless channel. *Proc. URSI International Symposium on Signals, Systems, and Electronics (ISSSE'98)*, Pisa, 1998, S. 295–300.

[WFH04] Windpassinger, C.; Fischer, R. F. H.; Huber, J. B.: Lattice-reduction-aided broadcast precoding. *IEEE Transactions on Communications*, Bd. 52, 2004, S. 2057–2060.

[WHL+03] Welling, I.; Harno, J.; Loizillon, F.; Stordahl, K.; Varoutas, D.: Techno-economic evaluation of 3G & WLAN business case feasibility under varying conditions. *Proc. 10th International Conference on Telecommunications (ICT'03)*, Bd. 1, Papeete, 2003, S. 33–38.

[WIF02] Wathan, F.; Irmer, R.; Fettweis, G.: On transmitter-based interference mitigation in TDD-downlink with frequency selective fading channel environment. *Proc. Asia-Pacific Conference on Communications (APCC)*, Bandung, 2002, S. 125–128.

[Wil98] Wilson, S. G.: *Digital modulation and coding.* London: Prentice Hall, 1998.

[Win04] Windpassinger, C.: *Detection and Precoding for Multiple Input and Multiple Output Channels.* Dissertation, University Erlangen-Nürnberg, 2004.

[WLMM03] Weber, T.; Liu, Y.; Maniatis, I.; Meurer, M.: Performance of a multiuser OFDM mobile radio system with joint detection. *Proc. 8th International OFDM-Workshop (InOWo'03)*, Hamburg, 2003, S. 191–195.

[WM02a] Weber, T.; Meurer, M.: Iterative multiuser detection for TD-CDMA exploiting data estimate refinement techniques. *Proc. IEEE 56th Vehicular Technology Conference (VTC'02-Fall)*, Bd. 3, Vancouver, 2002, S. 1642–1646.

[WM02b] Weber, T.; Meurer, M.: Turbo multiuser detection for TD-CDMA. *Kleinheubacher Berichte*, Bd. 45, Kleinheubach, 2002, S. 159–164.

[WM03a] Weber, T.; Maniatis, I.: Channel knowledge: A crucial prerequisite for MIMO transmission? *COST 273 TD(03)083*, Paris, 2003.

[WM03b] Weber, T.; Meurer, M.: Influence of channel estimation errors on joint detection and joint transmission. *Proc. Dresden Workshop on "Senderseitige Signalverarbeitung im Mobilfunk"*, Dresden, 2003.

[WM03c] Weber, T.; Meurer, M.: Joint detection and joint transmission - unexpected nondualities concerning the influence of channel estimation errors. *COST 273 TD(03)152*, Prag, 2003.

[WM03d] Weber, T.; Meurer, M.: Optimum joint transmission: Potentials and dualities. *Proc. 6th International Symposium on Wireless Personal Multimedia Communications (WPMC'03)*, Bd. 1, Yokosuka, 2003, S. 79–83.

[WM03e] Weber, T.; Meurer, M.: Potential of optimum joint transmission. *1. Diskussionssitzung der ITG-Fachgruppe Angewandte Informationstheorie*, Erlangen, 2003.

[WM04a] Weber, T.; Meurer, M.: Imperfect channel state information in MIMO-transmission. *Proc. IEEE 59th Vehicular Technology Conference (VTC'04-Spring)*, Mailand, 2004.

[WM04b] Weber, T.; Meurer, M.: Transmit nonlinear zero forcing for OFDM multiuser downlinks. *COST 273 TD(04)008*, Athen, 2004.

[WMGG67] Widrow, B.; Mantey, P. E.; Griffiths, L. J.; Goode, B. B.: Adaptive antenna systems. *Proceedings of the IEEE*, Bd. 55, 1967, S. 2143–2159.

[WMS03] Weber, T.; Meurer, M.; Sklavos, A.: Optimum nonlinear joint transmission. *COST 273 TD(03)008*, Barcelona, 2003.

[WMSL02] Weber, T.; Maniatis, I.; Sklavos, A.; Liu, Y.: Joint transmission and detection integrated network (JOINT), a generic proposal for beyond 3G systems. *Proc. 9th International Conference on Telecommunications (ICT'02)*, Bd. 3, Peking, 2002, S. 479–483.

[WMZ04a] Weber, T.; Meurer, M.; Zirwas, W.: Low Complexity Energy Efficient Joint Transmission for OFDM Multiuser Downlinks. *Proc. IEEE 15th International Symposium on Personal, Indoor and Mobile Radio Communications (PIMRC'04)*, Barcelona, 2004.

[WMZ04b] Weber, T.; Meurer, M.; Zirwas, W.: A MIMO based OFDM system concept for beyond 3G mobile radio systems. *COST 273 TD(04)084*, Göteborg, 2004.

[WMZ05] Weber, T.; Meurer, M.; Zirwas, W.: Subspace Based Channel Estimation. *COST 273 TD(05)004*, Bologna, 2005.

[WNM92] Wijayasuriya, S.; Norton, G.; McGeehan, J.: Sliding window decorrelating algorithm for DS–CDMA receivers. *IEE Electronics Letters*, Bd. 28, 1992, S. 1596–1598.

[WNM93] Wijayasuriya, S.; Norton, G.; McGeehan, J.: A novel algorithm for dynamic updating of decorrelator coeeficients in mobile DS–CDMA. *Proc. 4th International Symposium on Personal, Indoor and Mobile Radio Communications (PIMRC'93)*, Yokohama, 1993, S. 292–296.

[WNM96] Wijayasuriya, S.; Norton, G.; McGeehan, J.: A sliding window decorrelating receiver for multiuser DS–CDMA mobile radio networks. *IEEE Transactions on Vehicular Technology*, Bd. 45, 1996, S. 503–521.

[WO01] Weber, T.; Oster, J.: Hard- and soft-decision multi-step joint detection for TD-CDMA. *Proc. 2001 URSI International Symposium on Signals, Systems, and Electronics (ISSSE'01)*, Tokyo, 2001, S. 347–350.

[WOWB02] Weber, T.; Oster, J.; Weckerle, M.; Baier, P. W.: Turbo multiuser detection for TD-CDMA. *International Journal of Electronics and Communications (AEÜ)*, Bd. 54, 2002, S. 120–130.

[WP99] Wang, X.; Poor, H. V.: Iterative (turbo) soft interference cancellation and decoding for coded CDMA. *IEEE Transactions on Computers*, Bd. 47, 1999, S. 1046–1061.

[WR01] Walke, C. M.; Rembold, B.: Joint Detection and Joint Pre-Distortion techniques for SD/TD/CDMA systems. *Frequenz*, Bd. 55, 2001, S. 204–213.

[WS85] Widrow, B.; Stearns, S. D.: *Adaptive Signal Processing*. Englewood Cliffs: Prentice Hall, 1985.

[WSLW03] Weber, T.; Sklavos, A.; Liu, Y.; Weckerle, M.: The air interface concept JOINT for beyond 3G mobile radio networks. *Proc. 15th International Conference on Wireless Communications (WIRELESS 2003)*, Bd. 1, Calgary, 2003, S. 25–33.

[WSM04] Weber, T.; Sklavos, A.; Meurer, M.: Imperfect Channel State Information in MIMO-Transmission. *IEEE Transactions on Communications*, 2004. Submitted for publication.

[WVF03a] Windpassinger, C.; Vencel, T.; Fischer, R. F. H.: Real- vs. complex-valued equalisation in V-BLAST systems. *IEE Electronics Letters*, Bd. 39, 2003, S. 470–471.

[WVF03b] Windpassinger, C.; Vencel, T.; Fischer, Robert, F. H.: Precoding and loading for BLAST-like systems. *Proc. IEEE Global Telecommunications Conference (GLOBECOM'03)*, Anchorage, 2003, S. 3061–3065.

[WZW04a] Wellig, A.; Zory, J.; Wehn, N.: Energy- and area-efficient deinterleaving architecture for high-throughput wireless applications. *Proc. 14th PATMOS Workshop - International Workshop on Power And Timing Modeling, Optimization and Simulation*, Santorini, 2004.

[WZW04b] Wellig, A.; Zory, J.; Wehn, N.: Novel optimum reduced search mlse decoding algorithm enabling system-aware power savings. *Proc. IEEE Radio & Wireless Conference 2004 (RAWCON 2004)*, Atlanta, 2004.

[WZZY99] Wang, J.-B.; Zhao, M.; Zhou, S.-D.; Yao, Y.: A novel multipath transmission diversity scheme in TDD-CDMA systems. *IEICE Transactions on Communications*, Bd. E82-B, 1999, S. 1706–1707.

[XSR90] Xie, Z.; Short, R. T.; Rushforth, C. K.: A family of suboptimum detectors for coherent multiuser communications. *IEEE Journal on Selected Areas in Communications*, Bd. 8, 1990, S. 683–690.

[You79] Young, W. R.: Advanced mobile phone service: Introduction, background, and objectives. *The Bell System Technical Journal*, Bd. 58, 1979, S. 1–14.

[YR94] Yang, J.; Roy, S.: Joint transmitter-receiver optimization for multi-input multi-output systems with decision feedback. *IEEE Transactions on Information Theory*, Bd. 40, 1994, S. 1334–1347.

[YSJ+01] Yu, W.; Sutivang, A.; Julian, D.; Cover, T.; Chiang, M.: Writing on colored paper. *Proc. International Symposium on Information Theory (ISIT'01)*, Washington, DC, 2001.

[Zan92a] Zander, J.: Distributed cochannel interference control in cellular radio systems. *IEEE Transactions on Vehicular Technology*, Bd. 41, 1992, S. 305–311.

[Zan92b] Zander, J.: Performance of optimum transmitter power control in cellular radio systems. *IEEE Transactions on Vehicular Technology*, Bd. 41, 1992, S. 57–62.

[ZB98] Zhang, X.; Brady, D.: Asymptotic multiuser efficiency for decision-directed multiuser detection. *IEEE Transactions on Information Theory*, Bd. 44, 1998, S. 502–515.

[ZF86] Zurmühl, R.; Falk, S.: *Matrizen und ihre Anwendungen.* Bd. 2. 5. Auflage. Berlin: Springer-Verlag, 1986.

[ZF97] Zurmühl, R.; Falk, S.: *Matrizen und ihre Anwendungen.* Bd. 1. 7. Auflage. Berlin: Springer-Verlag, 1997.